

# Directed Evolution of Enantioselective Enzymes as Catalysts for Organic Synthesis

M.T. REETZ

*Max-Planck-Institut für Kohlenforschung, 45470 Mülheim/Ruhr, Germany*

This review constitutes a comprehensive and critical account of a fundamentally new approach to asymmetric catalysis, namely, the exploitation of the methods of directed evolution in the creation of enantioselective enzymes as biocatalysts in organic chemistry. The basis of the concept is the effective combination of molecular biological methods of gene mutagenesis and expression followed by high-throughput screening for assessing the enantioselectivity of thousands of samples. Following a brief introduction outlining the challenges in putting this new approach into practice, the molecular biological gene mutagenesis methods are introduced in a language that chemists can understand, followed by a description of high-throughput assays for enantioselectivity. Examples illustrating the concept are then presented, beginning with a detailed account of lipases followed by other hydrolases, aminotransferases, aldolases, and oxidases. The review ends with conclusions and perspectives.

**Abbreviations:** 3D, three-dimensional; ACS, acetyl coenzyme synthetase; ADO, assembly of designed oligonucleotides, a recombinant mutagenesis method; ANEH, epoxide hydrolase from *Aspergillus niger*; ATP, adenosine 5'-triphosphate; BSA, bovine serum albumin; BSLA, *Bacillus subtilis* lipase A; CAE, capillary array electrophoresis; CAST, complete active-site saturation test; CD, circular dichroism; CE, capillary electrophoresis; CHMO, cyclohexanone monooxygenase; CMC, combinatorial multiple-cassette mutagenesis; CS, citrate synthase; DNA, deoxyribonucleic acid, the genetic material of living things; DNA shuffling, a recombinant gene mutagenesis method; *ee*, enantiomeric excess; EH, epoxide hydrolase; EMDee, enzymatic method for determining enantiomeric excess; epPCR, error-prone polymerase chain reaction; ESI-MS, electrospray ionization mass spectrometry; *E* value, enantioselectivity factor in a kinetic resolution; FTIR, Fourier transform infrared; GC, gas chromatography; HLDH, horse-liver alcohol dehydrogenase; HPLC, high-performance liquid chromatography; HTS-FTIR, high-throughput Fourier transform infrared; IR, infrared; ITCHY, incremental truncation for the creation of hybrid enzymes;  $k_{\text{cat}}$ , catalytic rate constant of an enzyme-catalyzed reaction;  $k_{\text{cat}}/K_{\text{M}}$ , catalytic efficiency of an enzyme-catalyzed reaction; the greater the value, the more efficient is the conversion of the substrate into product; KDPG, D-2-keto-3-deoxy-6-phospho-6-gluconate aldolase;  $K_{\text{M}}$ , dissociation constant of the binding of an enzyme to a substrate; L-MDH, L-malate dehydrogenase; MAO-N, monoamine oxidase from *Aspergillus niger*; MM, molecular modeling; MS, mass spectrometry; MURA, mutagenic and unidirectional reassembly, a gene mutagenesis method; NAD, nicotinamide adenine dinucleotide, a coenzyme functioning as a hydrogen carrier in redox reactions; NADH, reduced form of NAD; NAD(P)H, reduced form of NAD(P), which is the phosphorylated form of NAD; NMR, nuclear magnetic resonance; OPUS<sup>TM</sup>, software for FTIR-based *ee*-assay (Bruker); PAMO, phenyl acetone monooxygenase; PC, personal computer; PCHMO, phenylcyclohexanone monooxygenase; PCR, polymerase chain reaction, a DNA amplification method;

PFE, esterase from *Pseudomonas fluorescens*;  $pK_a$ , negative logarithm of acidity constant; QM, quantum mechanics; Quick-*E*-Test, an assay for assessing the *E* value in the hydrolytic kinetic resolution of esters; (*R*), absolute configuration of a compound according to the Cahn–Ingold–Prelog convention; RDA-PCR, recombination-dependent exponential amplification-polymerase chain reaction, a gene mutagenesis method; RETT, recombined extension on truncated templates, a gene mutagenesis method; RID, random insertion/deletion mutagenesis; RNA, ribonucleic acid; (*S*), absolute configuration of a compound according to the Cahn–Ingold–Prelog convention; SCOPE, structure-based combinatorial protein engineering, a gene mutagenesis method; SCRATCHY, combination of ITCHY and DNA shuffling; SERRS, surface-enhanced resonance Raman scattering; SeSaM, sequence saturation mutagenesis; SHIPREC, sequence homology-independent protein recombination, a recombinant gene mutagenesis method; SIMPLEX expression, *in vitro* coupled transcription/translation; SISDC, sequence-independent site-directed chimeragenesis, a gene mutagenesis method; STEP, staggered extension process, a recombinant gene mutagenesis method; *Taq* polymerase, an enzyme from *Thermus aquaticus* used in PCR; TWISTER 1, microplate stacking device coupled to microplate plate reader in FTIR-based *ee* assay (Bruker); UV/Vis, ultraviolet/visible; WT, wild-type gene or protein.

## I. Introduction

The world market for chiral organic compounds such as pharmaceuticals, plant protecting agents, and fragrances continues to expand, requiring efficient methods for their synthesis (1,2). Although classical antipode resolution based on diastereomer formation and separation followed by enantiomer regeneration is still widely used in industry, catalytic methods have gained importance during the preceding two decades. Indeed, asymmetric catalysis constitutes the most elegant, efficient, and environmentally benign strategy to meet the synthetic goals. This requires the ready accessibility of highly enantioselective catalysts, which also need to be robust and active. When choosing this approach, organic chemists have four options: transition metal catalysts (3–5), organocatalysts (6), enzymes (7–11), or catalytic antibodies (12). The decision as to which option is best depends on a number of factors including cost of catalysts, catalyst stability, activity, and enantioselectivity, type of solvent, and ease of workup.

Enzymes have been used as catalysts in asymmetric transformations for at least a century, but their routine use in synthetic organic chemistry was not established until the 1980s. Since then the importance of this class of biocatalysts has continually increased, and an impressive number of industrial processes have been reported (7–11). In any investigation of new substrates (reactants), various commercially available enzyme kits can be screened. An important innovation in the field was the discovery that many enzymes perform well in organic solvents (13). Although a trend is clearly emerging in industry to consider biocatalysis more than in the past, one of the problems with using enzymes is the fact that they are substrate-specific. For a given reaction, enantioselectivity may be unacceptably low, or the substrate may not even be accepted by the enzyme. In principle, a type of “ligand tuning” guided by molecular modeling is possible, namely, the exchange of one or more amino acids at given positions in the enzyme by one of the remaining 19 proteinogenic amino acids using site-directed mutagenesis, a standard technique in molecular biology (14,15). Successful examples of enhancing the enantioselectivity of a given enzyme-catalyzed reaction by this method have been reported, but due to the complexity of enzymes, the procedure has not proven to be a straightforward tool.

Enantioselective enzyme-catalyzed reactions may involve the transformation of a prochiral substrate into a chiral product, in which case the selectivity is measured by the enantiomeric excess (*ee*). The transformations can also involve kinetic resolution of racemic substrates, in which case enantioselectivity is measured by the selectivity factor *E* reflecting the relative rates of reaction of the (*R*)- and (*S*)-enantiomer.

In the 1990s, a fundamentally new approach to the development of enantioselective catalysts for use in organic synthesis was introduced (16). It is based on the directed evolution of enzymes, a process which had previously been used to improve properties such as activity or stability (17–20). The basis of the concept is the combination of proper molecular biological methods for random gene mutagenesis and expression coupled with high-throughput screening systems for the rapid identification of enantioselective mutant enzymes. The idea is to start with a natural (wild-type, WT) enzyme showing an unacceptably low *ee* or *E* value for a given transformation of interest,  $A \rightarrow B$ , to create a library of mutants from which the most highly enantioselective variant is identified, and to repeat such cycles as often as necessary using in each case an improved mutant for the next round of mutagenesis (16). Because the inferior mutants are discarded, an evolutionary character of the overall process is simulated. In the process, random mutagenesis is performed on the gene (DNA segment) that encodes the desired enzyme (Fig. 1). Of course, in fortunate cases, the initial library of mutants may already contain a variant showing the desired level of enantioselectivity, which means that the search can be ended before the actual evolutionary process begins (21–24).

Experimentally, in each cycle the library of mutated genes is first inserted in a standard bacterial host such as *Escherichia coli* or *Bacillus subtilis*. Then bacterial colonies are plated on agar plates and harvested individually by a colony picker. Each colony is placed in a separate well of a microtiter plate containing nutrient broth, so that the bacteria grow and produce the protein of interest. Because each colony originates from a single cell, mixtures of mutant enzymes are avoided (provided that there is no undesired cross-contamination). A portion of each mutant occurring in the harvested bacterial colony is then robotically placed on a different microtiter plate, where the enantioselective reaction of interest is carried out. Because the enzyme variants and the corresponding mutant genes are spatially addressable, the genotype/phenotype relation is maintained, and tedious deconvolution is not necessary. The best mutant (positive hit) is then the starting point for the next cycle of gene mutagenesis, expression, and screening (Fig. 2). Knowledge of the structure or mechanism of the enzyme is not required (16,21–24). This approach is quite different from rational design based on site-directed mutagenesis, but it is nevertheless rational in a different sense due to the evolutionary character.

The general idea of “evolution in the test tube” was first proposed and illustrated experimentally by Spiegelman in 1965–1967, who performed an interesting “Darwinian experiment with a self-duplicating nucleic acid molecule” (RNA) outside a living cell (25). The term “directed evolution” was used as early as 1972 by Hansche, who screened naturally occurring mutants of a phosphatase in a population of  $10^9$  cells over 1000 generations in a continuous manner, thereby increasing enzyme activity (26). Following several other sporadic contributions (27), Eigen

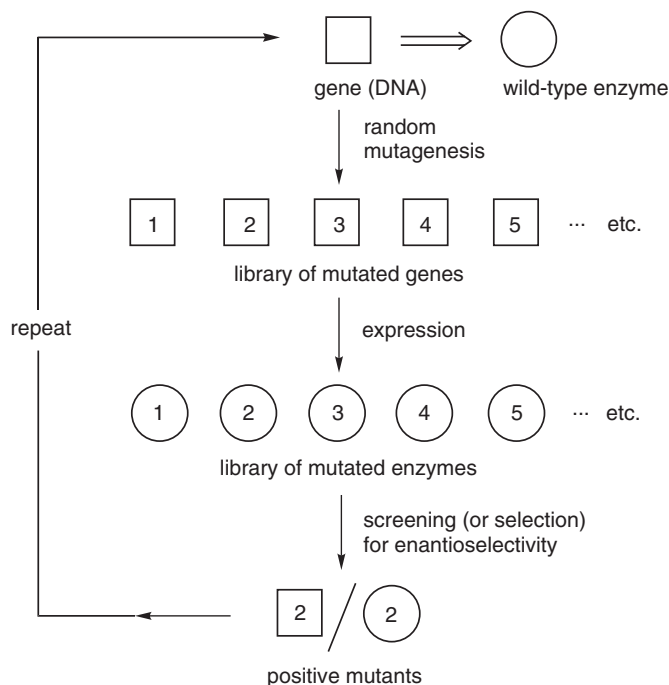


FIG. 1. Strategy for directed evolution of an enantioselective enzyme (22,24).

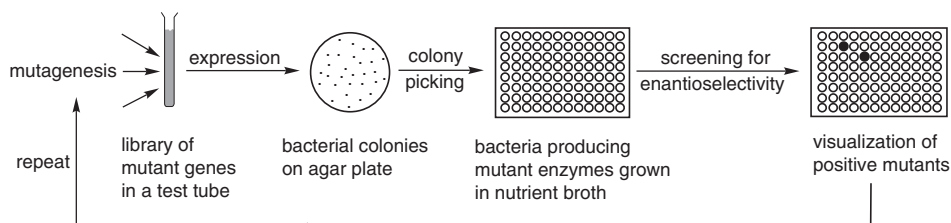


FIG. 2. The experimental stages of directed evolution of enantioselective enzymes (21,22).

predicted that it should be possible to construct an evolutionary machine comprising repeating cycles of mutant production, separation, and amplification of individual clones; evolution of optimal phenotypes; and identification of optimal genotypes (27,28). Following this suggestion, the 1980s witnessed significant progress in the development of efficient methods for gene mutagenesis and expression, and libraries of mutant enzymes were constructed and scanned for properties of interest, in most cases, activity (29a,b).

However, this process in itself is not yet directed evolution, because only one cycle of mutagenesis/screening is involved. Isolated cases involving at least two such cycles began to appear, being the first cases of true directed evolution of enzymes (29c), but it was not until the period of 1993–1997 that the idea of directed

evolution was fully appreciated and generalized experimentally, specifically by the groups of Arnold (30–32) and Stemmer (18,33–35). Using known and new methods of gene mutagenesis, some of which were developed in the laboratories of these authors, in combination with simple screening or selection systems, enzyme properties such as activity, thermal stability, and stability against hostile solvents were improved. This work opened a completely new field. Other groups concentrated mainly on devising new and more efficient mutagenesis methods that provide new avenues to high protein diversity (17–20).

These developments set the stage for the concept of directed evolution of enantioselective enzymes, which likewise makes use of repeating cycles of mutagenesis/expression/screening (Figs 1 and 2) (16,21–24). The challenges in this new field include the elaboration of strategies for looking through protein sequence space for enantioselectivity, on the one hand, and the development of efficient high-throughput screening systems for evaluating thousands of potentially enantioselective mutant enzymes, on the other.

This chapter is a summary of the present state of the art concerning the directed evolution of enantioselective enzymes as catalysts in organic chemistry. It begins with a description of the molecular biological methods of gene mutagenesis, presented in a way that chemists can easily follow, continues with a summary of high-throughput *ee* assays, and ends with a systematic report of all currently known examples of directed evolution of enantioselective enzymes.

## II. Mutagenesis Methods

To date, an impressive number of gene mutagenesis methods are available for application in directed evolution (17–20,36,37). However, it is currently not clear how they compare in terms of efficiency and ease of performance. It is also not obvious when and how to apply a given method in a directed evolution project (36–38). The fact that a few of the methods constitute proprietary intellectual property, such as DNA shuffling, poses a different kind of problem for potential users in industry. Some of the most important gene mutagenesis methods are described briefly here (for complete coverage, the reader is referred to recent reviews 17–20,36,37).

The use of mutator strains or the treatment of the isolated DNA with UV light or chemicals, as reported in the older literature and sometimes still used today, provides a means to target the whole gene for more or less random point mutagenesis, but it is not trivial to control such processes (17). Modern gene mutagenesis methods can be roughly assigned to two different categories, those based on point mutations and those making use of recombination (17–20,36,37).

### A. METHODS BASED ON POINT MUTATIONS

In 1989, a very practical mutagenesis method was described by Leung *et al.* (39), which was later improved by Cadwell and Joyce (40). Error-prone polymerase chain reaction (epPCR), as it is called, is based on the classical DNA amplification

method, PCR, developed by Mullis (41). By varying parameters such as the concentration of  $\text{MgCl}_2$  (or  $\text{MnCl}_2$ ) and/or nucleotide concentration, errors in DNA amplification are induced—which constitutes mutagenesis. The mutation rate can be adjusted empirically (e.g., so that on average one, two, or more amino acid exchange events occur in the expressed protein). Although epPCR is sometimes considered to induce point mutations randomly over the entire gene (and protein), this is actually not the case. Due to the degeneracy of the genetic code, *inter alia*, some amino acid exchanges are favored in a given enzyme whereas others are not accessible (17,42). It has been estimated that typically only about 25% of the theoretically possible mutants can be accessed by epPCR. Nevertheless, most directed evolution projects begin with epPCR because it is very easy to perform and provides a convenient platform from which the actual evolutionary optimization can begin. To eliminate or reduce amino acid bias in whole gene randomization, methods have been developed that however require a greater degree of effort, as in a process called sequence saturation mutagenesis (SeSaM) (42d). As pointed out by Lutz and Patrick (37), Stratagene's second-generation Mutazyme<sup>®</sup> polymerase in combination with *Taq* DNA polymerase can also provide a method for the construction of unbiased epPCR libraries.

The number of enzyme variants  $N$  at the theoretically maximum degree of diversity is given by the algorithm shown as:

$$N = \frac{19^M X!}{(X - M)! M!}, \quad (1)$$

where  $M$  is the total number of amino acid exchanges per enzyme molecule and  $X$  the number of amino acids per enzyme molecule (17). For the purpose of illustration, an enzyme composed of 300 amino acids theoretically has 5700 mutants if one amino acid is exchanged, but 16 million in the case of two simultaneous exchanges, and 30.5 billion if three amino acids are exchanged per enzyme molecule simultaneously (17,31,32). Such numbers are often cited to illustrate the problem of protein sequence space, which of course points to the difficulty in screening such large numbers of enzyme mutants.

In addition to epPCR, the generation of focused mutant libraries also provides the user with a useful tool in directed evolution (17–20). To apply such methods, several versions of which are available, information regarding the structure of the enzyme (X-ray data or homology model), the location and nature of the active site, and the mechanism may or may not be necessary. In the former case an intelligent decision is made on the basis of molecular modeling regarding the identification of a “hot spot,” a position in the amino acid sequence of the enzyme, which is believed to be important with respect to a given catalytic property. Following this choice, the position is randomized by saturation mutagenesis (17–20,43,44), a process developed by Wells *et al.* in 1985 (44a). It leads to an enzyme library containing the 20 theoretically different mutants corresponding to the 20 proteinogenic amino acids at a defined position. In general, this position is next to the binding site or near the catalytically active center, but this need not always be the case. To ensure >95% coverage (i.e., to make certain that all 20 mutants have been evaluated in an

appropriate screen), oversampling is necessary. It usually suffices to screen about 200 clones (i.e., to pick and evaluate this number of bacterial colonies on the agar plates). Of course, as an alternative, it is also possible to perform 19 appropriate experiments using conventional site-directed mutagenesis.

In another process, which does not require any knowledge of the 3D structure of the enzyme, every single position is randomized separately in a systematic manner (45,46). Thus, in the case of an enzyme composed of  $N$  amino acids,  $N$  libraries each containing about 300 clones are produced and screened. In still another strategy, “hot spots” are first identified by the epPCR screening process, and these are subsequently randomized separately (47,48).

Another way to generate a focused library of enzyme mutants is to perform cassette mutagenesis (17–20,44a,49). The user identifies (or predicts) a “hot region” in the enzyme, either on the basis of structural and mechanistic data or as a result of applying epPCR. As before, one usually focuses on a portion of the enzyme near the binding site and designs a cassette, which is a DNA fragment consisting of a defined number of nucleotides encoding the desired amino acids. If two amino acid positions are chosen for simultaneous randomization,  $20 \times 20 = 400$  theoretically different mutants are possible, and the necessary oversampling for 95% coverage can be handled using today’s screening methods ( $\sim 3000$  clones) (50). However, when the number of amino acid positions for randomization is increased, serious screening problems arise if the goal is complete coverage. For example, if four positions are randomized simultaneously, catalyst diversity is high ( $20 \times 20 \times 20 \times 20 = 160\,000$  different mutants), which is in principle desirable, but oversampling necessary for 95% coverage poses unsurmountable screening problems ( $> 3$  million clones) using today’s assays (50).

Of course, one can settle for much lower coverage, and the greatly reduced catalyst diversity in the screened mutants can still lead to the discovery of hits displaying improved catalytic profiles, as has been demonstrated, for example, in the directed evolution of enantioselective lipases (49). Hilvert used Hecht’s idea of binary patterning, according to which amino acid positions are identified on the basis of rational design and then partially randomized by restricting the type of amino acids to be introduced (polar, non-polar, etc.) (20a). It would be interesting to apply this tool to the evolution of enantioselectivity.

Selection, in the present context meaning a growth advantage of the bacterial host as a consequence of expressing mutant enzymes with improved catalytic profiles of interest to the chemist, is fundamentally different from screening (17–21,36). Selection—instead of screening—would allow much larger libraries to be scanned, but the development of efficient selection methods for *enantioselectivity* remains a challenge for the future (Section III).

## B. RECOMBINANT METHODS

Recombination in a genetic sense means the breaking and rejoining of DNA in new combinations. Such a process is crucial for all living species, because it significantly speeds up the Darwinian process (“sexual evolution”). When mimicking this process in the laboratory, the presence of a set of recombination enzymes, which ensure the

breakage and rejoining of DNA molecules is required. In the laboratory, sexual evolution can indeed be simulated by several recombinant methods. The most prominent version, pioneered by Stemmer in 1994, is called DNA shuffling (*18,33–35*). In general, one or more genes are first digested with a DNase to yield double-stranded oligonucleotide fragments of 10–50 base pairs, which are then amplified in a PCR-like process. Repeating cycles of strand separation and reannealing in the presence of a DNA polymerase followed by a final PCR-amplification step result in the reassembly of full-length mutant genes. Recombination is due to template switching (i.e., fragments from one copy of the gene prime on another copy).

DNA shuffling can be performed with one gene, with two or more natural genes, or with mutant genes (*Fig. 3*). A limitation is the requirement of relatively high homology. If homologous genes from different species are chosen, the process is called family shuffling, which appears to be particularly efficient because it provides high catalyst diversity (*18,35,51*). In all versions, a certain degree of self-hybridization of parental genes occurs, which lowers the quality of the mutant libraries (many colonies containing WT).

A number of other recombinant methods have been developed, each having advantages and (some) disadvantages. For example, a simple and efficient method is based on a staggered PCR-like reaction that has been called the staggered extension process (StEP) (*52*). In this method one defined primer is added to the template DNA, which may consist of two or more genes. An extremely abbreviated primer extension reaction catalyzed by DNA polymerase then produces short DNA fragments, which can anneal to different templates and are further extended during the next short cycle of primer extension. Such a process is repeated until full-length genes are formed, which are amplified by conventional PCR using external primers.

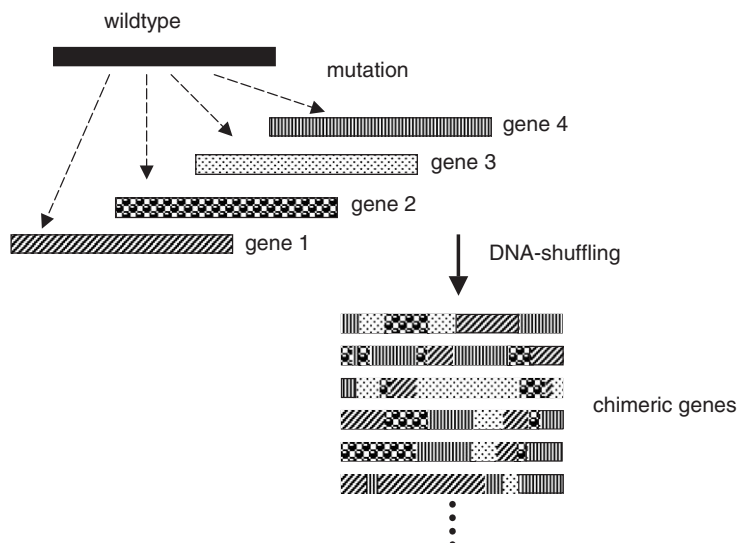


FIG. 3. Scheme for DNA shuffling illustrated for the case in which the parent genes originate from the WT by some form of mutagenesis (*18*).



Interesting new homology-dependent and -independent methods have been developed that are not discussed in detail here, including RDA-PCR (53), MURA (54), RETT (55), ITCHY (56), SISDC (57), SCOPE (58), SCATCHY (59), and SHIPREC (60). These and other methods have been reviewed critically by Lutz and Patrick (37). A novel method based on random insertion and deletion of arbitrary number of bases for codon-based random mutation (RID) was developed by Sisido, which introduces additional amino acids or deletes them in the WT (61). Of special note is the fact that some non-natural amino acids can also be introduced, although this process is more complicated.

Another conceptionally significant advance was described independently in 2002–2003 by three groups, the basic idea being rather simple (62–64). Necessary for digestion are not the genes themselves, but only the information regarding their sequences. When considering two or more genes (which in the case of traditional DNA shuffling are digested and reassembled), overlapping oligonucleotides encoding all of the degeneracy as determined by gene alignment and computer analysis are used as substrates in a polymerase-mediated reassembly process. The three studies describing the same phenomenon (but using different terms, namely, “degenerate homoduplex recombination” (62), “synthetic shuffling,” (63) and “assembly of designed oligonucleotides” (ADO) (64), are all based on an identical concept, although some differences exist. In all cases, libraries of gene mutants (and therefore enzyme variants following expression) are generated in which all “shuffled” variants are equally likely, regardless of how tightly parental diversity is linked. Low homology is tolerated, and undesired self-hybridization of parental genes is minimized, leading to higher quality libraries. In an interesting recent review, the advantages of this approach were analyzed on a statistical basis (37). The ADO method, which includes a certain degree of new non-parental diversity due to the oligonucleotide design strategy, is illustrated in Fig. 4 (64).

As a consequence of the high diversity and enhanced quality of the libraries of mutants generated by these new molecular biological methods, the screening effort is greatly reduced. Efficiency is attained in directed evolution by quality, not by quantity—a trend that has emerged clearly in the preceding few years (37). Of course, this includes the development of strategies for effectively scanning protein sequence space, which means that questions regarding the choice of the above mutagenesis methods need to be addressed (Section IV).

Should one begin a given directed evolution project by applying epPCR, systematic saturation mutagenesis, cassette mutagenesis, DNA shuffling, or yet another recombinant method? If it is epPCR, at what mutation rate and for how many cycles? The answers are not likely to be general. Nevertheless, trends and guidelines have started to appear, and more experience is expected to lead to further progress. Moreover, statistical and computational methods of diverse types, including molecular modeling and quantum mechanical analyses (MM/QM), genetic algorithms, quantitative evaluation of motion and catalysis in coupled networks, may be helpful in the process of directed evolution (15,65). Examples also exist in which directed evolution is used as an experimental instrument in attempts to deepen our understanding of how enzymes work. Indeed, the traditional area of rational design and the original form of directed evolution have begun to influence each other positively (Section IV).

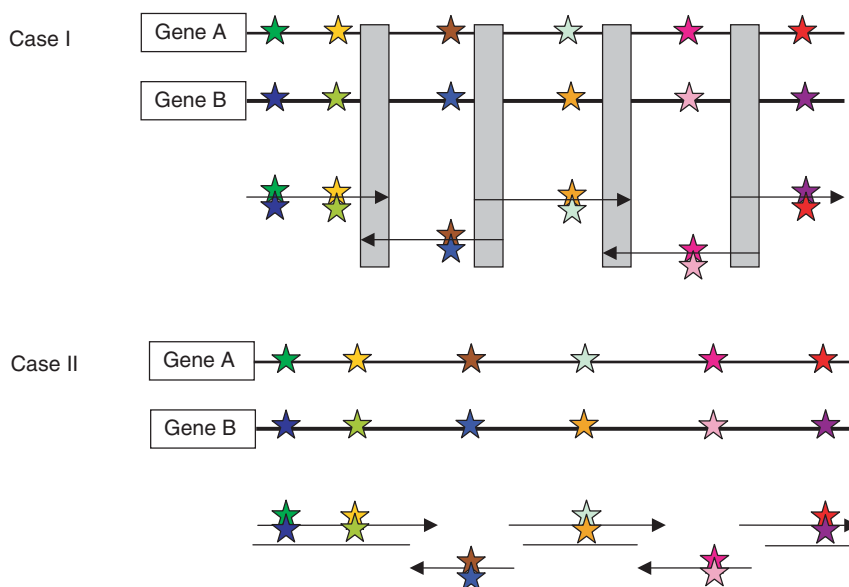


FIG. 4. General concept of ADO, two strategies for the linking of fragments being possible (cases I and II). In case I the two genes A and B to be virtually shuffled are aligned; the different colored stars refer to information which encoded different amino acids, whereas oligonucleotide fragments with both colored stars in the same position of the parent gene denote the synthetic oligonucleotide fragment with degenerate nucleotides. The gray blocks denote conserved regions of sequence, which can be used as the linking part with homologous recombination. Case II shows no homology between flanking oligos, which can be assembled by ligation between ssDNA with an unknown terminal sequence (64).

### III. High- and Medium-Throughput Screening Systems for Assaying the Enantioselectivity of Enzymatic Reactions

A crucial component in putting directed evolution of enantioselective enzymes into practice (as shown schematically in Figs 1 and 2) is the availability of efficient screening systems capable of rapidly evaluating thousands of mutant enzymes as catalysts in asymmetric transformations (66–70). Traditional forms of *ee* determination based on gas chromatography (GC) or HPLC using chirally modified columns can handle only a few dozen samples per day, not enough for directed evolution studies. The development of fast assays has thus become one of the focal points of research. Most of these assays can also be used in combinatorial asymmetric transition metal catalysis (66,71), and *vice versa*. Some of the screening systems originally developed for use in the area of transition metal catalysis can, in principle, be adapted for application in enzyme catalysis. More than a dozen high- and medium-throughput *ee* assays have been developed. In a somewhat arbitrary definition, medium throughput means several hundred *ee* determinations per day, whereas high throughput is currently considered to imply the evaluation of 1000–10 000 samples per day. No single *ee* assay is truly universal, but fortunately many are complementary.

This section focuses on the most practical *ee* assays currently available. For a comprehensive coverage, the reader is referred to recent reviews (66–70). As pointed out in Section II, selection systems based on growth advantage of the bacterial host are fundamentally different from screening systems, and can in principle “handle” millions of enzyme mutants. However, the development of selection systems, which respond to the *enantioselectivity* of a given enzyme-catalyzed reaction is difficult. To date, efficient selection systems of this kind are unknown, although a screening system based on differential cell growth as a consequence of enantioselective substrate transformation has been described (72). Phage display has been applied in the directed evolution of enantioselective enzymes (73), but thus far the problem of turnover remains. Colony-based *ee* screens (i.e., crude pre-tests on agar plates) are rare (66–70). All of the screening systems described in this section are carried out robotically in the spatially addressable wells of 96- or 384-microtiter plates following bacterial colony picking.

It is important to keep in mind that in directed evolution studies a formidable portion of a given enzyme library is composed of inactive mutants. Although this becomes apparent upon applying any *ee* assay, it is more efficient and economical to use a simple pre-test for *activity* that eliminates inactive mutants and therefore reduces the effort in using more elaborate screens for enantioselectivity. A wide variety of tests for activity have been developed, some designed to function directly on agar plates (which entails the least amount of effort), others being performed in the wells of microtiter plates following colony picking (17–20,66). Although most of these tests are very useful and easy to apply, it must be remembered that they are not completely reliable. This lack of reliability has to do with the fact that the protein expression rate may vary from mutant to mutant in a given library, leading to different amounts of enzyme from well to well of microtiter plates.

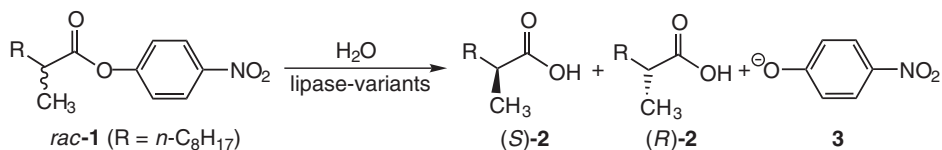
#### A. UV/VIS-BASED *EE* ASSAYS

All *ee* screening systems using UV/Vis spectroscopy as a detection system have a number of advantages, including the possibility of visual pre-screening for activity on microtiter plates in some cases. Moreover, if a reliable UV/Vis signal arises as a consequence of an enzymatic reaction, commercially available UV/Vis plate readers can be used to screen thousands of mutant enzymes catalyzing the reactions of interest in the wells of microtiter plates.

##### A.1. Assay for Screening Lipases or Esterases in the Kinetic Resolution of Chiral *p*-Nitrophenyl Esters

The first high-throughput *ee* assay used in the directed evolution of enantioselective enzymes was based on UV/Vis spectroscopy (16,74). It is a crude but useful screening system that is restricted to the hydrolytic kinetic resolution of racemic *p*-nitrophenyl esters catalyzed by lipases or esterases. The development of this assay arose from the desire to evolve highly enantioselective mutants of the lipase from *Pseudomonas aeruginosa* as potential biocatalysts in the hydrolytic kinetic resolution of the chiral ester *rac*-1. The wild type leads to an *E* value of only 1.1 in slight

favor of the (*S*)-acid **2**. Lipase-catalyzed hydrolysis in a buffered medium generates *p*-nitrophenolate (**3**), which shows a strong UV/Vis absorption at 405 nm. Thus, reactions can be carried out on microtiter plates, with a simple UV/Vis plate reader measuring absorption as a function of time (typically during the first 6–8 min). However, because the racemate delivers only information concerning the overall rate, the (*S*)- and (*R*)-substrates **1** were prepared and investigated *separately* pairwise on 96-well microtiter plates.



If the slopes of the absorption/time curves differ considerably, a positive hit is indicated (i.e., an enantioselective lipase-variant has been identified) (16). Figure 5 shows two typical experimental plots, illustrating the presence of a non-selective lipase (top) and a hit (bottom) (16). As a consequence of the crudeness of the test, quantitative evaluation is not possible. Therefore, the hits need to be investigated separately in laboratory-scale reactions and evaluated quantitatively by conventional chiral GC. About 800 plots of this kind can easily be recorded per day. A total of 40 000 lipase-variants were generated by epPCR, saturation mutagenesis, cassette mutagenesis, and DNA shuffling and screened in the model reaction,

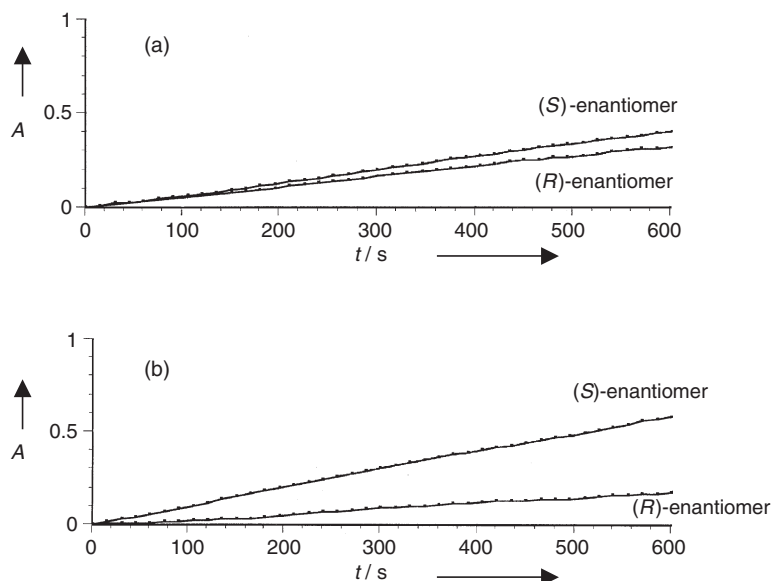


FIG. 5. Time course of the lipase-catalyzed hydrolysis of the (*R*)- and (*S*)-ester **1** measured with a UV/Vis plate reader. (a) WT lipase from *P. aeruginosa*, (b) improved mutant in the first-generation epPCR (16).

leading to the identification of several highly enantioselective variants (16,21–24) (Section IV.A.1).

An inherent disadvantage of this assay has to do with the fact that a built-in chromophore is required (*p*-nitrophenol), yet *p*-nitrophenyl esters will never be used in industrial applications. Methyl- or ethyl-esters do not yield hydrolysis products that are UV/Vis active. Moreover, because the (*S*)- and (*R*)-substrates are tested separately pairwise, the enzyme does not compete for the two substrates, and so some uncertainty is introduced. When considering this assay, the user has the option of either scanning through whole libraries of mutant lipases, or reducing the effort by first applying an appropriate pre-screen, in this case the conventional tributyrin test (66). Accordingly, the agar plates are charged with tributyrin, a well-known substrate for lipase-catalyzed ester hydrolysis. Due to the insolubility of tributyrin in the medium, the plates have a milky appearance. In the case of an active lipase mutant, hydrolysis occurs, and consequently clear spots (halos) appear (Fig. 6). Only these colonies are harvested for the actual UV/Vis-based *ee* screen.

#### A.2. *Quick-E-Test in the Lipase- or Esterase-Catalyzed Kinetic Resolution of Chiral p-Nitrophenyl Esters*

Another colorimetric assay for testing the enantioselectivity of lipases or esterases in ester hydrolysis reactions is based on a different principle (75). To simulate the state of competitive conditions of an enzymatic process, the so-called Quick-*E*-Test

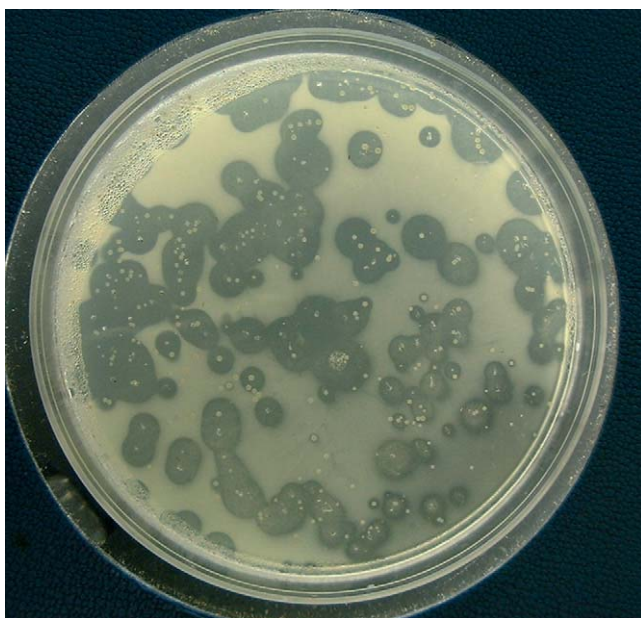
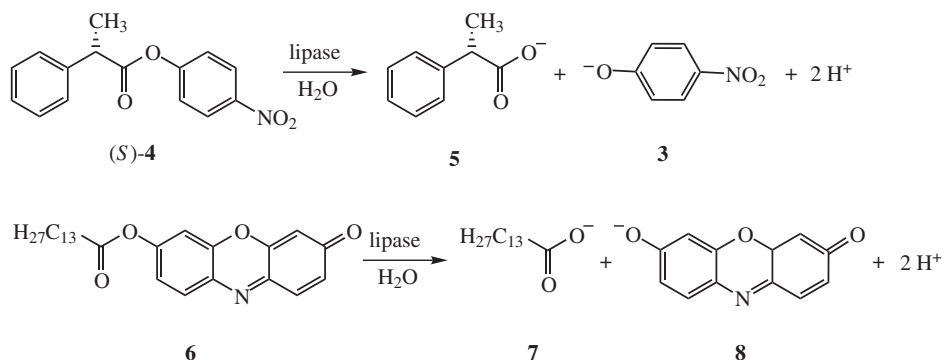


FIG. 6. Typical butyrin test for lipase activity in which the agar plate is placed on a black background for visualization. White dots represent bacterial colonies; those having no (even) black background contain inactive mutants (66a).

was developed, in which a mixture of the *p*-nitrophenyl ester of one enantiomeric form of a chiral ester **4** and a resorufin ester **6** is subjected to enzyme-catalyzed hydrolysis, the latter taking on the “role” of the enantiomer (75). The two hydrolyses are monitored by recording the UV/Vis absorption of the two products **3** and **8** at two distinctly different wavelengths (410 vs. 570 nm). Although this procedure makes a more precise determination of *E* values possible, it suffers from the same disadvantage noted previously, namely, the necessity of employing the *p*-nitrophenyl ester of the chiral acid.



### A.3. Screening Systems for Lipase- or Esterase-Catalyzed Reactions Based on pH-Indicators

Yet another principle forms the basis of a different UV/Vis test useful in determining the *ee* of lipases or esterases (76). It is based on the notion that hydrolysis of an ester leads to a change in acidity that is measurable by an appropriate pH indicator. Upon using a buffer (*N,N*-bis(2-hydroxyethyl)-2-aminoethane sulfonic acid) and a pH indicator (*p*-nitrophenol) having the same *pK<sub>a</sub>* value, a linear correlation between the amount of acid generated and the protonation of the indicator was established. In this case the two enantiomeric esters are investigated separately pairwise, the color change upon protonation in each case being monitored colorimetrically. Currently it is not quite clear how general and how precise this method actually is, since it was later observed that appreciable discrepancies between the *E* value obtained and the *E* value measured conventionally in control experiments exist in some cases (77).

A related assay was later reported which makes use of a different and more convenient indicator (bromothymol blue) (78). However, it is emphasized that all of the assays based on pH change reported so far refer to the use of isolated enzymes. In real applications, supernatants are likely to be used, as in directed evolution studies. In supernatants, however, pH variations may occur. Therefore, an optimized assay was later developed in which supernatants are employed (79). Thus, the pH of the buffer is adjusted to the acidity of the medium, enabling about 4000 samples in kinetic resolution investigations to be screened per day.

#### A.4. Enzyme-Coupled *ee* Screening Systems

In those cases in which the product of an enzymatic reaction under study can be transformed by another enzyme into a secondary product which gives rise to a spectroscopic signal, an enzyme-coupled assay is possible. This principle was first demonstrated using fluorescence as the spectroscopic detection method (80) (Section III.B). In a UV/Vis approach using this concept, the hydrolase-catalyzed kinetic resolution of chiral acetates was investigated using a high-throughput *ee* assay based on an enzyme-coupled test, the presence of a fluorogenic moiety or a UV/Vis chromophore not being necessary (81). The assay is based on the idea that the acetic acid formed in the hydrolysis of a chiral acetate can be transformed stoichiometrically into NADH via a series of coupled enzymatic reactions using commercially available enzyme kits (Fig. 7). The NADH is then easily detected by UV spectroscopy in the wells of microtiter plates using a standard plate reader. It has been estimated that about 13 000 samples can be evaluated per day, although in practice this has not yet been demonstrated.

The kinetic resolution of (*S,R*)-1-methoxy-2-propylacetate was investigated using various commercially available hydrolases. The agreement between the apparent selectivity factor  $E_{\text{app}}$  and the actual value  $E_{\text{true}}$  determined by GC turned out to be excellent at low enantioselectivity ( $E = 1.4\text{--}13$ ), but less so at higher enantioselectivity (20% variation at  $E = 80$ ). This limitation may cause problems when attempting to enhance enantioselectivity beyond  $E = 50$ .

Whenever the product concentration (e.g., of an alcohol) can be determined, the *ee* value is accessible by using an enzyme to catalyze a further reaction which can be monitored by UV/Vis spectroscopy. In the so-called EMDee method, a selective

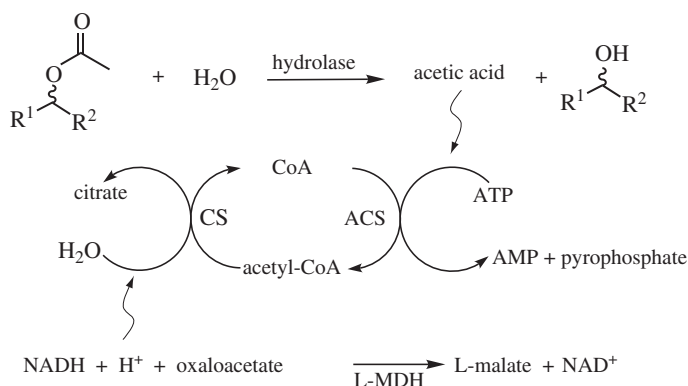
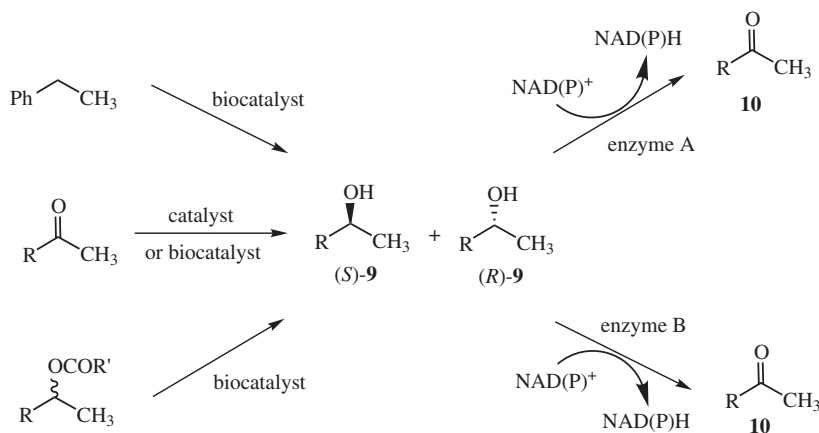


FIG. 7. Enzyme-coupled assay in which the hydrolase-catalyzed reaction releases acetic acid. The latter is converted by acetyl-CoA synthetase (ACS) into acetyl-CoA in the presence of (ATP) and coenzyme A (CoA). Citrate synthase (CS) catalyzes the reaction between acetyl-CoA and oxaloacetate to give citrate. The oxaloacetate required for this reaction is formed from L-malate and  $\text{NAD}^+$  in the presence of L-malate dehydrogenase (L-MDH). Initial rates of acetic acid formation can thus be determined by the increase in adsorption at 340 nm due to the increase in NADH concentration. Use of optically pure (*R*)- or (*S*)-acetates allows the determination of the apparent enantioselectivity  $E_{\text{app}}$  (81).



alcohol dehydrogenase is employed to specifically oxidize one enantiomer of a chiral alcohol (82,83). The oxidation rate can be measured by following the formation of NAD(P)H, which ultimately allows determination of the *ee*. The method has precision of  $\pm 10\%$  and can be adapted to high throughput. However, the product concentration must be determined by an alternative means when conversion is less than 100%.

In what appears to be a particularly innovative development in the area of UV/Vis-based *ee* screening systems, the determination of the enantiomeric purity of chiral alcohols **9** is based on a new concept of using two enantioselective enzymes to modify the product (84). The method allows the determination of *ee* values independent of the concentration, which may be of significant advantage in directed evolution projects. It can be used in three different biocatalytic processes, namely biohydroxylation of alkanes, reductase-catalyzed reduction of ketones, and lipase- or esterase-catalyzed ester hydrolysis.



To analyze the *ee* value of **9**, enantioselective NAD(P)<sup>+</sup>-dependent alcohol dehydrogenases A and B are each used to oxidize the alcohol. The reaction rates for enzyme A ( $v^a$ ) and enzyme B ( $v^b$ ) can be determined by following the formation of NAD(P)H through its absorption at 340 nm. The enantiomers of chiral alcohols are generally competing substrates for enantioselective alcohol dehydrogenases, so the reaction rates  $v^a$  and  $v^b$  can be expressed by simple equations that are routine in enzyme kinetics. When two selective alcohol dehydrogenases are used, the following equation for the *ee* value can be derived (84):

$$ee = \frac{[R] - [S]}{[R] + [S]} = \frac{V_{\max, S}^b / K_{m, S}^b + 1/K_I^a - V_{\max, R}^a / K_{m, R}^a - 1/K_I^b}{V_{\max, S}^b / K_{m, S}^b + 1/K_I^a - V_{\max, R}^a / K_{m, R}^a - 1/K_I^b} \quad (2)$$

In the application of this method, the kinetic constants  $V_{\max, R}^a$ ,  $V_{\max, S}^a$ ,  $K_{m, R}^a$ ,  $K_{m, S}^a$ ,  $V_{\max, R}^b$ ,  $V_{\max, S}^b$ ,  $K_{m, R}^b$ ,  $K_{m, S}^b$ ,  $K_I^a$ , and  $K_I^b$  can be readily established by separate oxidation of (R)-**9**, (S)-**9**, and mixtures of (R)- and (S)-**9** in known ratios with



enzymes A and B, respectively. In a model study, an enzyme preparation with a constant concentration was used to establish the kinetic constants and analyze unknown samples; the *ee* values could then be calculated. The use of  $V_{\max}$  is advantageous because this approach does not require the accurate determination of the enzyme concentration in each experiment.

The method was successfully applied to a series of alcohols **9**. Of the 83 measured *ee* values, 79 turned out to be within 10% of the true value, and four resulted in an error of  $\pm 12\%$ . As the authors stated, the method has several distinctive features (84):

- (a) The *ee* can be determined with satisfactory accuracy, independent of the concentration.
- (b) The enzymes do not have to be specific to (or highly active toward) the alcohol. A large number of alcohol dehydrogenases with broad substrate ranges are now available, and it is thus easy to find appropriate alcohol dehydrogenases for analysis of the *ee* value of a given alcohol.
- (c) The analysis method is very sensitive. The technique can be used to determine the *ee* value of a sample with a concentration as low as 200  $\mu\text{M}$  and is therefore particularly useful for biocatalyst screening, when product concentration is often low.
- (d) The analysis is performed with UV spectroscopy; no special instrument is required.
- (e) Experiments are performed in a 956-well microtiter plate, which allows analysis of the *ee* values of 48 samples within 5 min. Given a preparation time of 5 min, about 288 samples can be analyzed in an hour, which is a high enough throughput for most practical applications.
- (f) The method can be extended to measure the *ee* values of other types of compounds. Two enzymes of another type may be applied, coupled with detection by UV spectroscopy, MS, or even HPLC or GC for short analysis times.
- (g) The method also provides the possibility to measure concentration. For high concentrations, samples may be diluted and then analyzed, which makes the method useful for screening catalyst activities. However, as a note of caution, an accuracy of  $\pm 10\%$  may cause problems in the late stages of projects concerning the directed evolution of enantioselectivity (i.e., when going beyond *ee* > 90%).

#### A.5. Other UV/Vis-Based *ee* Assays

Several other UV/Vis-based *ee* assays have been developed, but their general application in directed evolution remains to be demonstrated (66–70). One of them is a well- designed screening system based on enzyme immunoassays (85). The success of the *ee* assay depends upon the availability of specific antibodies that are easily raised for almost any chiral product of interest. In a given reaction, two antibodies are needed, one that measures the product concentration and the other that measures the amount of one of the enantiomers. About 1000 *ee* determinations are possible per day, the precision amounting to  $\pm 9\%$  (85).

## B. ASSAYS USING FLUORESCENCE

Fluorescence-based assays either in the measurement of enzyme activity or in the quantification of enantioselectivity all have a high degree of sensitivity, which allows the use of very dilute substrate concentrations and extremely small amounts of enzymes. Basically, there are two different approaches. One involves the use of a substrate of interest to which a fluorescent-active (or potentially active) moiety is covalently attached. The second approach makes use of a fluorescence-based sensor, which gives rise to a signal as a consequence of the enzyme-catalyzed reaction of a substrate of interest.

One of the first fluorescence-based *ee* assays uses umbelliferone (**14**) as the built-in fluorophore and works for several different types of enzymatic reactions (70,86). In an initial investigation, the system was used to monitor the hydrolytic kinetic resolution of chiral acetates (e.g., *rac*-**11**) (Fig. 8). It is based on a sequence of two coupled enzymatic steps that converts a pair of enantiomeric alcohols formed by the asymmetric hydrolysis under study (e.g., (*R*)- and (*S*)-**12**) into a fluorescent product (e.g., **14**). In the first step, (*R*)- and (*S*)-**11** are subjected separately to hydrolysis in reactions catalyzed by a mutant enzyme (lipase or esterase). The goal of the assay is to measure the enantioselectivity of this kinetic resolution. The relative amount of (*R*)- and (*S*)-**12** produced after a given reaction time is a measure of the enantioselectivity and can be ascertained rapidly, but not directly.

Two subsequent chemical transformations are necessary. First, the enantiomeric alcohols (*R*)- and (*S*)-**12** are oxidized separately by horse-liver alcohol dehydrogenase

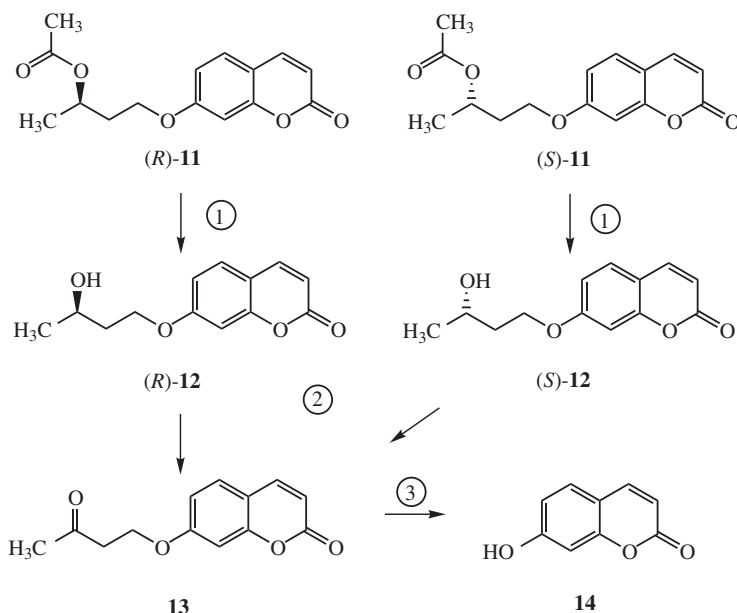


FIG. 8. Scheme for fluorescence-based assay used in the determination of enantioselectivity of ester hydrolysis (80).

(HLDH) to the ketone **13**, from which the fluorescent final product umbelliferone (**14**) is released in each case by the catalytic action of bovine serum albumin (BSA). Thus, by measurement of the fluorescence of **14** for the (*R*)- and the (*S*)-substrate separately, the relative amounts of (*R*)- and (*S*)-**12** can be determined.

Thirty different esterases and lipases were tested. The rate of release of **14** in the wells of standard microtiter plates was monitored by fluorescence (70,86). Control experiments ensured that the apparent rate of release of **14** is directly proportional to the rate of acetate hydrolysis. The predicted and observed *E* and *ee* values (as checked by standard HPLC assay on a chiral phase) were found to match within  $\pm 20\%$ . Only in one case was a larger discrepancy observed, a result that was believed to be caused by the occurrence of an unusually low value of  $K_M$  for one of the enantiomers.

Thus, because the test can be carried out on 96-well microtiter plates, high throughput is possible. Of course, the inherent disadvantage noted above for some of the colorimetric tests also applies here, namely, the fact that the optimization of a potential catalyst is focused on a specific substrate **11** modified by incorporation of a probe, in this case the fluorogenic moiety **14**. However, one can expect the test to be useful in directed evolution projects in which proof of principle is the goal. Moreover, this kind of approach can be used in very practical applications, namely as a pre-test for the activity of enzymes.

The general concept has been extended beyond the *ee* assay for lipases and esterases to include enzymes such as acylases, epoxide hydrolases (EHs), alcohol dehydrogenases, aldolases, and phosphatases (70,87). In many cases, the assay utilizes  $\text{NaIO}_4$ -mediated oxidation of a diol-moiety followed by base-catalyzed  $\beta$ -elimination to generate the fluorescent umbelliferone (**14**) (Fig. 9). Again, the most likely area of application is pre-screening, although adaption to include high-throughput *ee* determination seems possible.

In a different approach, fluorescence-based DNA microarrays are utilized (88). In a model study, chiral amino acids were used. Mixtures of a racemic amino acid are first subjected to acylation at the amino function with formation of *N*-Boc protected derivatives. The samples are then covalently attached to amine-functionalized glass slides in a spatially arrayed manner (Fig. 10). In a second step, the uncoupled surface amino functions are acylated exhaustively. The third step involves complete deprotection to afford the free amino function of the amino acid. Finally, in a fourth step, two *pseudo*-enantiomeric fluorescent probes are attached to the free amino groups on the surface of the array. An appreciable degree of kinetic resolution in the process of amide coupling is a requirement for the success of the *ee* assay (Horeau's principle). In the present case, the *ee* values are accessible by measuring the ratio of the relevant fluorescent intensities. About 8000 *ee* determinations are possible per day, precision amounting to  $\pm 10\%$  of the actual value (88). Although it was not explicitly demonstrated that this *ee* assay can be used to evaluate enzymes (e.g., proteases), this should in fact be possible. So far this approach has not been extended to other types of substrates.

A number of other *ee* assays relying on the use of fluorescence have been described, although their general utility in the high-throughput evaluation of enantioselective enzymes remains to be demonstrated in most cases (66–70). A high-throughput *ee*

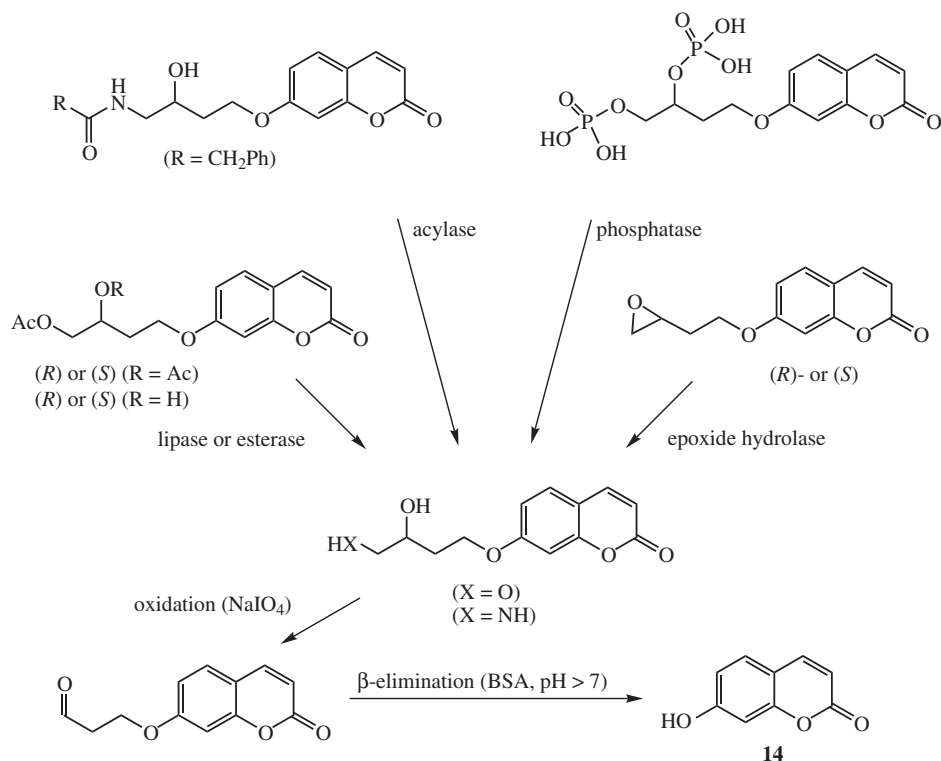


FIG. 9. Periodate-coupled fluorogenic *ee* assay for hydrolases based on the generation of umbelliferone (**14**) (70,86,87).

assay based on capillary array electrophoresis (CAE) (89) using fluorescence as the detection system is described in Section III.G.

### C. ASSAYS BASED ON MASS SPECTROMETRY

Enantiomers have identical mass spectra, and therefore the relative amounts of the (*R*)- and (*S*)-forms present in a given sample cannot be measured by conventional MS techniques. However, special MS-based approaches have been described that do in fact allow *ee* determination. In one method, two conditions have to be met (90,91): (a) a mass-tagged chiral derivatization agent is applied to the product mixture, and (b) in the process of derivatization, a significant degree of kinetic resolution needs to occur (Horeau's principle). The relative amounts of mass-tagged diastereomers can then be measured by MS, simply by integrating the appropriate peaks, the uncertainty in the *ee* value amounting to  $\pm 10\%$  (90,91).

Isotope labeling forms the basis of a different MS-based *ee*-assay (92,93). It involves a fundamentally new way to measure enantiopurity. The method has been parallelized for high throughput and used a number of times in the directed evolution of enantioselective enzymes (46,64,94–96). In this MS-based approach,

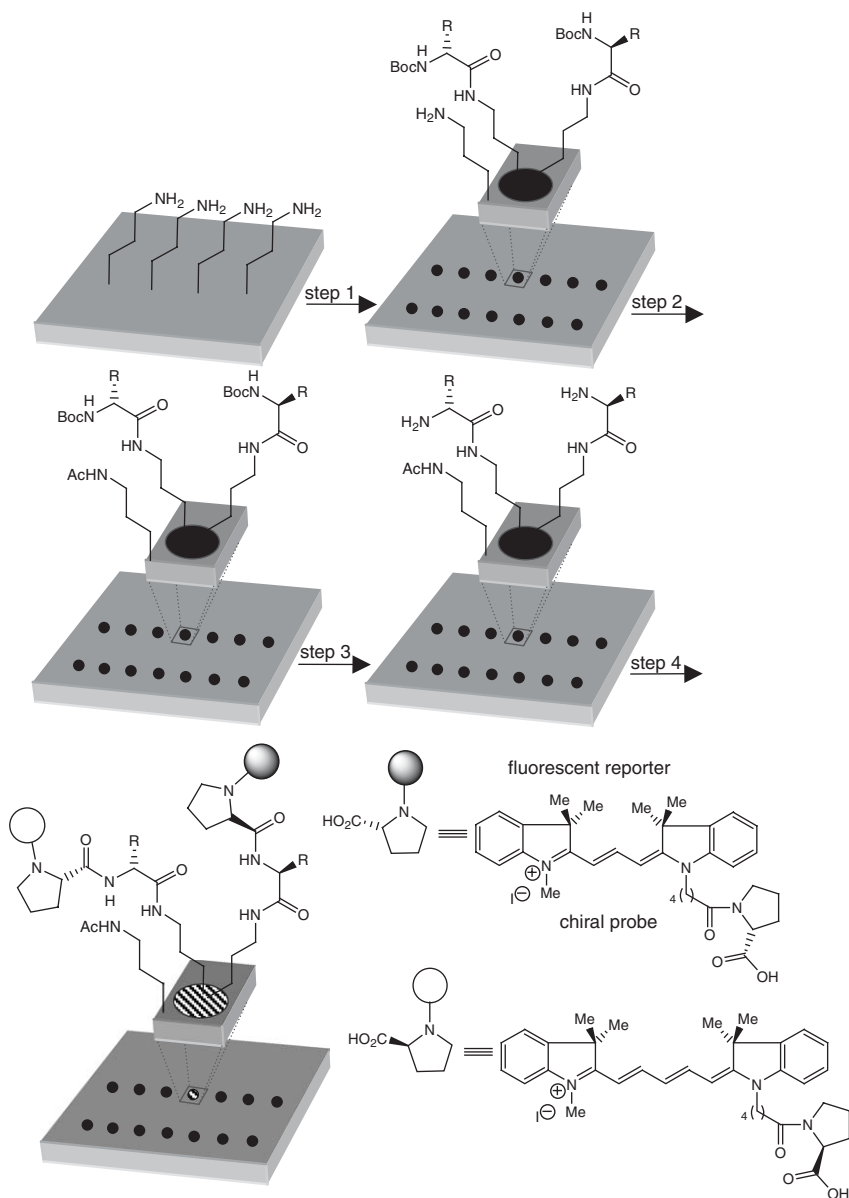


FIG. 10. Reaction microarrays in high-throughput *ee* determination of amino acids. Reagents and conditions: step (1) BocHNCH(R)CO<sub>2</sub>H, PyAOP, *i*Pr<sub>2</sub>NEt, DMF; step (2) Ac<sub>2</sub>O, pyridine; step (3) 10% CF<sub>3</sub>CO<sub>2</sub>H and 10% Et<sub>3</sub>SiH in CH<sub>2</sub>Cl<sub>2</sub>, then 3% Et<sub>3</sub>N in CH<sub>2</sub>Cl<sub>2</sub>; step (4) pentafluorophenyl diphenylphosphinate, *i*Pr<sub>2</sub>NEt, 1:1 mixture of the two fluorescent proline derivatives, DMF, -20°C (88).

derivatization reactions are not necessary, which makes the overall process easy. It makes use of deuterium-labeled *pseudo*-enantiomers or *pseudo*-*meso*-compounds. This practical method is restricted to investigations involving kinetic resolution of racemates and desymmetrization of prochiral compounds bearing reactive enantiotopic groups (Fig. 11) (92,93).

It is clear that the products of these transformations are *pseudo*-enantiomers differing in absolute configuration *and* in mass, with integration of the MS peaks and data processing affording the *ee* or *E* values. Any type of ionization can be employed, and electrospray ionization (ESI) is used most commonly. In some cases, the use of an internal standard is advisable if the determination of conversion is necessary. The uncertainty in the *ee* value amounts to less than  $\pm 5\%$ . In the original version, about 1000 *ee* values could be measured per day, but this has been increased to about 8000 per day as a result of a second-generation system based on an eight-channel multiplexed sprayer system (93).

The method is illustrated here using lipase-variants from *Bacillus subtilis*, produced by the methods of directed evolution and employed as catalysts in the desymmetrization of *meso*-1,4-diacetoxy-cyclopentene (64,94). The goal was to obtain enantioselective variants of this lipase, which are expressed in *E. coli*. Accordingly, the D<sub>3</sub>-labeled *pseudo*-*meso*-compound **15** (which is actually chiral) was selectively prepared and used as the substrate, the two products of the asymmetric transformation being non-labeled **16** and the D<sub>3</sub>-labeled *pseudo*-enantiomer D<sub>3</sub>-**16**. The products are easily distinguished by ESI-MS because they differ by three mass units. Upon integration of the respective peaks, the *ee* value is accessible.

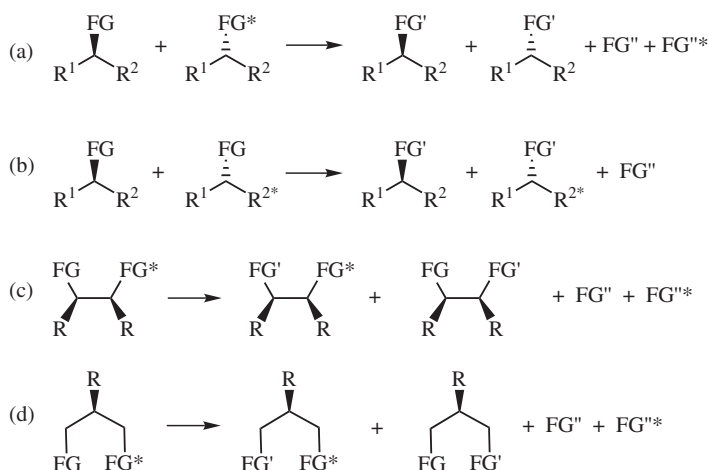
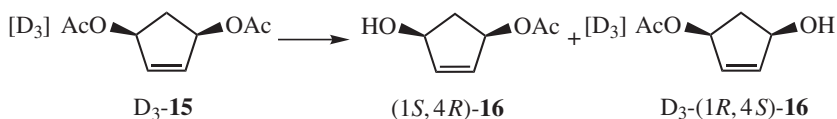
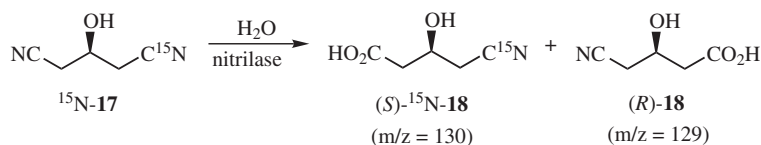


FIG. 11. (a) Asymmetric transformation of a mixture of *pseudo*-enantiomers involving cleavage of the functional groups FG and labeled FG\*. (b) Asymmetric transformation of a mixture of *pseudo*-enantiomers involving either cleavage or bond formation at the functional group FG; isotopic labeling at R<sup>2</sup> is indicated by the asterisk. (c) Asymmetric transformation of a *pseudo*-*meso* substrate involving cleavage of the functional groups FG and labeled FG\*. (d) Asymmetric transformation of a *pseudo*-prochiral substrate involving cleavage of the functional groups FG and labeled FG\* (92).



This screening system has also been applied successfully in the directed evolution of enantioselective EHs acting as catalysts in the kinetic resolution of chiral epoxides (95,96) (Section IV.A.4). Moreover, the firm Diversa has applied the MS-based method in the desymmetrization of a prochiral dinitrile (1,3-dicyano-2-hydroxypropane) catalyzed by mutant nitrilases (46). In this industrial application, one of the nitrile moieties was labeled selectively with  $^{15}\text{N}$  as in  $^{15}\text{N}\text{-17}$ , which means that the two *pseudo*-enantiomeric products (*S*)- $^{15}\text{N}\text{-18}$  and (*R*)-**18** differ by one mass unit. This is sufficient for the MS system to distinguish between the two products quantitatively (46).



It is emphasized that in the case of kinetic resolution, the MS measurements must be performed in the appropriate time window (near 50% conversion). If this is difficult to achieve due to different amounts or activities of the mutants being screened in the wells of microtiter plates, the system needs to be adapted in terms of time resolution. This means that samples for MS evaluation need to be taken as a function of time. Finally, it is useful to delineate the possibility of multi-substrate *ee* screening using the MS-based assay, which allows for enzyme fingerprinting with respect to the enantioselectivity of several substrates simultaneously.

#### D. ASSAYS BASED ON NMR SPECTROSCOPY

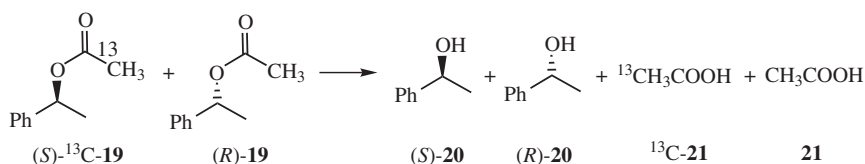
Nuclear magnetic resonance (NMR) measurements are usually considered to be slow processes, but recent advances in the design of flow-through NMR cells have allowed the method to be applied in combinatorial chemistry (97). These technological improvements were applied to the development of two NMR-based high-throughput *ee* assays for evaluating the products of enzyme- or transition metal-catalyzed reactions (98).

In one version, classical derivatization using a chiral reagent or NMR shift agent is simply parallelized and automated by the use of flow-through cells, with about 1400 *ee* measurements being possible per day with a precision of  $\pm 5\%$ . In the second embodiment, illustrated here in detail, a principle related to that of the MS system described in Section III.C is applied (98). Chiral or *meso*-substrates are labeled to produce *pseudo*-enantiomers or *pseudo-meso*-compounds that are then used in the actual screen. Application is thus restricted to kinetic resolution of racemates and

desymmetrization of prochiral compounds bearing reactive enantiotopic groups, as illustrated previously for the MS system (Fig. 11 in Section III.C).

In a typical application,  $^{13}\text{C}$ -labeling is used to distinguish between the (*R*)- and (*S*)-forms of a chiral compound. Essentially, any carbon atom in the compound of interest can be labeled (Fig. 11), but methyl groups in which the  $^1\text{H}$  signals are not split by  $^1\text{H}$ ,  $^1\text{H}$  coupling are preferred because the relevant peaks to be integrated are the singlet arising from the  $\text{CH}_3$ -group of one enantiomer and the doublet of the  $^{13}\text{CH}_3$ -group of the other.

A typical example that illustrates the method concerns the lipase- or esterase-catalyzed hydrolytic kinetic resolution of *rac*-1-phenyl ethyl acetate, derived from *rac*-1-phenyl ethanol (**20**). However, the acetate of any chiral alcohol or the acetamide of any chiral amine can be used. A 1:1 mixture of labeled and non-labeled compounds (*S*)- $^{13}\text{C}$ -**19** and (*R*)-**19** is prepared, which simulates a racemate. It is used in the actual catalytic hydrolytic kinetic resolution, which affords a mixture of true enantiomers (*S*)-**20** and (*R*)-**20** as well as labeled and non-labeled acetic acid  $^{13}\text{C}$ -**21** and **21**, respectively, together with non-reacted starting esters **19**. At 50% conversion (or at any other point of the kinetic resolution), the ratio of (*S*)- $^{13}\text{C}$ -**19** to (*R*)-**19** correlates with the enantiomeric purity of the non-reacted ester, and the ratio of  $^{13}\text{C}$ -**21** to **21** reveals the relative amounts of (*S*)-**20** and (*R*)-**20** (98).



The ratio of the two *pseudo*-enantiomers is accessible by simple integration of the respective peaks, which provides the *ee* and the *E* value (by use of an internal standard for conversion). The quantitative analysis can be accomplished automatically by a suitable software such as AMIX<sup>TM</sup> (available from Bruker Biospin GmbH, Rheinstetten, Germany). The presence of naturally occurring  $^{13}\text{C}$  in the non-labeled (*R*)-substrate is automatically considered in the data processing step. As demonstrated by control experiments, the agreement with the corresponding *ee* values obtained by independent GC analysis is excellent, the correlation coefficient being 0.9998 (98). The precision in the *ee* values amounts to  $\pm 2\%$ , as checked by independent GC analysis. In the case of the first version of the high-throughput *ee* assay based on traditional derivatization using chiral reagents such as Mosher's acid chloride, the same equipment and software can be used (98). Again, about 1400 samples can be handled per day, with the precision in the *ee* value in these cases being  $\pm 5\%$ . Thus, these two NMR-based *ee* screening systems are practical, precise, and rather general.

The method has been extended to include chemical shift imaging, which allows even higher throughput (99). In this embodiment, a 19-capillary through-flow system enables the simultaneous analysis of 19 samples. The enantiomeric purity of 5600 samples can be determined within one day, the precision being  $\pm 6\%$ . In this



NMR-tomographic method, any commercially available NMR spectrometer can be used. To inject samples from 384-format deep-well microtiter plates into the bundle automatically, an in-house-developed pipetting robot with a modified tray was used.

In a different NMR approach, deuterium-labeled *pseudo*-enantiomeric ketones are reduced to diastereomeric alcohols (theoretically by a hydrogenase), and the product ratio is measured by NMR spectroscopy (100). The method has yet to be tested in enzyme-catalyzed reactions.

#### E. ASSAYS BASED ON FTIR SPECTROSCOPY FOR ASSAYING LIPASES OR ESTERASES

The concept of exploiting isotopic labeling for distinguishing *pseudo*-enantiomers in the kinetic resolution of chiral compounds and in the desymmetrization of prochiral substrates bearing reactive enantiotopic groups (Fig. 11) can also be applied in some cases by use of Fourier transform infrared (FTIR) spectroscopy as the detection system (101). Because FTIR spectroscopy is inexpensive and available in almost all laboratories, the *ee* assay has great potential. Moreover, it is of particular interest in the analysis of enzymatic reactions because the *ee* or *E* values can be measured directly in culture supernatants without prior extractive work-up procedures. Of course, the method is restricted to substrates of the type shown in Fig. 11, which, however, must contain IR-active functional groups undergoing reactions. If all pre-requisites are fulfilled, up to 10 000 *ee* values can be measured per day with an accuracy of  $\pm 7\%$ , making this a particularly practical and economical method for evaluating large libraries of potentially enantioselective lipases or esterases (101).

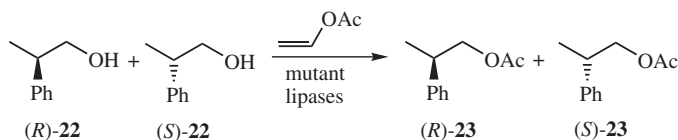
For the purpose of illustration, the lipase- or esterase-catalyzed kinetic resolution of esters is considered here, although the method is not restricted to this type of reaction.  $^{13}\text{C}$ -labeling of carbonyl groups is ideal for several reasons: carbonyl groups provide intensive vibrational bands in an IR spectrum, allowing easy and precise determination of the concentrations of the compounds by applying the Beer–Lambert law. In the spectral region between 1600 and 1800  $\text{cm}^{-1}$ , typical for carbonyl stretching vibrations, almost no absorptions of other functional groups appear, eliminating interference with other vibrational bands. The  $^{13}\text{C}$ -labeled compounds are easily prepared; the absorption maxima of the carbonyl stretching vibration is shifted by 40–50  $\text{cm}^{-1}$  to lower wave numbers by introducing a  $^{13}\text{C}$ -label, which prevents the overlap of the two carbonyl bands.

The analysis of IR spectra of different synthetic mixtures of  $^{13}\text{C}$ -labeled and non-labeled enantiomeric acetates poses no problems. After applying an automated baseline correction to the spectra and correcting the absorbance of one enantiomer in the synthetic mixtures by the absorbance of the other enantiomer at this position, the accuracy of the *pseudo*-enantiomeric system is excellent, specifically, within  $\pm 3\%$  in comparison to the *ee* values determined by chiral GC (101). Using commercially available HTS-FTIR systems, high-throughput measurements are easily possible. The analysis can be performed on a Tensor 27 FTIR spectrometer coupled to a HTS-XT system, which is able to analyze the samples on 96- or

384-well microtiter plates. The plates are equipped with a silicon plate for IR transmittance. Moreover, the *ee* values can be measured in culture supernatants, which is not possible in the case of the MS- or NMR-based assays. The manufacturer Bruker has already coupled the microplate stacking device TWISTER 1 to its microplate reader (101). In this combination which is controlled by OPUS<sup>®</sup> software, 40 IR microplates can be measured automatically. In order to perform the sample loading at high throughput, the auto-sampler microlab 4000 SP can be used. Both formats (96 and 384) of the Bruker silicon microplates are suitable for automatic loading of different types of samples (proteins, cells, and culture media). At least 9000 samples can be handled per day (101).

#### F. ASSAYS BASED ON GAS CHROMATOGRAPHY OR HPLC

Conventional chromatography (GC) using chiral stationary phases can handle only a few dozen *ee* determinations per day. However, if medium or high throughput is desired, speed-up using automation is possible, although generally at the expense of precision. This disadvantage is not a serious concern, because the purpose is to identify positive hits that can then be analyzed by a more precise system. In some cases, GC can be modified so that in optimal cases about 700–800 fairly exact *ee* and *E* determinations are possible per day. Such medium throughput may suffice in certain applications. The first such case concerned the lipase-catalyzed kinetic resolution of the chiral alcohol (*R*)- and (*S*)-**22** with formation of the acylated forms (*R*)- and (*S*)-**23** (102). Thousands of mutants of the lipase from *P. aeruginosa* were created by epPCR for use as catalysts in the model reaction and were then screened for enantioselectivity.



Although in principle it is possible to simply use several GC instruments each equipped with a sample manager and a separate PC, this is really not efficient because it is expensive, and at the same time data handling becomes tedious. The first successful construction consisted of two GC instruments (e.g., GC instruments and data bus (*HP-IB*) are commercially available from the firm Hewlett-Packard, Waldbronn, Germany), one prep-and-load sample manager (*PAL*) (commercially available from CTC, Schlieren, Switzerland) and one PC (102).

Recently, this system has been extended to include three GC instruments operated by one PC (Fig. 12) (103,104). Experience has shown that a single sample manager for all three GC instruments may cause problems because it is difficult to construct identical columns (104). Therefore, three sample managers were employed

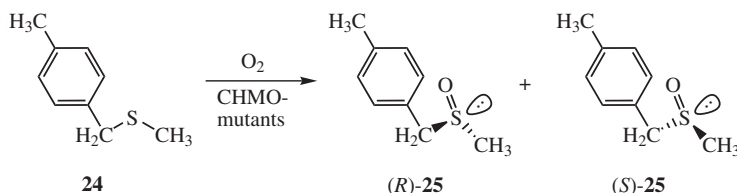


FIG. 12. Picture of optimized unit for *ee* determination based on three GC instruments driven by one PC (104).

separately, the final data being collected and analyzed (*ee* and/or *E*) by one PC. This screening system was first applied successfully in the analysis of chiral products arising from catalysis by mutant Baeyer-Villigerases. In this directed evolution project about 17 000 samples were screened (103).

HPLC can also be exploited for a medium-throughput *ee* analysis, although again the traditional forms need to be adapted. As before, speed is accomplished at the expense of precision, but systems can be implemented that allow the identification of positive hits, which then need to be analyzed more precisely by the use of conventional HPLC having longer columns (and longer analysis times). Presently, only medium throughput can be achieved, meaning the evaluation of 300–800 samples per day, which suffices in some applications.

The first medium-throughput HPLC-based *ee* assay was developed to identify hits in the directed evolution of enantioselective cyclohexanone monooxygenases (CHMO) as catalysts for the asymmetric O<sub>2</sub>-mediated oxidation of prochiral thio-ethers such as **24** (105). In this application, a commercially available HPLC instrument (Shimadzu LC 2010) was equipped with a sample manager and the appropriate software (Lab Solutions) to handle 96- or 384-well microtiter plates. Because enantiomeric separation of (*R*)-**25**/*(S)*-**25** has to be fast and efficient, exploratory experiments were performed with a variety of different chiral stationary phases, solvents, and conditions. An efficient system turned out to be benzoylated cellulose as the stationary phase with a mixture of *n*-heptane and ethanol as the mobile phase. For rapid analysis, columns 50 mm in length and 4.5 mm in diameter were used. This system allows for at least 800 *ee* determinations per day. Unfortunately, the *E. coli*-based expression system produces small amounts of indole, which leads to an overlap with the HPLC-peak of (*S*)-**25**. Although this can be considered in the quantitative evaluation, the *ee* values accessible under these conditions are not precise and were consequently used only to identify hits. These were subsequently analyzed precisely by a conventional HPLC setup using a longer column (250 mm) (105).



### G. ASSAYS BASED ON CAPILLARY ARRAY ELECTROPHORESIS

The GC- or HPLC-based techniques described above may well serve as practical medium-throughput assays in some cases, but high throughput encompassing thousands of *ee* values per day is outside of the realm of these assays. In sharp contrast, CAE has been modified to allow the high-throughput determination of enantiomeric purity (89,106). It is well known that traditional capillary electrophoresis (CE) in which the electrolyte contains chiral selectors, such as  $\beta$ -cyclodextrin derivatives ( $\beta$ -CDs), can be used to determine the enantiomeric purity of a given sample. The conventional form of this analytical technique allows for only a few dozen *ee* determinations per day. However, because of the analytical demands arising from the Human Genome Project, *inter alia*, CE has been revolutionized so that efficient techniques for instrumental miniaturization are now available, making super-high-throughput analysis of biomolecules possible for the first time.

Two different approaches for such analyses have emerged, namely, CAE (107) and CE on micro-chips (also called CAE on chips) (108). Both techniques can be used to carry out DNA sequence analyses and/or to analyze oligonucleotides, DNA-restriction fragments, amino acids, or PCR products. Many hundreds of thousands and more analytical data points can be accumulated per day. On the basis of these results, CAE was adapted to determine the enantiomeric purity of chiral amines, with fluorescence serving as the detection system (89,106). In optimal cases between 7000 and 20 000 *ee* determinations were shown to be possible with high accuracy. However, the instruments currently call for large financial investments. CAE on chips could be a cheap alternative, but this method requires more development if high-throughput *ee* determinations are to be included (106).

### H. ASSAYS BASED ON CIRCULAR DICHROISM

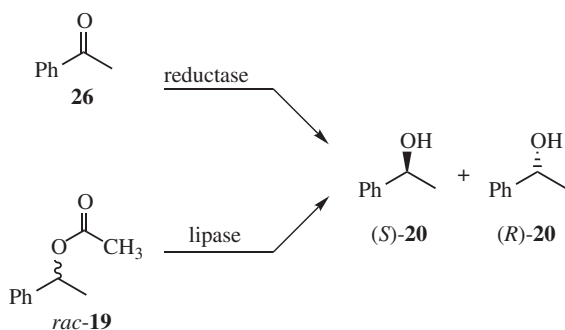
In some cases, circular dichroism (CD) is ideally suited for high-throughput *ee* assays, although to date it has not been used routinely in enzymatic reactions. An alternative to HPLC employing chiral columns, which separate the enantiomers of interest, involves the use of normal columns which simply separate the starting materials from the enantiomeric products, with *ee* of the mixture of enantiomers then being determined by CD spectroscopy (109). This classical method has been adapted to high-throughput *ee* screening (110–112). The method is based on the use of sensitive detectors for HPLC which determine in a parallel manner both the CD ( $\Delta\epsilon$ ) and the UV absorption ( $\epsilon$ ) of a sample at a fixed wavelength in a flow-through

system. The CD signal depends only on the enantiomeric composition of the chiral products, whereas the absorption is related to their concentrations. Thus, only short HPLC columns are necessary. Upon normalizing the CD value with respect to absorption, the so-called anisotropy factor  $g$  is obtained:

$$g = \frac{\Delta\epsilon}{\epsilon}. \quad (3)$$

Therefore, it is possible to determine the  $ee$  value without recourse to complicated calibration. The method is theoretically valid only if the  $g$  factor is independent of concentration and linear with respect to  $ee$ . These conditions may not hold if the chiral compounds form dimers or aggregates, because such enantiomeric or diastereomeric species would give rise to their own particular CD effects. Although such cases have yet to be reported, it is mandatory that this possibility be checked in each new system.

In work concerning the directed evolution of enantioselective enzymes, there was a need for fast and efficient ways to determine the enantiomeric purity of chiral alcohols, which can be produced enzymatically either by reduction of prochiral ketones (e.g., **26**) using reductases or by kinetic resolution of *rac*-acetates (e.g., **19**) by lipases (111). In both systems, the CD approach is theoretically possible. In the former case, an LC column would have to separate the educt **26** from the product (*S*)/(*R*)-**20**, whereas in the latter, (*S*)/(*R*)-**20** would have to be separated from (*S*)/(*R*)-**19**.



Because acetophenone (**26**) has a considerably higher extinction coefficient than 1-phenylethanol (**20**) at a similar wavelength (near 260 nm), separation of starting material from product is necessary. In preliminary experiments using enantiomerically pure product **20**, the maximum value of the CD-signal was determined. Mixtures of **20** having different enantiomer ratios (and therefore  $ee$  values) were prepared and analyzed precisely in control experiments by chiral GC. The same samples were studied by CD, resulting in the compilation of  $g$  values. A linear dependence of the  $g$  values on the  $ee$  values was observed, with a correlation factor of  $r = 0.99995$ , which translates into the following simple equation for enantioselectivity (111):

$$ee = 3176.4g - 8.0. \quad (4)$$

Although a reductase was not actually applied, separation of **26** from (*S*)/(*R*)-**20** was accomplished by use of reversed-phase silica as the column material and methanol/water as the eluant. In view of the observed dependence of the *g* factor on concentration, aggregation in this protic medium was excluded. In the HPLC setup, the mixture was fully separated within less than 1.5 min. By use of the JASCO-CD-1595 instrument in conjunction with a robotic autosampler, it was possible to perform about 700–900 rather exact *ee* determinations per day (111).

### I. OTHER *ee* ASSAYS

The infrared radiation caused by the heat of reaction of an enantioselective enzyme-catalyzed transformation can be detected by modern photovoltaic infrared (IT)-thermographic cameras equipped with focal-plane array detectors. Specifically, in the lipase-catalyzed enantioselective acylation of racemic 1-phenylethanol (**20**), the (*R*)- and (*S*)-substrates were allowed to react separately in the wells of microtiter plates, the (*R*)-alcohol showing hot spots in the IR-thermographic images (113,114). Thus, enantioselective enzymes can be identified in kinetic resolution. However, quantification has not been achieved thus far by this method, which means that only those mutants can be identified which have *E* values larger than 100 (113–115).

Another method for assaying the activity and stereoselectivity of enzymes at *in vitro* concentrations is based on surface-enhanced resonance Raman scattering (SERRS) using silver nanoparticles (116). Turnover of a substrate leads to the release of a surface targeting dye, which is detected by SERRS. In a model study, lipase-catalyzed kinetic resolution of a dye-labeled chiral ester was investigated. It is currently unclear how precise the method is when identifying mutants which lead to *E* values higher than 10. The assay appears to be well suited as a pre-test for activity.

## IV. Examples of Directed Evolution as a Means to Control the Enantioselectivity of Enzymes

In view of the availability of numerous mutagenesis methods and *ee* assays, it may seem that *in vitro* evolution of enantioselectivity of a given enzyme for a specific asymmetric reaction is a routine process. However, this is not (yet) the case, notwithstanding a great deal of progress. The problem is how to choose the optimal strategy when exploring protein sequence space. Which mutagenesis method should be used? High or low mutation rate? Focused or non-focused libraries? Large or small libraries? Moreover, the proper choice of an appropriate *ee* assay is also important, which may require some adaptation of a known screening system.

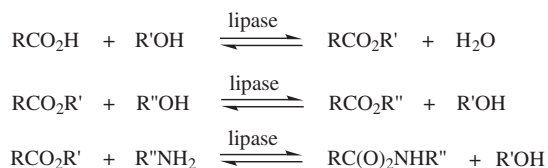
These questions have been addressed most systematically in a series of case studies involving a lipase (16,22–24). The results and conclusions of these studies are presented in detail here because they serve as a guide for future investigations (Section IV.A.1).

## A. HYDROLASES

A.1. *Lipase from Pseudomonas Aeruginosa*

The first case study of the directed evolution of an enantioselective enzyme involving repeating cycles of gene mutagenesis, expression, and screening resulting in evolutionary pressure was carried out with a lipase (16). Systematic investigations were conducted with this enzyme not only to provide proof of principle (16), but also to determine how the strategies concerning the use of various mutagenesis methods compare in terms of efficiency (21–24). The lessons learned were then applied to other studies.

Lipases (triacylglycerol ester hydrolases, EC 3.1.1.3) are ubiquitous enzymes that catalyze the hydrolysis of fats and oils (7,9–11,117,118). In addition to their biological function in bacteria, fungi, plants, and higher animals, lipases are biocatalysts that have received a great deal of attention in numerous industrial processes, including those related to oils and fats, detergents, baking, cheese-making, hard-surface cleaning, and leather and paper processing. Moreover, lipases are the most widely used enzymes in synthetic organic chemistry, catalyzing the chemo-, regio- and/or stereoselective hydrolysis of carboxylic acid esters or the reverse reaction in organic solvents. In the case of enantioselectivity, either desymmetrization of prochiral substrates or kinetic resolution of racemates are relevant, and numerous academic and industrial examples are known, including the BASF process for the production of chiral amines (119,120). More than a dozen lipases are currently available commercially.



The active site of lipases is characterized by a triad composed of serine, histidine, and aspartate, and acyl-enzyme complexes are the crucial intermediates in all lipase-catalyzed reactions (117,118) (Fig. 13).

To illustrate the feasibility of directed evolution of enantioselective enzymes, the field of lipases was considered (16). Then a decision had to be made regarding the choice of a specific lipase and the nature of the substrate to be investigated. Although the genes of many enzymes are available for public use, details of expression systems are often the property of companies that may or may not share them. Thus, none of the common commercially available lipases was chosen for the model study; rather, one of the less common representatives was chosen, namely, the lipase from *P. aeruginosa* (16). The existing expression system is effective enough to provide sufficient amounts of mutants on microtiter plates for screening, but not for the production of gram amounts (121), which means that this lipase is not likely to gain industrial importance. It is also not particularly stable, making isolation, purification, and the determination of precise kinetics data difficult.





was not available at the time. The UV/Vis-based screening system measuring the absorption of the liberated *p*-nitrophenolate was employed (Section III.A; Fig. 5). As a consequence of the first round of mutagenesis and screening, a variant displaying a selectivity factor of  $E = 2.1$  was identified. The corresponding mutant gene was then subjected once more to mutagenesis, and the process was repeated several times. The result after four generations was a variant (A) having an  $E$  value of 11.3 in favor of (*S*)-**2** (Fig. 14).

Figure 14 provides proof of principle, but a factor of  $E = 11.3$  is far from practical. A fifth round of epPCR increases the  $E$  value slightly, but such a strategy is far from optimal. Indeed, after experience was gained in this endeavor and in other directed evolution projects, it became clear that it is better to apply only two or three rounds of epPCR and then to switch to another mutagenesis method (21–24). One of these methods concerns the use of saturation mutagenesis, which requires an intelligent decision as to the choice of the position at which randomization is to be performed. It was assumed that the identified sites of amino acid exchange are “hot spots” that are important for increasing enantioselectivity, but that the specific amino acids identified by sequencing are not necessarily optimal (48). This assumption is reasonable because the size of the screened libraries was smaller than the theoretical number of enzyme variants and because the amino acid exchanges induced by epPCR are biased (i.e., the method is not truly random) (Section II.A). Therefore, several “mutation hot spots” were chosen for saturation experiments (36,48,74). The same strategy was developed independently in a study concerning the enhancement of the thermostability of a protease (47a,123), and it is now used routinely in directed evolution studies. One of the sensitive positions turned out to be 155 (Fig. 14), which was “saturated” by randomization using the appropriate oligonucleotides. This strategy led to variant B displaying an  $E$  value of 20 (48). The

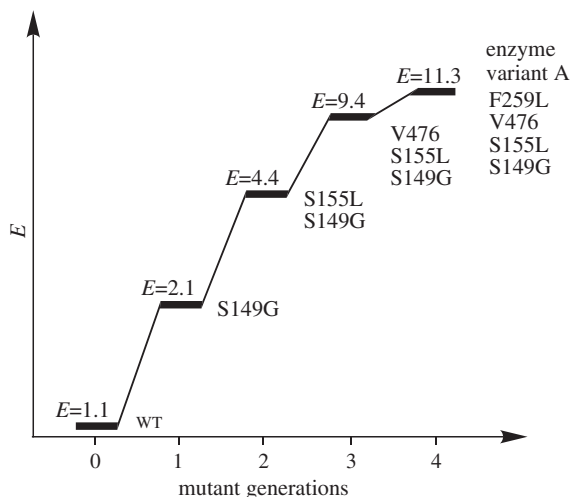


FIG. 14. Increasing the  $E$  values of the lipase-catalyzed hydrolysis of the chiral ester **1** by cumulative mutations caused by four rounds of epPCR (16,22,24).

gene encoding enzyme variant B was then subjected to another cycle of epPCR, resulting in an even better enzyme variant C having five mutations and a selectivity factor of  $E = 25$  in favor of the (*S*)-substrate.

Subsequently, DNA shuffling was considered, but it was not clear which mutant genes should be shuffled (a general problem in any directed evolution project!). DNA shuffling of the mutant genes produced by low-mutation-rate epPCR (Fig. 14) failed to achieve significant improvements, leading to the conclusion that higher gene diversity is necessary (49). Therefore, epPCR of the WT gene was repeated, this time at a higher mutation rate corresponding to an average of three amino acid exchange events per enzyme molecule. This process led to the identification of several improved enzyme variants, D and E ( $E = 3$  and 6.5) being the best (49). In the original project using a low mutation rate such selectivity factors were not obtained until the second cycle of epPCR (16). The probability of creating even better mutants by adjusting epPCR to very high mutation rate (e.g., 8–20 simultaneous amino acid exchanges) is likely due to higher catalyst diversity, but then the problem of screening needs to be addressed.

This result can be constructed as evidence for the hypothesis that epPCR at high error rate constitutes the better strategy. The genes encoding the variants C, D, and E were then subjected to conventional DNA shuffling. This process provided variant F having the highest enantioselectivity up to that point ( $E = 32$ ) (49). These observations support the hypothesis that enhanced gene diversity leads to better results in DNA shuffling.

Clearly, all of these strategies for navigating in protein sequence space are successful, but it is not obvious which ones are optimal.

As part of yet another strategy, the region of accessible protein sequence space was extended by developing a modified version of Stemmer's combinatorial multiple-cassette mutagenesis (CMCM) (49). The original form of CMCM is a special type of DNA shuffling using the WT gene and cassettes composed of defined sequences to be randomized (124). In the lipase project, two mutant genes encoding the enzyme variants D and E and a mutagenic oligocassette allowing simultaneous randomization at the "hot spots" 155 and 162 were subjected to DNA shuffling (Fig. 15). This resulted in the most enantioselective variant J to date, displaying a selectivity factor of  $E = 51$  (49). It is characterized by six mutations, most of which are remote from the active site (Ser 82) (see discussion below).

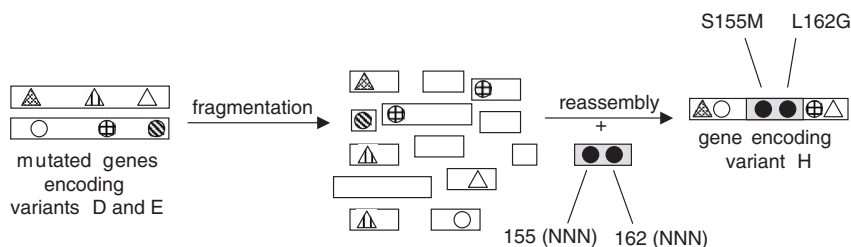


FIG. 15. Extended combinatorial multiple-cassette mutagenesis in the evolution of an (*S*)-selective lipase-variant from *P. aeruginosa* as a catalyst in the kinetic resolution of 1 (▲ position 20; △ position 161; □ position 234; ○ position 53; ⊕ position 180; ⊗ position 272) (49).

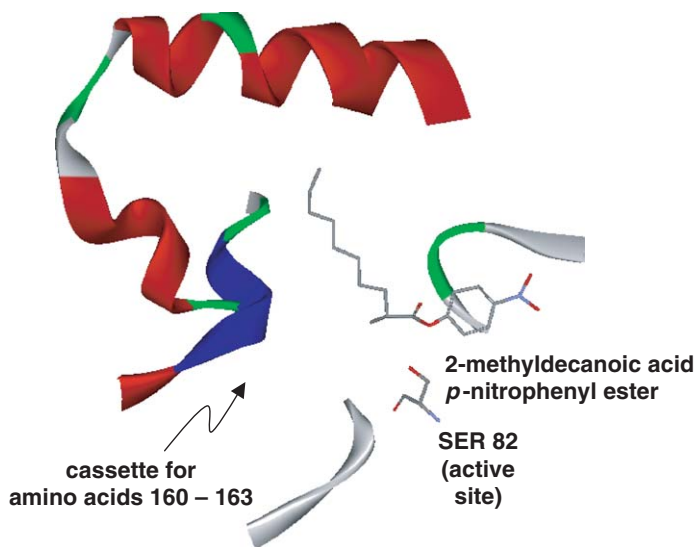


FIG. 16. Binding pocket of the lipase from *P. aeruginosa* for the acid part of 2-methyldecanoic acid *p*-nitrophenyl ester showing the geometric position of amino acids 160–163 which were randomized in cassette mutagenesis (49).

Finally, a focused library was generated by randomizing amino acids 160–163, a region next to the binding site (Fig. 16). This procedure constitutes a fusion of “rational design” and directed evolution. For this purpose cassette mutagenesis was applied, resulting in variant G with  $E = 30$  which is characterized by four mutations (E160A, S161D, L162G, and N163F) (49). In this case, only 5000 clones were screened, although for 95% coverage of the 160 000 theoretically different mutants, an oversampling of about 3 million clones would be necessary (see Section II.A for a detailed discussion concerning this point).

The results of these and other experiments are summarized in Fig. 17. A total of only 40 000 mutants was screened, which is actually a small number in our context. It is likely that upon exploration of larger portions of protein sequence space efficiently, even better lipase-variants can be identified. The assumption that millions of potential variants in the vast protein sequence space are highly enantioselective is not unfounded.

However, efficient directed evolution is not a matter of generating huge libraries which then require considerable efforts in screening for the desired property. The goal is to create a maximum in structural diversity while minimizing the size of the libraries (17,23,24,37).

The systematic studies regarding the directed evolution of the lipase from *P. aeruginosa* show that protein sequence space is best explored by applying the following strategies:

- (1) Generation of mutants by epPCR at low or preferably at high mutation rate.
- (2) Identification of hot spots and application of saturation mutagenesis.
- (3) Identification of hot regions empirically or by rational design and subsequent application of cassette mutagenesis.

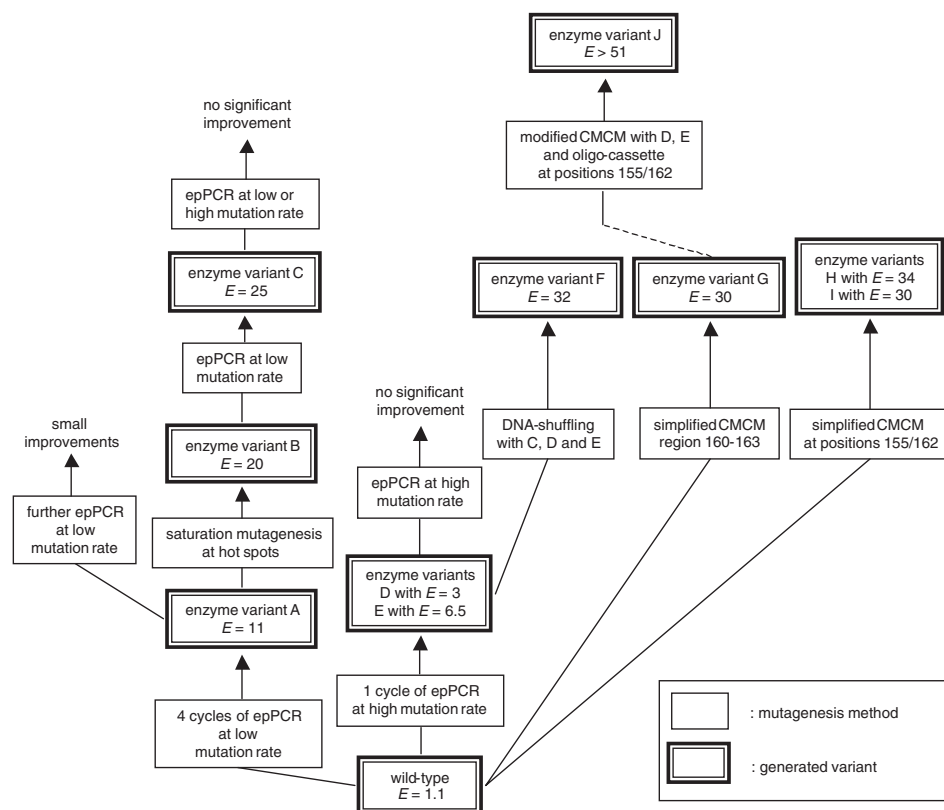


FIG. 17. Schematic summary of the directed evolution of enantioselective lipase-variants originating from the WT *P. aeruginosa* used as catalysts in the hydrolytic kinetic resolution of ester **1** (49).

- (4) Application of epPCR at high mutation rate followed by DNA shuffling of the mutants.
- (5) Extension of the process of CCM to cover focused positions in the enzyme (hot spots identified by earlier experiments).

Traditionally, one of the limitations of asymmetric biocatalysis is the fact that usually only one of the enantiomeric products (*R*) or (*S*) are accessible by applying a given enzyme (7–11). However, organic chemists need (*R*)- or (*S*)-selective (bio)catalysts on an optional basis. Therefore, efforts were undertaken to invert the sense of enantioselectivity in the hydrolytic kinetic resolution of ester **1** using the lipase from *P. aeruginosa* with preferential formation of (*R*)-**2** (21,36,125). The original library of enzyme variants produced by applying epPCR at low mutation rate to the WT gene of the lipase contained mainly *S*-selective enzymes; only a few showed a (very slight) preference for (*R*)-**2** (21,36). Therefore, the same experiment at a relatively high mutation rate corresponding to about 2–3 amino acid substitutions per enzyme molecule was performed (125). Upon screening an enzyme library of 15 000 clones, several (*S*)-selective variants were identified, but also

two (*R*)-selective lipases, 18F9 and 12G12, characterized by a single mutation (V232I) and four mutations (S112P, S147N, T150A, and T226A), respectively (125). The *E* values in favor of the (*R*)-product **2** were found to be 2.0 and 1.1, respectively. Furthermore, an active mutant 47E6 (with D113G, I142 T, S218L, and S268N) was identified, showing no preference for either of the two enantiomers (*E* = 1.0).

The gene corresponding to 18F9 served as the basis for another cycle of epPCR under otherwise identical conditions (125). As a result of the screening of 5000 clones, (*R*)-selective enzyme variants 18F9E1 (with M16L, A34 T, and V232I) and OE7 (with V55A, P86L, D113G, and V232I) were discovered, displaying *E* values of 3.7 and 3.0, respectively.

In a similar third cycle of epPCR using gene OE7, enzyme variant 3B6 (with V55A, P86L, D113G, V232I, S237 T, and Q275L) was generated, resulting in even higher (*R*) selectivity (*E* = 7.0). However, further rounds of epPCR-based mutagenesis failed to produce additional positive results.

In an initial attempt to apply DNA shuffling, genes 18F9, 12G12, and 47E6 were shuffled, with the hope that possible non-productive mutations would be eliminated. However, the hope was not realized, as no improvements were detected (125). Consequently, the size of the gene pool was increased, and genes 12G12, 47E6, 18F9, 3B6, and OE7 were subjected to DNA shuffling. Although no shift to significantly higher enantioselectivity resulted, three *R*-selective enzyme variants of comparable enantioselectivity were in fact found, namely, 14A5 (with V55A, P86L, D113G, S147N, T150A, V232I, S237 T, and Q275L), 11C8 (with V55A, P86L, A102 V, D113G, V232I, and S237 T) and 16A7 (with V55A, P86L, S71G, D113G, V232I, S237 T, and S268C), with the *E* values being 6.7, 6.5, and 7.0, respectively, in favor of (*R*)-**2**. Reporting negative results is important, because lessons can be learned from them.

Because initial attempts to apply saturation mutagenesis at selected hot spots failed to increase enantioselectivity markedly, DNA shuffling was reconsidered (125). With the hope of increasing diversity, gene 18F9E1, which had been generated earlier, was shuffled with gene 14A5. By inspection of a library of 5000 clones, several (*R*)-selective variants were found, the best one being 1G10 (with M16L, A34 T, P86L, D113G, S147N, T150A, V232I, and S237 T) displaying a selectivity factor of *E* = 20 in the model reaction *rac*-**1** → (*R*)-**2** (125).

By comparison of the mutations present in 18F9E1 and 14A5 with those of the new variant 1G10, it became clear that mutations V55A and Q275L have been eliminated by the process of DNA shuffling. Obviously, these two mutations exert a negative effect, which means that in the present case DNA shuffling plays the role of “correcting” non-productive mutational changes brought about earlier. New point mutations were not introduced. Finally, a single round of epPCR on top of this (using gene 1G10 at high mutation rate) resulted in yet another substantial improvement, with enantioselectivity in favor of (*R*)-**2** reaching *E* = 30 (125). In this case, the enzyme (15B10) has 11 amino acid substitutions (M16L, A34 T, P86L, T87S, V94A, D113G, S147N, T150A, L208 H, V232I, and S237 T). Relative to variant 1G10, three new mutations (T87S, V94A, and L208 H) were introduced. A total of 45 000 clones were screened in these efforts, which is again a relatively small number in our context.

This study seems to suggest (but not to prove) that evolution of pronounced (*R*)-selectivity in the present case requires greater structural change than in the case of (*S*)-selectivity, which seems to be reflected in the comparatively high number of amino acid exchanges. However, the application of other strategies could lead to a different conclusion. It is also interesting that the amino acid substitutions described herein occur at positions quite different from the hot spots that were uncovered in the case of the (*S*)-selective mutants.

Systematic investigations of the type described above provide two types of lessons. First, they shed some light on how to choose the right strategy for navigating in protein sequence space. Second, they provide novel data for theoretical studies concerning the origin of enantioselectivity. Most of the above results were obtained without prior knowledge of the 3D structure of the enzyme or of its mechanism. Rather, the Darwinian nature of the concept was relied on. However, insight into how enzymes function can be gained from directed evolution, provided a sound theoretical analysis is performed.

The lipase from *P. aeruginosa* is a hydrolase having the usual catalytic triad composed of aspartate, histidine, and serine (Fig. 13). In the case of the kinetic resolution of the chiral ester **1**, stereoselectivity is determined in the first step, which involves the formation of the oxyanion. Unfortunately, X-ray structural characterization of the (*S*)- and (*R*)-selective mutants are not available, because of the difficulties in expressing sufficient amounts and in handling the somewhat sensitive enzyme. Such crystallographic data would provide ideal information in attempts to unveil the source of enhanced enantioselectivity. However, consideration of the crystal structure of the WT lipase is in itself illuminating. It shows a conserved  $\alpha/\beta$  hydrolase fold typical of lipases and the presence of a lid and the usual catalytic triad composed of aspartate (D229), histidine (H251), and serine (S82) (126). Surprisingly, it turned out that many of the mutants have amino acid exchanges remote from the active site (21–24,48–50).

Attempts were made to isolate and purify the mutant (variant J) showing the highest enantioselectivity ( $E = 51$  in favor of (*S*)-**2**) (Fig. 17). However, as noted above, as a consequence of the low rate of expression and the relative instability of the WT and mutants of the lipase from *P. aeruginosa*, it was not possible to isolate pure mutant J. To determine a rough idea of activity, the supernatants were used to perform kinetics assuming similar amounts of protein in each case (22). The  $k_{\text{cat}}$  values of mutant J turned out to be  $9.6 \text{ s}^{-1}$  for (*S*)-**1** and  $1.2 \text{ s}^{-1}$  for (*R*)-**1**. In going from the wild type to variant J, the  $k_{\text{cat}}/K_{\text{m}}$  value [ $\text{l mol}^{-1} \text{ s}^{-1}$ ] increased significantly: for (*S*)-**1**,  $k_{\text{cat}}/K_{\text{m}} = 9.0 \times 10^2$  (wild type) and  $3.7 \times 10^5$  (variant J); for (*R*)-**1**,  $k_{\text{cat}}/K_{\text{m}} = 3.5 \times 10^2$  (wild type) and  $8.4 \times 10^3$  (variant J). Thus, although these are only rough numbers, they show that variant J is much more active than the WT.

To illuminate the source of enhanced (*S*)-selectivity, mutant J and other real and hypothetical mutants were subjected to a detailed MM/QM study (127). The six mutations (amino acid substitutions) of mutant J are D20N, S53P, S155M, L162G, T180I, and T234S, most occurring at positions remote from the active center (S82) (21–24,48). Remote effects had been observed in early investigations of protein engineering (29a), catalytic antibodies (12), and directed evolution (123,128–130),

but these were all cases in which thermal and/or chemical stability or activity was the focus of interest.

In contrast, enantioselectivity is a parameter that chemists, biochemists, and enzymologists traditionally associate with the active center and the binding region around it, in the tradition of Emil Fischer's hypothesis of lock-and-key or Koshland's model of induced fit (131). Indeed, all previous attempts to influence the enantioselectivity of an enzyme based on site-specific mutagenesis as suggested by rational design focused on the binding site (14,15). Thus, the present results seem to indicate a change in paradigm. However, on the basis of a careful theoretical analysis, they are not as surprising as one might first think (127). Other examples of distal mutations influencing enantioselectivity followed in later studies (Sections IV.A.2, IV.A.4, and IV.C). The present experimental results do not mean that the traditional approach based on site-directed mutagenesis at or near the active site is wrong; rather, they show that directed evolution covering the whole enzyme can lead to new effects.

The results of the detailed MM/QM study make several important conclusions plausible (127). First, only three of the six amino acid substitutions influence enantioselectivity. Second, there is no substantial difference in the binding energetics of the (*S*)- and (*R*)-substrate; rather, stereodifferentiation occurs as the oxyanion is formed. Thus, there is no substantial enantioselective molecular recognition in the formation of the Michaelis–Menten complex. Third, a novel relay mechanism starting at the surface of the enzyme and working inward toward the active site results in additional stabilization of the oxyanion by hydrogen bonding originating from a histidine in the case of (*S*)-1. This is in contrast to (*R*)-1, in which case the corresponding oxyanion cannot profit from such stabilization for steric reasons (Fig. 18). It is likely that the same effects operate in the transition state of the reaction leading to the oxyanion, a reasonable assumption that is the subject of an ongoing QM study (127). These results are fully in line with the conclusions of the (rough) kinetics data. They are also a perfect example of Pauling's hypothesis concerning the stabilization of the transition state as the primary factor in enzyme-catalyzed reactions (65*h*,131), a hypothesis that has been elaborated on by Garcia-Viloca, Gao, Karplus, and Truhlar (65*f*).

Such experimental and theoretical studies raise important questions concerning the *in vitro* evolution of enantioselectivity. Are remote mutations more important than those close to the active site, or is the opposite true? Is it more effective to allow randomization all over the enzyme rather than focusing on the region around the active site (or *vice versa*)? Currently, it is not possible to provide general answers. To be sure, in the performance of epPCR or any other mutagenesis method, which more or less covers the whole gene, there are statistically more remote amino acids for exchange events to occur than amino acids close to the active site. For this trivial reason, it is therefore not surprising to find an increased number of exchanged amino acids at distal sites (24,127,132). However, is it meaningful to prevent their occurrence by restricting amino acid randomization to regions next to the active site in the form of focused libraries? Some authors appear to favor such a conclusion (133). However, a rigid position on this issue may not be helpful. It may well be that if one were to perform single amino acid substitutions systematically at



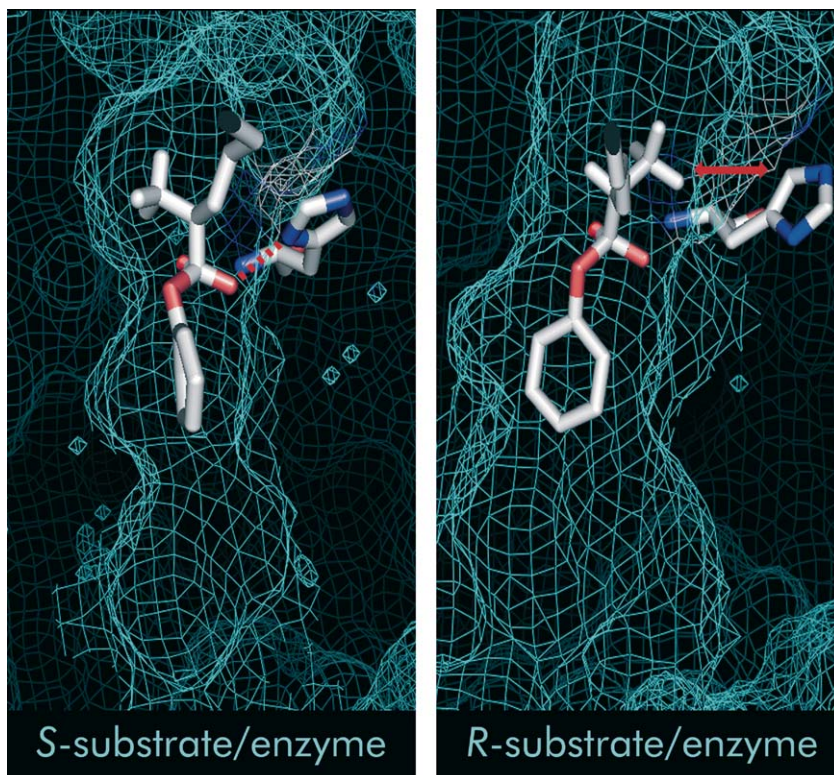


FIG. 18. The oxyanions originating from *rac*-**1** in the lipase-mutant J. Left: (*S*)-**1** as substrate; right: (*R*)-**1** as substrate, showing the different degree of additional stabilization by a histidine residue (24,127).

all positions of an enzyme such as the lipase from *P. aeruginosa* and to test all theoretically possible mutants in a given enantioselective reaction as in the kinetic resolution of substrate **1**, one would find mainly hits characterized by amino acid substitutions near the binding site or catalytically active center.

However, the situation becomes more complicated when several (sequential or simultaneous) amino acid exchange events are considered, because in such cases cooperativity (not just additivity) may occur as a result of unpredictable phenomena. This is certainly the case in the investigation just considered (24,127). Semi-rational design by focusing randomization exclusively around the active site would never have resulted in the creation of mutant J, nor in the discovery of the novel effects as described in the above MM/QM analysis. On the other hand, the success of the library created by randomization in the restricted region 160–163 in the form of cassette mutagenesis near the active site illustrates the value of focused libraries, because this resulted in an *E* value of 30 for variant G (49). This result shows that as long as the screening effort remains reasonable, it is worthwhile to test both strategies.



Relevant to this discussion is the recently developed method called the complete active-site saturation test (CAST), which is an efficient fusion of rational design and focused randomization (50,134). It is a method ideally suited to expand the range of substrate acceptance and thus touches on one of the most important unsolved problems of biocatalysis. CASTing requires two straightforward steps: the design and generation of relatively small focused libraries of enzyme mutants produced by randomization at several sets of two spatially close amino acid positions around the active site. The pairs of amino acids chosen for randomization are those that have their side chains pointing toward the binding pocket. The choice of two amino acid that are spatially close to one another allows for potential synergistic conformational effects arising from side chain interactions. This strategy constitutes a practical compromise between conventional saturation mutagenesis at single sites and simultaneous randomization at multiple sites using large cassettes. In the former case, the screening effort is low (oversampling 200 clones) but catalyst diversity is restricted, whereas in the latter case catalyst diversity is high but screening may require millions of clones to be assayed. CASTing generates 400 different mutants in each library, which requires only 3000 clones to be screened for 95% coverage (Section II.A). Upon applying CASTing to the lipase from *P. aeruginosa*, five mutant libraries A, B, C, D, and E were constructed in the above manner, leading to the generation of half a dozen mutants with unusually broad substrate acceptance (Fig. 19) (50).

Initial results show that CASTing can also be used to generate enantioselectivity (50). For example, in the hydrolytic kinetic resolution of 2-phenyl-propionic acid *p*-nitrophenyl ester catalyzed by the lipase from *P. aeruginosa*, a mutant resulted, having an *E* value of 25 (50). Moreover, in the case of substrate **1**, a mutant was readily generated having an *E* value of 39 in favor of (*S*)-**2** (135). This mutant is characterized by two amino acid exchanges, L159Y and L162G. Interestingly, the latter mutation had been identified in previous investigations (see above). Had one started the original directed evolution study using CASTing, positive results would have been achieved considerably faster. Mutants showing reversed enantioselectivity were also found (135). Of course, CASTing has no evolutionary character (similar to the first round of epPCR), but it is a powerful combinatorial approach that can be applied as a first step in any directed evolution project. In fact it is a viable alternative to epPCR in the initial phase, to be followed by further mutagenesis steps, which create evolutionary pressure. Re-casting is but one of many possibilities (i.e., to use the gene of one of the hits as the parent in a second round of CASTing).

## A.2. Other Lipases

The *Bacillus subtilis* lipase A (BSLA) is an unusual lipase because it lacks the so-called lid structural unit (136). Moreover, it is a small enzyme composed of only 181 amino acids. The initial results of an ongoing study are remarkable and illustrate the power of directed evolution (45,137). The desymmetrization of *meso*-1, 4-diacetoxy-2-cyclopentene (**15**) was chosen as the model reaction, and the MS-based *ee* assay using an appropriately D<sub>3</sub>-labeled substrate (Section III.C) provided a means to screen thousands of mutants.

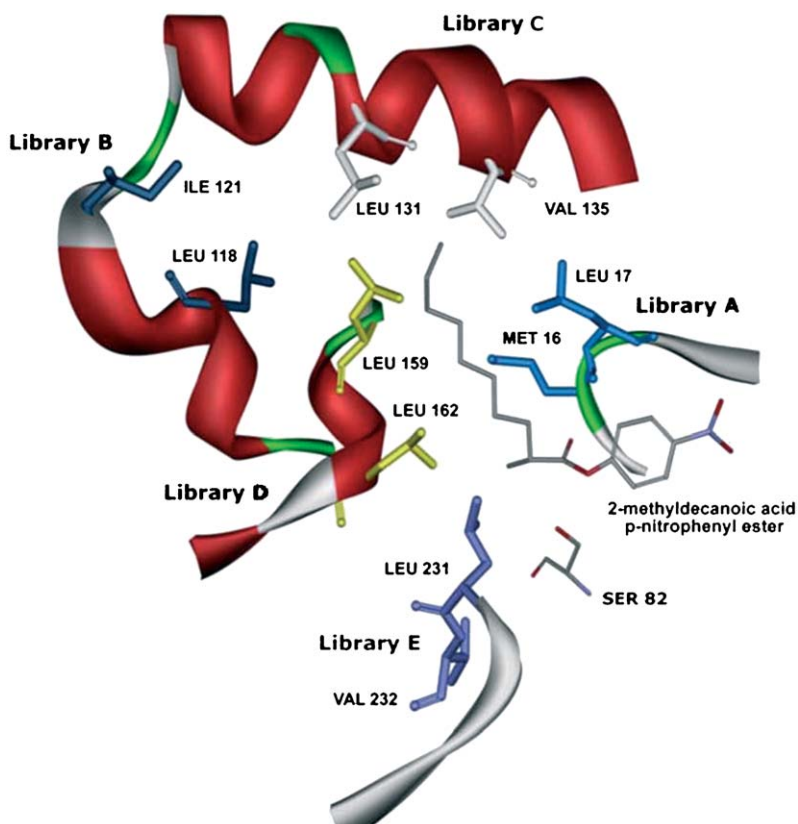
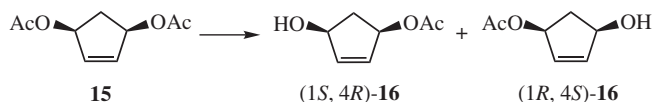


FIG. 19. CASTing of the lipase from *P. aeruginosa* leading to the construction of five libraries of mutants produced by simultaneous randomization at two amino acid sites: A, B, C, D, and E (for illustrative purposes binding of substrate **1** is shown) (50).

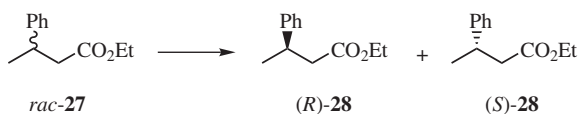


The WT lipase leads to an *ee* value of only 38% in favor of the (1*R*,4*S*) enantiomer. The application of low-error epPCR increased the enantioselectivity slightly, but high-error rate epPCR turned out to be more successful, with several mutants showing *ee* values of 54–58% (45,137). The results are in line with the experience gained in the *Pseudomonas aeruginosa* lipase project (Section IV.A.1). Of course, a library produced by high mutation rate can also contain hits that have only one amino acid exchange, and this was indeed observed in several cases.

In this ongoing project, a different strategy was also tested, namely, systematic saturation mutagenesis at all of the 181 positions (45,137). In such an approach, all 181 mini-libraries are screened (each about 200 clones for the purpose of

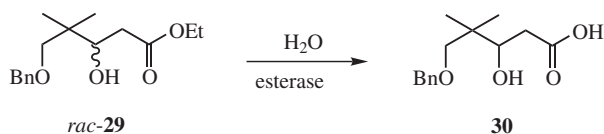
oversampling). Several mutants with slightly enhanced *ee* values were identified. Interestingly, some showed distinct reversed enantioselectivity favoring the (1*S*,4*R*)-enantiomer. Two of the most selective mutants displaying reversed enantioselectivity are characterized by single mutations at position 18, namely, N18S and N18Q leading to *ee* values of 82 and 83%, respectively (137). Position 18 is rather close to the binding site, but a detailed MM/QM interpretation has not yet been performed. The same lipase and substrate were also used to illustrate a new recombinant mutation method (ADO) (Section II.B), resulting in the discovery of several mutants showing improved enantioselectivity (64). Further optimization was not the purpose of the ADO study.

In yet another investigation regarding the control of stereoselectivity of a lipase by directed evolution, inversion of the sense of enantioselectivity was accomplished (138). The focus of this interesting study was the *Burkholderia cepacia* KWI-56 lipase as a catalyst in the hydrolytic kinetic resolution of *rac*-ethyl-3-phenylbutyrate (27). The WT shows (*S*)-selectivity with an *E* factor of 33. Using X-ray structural data characterizing the lipase, the authors made a decision concerning the choice of four amino acid residues (L17, F119, L167, and L266, all near the binding product), which they then subjected to randomization. However, less than complete randomization was performed; rather, it was restricted to the introduction of seven hydrophobic amino acids in a combinatorial manner. This procedure is related to binary patterning (20a). By use of a novel *in vitro* technique for the construction and screening of a protein library by single-molecule DNA amplification via PCR followed by *in vitro* coupled transcription/translation (SIMPLEX expression), a mutant lipase was identified showing reversed enantioselectivity ( $E_R = 38$ ). These impressive results call for a detailed theoretical analysis, *inter alia*, because the  $\Delta\Delta G^\ddagger$  achieved in going from the WT to the mutant is substantial ( $\sim 4$  kcal/mol).



### A.3. Esterases

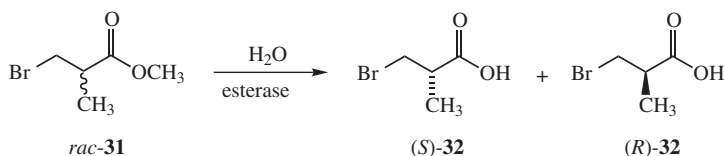
Esterases have a catalytic function and mechanism similar to those of lipases, but some structural aspects and the range of substrates differ (7–11). Most important, they lack the so-called lid prominent in almost all lipases. Nevertheless, one can expect that the lessons learned from the directed evolution of lipases also apply to esterases. So far, few efforts have been investigated in the directed evolution of enantioselective esterases, although earlier work by Arnold (17,32,139) had shown that the activity of esterases as catalysts in the hydrolysis of achiral esters can be enhanced. The first example involving the improvement of enantioselectivity concerned the hydrolytic kinetic resolution of the sterically hindered ester *rac*-29 catalyzed by the esterase from *P. fluorescens* (PFE) (140).



Instead of using the standard mutagenesis methods of modern molecular biology (Section II), the authors employed a mutator strain lacking DNA repair mechanisms, namely, *Epicurian coli* XL1-red. Although difficulties arose in the screening process, a mutant PFE-U3 was isolated that contains two point mutations (A209D and L181V). Following partial hydrolysis, the non-reacted ester **29** having an *ee* value of 25% was isolated. The value of this investigation is limited, because a second round of mutagenesis was not attempted, configurational assignments of **29/30** were not made, and the selectivity factor *E* was not determined (140).

In a related investigation, the same authors used the identical system but a different substrate, namely, 3-phenylbutyric acid ethyl ester (141). In this case, enantioselectivity of the WT (*E* = 3.5) was increased slightly, to *E* = 5.8 and 6.6, by the formation of two mutants, one having mutation D158N and the other L181Q. Again, as a consequence of the paucity of data, it difficult to draw any sound conclusions.

In a more detailed study, the same esterase (*P. fluorescens*) was again subjected to mutagenesis using the same mutator strain, but also by saturation mutagenesis at selected positions (133a). In addition to 3-phenylbutyric acid ethyl ester (**27**), 3-bromo-2-methyl-propionic acid methyl ester (*rac*-**31**) was chosen for the hydrolytic kinetic resolution, with the WT PFE showing an *E* factor of 12 in favor of the (*S*)-**32**.



Upon screening of only 288 colonies produced by the mutator strain, an improved mutant showing *E* = 21 was identified (T230I). Several other mutants displaying enantioselectivities similar to the WT were also discovered (133). These observations led to the logical conclusion that position 230 is a hot spot and that saturation mutagenesis might lead to further improvements. Indeed, from a 175-member library a mutant characterized by T230P was identified, showing an *E* value of 19. All of the other mutants were less selective or showed no activity. The same procedure was applied to the other substrate, 3-phenylbutyric acid ethyl ester, resulting in several mutants displaying moderate increases in enantioselectivity (*E* = 3.5 for WT to *E* = 6–12 for mutants) (133). In all three investigations, only very small libraries were scanned, which makes a statistical analysis difficult.

The authors analyzed the (limited) data on the basis of homology model derived by considering the X-ray structure of a different type of enzyme, a haloperoxidase

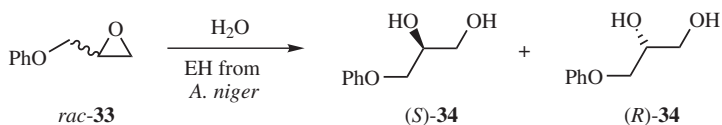
showing 46–51% amino acid sequence identity with PFE (133). They then discussed the possible role of the individual mutations. Assuming the correctness of the homology model, it appears that some of the mutations occur at distal positions, with others close to the binding site. It was concluded that the distal mutations increase enantioselectivity only moderately and that mutations near the active site exert stronger effects (133a).

In a later investigation this conclusion was reiterated (133b). However, although it may pertain in the particular case, the conclusion may be one-sided. As already pointed out in Section IV.A.1, one needs to distinguish between a situation in which single point mutations are compared (close, medium-close, distal), and one in which several mutations are involved, possibly leading to unpredictable cooperative effects (24,127,142). Thus, at this stage one needs to be open-minded (i.e., to investigate randomization over the whole enzyme) but also to design focused libraries as, for example, in CASTing studies (50,134).

#### A.4. Epoxide Hydrolases

Thus far only three reports regarding the directed evolution of enantioselective EHs have appeared (95,96,143), notwithstanding the fact that these enzymes, even as wild types, constitute important catalysts in synthetic organic chemistry (7–12,144,145). Indeed, since two EHs became commercially available recently, this type of biocatalysis offers exciting prospects for the practicing organic chemist.

The first two reported studies concern the epoxide hydrolase from *Aspergillus niger* (ANEH) (95,96). The enzyme had previously been purified to homogeneity, the gene cloned and expressed in *E. coli*, and the catalytic hydrolysis of epoxides optimized to high substrate concentrations. Initial attempts were made to enhance the enantioselectivity of the ANEH-catalyzed hydrolytic kinetic resolution of glycidyl phenyl ether (*rac*-33). The WT leads to an *E* value of only 4.6 in favor of (*S*)-34 (96).



To screen efficiently, the MS-based *ee* assay (Section III.C) was adapted to the present transformation (95,96). This means that a *pseudo*-racemate comprising a 1:1 mixture of (*S*)-33 and (*R*)-D<sub>5</sub>-33 was used in the screening. Several libraries of mutant ANEHs were prepared by applying epPCR under various conditions and transforming into *E. coli* BL21 (DE3). Single transformants were cultured in liquid media in 96-well format, and a pre-test for activity was first performed using bacterial cultures and the racemic epoxide 33. Of the first 20 000 clones that were pre-screened, almost 80% showed no appreciable activity, a result that underscores the value of the pre-test. The active mutants were then screened by the MS assay, leading to the identification of several dozen variants with improved enantioselectivity. Most of these exhibited *E* values ranging between 5 and 7, but several had

distinctly higher enantioselectivities. The most selective ANEH variant showed a selectivity factor of  $E = 10.8$  in the kinetic resolution of *rac*-**33** (96). Because only one round of epPCR was performed, an evolutionary process was not (yet) involved. Unfortunately, the expression system was observed to be genetically unstable (loss of plasmid DNA in a number of cases), and further optimization was temporarily halted at this stage (96).

The ANEH mutant displaying enhanced enantioselectivity ( $E = 10.8$ ) was sequenced and shown to be characterized by three mutations, A217V near the active site and K332E and A390E both at remote positions (96). The X-ray crystal structure of the WT ANEH had been analyzed earlier (146), revealing a dimer comprising identical subunits. Each monomeric unit contains the catalytic triad (two tyrosines and an aspartate), typical of most EHs. Asp192 attacks the epoxide nucleophilically with formation of a glycol-monoester intermediate that is hydrolyzed in a second step. Figure 20 shows the known 3D-structure of the monomer, displaying the active site, the two tyrosines that bind and activate the epoxide via H-bonding, and the three mutations of the most enantioselective ANEH-mutant (96).

It is clear that K332E and A390E occur at positions remote from the active center, whereas A217V appears to be rather close. The side chain of the amino acid

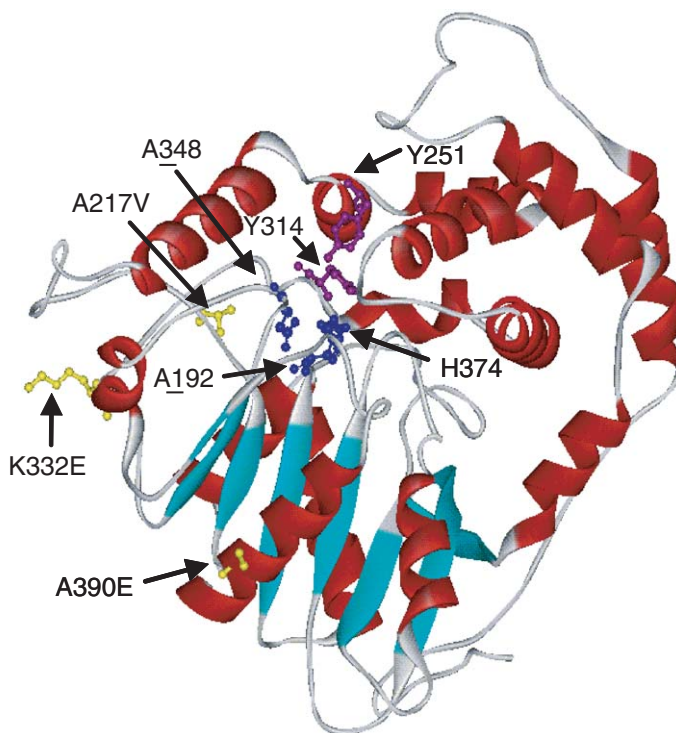


FIG. 20. Crystal structure of the monomer of the WT EH from *Aspergillus niger* (146) showing the catalytic triad (blue), the two tyrosines which activate the epoxide by H-bonding (purple) and the three amino acid substitutions (yellow) (96).

at position 217 is located about 9 Å from the nucleophilic active site D192. Molecular modeling using MOLOC molecular dynamics calculations of the WT ANEH with both enantiomers of **33** showed that the side chain of residue 217 is in van der Waals contact with the phenyl ring of the substrate. A preliminary model suggests that the larger valine side chain at residue 217 disfavors the (*R*) substrate due to a steric clash (96). The role of the remote substitutions K332E and A390E was reported to be more difficult to explain, requiring a more extensive theoretical analysis.

Parallel to these efforts, an efficient and reliable expression system for ANEH was developed (95). Subsequently, two libraries of mutants were generated by epPCR, comprising 3500 and 4 600 clones, respectively. Mutants were discovered displaying an expression level 3.4 times higher than the original WT and a 3.3-fold enhancement of catalytic activity as measured by the hydrolysis of 4-(*p*-nitrophenoxy)-1,2-epoxybutane (95). The distribution of ANEH activities from the clones of these two libraries is shown in Fig. 21.

In addition to the above two studies concerning ANEH (95,96), which set the stage for further improvements using the methods of directed evolution, another

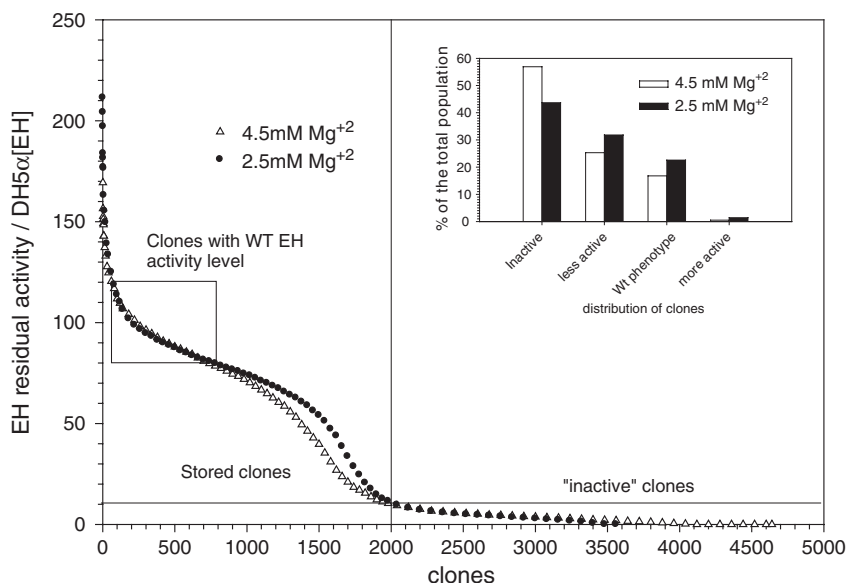


FIG. 21. Distribution of EH activities from 3500 and 4600 clones assayed from the 2.5 mM Mg<sup>2+</sup> (●) and 4.5 mM Mg<sup>2+</sup> (Δ) epPCR libraries, respectively. Clones were randomly picked after transformation in DH5α and grown overnight at 30°C in LB + 0.1 mg/mL ampicillin. A total of 44% of the clones from the 2.5 mM library and 57% of those from the 4.5 mM library were inactive, defined as less than 10% WT activity. The remainder of the clones, 2000 from each library, which exhibit a minimum of 10% of WT EH activity were stored for future analysis; 40% of the stored clones from each library showed WT EH activity, defined 100 ± 23% of WT activity. Two and one-half percent and 0.5% of the clones from the 2.5 and 4.5 mM libraries were more active than the wild type. Activity is expressed as percentage of WT activity (95).



investigation subsequently appeared which features the EH from *Agrobacterium radiobacter* as the enzyme and *p*-nitrophenyl glycidyl ether as the substrate (143). The WT shows an *E* value of only 3.4. Upon application of epPCR and DNA shuffling, several improved mutants were identified showing *E* factors ranging between 20 and 44. In almost all cases, the mutations occurred around the active site and in one of the  $\alpha$ -helices which follows the so-called nucleophile elbow (143). The latter mutation was believed to influence the position of the nucleophilic aspartate D107 (active site), although an MM/QM analysis was not performed. Whereas some of the mutations brought about by epPCR were shown to occur at remote sites, the process of subsequent DNA shuffling essentially eliminated these and resulted in focusing mutations around the active site and the said  $\alpha$ -helix. Thus, the remote mutations do not appear to influence enantioselectivity in this case, but the question whether they possibly help to maintain stability was not addressed.

Finally, it is interesting to note that in most cases enhanced enantioselectivity was shown to be due to a reduced value of  $k_{\text{cat}}/K_{\text{m}}$  for the non-preferred enantiomer (143). This result is contrasted with the results of directed evolution of the lipase from *Pseudomonas aeruginosa*, in which case the value of  $k_{\text{cat}}/K_{\text{m}}$  for the preferred enantiomer increased by two orders of magnitude (22,24). Thus, currently there seems to be no clear relationship between enhanced enantioselectivity and activity of evolved enzymes. However, in the case of the lipase, the screening system included both enantioselectivity and activity, which led to the creation of mutants showing higher enantioselectivity as well as enhanced activity (22,24).

### A.5. Hydantoinases

Hydantoinases belong to the E.C.3.5.2 group of cyclic amidases, enzymes that catalyze the hydrolysis of hydantoins (7–11,147). Because synthetic hydantoins are accessible by a variety of chemical syntheses, including Strecker reactions, enantioselective hydantoinase-catalyzed hydrolysis offers an attractive and general route to chiral amino acid derivatives. Moreover, because hydantoins are easily racemized chemically or enzymatically by appropriate racemases, dynamic kinetic resolution with potential 100% conversion and complete enantioselectivity is theoretically possible. Indeed, a number of such cases have been reported (147). However, if asymmetric induction is poor or if inversion of enantioselectivity is desired, directed evolution can come to the rescue. Such a case has been reported, specifically in the production of L-methionine as part of a whole cell system (*E. coli*) (Figure 22) (148).

Using epPCR followed by saturation mutagenesis at hot spots, the D-selective hydantoinase from *Arthrobacter* sp. DSM 9771 was converted into an L-selective variant showing a fivefold increase in activity. Whole *E. coli* cells expressing the evolved L-hydantoinase and a hydantoin racemase led to the production of 91 mM L-methionine from 100 mM of D,L-MTEH as starting substrate. The best L-selective mutant showed an *ee* value of 20% at about 30% conversion, compared to the wild type displaying *ee* = 40% in favor of the D-methionine derivative. With the help of an appropriate L-carbamoylase, L-methionine itself was produced. In the project,



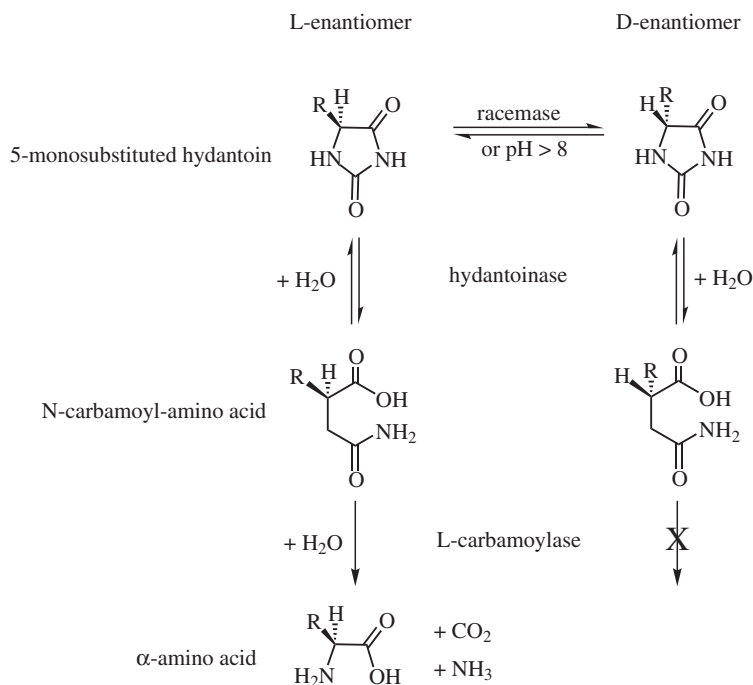


FIG. 22. Reactions and enzymes involved in the production of L-amino acids from racemic hydantoin by the three-enzyme hydantoinase process (148).

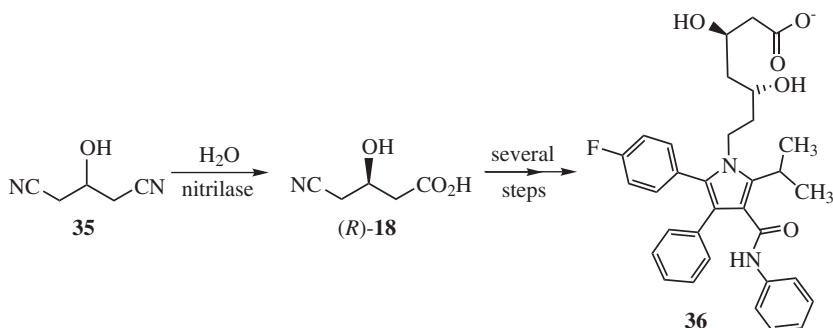
D-selective variants were also obtained (148). This academic/industrial collaboration led to the production of several highly selective hydantoinases of industrial interest (149).

#### A.6. Nitrilases

Nitrilases catalyze the synthetically important hydrolysis of nitriles with formation of the corresponding carboxylic acids (7–11). Enantioselectivity is relevant in the kinetic resolution of racemic nitriles or desymmetrization of prochiral dinitriles. Both versions have been applied successfully to a number of different substrates using one of the known currently available nitrilases. Recently, scientists at Diversa expanded the collection of nitrilases by metagenome panning (150). Nevertheless, in numerous cases the usual limitations of enzyme catalysis become visible, including poor or only moderate enantioselectivity and limited activity.

In the first reported case of the directed evolution of an enantioselective nitrilase, an additional limitation had to be overcome that is sometimes ignored when enzymes are used as catalysts in synthetic organic chemistry: product inhibition and/or decreased enantioselectivity at high substrate concentrations (46). A case in point concerns the desymmetrization of the prochiral dinitrile **35** with preferential formation of the (*R*)-configured acid **18**, which is known to be a chiral intermediate in the synthesis of the cholesterol-lowering therapeutic drug **36** (Lipitor,<sup>TM</sup>

Sortis,<sup>TM</sup> Torvast,<sup>TM</sup> etc), the first pharmaceutical product to exceed yearly sales exceeding the value of \$10 billion per year.



In the screening of genomic libraries prepared from environmental samples collected in various parts of the world, more than 200 new nitrilases were discovered that allow mild and selective hydrolysis of nitriles (150). One of them catalyzes the (*R*)-selective hydrolysis of **35** with an *ee* value of 94.5% at a substrate concentration of 100 mM (46). However, when experiments were done at a more practical concentration of 2.25 M, activity and enantioselectivity suffered (*ee* only 87.8%).

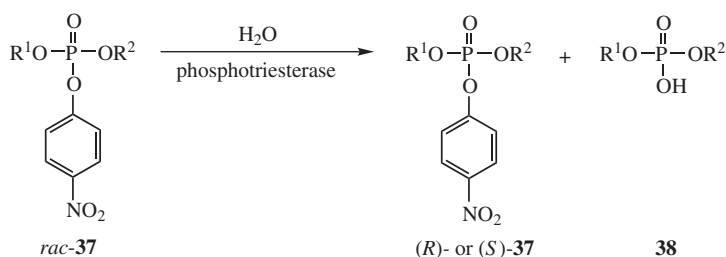
Therefore, directed evolution was applied to solve these problems. To screen for enantioselectivity, the Mülheim MS-based high-throughput *ee* assay (92,93) (Section III.C) was applied (46). In this case, the necessary isotope labeling focused on the use of <sup>15</sup>N in the *pseudo-meso* compound <sup>15</sup>N-(*R*)-**17** (see Section III.C for a detailed discussion). An (*S*)-selective nitrilase leads preferentially to <sup>15</sup>N-(*S*)-**18**, whereas an *R*-selective variant results in the *pseudo*-enantiomer (*R*)-**18**. They differ by one mass unit and can therefore be distinguished by MS, both qualitatively and quantitatively (by integration of the relevant peaks).

Saturation mutagenesis was then performed systematically at all positions of the 330- amino acid enzyme (46). The library contained 10 528 genetic variants and was screened with appropriate oversampling to ensure complete coverage. Of the 31 584 clones that were screened, 17 led to enhanced enantioselectivity over the WT enzyme. Each of these variants was then tested at 2.25 M substrate concentration. Many performed poorly at this high concentration, but several mutants having newly introduced serine, histidine, or threonine at position 190 (hot spot!) showed enhanced enantioselectivity. The A190 H mutant turned out to be the most enantioselective and active catalyst. Within 15 h, complete conversion of **35** was observed, affording (*R*)-**18** with 98% *ee*. This dramatic improvement is contrasted with the performance of the less active WT (88% *ee*). The system works even at 3 M substrate concentration with 90% conversion, 98.5% *ee*, and essentially no substrate inhibition. Volumetric productivity, which is of great importance in any industrial application, was thus enhanced by the process of directed evolution (46). Explanations on a molecular basis remain to be offered for these exciting observations (151).

### A.7. Phosphotriesterases

Chiral phosphates and/or phosphonic acid esters play an important role in biochemistry and organic chemistry; some derivatives are of value as agricultural insecticides, and others pose a threat as potential chemical warfare agents (152). The toxicological properties of such compounds are due to their capability for inactivation of the enzyme acetylcholinesterase and the concomitant loss of nerve function. In most cases, the biological effects arise exclusively or mainly from one enantiomeric form, with the mirror image compound showing no or reduced biological activity (152,153).

For these and other reasons, the development of asymmetric catalytic methods for the preparation of enantiopure phosphorus compounds is highly desirable. One approach is to perform hydrolytic kinetic resolution using phosphotriesterases as catalysts (152–154). A typical example is the production of chiral organophosphates (*R*)-37 or (*S*)-37.



It was shown that the phosphotriesterase from *P. diminuta* catalyzes the enantioselective hydrolysis of several racemic phosphates 37, the *S<sub>P</sub>* isomer reacting faster than the *R<sub>P</sub>* compound (153,154). Kinetics experiments showed that the value of  $k_{\text{cat}}/K_{\text{m}}$  is greater for the *S<sub>P</sub>* isomer than for the other by a factor of as much as 90, depending on the relative sizes of *R*<sup>1</sup> and *R*<sup>2</sup>. A simple model was proposed according to which the *p*-nitrophenol residue is placed in the leaving group binding pocket, whereas the alkoxy-residues *R*<sup>1</sup>O and *R*<sup>2</sup>O are assigned to a small and large binding pocket, respectively. On the basis of rational design and subsequent site-specific mutagenesis, it was possible to enhance (*S*) selectivity and to invert the sense of enantioselectivity in favor of the (*R*) substrate (153,154).

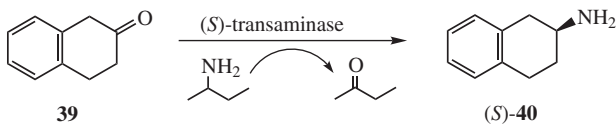
Clearly, this system is easily amenable to rational design, possibly because the reaction center and the stereogenic center are identical (P center). In most other biocatalytic systems, the stereogenic center is next to the reacting center or even farther away. Nevertheless, in the present system involving *rac*-37, an approach comprising rational design and randomization was also put into practice successfully (154). This was accomplished by first carrying out a restricted alanine-scan (155) (i.e., at pre-determined amino acid positions alanine was introduced). Whenever an effect on activity/enantioselectivity was observed, the position was defined as a hot spot. Subsequently, randomization at several hot spots was performed, which led to the identification of several highly (*S*)- or (*R*)-selective mutants (154). These impressive results were rationalized by the previously proposed model. A

similar procedure was applied to the generation of mutant phosphotriesterases as catalysts in the kinetic resolution of racemic phosphonates (156).

## B. AMINOTRANSFERASES

Aminotransferases are widely distributed enzymes in nature, participating in a number of metabolic pathways (7–11). They catalyze the transfer of an amino group originating from an amino acid donor to a 2-ketoacid acceptor. In effect, this statement implies the reductive animation of a keto moiety, although a redox process is not directly involved.

The mechanism is described by two steps. First, an amino group from the donor is transferred to the co-factor pyridoxal phosphate, with formation of a 2-keto acid and an enzyme-bound pyridoxamine phosphate intermediate. Second, this intermediate transfers the amino group to the 2-keto acid acceptor. The reaction is reversible, shows ping-pong kinetics, and has been used industrially in the production of amino acids (157). It can be driven in one direction by the appropriate choice of conditions (e.g., substrate concentration). Some of the aminotransferases accept simple amines instead of amino acids as amine donors, and highly enantioselective cases have been reported (158). However, this is obviously not always the case, with a counterexample being the transformation of  $\beta$ -tetralone (39) to (*S*)- $\beta$ -aminotetralin (40), with 2-aminobutane serving as the amine donor. The WT of an (*S*)-selective aminotransaminase led to an *ee* value of only 65%. In an early and important study, a single round of epPCR was performed, and about 10 000 clones were screened (no details) (158). This led to several active mutants with improved enantioselectivity in the range 84–94% *ee*. Some had only one amino acid exchange; others had two (e.g., M245V/R405G leading to *ee* = 94%). This combinatorial approach does not constitute an evolutionary process, but in view of the early work on the directed evolution of lipases (16) (Section IV.A), one can imagine that a second round of epPCR, DNA shuffling or CASTing could result in higher enantioselectivities. In a second study using a single round of epPCR, (*S*)-1-methoxypropan-2-amine was prepared with >99% *ee* and 97% conversion, a nice case in which evolutionary optimization is not necessary (159).

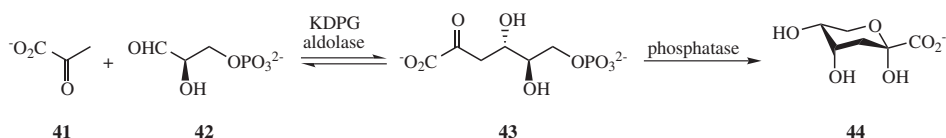


## C. ALDOLASES

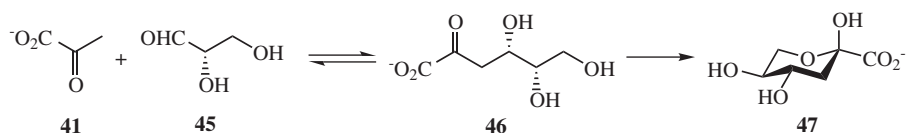
Carbon–carbon bond-forming reactions are of central importance in synthetic organic chemistry. Although a host of asymmetric transition metal-catalyzed (5) and organocatalyzed (6) reactions of this type are known, enzyme catalysts are often complementary and sometimes even superior. Aldolases allow the synthesis of many complex carbohydrates in one or two steps, with enantio- and diastereoselectivity

often being >95% (7–11,160). Of course, as in other enzyme-catalyzed processes, broad substrate acceptance and stereoselectivity are not general, so that directed evolution offers intriguing prospects.

The first such case was concerned with the limited substrate acceptance of D-2-keto-3-deoxy-6-phospho-gluconate (KDPG) aldolase (161). This catalyzes the (reversible) reaction of pyruvate (**41**) to certain chiral aldehydes such as **42**, with formation of aldol products such as **43**. It was known that this aldolase is highly specific for chiral-*phosphorylated* aldehydes with the D configuration at the C2 position leading stereoselectively to a precursor of the corresponding D sugar such as **44** (162):



Because the phosphorylated form of the starting aldehyde is expensive, and dephosphorylation by a phosphatase constitutes an additional step, it was of interest to obtain a mutant aldolase that accepts not only non-phosphorylated substrates, but also turns over the enantiomeric aldehyde **45** stereoselectively with formation of **46**, a precursor of carbohydrate **47** (161):



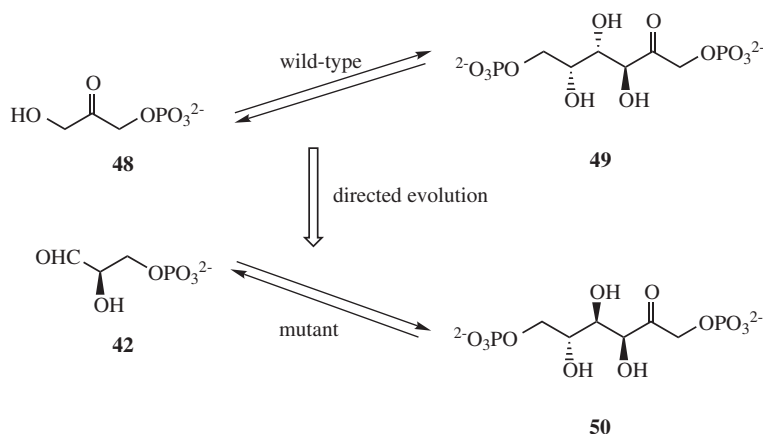
By applying the appropriate methods of directed evolution, it was indeed possible to turn the KDPG aldolase into an efficient mutant that induces reaction and turns over **45**, while maintaining perfect control over the creation of the new stereo center. Several rounds of epPCR and DNA shuffling led to a few highly active and stereoselective mutants. One of the best mutants turned out to have four mutations (T84A, I92F, V118A, and E138V), most of which occur at positions remote from the active site (161). A detailed explanation has not been proposed, but this investigation once more shows that directed evolution may lead to effects not predicted by current rational design. (Of course, this statement does not imply that research focusing solely on rational design based on traditional site-directed mutagenesis should be abandoned.)

In an interesting extension of this work, the Neu5Ac aldolase from *E. coli* was subjected to directed evolution to expand its catalytic activity for enantiomeric forms of the usual substrates to include *N*-acetyl-L-mannosamine and L-arabinose with formation of the synthetically important products L-sialic acid and L-3-deoxy-L-manno-oct-2-ulonic acid (L-KDO) (163). The evolved Neu5Ac aldolases were characterized by sequence analysis, kinetics, stereoselectivity, and in one case even by an X-ray structure analysis. Again, remote mutations were identified. It is significant

that the X-ray structure of one of the triple mutants at 2.3 Å resolution showed no significant difference in folding relative to that of the wild type.

In yet another intriguing directed evolution study, the stereochemical course of aldol additions was significantly altered in a different sense (164). Rather than evolving aldolase mutants that selectively accept stereoisomers of substrates, the configuration of the chiral aldehyde as substrate was kept constant and mutants were evolved which show opposite diastereoselectivity:

Such protein engineering was accomplished for the first time in a directed evolution study involving the so-called tagatose-1,6-bisphosphate aldolase (164). The WT catalyzes the aldol addition of **48** to **42** with selective formation of adduct **49**. Upon application of three rounds of DNA shuffling and screening of a total of only approximately 8000 mutants, an aldolase was obtained showing an 80-fold improvement in the value of  $k_{\text{cat}}/K_{\text{m}}$  in the reaction **42** + **48**  $\rightleftharpoons$  **50**; in other words, “tagatose aldolase” was turned into a “fructose aldolase.” A 100-fold change in stereoselectivity was observed. Subsequent saturation mutagenesis at some of the mutational positions failed to lead to further improvements. Investigations of this kind are of great importance to synthetic organic chemists interested in the synthesis of complex stereoisomeric products such as carbohydrates, and the example once again illustrates the power of directed evolution of enantioselective enzymes as catalysts in synthetic organic chemistry.



#### D. OXIDASES

Partial oxidation of organic substrates that is carried out catalytically in a chemo-, regio-, and stereoselective manner is an area of intense worldwide activity (4,5,9,165–167). Synthetic transition metal catalysts and enzymes have contributed successfully, but major challenges remain. Many of problematic transformations are not easily (or not all) accomplished by synthetic transition metal catalysts. Such cases form ideal targets for directed evolution.

### D.1. Cyclohexanone Monooxygenases as Baeyer-Villigerases

The Baeyer-Villiger (BV) reaction of ketones with hydroperoxides affording the corresponding esters or lactones constitutes a synthetically important transformation (168–170). The reaction is accelerated by acids, bases, or metal complexes, with enantioselective catalysis also being possible in some cases (169–171). Alternatively, flavin-dependent enzymes of the type CHMO can be used as biocatalysts in asymmetric BV reactions (172–175). In this enzymatic process, oxygen (in air) reacts with the enzyme-bound flavin (FAD) to form an intermediate hydroperoxide, which in the deprotonated form initiates the BV reaction by transferring one oxygen atom originating from  $O_2$  to the substrate (ketone), with the other being ultimately reduced to water (176–178). In this process, the flavin co-factor needs to be recycled by reduction, with the second co-factor NAD(P)H taking over this function. Consequently, when the isolated CHMO is used, NAD(P)H has to be recycled (Figure 23). Although NAD(P)H recycling systems are well known, it is currently more convenient to use whole CHMO cells.

This process has been employed successfully for a number of enantioselective BV reactions, including kinetic resolution of racemic ketones and desymmetrization of prochiral substrates (172–175). An example is the desymmetrization of 4-methylcyclohexanone, which affords the (*S*)-configured 7-membered lactone with 98% *ee* (172,175). Of course, many ketones fail to react with acceptable levels of enantioselectivity or are not even accepted by the enzyme.

It has been demonstrated recently that directed evolution is ideally suited to control the enantioselectivity of partial oxidations of this kind. The results are all the more significant because no X-ray data or homology models were available at the time to serve as a possible guide (103). In a model study using whole *E. coli* cells containing the CHMO from *Acinobacter* sp. NCIMB 9871, 4-hydroxy-cyclohexanone (**51**) was used as the substrate. The WT leads to the preferential formation of the primary product (*R*)-**52** which spontaneously rearranges to the thermodynamically more stable lactone (*R*)-**53**. The *ee* of this desymmetrization is

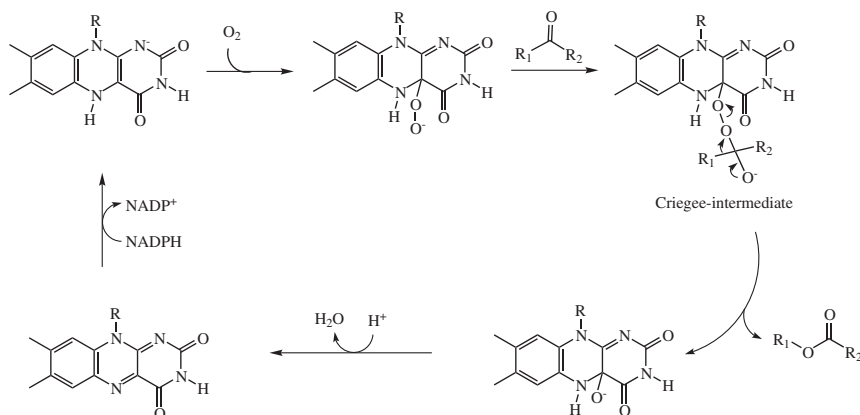
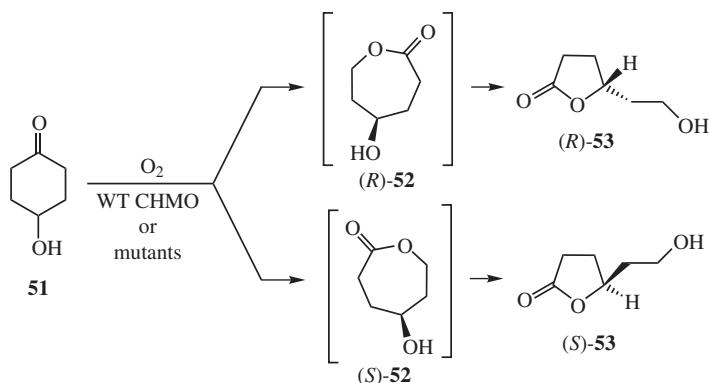


FIG. 23. Mechanism of CHMO-catalyzed Baeyer-Villiger reaction (173,177,178,182).



only 9%, and the sense of enantioselectivity (*R*) is opposite to the usually observed (*S*) selectivity displayed by simple 4-alkyl-substituted cyclohexanone derivatives (172–175).



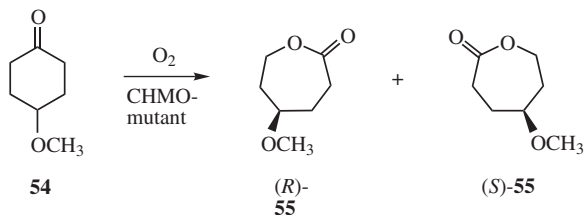
In the directed evolution study, epPCR at various mutation rates was applied, and the total number of clones screened was about 10 000. Of the positive hits identified, some were (*R*)-, others (*S*)-selective. Eight of them were sequenced (Table I) (103). Of particular interest is mutant 1-K2-F5, characterized by a single mutation F432S, because it leads to reversal of enantioselectivity (79% *ee* in favor of (*S*)-53).

Evolutionary optimization of (*R*) selectivity was then performed by using the genes of some of the (*R*)-selective mutants as starting points for a second round of epPCR (103). In each case only about 1600 mutants were screened. Although a systematic search was not a goal of this initial investigation, the strategy turned out to be successful. In the case of mutant 1-F1-F5 (*ee* = 40%), characterized by a single mutation L143F, a second round of epPCR led to a markedly improved mutant (2-D19-E6). It catalyzes the BV reaction of **51** with an *ee* value of 90% in favor of (*R*)-53. Sequencing revealed that four new amino acid exchange events had occurred (E292G, T433I, L435Q, and T464A) in addition to the already existing L143F mutation.

TABLE I  
CHMO Mutants Identified in the First Round of epPCR Showing Improved Enantioselectivity in the Air-Oxidation of **51** (Reaction Time: 24 h; Temperature, 23–25°C; Conversion >95%) (103)

Mutant	Amino acid exchanges	Favored enantiomer of <b>53</b>	<i>ee</i> (%)
Wild type	—	( <i>R</i> )	9
1-C2-B7	F432Y, K500R	( <i>R</i> )	34
1-F1-F5	L143F	( <i>R</i> )	40
1-E12-B5	F432I	( <i>R</i> )	49
1-H7-F4	L426P, A541V	( <i>R</i> )	54
1-H3-C9	L220Q, P428S, T433A	( <i>S</i> )	18
1-F4-B9	D41N, F505Y	( <i>S</i> )	46
1-K6-G2	K78E, F432S	( <i>S</i> )	78
1-K2-F5	F432S	( <i>S</i> )	79

Because the WT CHMO was known to react (*S*)-selectively with simple 4-substituted cyclohexanone derivatives (172–176), it was logical to test mutant 1-K2-F5 as a catalyst in the BV reaction of other ketones, because this should lead to enhanced degrees of (*S*) enantioselectivity. Indeed, when 4-methoxycyclohexanone (**54**) was subjected to the BV reaction catalyzed by mutant 1-K2-F5, almost complete enantioselectivity was observed in favor of the (*S*) lactone **55** (*ee* = 98.5%), in contrast to the WT, which is considerably less selective (*ee* = 78%) (103).



Moreover, other 4-substituted cyclohexanone derivatives such as the methyl-, ethyl-, chloro-, bromo-, and iodo-compounds react with enantioselectivities of 95–99% *ee* (103). This catalytic behavior is similar to that of the WT, a comparison that shows that the mutational change F432S does not simply shift, but rather expands the substrate range in which > 95% *ee* is achieved. In tests of a wide range of other substrates including cyclopentanone-derivatives, bicyclic ketones, functionalized cyclohexanone-derivatives, and cyclobutanone-derivatives, it was discovered that mutant 1-K2-F5 is astonishingly effective (179). Enantioselectivities of 90–99% were generally observed; no synthetic catalyst known to date can compete (169–171). All of these results were obtained without any structural knowledge of the catalysts.

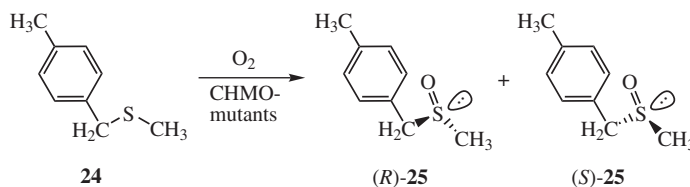
Several months after the publication of this work (103), a paper appeared describing the X-ray structure of another Baeyer-Villigerase, namely, phenyl acetone monooxygenase (PAMO) (180). It was originally found in the thermophilic bacterium *Thermobifida fusca* and is the first thermostable Baeyer-Villigerase (181), although it is characterized by very narrow substrate acceptance. The X-ray data representing PAMO, the first Baeyer-Villigerase to be characterized crystallographically, allowed the construction of a homology model for CHMO and the possibility of interpreting the previous mutational results (103) on a molecular level (182). Although such a theoretical analysis has not been completed, a cursory inspection suggests that the newly introduced serine at position 432 of mutant 1-K2-F5 forms a hydrogen bond with arginine at position 337. The originally identified mutation F432S can be understood because Arg337 stabilizes the involved Criegee intermediate (182).

Because PAMO is characterized by unusual thermal stability (180,181), it seemed attractive to exploit this information to engineer thermostable Baeyer-Villigerases showing broad substrate acceptance (182). As a first step toward this practical goal, PAMO was turned into a phenylcyclohexanone monooxygenase (PCHMO) by rational design (182). The best mutant accepts 2-phenylcyclohexanone, *inter alia*, and leads to an *E* value of 100 in kinetic resolution, while retaining high thermal

stability. The WT CHMO also shows high enantioselectivity in this reaction, but it is not very stable thermally. Thus, this investigation constitutes an important step toward developing robust (and thus industrially viable) Baeyer-Villigerases (182).

## D.2. Cyclohexanone Monooxygenases in Stereoselective Sulfoxidation

Because CHMOs can also be used as catalysts in the enantioselective air oxidation of some prochiral thioethers (173–175,183–185), directed evolution of the CHMO from *Acinetobacter* sp. NCIMB 9871 was applied in the case of difficult substrates such as **24** (105). The WT CHMO leads to an *ee* of only 14%.



Because the first round of epPCR does not constitute an evolutionary process, the original library of 10 000 clones used in the BV reaction (103) (Section IV.D.1) was screened for performance as potential catalysts in the sulfoxidation (105). In this case, screening posed a particularly difficult problem, which was finally solved by modifying an HPLC system allowing about 800 *ee* determinations per day (Section II.F). The screening led to the discovery of at least 20 mutants having *ee* values in the range 85–99%, some being (*R*)- and others being (*S*)-selective. Five mutants resulting in *ee* values of >95% were sequenced (Table II) (105).

Two mutants (1-D10-F6 and 1-K15-C1) are (*R*)-selective, whereas the other three variants (1-C5-H3, 1-H8-A1, and 1-J8-C5) induce the opposite enantioselectivity in favor of (*S*)-**25**. Sequencing studies show that between one and four amino acid exchanges occurred. In general, the mutants are different from those that were previously identified as hits in the BV reaction of prochiral cyclohexanone

TABLE II

*Selected Mutant CHMOs from Acinetobacter sp. NCIMB 9871 for the Enantioselective Air-Oxidation of Thio-Ether 24 (24 h; 23–25°C) Using Whole Cells (105)*

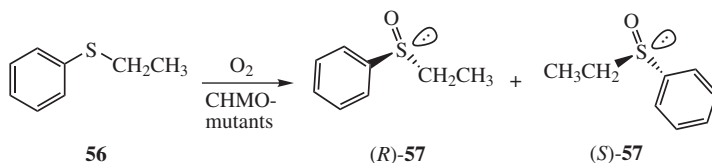
Mutant	Amino acid exchanges	Yield of <b>25</b> (%)	Configuration	<i>ee</i> (%)	Sulfone as side product (%)
Wild type	—	75	( <i>R</i> )	14.0 <sup>a</sup>	<1
1-D10-F6	D384H	75	( <i>R</i> )	98.9	7.9
1-K15-C1	F432S	55	( <i>R</i> )	98.7	20.0
1-C5-H3	K229I, L248P	77	( <i>S</i> )	98.1	5.6
1-H8-A1	Y132C, F246I, V361A, T415A	52	( <i>S</i> )	99.7	26.6
1-J8-C5	F16L, F277S	84	( <i>S</i> )	95.2	5.6

<sup>a</sup> Only 5% *ee* results when using the enzyme extract.

derivatives, a result that is not surprising. In contrast, mutant 1-K15-C1, which leads to 98.7% *ee* in favor of (*R*)-**25**, is characterized by amino acid exchange F432S. It is therefore identical to mutant 1-K2-F5 previously identified as a highly enantioselective biocatalyst in the asymmetric BV reaction of a wide range of 4-substituted cyclohexanone derivatives (Section IV.D.1). Thus, one and the same single mutational change at position 432, namely, the exchange of phenylalanine by serine, leads to a surprisingly versatile biocatalyst (105). It was identified twice by screening the same 10 000-membered library in two completely different reaction types! It is remarkable that these results were obtained following a single round of epPCR, which is not an evolutionary process.

In the sulfoxidation, small to appreciable amounts of over oxidation with formation of undesired sulfone were observed, a result that implies that kinetic resolution may be involved in influencing the overall stereochemical result (105). This was shown to be the case. Indeed, some of the mutants are also excellent catalysts in the kinetic resolution of racemic sulfoxides such as **25** (105). Directed evolution was then applied successfully to eliminate undesired sulfone formation, specifically, by going through a second cycle of epPCR (105). This is significant because it shows for the first time that an undesired side reaction can be eliminated by directed evolution.

Although a systematic study of the mutants as catalysts in the sulfoxidation of a wide variety of thioethers has not been completed, initial results are promising (105). For example, when thioether **56** was used as the substrate, previously identified mutant 1-C5-H3 induced complete reversal of enantioselectivity. The WT CHMO resulted in 47% *ee* in favor of (*R*)-**57**, whereas 1-C5-H3 led to 98.9% *ee* in favor of (*S*)-**57** (105). An interpretation of the results on a molecular basis remains to be offered. Since a homology model of the CHMO has been generated (183), this may in fact be possible.

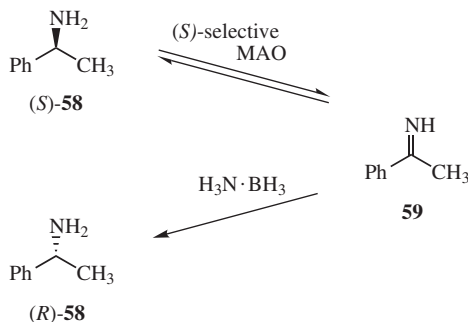


### D.3. Monoamine Oxidases

Monoamine oxidases are enzymes that catalyze the racemization of  $\alpha$ -amino acids (186). Both L- and D-selective monoamine oxidases are known (i.e., they catalyze the racemization of either (*S*)- or (*R*)-enantiomers of amino acids). This property has been exploited to obtain enantiomerically pure (*R*) and (*S*) amino acids by using an appropriate achiral reducing agent such as  $\text{NaBH}_4$ ,  $\text{NaB(CN)H}_3$ , or  $\text{H}_3\text{N}\cdot\text{BH}_3$  in combination with an L- or D-selective monoamine oxidase (187).

It was of interest to extend this synthetically interesting procedure to the production of chiral amines such as  $\alpha$ -methylbenzylamine (**58**) (188). Unfortunately, the enzymes display somewhat low activity toward substrates of this kind.

For example, the monoamine oxidase from *Aspergillus niger* (MAO-N) racemizes **58**, with  $k_{\text{cat}}$  being only  $0.17 \text{ min}^{-1}$ , although enantioselectivity is not bad [(*S*)-versus (*R*)-selectivity amounts to 17:1] (188).



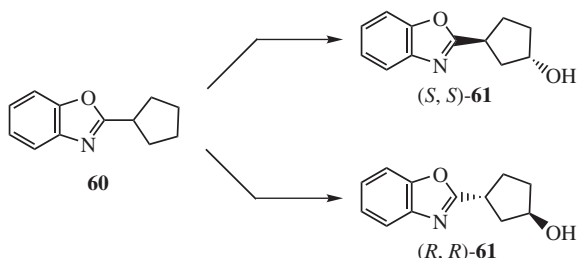
After multiple cycles of mutagenesis using the *E. coli* XL1-Red mutator strain followed by transformation of the plasmid library into *E. coli*, a total of about 150 000 bacterial colonies were assayed for activity using a colorimetric pre-screen (188). Following the identification of 35 clones with improved activity for (*S*)-**58**, they were grown on a small scale and assayed against both (*S*)- and (*R*)-**58** as cell-free extracts. The best mutant showed a 47-fold increase in activity and a 5.8-fold enhancement of (*S*)-enantioselectivity. Sequencing of the best mutant revealed a single amino acid substitution N336S (188). Later it was shown that this mutant displays a fairly broad substrate acceptance. The result illustrates the synthetic power of this approach (189). It may be an alternative to the industrially practiced lipase-catalyzed kinetic resolution of chiral amines (BASF process) (119,190), a reaction type that can also be performed using dynamic kinetic resolution (191–193).

#### D.4. Cytochrome P450 Enzymes

Enzymes of the type cytochrome P450 occur widely in nature, catalyzing the O<sub>2</sub>-driven oxidation of an immense variety of organic substrates (7,194,195). The mechanism of these Fe-heme-containing enzymes has been investigated extensively (195), and many have been used as whole-cell catalysts in organic chemistry, as in the CH-activating hydroxylation of steroids (196). Directed evolution has been applied to the bacterial cytochrome P450 BM-3 from *Bacillus megaterium* with the aim of turning the WT into a practical mutant showing high activity and stability toward simple linear alkanes (197,198).

In follow-up work, a rational approach was chosen to improve the regioselectivity of the hydroxylation of *n*-octane (199). Previous work had shown that a mixture of 2-, 3-, and 4-octanols are obtained. The design and construction of a mutant selective for 2-octanol was successful, leading to approximately 80% regioselectivity in favor of 2-octanol (199). The enantiopurity turned out to be only 40% *ee* (*S*), but enantioselectivity was not the goal of the investigation. In a series of epPCR and DNA shuffling experiments, mutants showing the same degree of

enantioselectivity were identified (199). However, the screening system was not designed to measure enantioselectivity. In a later study, some of the mutants were screened as catalysts for the hydroxylation of substrate **60** (200). This work led to the identification of (*S,S*)- and (*R,R*)-mutants leading to (*S,S*)-**61** and (*R,R*)-**61**, respectively, with enantioselectivity being in the range of 84–88% *ee* with diastereoselectivity of 94–96% (200). It would be interesting to perform directed evolution investigations of substrates of this kind.



## V. Conclusions and Perspective

Directed evolution of enantioselective enzymes has emerged as a fundamentally new approach to asymmetric catalysis in synthetic organic chemistry. It involves the proper combination of gene mutagenesis, expression, and high-throughput analysis of enantiomeric purity. A range of mutagenesis methods is available, and strategies have been developed for applying them efficiently when exploring protein sequences. Most directed evolution projects begin with epPCR or DNA shuffling, but the generation of focused libraries may also be a useful starting point. Along these lines, CASTing offers interesting prospects with respect to the enlargement of substrate acceptance and the enhancement of enantioselectivity. Prior to the study of enantioselectivity, parameters such as activity, thermostability, and stability in hostile solvents had already been enhanced by the methods of directed evolution. It is now possible to combine these parameters by applying the appropriate screens. This can be accomplished in one step (e.g., activity and enantioselectivity together), or in consecutive steps (first activity and then enantioselectivity, or *vice versa*). A well-known motto is you get what you screen for. Moreover, the first cases have been reported in which directed evolution has been used to reduce product inhibition, or to eliminate the formation of undesired side-products. Several industrial examples of directed evolution of enantioselective and robust enzymes have been described.

Future work is expected to concentrate on generalizations to include enzymes not yet investigated and on the development of even more efficient strategies for scanning protein sequence space, including computational approaches such as genetic algorithms or neural networks. Directed evolution is also beginning to have an impact on introducing promiscuity into enzymes (i.e., to engineer proteins so that they will catalyze reaction types different from the natural function) (201). Another challenge is the development of selection rather than screening when evolving enantioselective enzymes. Furthermore, the idea of directed evolution of enantioselective hybrid

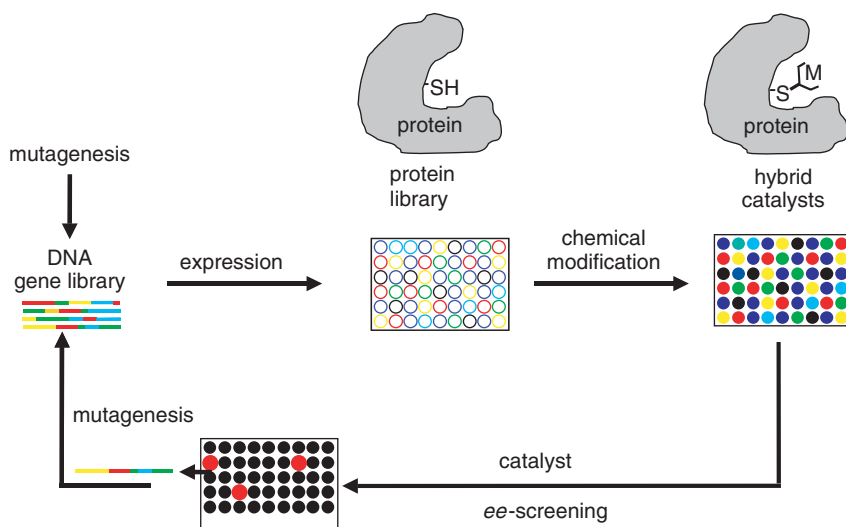


FIG. 24. General scheme of the directed evolution of hybrid catalysts (22,132,202,203).

catalysts comprising a synthetic transition metal center in a protein host may also offer intriguing prospects because this would allow the tuning of synthetic catalysts by the methods of molecular biology in a Darwinian sense (Fig. 24) (22,132,202,203).

## References

1. Collins, A.N., Sheldrake, G.N., and Crosby, J. (Eds.), "Chirality in Industry II: Developments in the Commercial Manufacture and Applications of Optically Active Compounds." Wiley, Chichester, 1997.
2. Rouhi, A.M., *Chem. Eng. News* **81**, 45 (2003).
3. Noyori, R., *Angew. Chem. Int. Ed.* **41**, 2008 (2002).
4. Sharpless, K.B., *Angew. Chem.* **114**, 2126–2135 (2002); *Angew. Chem. Int. Ed.* **41**, 2024–2032 (2002).
5. Jacobsen, E.N., Pfaltz, A., and Yamamoto, H. (Eds.), "Comprehensive Asymmetric Catalysis." Vol. I–III, Springer, Berlin, 1999.
6. Reviews of organocatalysis:
  - (a) List, B., *Tetrahedron* **58**, 5573–5590 (2002);
  - (b) Berkessel, A., and Gröger, H. (Eds.), "Asymmetric Organocatalysis." VCH, Weinheim, 2004;
  - (c) Dalko, P.I., and Moisan, L., *Angew. Chem.* **113**, 3840–3864 (2001); *Angew. Chem. Int. Ed.* **40**, 3726–3748 (2001).
7. (a) Drauz, K., and Waldmann, H. (Eds.), "Enzyme Catalysis in Organic Synthesis: A Comprehensive Handbook." Vol. I–III, VCH, Weinheim, 2nd Edition, 2002;
  - (b) Faber, K. (Ed.), "Biotransformations in Organic Chemistry.", 2nd Edition, Springer, Berlin, 2000.
8. (a) Schmid, A., Dordick, J.S., Hauer, B., Kiener, A., Wubbolts, M., and Witholt, B., *Nature* **409**, 258–268 (2001);
  - (b) Rasor, J.P., and Voss, E., *Appl. Catal. A* **221**, 145–158 (2001);
  - (c) Straathof, A.J.J., Panke, S., and Schmid, A., *Curr. Opin. Biotechnol.* **13**, 548–556 (2002);



- (d) Liese, A., and Filho, M.V., *Curr. Opin. Biotechnol.* **10**, 595–603 (1999);
- (e) Panke, S., Held, M., and Wubbolts, M., *Curr. Opin. Biotechnol.* **15**, 272–279 (2004);
- (f) Montézin, M., Sonet, J.-M., and Lefèvre, F., *PharmaChem* **3**, 7–10 (2004);
- (g) For a comparison of certain transition metal catalyzed reactions with those catalyzed by enzymes or catalytic antibodies, see: Jacobsen, E.N., and Finney, N.S., *Chem. Biol.* **1**, 85–90 (1994).
- 9. Liese, A., Seelbach, K., and Wandrey, C. (Eds.), “Industrial Biotransformations.” Wiley-VCH, Weinheim, 2000.
- 10. Davies, H.G., Green, R.H.Kelly, D.R., and Roberts, S.M. (Eds.), “Biotransformations in Preparative Organic Chemistry.” Academic Press, London, 1989.
- 11. Koeller, K.M., and Wong, C.-H., *Nature* **409**, 232–240 (2001).
- 12. Schultz, P.G., Yin, J., and Lerner, R.A., *Angew. Chem.* **114**, 4607–4618 (2002); *Angew. Chem. Int. Ed.* **41**, 4427–4437 (2002).
- 13. Klibanov, A.M., *Nature* **409**, 241 (2001).
- 14. Imanaka, T., and Atomi, H., in “Enzyme Catalysis in Organic Synthesis: A Comprehensive Handbook” (K. Drauz and H. Waldmann, Eds.), Vol. I, p. 67, VCH, Weinheim, 2nd Edition, 2002.
- 15. (a) Cedrone, F., Ménez, A., and Québécois, E., *Curr. Opin. Struct. Biol.* **10**, 405 (2000);  
(b) Harris, J.L., and Craik, C.S., *Curr. Opin. Chem. Biol.* **2**, 127 (1998);  
(c) Kazlauskas, R.J., *Curr. Opin. Biotechnol.* **4**, 81 (2000);  
(d) Li, Q.-S., Schwaneberg, U., Fischer, M., Schmitt, J., Pleiss, J., Lutz-Wahl, S., and Schmid, R.D., *Biochim. Biophys. Acta* **1545**, 114 (2001).
- 16. (a) Reetz, M.T., Zonta, A., Schimossek, K., Liebeton, K., and Jaeger, K.-E., *Angew. Chem. Int. Ed.* **36**, 2830 (1997);  
(b) Reetz, M.T., Zonta, A., Schimossek, K., Liebeton, K., Jaeger, K.-E., DE-A 197 31 990.4 (1997).
- 17. Arnold, F.H., and Georgiou, G. (Eds.), “Directed Enzyme Evolution: Screening and Selection Methods.” Vol. 230, Humana Press, Totowa N J, 2003.
- 18. Powell, K.A., Ramer, S.W., del Cardayré, S.B., Stemmer, W.P.C., Tobin, M.B., Longchamp, P.F., and Huisman, G.W., *Angew. Chem. Int. Ed.* **40**, 3948 (2001).
- 19. (a) Brakmann, S., and Johnsson, K. (Eds.), “Directed Molecular Evolution of Proteins (or How to Improve Enzymes for Biocatalysis).” Wiley-VCH, Weinheim, 2002;  
(b) Brakmann, S., and Schwienhorst, A. (Eds.), “Evolutionary Methods in Biotechnology (Clever Tricks for Directed Evolution).” Wiley-VCH, Weinheim, 2004.
- 20. (a) Taylor, S.V., Kast, P., and Hilvert, D., *Angew. Chem. Int. Ed.* **40**, 3310 (2001);  
(b) Stevenson, J.D., and Benkovic, S.J., *Perkin Trans. J. Chem. Soc.* **2**, 1483 (2002);  
(c) Brakmann, S., *ChemBioChem* **2**, 865 (2001);  
(d) Neylon, C., *Nucleic Acids Res.* **32**, 1448 (2004);  
(e) Sutherland, J.D., *Curr. Opin. Chem. Biol.* **4**, 263 (2000);  
(f) Schellenberger, V., *ASM News* **64**, 634 (1998);  
(g) Turner, N.J., *Trends Biotechnol.* **21**, 474 (2003).
- 21. Reetz, M.T., and Jaeger, K.-E., *Chem.-Eur. J.* **6**, 407 (2000).
- 22. Reetz, M.T., *Tetrahedron* **58**, 6595 (2002).
- 23. Reetz, M.T., in “Methods in Enzymology” (D.E. Robertson and J.P. Noel, Eds.), Vol. 388, p. 238, Elsevier Academic Press, San Diego, 2004.
- 24. Reetz, M.T., *Proc. Natl. Acad. Sci. USA* **101**, 5716 (2004).
- 25. Mills, D.R., Peterson, R.L., and Spiegelman, S., *Proc. Natl. Acad. Sci. USA* **58**, 217 (1967).
- 26. Francis, J.C., and Hansche, P.E., *Genetics* **70**, 59 (1972).
- 27. For an interesting historical account including recent developments, see: Koltermann, A., and Kettling, U., *Biophys. Chem.* **66**, 159 (1997).
- 28. Eigen, M., and Gardiner, W., *Pure Appl. Chem.* **56**, 967 (1984).
- 29. See for example:  
(a) Cunningham, B.C., and Wells, J.A., *Protein Eng.* **1**, 319 (1987);  
(b) Lehtovaara, P.M., Koivula, A.K., Bamford, J., and Knowles, J.K.C., *Protein Eng.* **2**, 63 (1988);  
(c) Liao, H., McKenzie, T., and Hageman, R., *Proc. Natl. Acad. Sci. USA* **83**, 576 (1986).

30. Chen, K., and Arnold, F.H., *Proc. Natl. Acad. Sci. USA* **90**, 5618 (1993).
31. (a) You, L., and Arnold, F.H., *Protein Eng.* **9**, 77 (1996);  
(b) Arnold, F.H., *Chem. Eng. Sci.* **51**, 5091 (1996).
32. Arnold, F.H., *Acc. Chem. Res.* **31**, 125 (1998).
33. Stemmer, W.P.C., *Nature* **370**, 389 (1994).
34. Stemmer, W.P.C., *Proc. Natl. Acad. Sci. USA* **91**, 10747 (1994).
35. Cramer, A., Raillard, S.-A., Bermudez, E., and Stemmer, W.P.C., *Nature* **391**, 288 (1998).
36. Reetz, M.T., and Jaeger, K.-E., *Top. Curr. Chem.* **200**, 31 (1999).
37. Lutz, S., and Patrick, W.M., *Curr. Opin. Biotechnol.* **15**, 291 (2004).
38. For an illuminating comparison of directed evolution approaches using the  $\beta$ -glucuronidase model system, see: Rowe, L.A., Geddie, M.L., Alexander, O.B., and Matsumura, I., *J. Mol. Biol.* **332**, 851 (2003).
39. Leung, D.W., Chen, E., and Goeddel, D.V., *Technique* **1**, 11 (1989).
40. Cadwell, R.C., and Joyce, G.F., *PCR Methods Appl.* **2**, 28 (1992).
41. Mullis, K.B., *Angew. Chem. Int. Ed. Engl.* **33**, 1209 (1994).
42. (a) Hughes, M.D., Nagel, D.A., Santos, A.F., Sutherland, A.J., and Hine, A.V., *J. Mol. Biol.* **331**, 973 (2003);  
(b) Cirino, P.C., Mayer, K.M., and Umeno, D., in "Directed Evolution Library Creation" (F.H. Arnold and G. Georgiou, Eds.), Vol. 231, pp. 3–10, Humana Press, Totowa, N J, 2003;  
(c) Eggert, T., Reetz, M.T., and Jaeger, K.-E., in "Enzyme Functionality—Design, Engineering, and Screening" (A. Svendsen, Ed.), pp. 375–390, Marcel Dekker, New York, 2004;  
(d) Wong, T.S., Tee, K.L., Hauer, B., and Schwaneberg, U., *Nucleic Acids Res.* **32**, e26 (2004).
43. Georgescu, R., Bandara, G., and Sun, L., in "Directed Evolution Library Creation" (F.H. Arnold and G. Georgiou, Eds.), pp. 75–84, Humana Press, Totowa, N J, 2003.
44. (a) Wells, J.A., Vasser, M., and Powers, D.B., *Gene* **34**, 315 (1985);  
(b) Baretino, D., Feigenbutz, M., Valcarcel, R., and Stunnenberg, H.G., *Nucleic Acids Res.* **22**, 541 (1994).
45. Funke, S.A., Eipper, A., Reetz, M.T., Otte, N., Thiel, W., van Pouderoyen, G., Dijkstra, B.W., Jaeger, K.-E., and Eggert, T., *Biocatal. Biotransform.* **21**, 67 (2003).
46. DeSantis, G., Wong, K., Farwell, B., Chatman, K., Zhu, Z., Tomlinson, G., Huang, H., Tan, X., Bibbs, L., Chen, P., Kretz, K., and Burk, M.J., *J. Am. Chem. Soc.* **125**, 11476 (2003).
47. (a) Miyazaki, K., and Arnold, F.H., *J. Mol. Evol.* **49**, 716 (1999);  
(b) Sneed, J.L. and Loeb, L.A., in "Directed Evolution Library Creation" (F.H. Arnold and G. Georgiou, Eds.), Vol. 231, p. 65, Humana Press, Totowa, N J, 2003; and literature cited therein.
48. Liebeton, K., Zonta, A., Schimossek, K., Nardini, M., Lang, D., Dijkstra, B.W., Reetz, M.T., and Jaeger, K.-E., *Chem. Biol.* **7**, 709 (2000).
49. Reetz, M.T., Wilensek, S., Zha, D., and Jaeger, K.-E., *Angew. Chem. Int. Ed.* **40**, 3589 (2001).
50. Reetz, M.T., Bocola, M., Carballeira, J.D., Zha, D., and Vogel, A., *Angew. Chem. Int. Ed.* **44**, 4192 (2005).
51. Suen, W.-C., Zhang, N., Xiao, L., Madison, V., and Zaks, A., *Prot. Eng. Des. Sel.* **17**, 133 (2004).
52. Zhao, H., Giver, L., Shao, Z., Affholter, J.A., and Arnold, F.H., *Nat. Biotechnol.* **16**, 258 (1998).
53. Ikeuchi, A., Kawarasaki, Y., Shinbata, T., and Yamane, T., *Biotechnol. Prog.* **19**, 1460 (2003).
54. Song, J.K., Chung, B., Oh, Y.H., and Rhee, J.S., *Appl. Environ. Microbiol.* **68**, 6146 (2002).
55. Lee, S.H., Ryu, E.J., Kang, M.J., Wang, E.-S., Piao, Z., Choi, Y.J., Jung, K.H., Jeon, J.Y.J., and Shin, Y.C., *J. Mol. Catal. B: Enzymes* **26**, 119 (2003).
56. (a) Ostermeier, M., Shim, J.H., and Benkovic, S.J., *Nat. Biotechnol.* **17**, 1205 (1999);  
(b) Lutz, S., Ostermeier, M., and Benkovic, S.J., *Nucleic Acids Res.* **29**, e16 (2001).
57. Higara, K., and Arnold, F.H., *J. Mol. Biol.* **330**, 287 (2003).
58. O'Maille, P.E., Bakhtina, M., and Tsai, M.D., *J. Mol. Biol.* **321**, 677 (2002).
59. Kawarasaki, Y., Griswold, K.E., Stevenson, J.D., Selzer, T., Benkovic, S.J., Iverson, B.L., and Georgiou, G., *Nucleic Acids Res.* **31**, e126 (2003).

60. Sieber, V., Martinez, C.A., and Arnold, F.H., *Nat. Biotechnol.* **19**, 456 (2001).
61. Murakami, H., Hohsaka, T., and Sisido, M., *Nat. Biotechnol.* **20**, 76 (2002).
62. Coco, W.M., Encell, L.P., Levinson, W.E., Crist, M.J., Loomis, A.K., Licato, L.L., Arensdorf, J.J., Sica, N., Pienkos, P.T., and Monticello, D.J., *Nat. Biotechnol.* **20**, 1246 (2002).
63. Ness, J.E., Kim, S., Gottman, A., Pak, R., Krebber, A., Borchert, T.V., Govindarajan, S., Mundorff, E.C., and Minshull, J., *Nat. Biotechnol.* **20**, 1251 (2002).
64. Zha, D., Eipper, A., and Reetz, M.T., *ChemBioChem* **4**, 34 (2003).
65. (a) Arnold, F.H., *Nature* **409**, 253 (2001);  
(b) Moore, G.L., and Maranas, C.D., *AIChE J* **51**, 262 (2004);  
(c) Bogard, L.E., and Deem, M.W., *Proc. Natl. Acad. Sci. USA* **96**, 2591 (1999);  
(d) Dwyer, M.A., Looger, L.L., and Hellinga, H.W., *Science* **304**, 1967 (2004);  
(e) Otey, C.R., Silberg, J.J., Voigt, C.A., Endelman, J.B., Bandara, G., and Arnold, F.H., *Chem. Biol.* **11**, 309 (2004);  
(f) Garcia-Viloca, M., Gao, J., Karplus, M., and Truhlar, D., *Science* **303**, 186 (2004);  
(g) Gerlt, J.A., and Babbitt, P.C., *Genom. Biol.* **1**(5), 1 (2000);  
(h) Benkovic, S.J., and Hammes-Schiffer, S., *Science* **301**, 1196 (2003);  
(i) Williams, D.H., Stephens, E., O'Brien, D.P., and Zhou, M., *Angew. Chem. Int. Ed.* **43**, 6596 (2004);  
(j) Bosley, A.D., and Ostermeier, M., *Biomol. Eng.* **22**, 57 (2005).
66. (a) Reetz, M.T., *Angew. Chem. Int. Ed.* **40**, 284 (2001);  
(b) Reetz, M.T., *Angew. Chem. Int. Ed.* **41**, 1335 (2002).
67. (a) Reetz, M.T., in "Methods in Molecular Biology" (F.H. Arnold and G. Georgiou, Eds.), Vol. 230, pp. 259–282, Humana Press, Totowa, N J, 2003;  
(b) Reetz, M.T., in "Methods in Molecular Biology" (F.H. Arnold and G. Georgiou, Eds.), Vol. 230, pp. 283–290, Humana Press, Totowa, N J, 2003.
68. Reetz, M.T., in "Enzyme Functionality—Design, Engineering, and Screening" (A. Svendsen, Ed.), pp. 559–598, Marcel Dekker, New York, 2004.
69. Reetz, M.T., in "Evolutionary Methods in Biotechnology" (S. Brakmann and A. Schwienhorst, Eds.), pp. 113–141, Wiley-VCH, Weinheim, 2004.
70. (a) Wahler, D., and Reymond, J.-L., *Curr. Opin. Biotechnol.* **12**, 535 (2001);  
(b) Schmidt, M., and Bornscheuer, U.T., *Biomol. Eng.* **22**, 51 (2005).
71. Dahmen, S., and Bräse, S., *Synthesis* 1431 (2001).
72. Reetz, M.T., and Rüggeberg, C.J., *Chem. Commun.*, 1428 (2002).
73. (a) Dröge, M.J., Rüggeberg, C.J., van der Sloot, A.M., Schimmel, J., Dijkstra, R.S., Verhaert, R.M.D., Reetz, M.T., and Quax, W.J., *J. Biotechnol.* **4**, 19 (2003);  
(b) Reetz, M.T., Rüggeberg, C.J., Dröge, M.J., and Quax, W.J., *Tetrahedron* **58**, 8465 (2002).
74. (a) Reetz, M.T., *Pure Appl. Chem.* **71**, 1503 (1999);  
(b) Reetz, M.T., *Pure Appl. Chem.* **72**, 1615 (2000).
75. Janes, L.E., and Kazlauskas, R.J., *J. Org. Chem.* **62**, 4560 (1997).
76. Janes, L.E., Löwendahl, A.C., and Kazlauskas, R.J., *Chem.-Eur. J.* **4**, 2324 (1998).
77. Liu, A.M.F., Somers, N.A., Kazlauskas, R.J., Brush, T.S., Zocher, F., Enzelberger, M.M., Bornscheuer, U.T., Horsman, G.P., Mezzetti, A., Schmidt-Dannert, C., and Schmid, R.D., *Tetrahedron: Asymmetry* **12**, 545 (2001).
78. Moris-Varas, F., Shah, A., Aikens, J., Nadkarni, N.P., Rozzell, J.D., and Demirjian, D.C., *Bioorg. Med. Chem.* **7**, 2183 (1999).
79. Rüggeberg, C.J., Dissertation, Ruhr-Universität Bochum (2001).
80. Klein, G., and Reymond, J.-L., *Helv. Chim. Acta* **82**, 400 (1999).
81. Baumann, M., Stürmer, R., and Bornscheuer, U.T., *Angew. Chem. Int. Ed.* **40**, 4201 (2001).
82. Abato, P., and Seto, C.T., *J. Am. Chem. Soc.* **123**, 9206 (2001).
83. Onaran, M.B., and Seto, C.T., *J. Org. Chem.* **68**, 8136 (2003).
84. Li, Z., Bütikofer, L., and Witholt, B., *Angew. Chem. Int. Ed.* **43**, 1698 (2004).
85. Taran, F., Gauchet, C., Mohar, B., Meunier, S., Valleix, A., Renard, P.Y., Crémignon, C., Grassi, J., Wagner, A., and Mioskowski, C., *Angew. Chem. Int. Ed.* **41**, 124 (2002).
86. Badalassi, F., Wahler, D., Klein, G., Crotti, P., and Reymond, J.-L., *Angew. Chem. Int. Ed.* **39**, 4067 (2000).

87. Reymond, J.-L., and Wahler, D., *ChemBioChem* **3**, 701 (2002).
88. Korbel, G.A., Lalic, G., and Shair, M.D., *J. Am. Chem. Soc.* **123**, 361 (2001).
89. Reetz, M.T., Kühling, K.M., Deege, A., Hinrichs, H., and Belder, D., *Angew. Chem. Int. Ed.* **39**, 3891 (2000).
90. Guo, J., Wu, J., Siuzdak, G., and Finn, M.G., *Angew. Chem. Int. Ed.* **38**, 1755 (1999).
91. Yao, S., Meng, J.-C., Siuzdak, G., and Finn, M.G., *J. Org. Chem.* **68**, 2540 (2003).
92. (a) Reetz, M.T., Becker, M.H., Klein, H.-W., and Stöckigt, D., *Angew. Chem. Int. Ed.* **38**, 1758 (1999);  
(b) Reetz, M.T., Becker, M.H., Stöckigt, D., Klein, H.-W., DE-A 199 13 858.3.
93. Schrader, W., Eipper, A., Pugh, D.J., and Reetz, M.T., *Can. J. Chem.* **80**, 626 (2002).
94. Eipper, A., Dissertation, Ruhr-Universität Bochum (2002).
95. Cedrone, F., Niel, S., Roca, S., Bhatnagar, T., Ait-Abdelkader, N., Torre, C., Krumm, H., Maichele, A., Reetz, M.T., and Baratti, J.C., *Biocatal. Biotransform.* **21**, 357 (2003).
96. Reetz, M.T., Torre, C., Eipper, A., Lohmer, R., Hermes, M., Brunner, B., Maichele, A., Bocola, M., Arand, M., Cronin, A., Genzel, Y., Archelas, A., and Furstoss, R., *Org. Lett.* **6**, 177 (2004).
97. (a) Shapiro, M.J., and Gounarides, J.S., *Prog. Nucl. Magn. Reson. Spectrosc.* **35**, 153 (1999);  
(b) Gavaghan, C.L., Nicholson, J.K., Connor, S.C., Wilson, I.D., Wright, B., and Holmes, E., *Anal. Biochem.* **291**, 245 (2001).
98. Reetz, M.T., Eipper, A., Tielmann, P., and Mynott, R., *Adv. Synth. Catal.* **344**, 1008 (2002).
99. Reetz, M.T., Tielmann, P., Eipper, A., Ross, A., and Schlotterbeck, G., *Chem. Commun.*, 1366 (2004).
100. Evans, M.A., and Morken, J.P., *J. Am. Chem. Soc.* **124**, 9020 (2002).
101. Tielmann, P., Boese, M., Luft, M., and Reetz, M.T., *Chem.-Eur. J.* **9**, 3882 (2003).
102. Reetz, M.T., Kühling, K.M., Wilensek, S., Husmann, H., Häusig, U.W., and Hermes, M., *Catal. Today* **67**, 389 (2001).
103. Reetz, M.T., Brunner, B., Schneider, T., Schulz, F., Clouthier, C.M., and Kayser, M.M., *Angew. Chem. Int. Ed.* **43**, 4075 (2004).
104. Schneider, T., Dissertation, Ruhr-Universität Bochum (2005).
105. Reetz, M.T., Daligault, F., Brunner, B., Hinrichs, H., and Deege, A., *Angew. Chem. Int. Ed.* **43**, 4078 (2004).
106. Kühling, K.M., Dissertation, Ruhr-Universität Bochum (1999).
107. (a) Huang, X.C., Quesada, M.A., and Mathies, R.A., *Anal. Chem.* **64**, 2149 (1992);  
(b) Xue, G., Pang, H., and Yeung, E.S., *Anal. Chem.* **71**, 2642 (1999).
108. Harrison, D.J., Fluri, K., Seiler, K., Fan, Z., Effenhauser, C.S., and Manz, A., *Science* **261**, 895 (1993).
109. Salvadori, P., Bertucci, C., and Rosini, C., *Chirality* **3**, 376 (1991).
110. Ding, K., Ishii, A., and Mikami, K., *Angew. Chem. Int. Ed.* **38**, 497 (1999).
111. Reetz, M.T., Kühling, K.M., Hinrichs, H., and Deege, A., *Chirality* **12**, 479 (2000).
112. Angelaud, R., Matsumoto, Y., Korenaga, T., Kudo, K., Senda, M., and Mikami, K., *Chirality* **12**, 544 (2000).
113. Reetz, M.T., Becker, M.H., Kühling, K.M., and Holzwarth, A., *Angew. Chem. Int. Ed.* **37**, 2647 (1998).
114. Reetz, M.T., Hermes, M., and Becker, M.H., *Appl. Microbiol. Biotechnol.* **55**, 531 (2001).
115. Millot, N., Borman, P., Anson, M.S., Campbell, I.B., Macdonald, S.J.F., and Mahmoudian, M., *Org. Process Res. Dev.* **6**, 463 (2002).
116. Moore, B.D., Stevenson, L., Watt, A., Flitsch, S., Turner, N.J., Cassidy, C., and Graham, D., *Nature Biotechnol.* **22**, 1133 (2004).
117. (a) Schmid, R.D., and Verger, R., *Angew. Chem. Int. Ed.* **37**, 1608 (1998);  
(b) Krishna, S.H., and Karanth, N.G., *Catal. Rev.* **44**, 499 (2002);  
(c) Berglund, P., and Hult, K., in "Stereoselective Biocatalysis" (R.N. Patel, and N. Ramesh, Eds.), pp. 633–657, Marcel Dekker, New York, 2000;  
(d) QM-Studies of serine hydrolases: Hu, C.-H., Brinck, T., and Hult, K., *Int. J. Quantum Chem.*, 89 (1997);  
(e) Mechanism of serine proteases: Hedstrom, L., *Chem. Rev.* **102**, 4501 (2002).

118. Reetz, M.T., *Curr. Opin. Chem. Biol.* **6**, 145 (2002).
119. Hieber, G., and Ditrich, K., *Chim. Oggi* **19**(6), 16 (2001).
120. Breuer, M., Ditrich, K., Habicher, T., Hauer, B., Keßeler, M., Stürmer, R., and Zelinski, T., *Angew. Chem. Int. Ed.* **43**, 788 (2004).
121. (a) Jaeger, K.-E., Ransac, S., Dijkstra, B.W., Colson, C., van Heuvel, M., and Misset, O., *FEMS Microbiol. Rev.* **15**, 29 (1994);  
(b) Jaeger, K.-E., Wohlfarth, S., and Winkler, UK, in "Lipases: Structure, Mechanism and Genetic Engineering" (L. Alberghina, R.D. Schmid, and R. Verger, Eds.), Vol. 16, pp. 381–384, Verlag Chemie, Weinheim, 1991.
122. In some previous papers (22,24,48) a mistake was made in calculating the number of theoretical mutants when three amino acids are exchanged simultaneously (it should be 26 billion and not 52 billion).
123. Arnold, F.H., Wintrode, P.L., Miyazaki, K., and Gershenson, A., *Trends Biochem. Sci.* **26**, 100 (2001).
124. Crameri, A., and Stemmer, W.P.C., *BioTechniques* **18**, 194 (1995).
125. Zha, D., Wilensek, S., Hermes, M., Jaeger, K.-E., and Reetz, M.T., *Chem. Commun.*, 2664 (2001).
126. Nardini, M., Lang, D.A., Liebeton, K., Jaeger, K.-E., and Dijkstra, B.W., *J. Biol. Chem.* **275**, 31219 (2000).
127. Bocola, M., Otte, N., Jaeger, K.-E., Reetz, M.T., and Thiel, W., *ChemBioChem* **5**, 214 (2004).
128. Zhao, H., and Arnold, F.H., *Protein Eng.* **12**, 47 (1999).
129. Iffland, A., Tafelmeyer, P., Saudan, C., and Johnsson, K., *Biochem.* **39**, 10790 (2000).
130. (a) Kumar, M., Kannan, K.K., Hosur, M.V., Bhavesh, N.S., Chatterjee, A., Mittal, R., and Hosur, R.V., *Biochem. Biophys. Res. Commun.* **294**, 395 (2002);  
(b) Agarwal, P.K., Billeter, S.R., Rajagopalan, P.T.R., Benkovic, S.J., and Hammes-Schiffer, S., *Proc. Natl. Acad. Sci. USA* **99**, 2794 (2002).
131. Fersht, A. (Ed.), "Structure and Mechanism in Protein Science." W. H. Freeman, New York, 1999.
132. Reetz, M.T., in "Pharmacochemistry Library" (H. van der Goot, Ed.), Vol. 32, pp. 27–37, Elsevier, Amsterdam, 2002.
133. (a) Horsman, G.P., Liu, A.M.F., Henke, E., Bornscheuer, U.T., and Kazlauskas, R.J., *Chem.-Eur. J.* **9**, 1933 (2003);  
(b) Park, S., Morley, K.L., Horsman, G.P., Holmquist, M., Hult, K., and Kazlauskas, R.J., *Chem. Biol.* **12**, 45 (2005).
134. Reetz, M.T., Bocola, M., Carballeira, J.D., and Vogel, A., Abstract, Biotrans Conference, Hamburg, July 3–8, 2004.
135. Reetz, M.T., Carballeira, J.D., and Vogel, A., unpublished.
136. Van Pouderoyen, G., Eggert, T., Jaeger, K.-E., and Dijkstra, B.W., *J. Mol. Biol.* **309**, 215 (2001).
137. Krumm, H., Dissertation, Ruhr-Universität Bochum (2004).
138. Koga, Y., Kato, K., Nakano, H., and Yamane, T., *J. Mol. Biol.* **331**, 585 (2003).
139. Moore, J.C., and Arnold, F.H., *Nature Biotechnol.* **14**, 458 (1996).
140. Bornscheuer, U.T., Altenbuchner, J., and Meyer, H.H., *Biotechnol. Bioeng.* **58**, 554 (1998).
141. Henke, E., and Bornscheuer, U.T., *Biol. Chem.* **380**, 1029 (1999).
142. Otte, N., dissertation in preparation, Heinrich-Heine-Universität Düsseldorf (2005).
143. Van Loo, B., Spelberg, J.H.L., Kingma, J., Sonke, T., Wubbolts, M.G., and Janssen, D.B., *Chem. Biol.* **11**, 981 (2004).
144. Steinreiber, A., Mayer, S.F., and Faber, K., *Synthesis*, 2035 (2001).
145. Archelas, A., and Furstoss, R., *Curr. Opin. Chem. Biol.* **5**, 112 (2001).
146. Zou, J.Y., Hallberg, B.M., Bergfors, T., Oesch, F., Arand, M., Mowbray, S.L., and Jones, T.A., *Structure* **8**, 111 (2000).
147. Syldatk, C., May, O., Altenbuchner, J., Mattes, R., and Siemann, M., *Appl. Microbiol. Biotechnol.* **51**, 293 (1999).
148. May, O., Nguyen, P.T., and Arnold, F.H., *Nat. Biotechnol.* **18**, 317 (2000).
149. May, O., (Degussa-Hüls), personal communication (2005).

150. DeSantis, G., Zhu, Z., Greenberg, W.A., Wong, K., Chaplin, J., Hanson, S.R., Farwell, B., Nicholson, L.W., Rand, C.L., Weiner, D.P., Robertson, D.E., and Burk, M.J., *J. Am. Chem. Soc.* **124**, 9024 (2002).
151. Burk, M., personal communication (2004).
152. Benschop, H.P., and de Jong, L.P.A., *Acc. Chem. Res.* **21**, 368 (1988).
153. Wu, F., Li, W.-S., Chen-Goodspeed, M., Sogorb, M.A., and Raushel, F.M., *J. Am. Chem. Soc.* **122**, 10206 (2000).
154. (a) Chen-Goodspeed, M., Sogorb, M.A., Wu, F., Hong, S.-B., and Raushel, F.M., *Biochemistry* **40**, 1325 (2001);  
(b) Chen-Goodspeed, M., Sogorb, M.A., Wu, F., and Raushel, F.M., *Biochemistry* **40**, 1332 (2001).
155. (a) Cunningham, B.C., and Wells, J.A., *Science* **244**, 1081 (1989);  
(b) Morrison, K.L., and Weiss, G.A., *Curr. Opin. Chem. Biol.* **5**, 302 (2001).
156. Hill, C.M., Li, W.-S., Thoden, J.B., Holden, H.M., and Raushel, F.M., *J. Am. Chem. Soc.* **125**, 8990 (2003).
157. (a) Rozzell, J.D., and Bommarius, A.S., in "Enzyme Catalysis in Organic Synthesis: A Comprehensive Handbook" (K. Drauz and H. Waldmann, Eds.) Vol. II, pp. 873–893, VCH, Weinheim, 2nd Edition, 2002;  
(b) Li, T., Kootstra, A.B., and Fotheringham, I.G., *Org. Process Res. Dev.* **6**, 533 (2002).
158. Matcham, G.W., and Bowen, A.R.S., *Chim. Oggi* **14**(6), 20 (1996).
159. Matcham, G., Bhatia, M., Lang, W., Lewis, C., Nelson, R., Wang, A., and Wu, W., *Chimia* **53**, 584 (1999).
160. (a) Fessner, W.-D., and Walter, C., *Top. Curr. Chem.* **184**, 97 (1996);  
(b) Silvestri, M.G., DeSantis, G., Mitchell, M., and Wong, C.-H., in "Topics in Stereochemistry" (S.E. Denmark, Ed.), Vol. 23, pp. 267–342, Wiley, Weinheim, 2003.
161. Fong, S., Machajewski, T.D., Mak, C.C., and Wong, C.-H., *Chem. Biol.* **7**, 873 (2000).
162. Shelton, M.C., Cotterill, I.C., Novak, S.T.A., Poonawala, R.M., Sudarshan, S., and Toone, E.J., *J. Am. Chem. Soc.* **118**, 2117 (1996).
163. Wada, M., Hsu, C.-C., Franke, D., Mitchell, M., Heine, A., Wilson, I., and Wong, C.-H., *Bioorg. Med. Chem.* **11**, 2091 (2003).
164. Williams, G.J., Domann, S., Nelson, A., and Berry, A., *Proc. Natl. Acad. Sci. USA* **100**, 3143 (2003).
165. Li, Z., van Beilen, J.B., Duetz, W.A., Schmid, A., de Raadt, A., Griengl, H., and Witholt, B., *Curr. Opin. Chem. Biol.* **6**, 136 (2002).
166. Cornils, B., and Herrmann, W.A. (Eds.), "Applied Homogeneous Catalysis with Organometallic Compounds." Vol. 1–2, Wiley-VCH, Weinheim (1996).
167. Holland, H.L., and Weber, H.K., *Curr. Opin. Biotechnol.* **11**, 547 (2000).
168. Krow, G.R., *Org. React.* **43**, 251 (1993).
169. (a) Bolm, C., Schlingloff, G., and Weickhardt, K., *Angew. Chem. Int. Ed. Engl.* **33**, 1848 (1994);  
(b) Bolm, C., Palazzi, C., and Beckmann, O., in "Transition Metals for Organic Chemistry: Building Blocks and Fine Chemicals" (M. Beller, and C. Bolm, Eds.), Vol. 2, pp. 267–274, Wiley-VCH, Weinheim, 2nd Edition, 2004  
(c) Bolm, C., Palazzi, C., and Beckmann, O., in "Transition Metals for Organic Chemistry: Building Blocks and Fine Chemicals" (M. Beller, and C. Bolm, Eds.), Vol. 2, pp. 267–274, Wiley-VCH, Weinheim, 2nd Edition, 2004.
170. Strukul, G., *Angew. Chem. Int. Ed.* **37**, 1198 (1998).
171. Ito, K., Ishii, A., Kuroda, T., and Katsuki, T., *Synlett* **643** (2003).
172. Taschner, M.J., and Black, D.J., *J. Am. Chem. Soc.* **110**, 6892 (1988).
173. Flitsch, S., and Grogan, G., in "Enzyme Catalysis in Organic Synthesis: A Comprehensive Handbook" (K. Drauz and H. Waldmann, Eds.) Vol. III, pp. 1202–1280, VCH, Weinheim, 2nd Edition, 2002.
174. Stewart, J.D., Reed, K.W., Zhu, J., Chen, G., and Kayser, M.M., *J. Org. Chem.* **61**, 7652 (1996).
175. (a) Mihovilovic, M.D., Chen, G., Wang, S., Kyte, B., Rochon, F., Kayser, M.M., and Stewart, J.D., *J. Org. Chem.* **66**, 733 (2001);  
(b) Mihovilovic, M.D., Müller, B., Schulze, A., Stanetty, P., and Kayser, M.M., *Eur. J. Org. Chem.*, 2243 (2003).

176. Donoghue, N.A., Norris, D.B., and Trudgill, P.W., *Eur. J. Biochem.* **63**, 175 (1976).
177. Walsh, C.T., and Chen, Y.-C.J., *Angew. Chem. Int. Ed. Engl.* **27**, 333 (1988).
178. Sheng, D., Ballou, D.P., and Massey, V., *Biochemistry* **40**, 11156 (2001).
179. Mikovilovic, M.D., Reetz, M.T., Rudroff, F., Snajdrova, R., and Winninger, A. unpublished.
180. Malito, E., Afieri, A., Fraaije, M.W., and Mattevi, A., *Proc. Natl. Acad. Sci. USA* **101**, 13157 (2004).
181. Fraaije, M.W., Wu, J., Heuts, D.P.H.M., van Hellemond, E.W., Spelberg, J.H.L., and Janssen, D.B., *Appl. Microbiol. Biotechnol.* **66**, 393 (2005).
182. Bocola, M., Schulz, F., Leca, F., Vogel, A., Fraaije, M.W., and Reetz, M.T., *Adv. Synth. Catal.* **347**, 979 (2005).
183. Carrea, G., Redigolo, B., Riva, S., Colonna, S., Gaggero, N., Battistel, E., and Bianchi, D., *Tetrahedron: Asymmetry* **3**, 1063 (1992).
184. Alphand, V., Gaggero, N., Colonna, S., Pasta, P., and Furstoss, R., *Tetrahedron* **53**, 9695 (1997).
185. Chen, G., Kayser, M.M., Mihovilovic, M.D., Mrstik, M.E., Martinez, C.A., and Stewart, J.D., *New J. Chem.* **23**, 827 (1999).
186. Dostert, P.L., Benedetti, M.S., and Tipton, K.F., *Med. Chem. Res.* **9**, 45 (1989).
187. Beard, T.M., and Turner, N.J., *Chem. Commun.* 246 (2002).
188. Alexeeva, M., Enright, A., Dawson, M.J., Mahmoudian, M., and Turner, N.J., *Angew. Chem. Int. Ed.* **41**, 3177 (2002).
189. Carr, R., Alexeeva, M., Enright, A., Eve, T.S.C., Dawson, M.J., and Turner, N.J., *Angew. Chem. Int. Ed.* **42**, 4807 (2003).
190. Balkenhohl, F., Ditrach, K., Hauer, B., and Ladner, W., *J. Prakt. Chem./Chem.-Ztg.* **339**, 381 (1997).
191. Reetz, M.T., and Schimossek, K., *Chimia* **50**, 668 (1996).
192. Choi, Y.K., Kim, M.J., Ahn, Y., and Kim, M.-J., *Org. Lett.* **3**, 4099 (2001).
193. Recent reviews of enzyme-based dynamic kinetic resolution:  
(a) Pàmies, O., and Bäckvall, J.-E., *Chem. Rev.* **103**, 3247 (2003);  
(b) Kim, M.-J., Kim, H.M., Kim, D., Ahn, Y., and Park, J., *Green Chem* **6**, 471 (2004).
194. Sono, M., Roach, M.P., Coulter, E.D., and Dawson, J.H., *Chem. Rev.* **96**, 2841 (1996).
195. (a) Urlacher, V., and Schmid, R.D., *Curr. Opin. Biotechnol.* **13**, 557 (2002);  
(b) Meunier, B., de Visser, S.P., and Shaik, S., *Chem. Rev.* **104**, 3947 (2004).
196. Holland, H.L., in "Biotechnology" (H.-J. Rehm, G. Reed, A. Pühler, and P. Stadler, Eds.), Vol. 8a, pp. 475–533, VCH, Weinheim, 2nd Edition, 1998.
197. Farinas, E.T., Schwaneberg, U., Glieder, A., and Arnold, F.H., *Adv. Synth. Catal.* **343**, 601 (2001).
198. Glieder, A., Farinas, E.T., and Arnold, F.H., *Nat. Biotechnol.* **20**, 1135 (2002).
199. Peters, M.W., Meinhold, P., Glieder, A., and Arnold, F.H., *J. Am. Chem. Soc.* **125**, 13442 (2003).
200. Münzer, D.F., Meinhold, P., Peters, M.W., Feichtenhofer, S., Griengl, H., Arnold, F.H., Glieder, A., and de Raadt, A., *Chem. Commun.*, 2597 (2005).
201. (a) Aharoni, A., Gaidukov, L., Khersonsky, O., McQ Gould, S., Roodveldt, C., and Tawfik, D.S., *Nat. Genet.* **37**, 73 (2005);  
(b) Raillard, S.-A., Krebber, A., Chen, Y., Ness, J.E., Bermudez, E., Trinidad, R., Fullem, R., Davis, C., Welch, M., Seffernick, J., Wackett, L.P., Stemmer, W.P.C., and Minshull, J., *Chem. Biol.* **8**, 891 (2001);  
(c) O'Brien, P.J., and Herschlag, D., *Chem. Biol.* **6**, R91 (1999);  
(d) Copley, S.D., *Curr. Opin. Chem. Biol.* **7**, 265 (2003);  
(e) Bornscheuer, U.T., and Kazlauskas, R.J., *Angew. Chem. Int. Ed.* **43**, 6032 (2004).
202. Reetz, M.T., Rentzsch, M., Pletsch, A., and Maywald, M., *Chimia* **56**, 721 (2002).
203. Reetz, M.T., "Optimierung von synthetischen Katalysatoren durch gerichtete Evolution." DE-A 101 29 187.6 (2001).



# Dendrimers in Catalysis

JOOST N.H. REEK, SILVIA ARÉVALO, RIEKO VAN HEERBEEK, PAUL C.J. KAMER and PIET W.N.M. VAN LEEUWEN

*Van't Hoff Institute for Molecular Sciences, University of Amsterdam, Nieuwe Achtergracht 166, 1018 WV, Amsterdam, The Netherlands*

Dendrimers are well-defined hyperbranched macromolecules, with the larger ones having characteristic globular structures. These novel materials have been investigated intensively in recent decades, and among other potential applications, they are suitable as soluble supports for homogeneous transition metal complex catalysts. These catalysts offer the advantage of easy separation from products and recycling as well as the potential advantages of unique catalytic properties, including high activity, selectivity, and stability. In this chapter, the current state of research in dendrimer catalysis is reviewed, with emphasis on the importance of the location of the catalyst in the dendritic framework (e.g., at the core or at the periphery). Several approaches to the separation of dendrimer catalysts are evaluated, and unique dendritic effects in catalysis are discussed.

**Abbreviations:** *BINAP*, 2, 2'-bis(diphenylphosphino)-1, 1'-binaphthyl; *BINOL*, 1-1'-binaphthol; *C<sub>r</sub>*, relative concentration; *CFMR*, continuous-flow membrane reactor; *Cy*, cyclohexyl; *DAB*, polyamino; *dba*, dibutylamine; *DMF*, *N*, *N*-dimethylformamide; *dppf*, diphenylphosphineferrocene; *EDC*, ethyl-*N*, *N*-dimethylaminopropylcarbodiimide; *ee*, enantiomeric excess; *Fu*, furanyl; *G0*, generation 0 dendrimer; *G1*, first-generation dendrimer; *G2*, second-generation dendrimer; *G3*, third-generation dendrimer; *G4*, fourth-generation dendrimer; *HP-NMR*, high pressure nuclear magnetic resonance; *ICP-AES*, induced coupled plasma atomic emission spectroscopy; *LG*, leaving group; *MAO*, methylaluminumoxane; *MW*, molecular weight; *nbd*, norbornadiene; *NCN*, 2, 6-bis[(dimethylamino)methyl]phenyl anion; *N<sub>r</sub>*, number of residence times (reactor volume divided by the flow rate); *Nu*, nucleophile; *PAMAM*, polyamidoamine; *PPI*, polypropyleneimine; *POM*, polyoxometalate; *POSS*, polyhedral oligomeric silsesquioxane; *PS*, polystyrene; *PTC*, phase transfer catalyst; *RCM*, ring closing metathesis; *ROM*, ring opening metathesis; *ROMP*, ring opening metathesis polymerization; *R<sub>f</sub>*, retention factor (on TLC); *SEC*, size-exclusion chromatography; *STY*, space time yield (mass of product formed per volume of the reactor and time); *TADDOL*,  $\alpha$ ,  $\alpha$ ,  $\alpha'$ ,  $\alpha'$ -tetraaryl-1, 3-dioxolane-4, 5-dimethanol; *TPPTS*, tri(m-sulphophenyl)-phosphine; *TsDPEN*, *N*-(4-toluenesulfonyl)-1, 2, diphenylethylenediamine; *t<sub>1/2</sub>*, half-life time; *tmada*, tetramethylethylenediamine; *TOF*, turnover frequency.

## I. Introduction

Dendrimers are well-defined hyperbranched macromolecules, and the larger ones have characteristic globular structures. Dendrimer chemistry has become extremely popular since the preceding decades, and several potential applications of dendrimers, including catalysis (1), are well documented in several reviews (2). Recent

developments of synthetic procedures have made functionalized dendrimers readily available in large enough quantities to facilitate the rapid development of dendrimer chemistry. In catalysis, dendrimers have been proposed to bridge the gap between homogeneous catalysis and surface catalysis, because their sizes enable separation from reaction products by modern membrane techniques. These novel soluble catalysts can be used in continuous-flow membrane reactors, which offer major advantages, particularly for reactions that benefit from low substrate (reactant) concentrations or suffer from side reactions of the products. Dendrimers functionalized at their cores offer the prospect of mimicking the properties of enzymes (which are regarded as their natural counterparts), and such dendrimers may give catalysts with unique activities or stabilities.

Here we review recent progress and breakthroughs in research with promising, novel transition metal-functionalized dendrimer catalysts and discuss aspects of catalyst recycling and unique dendritic effects in catalysis.

In 1994, Tomalia and Dvornic (3) pointed out the promising opportunities offered by surface-functionalized dendrimer catalysts, which have often been proposed to bridge the gap between homogeneous, single site catalysts and heterogeneous, multi-site catalysts. Because heterogeneous systems generally contain at least  $10^{12}$  active sites per conglomerated particle (4), it is fair to state that dendritic catalysts containing at most 1000 active sites per molecule are closer to the monomeric homogeneous systems than to heterogeneous systems, both with respect to the number of sites per particle and in diffusion phenomena. A better formulation is that functionalized dendrimers offer the potential to combine the advantages of both homogeneous and heterogeneous catalysis. In principle, dendritic catalysts can show the activity and selectivity of a conventional homogeneous catalyst, and they can be recovered easily from the reaction medium. In contrast, catalysts supported on highly cross-linked polymer beads generally suffer from lower activity than their homogeneous analogues, because of reduced accessibility (5). The accessibility is related to the solvent-dependent swelling properties of the polymer, which can strongly influence the catalytic performance. Other advantages of dendritic catalysis include the opportunity to fine-tune the catalytic centers by ligand design and the opportunity to perform mechanistic studies of these uniformly distributed catalytic sites attached to the support.

The dendrimer framework also plays an important role. The catalytic performance measured by activity, selectivity, stability, and recyclability depends on the dendritic architecture, and it is important to distinguish periphery-functionalized, core-functionalized, and focal point-functionalized dendrimers (Fig. 1). Periphery-functionalized dendrimers have catalytic groups located at the surface where they are directly available to the substrate. In contrast, when a dendrimer is functionalized at its core, the substrate has to penetrate the dendrimer support before it reaches the active center, and this transport process can limit the rate of a catalytic reaction if large and congested dendrimers are involved.

The accessible peripheral catalytic groups enable reaction rates that are comparable to those of homogeneous systems, but the periphery-functionalized dendrimers contain multiple reaction sites and may have extremely high local catalyst concentrations, which can lead to cooperative effects in reactions that proceed via a

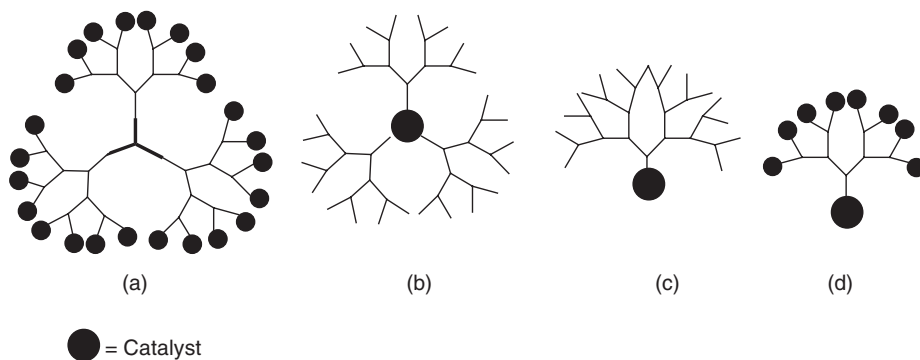


FIG. 1. Different dendritic architectures: catalyst located at the periphery (a), core (b), focal point of a wedge (c) and periphery of a wedge (d).

bimetallic mechanism (6). This may be a potential detriment of periphery-functionalized dendrimers because several deactivation pathways operate via bimetallic mechanisms (e.g., ruthenium-catalyzed metathesis (7), palladium-catalyzed reductive coupling of benzene and chlorobenzene (8), and reactions involving radicals (9)).

In core- (and focal point-) functionalized dendrimers, the catalyst may benefit from the site isolation created by the environment of the dendritic structure. Site-isolation effects in dendrimers can also be beneficial for other functionalities (a review of this topic has appeared in Reference (10)). When reactions are deactivated by excess ligand and when a bimetallic deactivation mechanism is operative, core-functionalized dendrimers can minimize the deactivation.

Another noteworthy difference between core- and periphery-functionalized dendrimers is that much higher costs are involved in the application of core-functionalized dendrimers due to their higher molecular weight per catalytic site. Furthermore, applications may be limited by the solubility of the dendrimer. (To dissolve 1 mmol of catalyst/L, 20 g/L of core-functionalized dendrimer is required (MW 20 000 Da, 1 active site) compared to 1 g/L of periphery-functionalized dendrimer (MW 20 000 Da, 20 active sites). On the other hand, for core-functionalized systems, the solubility of the dendritic catalyst can be optimized by changing the peripheral groups.

Dendritic catalysts can be recycled by using techniques similar to those applied with their monomeric analogues, such as precipitation, two-phase catalysis, and immobilization on insoluble supports. Furthermore, the large size and the globular structure of the dendrimer can be utilized to facilitate catalyst-product separation by means of nanofiltration. Nanofiltration can be performed batch wise or in a continuous-flow membrane reactor (CFMR). The latter offers significant advantages; the conditions such as reactant concentrations and reactant residence time can be controlled accurately. These advantages are especially important in reactions in which the product can react further with the catalytically active center to form side products.

Membrane reactors have been investigated since the 1970s (11). Although membranes can have several functions in a reactor, the most obvious is the separation of reaction components. Initially, the focus has been mainly on polymeric membranes applied in enzymatic reactions, and ultrafiltration of enzymes is commercially applied on a large scale for the synthesis of fine chemicals (e.g., L-methionine) (12). Membrane materials have been improved significantly over those applied initially, and nanofiltration membranes suitable to retain relatively small compounds are now available commercially (e.g., mass cut-off of 400–750 Da).

Two forms of leaching have to be considered when dendritic transition metal catalysts are used in membrane reactors: depletion of the dendritic catalyst through the membrane and metal dissociation from the dendrimer resulting in further leaching of the unsupported metal through the membrane. In Fig 2, the theoretical activities of dendritic catalysts are given for various retention factors.<sup>1</sup> For example, if a dendritic catalyst has a retention factor of 0.95, only 25% of the catalyst would remain in the reactor after the reactor had been flushed with 30 times its volume. For practical applications, the overall retention of the dendritic catalyst must be extremely high (typically, > 99.9%) to maintain the material in a CFMR for long reaction times. The required retention obviously depends on the application; processes for the commodity chemical industry generally require higher numbers of

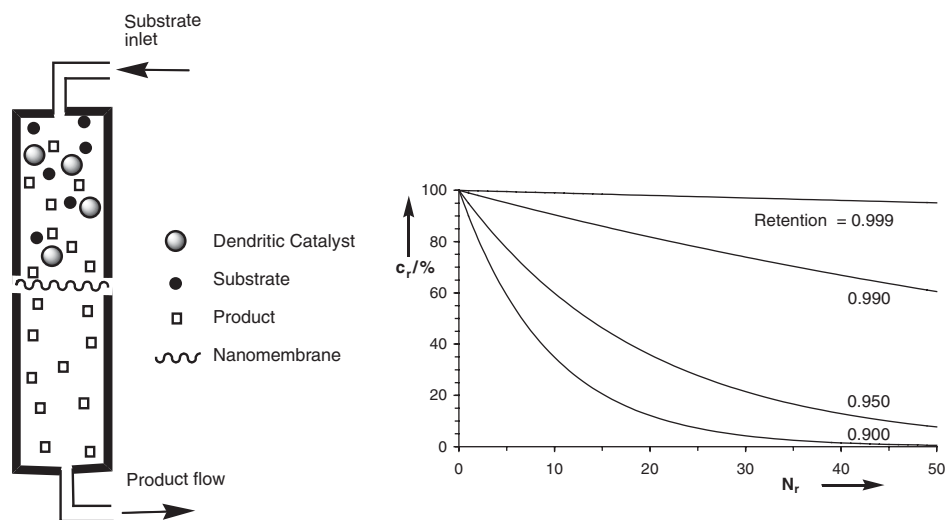


FIG. 2. Schematic presentation of a membrane reactor (left) and theoretical relative concentrations ( $C_r$ ) of the dendritic species versus the substrate flow (in residence times  $N_r$ ) calculated for various retention factors.

<sup>1</sup> **Retention factors** were calculated using the equation: retention factor =  $1 + \{\ln[a/(a+b)]/x\}$ , where  $a$  is the amount of dendrimer inside the reactor after the experiment;  $b$  the amount of dendrimer that went through the membrane;  $x$  the number of reactor volumes flushed with substrate solution.

turnovers and, therefore, more efficient catalyst recycling than those for high-value-added fine chemicals.

In the first part of this overview, we focus on the recycling of dendritic catalysts. This part of the review is divided according to the various recycling approaches, and the sections are organized by way of the reactions catalyzed. In the second part, we describe examples in which attachment of the catalyst to the dendrimer framework results in modified performance. (Although we attempted to make a clear division between catalyst recycling and dendritic effects, these two properties cannot always be addressed separately.)

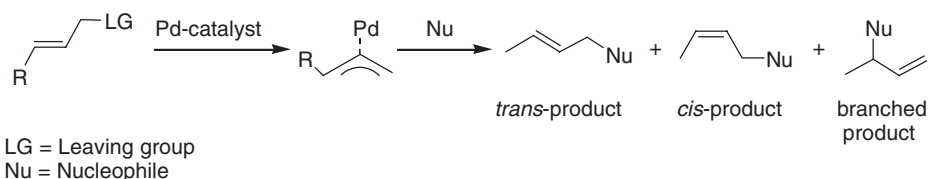
## II. Catalyst Recycling in Applications of Dendrimer-Supported Catalysts

### A. CATALYST RECYCLING USING NANOFILTRATION IN A CONTINUOUS-FLOW MEMBRANE REACTOR

Kragl (13) pioneered the use of membranes to recycle dendritic catalysts. Initially, he used soluble polymeric catalysts in a CFMR for the enantioselective addition of  $\text{Et}_2\text{Zn}$  to benzaldehyde. The ligand  $\alpha,\alpha$ -diphenyl-(L)-prolinol was coupled to a copolymer prepared from 2-hydroxyethyl methyl acrylate and octadecyl methyl acrylate (molecular weight 96,000 Da). The polymer was retained with a retention factor  $>0.998$  when a polyamide ultrafiltration membrane (Hoechst Nadir UF PA20) was used. The enantioselectivity obtained with the polymer-supported catalyst was lower than that obtained with the monomeric ligand (80% ee vs 97% ee), but the activity of the catalyst was similar to that of the monomeric catalyst. This result is in contrast to observations with catalysts in which the ligand was coupled to an insoluble support, which led to a 20% reduction of the catalytic activity.

#### A.1. Allylic Substitution using Dendritic Catalysts in a CFMR

**A.1.1. Covalently Functionalized Dendrimers Applied in a CFMR.** The palladium-catalyzed allylic substitution reaction has been investigated extensively in the preceding decades and provides an important tool for the formation of carbon–carbon and carbon–heteroatom bonds (14). The product is formed after attack of a nucleophile to an  $(\eta^3\text{-allyl})\text{Pd}(\text{II})$  species, formed by oxidative addition of the unsaturated substrate to palladium(0) (Scheme 1). To date several nucleophiles have been used, mostly resulting in the formation of carbon–carbon and



SCHEME 1.

carbon–nitrogen bonds. The majority of the reported investigations focused on the enantioselectivity and regioselectivity of the reaction. Recently, the recycling of this type of palladium catalyst has received some attention (15).

Reetz *et al.* (16) functionalized commercially available DAB-dendrimers with diphenylphosphine groups at the periphery (**1**) via a double phosphination of the amines with diphenylphosphine and formaldehyde. The transition metal complexes **1a–1e** have been prepared in which the dendrimer-N-(CH<sub>2</sub>PPh<sub>2</sub>)<sub>2</sub> groups act as bidentate ligands.

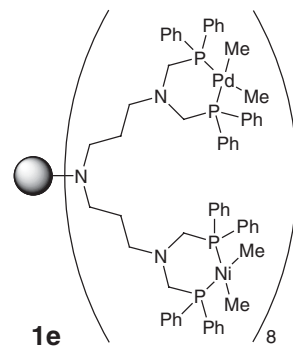
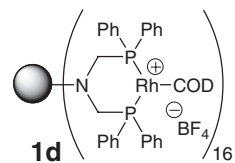
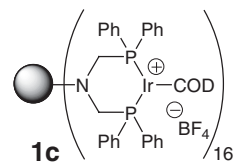
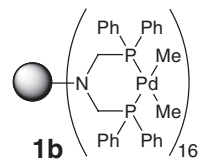
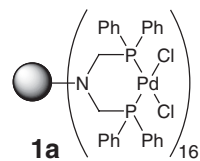
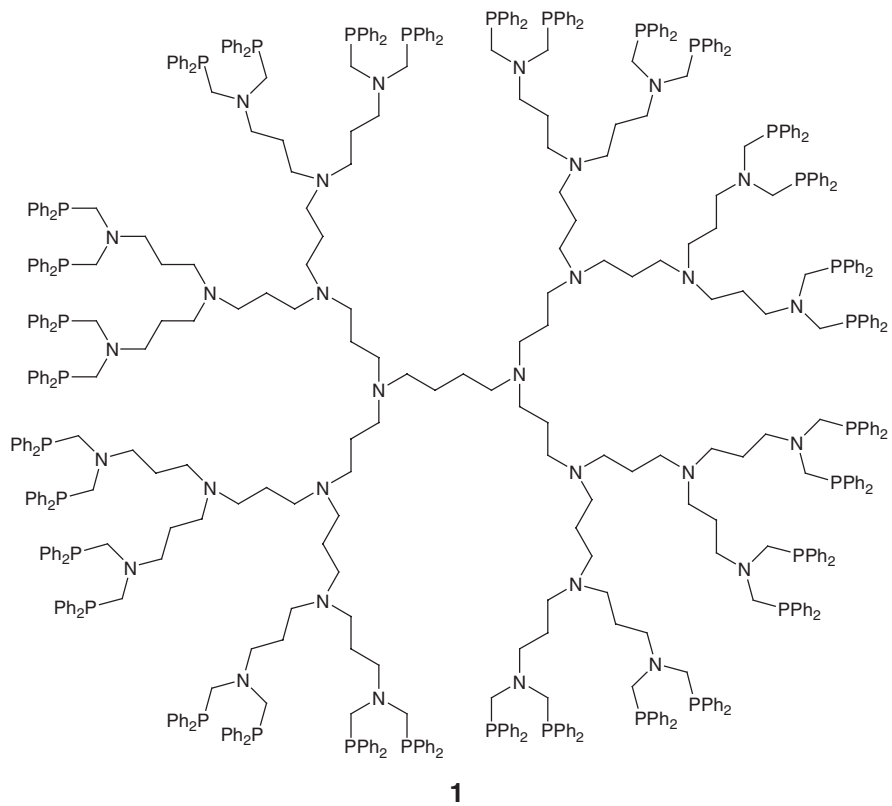
Brinkmann *et al.* (17) reported the use of these phosphine-containing dendritic catalysts for allylic substitution reactions in a CFMR. Retention factors up to 0.999 were measured for the third-generation dendrimer **1b** (molecular weight = 10,212 Da). Although the dendrimer remained in the reactor, palladium leaching was observed. Apparently, metal–ligand dissociation resulted in low-molecular-weight palladium species that were washed out of the reactor. During the reaction, leaching was compensated by addition of allylpalladium chloride to the feed solution. In this manner, dendrimer **1b** was applied in palladium-catalyzed allylic substitution, and the CFMR could be operated for more than 60 residence times with a conversion of as much as 12%. In this process, the product was obviously contaminated with palladium.

Better results were obtained by using *in situ* prepared palladium complexes of a G4 dendrimer (calculated molecular weight 20 564 Da for 100% palladium loading of the 32 diphosphines). After 100 residence times, the conversion had decreased from 100% to approximately 75% (Fig. 3). A small amount of palladium was leached from the catalyst during this experiment (0.14% per residence time), which only partly explains the decrease in conversion. The formation of inactive PdCl<sub>2</sub> was proposed to account for the additional drop in activity. A sound conclusion about the effect of this dendritic catalyst requires more experiments.

De Groot *et al.* (18) prepared phosphine-functionalized carbosilane dendrimers of different generations (4, 8, 24, and 36 phosphine end groups) and used their palladium complexes as catalysts for the allylic alkylation of allyl trifluoroacetate with diethyl sodio-2-methylmalonate.

In a batch process, all dendritic catalysts showed very high activity. When a substrate-to-Pd molar ratio of 2000 was used, the conversions after 5 min were 49, 55, 45, and 47% when dendrimers with 4, 36, 8, and 24 phosphine ligands were used, respectively. These results show that all the active sites located at the periphery of the dendrimer support acted independently as catalysts.

The palladium catalyst supported on the dendrimer with 24 phosphine end groups (**2**) was used in a CFMR. In the continuous process a solution of allyl trifluoroacetate and sodium diethyl 2-methylmalonate in THF (including *n*-decane as an internal standard) was pumped through the reactor. Figure 4 shows the conversion as a function of the amount of substrate solution (expressed in reactor volumes) pumped through the reactor. The reaction started immediately after the addition of the catalyst, and the maximum conversion was reached after two reactor volumes had passed, whereupon a drop in conversion was observed. It was inferred from the retention of the dendrimer (99.7% in dichloromethane) that the decrease was not caused by dendrimer depletion, and it was therefore ascribed to the



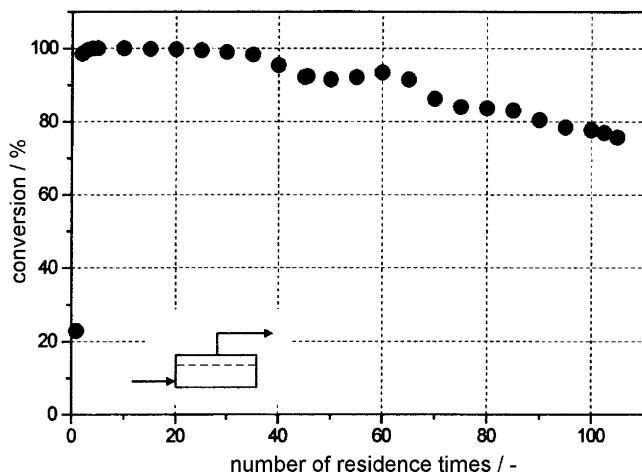
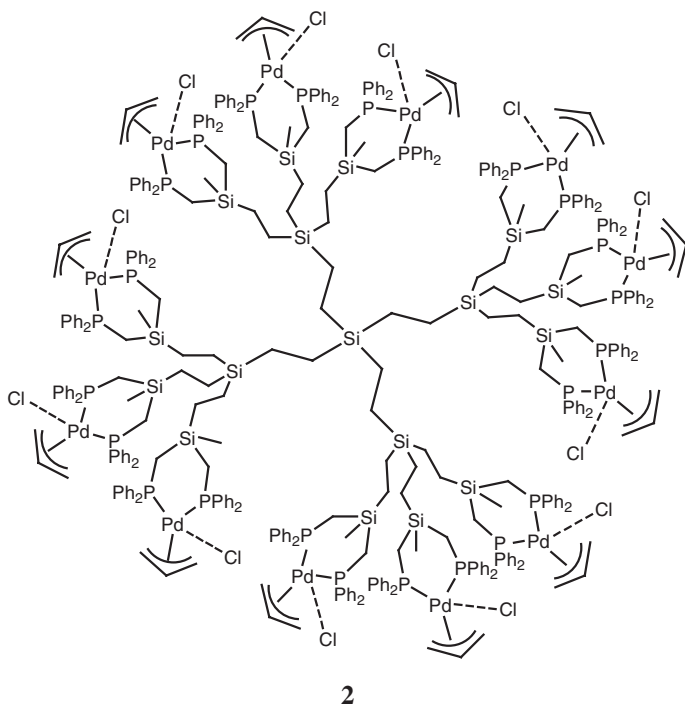


FIG. 3. Allylic substitution in a CFMR with **1b** as the catalyst (17).



decomposition of the palladium catalyst. Analysis of the reaction mixture by induced coupled plasma atomic emission spectroscopy (ICP-AES) showed that after the reaction all the palladium had passed through the membrane, but samples taken from the product stream were not catalytically active, indicating that no *active*



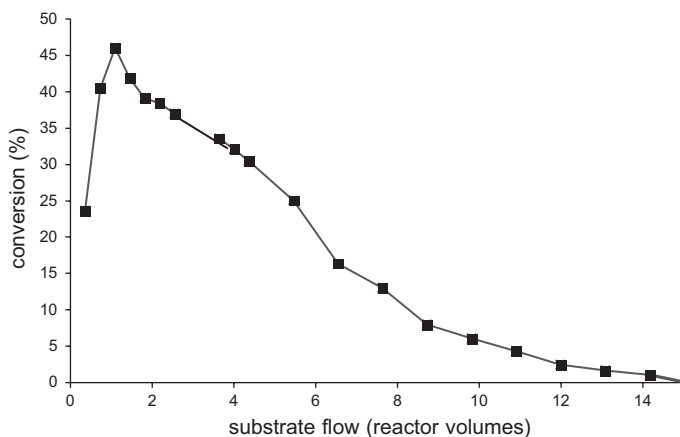


FIG. 4. Application of dendritic ligand **2** in the continuous allylic alkylation of allyl trifluoroacetate and sodium diethyl 2-methylmalonate in a membrane reactor (Koch MPF-60 NF membrane, molecular weight cut-off = 400 Da) (18a).

palladium catalyst had passed through the membrane. Batch experiments performed in the presence of pieces of membrane material gave results similar to those observed without the membrane pieces in the reactor, suggesting that the membrane material did not play a role in the deactivation process.

When dendritic catalyst **2** was applied in the allylic amination of crotyl acetate and piperidine in the CFMR, a similar rapid deactivation of the catalyst was observed.

Several experiments were carried out to provide insight into the deactivation process. The decomposition of the model compound  $\{(\text{CH}_3)_2\text{Si}(\text{CH}_2\text{PPh}_2)_2\}(\eta^3\text{-C}_3\text{H}_7)\text{PdCl}$  was monitored by  $^1\text{H}$ -, and  $^{31}\text{P}\{^1\text{H}\}$ -NMR spectroscopy, and the formation of  $\{(\text{CH}_3)_2\text{Si}(\text{CH}_2\text{PPh}_2)_2\}\text{PdCl}_2$  was observed. However, in the allylic amination of crotyl acetate and piperidine,  $\{(\text{CH}_3)_2\text{Si}(\text{CH}_2\text{PPh}_2)_2\}\text{PdCl}_2$  was found to be only slightly less active than  $\{(\text{CH}_3)_2\text{Si}(\text{CH}_2\text{PPh}_2)_2\}(\eta^3\text{-C}_3\text{H}_7)\text{PdCl}$ . Complete conversion was reached after 2 h. Therefore, the formation of  $\{(\text{CH}_3)_2\text{Si}(\text{CH}_2\text{PPh}_2)_2\}\text{PdCl}_2$  by reaction with the solvent cannot account for the fast deactivation of the catalyst (as had been suggested by Brinkmann *et al.* (17)). To study other possible deactivation pathways, the stability of the dendritic catalyst **2** was investigated by performing retention measurements in dichloromethane. The retention of catalyst **2** was 99.7% after flushing the reactor with 10 reactor volumes. This result indicates that the catalyst, which was in the Pd(II) state, was stable under these conditions. During the catalytic cycle the catalyst also becomes Pd(0), so retention measurements of the catalyst in the Pd(0) state were attempted. The addition of one or more equivalents of diethylamine, which converts Pd(II) into Pd(0) (after nucleophilic attack), did not result in leaching of palladium (99.5% retention). Apparently, the catalyst was stable under conditions very similar to those of the catalysis experiments; only the allyl acetate substrate was absent. It was therefore concluded that the presence of allyl acetate facilitated the decomposition.

Dendrimers with a 1,2-ethanediyl spacer between the terminal silicon atom and the phosphorus atom (**3** and **4**) were also prepared by the group of van Leeuwen (18b). The larger dendrimer (**4**) was applied as a ligand in the continuous allylic amination reaction. Figure 5a shows that this dendritic catalyst is much more stable than the one incorporating dendritic catalyst **2** (maximum conversion reached after pumping 5 reactor volumes of substrate solution through the reactor) and that the rate of product formation was nearly constant during the next 10 reactor volumes. At the end of the experiment in the flow system, the conversion was still more than 70% of the maximum; the decrease in conversion corresponds to a retention of more than 98% of the dendritic catalyst. Under similar conditions when the P/Pd ratio was 4 (Fig. 5b) instead of the value of 2 used in the previous experiment (Fig. 5a), the maximum conversion obtained during the reaction was higher, showing that the dendritic catalyst was more active (since the palladium concentration was the same in both experiments) and also more stable. The small decrease in conversion during this experiment is attributed entirely to depletion of very small amounts of dendritic catalyst. On the basis of the curve shown in Fig 5b, the retention of the dendritic complex is estimated to be 98.5–99%, which is in the range of the expected values. We emphasize that the stability of the palladium catalyst is sensitive to relatively small changes of the dendritic backbone.

When the catalyst is located in the core of a dendrimer, its stability can also be increased by site-isolation effects. Core-functionalized dendritic catalysts supported on a carbosilane backbone were reported by Oosterom *et al.* (19). A novel route was developed to synthesize dendritic wedges with arylbromide as the focal point. These wedges were divergently coupled to a ferrocenyl diphosphine core to form dppf-like ligands (**5**). Other core-functionalized phosphine dendritic ligands have also been prepared by the same strategy (20).

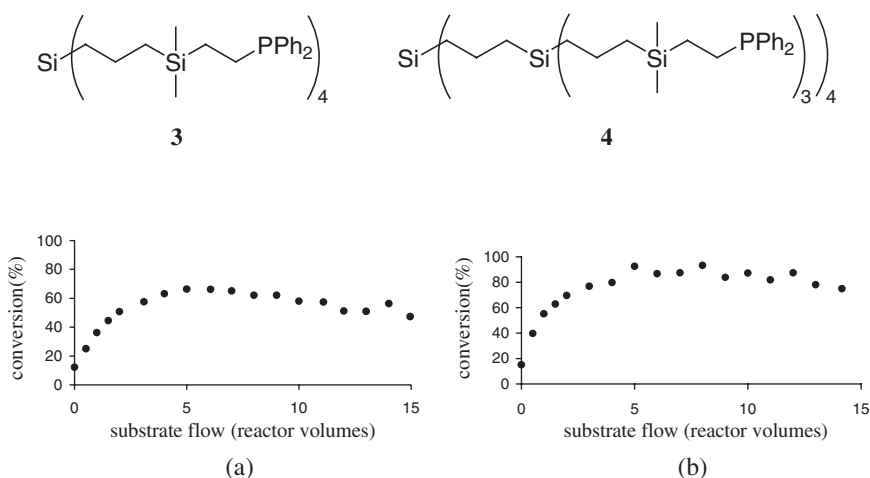
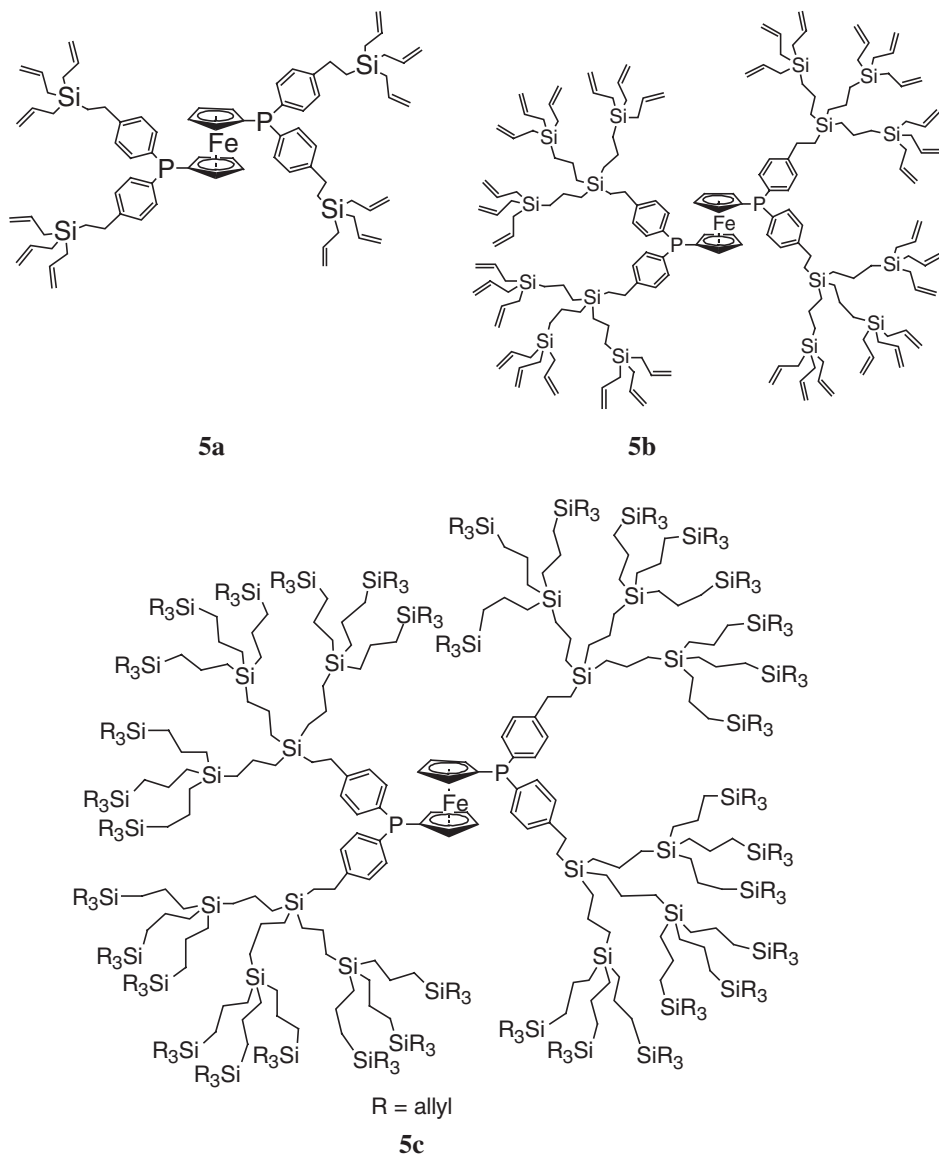


FIG. 5. Application of dendrimeric ligand **4** in the allylic amination of crotyl acetate and piperidine using a CFMR (% conversion of crotyl acetate in the product stream vs substrate flow), (a) P/Pd = 2, (b) P/Pd = 4, Koch MPF-60 NF membrane, molecular weight cut-off = 400 Da (18b).



Bidentate palladium complexes of **5** were formed upon the addition of  $\text{PdCl}_2$ , as shown by  $^{31}\text{P}$ -NMR spectroscopy, and even for the largest dendrimers steric interactions between the dendritic branches did not prevent the facile formation of the bidentate complex. Crotylpalladium chloride complexes were prepared *in situ* from these dendrimers and used as catalysts for allylic alkylation reactions. The regioselectivity for the branched product for the alkylation of 3-phenylallyl acetate with diethyl sodio-2-methylmalonate increased when the higher-generation dendrimers were used, albeit at the cost of a lower activity.

The recyclability of a catalyst incorporating dendritic ligand **5c** was tested by performing an allylic alkylation reaction in a CFMR. A mixture of the third-generation dendrimer **5c** and crotylpalladium chloride dimer in THF was incubated and injected into the reactor at room temperature. Subsequently, the reactor was fed with a solution of allyl trifluoroacetate, diethyl sodio-2-methylmalonate, and decane as an internal standard. Figure 6 shows that the conversion of substrate increased rapidly within the first 30 min until it stabilized at approximately 45%. The catalytic activity remained almost constant for 8 h, and in that period 20 reactor volumes of substrate solution had been pumped through the reactor. These data show that the core-functionalized dendritic complex was highly stable and active during the course of the experiment, especially compared to dendrimer **2**. The stability of the core-functionalized catalyst might be attributed to site-isolation effects, as a result of efficient encapsulation by the dendritic shell.

*A.1.2. Non-covalently Functionalized Dendrimers Applied in a CFMR.* In most systems reported so far, the catalyst is covalently linked to the dendritic support. An interesting alternative approach is the non-covalent anchoring of the catalyst to the dendrimers by using well-defined binding sites. The reversible nature of the non-covalent approach allows controlled de- and re-functionalization of the support, which enables the easy reuse of the support and simplifies the variation of catalyst loading even during catalysis. Such a novel non-covalent binding approach was recently reported in which phosphine ligands were anchored in the periphery of poly(propylene imine) dendrimers (**21**) via functional groups on the ligand that are complementary to those of the dendrimer support. The dendrimer provided directional binding sites for the strong but reversible binding of 32 guest molecules functionalized with the complementary binding pattern. The binding is based on a combination of multiple hydrogen bonds and ionic interactions (Fig. 7).

The binding constant of the anchor into the periphery of the dendrimer and that of the palladium to the ligand are very high; the guest–Pd–dendrimer complex remained intact during size-exclusion chromatography (SEC). The dendrimer containing 32 phosphine-functionalized guest molecules was used as a multidentate ligand in the palladium-catalyzed allylic amination with crotyl acetate and piperidine as the reactants. The reaction was fast; with a substrate to Pd ratio of 30, the

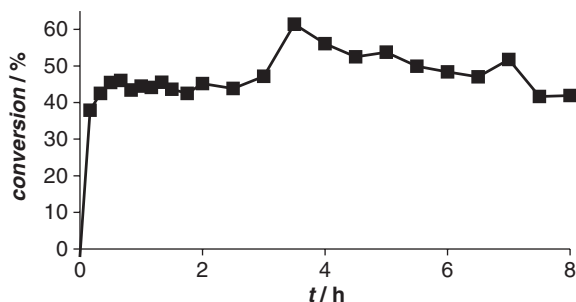


FIG. 6. Allylic alkylation in a continuous flow membrane reactor using dendritic ligand **5c** (flow rate 50 mL h<sup>-1</sup>; reactor volume 20 mL, Koch MPF-60 NF membrane, molecular weight cut-off = 400 Da; slight increases are due to pump failures) (*19b*).

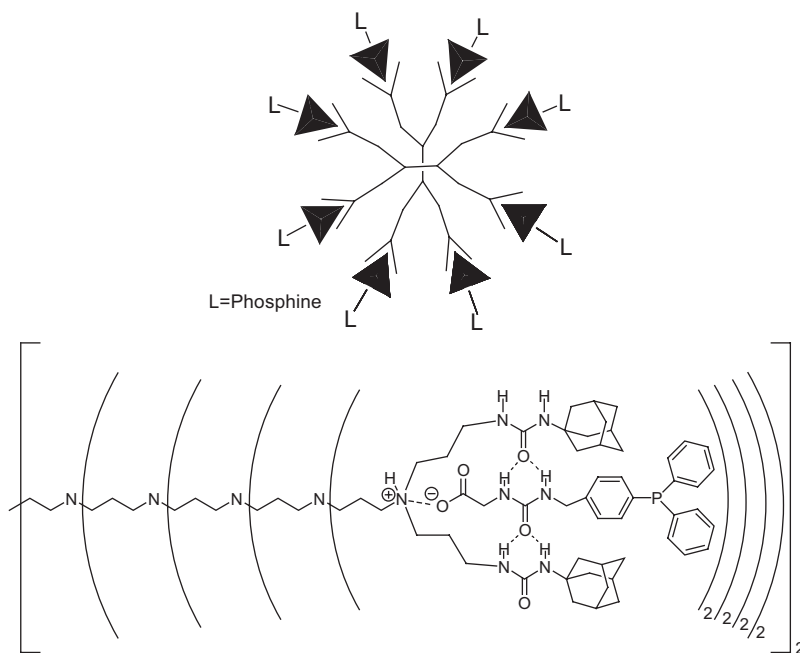


FIG. 7. Schematic representation of the non-covalent immobilization of ligands to a dendrimer support and the actual supramolecular dendritic complex containing 32 phosphine ligands (21).

conversion was more than 80% after 10 min. Approximately, the same rate and selectivity (branched/trans/cis ratio = 61:33:6) were observed for the monomeric palladium complex in the absence of the dendrimer.

The supramolecular guest–Pd–dendrimer complex was found to have a retention of 99.4% in a CFMR and was investigated as a catalyst for the allylic amination reaction. A solution of crotyl acetate and piperidine in dichloromethane was pumped through the reactor. The conversion reached its maximum (*ca.* 80%) after approximately 1.5 h (which is equivalent to 2–3 reactor volumes of substrate solution pumped through the reactor). The conversion remained fairly constant during the course of the experiment (Fig. 8). A small decrease in conversion was observed, which was attributed to the slow deactivation of the catalyst. This experiment, however, clearly demonstrated that the non-covalently functionalized dendrimers are suitable as soluble and recyclable supports for catalysts.

#### A.2. Hydrovinylation using Dendritic Catalysts in a CFMR

The hydrovinylation reaction, the codimerization of ethene and styrene (Scheme 2), provides easy access to chiral building blocks from inexpensive hydrocarbon feedstocks, which can be used further for the preparation of fine chemicals. Key problems in this reaction include the selectivity of the reaction and the stability of the catalyst. The main side reactions are oligomerization and isomerization of the product to internal achiral alkenes. The latter reaction can be suppressed by

keeping the conversion low. Performance of this reaction in a CFMR is therefore of interest because it can combine a high space-time yield with a low conversion and thus a high selectivity (22).

Eggeling *et al.* (23) functionalized carbosilane dendrimers with hemilabile P,O-ligands at the surface (6). The palladium allyl complexes of this compound were used as catalyst for the hydrovinylation reaction. In a batch process, the dendritic catalysts were found to be less active than the monomeric analogues, a result that was attributed to a combination of enhanced catalyst deactivation and increased steric hindrance. Isomerization of the product occurred at high conversion but was largely suppressed by stopping the reaction at low conversion. Retention of the multidentate ligand of **6a** (without palladium) was only 85%, but it was inferred to be sufficient for initial experiments in a CFMR. The results of such experiments, displayed in Fig. 9a, clearly show a rapid decrease in conversion. This drop was explained in part by leaching and in part by deactivation of the catalyst, which was

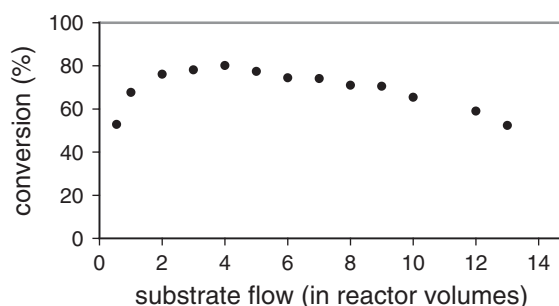
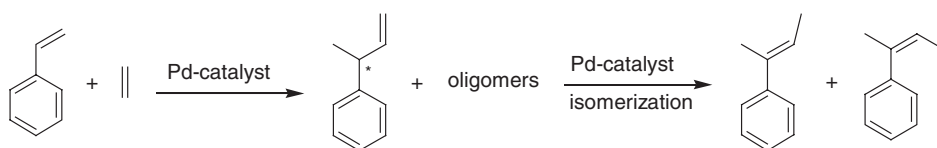
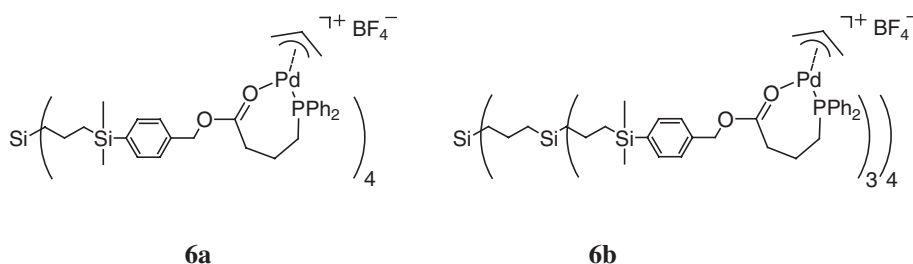


FIG. 8. Application of a non-covalently functionalized dendrimer (see fig. 7) in a CFMR in the allylic amination of crotyl acetate and piperidine in dichloromethane (Koch MPF-60 NF membrane, molecular weight cut-off = 400 Da) (21).



SCHEME 2.



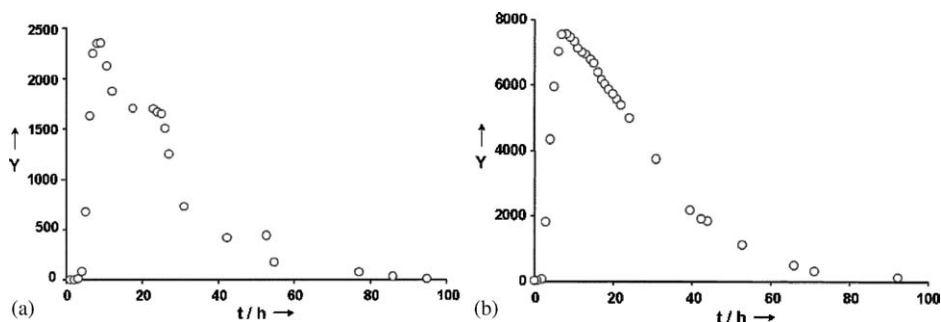


FIG. 9. Hydrovinylation in a CFMR using **6a** (a) and **6b** (b): Conditions:  $T = 23^{\circ}\text{C}$ ,  $p = 30$  bar, flow rates: ethene solution  $2.5\text{ mL h}^{-1}$  (10 M), styrene solution  $2.5\text{ mL h}^{-1}$  (1.8 M),  $\tau = 4$  h, MPF-60 NF membrane (Koch Int., Düsseldorf, Ger.). Y, space time yield ( $\text{mg L}^{-1}\text{ h}^{-1}$ ), for **6a**: 0.05 mmol Pd, L/Pd = 1; for **6b**, 0.13 mmol Pd, L/Pd = 1 (23).

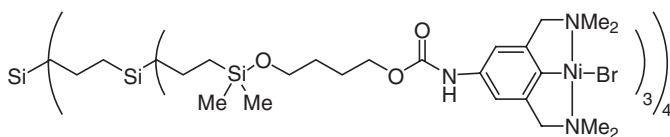
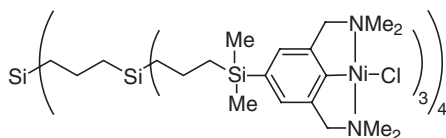
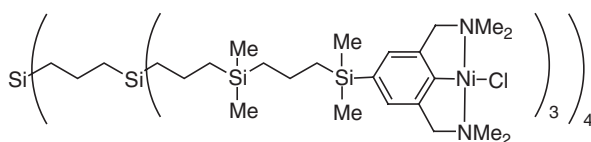
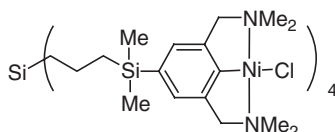
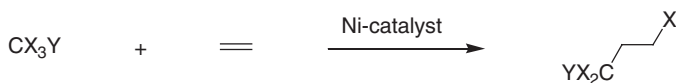
corroborated by the observation of palladium precipitated on the membrane. More importantly, in the hydrovinylation of styrene, the selectivity to the desired chiral 3-phenylbut-1-ene was high when the continuous-flow reactor was used.

In a subsequent experiment, the larger dendritic catalyst **6b** was used under optimized conditions, which was expected to result in a slower loss of activity. The results (Fig. 9b) did not show much improvement, indicating that catalyst deactivation was still a major problem. Indeed the number of turnovers (catalytic reaction events) of catalyst **6b** was only 260 in the continuous process compared with the value of 3273 determined in the batch reaction experiment; in contrast, the monomeric model compound showed a number of turnovers of 6027.

### A.3. Nickel-Catalyzed Kharasch Addition in a CFMR

An early example of a dendritic catalyst was reported by Knapen *et al.* (24), who functionalized G0 (generation zero) and G1 carbosilane dendrimers with up to 12 NCN pincer-nickel(II) groups (**7a**). These dendrimers were applied as catalysts in the Kharasch addition of organic halides to alkenes (Scheme 3).

Preliminary results obtained with compound **7a** in a CFMR indicated that the dendrimer decomposed (25), which was ascribed to hydrolysis of the Si–O bond of the linker between ligand and carbosilane backbone. The catalytically active complexes were disconnected from the support and subsequently washed out of the reactor. In species **7b–7d**, the NCN ligands are directly attached to the carbosilane backbone and therefore much more stable (26). The retentions for catalysts **7d** and **7c** were measured to be 97.4 and 99.75%, respectively, indicating that **7c** is sufficiently large for application in a CFMR without significant depletion of the catalyst after 100 cycles. During the experiments in the CFMR, the precipitation of *insoluble* purple species was noted. In an additional experiment, **7c** was applied in the CFMR with a continuous feed of  $[\text{Bu}_4\text{N}]\text{Br}$  to prevent catalyst precipitation (Fig. 10). Notwithstanding the fact that **7c** was successfully retained in the reactor and that precipitation was avoided, a fast decrease of the conversion was observed. The maximum activity (space-time yield) was reached after 600 min (after 15 cycles), and after 1800 min (45 cycles), the activity had dropped to nearly zero. ICP mass

**7a****7b****7c****7d**

SCHEME 3.

spectrometric analysis showed that the retention of **7c** under catalytic conditions was 98.6%, which indicates that the drop in activity resulted from catalyst deactivation.

#### A.4. Rhodium-Catalyzed Hydrogenation in a CFMR

One of the success stories of transition metal catalysis is the rhodium-complex-catalyzed hydrogenation reaction. Asymmetric hydrogenation with a rhodium catalyst has been commercialized for the production of L-Dopa, and in 2001 the inventor, Knowles, together with Noyori and Sharpless, was awarded the Nobel Prize in chemistry. After the initial invention, (enantioselective) hydrogenation has been subject to intensive investigations (27). In general, hydrogenation reactions proceed



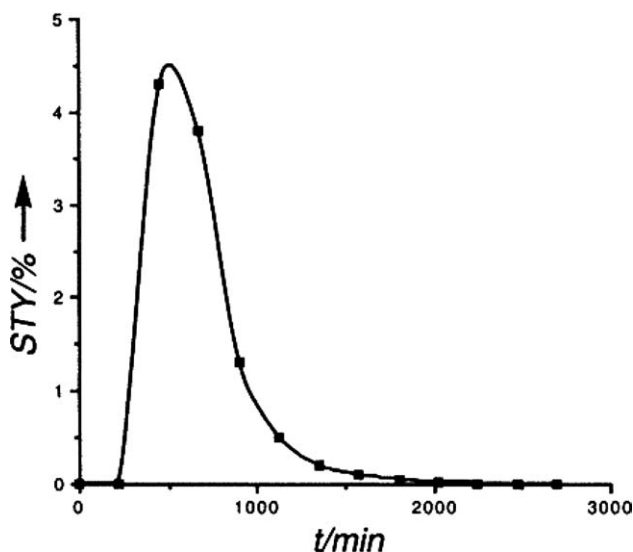
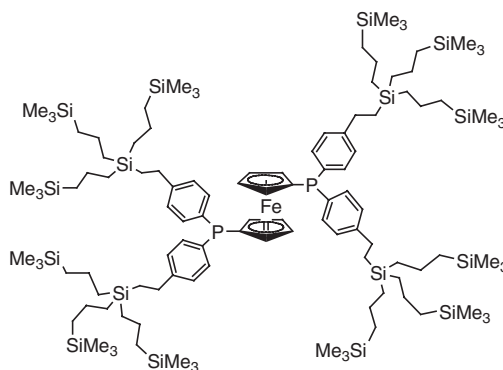


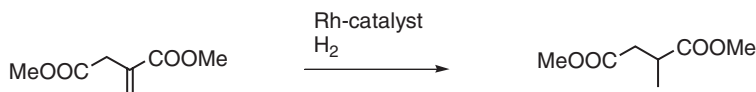
FIG. 10. The application of **7c** as catalyst for the Kharasch addition of methyl methacrylate and carbon tetrachloride in a CFMR using a SelRO-MPF-50 nanofiltration membrane. (Residence time (or cycle) is 43 min) (26).



**8**

under mild conditions; therefore, this reaction can be applied in a membrane reactor. For this purpose a rhodium complex of dendritic ligand **8** was used and compared with dppf (20).

The rhodium complexes were prepared *in situ* from the rhodium precursor  $[\text{Rh}(\text{nbd})_2](\text{ClO}_4)$  (nbd = 2,5-norbornadiene) and applied in the hydrogenation experiments under an initial hydrogen pressure of 5 bar at 35°C. The dendrimer structure had almost no effect on the activity of the catalyst in the batch-wise rhodium-catalyzed hydrogenation of dimethyl itaconate (Scheme 4).



SCHEME 4.

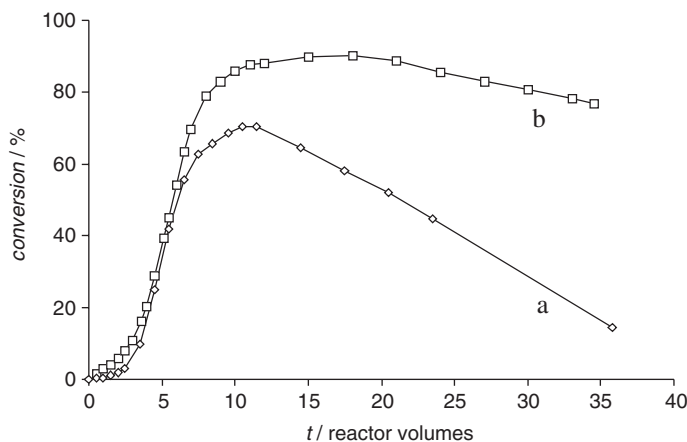


FIG. 11. The continuous hydrogenation of dimethyl itaconate using dpf (a) and the dendritic ligand **8**, (b) conversion (in %) versus time (expressed in reactor volumes pumped through the reactor) (20).

Before the start of the continuous reaction, the substrate solution was saturated with hydrogen by stirring under 5 bar of  $\text{H}_2$  for 16 h. Subsequently, a premixed solution of the ligand and the rhodium precursor  $[\text{Rh}(\text{nbd})_2](\text{ClO}_4)$  was injected into the membrane autoclave, after which the substrate solution was pumped through the reactor.

Figure 11 shows the conversion of dimethyl itaconate versus time for two experiments carried out with dpf and dendritic ligand **8** under identical conditions. The hydrogenation with dpf increased to a maximum conversion of approximately 70% after the flow of approximately 10 reactor volumes, after which it rapidly decreased to only 15% after 35 reactor volumes. In contrast, after reaching a maximum at approximately 85%, the conversion in the reaction with dendritic ligand **8** remained high, still showing a conversion of 77% after 35 reactor volumes. The amounts of metal and ligand depletion during the catalytic experiment were determined by ICP-AES analysis. The amount of metal leaching is similar to that of the phosphine, indicating that the ligand–metal interaction was sufficiently strong to suppress metal leaching. The ICP-AES analyses show that the loss of both ligand and rhodium from the reactor in the hydrogenation experiment with dendritic ligand **8** was much less than that for dpf. The experimental curves in Fig. 11 can be explained completely by the retentions (determined from the ICP-AES analyses) of 97% for the dpf–rhodium(nbd) complex and 99.8% for the dendritic catalyst. A

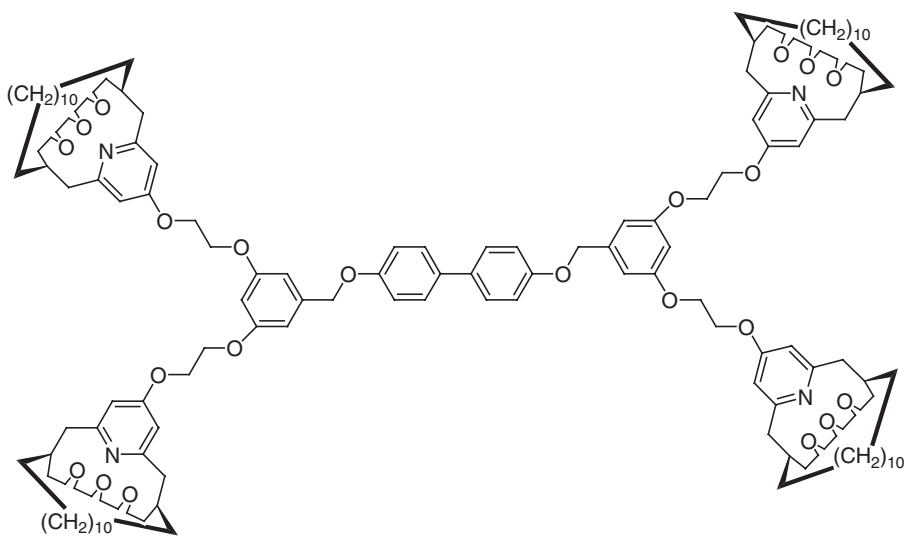
further improvement of the recyclability of these catalysts might be expected if larger dendrimers were used.

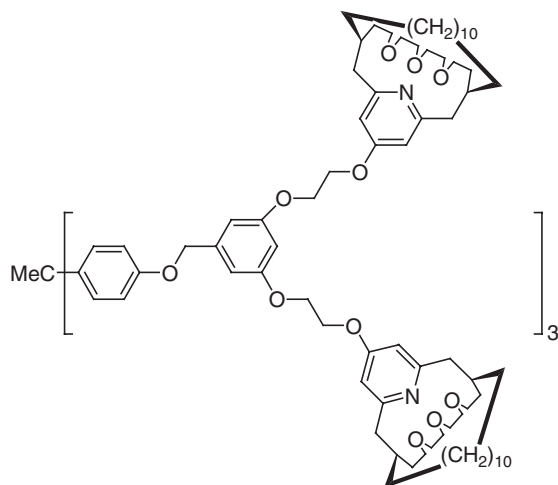
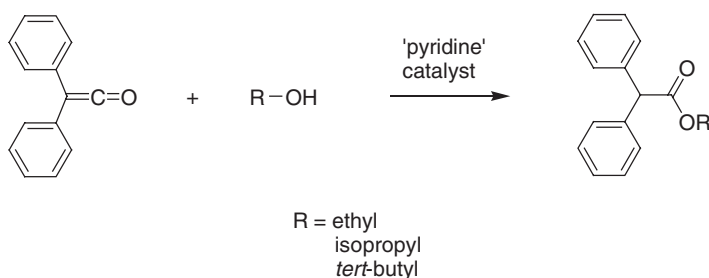
## B. CATALYST RECYCLING USING NANOFILTRATION IN BATCH PROCESSES

An alternative to the CFMR is the use of the nanofiltration technique in a batch process. In such a process the dendritic catalyst is separated from the reaction mixture after completion of the reaction. The typical advantages of continuous-flow experiments obviously do not apply in these experiments. On the other hand, the requirements with respect to stability and retention of the dendritic system are less stringent. The problem of metal leaching applies to the state of the catalyst after reaction, as catalyst leaching can take place only during the recycling procedure. The majority of reported batch-wise nanofiltration experiments with dendritic catalysts were performed primarily to assess whether these catalysts can be operated in a CFMR. However, the results obtained in a batch-wise process cannot be extrapolated to a CFMR. A typical example of a system for which large differences between batch and continuous operation may be encountered is a carbonylation reaction; in a flow system, metal carbonyl species may form that are leached in the presence of CO, but during the batch-wise recycling in the absence of CO, all the metal may return to the immobilized ligand.

### B.1. Acylation Reactions

Marquardt and Luning (28) immobilized concave pyridines on two types of dendrimers (9 and 10) to obtain a recoverable acylation catalyst. For comparison



**10**

SCHEME 5.

they also immobilized the concave pyridines on a Merrifield resin and a soluble poly(vinyl benzylchloride) polymer. Complete functionalization of the dendrimers was achieved, whereas only 9% of the Merrifield resin and 29% of the poly(vinyl benzylchloride) polymer functional groups reacted with the concave pyridine. The enhanced selectivity in an intermolecular competition acylation experiment with ethanol, isopropanol, and *tert*-butyl alcohol (Scheme 5), which was caused by the concave pyridines on the four different supports, was investigated (Table I).

The observed selectivity of the acylation with diphenylketene for the ethyl, isopropyl, and *tert*-butyl ester products of the monomeric concave pyridine, **9** and **10**, was almost the same. Lower selectivities were found when the modified Merrifield resin and poly(vinyl benzylchloride) polymer were used. Dendrimer **10** (MW = 3,863 Da) could be recovered from the reaction mixture in 70–90% yield by nanofiltration over a membrane.

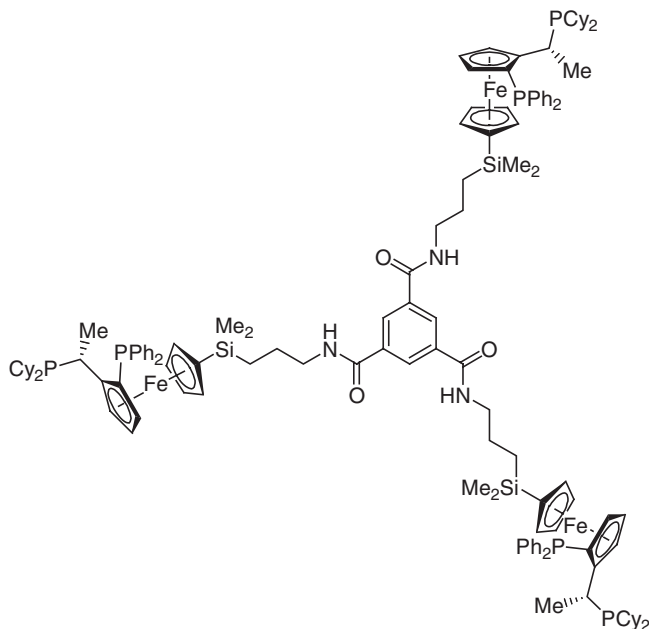
TABLE I  
*Intermolecular Competition Acylation Experiment of Ethanol, Isopropanol and tert-Butanol  
 with Diphenylketene*

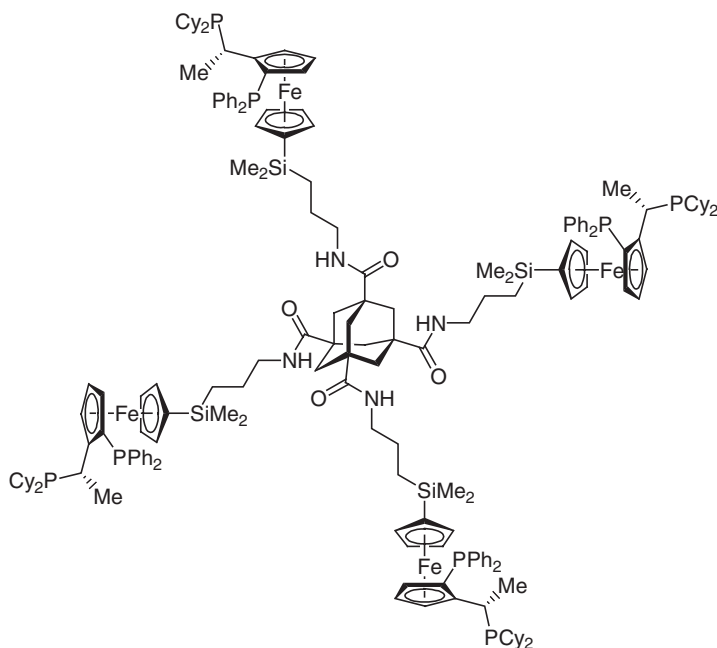
Immobilized pyridine	Ethyl ester	Isopropyl ester	tert-butyl ester
<b>9</b>	12.0	1	0
<b>10</b>	11.4	1	0
Merrifield resin	7.4	1	0
poly(Vinyl benzylchloride) polymer	9.5	1	0

Conditions: [alcohol] = [catalyst] = 50 mM; [ketene] = 5 m.

## B.2. Asymmetric Hydrogenation

Köllner *et al.* (29) prepared a Josiphos derivative containing an amine functionality that was reacted with benzene-1,3,5-tricarboxylic acid trichloride (**11**) and adamantane-1,3,5,7-tetracarboxylic acid tetrachloride (**12**). The second generation of these two types of dendrimers (**13** and **14**) were synthesized convergently through esterification of benzene-1,3,5-tricarboxylic acid trichloride and adamantane-1,3,5,7-tetracarboxylic acid with a phenol bearing the Josiphos derivative in the 1,3 positions. The rhodium complexes of the dendrimers were used as chiral dendritic catalysts in the asymmetric hydrogenation of dimethyl itaconate in methanol (1 mol% catalyst, 1 bar H<sub>2</sub> partial pressure). The enantioselectivities were only





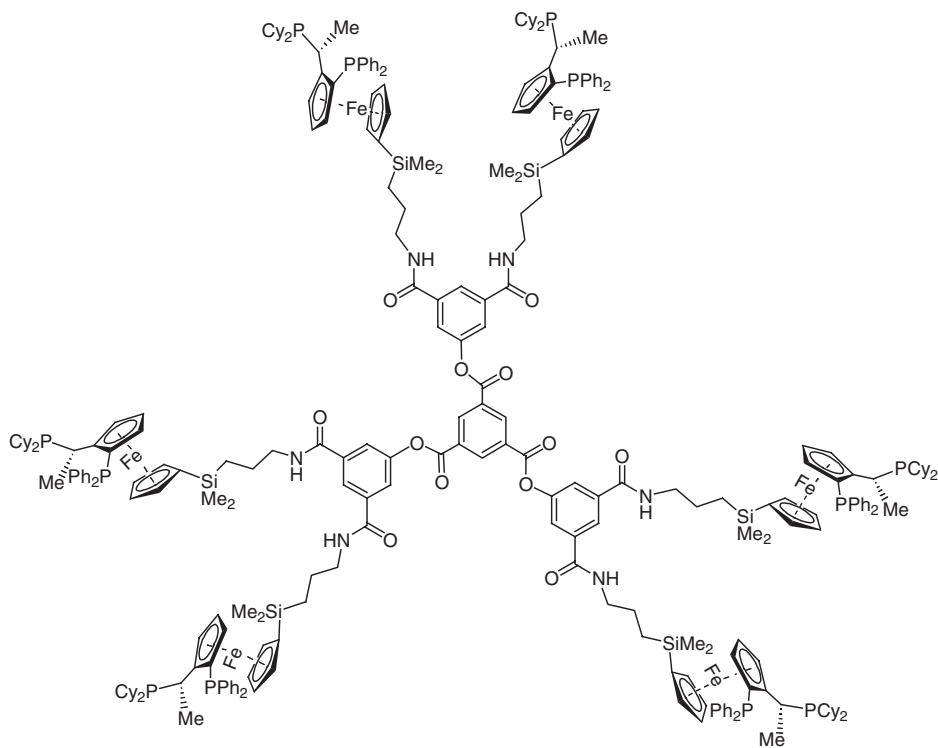
12

slightly lower than those obtained with the Josiphos parent compound (Table II). Preliminary nanofiltration experiments with dendrimers **13** and **14** (MD 4.8 and 6.5 kDa, respectively) with a Millipore Centricon-3 membrane having a pore size of 3 kDa and methanol as the solvent showed complete retention of the dendrimers.

### B.3. Asymmetric Borohydride Reductions

Schmitzer *et al.* (30) synthesized four generations of peripherally D-gluconolactone functionalized polyamidoamine (PAMAM) dendrimers (**15–18**), which were used as chiral ligands for the sodium borohydride reduction of prochiral aromatic ketones, either in water (homogeneous) or in tetrahydrofuran (heterogeneous) (Scheme 6). In the latter case, high enantioselectivities were achieved with the third-generation dendrimer (**16**), even for aliphatic ketones that are notorious for giving products with low enantioselectivities. The asymmetric reduction of acetophenone with a stoichiometric amount of sodium borohydride was investigated in the presence of water and of THF.

In water, the third-generation (**16**) and fourth-generation dendrimers (**17**) induced chirality toward the (*S*)-enantiomer (50% ee for **16** and 98% ee for **17**). In THF high enantiomeric excess was achieved only with the third-generation dendrimer (99% (*S*) ee for **16** and 3% (*S*) ee for **17**). Dendrimer **16** was recovered from the heterogeneous reaction mixture by nanofiltration on a Millipore microporous membrane system. After regeneration of the catalytic activity by treatment with



13

HCl/methanol, it could be reused, yielding the same results (for as many as 10 times).

#### B.4. Kharash Addition

Albrecht *et al.* (31) synthesized a series of polybenzyl ether dendrimers containing a pincer metal (Ni, Pt) at the focal point of the wedge (**19–22**). Coordination of SO<sub>2</sub> to the pincer-platinum complex resulted in a change in color of the dendrimer solutions from colorless to orange, a property that facilitates the investigation of the recoverability of these dendrimers by membrane filtration. The generation-dependent leaching of the dendrimers from a membrane-capped immersion vial was followed in time by UV–Vis spectroscopy. The retention of the first-generation dendrimer (**19**) was moderate (half-life  $t_{1/2}$  = 108 h). The second-generation dendrimer (**20**) displayed a  $t_{1/2}$  of ca. 300 h, whereas the third-generation dendrimer (**21**) was characterized by a  $t_{1/2}$  of > 1500 h. The third-generation nickel-pincer functionalized dendrimer (**22**) was applied in the Kharasch addition of CCl<sub>4</sub> to methyl methacrylate. The dendritic catalyst **22** (0.33 mol%) showed the same reaction rate and number of turnovers as the parent nickel-pincer complex (31). The dendritic nickel catalyst could be recovered when the reaction was performed in the

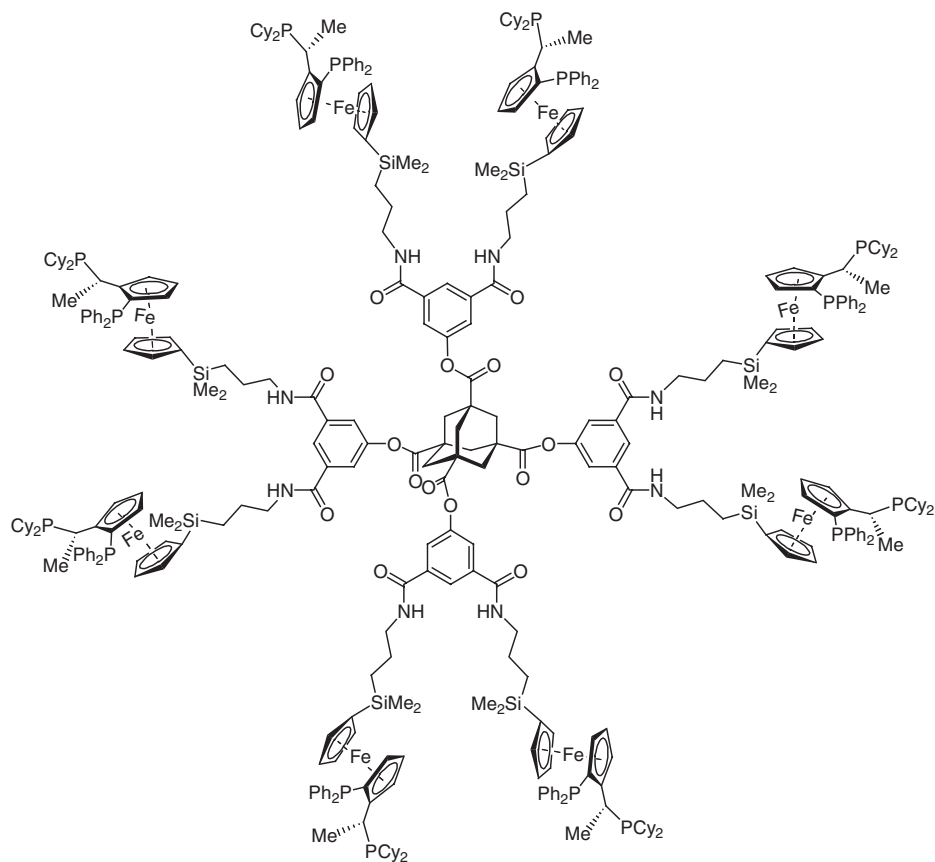
**14**

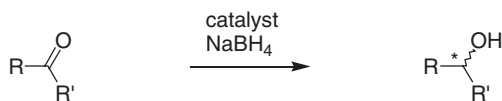
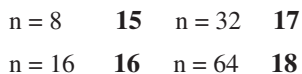
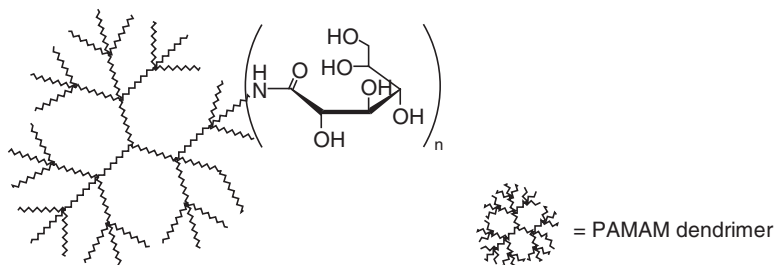
TABLE II  
Asymmetric Hydrogenation of Dimethyl Itaconate

Ligand	Enantiomeric excess (%)
Josiphos	99.0
<b>11</b>	98.6
<b>12</b>	98.7
<b>13</b>	98.1
<b>14</b>	98.0

Conditions: 1 mol% Rh catalyst, 1 bar H<sub>2</sub> pressure, MeOH.

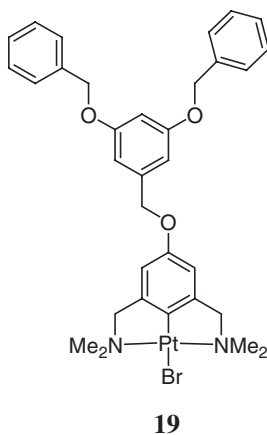
membrane-capped immersion vial by a simple washing procedure. We note that this recycling procedure of the dendritic catalyst is based on diffusion only, which limits the product flux.





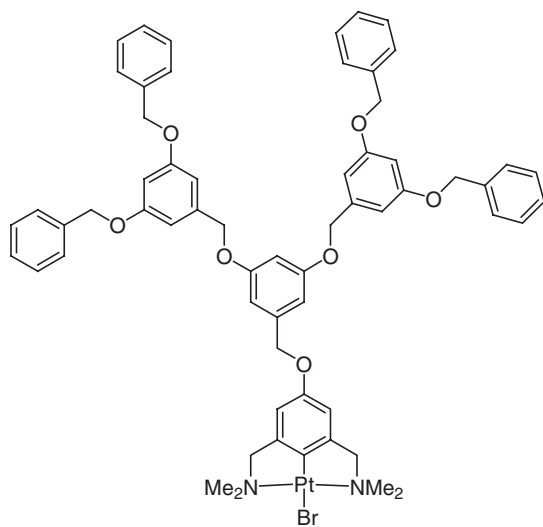
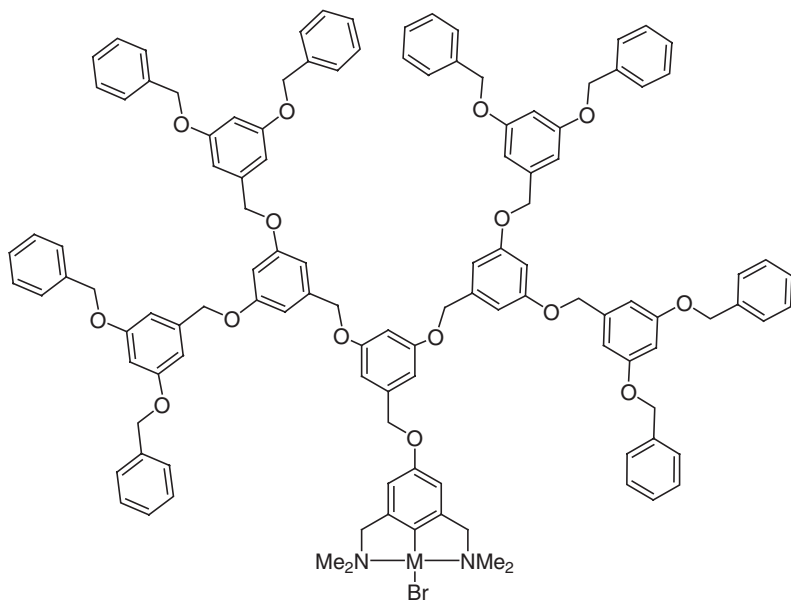
R, R' = aromatic, aliphatic

SCHEME 6.



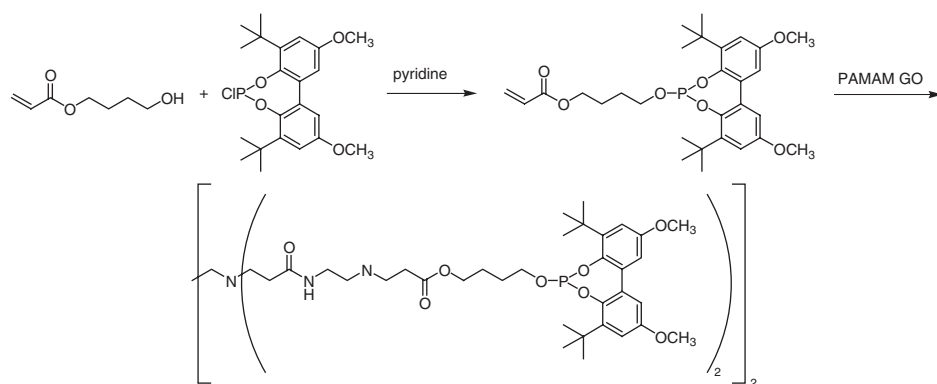
### B.5. Hydroformylation

Tulchinsky and Miller (32) patented dendritic macromolecules, their metal complexes, and their use in catalytic processes such as hydroformylation. Dendrimers containing organophosphites, organophosphonites, and/or organophosphinites were

**20****21** M = Pt**22** M = Ni

claimed. Examples of the synthesis of five generations of phosphite-functionalized PAMAM dendrimers, their use in hydroformylation, and separation via nanofiltration were described. A ligand precursor was synthesized by reaction of 4-hydroxybutyl acrylate with (3,3'-di-*tert*-butyl-5,5'-dimethoxy-1,1'-biphenyl-2,2'-diyl) phosphorochloride in the presence of pyridine. The precursor was subsequently reacted with five generations of PAMAM dendrimers (G0–G4, Michael addition) yielding G0–G4 dendrophites (Scheme 7; the zeroth generation is shown). The dendrophites were used in the hydroformylation of propene. A decrease in reaction rate was observed upon increasing the generation of dendrophite, whereas the linear-to-branched ratio of the product was the same for all systems (Table III).

After the hydroformylation reaction, product mixtures were passed through nanofiltration (reverse osmosis) membranes MPF-50 (available from Membrane Products Kiryat Weizmann Ltd., Israel), which are cross-linked GKSS membranes with an active layer thickness of 1  $\mu\text{m}$  and 10  $\mu\text{m}$  (available from GKSS, Forschungszentrum Geesthach GmbH, Germany) with Texanol<sup>®</sup> used as the solvent. No detectable dendritic material was found in the permeate solutions, indicating that under these conditions the dendrimer is stable. The retention of rhodium and the permeate flux rate were measured (Table IV). The experiment was also



SCHEME 7.

TABLE III  
*Hydroformylation of Propene using Dendrophites G0–G4*

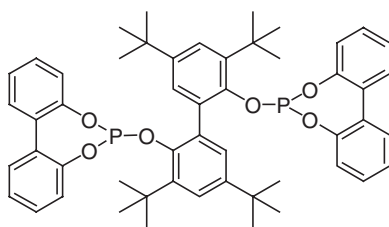
Ligand	Rate ( $\text{mol L}^{-1} \text{h}^{-1}$ )	l/b ratio
Dendrophite G0	3.2	1.32
Dendrophite G1	2.9	1.38
Dendrophite G2	2.0	1.41
Dendrophite G3	1.9	1.38
Dendrophite G4	1.8	1.40

Conditions: 0.039 mmol Rh; P/Rh = 8:1;  $p$  = 6.89 bars, propene:CO:H = 1:1:1;  $T$  = 70°C; 15 g Texanol<sup>®</sup> solution in a 100 mL reactor.

TABLE IV  
Rhodium Retention and Flux Rate Measured for the Nanofiltration of Hydroformylation Mixtures

Ligand	MPF-50		GKSS (1 $\mu$ m)		GKSS (10 $\mu$ m)	
	% Rh retention	Flux rate	% Rh retention	Flux rate	% Rh retention	Flux rate
G0	99.59	6.11	99.60	28.51	99.84	8.14
G1	99.74	13.85	99.86	21.18	99.86	12.22
G2	99.88	4.48	99.95	5.70	99.96	7.33
G3	99.92	4.07	99.94	9.77	99.96	9.77
G4	99.89	2.57	99.93	2.57	99.94	2.73
23	65	12.2–20.4	n. d.	n. d.	88	6.1–8.1

Flux rate:  $\text{L m}^{-2} \text{d}^{-1}$ . Conditions: Flow rate:  $100 \text{ mL min}^{-1}$ ;  $p = 20.67 \text{ bar}$  for MPF-50 and GKSS (1  $\mu$ m);  $p = 10.33 \text{ bar}$  for GKSS (10  $\mu$ m); solvent: Texanol<sup>®</sup>.



23

performed with a bidentate phosphite ligand (**23**), with the results showing a lower retention than observed with the higher generations of dendrimers. The use of the GKSS (10  $\mu$ m) membrane led to the highest retentions.

Remarkably, rhodium leaching was almost completely suppressed when these dendrimers were used, which may be explained in several ways. For example, one explanation is that the ligands on the dendritic surface were in such close proximity to each other that a chelating effect prevented leaching. Another explanation is that the binding of rhodium to polar groups (e.g., amides and esters) present in the dendritic backbone during the recycling procedure, which was performed under syngas-deficient conditions, minimized the leaching. The best retentions were found for the third- and not the fourth-generation dendrimers. Furthermore, a significant drop in the flux rate was observed when the fourth-generation dendrimer was used.

The same nanofiltration experiments were performed with a 50-Å ultrafiltration membrane (available from US Filter/Membralox, Warrendale, PA, USA), this time with a monodentate phosphite ligand (**24**) used for comparison and toluene as the solvent (Table V). Both higher retentions and flux rates for the dendrimers were obtained relative to what was observed with the reverse osmosis membranes. Dendrophite G4 was used in three subsequent reactions carried out with this procedure.

Recycling experiments were performed with the second- and third-generation dendrophites. Hydroformylation of propene was carried out in toluene, followed by

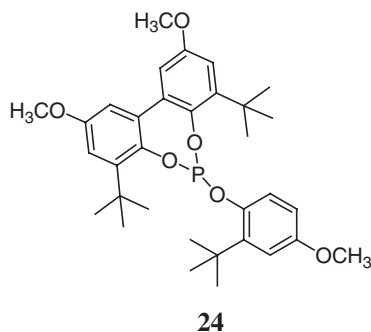


TABLE V  
*Rhodium Retention and Flux Rate Measurements using a 50 Å Ultrafiltration Membrane*

Ligand	Cycle	% Rh retention	Flux rate
24	1 <sup>st</sup>	83–86	171.04
Dendrophite G2	1 <sup>st</sup>	99.994	81.45
Dendrophite G3	1 <sup>st</sup>	99.997	77.38
Dendrophite G4	1 <sup>st</sup>	99.9975	52.94
Dendrophite G4	2 <sup>nd</sup>	99.9974	89.59
Dendrophite G4	3 <sup>rd</sup>	99.994	85.52

Flux rate:  $\text{L m}^{-2} \text{d}^{-1}$ . Conditions: flow rate:  $100 \text{ mL min}^{-1}$ ; solvent: toluene.

separation of the dendritic catalyst from the reaction mixture by passing it over the 50-Å ultrafiltration membrane. The catalyst solution was used in a second hydroformylation reaction. The differences in reaction rate between the two runs were only 2% and 3% for the second- and third-generation dendrimers, respectively.

### C. DENDRITIC CATALYST RECYCLING BY PRECIPITATION

Separation of catalysts from high-value products such as fine chemicals or pharmaceuticals is often accomplished by precipitating the catalyst from the product solution. Recycling of these catalysts is feasible, provided that they do not decompose. In industry, catalyst recovery by means of catalyst precipitation is applied only in relatively small batch processes. An example of such a process is the production of (–)-menthol (33) in which an Rh-BINAP isomerization catalyst converts the allylic amine substrate into (*R*)-citronellal (after hydrolysis of the enamine) in high yield (99%) and with high enantioselectivity (98.5% ee). After distillation of the solvent (THF) and product, the catalyst is recovered from the residue by precipitation with *n*-heptane.

The physical properties of dendrimers such as solubility, arising from their hyperbranched globular shapes and the peripheral groups, can be modified by end-group modification. In core-functionalized dendrimers, the immiscibility of the wedges with a solvent enables precipitation and subsequent separation by filtration.

In periphery-functionalized dendritic catalysts, the functional groups at the surface determine the solubility and miscibility and thus the precipitation properties. Many dendrimers functionalized with organometallic complexes do not dissolve in apolar solvents, and the presence of multiple metal centers at the periphery facilitates precipitation upon addition of this type of solvent. It is emphasized that the use of dendrimer-immobilized catalysts with the goal of recovery through precipitation is worthwhile only if the tendency to precipitation of the dendritic system exceeds that of its non-dendritic equivalent.

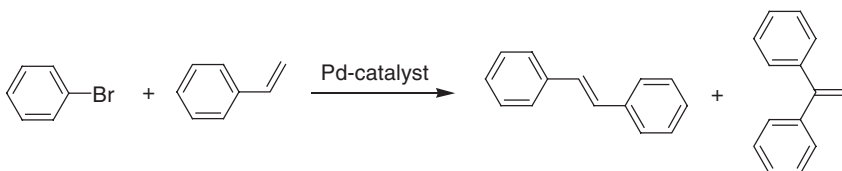
### C.1. Heck and Sonogashira Reaction

Reetz *et al.* (16) were the first to recover and recycle a dendritic catalyst through a precipitation procedure. The dimethylpalladium complex of the phosphine-functionalized DAB-dendr-[N(CH<sub>2</sub>PPh<sub>2</sub>)<sub>2</sub>]<sub>16</sub> dendrimer (**1a**) is an active catalyst for the Heck reaction of bromobenzene and styrene to give *trans*-stilbene (89% *trans*-stilbene and 11% 1,1-diphenylethylene, at a conversion of 85–90%, Scheme 8).

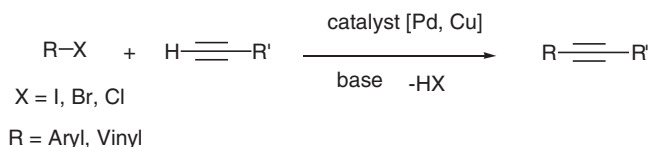
In contrast to the behavior of the monomeric catalyst, no decomposition to palladium metal was observed when dendrimer **1a** was used. The dendritic complex was recovered from the reaction mixture by precipitation with diethyl ether (yield >98%) and subsequent filtration. The precise structure of the recovered palladium complex was not determined, but the palladium-containing dendrimer showed only a small decrease in activity.

Heuzé *et al.* (34) synthesized three generations of bis(*tert*-butylphosphine)- and bis(cyclohexylphosphine)-functionalized Pd(II) DAB dendritic complexes that serve as copper-free recoverable catalysts for the Sonogashira coupling between aryl halides and alkynes (Scheme 9).

Treatment of the dendritic phosphines DAB-dendr-[N(CH<sub>2</sub>-NCH<sub>2</sub>PR<sub>2</sub>)<sub>2</sub>]<sub>x</sub> with Pd(OAc)<sub>2</sub> gave the Pd(II) dendrimers DAB-dendr-[N(CH<sub>2</sub>-NCH<sub>2</sub>PR<sub>2</sub>)<sub>2</sub>Pd(OAc)<sub>2</sub>]<sub>x</sub>



SCHEME 8.



SCHEME 9.

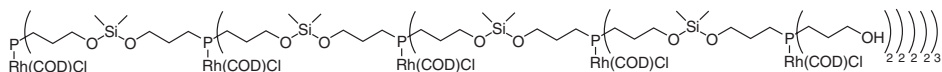
(R = Cy, tBu; x = 4, 8, 16). These new palladodendritic catalysts exhibit very good activity under mild conditions with aryl iodides and bromides in the Sonogashira reaction. The catalytic activity of systems with tBu substituents on the phosphines was much higher than those with Cy substituents. However, a similar negative dendritic effect was observed for both families, i.e., the third-generation catalysts are the less active ones. This observation is attributed to the increasing steric bulk around the active metal centers.

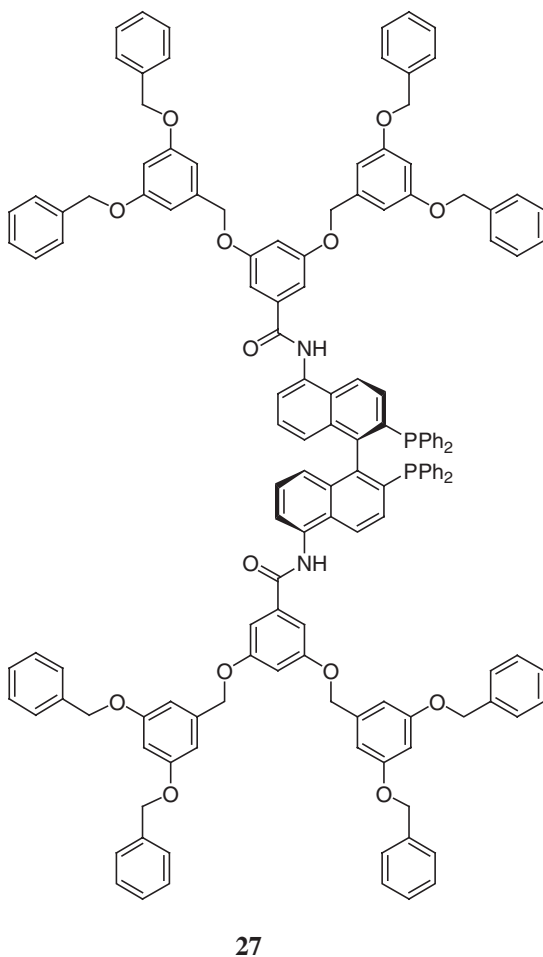
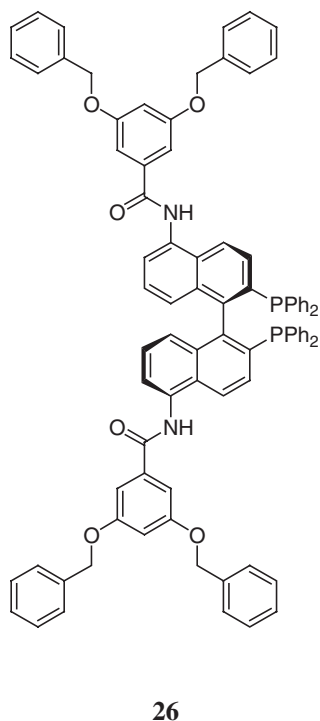
Recovery of the metallodendritic catalysts with Cy substituents was achieved by precipitation with pentane, and the dendrimers were reused five times without significant loss of activity. However, the tBu-substituted catalysts could not be recovered by this method as a consequence of their high solubility in pentane.

### C.2. Hydrogenation

Kakkar *et al.* (35) prepared organophosphine dendrimers up to the fourth generation (25) using phosphorus both as the branching point and as the ligand. The corresponding Rh(I) organometallic dendrimers (having Rh(I) coordinated to every branching point) were obtained by a reaction with  $[(\mu\text{-Cl})(\text{COD})\text{Rh}]_2$ . All Rh(I) organometallic dendrimers were found to be efficient catalysts for alkene hydrogenation reactions. Dendrimers of generations 1–4 (containing, respectively, 4, 10, 22, and 46 Rh(I) metal sites) were employed in the hydrogenation of 1-decene in THF under standard conditions (25°C, 20 bar  $\text{H}_2$ , 30 min, metal-to-substrate ratio = 1:200). The activity of each of the dendritic catalysts was similar to that of the monomeric analogue  $\text{Rh}(\text{COD})(\text{Cl})\text{P}\{(\text{CH}_2)_3\text{OH}\}_3$  (TOF  $\approx 400 \text{ h}^{-1}$ ), and there was only a slight decrease in activity observed for the larger systems. The recoverability and stability of the fourth-generation dendrimer (having 46 Rh(I) centers) was tested. Pentane extraction of the hydrogenation product from the reaction mixture followed by recrystallization from a THF/hexanes mixture resulted in recovery of this organometallic dendrimer. The recovered dendrimer was applied in a second hydrogenation run under the same conditions, giving an activity of 95% of that observed in the first run. Unfortunately, the same recycling procedure was not tested for the dendrimers of the earlier generations.

BINAP core-functionalized dendrimers were synthesized by Fan *et al.* (36), via condensation of Fréchet's polybenzyl ether dendritic wedges to 5,5'-diamino-BINAP (26–28). The various generations of BINAP core-functionalized dendrimers were tested in the ruthenium-catalyzed asymmetric hydrogenation of 2-[p-(2-methyl-propyl)phenyl]acrylic acid in the presence of 80 bar  $\text{H}_2$  pressure and in a 1:1 (v/v) methanol/toluene mixture. As later generations of the *in situ* prepared cymeneruthenium chloride dendritic catalysts were used, higher activities were observed (TOF values were 6.5, 8.3, and  $214 \text{ h}^{-1}$  respectively). Relative to those of the BINAP



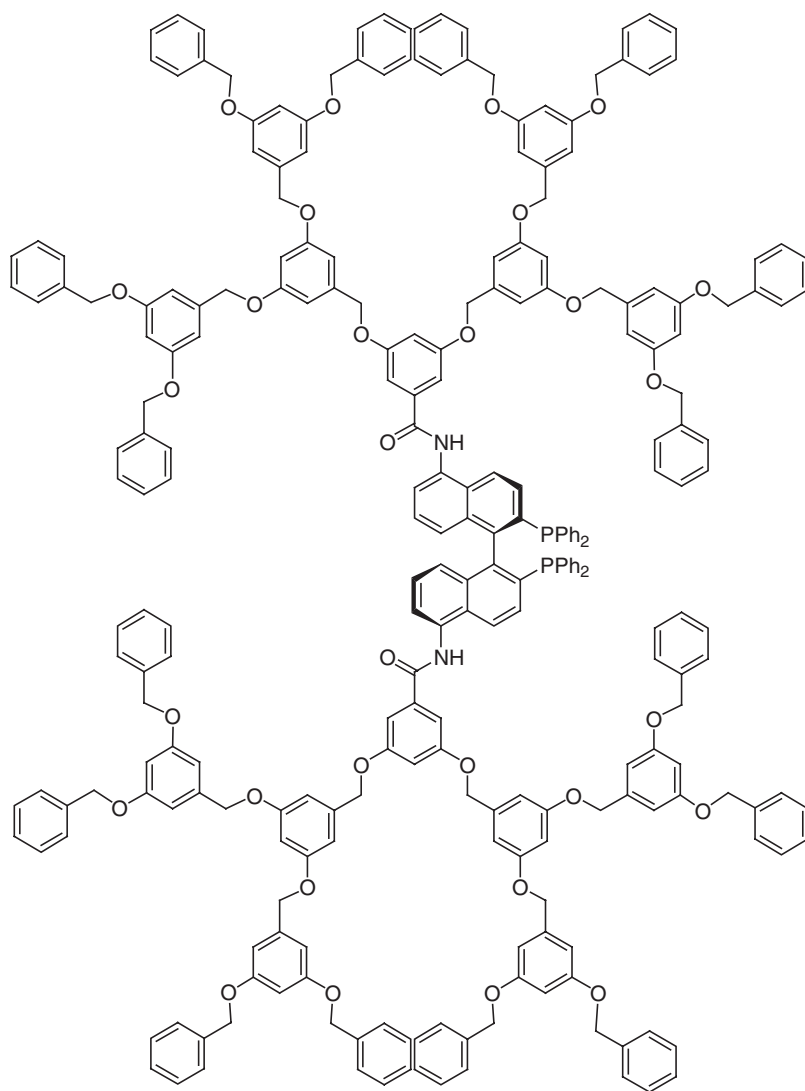


system (TOF  $6.3 \text{ h}^{-1}$ , ee 89.8% (S)) higher activities and (opposite) enantioselectivities were found for the dendritic catalysts (ee: **26** 91.8% (R), **27** 92.6% (R) and **28** 91.6% (R)). The dendritic catalyst composed of dendrimer **28** was quantitatively recovered by precipitation with methanol. The catalyst was reused three times, showing constant activity and enantioselectivity.

### C.3. Oxidation

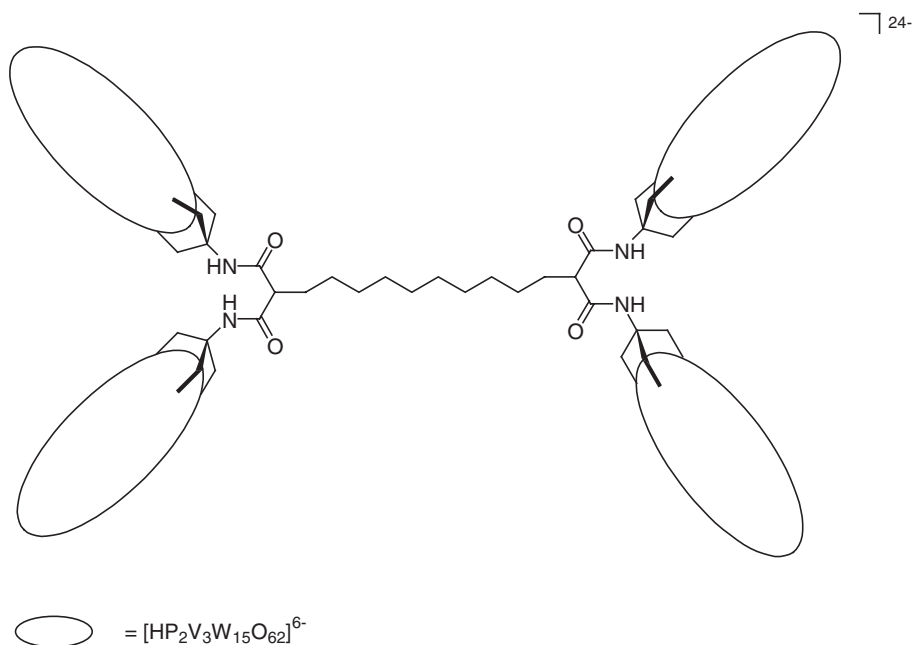
Zeng *et al.* (37) reported the synthesis and catalytic activity of tetra(polyoxometalate) dendrimers. The catalytically active polyoxometalate (POM)  $(n\text{Bu}_4\text{N})_5 [\text{H}_4\text{P}_2\text{V}_3\text{W}_{15}\text{O}_{62}]$  was esterified with two types of dendrimers containing four tris(hydroxymethyl) groups (**29** and **30**). Via an ion-exchange process, the dendrimer counterions  $n\text{Bu}_4\text{N}^+$  were fully replaced by  $\text{H}^+$ . The POM-functionalized dendrimer **29** and its  $\text{H}^+$ -exchanged form (**29-H**) were used as catalysts in the





28

oxidation of tetrahydrothiophene by  $t\text{BuOOH}$  in acetonitrile and in toluene. The oxidation activity of dendrimers **29-H** and **29** in the presence of *p*-toluenesulfonic acid was higher than that of the reaction in the absence of dendrimer with *p*-toluenesulfonic acid. POM dendrimer **29** by itself showed hardly any activity. The POM dendrimers **29-H** and **29** were recovered from the reaction mixture by precipitation after the addition of diethyl ether, and the recycled catalyst did not show any loss in activity.



## 29

Another example of dendritic POM complexes used as recoverable oxidation catalysts was reported by Plault *et al.* (38). A series of ionic polyammonium dendrimers containing between 1 and 6 POM units were prepared and used to catalyze the epoxidation of cyclooctene in a biphasic water/ $\text{CDCl}_3$  system. A comparison of the homogeneous mono-, bis-, tris-, and tetra(POM) catalysts indicated that there was no dendritic effect on the reaction kinetics within this series. However, a dendritic effect was found in the recovery of the catalysts. The dendritic catalysts were precipitated from the organic phase by addition of pentane. The recovery of the tri- and tetra-(POM) catalysts was easier (80–85% and 96%, respectively) than that of the mono(POM) catalyst.

#### C.4. Stille Couplings, Knoevenagel Condensations, and Michael Addition Reactions

Maraval *et al.* (39) synthesized core- and periphery-functionalized ruthenium and palladium dendritic diphosphines (Fig. 12) that were applied in three reactions (Stille coupling, Knoevenagel condensation, and diastereoselective Michael addition). The catalyst was recovered by using the precipitation strategy.

The third-generation dendrimer palladium complex (31, containing 24  $\text{PdCl}_2$  groups) was applied in the Stille coupling of methyl-2-iodobenzoate with 2-(tributylstannyl)thiophene in DMF (Scheme 10; 1 mol% catalyst). In contrast to what was observed with the monomer  $(\text{PPh}_3)_2\text{PdCl}_2$ , no palladium metal formation was

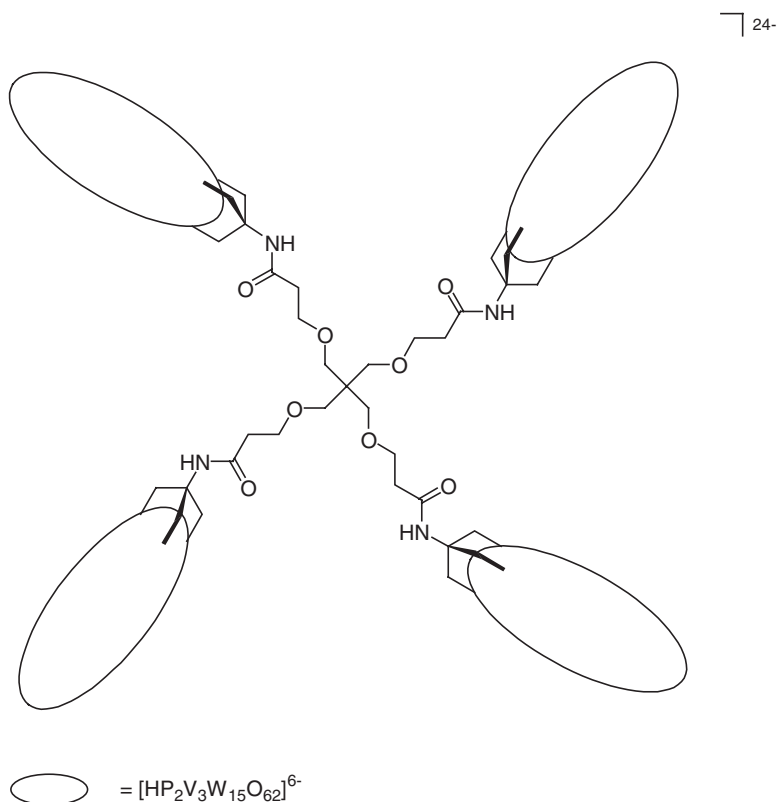
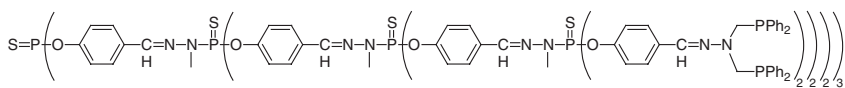
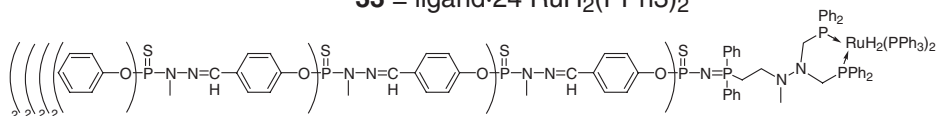
**30****31** = ligand·24 PdCl<sub>2</sub>**32** = ligand·12 Pd(OAc)<sub>2</sub>**33** = ligand·24 RuH<sub>2</sub>(PPh<sub>3</sub>)<sub>2</sub>**34**

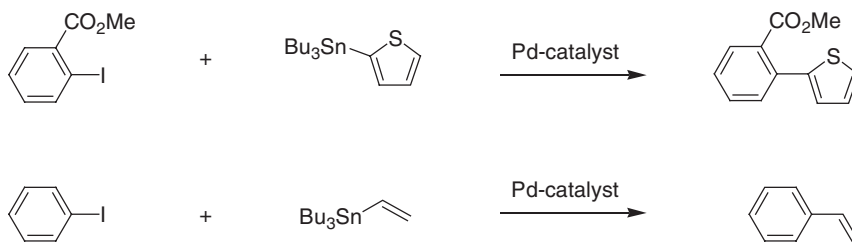
FIG. 12. Periphery- and core-functionalized ruthenium and palladium dendritic diphosphines.

observed when dendrimer **31** was applied. The dendrimer was precipitated by the addition of diethyl ether to the reaction mixture and recovered by filtration. No significant loss of activity was observed in three consecutive runs (80% conversion

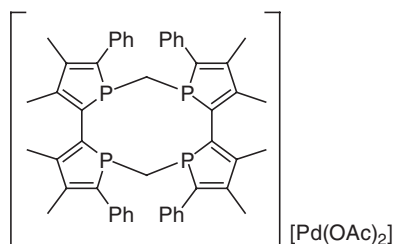
after 12 h). NMR analysis of the isolated dendrimer complex clearly indicated that no degradation had occurred.

Application of the same dendrimer **31** in the Stille coupling of iodobenzene with tributylvinyltin in DMF (Scheme 10; 5 mol% catalyst) showed an activity equal to that of the tetraphosphole macrocycle complex  $(\text{Fu}_3\text{P})_4\text{Pd}(\text{OAc})_2$  (**31b**; 100% conversion after 15 min). In contrast to the monomer, the dendritic catalyst could be recycled, but when recycled it showed a decrease in activity (95% conversion after 15 min). A better performance was achieved with the *in situ* prepared catalyst **32** by mixing the third-generation diphosphine dendrimer with  $\text{Pd}(\text{OAc})_2$  (P/Pd ratio = 4/1). An activity similar to that of the monomeric complex  $(\text{Fu}_3\text{P})_4\text{Pd}(\text{OAc})_2$  was observed (100% conversion after 15 min), even after three consecutive runs.

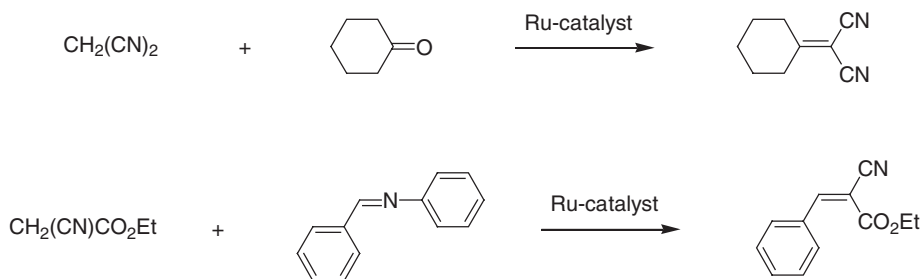
The phosphine-containing dendrimers were also applied as dendritic ligands in the ruthenium-catalyzed Knoevenagel reaction of malonitrile and cyclohexanone in THF solvent (Scheme 11). The application of 1 mol% phosphine-containing ruthenium dihydride-functionalized dendrimer (**33**) in the Knoevenagel reaction resulted in complete conversion to the unsaturated nitrile product in 24 h. Remarkably, the activity of dendrimer **33** is higher than that of the monomer complex  $[\text{Me}_2\text{N}-\text{N}(\text{CH}_2\text{PPh}_2)_2\text{RuH}_2(\text{PPh}_3)_2]$ , which gave only 80% conversion after 24 h. The monomer complex could not be recovered by the precipitation method, whereas dendrimer **33** was efficiently recycled after precipitation with diethyl



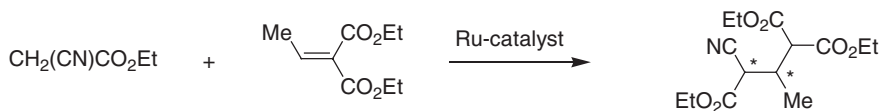
SCHEME 10.



**31b**



SCHEME 11.



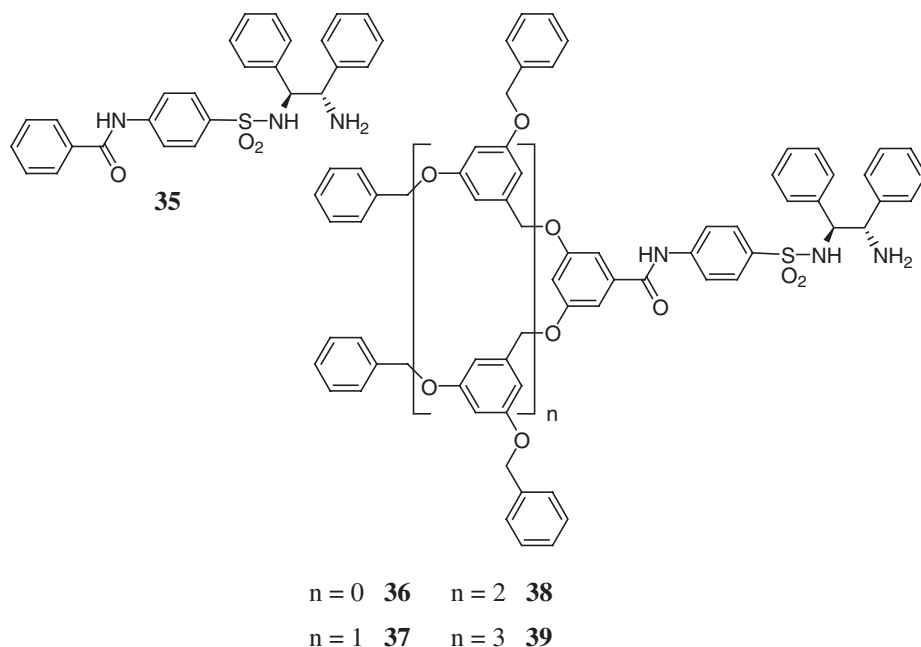
SCHEME 12.

ether and used in three runs without a significant loss of activity. The same efficient recoverability of dendrimer **33** (1 mol%) over three consecutive runs was found in the Knoevenagel condensation of ethyl cyanoacetate and N-benzylideneaniline to give ethyl benzylidenecyanoacetate (Scheme 11).

The phosphine-containing ruthenium dihydride dendrimer **33** was found to be an active catalyst for the diastereoselective Michael addition of ethyl cyanoacetate to diethyl ethylidenemalonate in THF (Scheme 12). The dendritic catalyst showed an activity and selectivity similar to those of the reference compound  $\text{RuH}_2(\text{PPh}_3)_4$  (100% conversion after 24 h and a diastereoselectivity of 7/3) (**40**). The dendritic catalyst was recycled twice by precipitation with diethyl ether without loss of activity or selectivity. Complex **34** showed similar activity and recoverability over three runs like that of complex **33**.

### C.5. Asymmetric Transfer Hydrogenation

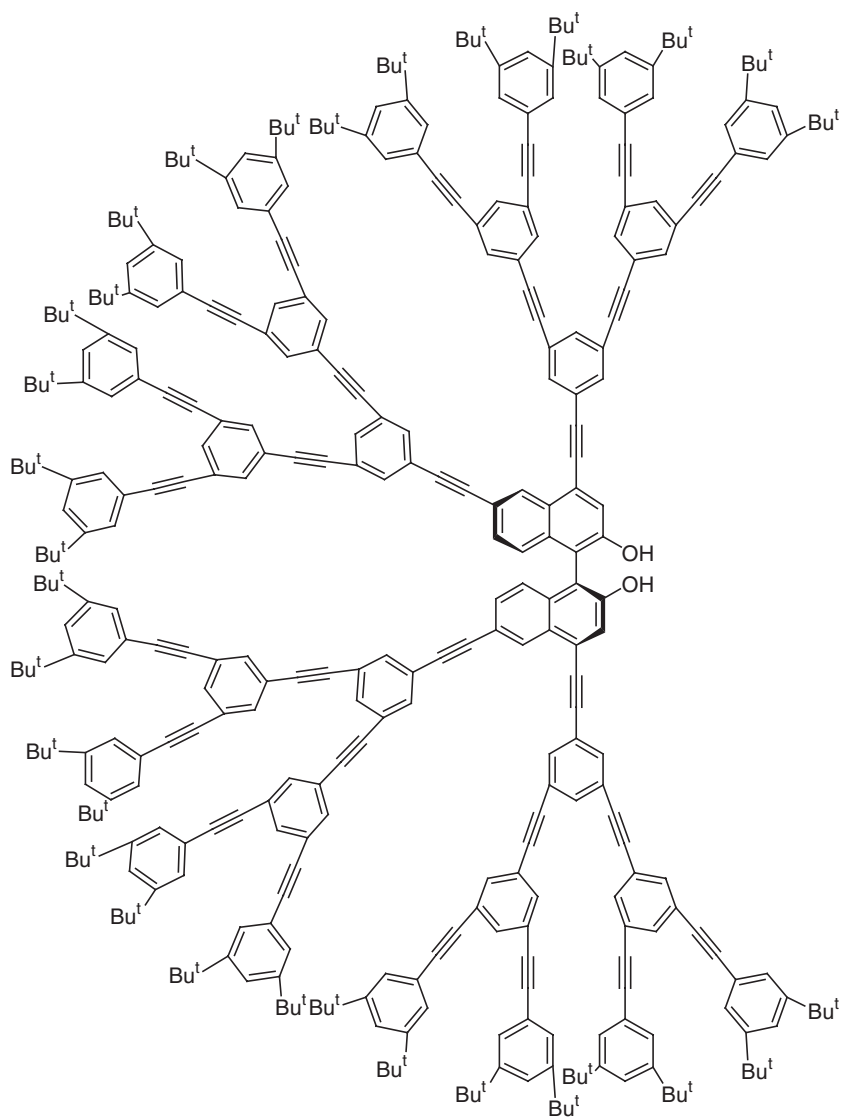
Chen *et al.* (**41**) reported the asymmetric transfer hydrogenation of acetophenone by using four generations of core-functionalized dendritic catalysts. Polybenzyl ether dendritic wedges were attached to an amine analogue of the [(*S,S*)-TsDPEN] ligand (**36–39**). The cymene ruthenium chloride dendritic catalysts were used for the transfer hydrogenation, which was performed in  $\text{CH}_2\text{Cl}_2$  with formic acid as the hydrogen donor. The dendritic catalysts gave similar activities with slightly shorter induction periods than the reference compound **35**. Each of the catalysts induced a high enantioselectivity (ee > 96%). The third- and fourth-generation dendritic catalysts were recycled four and five times, respectively, by evaporation of the  $\text{CH}_2\text{Cl}_2$  followed by the addition of dry methanol, centrifugation, removal of the methanol, and subsequent washing with methanol. After three cycles only a small loss in



activity was observed, and the enantioselectivities were still high. In the fifth run a loss in activity, but not in enantioselectivity, was found for the third-generation dendritic catalyst **38** (52% conversion after 20 h, ee 95.0%). In contrast, the fourth-generation dendritic catalyst **39** still displayed satisfactory activity (73% conversion after 20 h, ee 96.3%). The fourth-generation dendritic catalyst was even used in a sixth run, in which the activity and enantioselectivity were lower (52% conversion after 20 h, ee 87.0%). The higher stability of catalyst **39** was proposed to be a consequence of a site-isolation effect imposed by the large dendrimer.

### C.6. Asymmetric Additions of Diethylzinc to Aldehydes

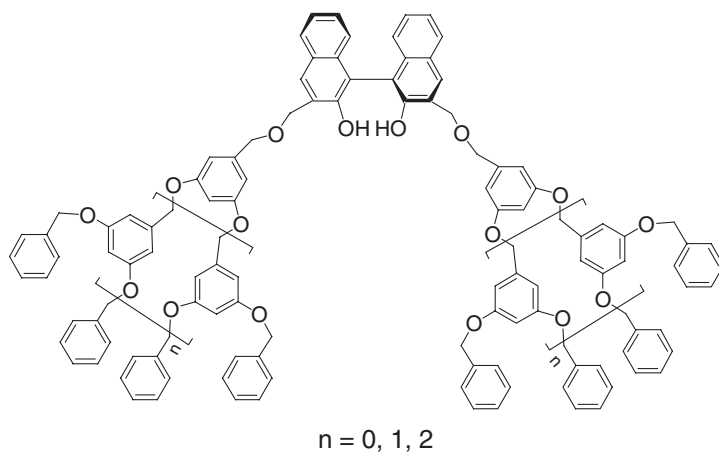
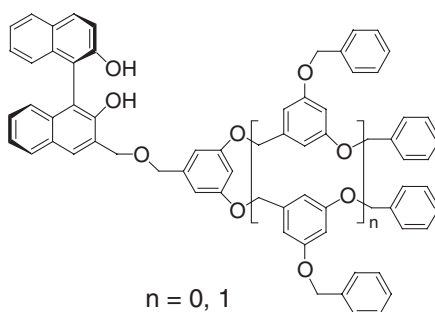
Hu *et al.* (42) reported chiral BINOL core-functionalized phenylacetylene-containing dendrimers (*S*)-**40**, which were used as catalysts in the asymmetric diethylzinc in addition to benzaldehyde. The reaction performed in the presence of (*S*)-**40** (5 mol%) displayed a much higher conversion after 24 h than the parent monomer BINOL, 98.6% and 37%, respectively. (*S*)-**40** gave rise to the formation of the opposite enantiomeric product. These results were explained by the site-isolation effect of (*S*)-**40**, which prevents aggregation of the zinc species through Zn–O–Zn linkages. These aggregates result in reduced Lewis acidity of the zinc/BINOL complex. Complexation of Ti(O–i-Pr)<sub>4</sub> to (*S*)-**40** (20 mol%) and BINOL resulted in comparable activities and enantioselectivities for the addition of diethylzinc to benzaldehyde (100% conversion, 89% ee) as well as to 1-naphthaldehyde (100% conversion, 90% ee). It is likely that similar catalytically



(S)-40

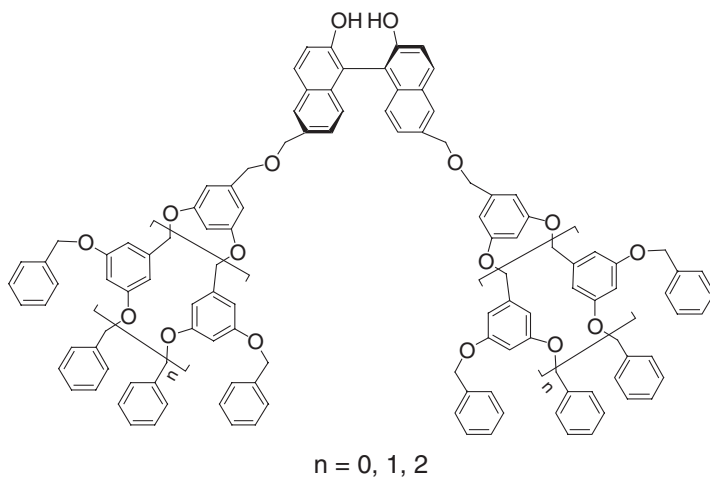
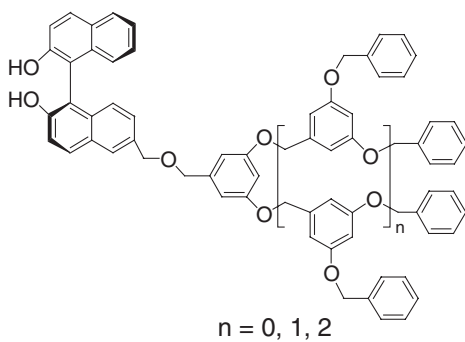
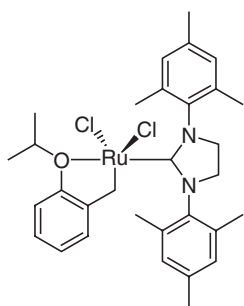
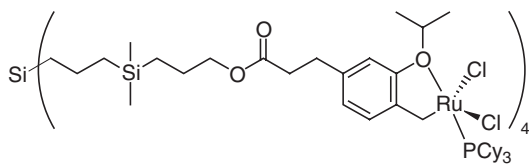
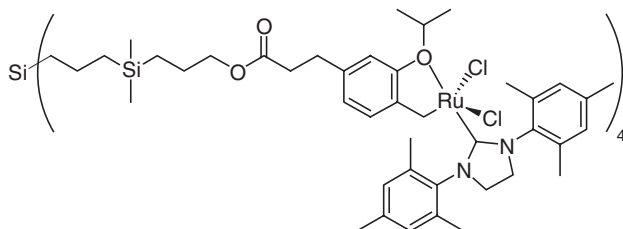
active (monomeric) species are formed from these complexes. (S)-40 could be recovered easily from the reaction mixture by precipitation with methanol. Unfortunately, no recycling experiments were reported.

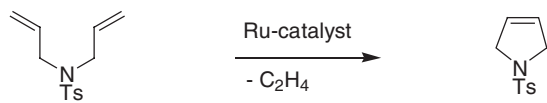
Liu *et al.* (43) prepared chiral BINOL ligands bearing dendritic Fréchet-type polybenzyl ether wedges ((R)-41–(R)-44), which were assessed in enantioselective Lewis acid-catalyzed addition of Et<sub>2</sub>Zn to benzaldehyde.

**41****42**

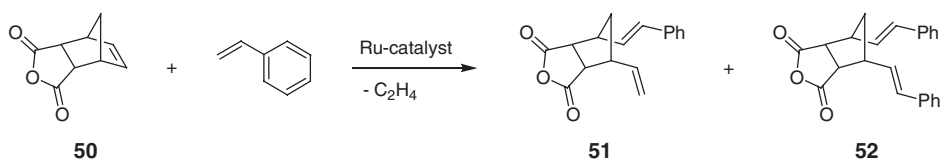
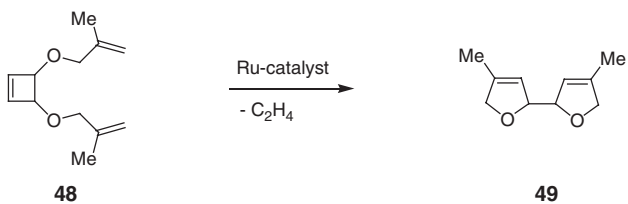
Differences in the effect of linking positions on enantioselectivity were observed for these dendritic ligand-derived catalysts. The catalytic experiments were carried out in toluene at 0°C in the presence of  $\text{Ti}(\text{O}-i\text{-Pr})_4$ . High conversions (up to 99%) and good enantioselectivities were observed for ligands (*R*)-**42**–(*R*)-**44**. Dendrimers (*R*)-**42** provided higher enantioselectivities than (*R*)-**41** with dendritic wedges at 3,3'-positions (80% vs 54% ee for the second-generation dendrimers). This difference was probably a consequence of the relatively open space around the active site of (*R*)-**42**, which may decrease the negative effect of the bulky dendritic wedges. Ligands (*R*)-**43** and (*R*)-**44** bear dendritic wedges at the 6,6'-positions or 6-position on the binaphthyl backbone, which are situated at a large distance from the catalytic center. Ligands (*R*)-**43** gave the highest enantioselectivity (up to 87% ee), which is similar to that observed with BINOL (85% ee). Moreover, the third-generation ligand G3-(*R*)-**43** was quantitatively precipitated by addition of methanol and recovered via filtration, and it could be reused without significant loss in performance.



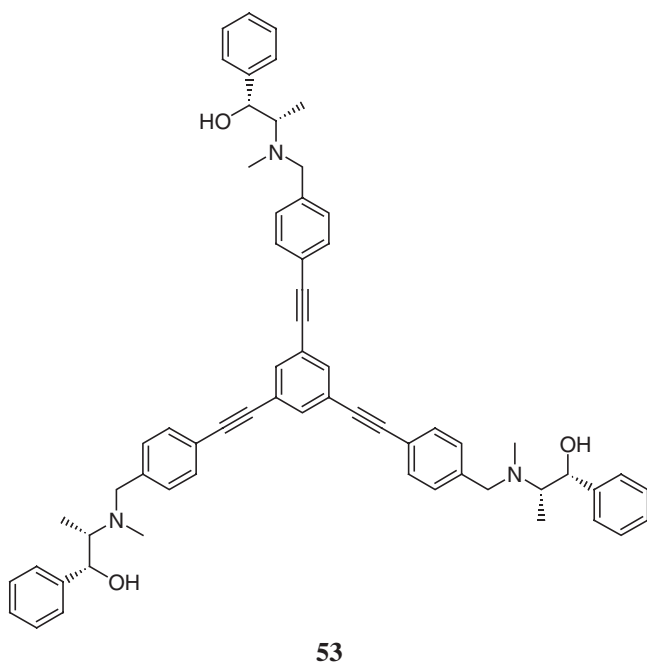
**43****44****45****46****47**

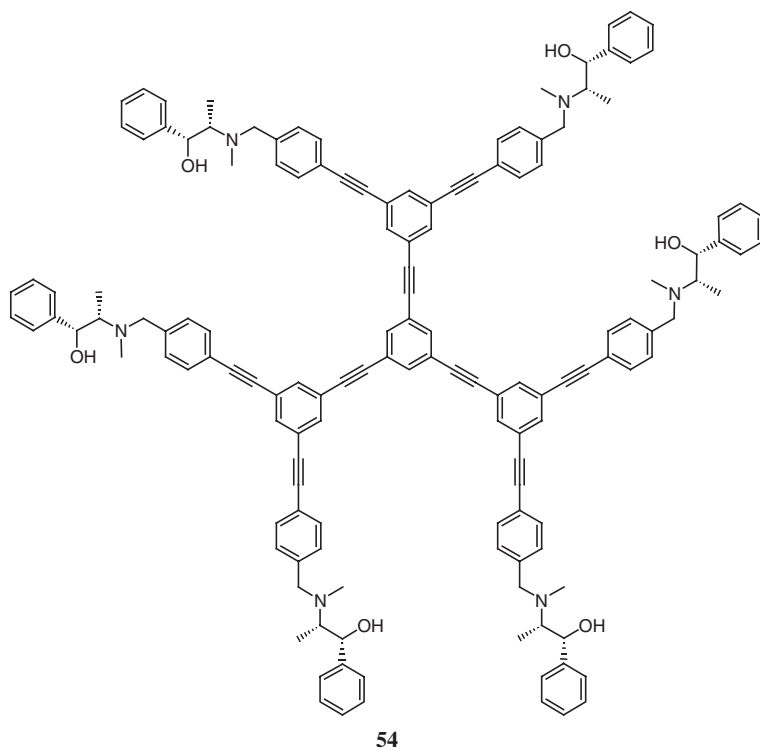


SCHEME 13.



SCHEME 14.





#### D. CATALYST RECOVERY BY COLUMN CHROMATOGRAPHY

##### D.1. Metathesis

Garber *et al.* (44) took advantage of the unique properties of dendrimers to enhance the separation of dendritic metathesis catalysts and products in a silica column. A mononuclear ruthenium catalyst with an imidazolin-2-ylidene carbene ligand was synthesized for the application in the ring-closing metathesis (RCM) of dienes into hetero- and carbocyclic-trisubstituted alkenes (Scheme 13). The catalytically active species is formed by reaction of ligand **45** with the substrate with the formation of 2-isopropoxystyrene. The imidazolin-2-ylidene carbene ligand gave a more active catalytic species than the tricyclohexylphosphine ligand. By addition of 2-isopropoxystyrene to the reaction mixture after the reaction had been completed, catalyst **45** was recovered by column chromatography (silica, >95% yield). Reuse of the catalyst in a consecutive run gave no significant loss in activity. In contrast, when the tricyclohexylphosphine-ligated complex was used, recycling resulted in loss in activity.

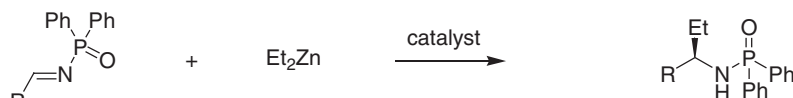
The monomeric catalyst fraction showed similar  $R_f$  values as the metathesis products, which complicated the chromatographic separation and recycling procedure. Immobilization of the ruthenium catalyst on a dendrimer was anticipated to facilitate the chromatographic separation. Indeed, the presence of multiple (polar) organometallic sites on the dendrimer periphery resulted in stronger adsorption interactions between the dendritic catalyst and the silica and thus a better separation from the product. Two types of dendritic catalysts were prepared in which

either tricyclohexylphosphine (**46**) or an imidazolin-2-ylidene carbene (**47**) acted as a ligand. Dendritic catalyst **46** was applied in the RCM reaction of diallyl tosylamine (1.25 mol% **46**, CH<sub>2</sub>Cl<sub>2</sub>, 40°C, 15 min). The catalyst was recycled five times by column chromatography with a silica column and CH<sub>2</sub>Cl<sub>2</sub> was used as eluent to isolate the cyclic product and ether was used for the elution of the dendritic catalyst. The cyclic product was isolated in more than 87% yield in each of the reactions. Although significant amounts of ruthenium metal had been lost from the recovered dendritic catalyst (13% after the first run), this loss did not affect the ring-closure activity (48% ruthenium content in the sixth cycle gave 87% yield after 15 min). The dendritic catalyst **47** exhibited a higher activity than catalyst **46**. In contrast to catalyst **46** and its mononuclear analogue, catalyst **47** catalyzed the ring-closing metathesis of diene carbinol, giving the product in a 78% yield. This dendritic catalyst was recovered in 90% yield after column chromatography with an 8% loss of the ruthenium loading. Catalyst **47** was also effective for the tandem ROM/RCM of catalysts **48** and **49** (94% yield, 90% catalyst recovery, 8% ruthenium loss; Scheme 14) and the ROM/CM of catalyst **50** with styrene to catalyst **51** (70% yield) and catalyst **52** (18% yield) (> 98% *trans*-alkenes, 95% catalyst recovery, 5% ruthenium loss; Scheme 14). In contrast to the mononuclear complex **45**, dendritic catalyst **47** was completely separated from the reaction products by column chromatography.

We emphasize that in these systems the ruthenium catalysts are released from the dendritic support during the reaction, and the activities are therefore high. However, at the same time this release limits the application of this type of system to batch reactors.

## D.2. Asymmetric Dialkyl Zinc Addition

Sato *et al.* (**45**) synthesized two generations of poly(phenylacetylene) dendrimers derivatized with (1*R*, 2*S*)-ephedrine, which were used as ligands for the asymmetric diethylzinc addition to aryl *N*-diphenylphosphinyl imines (phenyl, 2-naphthyl, *p*-tolyl; Scheme 15). Slightly higher enantioselectivities were achieved with ligand **53** than with **54** in the diethylzinc addition to phenyl, 2-naphthyl, and *p*-tolyl *N*-diphenylphosphinyl imine (89%, 94%, 89% ee for **53** and 87%, 90%, 85% ee for **54**, respectively). After the reaction of diethylzinc with phenyl *N*-diphenylphosphinyl imine, ligand **54** was recovered from the reaction mixture in 80% yield by thin layer chromatography on silica gel. The dendritic ligand was used in a consecutive reaction with a small loss in enantioselectivity (87% ee in the first run, 81% ee in the second).



R = phenyl, tolyl, 2-naphthyl

SCHEME 15.

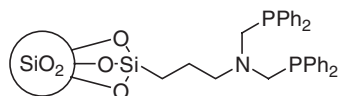
The same dendritic ligands were used for the addition of diisopropylzinc and diethylzinc to aldehydes (phenyl, 2-naphthyl, *p*-tolyl) (46). The two ligands were equally selective for the (*R*)-alcohol product ( $77\% \leq ee \leq 86\%$ , depending on the substrate). Dendrimer **53** was recovered after the reaction between diethylzinc and benzaldehyde and was reused in a consecutive run, giving the same enantioselectivity.

## E. RECOVERY OF HETEROGENEOUS DENDRITIC CATALYSTS

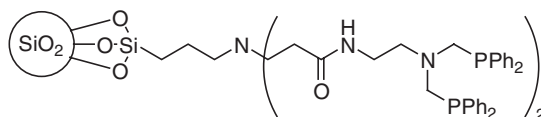
### E.1. Supported Dendritic Catalysts for Alkene Hydroformylation

Bourque *et al.* (47) prepared phosphine-functionalized PAMAM poly(amido amine) branches at the surfaces of silica particles. Primary amines were converted stepwise into G0–G4. Phosphination of the terminal amine groups occurred completely for G0–G2 (55–57), but steric crowding prevented complete functionalization of G3 and G4. Subsequent reaction with  $[\text{RhCl}(\text{CO})_2]_2$  gave the corresponding metal complexes, which were tested in the rhodium-catalyzed hydroformylation of alkenes. With styrene as a substrate, the dendritic catalysts 55–57 afforded aldehydes in nearly quantitative yield, even at room temperature ( $\text{TOF} = 10\text{--}20 \text{ mmol of substrate (mmol Rh)}^{-1} \text{ h}^{-1}$ ). These catalysts were characterized by high regioselectivity to the branched product (linear to branched ratios were as high as 1:30). The third- and fourth-generation catalysts showed considerable activity only at elevated temperatures.

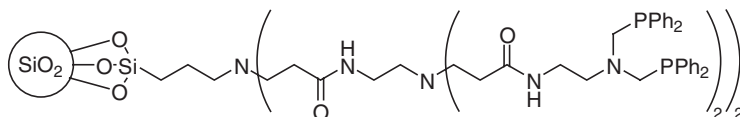
To investigate the impact of steric congestion on the hydroformylation reaction, the authors prepared a new series of ligands differing in flexibility as a result of



**55**



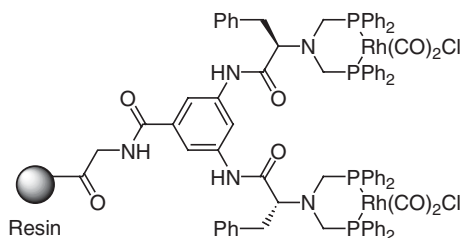
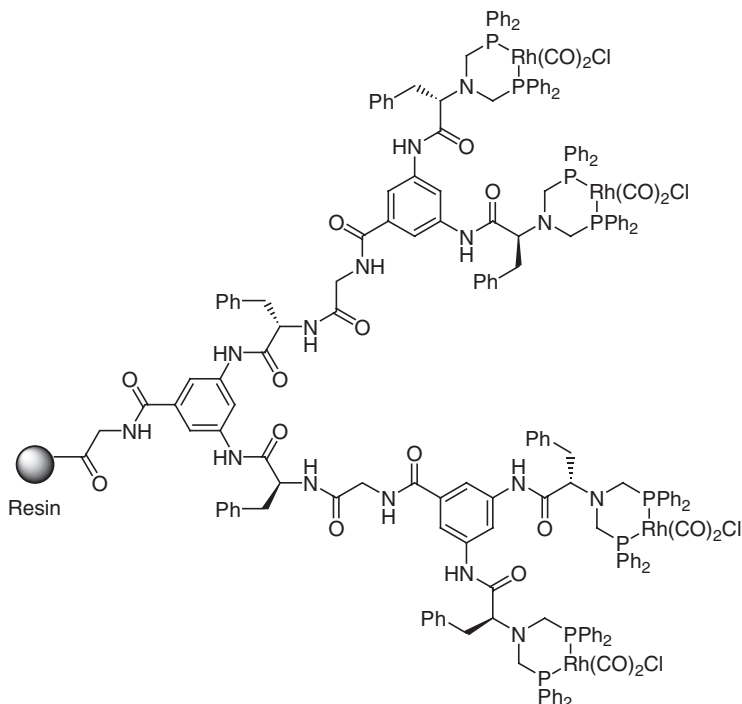
**56**

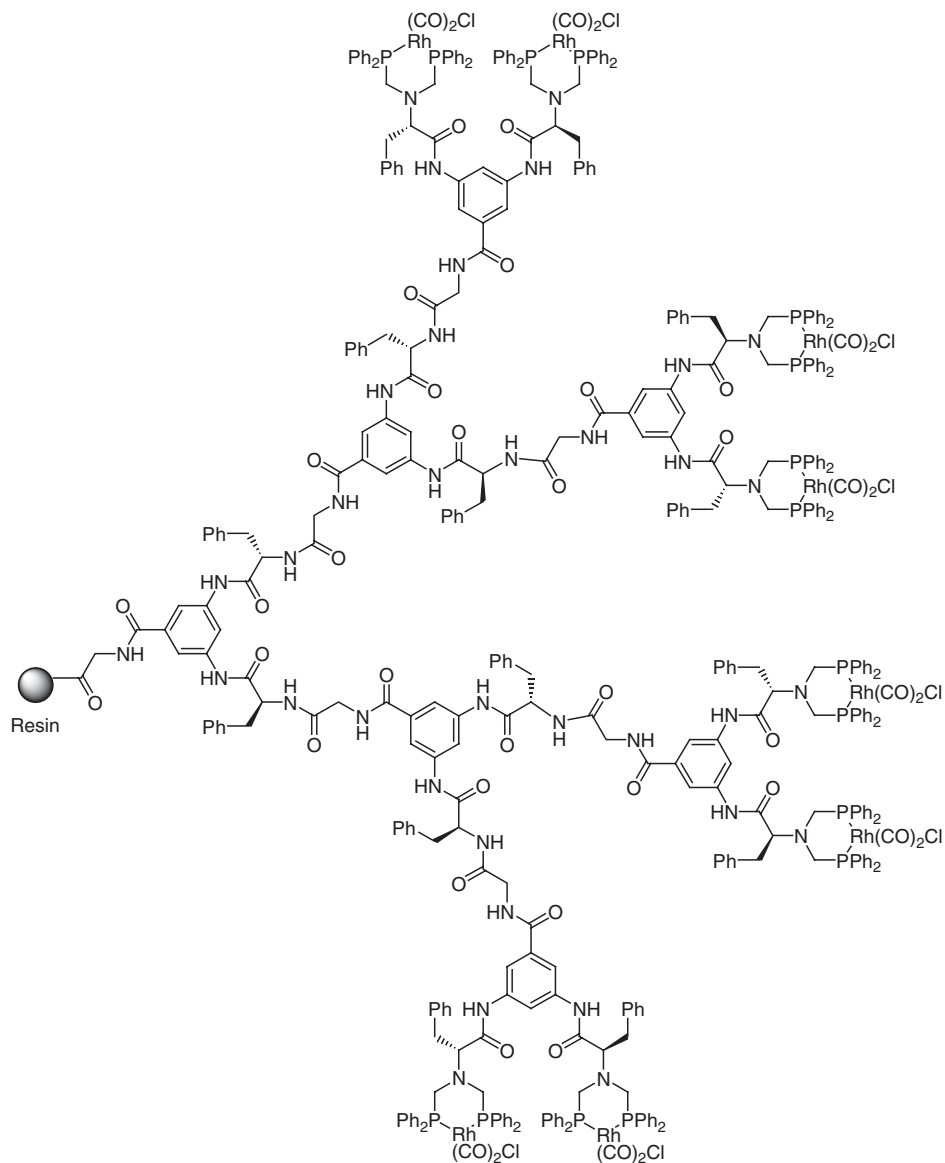


**57**

variations in spacer length (48). From a comparison of the catalytic activities observed with these ligands, they concluded that steric congestion indeed lowered the activity, which is in contrast with the results obtained with homogeneous dendritic systems (49). The reusability of the immobilized catalysts was tested in recycling experiments. Recovery of the catalyst was relatively easy, because the particles were large enough to be separated by microporous filtration. No significant loss of activity or selectivity was observed in five consecutive runs.

Arya *et al.* (50) immobilized similar dendrimers for the alkene hydroformylation on polystyrene (PS) beads, using solid-phase synthesis (58–60). The rhodium-catalyzed hydroformylation of styrene was investigated, and recycling experiments

**58****59**

**60**

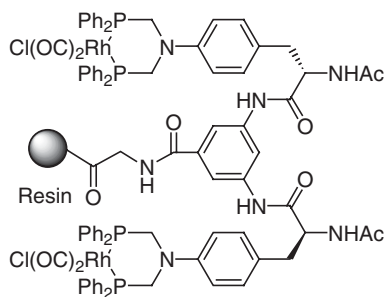
were performed with all three immobilized dendrimers over six consecutive runs. When the total pressure was 68.9 bar CO/H<sub>2</sub> (1:1) at 45°C, dendrimers **58** and **60** gave complete conversion after 22 h for the first four cycles. Unfortunately, no further details were given about the stability or activity of the system. The branched-to-linear ratio of the product varied between 9:1 and 16:1. In the fifth and

sixth runs, a drop in activity was observed for both dendrimers **59** (98% and 88% of the initial values, respectively, after 22 h) and **60** (78% and 47% of the initial values, respectively, after 22 h). The activities of the second- and third-generation catalysts **59** and **60** surpassed that of the first-generation catalyst **58** (85% conversion after 23 h in the third run). The second-generation catalyst **59** was subsequently investigated in three hydroformylation recycling experiments with the substrates vinyl acetate, vinyl benzoate, and *p*-methoxy styrene. The immobilized dendrimer was recycled three times without loss of activity or regioselectivity. Vinyl acetate as a substrate gave a branched-to-linear ratio of 15:1 in three subsequent runs.

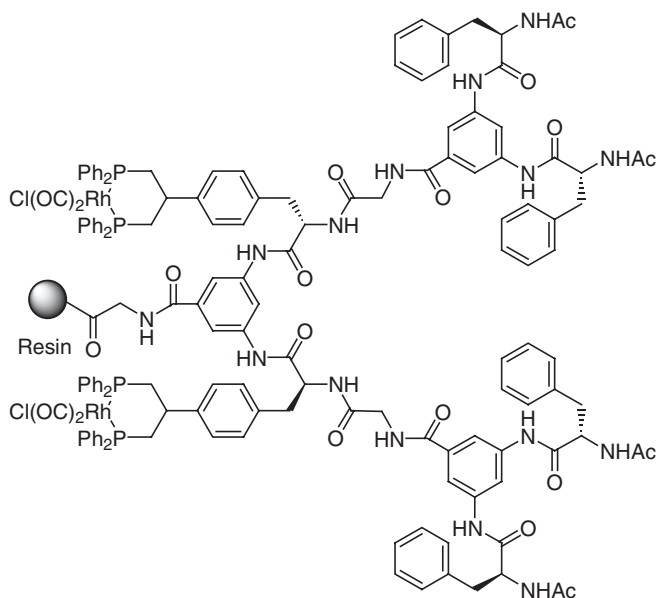
Arya *et al.* (**51**) used solid-phase synthesis to prepare immobilized dendritic catalysts with the rhodium center placed on different interior sites to mimic proteins and enzymes with catalytic sites in the inner core. Two generations of PS-immobilized rhodium-complexed dendrimer **61** and the more shielded **62**, were synthesized and used in the rhodium-catalyzed hydroformylation of styrene, *p*-methoxystyrene, vinyl acetate, and vinyl benzoate at a total pressure of 68.9 bar of 1:1 CO/H<sub>2</sub> at 45°C in the presence of CH<sub>2</sub>Cl<sub>2</sub>. With styrene as the substrate, dendrimers **61** and **62** were each recycled four times without significant loss in activity or selectivity (>99% conversion after 20 h; branched-to-linear ratio of product  $\approx$  18:1). When *p*-methoxystyrene was used as a substrate, the first three cycles did not suffer from any measureable deactivation (>99% conversion after 20 h, branched-to-linear ratio of product  $\approx$  17:1). Neither for dendrimer **61** nor for **62** did the fourth cycle reach full conversion after 20 h, but the more shielded dendritic catalyst did give a higher conversion than the other (56% conversion for **61**, 85% for **62**). In the hydroformylation of vinyl acetate, dendrimers **61** and **62** gave similar results. Comparable selectivities (branched-to-linear ratio of products  $\approx$  17:1) and slightly declining activities per cycle were observed (99% conversion for the second cycle relative to 85% conversion for the fifth cycle). With vinyl benzoate as substrate, the immobilized dendrimers **61** and **62** could be recycled with constant activity and selectivity for three cycles (>99% conversion after 20 h, branched-to-linear product ratio  $\approx$  25:1). In the fourth and fifth cycles, deactivation of each catalyst was observed. A dramatic drop in activity was found for dendrimer **61** (fourth cycle, conversion = 43%; fifth cycle, conversion = 20%). A smaller decline in activity was observed for dendrimer **62**, which was speculated to be a consequence of the larger dendritic environment (fourth cycle, conversion = 91%; fifth cycle, conversion = 83%). Determination of the numbers of turnovers characterizing the two systems should provide a conclusive test for the interpretation of this dendritic effect.

The same authors recently described the synthesis of similar rhodium-complexed dendrimers supported on a resin having both interior and exterior functional groups. These were tested as catalysts for the hydroformylation of aryl alkenes and vinyl esters (**52**). The results show that the reactions proceeded with high selectivity for the branched aldehydes, with excellent yields, even up to the tenth cycle. The hydroformylation experiments were carried out with first- and a second-generation rhodium-complexed dendrimers as catalysts, with a mixture of 34.5 bar of CO and 34.5 bar of H<sub>2</sub> in dichloromethane at room temperature. Each catalyst was easily recovered by simple filtration and was reusable for at least six more cycles without





61



62

loss of activity or regioselectivity. The second-generation dendrimer was found to be more reactive than the first-generation dendrimer when styrene was the substrate. The branched-to-linear ratio of the aldehyde products ranged from 39:1 to 36:1 at > 99% conversions, even up to the tenth cycle. Similar results were obtained for the hydroformylation of 4-isobutylstyrene, 4-vinylanisole, and 2-vinyl-6-methoxynaphthalene. These results indicate a dramatic improvement over the previously described Rh-complexed dendrimers reported by these authors (50,51) for the hydroformylation reactions. Unfortunately, the authors did not specify the P/Rh ratios used or the TOF observed. The improved catalytic behavior may be attributed to cooperative catalytic effects of the multiple coordination sites on the interior and exterior functional groups of these dendrimers.

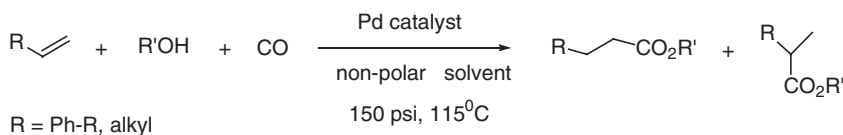
### E.2. Supported Dendritic Catalysts for Carbonylation, Hydroesterification, Oxidation, and Heck Reactions

Alper *et al.* (53) investigated the use of phosphine-functionalized PAMAM dendrimer immobilized on silica (55–57) as ligands in the palladium-catalyzed Heck reaction. Good yields were found in the reaction of bromobenzene with styrene at temperatures of 110–140°C for the dendrimer generations 0, 1, and 2, with generation 2 being the most active. The lower activities observed for generations 3 and 4 dendrimers was attributed to surface congestion. Again, this crowding problem was solved by using longer spacers between the dendritic branch points (43). The effect of the base on the reaction rate was investigated with the second-generation dendrimer in the reaction between bromobenzene and styrene. The use of triethylamine resulted in very low reaction rates, and sodium acetate and potassium carbonate gave the best yields. A drop in activity was found when the catalyst was used in a second cycle ( $K_2CO_3$ : 53% *trans*-stilbene in the first cycle, 43% in the second cycle; NaOAc: 39–69% in the first cycle, 20–45% in the second cycle).

Antebi *et al.* (54) investigated the carbonylation of iodoarenes to their methyl esters with Pd-PPh<sub>2</sub>-PAMAM-SiO<sub>2</sub> dendrimers of generations 0–3 as catalysts. These dendrimers were prepared by complexation of the phosphino-PAMAM dendrimers supported on SiO<sub>2</sub> 55–57 with either Pd(RCN)<sub>2</sub>Cl<sub>2</sub> (R = Me, Ph) or Pd(tmeda)Me<sub>2</sub>. The catalytic studies were carried out with methanol as the solvent, at a low pressure of CO, at 100°C, and with Et<sub>3</sub>N as a base. High yields were obtained, and the catalysts could be recycled 4 to 5 times without significant loss of activity. The results show that the activity decreased as the dendrimer generation increased. The carbonylation reaction is applicable to iodoarenes with both electron-withdrawing and electron-donating groups.

Similar 0–4 generations silica-supported Pd-PAMAM dendrimers with various spacer lengths were used by Alper *et al.* as recyclable catalysts for the hydroesterification reaction of alkenes (55) and the oxidation of terminal alkenes to methyl ketones (56). The hydroesterification experiments (Scheme 16) showed that (PPh<sub>3</sub>)<sub>2</sub>Pd-PPh<sub>2</sub>-PAMAM-SiO<sub>2</sub> complexes were highly active catalysts for styrene derivatives and linear long-chain alkenes (numbers of turnovers up to 1200).

These palladium-functionalized dendrimers show selectivity for the linear reaction product. A drop in activity was found when the catalysts were reused (1-decene as substrate/G(4)Pd(PPh<sub>3</sub>)<sub>2</sub> dendrimer as catalyst: 92, 75, 73, and 45% yield for the first, second, third, and fourth, respectively). The (dba)Pd-PPh<sub>2</sub>-PAMAM-SiO<sub>2</sub> dendrimers of generations 0–4 showed activity for the oxidation of terminal alkenes under mild conditions. The catalytic activity was found to be dependent on



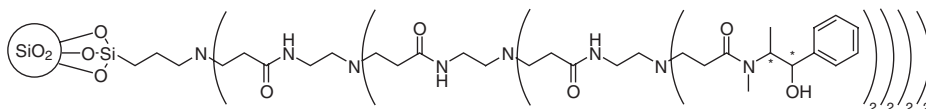
SCHEME 16.

the dendrimer generation. The higher generations were less active, giving lower conversions with 1-octene as the substrate. Only the first-generation dendrimer complex gave the methyl ketone in satisfactory yields (42%, 33%, traces, and no detectable yields for the zeroth, first, second, and third generations, respectively). These poor activities were attributed to steric congestion of the dendrimer. Oxidation was selective for the terminal double bond versus an internal unsaturated bond. These dendritic catalysts could be recycled; the G0 dendrimer was reused up to eight times, giving good yields of 2-octanone, whereas G1 and G2 complexes were reused only four times.

### E.3. *Supported Dendritic Catalysts for the Asymmetric Addition of Diethylzinc*

Chung *et al.* (57) synthesized silica-supported PAMAM dendrimers up to the fourth generation containing an (–)-ephedrine auxiliary (63) for the diethylzinc addition to benzaldehyde. Silica particles with a low and a high PAMAM loading were prepared starting from 0.24 and 0.9 mmol/g of amine initiator sites, respectively. Amine end group analysis showed that propagation of dendrimer growth became increasingly difficult with an increase in the generation, probably as a result of steric crowding. Larger deviations from the theoretical amine end group values were found for the highly loaded materials. The activity and (stereo) selectivity in the diethylzinc addition to benzaldehyde of the two types of modified silica were investigated (5 mol% catalyst, 2.2 eq. of diethylzinc, 0°C, toluene solvent, 48 h). In the case of the high loading, a gradual decrease in activity, selectivity, and enantioselectivity upon going to higher generation dendrimer-modified surfaces was observed. The diminished activity and selectivity were explained by a diffusional resistance induced by the irregular hyper-branched structure. The irregular branching, caused by incomplete functionalization during the dendrimer growth, is believed to generate different chiral environments leading to loss in enantioselectivity. However, the occurrence of the background reaction (no ligand: 45% conversion, 57% selectivity, racemic mixture) can partly account for these results.

A different trend was found for the low-loaded silica supports. The activity, selectivity, and enantioselectivity were found to increase upon going to the third generation. Under optimized reaction conditions, the third-generation silica-supported dendrimer gave results in the addition reaction identical to those observed with the homogeneous monomer (–)-ephedrine. The fourth generation showed a slightly lower activity and stereoselectivity, probably as a consequence of hindered access of the reagents to the catalytic sites. This effect was also found for similar dendritic catalysts in solution (58). The third-generation silica-supported



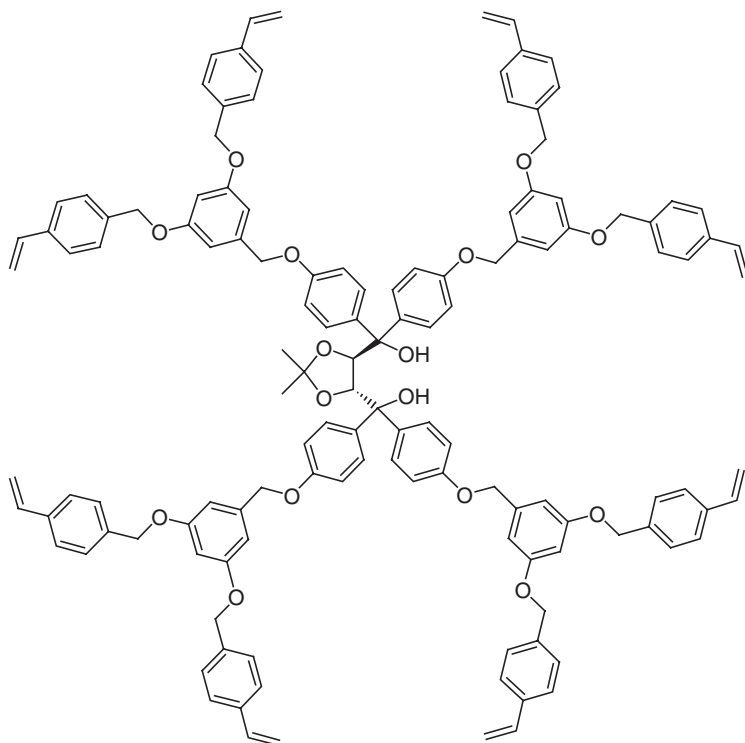
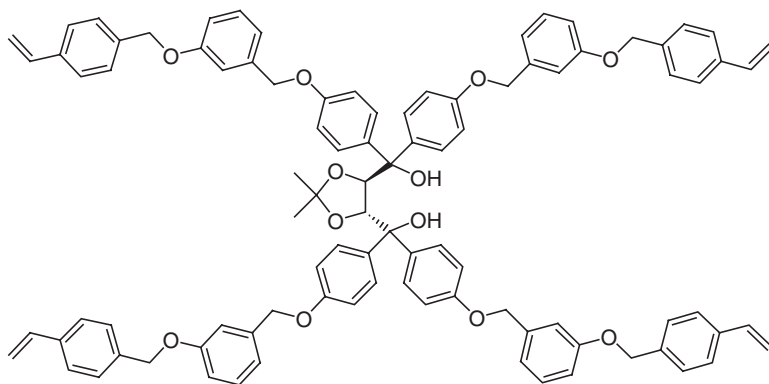
dendrimer was recycled three times without loss in activity, selectivity, or enantioselectivity.

Rheiner *et al.* (59) developed strategies to incorporate dendritic ligands incorporating TADDOL and BINOL moieties in a crosslinked polystyrene matrix. A first- and a second-generation TADDOL core-functionalized polybenzyl ether dendrimer with peripheral styryl groups (8 and 16, respectively) were synthesized and incorporated in a polystyrene matrix via a suspension copolymerization. The Ti-TADDOLate derivatives were synthesized by reacting the beads with  $\text{Ti}(\text{OiPr})_4$ . The polymer-incorporated dendritic Ti-TADDOLates are more active catalysts for the diethylzinc addition to benzaldehyde than a conventional PS-bound Ti-TADDOLate. The higher activity was attributed to the dendritic structure preventing the burial of the catalytic sites in the polystyrene matrix. Enantioselectivities comparable with those of the homogeneous Ti-TADDOLate were observed when 0.2 equivalents of the Ti-TADDOLates were used (*S/R*: homogeneous, 99:1; supported, 98:2). Higher enantioselectivities were obtained when the Ti-TADDOLate content in the polymer was lower as a result of the lower degree of cross-linking of the PS. No difference between the first- and second-generation dendrimers was observed.

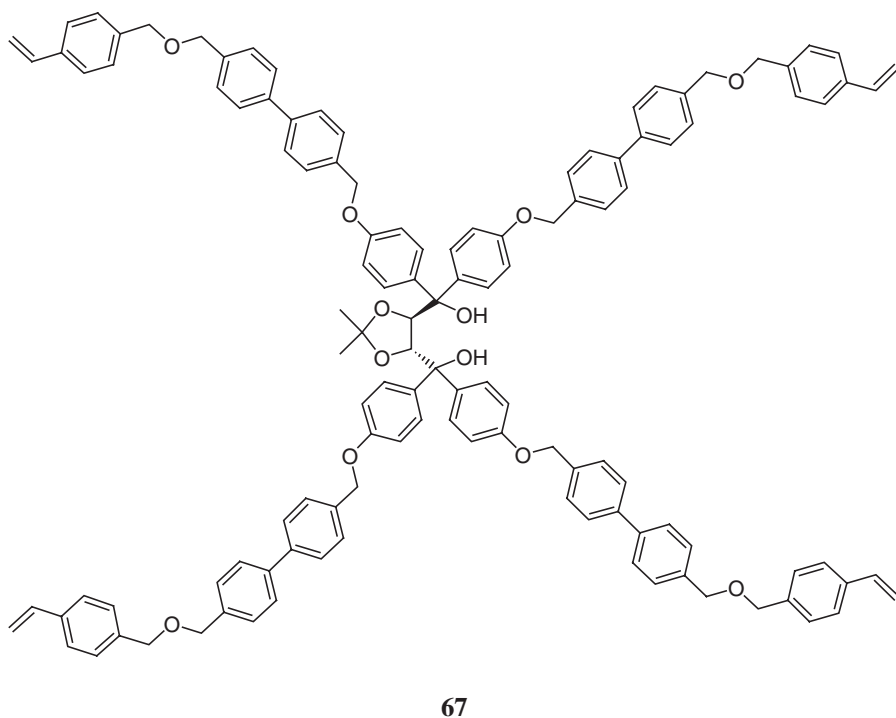
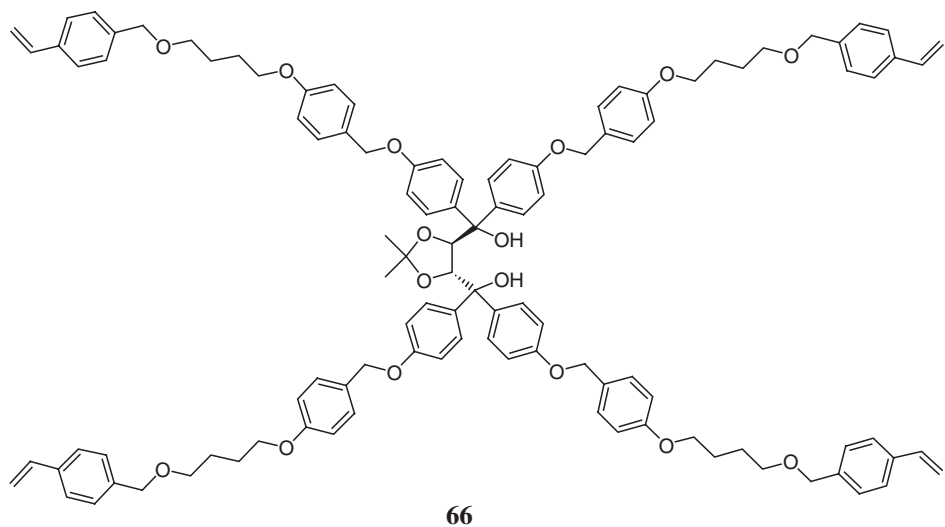
Sellner *et al.* (60) investigated these systems in more detail using cross-linkable TADDOL derivatives containing a variety of flexible linkers with peripheral styryl groups, including a dendritic analogue (64–67). The derivatized TADDOL systems were copolymerized with styrene and treated with  $\text{Ti}(\text{OiPr})_4$  to yield the polymer-bound Ti-TADDOLates p-64–p-67 (diameter in non-solvent-swollen state  $\sim 400\text{ }\mu\text{m}$ ). The enantioselectivities in the reaction of diethylzinc with benzaldehyde (0.2 equivalents, toluene,  $-20^\circ\text{C}$ , 2 h) with the application of the various polymer-bound Ti-TADDOLates with a loading of 0.1 mmol/g over 20 cycles was investigated. The best results were obtained with the PS beads cross-linked with dendritic TADDOL derivative p-64, yielding a similar enantioselectivity (*S/R* = 98:2) over 20 consecutive cycles. A kinetics investigation comparing the homogeneous TADDOL-Ti-complex and polymer-bound Ti-complex p-64 revealed that the activity of p-64 was slightly higher. Longer chain lengths of the linkers resulted in a dramatic drop in both selectivity and activity. Furthermore, the swelling properties of p-65, p-66, and p-67 decreased after multiple uses, whereas p-64 kept its high swelling properties.

Sellner *et al.* (61) applied another immobilization technique using a BINOL ligand. The cross-linkable peripheral styryl-functionalized BINOLs 68–70 and dendritic first-generation 71 and second-generation 72 were copolymerized with styrene and treated with  $\text{Ti}(\text{OiPr})_4$ . The recyclability over 20 cycles of the resultant Ti-BINOLates (loading 0.13 mmol/g) was investigated in the diethylzinc addition reaction to benzaldehyde. The best results were obtained with the immobilized dendritic BINOLate p-71 giving similar enantioselectivities (*S/R* = 93:7) over 20 cycles.

The cross-linked dendritic BINOLate p-71 (20 mol%) was also used as a supported catalyst in the asymmetric cyanosilylation of pivalaldehyde in  $\text{CH}_2\text{Cl}_2$ . The catalyst was reused several times after separation from the reaction mixture by filtration. In 20 consecutive reactions, the cyanohydrine product was formed in  $>90\%$  yield. Initially, an increase in enantioselectivity was observed from 72%

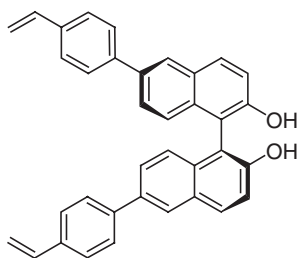
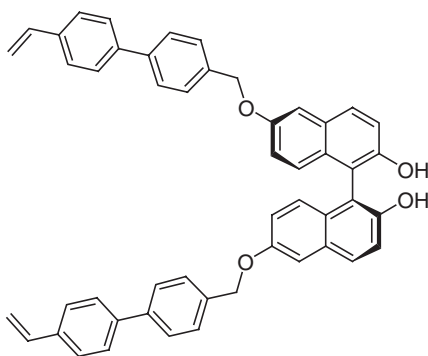
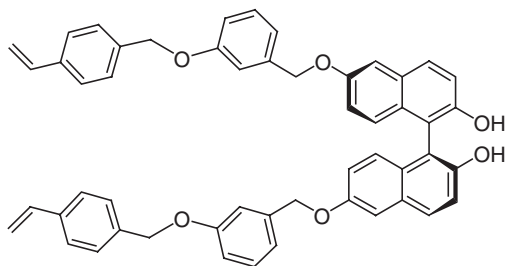
**64****65**

(*S*-enantiomer, comparable with the homogeneous BINOL-Ti catalyst) in the first run to 83% after the fifth run. After the 8th run, a gradual decrease in enantioselectivity was observed that was attributed to leaching of the metal. Reloading the vacant sites with  $\text{Ti}(\text{OiPr})_4$  caused a gradual increase of the enantioselectivity.

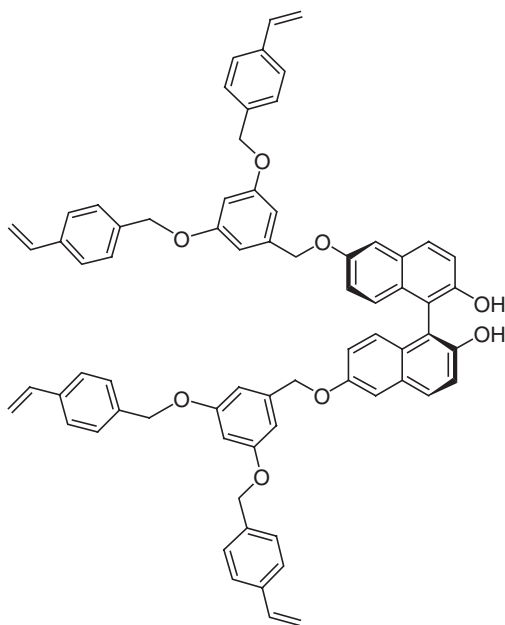


#### E.4. Scandium Cross-Linked Dendrimers as Lewis Acid Catalysts

Reetz and Giebel (62) anchored sulfonated poly(propylene imine) dendrimers by a cross-linking reaction with  $\text{Sc}(\text{OTf})_3$ , resulting in a non-porous material

**68****69****70**

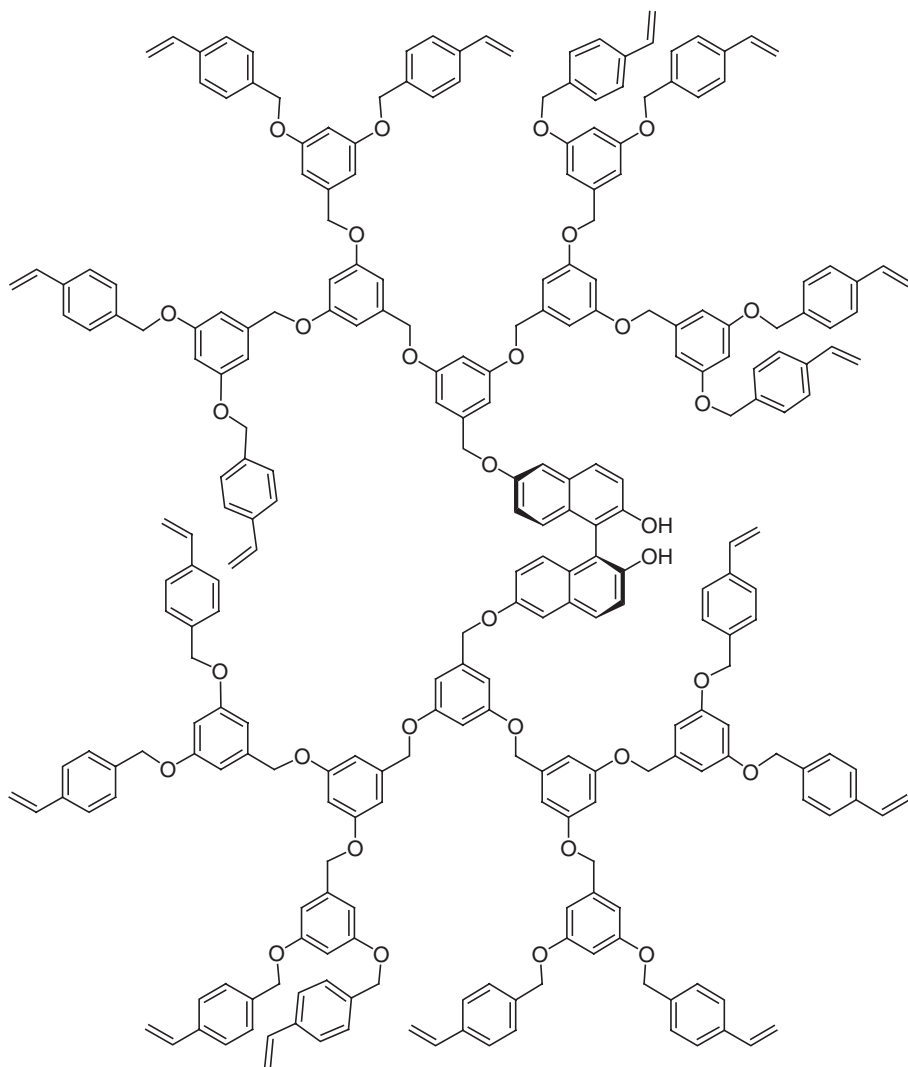
(73, Fig. 13). The cross-linked scandium-modified dendrimer was tested in a number of Lewis acid-catalyzed reactions, including Mukaiyama aldol additions to aldehydes and aldimines, Diels–Alder reactions, and Friedel–Crafts acylations. The dendritic catalyst was recovered by a simple filtration. The Mukaiyama aldol

**71**

addition was performed in a two-phase system, with stirring of benzaldehyde, aniline, and trimethyl-(1-phenyl-propenyloxy)-silane at room temperature in the presence of the dendritic material **73** (the system contained 7 mol% scandium). The aldimine product,  $\beta$ -amino ketone, was the only product observed (89% yield). After recycling of the catalysts, similar results (over three runs 88–89% yield) were obtained. ICP analysis of the filtrate and the absence of catalytic activity of the filtrate demonstrated that no scandium had leached from the dendritic material. The chemoselectivity of the dendritic material for the aldimine adduct is much better than that of the “monomeric”  $\text{Sc}(\text{OTf})_3$  homogeneous catalyst that gave rise to a 86:14 product mixture of the  $\beta$ -amino ketone over  $\beta$ -alcohol ketone. This increase in selectivity was attributed to the ligand effect.

In the Mukaiyama aldol additions of trimethyl-(1-phenyl-propenyloxy)-silane to give benzaldehyde and cinnamaldehyde catalyzed by 7 mol% supported scandium catalyst, a 1:1 mixture of diastereomers was obtained. Again, the dendritic catalyst could be recycled easily without any loss in performance. The scandium cross-linked dendritic material appeared to be an efficient catalyst for the Diels–Alder reaction between methyl vinyl ketone and cyclopentadiene. The Diels–Alder adduct was formed in dichloromethane at 0°C in 79% yield with an *endo/exo* ratio of 85:15. The material was also used as a Friedel–Crafts acylation catalyst (containing 7 mol% scandium) for the formation of *p*-methoxyacetophenone (in a 73% yield) from anisole, acetic acid anhydride, and lithium perchlorate at 50°C in nitromethane.





72

### E.5. Dendrimer-Bound Pd(II) Complex for Selective Hydrogenations

Mizugaki *et al.* (63) synthesized dendritic complex **1a** and carried out catalytic investigations of the selective hydrogenation of conjugated dienes to monoenes. The reactions were performed in ethanol as a solvent in which the dendritic catalyst was not soluble. The hydrogenation activity was monitored by the hydrogen uptake as a function of time. In the hydrogenation of cyclopentadiene, complex **1a** displayed considerable activity for the monoene ( $1.39 \text{ mL H}_2 \text{ min}^{-1}$ ). The subsequent

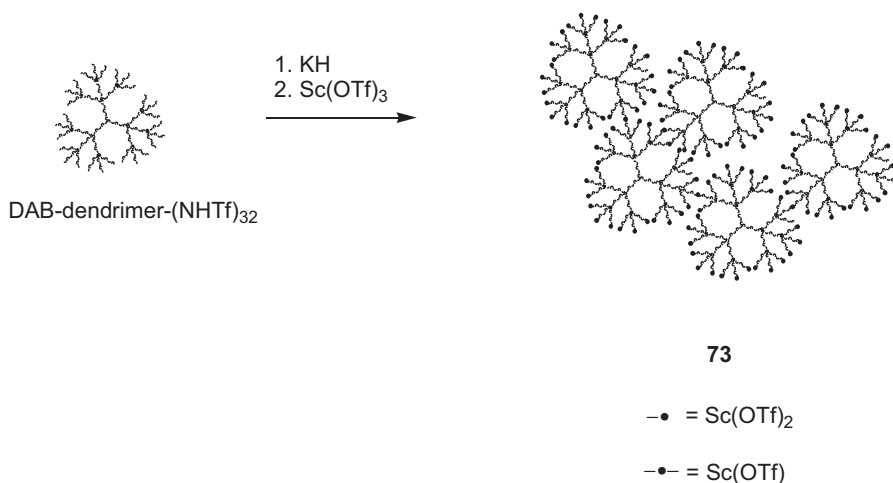
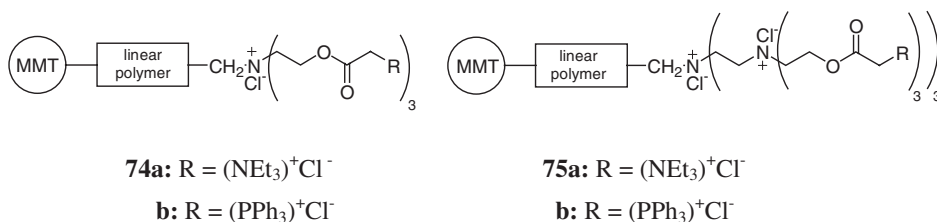


FIG. 13. Schematic representation of a scandium triflate cross-linked fourth generation poly(propylene imine) dendrimer (DAB).



hydrogenation to cyclopentane was significantly slower (0.1 mL H<sub>2</sub> min<sup>-1</sup>). The supported solid catalysts Pd/Al<sub>2</sub>O<sub>3</sub> and Pd/C showed higher activity, but no selectivity toward the monoene product. The monomeric complex PhN(CH<sub>2</sub>PPh<sub>2</sub>)<sub>2</sub>PdCl<sub>2</sub> was barely active, but the addition of triethylamine resulted in a moderate activity compared with that of **1a**. Cyclooctadiene was monohydrogenated with an initial rate of 1.80 mL H<sub>2</sub> min<sup>-1</sup> to cyclooctene. Complex **1a** was recovered from the reaction mixture by centrifugation, washed, dried, and reused in a consecutive run without considerable loss in activity (1.76 mL H<sub>2</sub> min<sup>-1</sup>).

#### E.6. Dendrimers Supported on Montmorillonite

Kenawy (64) immobilized ammonium and phosphonium peripheral functionalized dendritic branches on a montmorillonite supported chloromethylstyrene/methyl methacrylate copolymer (**74–75**). These polymer/montmorillonite-supported dendrimers were used as phase transfer catalysts (PTC) for the nucleophilic substitution reaction between *n*-butyl bromide and thiocyanate, cyanide, and nitrite anions in a toluene or a benzene/water system. These PT catalysts could be recycled by filtration of the functionalized montmorillonite from the reaction mixture. Generally,

higher activities were found at elevated (reflux) temperatures. The phosphonium-functionalized systems were found to be more active than the ammonium chloride analogues. A recycling experiment was performed in the reaction of *n*-butyl bromide with thiocyanate in benzene/water at reflux temperature (10% PTC **74b**). In three consecutive runs, only a small decline in activity was observed (yield after 15 h, respectively, 100, 96, and 96%). A similar experiment was performed with PTC **75b** in toluene/water (5% PTC). At reflux temperature, after 9 h a yield of 99% was obtained, whereas in a consecutive run a slightly lower yield (95%) was obtained.

## F. DENDRITIC CATALYSTS APPLIED IN TWO-PHASE CATALYSIS

The use of biphasic systems, in which the catalyst and product are dissolved in different phases facilitating separation and recycling, has been a subject of wide interest. Research in this area has been stimulated by the successful application of the two-phase rhodium-TPPTS Ruhrchemie/Rhone Poulenc process for hydroformylation of propene for the production of butanal (**65**). Recently, Horváth and Rabai (**66**) introduced fluorous phases as an alternative to water, which triggered the development of catalysts that are soluble in the fluorous phase. Solubilization of the ligand in the desired phase by attaching either water-soluble groups or fluorous tails is generally sufficient to allow efficient recovery and recycling of the catalyst. Therefore, there is no urgent need to introduce a dendritic structure into these types of processes. Consequently, the number of reports of the application of dendrimers in two-phase catalysis is limited.

### F.1. Water-Soluble Dendritic Catalysts for Alkene Hydroformylation

Gong *et al.* (**67**) synthesized four different water-soluble third-generation monodentate phosphine containing PAMAM dendrimers (Fig. 14, **76–79**). In the

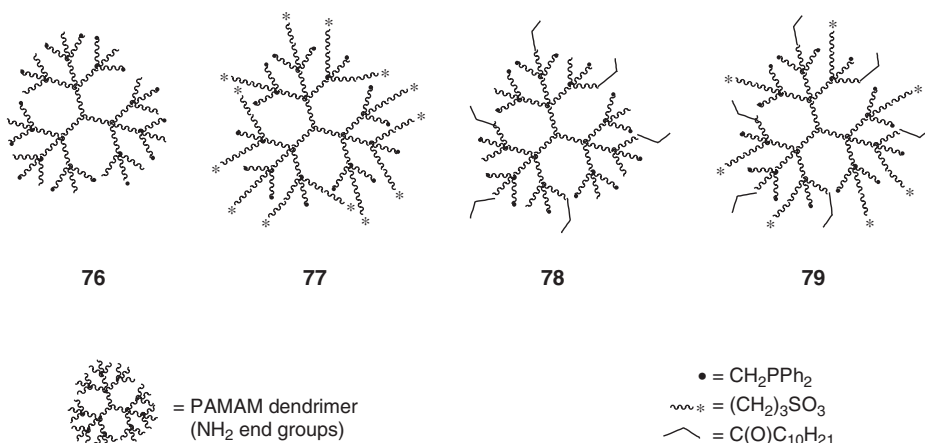


FIG. 14. Schematic representation of four types water-soluble PAMAM dendrimers containing phosphine ligands.

dendrimers **76** and **78**, the peripheral amine groups contribute to water solubility of the dendrimers, whereas in the analogues **77** and **79** the introduction of sulfonic acid groups assured the solubility in water. The hydroformylation of styrene and of 1-octene with the rhodium complexes of the dendrimers with varying Rh/P ratios was investigated (40°C, water/toluene, CO/H<sub>2</sub> = 1:1 (20 bar)). A higher branched-to-linear product ratio relative to that observed with the reference ligand TPPTS was found (68). Hydroformylation of styrene with **76** (Rh/P = 1:3) afforded a branched-to-linear product ratio of 14:1 compared to 6:94 for TPPTS. A branched-to-linear ratio of 1:2 was found for the hydroformylation of 1-octene when **76** was applied as the ligand, whereas TPPTS gave a ratio of 3:7 (69). Increasing the phosphorus-to-rhodium ratio resulted in a lower activity but a higher branched-to-linear ratio. Moreover, higher phosphorus-to-rhodium ratios suppressed rhodium leaching into the organic phase (P/Rh ratios were 2, 3, and 4). Raising the reaction temperature facilitated the leaching of rhodium into the organic phase. The dendritic catalyst was separated from the product phase; however, no recycling experiments using these water-soluble dendritic catalysts have been reported.

## F.2. Dendrimer-Encapsulated Palladium Nanoparticles for Hydrogenations

Zhao *et al.* (70) developed a method for the synthesis of dendrimer-encapsulated metal nanoparticles based on sorbing metal ions into (modified) PAMAM dendrimers followed by a reduction. Dendrimers encapsulating copper, palladium, and platinum nanoparticles have been prepared. Hydroxyl-terminated PAMAM dendrimers were used to prepare encapsulated palladium (PAMAM generations 4, 6, and 8) and platinum (PAMAM generations 4 and 6) nanoparticles. The dendrimer-encapsulated palladium and platinum nanocomposites catalyzed the hydrogenation reaction of allyl alcohol and N-isopropyl acrylamide in water (71).

Extending this work, Chechik *et al.* (72), prepared self-assembled inverted micelles that encapsulated palladium nanoparticles. The self-assembled inverted micelles were synthesized in an acid-base reaction between an amine-terminated fourth-generation PAMAM palladium-encapsulated dendrimer and dodecanoic acid (Fig. 15). With allyl alcohol as the substrate, the hydrogenation activity of the palladium nanoparticle-encapsulated inverted micelles was compared with the activity of the hydroxy-terminated dendrimer-encapsulated palladium nanoparticles in water. The amine-terminated dendrimer-encapsulated palladium nanoparticles were solubilized in toluene containing 2% (w/w) of dodecanoic acid. The 0.05 mol% inverted micelle palladium catalyst gave a TOF of approximately 760 mol H<sub>2</sub> (mol Pd)<sup>-1</sup> h<sup>-1</sup> at 20°C, whereas the water-soluble catalyst gave a TOF of 218 mol H<sub>2</sub> (mol Pd)<sup>-1</sup> h<sup>-1</sup>. The inverted micelle could be extracted back into the aqueous phase at pH 2, after which it could be re-introduced in the toluene/dodecanoic acid mixture after dialysis.

Using a similar approach, Chechik and Crooks (73), modified the PAMAM dendrimer-encapsulated palladium nanoparticles with perfluoropolyether tails utilizing non-covalent ion-pair interactions. The catalytic hydrogenation of six substrates under biphasic conditions (toluene/ perfluoro-2-butyltetrahydrofuran FC-75) was investigated. Allyl alcohol, methyl acrylate, vinyl isopropenyl ether, and

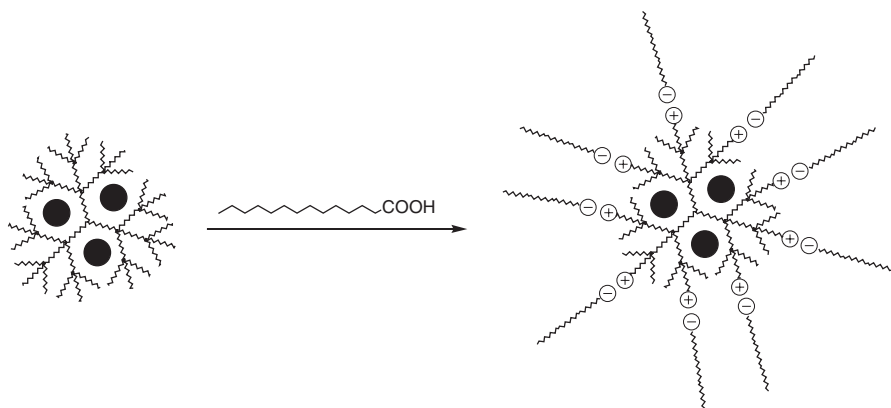
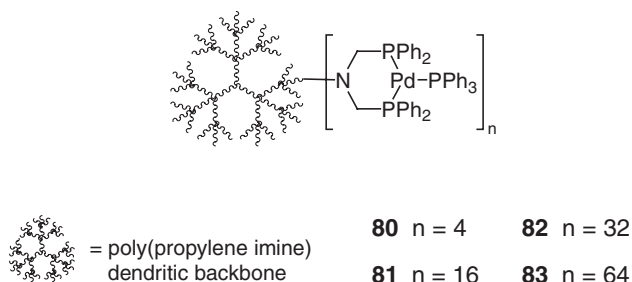


FIG. 15. Schematic representation of the formation of an inverse micelle from a PAMAM dendrimer-encapsulated palladium nanoparticle.



cyclohexene were hydrogenated with different turnover frequencies (400, 50, 10, and 3 mol  $\text{H}_2$  (mol Pd) $^{-1}$  h $^{-1}$ , respectively). The difference in activity is explained in part by the polar nano-environment within the dendrimer. The hydrogenation of 1-hexene resulted in the formation of hexane and the isomerized products 2- and 3-hexene. 1,3-Cyclooctadiene was hydrogenated selectively to cyclooctene (99%). The Pd/dendrimer nanocomposite could be recycled up to 12 times without a significant loss in activity. No leaching of the catalyst into the organic phase was observed within experimental error.

### F.3. Two-Phase Allylic Aminations and Heck Reactions using Thermomorphic Dendritic Catalysts

Mizugaki *et al.* (74) have recently utilized thermomorphic properties of Pd(0)-complexed phosphinated dendrimers for dendritic catalyst recycling. Using the method developed by Reetz (16), they prepared dendritic ligands containing, respectively, 2, 8, 16, and 32 chelating diphosphines. Palladium dichloride was complexed to the dendrimers, and a reduction in the presence of triphenylphosphine gave the Pd(0)-complexed dendrimers (**80–83**). The dendritic complexes were active

as catalyst in the allylic amination reaction of *trans*-cinnamyl acetate with morpholine in DMSO at 40°C, yielding the linear and branched allylic amines (quantitative yield after 30 min for dendrimer **81**, linear-to-branched ratio = 90:10). No change in regioselectivity was observed for the dendrimers of different generations. A change in the regioselectivity was observed when *cis*-3-acetoxy-5-carbomethoxycyclohex-1-ene was used as the allylic substrate and morpholine as the nucleophile. As a result of the steric congestion of the surface of the higher generation dendrimers, an increase in the selectivity toward the *cis*-product (up to 94% for **83**) was observed (tetra(triphenylphosphine) palladium gave 8% of the *cis*-product). The dendritic catalysts **80–83** could be dissolved only in polar solvents such as DMSO and DMF (in contrast to tetrakis(triphenylphosphine) palladium). This characteristic allowed the reactions to be performed in a biphasic system. Recycling experiments were performed with the dendrimers **80–83** catalyzing the allylic amination of *trans*-cinnamyl acetate with dibutylamine. The reaction was performed in a biphasic mixture of DMF and heptane, which became homogeneous at 75°C. After the reaction, the dendritic catalyst was recovered by cooling the reaction mixture to room temperature and decantation of the heptane phase containing the products. The catalytic activity remained high for three runs giving yields of 66% in the first, 99% in the second, and 99% in the third and fourth runs. Product distribution over the two phases decreased the yield of the first catalytic cycle.

Another example of a thermomorphic dendritic system was recently described by Ooe *et al.* (75). The immobilization of a palladium complex within the cavity of poly(propylene imine) dendrimers through ionic bonds afforded dendrimer-encapsulated palladium catalysts that act as unique nanoreactors for Heck reactions and allylic aminations. Peripheral amino groups on the third to fifth generation of PPI dendrimers were modified to give surface-alkylated and arylated dendrimers. 4-Diphenylphosphinobenzoic acid was used as the phosphine ligand to fix the palladium complex inside the dendrimers through ionic bonds between the carboxyl group and an internal amino group of the dendrimer (Fig. 16).

The dendritic palladium complexes efficiently catalyzed the Heck reaction of iodobenzene with *n*-butylacrylate in toluene at 100°C, whereas the reaction hardly

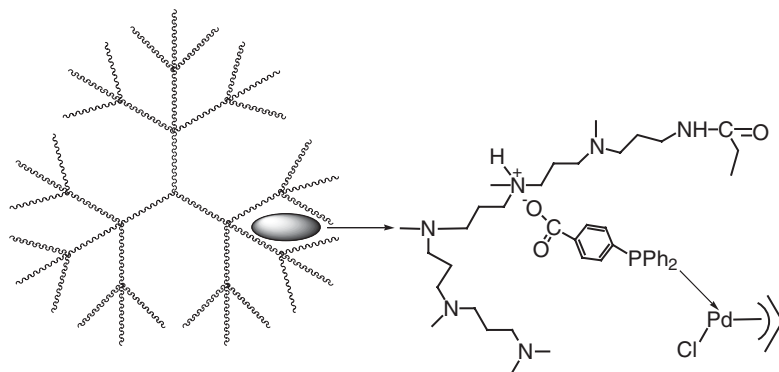


FIG. 16. Proposed structure of dendrimer-encapsulated palladium complex.

occurred in the absence of the dendrimer. The reaction yields increased with increasing generation of the dendrimers (59, 89, and 92% yields for the third, fourth, and fifth generations, respectively), with the generation effect being more pronounced between the third and fourth generations. When the fifth-generation dendrimer was used, the reaction rate decreased as the P/Pd ratio increased. It can be concluded that this dendrimer acts as an effective nanoreactor with high catalytic activity and stability for the Pd(0) species in a low P/Pd ratio. The high density of amine groups inside the dendrimer provides a polar nanoenvironment around the active palladium species, and even Pd-N coordination can occur—and consequently high catalytic activities have been obtained.

The fifth-generation dendrimer can also be used for other Heck reactions, such as the reaction of *p*-diiodobenzene with *n*-butylacrylate. In these experiments, the monosubstituted product was obtained in 92% selectivity, whereas a nearly equimolar mixture of mono and disubstituted products was obtained without dendrimer. A similar behavior was also observed using styrene and *p*-diiodobenzene as the substrates.

The allylic amination of cinnamyl methyl carbonate with morpholine was also catalyzed by these dendrimer-encapsulated palladium complexes. In this case, the reaction rates increased with decreasing generations of the dendrimers (78, 67, and 52% yields for third, fourth, and fifth generations, respectively). The surface congestion of the higher-generation dendrimers can suppress the penetration of substrates into the dendrimers. However, such an effect was not observed for the Heck reaction. The thermomorphic behavior of DMF and heptane was used as a tool for catalyst recycling. In the allylic amination of cinnamyl methyl carbonate with piperidine, DMF and heptane formed a homogeneous mixture during the reaction, and immediate phase separation was observed after cooling of the reaction mixture. After decantation of the heptane phase, the DMF phase containing the dendritic catalyst was recycled and reused with retention of activity.

### III. Dendritic Effects in Catalysis

Already at an early stage in the research with dendritic catalysis, these novel systems were proposed to form a promising class of recyclable catalysts. Furthermore, new, interesting properties were proposed to arise by catalyst attachment to these large, structurally well-defined polymers. In the previous section we summarized the results obtained so far in the recycling of dendritic catalysts, and here we describe some of the dendritic effects observed in catalysis. Both negative and positive effects are discussed, in an attempt to provide a balanced view of the current state of affairs.

#### A. DENDRIMERS AS SOLUBLE SUPPORTS

The properties induced by the dendritic framework depend on the location of the functional groups within the structure. Periphery-functionalized dendrimers offer high accessibility of the metal complex, which allows reaction rates that are

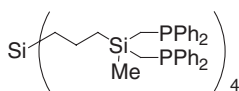
comparable with those in homogeneous solutions. However, these systems contain multiple reaction sites and ligands that provide high local catalyst and ligand concentrations. Thus, dendrimers can stabilize systems when excess ligand is required, as well as favor reactions that proceed by bimetallic mechanisms. On the other hand, bimetallic mechanisms operate in several deactivation mechanisms, which will be favored in periphery-functionalized dendrimers.

A general trend observed in many of the reports concerning catalysis with periphery-functionalized dendrimers is that the activity of the catalysts decreases with the dendrimer generation, which is usually attributed to the increasing steric bulk around the metal centers as the dendrimer generation increases. Some of these negative effects have already been discussed in Section II.

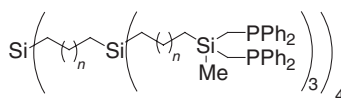
An early example of a dendritic catalyst was reported by Knapen *et al.* (24), who functionalized G0 and G1 carbosilane dendrimers with up to 12 NCN pincer-nickel(II) groups (7a) and applied them as catalysts in the Kharasch addition of organic halides to alkenes (Scheme 3).

The catalytic activity of the dendritic catalyst was slightly lower than that of the monomeric parent compound; 80% of the activity was found for G0 (four Ni centers) and 70% for G1 (7a, 12 Ni centers). The selectivity was the same in all experiments, resulting in a clean and regiospecific formation of the 1:1 addition product. It was proposed that the lower rates were a consequence of the high local concentration of nickel centers. In a subsequent paper (76), this effect was investigated in more detail with dendrimers having various spacer lengths. An even larger decrease in activity was observed with larger dendritic catalysts, which was attributed to surface congestion. This interpretation was strongly supported by the results of the experiments with more flexible dendrimers. The more flexible system 7c (with 12 active sites) yielded a much better catalyst for the Kharasch addition reaction than 7b (the TOF increased from 39 for 7b to 85 for 7c). It was proposed that the catalyst deactivation was caused by an interaction between neighboring Ni<sup>II</sup>/Ni<sup>III</sup> sites, which obviously is more pronounced in systems that are characterized by larger surface congestion. In a subsequent detailed report, this deactivation process was supported by EPR measurements and investigations with model compounds. During the reaction, a purple precipitate was formed that contained inactive Ni(III) species (26).

Rhodium complexes of the phosphine-functionalized carbosilane dendrimers are active for the hydroformylation of alkenes. The influence of the flexibility of the dendritic backbone on the catalytic performance was characterized by comparing dendritic ligands 84a–84c (conditions: toluene, 80°C, 20 bar CO/H<sub>2</sub>) (49).



84a

84b:  $n = 0$ 84c:  $n = 1$

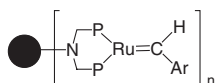


Remarkably, an increase in steric congestion ongoing from dendrimer **84a** to **84b**, and finally to **84c** did not affect the catalytic performance in this reaction, which is in contrast with the results representing the Kharasch addition reaction.

Ropartz *et al.* (77) described a positive dendritic effect for the rhodium-catalyzed hydroformylation of terminal alkenes with polyhedral oligomeric silsesquioxane (POSS) dendrimers functionalized with diphenylphosphine. The rhodium complexes of dendritic ligands G1-16ethylPPh<sub>2</sub> and G2-propyl-48ethylPPh<sub>2</sub> led to unexpectedly high regioselectivity for the linear aldehyde 1-nonanal (86%, 1:b ratios up to 14:1) for the hydroformylation of 1-octene. Small monomeric analogues did not show such selectivity, a result that clearly points to the positive dendritic effect. Remarkably, only the dendritic framework with a spacer of five atoms (CH<sub>2</sub>CH<sub>2</sub>SiCH<sub>2</sub>CH<sub>2</sub>) between the P atoms led to high selectivity. Other structures with three-atom spacers were too compact (G1-16methylPPh<sub>2</sub>), and those with seven-atom spacers were not sufficiently constrained (G1-16ethoxyPPh<sub>2</sub> and G1-16propylPPh<sub>2</sub>) to give a high regioselectivity for the linear aldehyde. The composition of the dendritic framework was also inferred to be important, because, when a carbon atom was replaced by an oxygen atom in the β position to the phosphorus atoms (from G1-16ethylPPh<sub>2</sub> to G1-16methoxyPPh<sub>2</sub>), the selectivity was reduced. It is believed that the lower regioselectivity in this case could arise from a different geometry of the Rh/dendritic ligand.

Gatard *et al.* (78) reported the synthesis of dendritic ruthenium benzylidene complexes and their use as catalysts for the ROMP of norbornene to form star-shaped metallodendritic polymers. The reaction of 1–4-generation dendritic diposphine DAB-dendr-[N(CH<sub>2</sub>PCy<sub>2</sub>)<sub>2</sub>]<sub>n</sub> (*n* = 4, 8, 16, 32) with [Ru{η<sup>2</sup>-(=CH-*o*-PhO-*i*-Pr)Cl<sub>2</sub>(PPh<sub>3</sub>)}] gives the dendritic chelating diposphine Ru-benzylidene complexes 1–4 generation DAB-dendr-[N(CH<sub>2</sub>PCy<sub>2</sub>)<sub>2</sub>Ru(=CHAr)Cl<sub>2</sub>]<sub>n</sub> (*n* = 4, 8, 16, 32) (**85**) with Ar = *o*-*i*-Pr-C<sub>6</sub>H<sub>4</sub>. ROMP of norbornene was carried out at 25°C in CDCl<sub>3</sub> with the 1–3-generation dendritic ruthenium carbene complexes.

A dramatic positive dendritic effect was observed, with the reaction proceeding more rapidly with the metallodendritic ruthenium complexes than with the monomeric ruthenium model compound (conversions after 3.5 h: G1, 94%; G2, 65%; G3, 59%; model compound, traces). A possible reason for this effect could be the labilization of metal–ligand bonds in the dendrimers by interbranch collisions of the metal groups. Among the metallodendrimers, the most active initiator is the first-generation complex, and the activity slowly and regularly decreased as the dendrimer generation increased. This negative dendritic effect is attributed to the increased bulk around the ruthenium centers when the generation increases. The



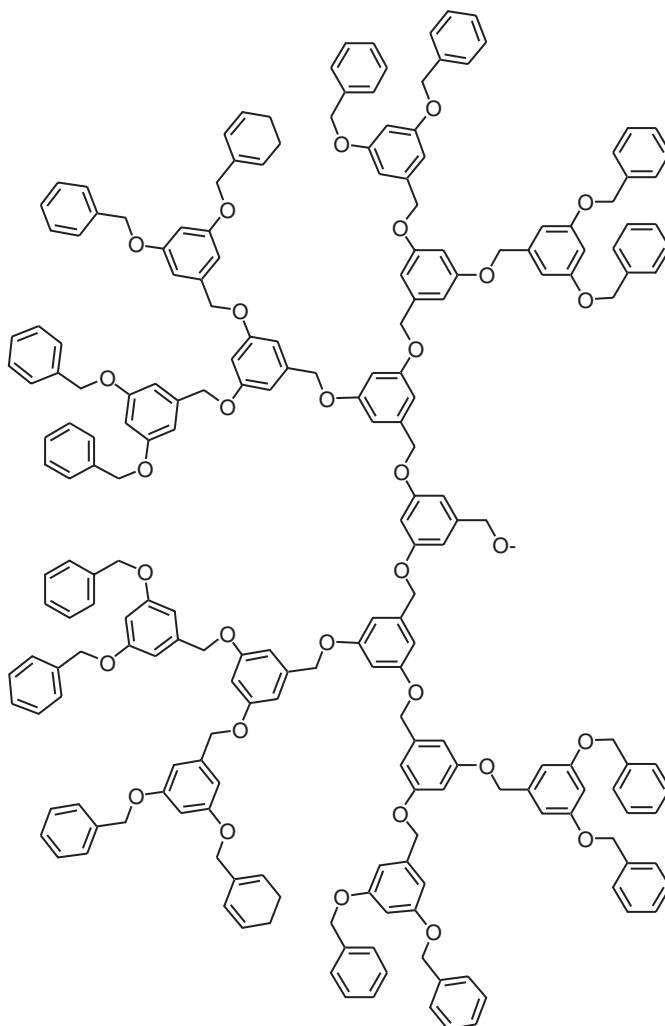
● = DAB dendrimer

*n* = 4, 8, 16, 32

steric bulk is proposed to slow down the approach of the incoming norbornene monomer to the ruthenium center.

In core- (and focal point-) functionalized dendrimers, the catalyst can especially benefit from the specific microenvironment created by dendritic structures. Site-isolation effects can be beneficial for reactions that are deactivated by excess ligand, and can also prevent bimetallic deactivation pathways.

The first example of a catalytic reaction at the core of dendrimers was provided by Fréchet (79) using dendritic alcoholates such as **86** as macro-initiators for anionic ring-opening polymerization of  $\epsilon$ -caprolactone. Usually the alkali

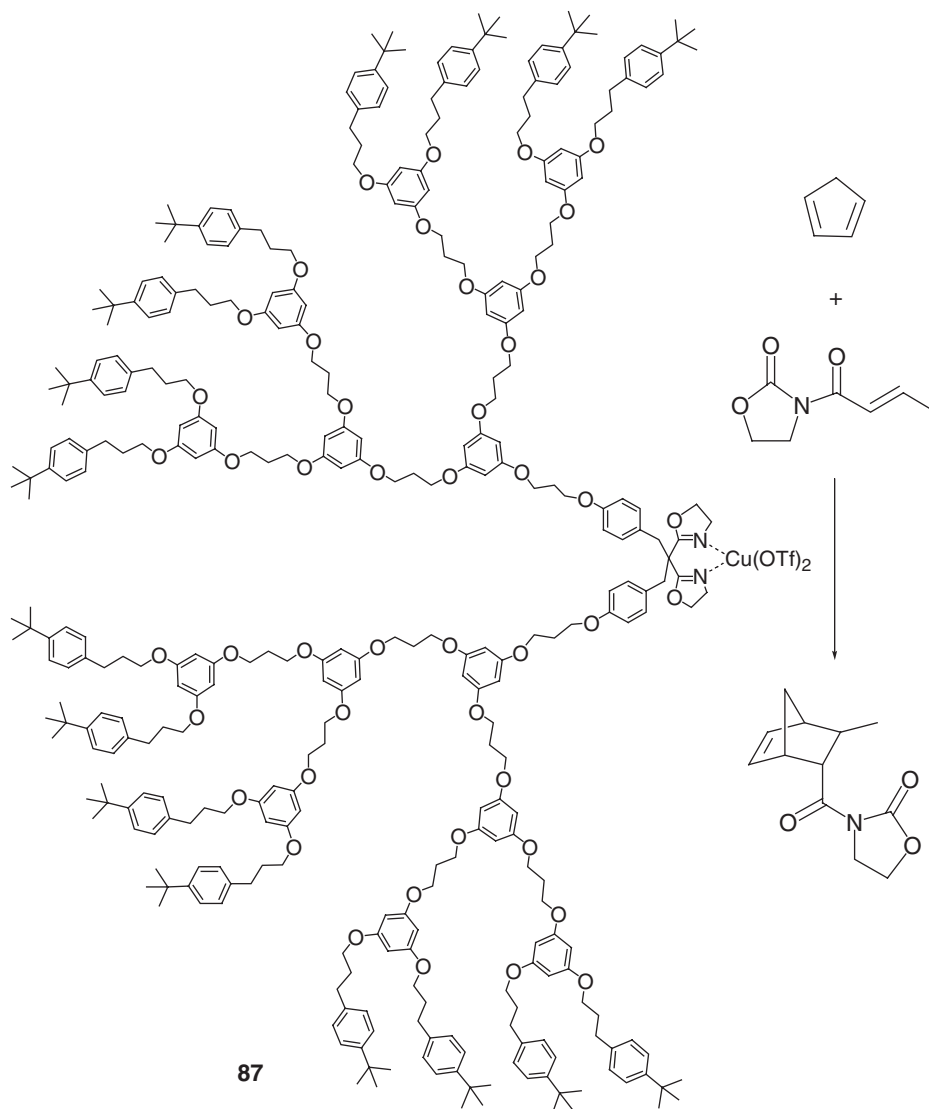


metal alcoholates yield low-molecular-weight (MW) polymers with broad MW distribution in the polymerization of  $\epsilon$ -caprolactone. Earlier research had shown that steric bulk around the reaction center leads to suppression of side reactions as well as to a decrease of “backbiting,” which is responsible for low-MW products. Furthermore, solubility limitations usually result in low-MW polymers. The dendritic species demonstrated to be suitable initiators because of their excellent solubility in THF and their steric bulk prevented “backbiting.” The G4 alcoholate **86** acts as a highly effective initiator producing high-MW polymers with a narrow MW distribution of 1.07. The initiator efficiency was estimated to be close to 100%, which confirms the high accessibility of the reactive core. The G1 analogue produced only oligomers with very low conversions. Thus, the large dendrimers prevent termination of the polymerization by shielding the growing tip from reacting with a chain of another growing tip.

Chow (80) reported the preparation of a series of poly(alkyl aryl ether) dendrons (G0 to G3; G3 (**87**) is shown in Scheme 17) functionalized with dendritic *bis* (oxazoline) ligands at the focal point. Cu<sup>II</sup> complexes of these dendrimers catalyze the Diels–Alder reaction between cyclopentadiene and N-2-butenoyl-2-oxazolidinone. A detailed study revealed that the reaction follows enzyme-like Michaelis–Menten kinetics. A reversible formation of the copper dienophile complex is followed by the rate-limiting conversion to the Diels–Alder adducts. The association constants of the catalyst–dienophile complex ( $k_1/k_{-1}$ ) decreased slightly with increasing generation dendrimer. The geometry at the metal center changes upon complexation of the dienophile at the focal point. This results in an increase in steric repulsion between the dendritic wedges, which is more pronounced for the larger systems. Because the dienophile was used in large excess in the catalytic experiments, the copper was present as a dienophile complex in all the catalysts. Thus, under these conditions no effect of this difference on the catalytic activity was expected. Indeed the activities of the dendritic catalysts G0–G2 were very similar. However, when G3 was used, a markedly lower activity was observed. The size of this dendritic system results in a change in spatial structure around the catalytic core, from planar to globular. The decrease in reaction rate is proposed to be to the result of a decrease in substrate accessibility; therefore G3 behaves more like a core-functionalized dendrimer.

This encapsulation effect was further characterized by determination of the substrate selectivity using substrates of different sizes. Dienophiles with various tail lengths were applied in a 1:1 molar ratio to react with cyclopentadiene in the presence of a catalyst. The smaller dienophile reacted slightly faster than the bulkier one with each of the catalysts investigated (non-dendritic parent complex, G1.Cu(OTf)<sub>2</sub>, and G3.Cu(OTf)<sub>2</sub>). More importantly, G3.Cu(OTf)<sub>2</sub> ( $k_{\text{rel}} = 1.18$ ) displayed higher substrate selectivity than G1.Cu(OTf)<sub>2</sub> ( $k_{\text{rel}} = 1.05$ ).

Another example of a dendritic effect observed for a core-functionalized dendritic catalyst was described by Oosterom *et al.* (19) for allylic alkylation reactions (Section II). The palladium complexes of **5** catalyzed the alkylation of 3-phenylallyl acetate with sodium diethyl methylmalonate. It was observed that the reaction rate decreased and the fraction of branched product increased with increasing generation number.

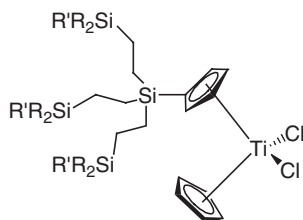


SCHEME 17.

Andrés *et al.* (81) reported the synthesis of titanium and zirconium metallocenes bearing one or two first-generation carbosilane dendritic wedges, together with their behavior in ethene polymerization with MAO as a cocatalyst. Reaction of wedges  $(\text{R}_2\text{R}'\text{SiCH}_2\text{CH}_2)_3\text{SiCl}$  with  $\text{K}(\text{C}_5\text{H}_5)$  and subsequent treatment with  $\text{KH}$  gave the dendronized cyclopentadienes  $\text{K}[(\text{R}_2\text{R}''\text{SiCH}_2\text{CH}_2)_3\text{Si}(\text{C}_5\text{H}_4)]$ , which were allowed to react with  $\text{CpTiCl}_3$  for the preparation of the mixed-ring titanocenes **88–89**, and with  $\text{MCl}_4$  ( $\text{M} = \text{Ti}, \text{Zr}$ ) for the synthesis of the symmetrically substituted metallocenes **90** and **91**.

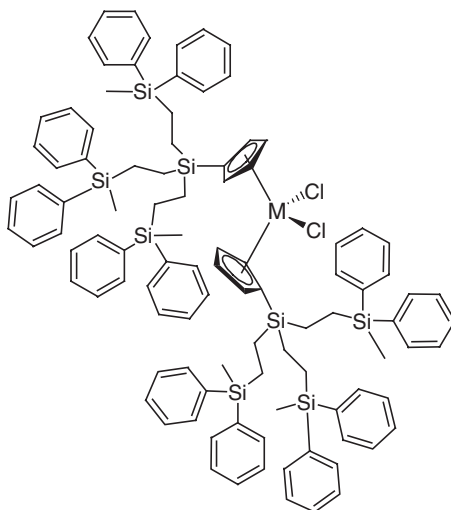
Complexes **88–91** catalyzed the polymerization of ethene upon activation with MAO. Every dendritic catalyst displayed a lower activity than its reference complex  $\text{Cp}_2\text{ZrCl}_2$  or  $\text{Cp}_2\text{TiCl}_2$ . It was found that the replacement of a  $\text{C}_5\text{H}_5^-$  ligand by a dendritic cyclopentadienide (**88** or **89**) caused a moderate decrease in activity (4,320; 2,064 and 1,720 kg/mol/h for  $\text{CpTiCl}_3$ , **88**, and **89**, respectively), which could be attributed to steric hindrance. The bis-dendritic Cp system **90** gave a lower activity (576 kgmol<sup>-1</sup>h<sup>-1</sup>). Interaction between a pair of dendritic wedges may restrict the conformations in which they are kept far away from the metal center.

In the case of the bis-dendritic zirconium complex **91**, a much smaller decrease in activity was observed relative to the reference zirconium complex, probably because of the bigger size of zirconium. Titanium dendrimers **88–90** gave polymers of higher molecular weights than those produced with  $\text{CpTiCl}_3$ . The polydispersity



$\text{R} = \text{R}' = \text{Et}$  **88**

$\text{R} = \text{Ph}; \text{R}' = \text{Me}$  **89**



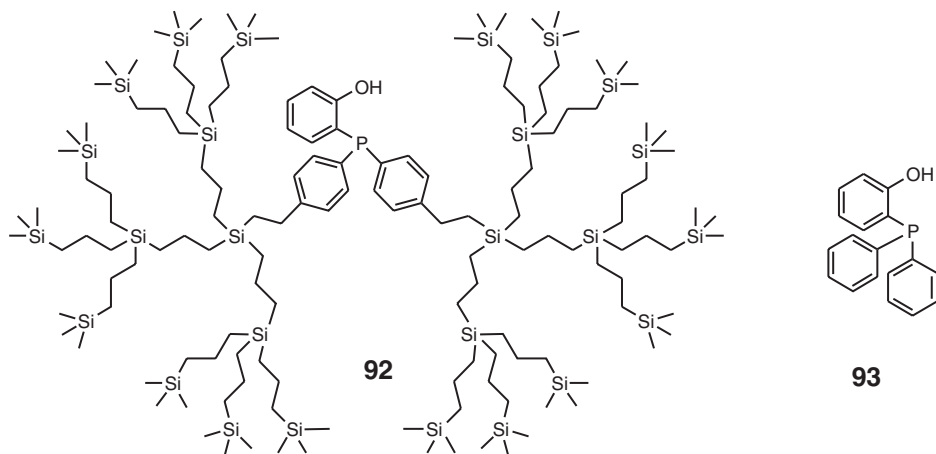
$\text{M} = \text{Ti}$  **90**

$\text{M} = \text{Zr}$  **91**

values increased with the number of dendritic substituents on the catalyst (1.86, 2.51, 3.33, and 5.81 for reference complex, **88**, **89**, and **90**, respectively). These values reflect the appearance of bimodal molecular weight distributions, especially for polyethylene produced by **90**. This fact could be attributed to a multi-state catalyst with slow interconversion of states or to the presence of traces of impurities, such as unsubstituted metal complexes.

Müller *et al.* (82) reported a site-isolation effect observed for a core-functionalized dendritic (P,O)Ni catalyst for the oligomerization of ethene. It was found that embedding a (P,O)Ni catalyst in a dendritic framework (**92**) suppressed the formation of inactive bis(P,O)Ni complexes in toluene, thereby enhancing the productivity of the catalyst. Catalysis experiments performed with **92** and parent ligand **93** in toluene show that the dendritic catalyst produced higher yields of oligomers than **93** (5.39 g oligomer,  $\text{TOF}_{\text{avg}} = 7700 \text{ h}^{-1}$  vs 2.52 g,  $\text{TOF}_{\text{avg}} = 3600 \text{ h}^{-1}$ ). Formation of bis(P,O)Ni complexes is favored in polar solvents such as methanol. The dendritic effect observed in methanol is subtle, because both **92** and **93** form bis(P,O)Ni complexes in solution. In contrast to the parent compound, the bis(P,O)Ni complex derived from dendrimer ligand **92** is able to dissociate to form active mono-ligated species under reaction conditions, as was evident from HP-NMR experiments, resulting in a dendritic catalyst that is far more active than the parent compound.

Enantioselective catalysis with dendrimers (83) offers appealing prospects in the search for “dendritic effects;” however, so far there are relatively few reports of applications of dendrimers in asymmetric catalysis. The traditional concepts of chirality for small molecules are not sufficient to explain the chiroptical properties of some of the chiral dendrimers. Some studies show that the local chirality in the core of a dendrimer can result in a cryptochiral dendrimer that exhibits no optical activity. Furthermore, in periphery-functionalized systems with chiral groups, the optical rotation can depend strongly on the number of end groups. In general, the rigidity of the system and the dense packing of chiral groups can have a dramatic



influence on the stereochemical properties. Steric hindrance of the chiral end groups at the periphery of a dendrimer can result in an increased resistance to the attainment of their preferred conformation of all terminal groups, which will have a direct influence on enantioselective catalysis.

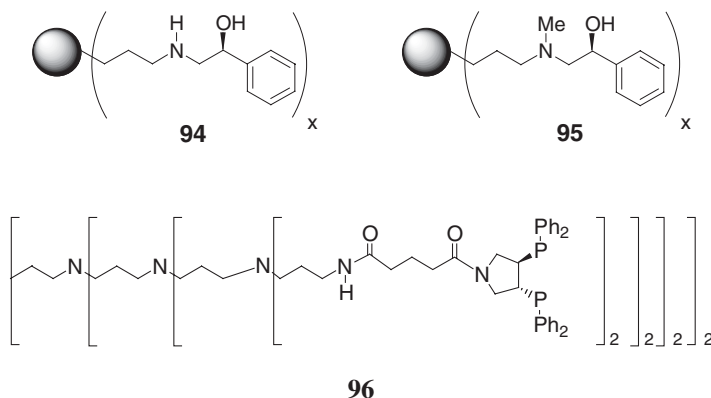
Meijer *et al.* (84) investigated the asymmetric addition of  $\text{Et}_2\text{Zn}$  to benzaldehyde catalyzed by PPI dendrimers functionalized with chiral amino alcohol ligands (94–95).

Their results show that the chemical yields of 1-phenylpropanol and the enantioselectivities decreased with increasing generation of the dendrimer; when G5 was used, almost no enantioselectivity was observed (57% yield, 7% ee), a result that was attributed to the dense packing of the chiral end groups at the periphery.

Similar results were obtained by Suzuki *et al.* (85) in their investigation of enantioselective addition of  $\text{Et}_2\text{Zn}$  to various N-diphenylphosphinylimines with PAMAM dendrimers functionalized with 4 and 8 chiral amino alcohol groups. They observed 92% ee for the monomeric ligand, 43% ee for G0, and 30–39% ee for G1 when using N-diphenylphosphinylbenzaldimine as the substrate. Again, a high local concentration of chiral active sites leads to a decrease in enantioselectivity.

Significantly, the more rigid dendrimers 53–54 and 11–14 (described in Section II) prepared by Sato (45) and Kolner (29) showed no drop in enantioselectivity for higher generations of the dendrimer for the addition of  $\text{Et}_2\text{Zn}$  to N-diphenylphosphinylimines and the hydrogenation of dimethylitaconate, respectively. This result clearly suggests that in those systems the catalysts work as independent sites without significant obstruction by steric congestion.

Recently Engel *et al.* (86) prepared the rhodium complexes of a series of chiral phosphine-functionalized PPI dendrimers and investigated their catalytic properties in the asymmetric hydrogenation of Z-methyl- $\alpha$ -acetamidocinammate and of dimethylitaconate. The reaction of carboxyl-linked  $\text{C}_2$ -chiral pyrphos ligand (3,4-bis(diphenylphosphino)pyrrolidine) with PPI dendrimers of generations 0–4 with ethyl-N,N-dimethylaminopropylcarbodiimide (EDC)/1-hydroxybenzotriazol as a coupling agent gave pyrphos-functionalized dendrimers (3G 96).

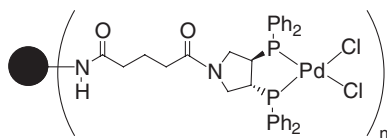


Subsequent metallation of the multi-site phosphines with  $[\text{Rh}(\text{COD})_2]\text{BF}_4$  led to dendrimers containing up to 32 cationic rhodium metal centers (for G4). These dendrimers were used as catalysts for the asymmetric hydrogenation of methyl acetamidocinnamate. It was found that the activity and enantioselectivity decreased upon going from G0 (93% ee) to G4 (88% ee). The results of the asymmetric hydrogenation of dimethylitaconate show a more pronounced dependence of the catalyst performance on the dendrimer size. The activity and selectivity were found to decrease upon going to the higher generations (74% ee for G0, 59% ee for G4). The reduction in activity observed for both hydrogenations is attributed to the reduced accessibility of all the metal centers in the higher-generation dendrimers, and the negative dendritic effect in enantioselectivity may be a consequence of the flexibility of the dendritic backbone, which renders the immediate environment of the catalytic centers less uniform.

In a subsequent paper (87), the same authors investigated the palladium-catalyzed allylic aminations with pyrphos-functionized PPI and PAMAM dendrimers as multidentate ligands. Zero to four generation PPI-(pyrphosPdCl<sub>2</sub>)<sub>x</sub> and PAMAM-(pyrphosPdCl<sub>2</sub>)<sub>x</sub> neutral dendrimers (97) showed a strong positive dendritic effect on the selectivity of the allylic amination of 1,3-diphenyl-1-acetoxypipropene with morpholine (at 45°C in DMSO).

A remarkable increase in catalyst selectivity was observed as a function of the dendrimer generation. This increase in ee values was less pronounced for the PPI-derived catalysts (40% ee for G4-PPI(pyrphosPdCl<sub>2</sub>)<sub>64</sub>) than for the more rigid PAMAM-containing dendritic catalysts, for which an increase in selectivity from 9% ee for a mononuclear reference system to 69% ee for G4-PAMAM (pyrphosPdCl<sub>2</sub>)<sub>64</sub> was observed.

Since the pioneering studies of asymmetric catalysis with core-functionalized dendrimers reported by Brunner (88) and Bolm (89), several noteworthy investigations have been described in this field. Some examples of the dendritic effects observed in enantioselective catalysis with dendrimers having active sites in the core were discussed in Section II, such as the catalytic experiments with TADDOL-cored dendrimers described by Seebach *et al.* (59); the asymmetric addition of Et<sub>2</sub>Zn to aldehydes catalyzed by core-functionalized phenylacetylene-containing dendrimers reported by Hu *et al.* (42); the asymmetric hydrogenation investigations with (R)-BINAP core-functionalized dendrimers synthesized by Fan *et al.* (36); or the results



● = PPI, PAMAM  
n = 4, 8, 16, 32, 64



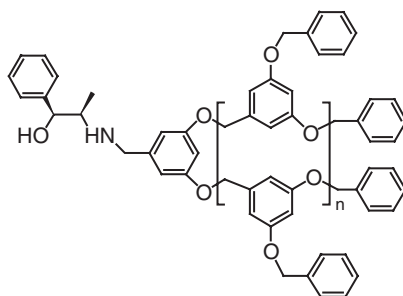
concerning the asymmetric transfer hydrogenation with polybenzylether-containing dendrimers with [(S,S)-TsDPEN] ligands in the core reported by Chen *et al.* (41).

The latter authors (90) subsequently prepared the Ru(II) complexes of dendritic ligands based on (1S, 2R)-norephedrine and used them as catalysts for asymmetric transfer hydrogenation. N-alkylation of (1S, 2S)-norephedrine with polybenzyl ether Fréchet-type wedges bearing benzylic bromo groups at the focal point led to dendritic ligands **98–100**. The catalysts were generated *in situ* by refluxing [RuCl<sub>2</sub>(*p*-cymene)]<sub>2</sub> and the dendritic ligands in isopropanol for 1 h. Asymmetric transfer hydrogenation reactions were carried out at 25°C in isopropanol with acetophenone as a substrate. In comparison with a ruthenium monomeric catalyst analogue, an enhancement of reactivity and similar enantioselectivity was observed for the first-generation catalyst Ru-**98** (70% yield, 93% ee for monomer; 88% yield, 92% ee for Ru-**98**). However, the second- and third-generation dendritic catalysts Ru-**99** and Ru-**100** led to a decrease in activity and enantioselectivity, probably as a consequence of their low solubility in isopropanol.

The addition of CH<sub>2</sub>Cl<sub>2</sub> as co-solvent to the Ru-**99** system improved the solubility, and as a consequence a great enhancement in reactivity and enantioselectivity was observed (63% yield, 87% ee for monomer; 82% yield, 90% ee for Ru-**99**). Moreover, use of the dendritic catalyst Ru-**100** for a prolonged reaction time (up to 25 h) did not result in lower ee values, as is usually observed for the unsupported species because of the reversibility of the transfer hydrogenation in isopropanol. The fact that the ee was retained upon use of the dendritic species is interesting, but the origin of the effect is unclear and might be explained simply by the lower reactivity.

To improve the solubility of the dendritic catalysts, other series of dendritic ligands with 2-methoxyethyl groups instead of benzyl groups were synthesized (**101–103**).

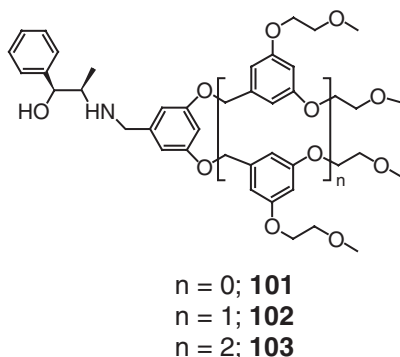
It was found that Ru-**101** and Ru-**102** maintained the enantioselectivity, and a dendritic acceleration effect was also observed in comparison with the performance of the monomeric analogue (70% yield, 93% ee for monomer; 75% yield, 92% ee for Ru-**101**; 90% yield, 93% ee for Ru-**102**). However, the higher-generation



n = 0; **98**

n = 1; **99**

n = 2; **100**



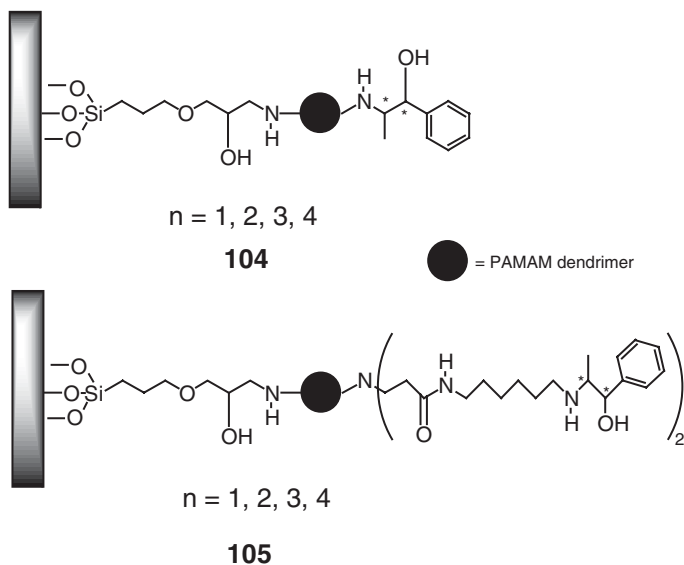
dendrimer Ru-**103** gave low catalytic activity and enantioselectivity associated with its poor solubility in isopropanol. By adding  $\text{CH}_2\text{Cl}_2$  to the reaction mixture, Ru-**103** gave rise to much better activity and selectivity.

### B. DENDRIMERS SUPPORTED ON A SOLID PHASE

Catalysis using immobilized dendritic catalysts on solid supports was discussed in Section II.E. Some interesting dendritic effects were also observed for this class of dendritic materials. For example, Chung *et al.* (57) investigated the  $\text{Et}_2\text{Zn}$  addition to benzaldehyde with silica-supported PAMAM dendrimers up to the fourth generation containing an (–)-ephedrine auxiliary. They observed a decrease in catalytic activity, selectivity, and enantioselectivity upon going to higher-generation dendrimer-modified surfaces when highly loaded silica supports were used. The loss in enantioselectivity was attributed to the presence of different chiral environments generated by incomplete functionalization during dendrimer synthesis. A diffusional resistance induced by irregularities in the hyper-branched structure explained the decrease in activity and selectivity. However, an opposite trend was observed for lightly loaded silica supports. The activity, selectivity, and enantioselectivity increased upon going to the third generation.

In a subsequent paper, the authors developed another type of silica-supported dendritic chiral catalyst that was anticipated to suppress the background racemic reaction caused by the surface silanol groups, and to diminish the multiple interactions between chiral groups at the periphery of the dendrimer (91). The silica-supported chiral dendrimers were synthesized in four steps: (1) grafting of an epoxide linker on a silica support, (2) immobilization of the *n*th generation PAMAM dendrimer, (3) introduction of a long alkyl spacer, and (4) introduction of chiral auxiliaries at the periphery of the dendrimer with (1*R*, 2*R*)-(+)-1-phenylpropene oxide. Two families of dendritic chiral catalysts with different spacer lengths were prepared (nG-**104** and nG-**105**).

Important differences were found between the two series of catalysts in promoting the addition of  $\text{Et}_2\text{Zn}$  to benzaldehyde. A decrease in conversion, selectivity, and enantiomeric excess upon increasing the dendrimer generation was observed

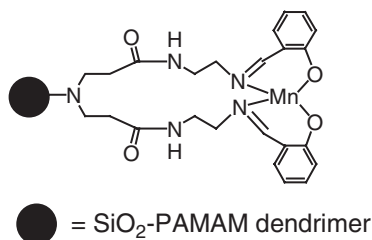


when nG-**104** dendrimers were used (79.7% yield, 96.4% selectivity, 13.2% ee for G1; 65.5% yield, 87.2% selectivity, 2.3% ee for G4). The denser packing in the higher-generation dendrimers restricts the access of reagents (decrease in activity) and leads to the presence of a number of different frozen-in conformations (poor enantioselectivity).

The reactions with nG-**105** dendrimers show a different trend. Enhanced catalytic performance was observed with increasing dendrimer generation (77.3% yield, 97.2% selectivity, 15.5% ee for G1; 85% yield, 98% selectivity, 37% ee for G4). This comparison indicates that the introduction of an alkyl spacer not only facilitates the access of reactant to the catalytic active sites but also prevents the formation of frozen-in conformations and thus different chiral active sites. However, when the fifth-generation dendrimer is reached, the multiple interactions between end groups become more pronounced, which leads to a decrease in the catalyst performance (68% yield, 95.3% selectivity, 17.6% ee).

Bu *et al.* (92) described the immobilization of an Mn(II) salen complex on the periphery of 0–4 generation PAMAM-SiO<sub>2</sub> dendrimers (**106**) and their use as catalysts for alkene epoxidation.

They reported a remarkable enhancement of the catalytic activity in the epoxidation of styrene upon increasing the dendrimer generation, which suggests that the length of the dendritic backbone chain plays an important role in increasing the accessibility of the reactant molecules to the catalytic active sites of the immobilized Mn(II) salen complex (yields of 20.2, 25.6, 36, 53.4, and 75% for G0-, G1-, G2-, G3-, and G4-Mn dendrimers, respectively). It was found that the manganese loadings are not as high as the expected values, and the amount of manganese loading of G4-Mn was even slightly lower than that of G3-Mn. However, G4-Mn exhibited a much higher catalytic activity than G3-Mn. These results suggest that the length of



106

the dendritic backbone plays a more important role in the catalytic performance than the number of catalytic sites. These silica-supported dendritic catalysts could be recycled and reused without significant loss in activity.

#### IV. Conclusions

There are reports of numerous examples of dendritic transition metal catalysts incorporating various dendritic backbones functionalized at various locations. Dendritic effects in catalysis include increased or decreased activity, selectivity, and stability. It is clear from the contributions of many research groups that dendrimers are suitable supports for recyclable transition metal catalysts. Separation and/or recycle of the catalysts are possible with these functionalized dendrimers; for example, separation results from precipitation of the dendrimer from the product liquid; two-phase catalysis allows separation and recycle of the catalyst when the products and catalyst are concentrated in two immiscible liquid phases; and immobilization of the dendrimer in an insoluble support (such as crosslinked polystyrene or silica) allows use of a fixed-bed reactor holding the catalyst and excluding it from the product stream. Furthermore, the large size and the globular structure of the dendrimers enable efficient separation by nanofiltration techniques. Nanofiltration can be performed either batch wise or in a continuous-flow membrane reactor (CFMR).

The common problems involved in catalyst recycle also pertain to dendritic catalysts. These include dendrimer or catalyst decomposition, dendrimer leaching, metal leaching, and catalyst deactivation. The demands are usually most stringent for applications in continuous processes. Some of the problems such as metal leaching and lack of catalyst stability can be alleviated by proper choice of ligands and dendrimer backbones. This point emphasizes the importance of ligand and catalyst design and the need for identification of the catalytically active species. It is significant that small changes in the dendritic architecture can have a huge impact on the stability of catalytic systems.

Whether dendritic catalysis can compete successfully in commercial applications with other systems remains to be seen. Two-phase catalysis and catalysis by

polymer-supported metal complexes have found successful industrial applications, but dendrimer-supported catalysts still have not. Dendrimer supports are still relatively expensive, but for applications that do not require the well-defined structure of the dendrimer support, hyperbranched polymers can offer a cheaper alternative. The price per active site of this type of material is competitive with the prices of supports such as crosslinked polystyrene and silica. However, it is important to realize that high turnover numbers are required before these sophisticated systems become attractive for commercial applications.

Although dendritic catalysts have been used in several reactions, more experiments are required to provide deeper insight into dendritic effects in catalysis and catalyst recycling. Optimal advantage of dendrimers as soluble supports for catalysts can be obtained when they are applied in a continuous-flow membrane reactor. The progress in membrane technology will be important to future development of sophisticated reactors for the application of dendritic catalysts. Dendritic systems functionalized with different catalytic sites at several well-defined locations can potentially be used for tandem reactions, making these membrane processes more efficient. However, so far the area of cascade reactions using dendrimers is largely unexplored.

## References

- (a) Astruc, D., and Chardac, F., *Chem. Rev.* **101**, 2991 (2001);
  - (b) Kreiter, R., Kleij, A.W., Klein Gebbink, R.J.M., and van Koten, G., in "Dendrimers IV: Metal Coordination, Self Assembly, Catalysis." (F. Vögtle, and C.A. Schalley, Eds.), Vol. 217, p. 163. Springer, Berlin, 2001;
  - (c) Oosterom, G.E., Reek, J.N.H., Kamer, P.C.J., and van Leeuwen, P.W.N.M., *Angew. Chem. Int. Ed.* **40**, 1828 (2001);
  - (d) Crooks, R.M., Zhao, M., Sun, L., Chechik, V., and Yueng, L.K., *Acc. Chem. Res.* **34**, 181 (2001);
  - (e) Reek, J.N.H., de Groot, D., Oosterom, G.E., Kamer, P.C.J., and van Leeuwen, P.W.N.M., *Rev. Mol. Biotechn.* **90**, 159 (2002);
  - (f) Reek, J.N.H., de Groot, D., Oosterom, G.E., Kamer, P.C.J., and van Leeuwen, P.W.N.M., *Comp. Rend. Chim.* **6**, 1061 (2003);
  - (g) van Heerbeek, R., Kamer, P.C.J., van Leeuwen, P.W.N.M., and Reek, J.N.H., *Chem. Rev.* **102**, 3717 (2002);
  - (h) Caminade, A.-M., Maraval, V., Regis, L., and Majoral, J.-P., *Current Organic Chemistry* **6**, 739 (2002).
- (a) Newkome, G. R., Moorefield, C. N., and Vögtle, F., in "Dendritic Molecules" Verlag Chemie, Weinheim, 1996;
  - (b) Vögtle, F., *Top. Curr. Chem.* **197** (1998);
  - (c) Majoral, J.-P., and Caminade, A.-M., *Chem. Rev.* **99**, 845 (1999);
  - (d) Bosman, A.W., Janssen, H.M., and Meijer, E.W., *Chem. Rev.* **99**, 1665 (1999).
- Tomalia, D.A., and Dvornic, P.R., *Nature* **372**, 617 (1994).
- A silica particle of 10 nm (a lower limit for a slurry reactor) loaded with 1% of rhodium contains approximately  $10^{12}$  metal atoms.
- Inoue, K., *Prog. Polym. Sci.* **25**, 453 (2000).
- (a) Adams, R.D., and Cotton, F.A. (Eds.), "Catalysis by Di- and Polynuclear Metal Cluster Complexes." Wiley-VCH Inc., New York, 1998;

- (b) Broussard, M.E., Juma, B., Train, S.G., Peng, W.-J., Laneman, S.A., and Stanley, G.G., *Science* **260**, 1784 (1993).
7. Ulman, M., and Grubbs, R.H., *J. Org. Chem.* **64**, 7202 (1999).
8. Mukhopadhyah, S., Rothenberg, G., Gitis, D., and Sasson, Y., *J. Org. Chem.* **65**, 3107 (2000).
9. Van de Kuil, L.A., Grove, D.M., Gossage, R.A., Zwikker, J.W., Jenneskens, L.W., Drenth, W., and van Koten, G., *Organometallics* **16**, 4985 (1997).
10. (a) Hecht, S., and Fréchet, J.M.J., *Angew. Chem. Int. Ed.* **40**, 74 (2001);  
(b) Gorman, C.B., and Smith, J.C., *Acc. Chem. Res.* **34**, 60 (2001).
11. Sirkar, K.K., Shanbhag, P.V., and Kovvali, A.S., *Ind. Eng. Chem. Res.* **38**, 3715 (1999).
12. (a) Kragl, U., Vasic-Racki, D., and Wandrey, C., *Chem.-Ing.-Tech.* **64**, 499 (1992);  
(b) Kragl, U., Vasic-Racki, D., and Wandrey, C., *Indian J. Chem.* **32B**, 103 (1993);  
(c) Bommarius, A.S., in "Biotechnology, Bioprocessing." (H.-J. Rehm, G. Reed, A. Pühler, P. Stadler, and G. Stephanopoulos, Eds.), Vol. 3, p. 427. VCH, Weinheim, 1993;  
(d) Prazeres, D.M.F., and Cabral, J.M.S., *Enzyme Microb. Technol.* **16**, 738 (1994);  
(e) Kragl, U., in "Industrial Enzymology." (T. Godfrey, and S. West, Eds.), MacMillan, Hampshire, 1996.
13. Kragl, U., and Dreisbach, C., *Angew. Chem. Int. Ed. Engl.* **35**, 642 (1996).
14. (a) Tsuji, J., Takahashi, H., and Morikawa, M., *Tetrahedron Lett.*, 4387 (1965);  
(b) Trost, B.M., and Verhoeven, T.R., in "Comprehensive Organometallic Chemistry." (G. Wilkinson, Ed.), Vol. 8, p. 799. Pergamon, Oxford, 1982;  
(c) Pfalz, A., *Acc. Chem. Res.* **26**, 339 (1993);  
(d) Sjörgren, M.P.T., Hansson, S., Åkermark, B., and Vitagliano, A., *Organometallics* **13**, 1963 (1994);  
(e) Trost, B.M., and van Vranken, D.V., *Chem. Rev.* **96**, 395 (1996);  
(f) Pregosin, P.S., and Salzmann, R., *Coord. Chem. Rev.* **155**, 35 (1996);  
(g) Blöchl, P.E., and Togni, A., *Organometallics* **15**, 4125 (1996);  
(h) Helmchen, G., Kudis, S., Sennhenn, P., and Steinhagen, H., *Pure and Applied Chem.* **69**, 513 (1997).
15. (a) Gotov, B., Toma, S., and Macquarrie, D.J., *New J. Chem.* **24**, 597 (2000);  
(b) Johnson, B. F. G., Raynor, S. A., Shephard, D. S., Maschmeyer, T., Thomas, J. M., Sankar, G., Bromley, S., Oldroyd, R., Gladden, L., and Mantle, M. D., *Chem. Commun.* 1167 (1999).
16. Reetz, M.T., Lohmer, G., and Schwickardi, R., *Angew. Chem. Int. Ed.* **36**, 1526 (1997).
17. Brinkmann, N., Giebel, D., Lohmer, G., Reetz, M.T., and Kragl, U., *J. Catal.* **183**, 163 (1999).
18. (a) De Groot, D., Eggeling, E. B., de Wilde, J. C., Kooijman, H., van Haaren, R. J., van der Made, A. W., Spek, A. L., Vogt, D., Reek, J. N. H., Kamer, P. C. J., and van Leeuwen, P. W. N. M., *Chem. Commun.*, 1623 (1999);  
(b) De Groot, D., Reek, J.N.H., Kamer, P.C.J., and van Leeuwen, P.W.N.M., *Eur. J. Org. Chem.* **6**, 1085 (2002).
19. (a) Oosterom, G. E., van Haaren, R. J., Reek, J. N. H., Kamer, P. C. J., and van Leeuwen, P. W. N. M., *Chem. Commun.*, 1119 (1999);  
(b) Reek, J. N. H., De Groot, D., Oosterom, G. E., van Heerbeek, R., Kamer, P. C. J., and van Leeuwen, P. W. N. M., *PMSE*, 087 (2001).
20. Oosterom, G.E., Steffens, S., Reek, J.N.H., Kamer, P.C.J., and van Leeuwen, P.W.N.M., *Top. Catal.* **19**, 61 (2002).
21. De Groot, D., de Waal, B.F.M., Reek, J.N.H., Schenning, A.P.H.J., Kamer, P.C.J., Meijer, E.W., and van Leeuwen, P.W.N.M., *J. Am. Chem. Soc.* **123**, 8453 (2001).
22. Hovestad, N.J., Eggeling, E.B., Heidbüchel, H.J., Jastrzebski, J.T.B.H., Kragl, U., Keim, W., Vogt, D., and van Koten, G., *Angew. Chem. Int. Ed.* **38**, 1655 (1999).
23. Eggeling, E.B., Hovestad, N.J., Jastrzebski, J.T.B.H., Vogt, D., and van Koten, G., *J. Org. Chem.* **65**, 8857 (2000).
24. Knapen, J.W.J., van der Made, A.W., de Wilde, J.C., van Leeuwen, P.W.N.M., Wijkens, P., Grove, D.M., and van Koten, G., *Nature* **372**, 659 (1994).
25. Kragl, U., "Membrane reactors for dendritic catalysts": Proceedings of the 1st International Dendrimer Symposium (Frankfurt, Germany), 1999.

26. Kleij, A.W., Gossage, R.A., Klein Gebbink, R.J.M., Brinkman, N., Kragl, U., Reyerse, E.J., Lutz, M., Spek, A.L., and van Koten, G., *J. Am. Chem. Soc.* **122**, 12112 (2000).
27. (a) Bogdan, P.L., Irwin, J.J., and Bosnich, B., *Organometallics* **8**, 1450 (1989);  
(b) Halpern, J., *Science* **217**, 401 (1982);  
(c) Brown, J. M., Chaloner, P. A., and Morris, G. A., *J. Chem. Soc. Chem. Commun.*, 644 (1983);  
(d) Dickson, R.S., in "Catalysis by Metal Complexes." (R. Ugo, and B.R. James, Eds.), Vol. 8, Reidel, Dordrecht, 1985;  
(e) Landis, C.R., and Halpern, J., *J. Am. Chem. Soc.* **109**, 1746 (1987);  
(f) Weissmehl, K., and Arpe, H.-J., in "Industrielle Organische Chemie" VCH, Weinheim, 1988;  
(g) Mortreux, A., and Petit, F., in "Catalysis by Metal Complexes." (R. Ugo, and B.R. James, Eds.), Reidel, Dordrecht, 1988;  
(h) Brown, J.M., *Chem. Rev.* **22**, 25 (1993);  
(i) Noyori, R., and Hashiguchi, S., in "Applied Homogeneous Catalysis with Organometallic Compounds." (B. Cornils, and W.A. Hermann, Eds.), Vol. 1, p. 552. VCH, Weinheim, 1996;  
(j) Kimmich, B.F.M., Somsook, E., and Landis, C.R., *J. Am. Chem. Soc.* **120**, 10115 (1998);  
(k) Landis, C.R., and Brauch, T.W., *Inorg. Chim. Acta* **270**, 285 (1998);  
(l) Rajanbabu, T.V., Radetich, B., You, K.K., Ayers, T.A., Casalnuovo, A.L., and Calabrese, J.C., *J. Org. Chem.* **64**, 3429 (1999);  
(m) Landis, C.R., Hilfenhausen, P., and Feldgus, S., *J. Am. Chem. Soc.* **121**, 8741 (1999);  
(n) Feldgus, S., and Landis, C.R., *J. Am. Chem. Soc.* **122**, 12714 (2000);  
(o) Knowles, W.S., *Angew. Chem. Int. Ed.* **41**, 1999 (2002).
28. Marquardt, T., and Lüning, U., *Chem. Commun.*, 1681 (1997).
29. Köllner, C., Pugin, B., and Togni, A., *J. Am. Chem. Soc.* **120**, 10274 (1998).
30. Schmitzer, A.R., Franceschi, S., Perez, E., Rico-Lattes, I., Lattes, A., Thion, L., Erard, M., and Vidal, C., *J. Am. Chem. Soc.* **123**, 5956 (2001).
31. Albrecht, M., Hovestad, N.J., Boersma, J., and van Koten, G., *Chem. Eur. J.* **7**, 1289 (2001).
32. Tulchinsky, M. L., and Miller, D. J. US 6350819, 2002, *Chem. Abstr.* **136**, 200619 (2002).
33. Frohning, C.D., and Kohlpaintner, C.W., in "Applied Homogeneous Catalysis with Organometallic Compounds: a comprehensive handbook in two volumes." (B. Cornils, and W.A. Herrmann, Eds.), Vol. 1, p. 27. VCH, Weinheim, 1996.
34. (a) Heuzé, K., Méry, D., Gauss, D., and Astruc, D., *Chem. Commun.*, 2274 (2003);  
(b) Heuzé, K., Méry, D., Gauss, D., Blais, J.-C., and Astruc, D., *Chem. Eur. J.* **10**, 3936 (2004).
35. Petrucci-Samija, M., Guillemette, V., Dasgupta, M., and Kakkar, A.K., *J. Am. Chem. Soc.* **121**, 1968 (1999).
36. Fan, Q.-H., Chen, Y.-M., Chen, X.-M., Jiang, D.-Z., Xi, F., and Chan, A.S.C., *Chem. Commun.*, 789 (2000).
37. Zeng, H., Newkome, G.R., and Hill, C.L., *Angew. Chem. Int. Ed.* **39**, 1772 (2000).
38. Plault, L., Hauseler, A., Nlate, S., Astruc, D., Ruiz, J., Gatard, S., and Neumann, R., *Angew. Chem. Int. Ed.* **43**, 2924 (2004).
39. Maraval, V., Caminade, A.-M., and Majoral, J.-P., *Organometallics* **19**, 4025 (2000).
40. Murahashi, S.I., Naota, T., Taki, H., Mizono, M., Takaya, H., Komiya, S., Mizuho, Y., Oyasato, N., Hitaoka, M., Hirano, M., and Fukuoka, A., *J. Am. Chem. Soc.* **117**, 12436 (1995).
41. Chen, Y.-C., Wu, T.-F., Deng, J.-G., Liu, H., Jiang, Y.-Z., Choi, M.C.K., and Chan, A.S.C., *Chem. Commun.*, 1488 (2001).
42. Hu, Q.-S., Pugh, V., Sabat, M., and Pu, L., *J. Org. Chem.* **64**, 7528 (1999).
43. Liu, G.-H., Tang, W.-J., and Fan, Q.-H., *Tetrahedron* **59**, 8603 (2003).
44. Garber, S.B., Kingsbury, J.S., Gray, B.L., and Hoveyda, A.H., *J. Am. Chem. Soc.* **122**, 8168 (2000).
45. Sato, I., Kodaka, R., Shibata, T., Hirokawa, Y., Shirai, N., Ohtake, K., and Soai, K., *Tetrahedron: Asymmetry* **11**, 2271 (2000).
46. Sato, I., Shibata, T., Ohtake, K., Kodaka, R., Hirokawa, Y., Shirai, N., and Soai, K., *Tetrahedron Lett.* **41**, 3123 (2000).
47. Bourque, S.C., Maltais, F., Xiao, W.-J., Tardif, O., Alper, H., Arya, P., and Manzer, L.E., *J. Am. Chem. Soc.* **121**, 3035 (1999).
48. Bourque, S.C., and Alper, H., *J. Am. Chem. Soc.* **122**, 956 (2000).

49. De Groot, D., Emmerink, P. G., Coucke, C., Reek, J. N. H., Kamer, P. C. J., and van Leeuwen, P. W. N. M., *Inorg. Chem. Commun.* 711 (2000).
50. Arya, P., Rao, N.V., Singkhonrat, J., Alper, H., Bourque, S.C., and Manzer, L.E., *J. Org. Chem.* **65**, 1881 (2000).
51. Arya, P., Panda, G., Rao, N.V., Alper, H., Bourque, S.C., and Manzer, L.E., *J. Am. Chem. Soc.* **123**, 2889 (2001).
52. Lu, S.-M., and Alper, H., *J. Am. Chem. Soc.* **125**, 13126 (2003).
53. Alper, H., Ayra, P., Bourque, S.C., Jefferson, G.R., and Manzer, L.E., *Can. J. Chem.* **78**, 920 (2000).
54. Antebi, S., Arya, P., Manzer, L.E., and Alper, H., *J. Org. Chem.* **67**, 6623 (2002).
55. Reynhardt, J.P.K., and Alper, H., *J. Org. Chem.* **68**, 8353 (2003).
56. Zweni, P.P., and Alper, H., *Adv. Synth. Catal.* **346**, 849 (2004).
57. Chung, Y.-M., and Rhee, H.-K., *Chem. Commun.*, 238 (2002).
58. Sanders-Hoven, M.S.T.H., Jansen, J.F.G.A., Vekemans, J.A.J.M., and Meijer, E.W., *Mater. Sci. Eng.* **210**, 180 (1995).
59. (a) Rheiner, P.B., and Seebach, D., *Polym. Mater. Sci. Eng.* **77**, 130 (1997);  
(b) Rheiner, P.B., Sellner, H., and Seebach, D., *Helv. Chim. Acta* **80**, 2027 (1997).
60. Sellner, H., and Seebach, D., *Angew. Chem. Int. Ed.* **8**, 1918 (1999).
61. Sellner, H., Faber, C., Rheiner, P.B., and Seebach, D., *Chem. Eur. J.* **6**, 3692 (2000).
62. Reetz, M.T., and Giebel, D., *Angew. Chem. Int. Ed.* **39**, 2498 (2000).
63. Mizugaki, T., Ooe, M., Ebitani, K., and Kaneda, K., *J. Mol. Catal. A: Chem.* **145**, 329 (1999).
64. Kenawy, E.-R.J.M.S., *Pure Appl. Chem. A* **35**, 657 (1998).
65. Cornils, B., and Herrmann, W. A., (Eds.), in "Applied Homogeneous Catalysis with Organometallic Compounds: a Comprehensive Handbook in Three Volumes" VCH, Weinheim, 2002.
66. (a) Horvath, I.T., and Rabai, J., *Science* **266**, 72 (1994);  
(b) Horvath, I.T., *Acc. Chem. Res.* **31**, 641 (1998).
67. Gong, A., Fan, Q., Chen, Y., Liu, H., Chen, C., and Xi, F., *J. Mol. Catal. A Chem.* **159**, 225 (2000).
68. (a) Horvath, I.T., and Rabai, J., *Science* **266**, 72 (1994);  
(b) Horvath, I.T., *Acc. Chem. Res.* **31**, 641 (1998).
69. Hanson, B. E., Ding, H., and Kohlpaintner, C. W., *Catal. Today* 421 (1998).
70. Zhao, M., Sun, L., and Crooks, R.M., *J. Am. Chem. Soc.* **120**, 4877 (1998).
71. Zhao, M., and Crooks, R.M., *Angew. Chem. Int. Ed.* **38**, 364 (1999).
72. Chechik, V., Zhao, M., and Crooks, R.M., *J. Am. Chem. Soc.* **121**, 4910 (1999).
73. Chechik, V., and Crooks, R.M., *J. Am. Chem. Soc.* **122**, 1243 (2000).
74. Mizugaki, M., Murata, M., Ooe, M., Ebitani, K., and Kaneda, K., *Chem. Commun.*, 52 (2002).
75. Ooe, M., Murata, M., Mizugaki, T., Ebitani, K., and Kaneda, K., *J. Am. Chem. Soc.* **126**, 1604 (2004).
76. Kleij, A.W., Gossage, R.A., Jastrzebski, J.T.B.H., Boersma, J., and van Koten, G., *Angew. Chem. Int. Ed.* **39**, 176 (2000).
77. Ropartz, L., Haxton, K. J., Foster, D. F., Morris, R. E., Slawin, A. M. Z., and Cole-Hamilton, D. J., *J. Chem. Soc., Dalton Trans.*, 4323 (2002).
78. Gatard, S., Kahlal, S., Méry, D., Nlate, S., Cloutet, E., Saillard, J.-Y., and Astruc, D., *Organometallics* **23**, 1313 (2004).
79. Gitsov, I., Ivanova, P.T., and Fréchet, J.M.J., *Macromol. Rapid Commun.* **15**, 387 (1994).
80. (a) Chow, H.-F., and Mak, C.C., *J. Org. Chem.* **62**, 5116 (1997);  
(b) Mak, C.C., and Chow, H.-F., *Macromolecules* **30**, 1228 (1997).
81. Andrés, R., de Jesús, E., de la Mata, F. J., Flores, J.C., and Gómez, R., *Eur. J. Inorg. Chem.*, 2281 (2002).
82. Muller, C., Ackerman, L.J., Reek, J.N.H., Kamer, P.C.J., and van Leeuwen, P.W.N.M., *J. Am. Chem. Soc.* **126**, 14960 (2004).
83. Seebach, D., Rheiner, P.B., Greiveldinger, G., Butz, T., and Sellner, H., *Top. Curr. Chem.* **197**, 125 (1998).
84. Sanders-Hoven, M.S.T.H., Jansen, J.F.G.A., Vekemans, J.A.J.M., and Meijer, E.W., *Polym. Mater. Sci. Eng.* **210**, 180 (1995).



85. Suzuki, T., Hirokawa, Y., Ohtake, K., Shibata, T., and Soai, K., *Tetrahedron: Asymmetry* **8**, 4033 (1997).
86. Engel, G.D., and Gade, L.H., *Chem. Eur. J.* **8**, 4319 (2002).
87. Ribourdouille, Y., Engel, G. D., Richard-Ploutet, M., and Gade, L. H., *Chem. Commun.*, 1228 (2003).
88. (a) Brunner, H.J., *Organomet. Chem.* **500**, 39 (1995);  
(b) Brunner, H., and Altmann, S., *Chem. Ber.* **127**, 2285 (1994);  
(c) Brunner, H., Fürst, J., Nagel, U., and Fischer, A.Z., *Naturforschung* **49 B**, 1305 (1994).
89. Bolm, C., Derrien, N., and Seger, A., *Synlett*, 387 (1996).
90. Liu, P.-N., Chen, Y.-C., Li, X.-Q., Tu, Y.-Q., and Deng, J.-G., *Tetrahedron: Asymmetry* **14**, 2481 (2003).
91. Chung, Y.-M., and Rhee, H.-K., *Catal. Lett.* **82**, 249 (2002).
92. Bu, J., Judeh, Z.M.A., Ching, C.B., and Kawi, S., *Catal. Lett.* **85**, 183 (2003).

# Catalysis in Ionic Liquids

Z. CONRAD ZHANG

*AKZO Nobel Chemicals, Inc., 1 Livingstone Avenue, Dobbs Ferry, New York 10522, USA*

Ionic liquids, salts with melting points less than about 100°C, present a wide range of properties for applications as catalysts, and there has been a spate of research recently concerned with catalytic applications of low-temperature ionic liquids. These typically consist of an organic cationic component with one or multiple heteroatoms, such as N, P, or S, and an inorganic or organic anion. The inertness of many ionic liquids toward most known catalysts makes them superior to water as solvents for catalysts, and from an environmental point of view, their low vapor pressures make them attractive as replacements for organic solvents. Other unique properties of ionic liquids, including the high thermal stability, broad ranges of temperatures over which they are liquids, the tunability of their acidities, and their excellent retention of polar or charged catalysts make them appealing media for a broad range of catalytic applications. Reusable catalyst–ionic liquid systems make possible facile catalyst–product separation, providing economic incentives for the development of such systems for new processes and as replacements for the existing ones.

**Abbreviations:** acac, acetylacetonate; AD, asymmetric dihydroxylation; AMIM, 1-alkyl-3-methylimidazolium; ATRP, atom transfer radical polymerization; BA, butyl acrylate; BDMIM, 1-butyl-2, 3-dimethylimidazolium; BDP, dibutylphosphonate; bdpp, 2, 4-bis(diphenylphosphino)pentane; BINAP, 2, 2'-bis(diphenylphosphino)-1, 1'-binaphthyl; BMIM, 1-butyl-3-methylimidazolium; Bn, benzyl; BuPy, *n*-butylpyridinium; CALB, *Candida antarctica* lipase B; cod, cyclooctadiene; Cy, cyclohexyl; cyt, cytochrome; DABCO, 1, 4-diazabicyclo[2.2.2] octane; dba, dibenzylideneacetone; DBIM, 1, 3-dibutylimidazolium; DMF, dimethylfuran; DMIM, 1-decyl-3-methylimidazolium; DSC, differential scanning calorimetry; EADC, ethylaluminum dichloride; EEIM, 1-ethyl-3-ethylimidazolium; EMIM, 1-ethyl-3-methylimidazolium; EMIMF, 1-ethyl-3-methylimidazolium fluoride; GOD, glucose oxidase; HBIM, hydrogen butylimidazolium; hfacac, hexafluoroacetylacetonate; HMIM, 1-H-3-methylimidazolium; HOMIM, 3-hexyloxymethyl-1-methylimidazolium; IM, imidazolium; IR, infrared; MBMIM, methyl-1-butyl-3-methylimidazolium; MIM, methylimidazolium; MMA, methyl methacrylate; MMIM, 1-methyl-3-methylimidazolium; Mn, number average molecular weight; MOEMIM, 1-methoxyethyl-3-methylimidazolium; MP, microperoxidase; MTBE, methyl-*tert*-butylether; MTO, methyltrioxorhenium; MTOA, methyltriocetylammmonium; Mw, weight average molecular weight; nbd, norbornadiene; OMIM, 1-octyl-3-methylimidazolium; o-Tol, ortho-tolyl; PCL, *Pseudomonas cepacia* lipase; PDI, polydispersity index; PPA, poly(phenylacetylene); PPTS, pyridinium *p*-toluenesulfonate; PS-C, *Pseudomonas cepacia*; pta, 1, 3, 5-triaza-7-phosphadamantane; QB, quininium bromide; (QN)<sub>2</sub>PHAL, 1, 4-bis(9-*O*-quininyl)phthalazine; Q<sup>+</sup>OOH<sup>-</sup>, dialkylimidazolium hydroperoxide; RCM, ring-closing metathesis; ROP, ring-opening polymerization; ScCO<sub>2</sub>, supercritical carbon dioxide; TBA, tetrabutylammmonium; TBAB, tetrabutylammmonium bromide; Tf<sub>2</sub>N, bis(trifluoromethanesulfonyl)amide; TfO, trifluoromethanesulfonate; TfOH, trifluoromethanesulfonic acid; TGA, thermogravimetric analysis; THF, tetrahydrofuran; THP, tetrahydropyran; TMAC, trimethylammmonium chloride; TOF, turnover frequency; TPP, triphenyl phosphine; tppti, tri(*m*-sulfonyl)triphenyl phosphine tris(1-butyl-3-methylimidazolium); tppts, tri(*m*-sulfonyl)triphenyl phosphine trisodium; TPPTS triphenylphosphine

trisulfonate sodium salt; TSIL, task-specific ionic liquid; TsO, tosylate; TsOH *p*-toluenesulfonic acid; UV, ultraviolet; UCST, upper critical solution temperature; ViEIM, 1-vinyl-3-ethyl-imidazolium; VO(salen)@IL, a vanadyl salen complex chemically attached to an ionic liquid.

## I. Introduction

Ionic liquids are salts that are often defined as those with melting points  $< 100^{\circ}\text{C}$  (*1*); many are liquids even at room temperature. These salts present a wide range of properties for applications as new solvents and catalysts. A large number of new ionic liquids have been reported recently, and the scope of their potential applications has been expanding rapidly. For catalytic applications, ionic liquids can be viewed as salts that are stable in the liquid state under the process conditions.

One distinctive difference between the low-melting ionic liquids and conventional molten salts is reflected in their compositions. A low-temperature ionic liquid typically consists of an organic cationic component with one or multiple heteroatoms, such as N, P, or S, and an inorganic or organic anion, whereas conventional molten salts are typically inorganic, commonly mixed metal halides. Ionic liquids have considerably lower melting points than most conventional molten salts, although a number of low-melting molten salts exist. The conventional molten salts are typically corrosive at high temperatures and therefore find only limited applications in catalytic processes. Many ionic liquids are known to be thermally stable up to  $300^{\circ}\text{C}$  or somewhat higher temperatures, but the decomposition temperature of an ionic liquid can be significantly lowered by impurities. In general, the melting and stable temperature ranges of most ionic liquids have been found to be well suited to a broad range of catalytic processes.

The history of the development of ionic liquids has been reviewed (*2*) and is not addressed here.

Successful homogeneous catalysts offer advantages that may include high selectivity, high activity, low investment cost, and flexibility of operation under mild conditions that facilitate rapid mixing and heat removal. For selective synthesis of fine chemicals and medicinal products, organometallic homogeneous catalysts are particularly attractive because of their well-characterized, uniform active sites and the tunability of their steric and electronic properties by variation of the metal and/or the ligands (*3,4*).

However, homogeneous catalytic processes typically suffer from the disadvantages of corrosion and expensive separation of the catalyst from the products, and in many cases, the need for an organic solvent poses serious challenges to the commercialization of the processes. Because of these disadvantages, it may be economical to isolate the catalyst in a phase separate from that containing most of the reactants, for example, by the use of liquid–liquid two-phase systems. In such systems, the catalyst is confined in a polar liquid phase in which the organic products are poorly soluble. The use of aqueous (*5*) or fluorous (*6*) phases for the catalyst has been investigated thoroughly. Water-soluble sulfonated arylphosphorus-containing ligands have enabled various biphasic catalytic reactions to be conducted on an industrial scale (*6,7*).

The concept of this biphasic catalysis implies that the organometallic catalyst is soluble in only one phase whereas the reactants and products are confined almost entirely to the other phase. In most cases, the catalyst phase can be reused, and the products and reactants are simply removed from the reaction mixture by decantation. In successful processes involving biphasic catalysis, the advantages of homogeneous catalysis listed above may be realized without the disadvantages of expensive separation of catalysts from products.

The use of an aqueous phase for catalyst isolation has met with some obvious limitations. Water is a coordinating proton-donor solvent with a high polarity and may be reactive with the metal catalyst and thereby interfere with the desired chemistry. Another disadvantage of aqueous-organic systems is that the ligands on the catalyst have to be modified to give the catalyst the needed solubility in water, and the low solubility of some organic reactants in water limits the attainable reaction rates. Solubilities of reactants in an aqueous phase may be quite limited and reaction rates may be correspondingly low when the reactants are introduced from the gas phase.

Potential applications of fluorous phases are also limited by the low solubilities of reactants in them (8–10), and modifications of catalysts with fluorous ligands necessary for some applications are expected to be expensive (6).

An area of broad interest in catalysis is the search for viable replacements for the widely used Brønsted liquid acids such as HF and H<sub>2</sub>SO<sub>4</sub> and solid Lewis acids such as AlCl<sub>3</sub> and MgCl<sub>2</sub>. The liquid acids are corrosive and also costly, because of the need to work up the products by neutralization and repeated washing. In many cases, the contamination of the products by these acids induces degradation over time and limits the application of the products. The cost of multi-step washing can be quite high. Acidic ionic liquids therefore offer potential alternatives for such reactions (11).

Ionic liquids in general have higher densities than most organic reactants and products. They are also quite different in other physical and chemical properties, as discussed below. Therefore, they usually have limited miscibility with most reactants and products of practical interest. Ionic liquids have been used to carry catalysts that are charged or bear polar functional groups; the catalysts are retained in the ionic liquid phase after separation of the product phase. It has even been reported that an inert ionic liquid could be used as a medium to make and stabilize metallic nanoclusters (12).

Most catalytic applications of ionic liquids involve a biphasic or multiphasic system, with the ionic liquids being readily and economically separated from the products and in most cases reusable. Some ionic liquids can also function as catalysts themselves.

There is a wide range of possibilities for adjusting the solubility characteristics of ionic liquids, and this is one of their potential advantages for optimized performance in biphasic or multiphasic catalysis (1). Because of the generally weak coordinating ability of the anions, most catalysts can be isolated in the solvent in a stable state without loss of activity. The product selectivity can sometimes be improved as well by the phase isolation. Because the catalyst is concentrated in the ionic phase, the reaction volume can be much smaller than in classical

homogeneous processes in which the catalyst concentration in an organic solvent is typically low.

Dissolving a metal halide Lewis acid in a stable ionic liquid may increase the catalytic activity of the Lewis acid. Most of these Lewis acids have good solubilities in ionic liquids.

An early success has appeared in a commercial process for the manufacture of alkoxyphenylphosphine. This process ingeniously utilizes the low melting point of an ionic liquid and the facile formation of the liquid from a precursor during the process (13). In the process, HCl is a product. Triethylamine was used in the former process, together with the feed, to scavenge the HCl. The process slurry became increasingly viscous from the formation of triethylammonium chloride. The new BASF BASIL process uses *N*-methylimidazole to scavenge the HCl, resulting in the formation of the ionic liquid *N*-methylimidazolium chloride, which has a melting point of 75°C, below the operating temperature. Remarkably, the production rate of the new process involving the ionic liquid is accelerated by a factor of 80 000.

Another example is butene dimerization catalyzed by nickel complexes in acidic chloroaluminates (14). This reaction has been performed on a continuous basis on the pilot scale by IFP (Difasol process). Relative to the industrial process involving homogeneous catalysis (Dimersol process), the overall yield in dimers is increased. Similarly, selective hydrogenation of diene can be performed in ionic liquids, because the solubility of dienes is higher than that of monoene, which is higher than that of paraffins. In the case of the Difasol process, a reduction of the volume of the reaction section by a factor of up to 40 can be achieved. This new Difasol technology enables lower dimer (e.g., octenes) production costs (14).

With the continued explosion of academic and industrial activities surrounding ionic liquids for many different applications, the potential for catalytic processes using ionic liquids has been increasingly recognized (1,15–18). A number of excellent reviews have appeared (19), including the reviews related to biocatalytic applications of ionic liquids (20,21).

The review presented here is intended to update the development of the fundamental understanding of ionic liquids as applied to catalytic processes.

## II. Ionic Liquids for Catalysis and Process Engineering

### A. GENERAL FEATURES OF IONIC LIQUIDS IN CATALYSIS

Ionic liquids represent a unique class of reaction media for catalytic processes, and their application in catalysis has entered a period of exploding growth. The number of catalytic reactions involving ionic liquids continues to increase rapidly. These liquids offer promising solutions to the problems associated with conventional organic solvents; the potential advantages may include enhanced reaction rates, improved chemo- and regioselectivities, and facile separation of products and catalyst recovery.

Because most transition metal complexes are soluble in ionic liquids, the ionic liquids are particularly suited for the isolation of catalysts in biphasic synthesis.

The modification of ligands to introduce charged groups has been carried out to prevent leaching of the catalyst from the ionic liquid phase to the organic phase. The catalytic reaction takes place in the ionic liquid phase or at the interface between the phases, where the catalyst is homogeneously distributed. It is desirable to have a high solubility of the reactants combined with a low solubility of the desired products in the ionic liquid phase. In such a system, the continuous removal of reaction products from the ionic liquid phase can lead to high yields because it minimizes the approach to equilibrium of the reaction in the phase where the reaction occurs and also reduces consecutive reactions.

Ionic liquids offer a broad spectrum of solvent properties that can be readily distinguished from those of the typical conventional organic solvents. The possibilities for tailoring properties of ionic liquids by the selection of their structures are particularly attractive.

When the solubility of reactants in ionic liquids is limited, mixed organic solvents and ionic liquids can be used advantageously to achieve homogeneous systems in which the reactants and catalysts have the best solubility. The product separation can be facilitated by the removal of the organic solvent from the mixed solvent containing the ionic liquid (e.g., by extraction or distillation), because the solubility of the product in the ionic liquid is reduced upon the removal of the organic solvent.

In catalytic reactions, ionic liquids with controllable coordinating strengths and/or reactivities toward the catalyst are particularly important. The coordinating strength of the ionic liquids depends on the nature of the anions and on the metal complex involved in the catalysis. With a large selection of available anions, it is possible to tailor the ionic liquid to suit specific chemical reactions, and variation of the structure and the composition of the cations and anions can alter the solubility of organic reactants in the ionic liquid.

The subject of ionic liquids applied to separation of gases and liquids has been reviewed recently (22). Although the separation of products from ionic liquids deserves significant consideration in catalytic processing, it is discussed in this review only when it is relevant to a specific example.

Some general features of ionic liquids relevant to catalysis are summarized below (15,16,22,23):

- (1) The melting point of an ionic liquid is typically below 100°C and often near ambient temperature. It is often important that there is a wide range of temperature over which the liquid is maintained to allow operational flexibility. Ionic liquids offer a desirable liquid range of up to 300°C.
- (2) Ionic liquids essentially lack measurable vapor pressures. Therefore, they emit almost no volatile organic compounds and allow product removal simply by distillation. There is little product contamination by ionic liquids. As a result, recycling of the ionic liquids and catalysts becomes feasible.
- (3) Ionic liquids have much higher heat capacities and thermal conductivities than most organic solvents. These properties facilitate heat transfer for many chemical reactions.
- (4) These liquids are inert and stable toward various organic chemicals under the typical process conditions. Importantly, many ionic liquids are also inert in

- reactions involving polar or charged intermediates such as carbocations or carbanions, so that such intermediates may be long-lived in these media.
- (5) Ionic liquids have higher densities than organic liquids, and thus exist as the lower phase in a biphasic system. They are also generally more viscous than conventional organic solvents; the phase separation from organic solvents is often more rapid than with two solvents of similar viscosity.
  - (6) Some ionic liquids have tunable Lewis acidities and basicities. The tuning can be achieved simply by varying the anion fraction in the overall ionic liquid composition. In some cases, Brønsted acidity can also be introduced into stable ionic liquids. Many publications show the broad applicability of acidic or basic ionic liquid media in catalysis replacing corrosive liquids and solid catalysts.
  - (7) Ionic liquids are generally polar, but the component ions are weakly coordinating. Therefore, most ionic liquids are compatible with organometallics and metal catalysts; the active site is only little affected by the anions of the ionic liquids and remains easily accessible to organic reactants. Furthermore, ionic liquids are also chemically inert toward reactive intermediates. In contrast to aqueous phases, ionic liquids allow the use of most conventional ligands. Most known catalysts, when used in ionic liquids, typically exhibit reactivities different from those in conventional solvents. There are numerous examples showing that reactions are accelerated in suitable ionic liquids and proceed with selectivities superior to those observed when the reaction occurs in a conventional organic solvent. In a number of cases, improved catalyst stability has also been observed in ionic liquids.
  - (8) Ionic liquids display good solubility for some organic compounds, typically aromatics, but poor solubility for many saturated hydrocarbons, and solubilities of gases also depend on their properties. It has therefore been possible to run chemical reactions with reactants that are more soluble in the ionic liquids than products.
  - (9) There is a broad spectrum of physical and chemical properties among ionic liquids, allowing their tailoring for a wide range of applications (23).
  - (10) Catalysis in ionic liquids is not limited to biphasic reaction systems. When the reaction mixture is homogeneous, an extraction solvent that is immiscible with the ionic liquid can be used to remove the product. A number of organic solvents display little or only limited miscibility with these liquids. However, this advantage is of limited value in practice, because one major incentive for using ionic liquids is to avoid volatile organic compounds.

## B. ISOLATION OF CATALYSTS

In conventional solid–liquid or solid–gas heterogeneous catalytic systems, the catalyst is conveniently separated from the fluid-phase reaction product. When an ionic liquid is used as a phase to isolate a catalyst, the catalyst is fully dispersed and mobile and may be fully involved in the reaction. When a homogeneous catalyst is isolated by anchoring onto the surface of a solid support (e.g., by reaction with OH groups), the result may be a stable catalyst that is not leached into the reactant

phase during catalysis (24). When an ionic liquid is used as a phase to isolate the catalyst, the typical catalyst experiences little direct bonding to the ionic liquid and maintains a high dispersion and accessibility; polarity and charge play a rather important role.

Although most ionic liquids have high viscosities at room temperature, viscosity can drop dramatically with a small increase in temperature (25). The density of an ionic liquid also drops with increasing temperature. Because reactions are typically carried out at temperatures above ambient, the miscibility of an ionic liquid with reactants and products can be expected to increase as the temperature is raised to that of the reaction. The result may be an enhanced reaction rate by reduction of the mass transfer resistance between reactants and the catalyst that are separated in two phases at ambient temperature. Furthermore, as the miscibility of ionic liquids with various organic solvents can be tuned, an ideal situation could be reached by selecting an ionic liquid in which reactants are more soluble than the product, resulting in a minimal mass transfer resistance for the reactants to reach the catalyst in the ionic liquid—then, at the end of a catalytic process, the product and ionic liquid can be readily separated from each other at reduced temperatures, allowing easy recycling and reuse of the catalytic ionic liquid phase.

An example illustrates how the miscibility of water with ionic liquids can be engineered to allow a temperature-controlled reversible single-phase–biphase transition (26). In such a system, the ionic liquid [OMIM]BF<sub>4</sub> and water exist as separate phases at room temperature; a catalyst preferentially stays in the ionic liquid phase rather than the water phase. When hydrogenation reactions were conducted at a higher temperature, 80°C, the two phases became completely miscible, allowing homogeneous catalysis. Upon cooling, the phase separation occurs again, with the catalyst in the ionic liquid phase and water serving as an extractant for water-soluble products.

### C. PRODUCT SEPARATION AND CATALYST RECYCLING

In an ideal case, an ionic liquid dissolves the catalyst and displays a partial miscibility with the reactants under reaction conditions (giving a relatively high reaction rate) and negligible miscibility with the product (giving enhanced selectivity and yield). At the termination of the reaction, the product can be removed by simple decantation without the need to extract the catalyst. This mode of operation eliminates heating and therefore results in reduced loss of catalyst by thermal decomposition (1).

When the products are partially or totally miscible in the ionic liquid, the separation of the products can be more complicated. It is however possible to reduce the solubility of typical organic products in the ionic liquid by introducing a more polar solvent that can be separated by distillation afterward at a lower temperature (27). Because of the low vapor pressure of the ionic liquid, direct distillation can be applied without azeotrope formation (28). However, such operation is often limited to highly volatile or thermally labile products because of the general thermal instability of organometallic catalysts.



As an alternative to distillation, extraction with a co-solvent that is poorly miscible with the ionic liquid has often been used. There are many solvents that can be used to extract product from the ionic liquid phase, whether from a monophasic reaction or from a partially miscible system. Typical solvents are alkanes and ethers (15). Supercritical CO<sub>2</sub> (scCO<sub>2</sub>) was recently shown to be a potential alternative solvent for extraction of organics from ionic liquids (22). CO<sub>2</sub> has a remarkably high solubility in ionic liquids. The scCO<sub>2</sub> dissolves quite well in ionic liquids to facilitate extraction, but there is no appreciable ionic liquid solubilization in the CO<sub>2</sub> phase in the supercritical state. As a result, pure products can be recovered. For example, about 0.5 mol fraction of CO<sub>2</sub> was dissolved at 40°C and 50 bar pressure in [BMIM]PF<sub>6</sub>, but the total volume was only swelled by 10%. Therefore, supercritical CO<sub>2</sub> may be applied to extract a wide variety of solutes from ionic liquids, without product contamination by the ionic liquid (29).

However, because water has a high polarity, the solubility of CO<sub>2</sub> in ionic liquids, exemplified by [BMIM]PF<sub>6</sub> is markedly reduced by the presence of water (30).

CO<sub>2</sub> has been proposed to function as a separation switch for ionic-liquid–organic mixtures (31). The concept of task-specific ionic liquids (TSILs) was also suggested for CO<sub>2</sub> assisting in the capturing of the organics (32). In recent works, the solubility of supercritical CO<sub>2</sub> at various densities in ionic liquid was explored for the lipase-catalyzed resolution of chiral secondary alcohols (33). The process combines biocatalytic esterification with highly efficient enantiomer separation in a continuous flow system avoiding the use of organic solvents completely. In this process, the racemic alcohol and the acylating agent are transported into the reactor by use of scCO<sub>2</sub> as the mobile phase. One of the enantiomers is esterified selectively by the lipase in the ionic liquid, and the mixture of products is continuously extracted with the scCO<sub>2</sub> stream. Ester and unreacted alcohol are then separated downstream by controlled density reduction by variation of temperature and/or pressure. The acylating agent was chosen so that the ester can have either higher or lower solubility in scCO<sub>2</sub> than the corresponding alcohol, which is crucial for efficient extractive separation.

It has recently been demonstrated that solutes can be extracted from ionic liquids by pervaporation. This technique is based on the preferential partitioning of the solute from a liquid feed into a dense, non-porous membrane. The ionic liquids do not permeate the membrane. This technique can be applied to the recovery of volatile solutes from temperature-sensitive reactions such as bioconversions carried out in ionic liquids (34).

### III. Structures and Properties of Ionic Liquids

The physical and chemical properties of ionic liquids are governed by the nature of both the cations and the anions (35,36). Numerous ionic liquids have been reported, and a large number of potential ionic liquids have been suggested (37), but for catalytic applications relatively few have been investigated. Among the less well studied for catalysis include [BMIM][Co(CO)<sub>4</sub>] (38), [Bu<sub>3</sub>PEt][TsO] (m.p. = 83°C), and [Ph<sub>3</sub>PEt][TsO] (m.p. = 95°C), as well as ionic liquids consisting of organic

anions [e.g.,  $\alpha$ -cyano-4-hydrpxycinnamate and sinapinate (39), bis(oxalato)borate, bis(malonato)borate, bis(salicylato)borate, etc. (40)].

A number of ionic liquids incorporating new cations and anions have shown decreased viscosity and stability (1). There is no doubt that more applications of ionic liquids in catalysis are yet to be developed.

Heretofore, ionic liquids incorporating the 1,3-dialkylimidazolium cation have been preferred as they interact weakly with the anions and are more thermally stable than the quaternary ammonium cations. Recently, the physical properties of 1,2,3,4-tetraalkylimidazolium- and 1,3-dialkylimidazolium-containing ionic liquids in combination with various hydrophobic and hydrophilic anions have been systematically investigated (36,41). The melting point, thermal stability, density, viscosity, and other physical properties have been correlated with alkyl chain length of the imidazolium cation and the nature of the anion. The anion mainly determines water miscibility and has the most dramatic effect on the properties. An increase in the alkyl chain length of the cations from butyl to octyl, for example, increases the hydrophobicity and viscosity of the ionic liquid, whereas densities and surface tension values decrease, as expected.

According to their miscibility with water, ionic liquids are also frequently classified as hydrophilic or hydrophobic. The hydrophilic ionic liquids are typically salts composed of halide, acetate, nitrate, trifluoroacetate, and, in some cases, tetrafluoroborate anions, in particular their salts with [AMIM]<sup>+</sup> having short alkyl chains, as these ionic liquids are totally miscible with water. The ionic liquids composed of PF<sub>6</sub><sup>-</sup> and (CF<sub>3</sub>SO<sub>2</sub>)<sub>2</sub>N<sup>-</sup> with [AMIM]<sup>+</sup> are immiscible with water in bulk, and are therefore referred to as hydrophobic ionic liquids. The ionic liquids consisting of BF<sub>4</sub><sup>-</sup> and CF<sub>3</sub>SO<sub>3</sub><sup>-</sup> ions with [AMIM]<sup>+</sup> can be totally miscible or immiscible depending on the substituents on the cation, and they are therefore sometimes called tunable ionic liquids (22). A recent review covers relevant properties of some ionic liquids for catalysis (42,43).

#### A. HYDROGEN BOND BASICITY OF ANIONS

By using an approach based on linear free energy relationships, a recent study of 17 different ionic liquids led to an extensive comparison of their multiple solvation interactions with a large number of probe molecules (39). Although the dispersion forces were nearly constant for all the ionic liquids in this investigation, the hydrogen bond basicity (a measure of hydrogen bonding Gibbs Free energy of bases with HF (44)) and dipolarity terms seemed to vary for each ionic liquid (Fig. 1).

The following observations were made:

- (1) The ionic liquids incorporating various anions associated with the same cation [BMIM]<sup>+</sup> exhibited different basicity and dipolarity values. The effect of the cation on hydrogen bond basicity and dipolarity was quite small. Therefore, it was inferred that the anion has a greater influence than the cation on the overall hydrogen bond basicities of the ionic liquids.
- (2) Ionic liquids in which a cationic moiety has an electron-rich aromatic  $\pi$ -system showed stronger interactions with solute molecules capable of undergoing  $\pi$ - $\pi$  and  $n$ - $\pi$  interactions (e.g., 2-chloroaniline, *p*-cresol, aniline) than with others.

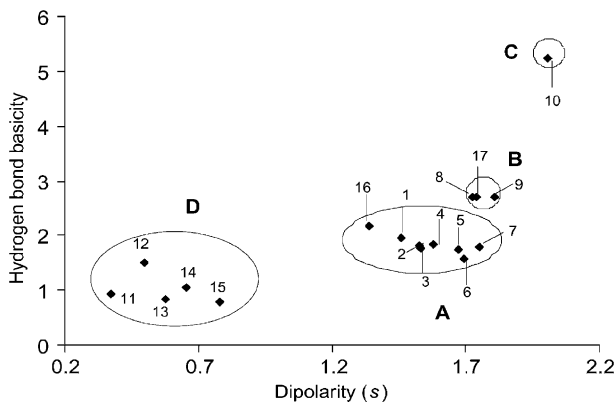


FIG. 1. Grouping based on the hydrogen bond basicity and dipolarity characteristics of 17 ionic liquids. (1) [BMIM][BF<sub>4</sub>]; (2) [C8m4im][NTf<sub>2</sub>]; (3) [BMPY][NTf<sub>2</sub>]; (4) [C6m4im][NTf<sub>2</sub>]; (5) [BMIM][NTf<sub>2</sub>]; (6) [BMIM][PF<sub>6</sub>]; (7) [Bm2im][NTf<sub>2</sub>]; (8) [BMIM][TfO]; (9) [BMIM][SbF<sub>6</sub>]; (10) [BMIM][Cl]; (11) [NH<sub>2</sub>m<sub>2</sub>][PA]; (12) [NHb<sub>3</sub>][PA]; (13) [NHb<sub>3</sub>][OHPA]; (14) [NH<sub>2</sub>e<sub>3</sub>][PA]; (15) [NHb<sub>3</sub>][Ac]; (16) [NHb<sub>3</sub>][CHCA]; (17) [NHb<sub>3</sub>][SA]. Reproduced with permission from Anderson *et al.*(39). The hydrogen bond basicity is defined according to the solvation model of Abraham.

(3) The chloride ion (with non-bonding electrons), in combination with the [BMIM]<sup>+</sup> ion, exhibited significant ability to interact with  $\pi$ -systems of probe molecules. Similar behavior, but of a much smaller magnitude, was observed for the [BMIM]SbF<sub>6</sub> and [BMIM]TfO salts, both having anions exhibiting large hydrogen bond basicity. It was also concluded that probe molecules that interact with the ionic liquids primarily via dispersion interactions behave similarly. Although dispersion interactions between solutes and ionic liquids are important, they usually cannot be used to distinguish between ionic liquids.

The authors applied the observed trends in hydrogen bond basicity of the anions to rationalize some published results. One was related to the solubility of cellulose in [BMIM]Cl ionic liquid up to 25 wt%, although cellulose is not soluble in [BMIM]BF<sub>4</sub> and [BMIM]PF<sub>6</sub> (45). This difference was attributed to the large hydrogen bond basicity of the [BMIM]Cl ionic liquid. Similarly, the high solubility of  $\alpha$ -,  $\beta$ -, and  $\gamma$ -cyclodextrins in [BMIM]Cl was explained. In general, the role of the chloride ion (and its high hydrogen bond basicity) is crucial in achieving dissolution of compounds capable of hydrogen bonding to the ionic liquid. The hydrogen bond basicity related to the anions also satisfactorily accounts for a number of observations in catalytic reactions that show large differences among the ionic liquids [BMIM]PF<sub>6</sub>, [BMIM]BF<sub>4</sub>, and [BMIM]TfO with basicities decreasing in this order. The observed high activity of rhodium-catalyzed biphasic hydrogenation of 1-pentene in [BMIM]SbF<sub>6</sub> compared with that in acetone and in [BMIM]PF<sub>6</sub> and [BMIM]BF<sub>4</sub> was similarly rationalized in terms of the fact that [BMIM]SbF<sub>6</sub> has the highest hydrogen bond basicity among the solvents.

Recently, the ionic liquids [EMIM]NbF<sub>6</sub> and [EMIM]TaF<sub>6</sub> have been reported (46). These melt at temperatures slightly below room temperature and have the

expected high densities. The viscosity of each is about 50 cP, among the lowest associated with ionic liquids.

## B. CATIONS

The cations in ionic liquids are generally bulky monovalent organics. The typical cations of ionic liquids, not including the familiar alkylammonium and alkylphosphonium ions, are shown in Fig. 2. It is primarily the cations, which account for the low melting points of ionic liquids. The dialkylimidazolium ions, such as 1-butyl-3-methyl imidazolium [BMIM]<sup>+</sup>, have been widely investigated because low-melting ionic liquids can be made readily from such cations and because of their thermal and chemical stability.

A number of other substituted imidazolium ions have also been reported. [MIM-C<sub>2</sub>H<sub>5</sub>OCH<sub>3</sub>]<sup>+</sup>Br and [MIM-CH<sub>3</sub>OCH<sub>3</sub>]<sup>+</sup>Br, liquids at room temperature, were recently reported to be good solvents for carbohydrates and proteins (47). The diversity of organic cations was extended even to include the antifungal drug miconazole, which contains an imidazole ring. By the reaction of the miconazole with alkyl iodide, bioactive cations were obtained that were subsequently used to form ionic liquids with PF<sub>6</sub><sup>-</sup> (9).

Cholin chloride, shown in Scheme 1, was recently shown to be a versatile cationic precursor for the preparation of a wide variety of ionic liquids (48). This precursor is particularly interesting, as cholin is a vitamin B4 additive to animal food. Therefore, it is not expected to be restricted in applications by health-related concerns, whereas a number of other ionic liquids remain to be fully evaluated for their environmental and health effects, including the ones based on imidazolium ions.

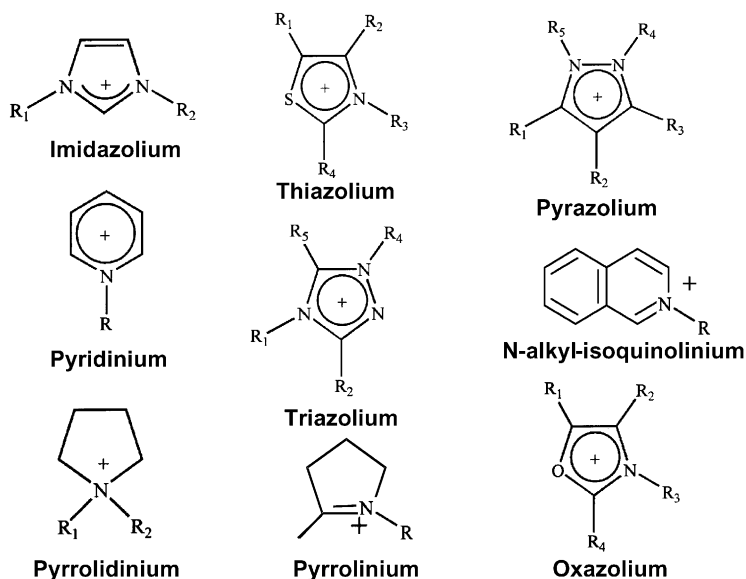
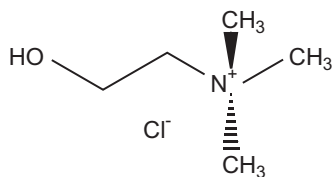


FIG. 2. Typical cations used in ionic liquids, excluding alkylammonium and alkylphosphonium ions.



SCHEME 1.

The cholin chloride-containing ionic liquids are made simply by mixing it with a metal halide or a compound such as a weak base, alcohol, or carboxylic acid. The melting points of cholin metal halide (e.g.,  $\text{ZnCl}_2$ ,  $\text{FeCl}_3$ , or  $\text{SnCl}_2$ ) ionic liquids are typically below  $50^\circ\text{C}$  when the metal halide mole fraction is 67%. The melting points of cholin-containing ionic liquids from neutral molecules, such as urea and polyols, are below room temperature. However, this type of ionic liquid is expected to have less thermal stability than the imidazolium-containing ionic liquids. The low-temperature Diels–Alder reactions have been successfully demonstrated with the cholin  $\text{Cl-ZnCl}_2\text{-FeCl}_3$  liquid, showing high yields and regioselectivities without solvent residues in the products after decantation.

### C. ANIONS

Anions in ionic liquids are typically monovalent, although a few higher-valent anions such as phosphates have been reported (49). There is an opportunity for any monovalent anion to join the ionic liquid universe if it is not thermally unstable. Some typical anions found in ionic liquids include  $\text{BF}_4^-$ ,  $\text{PF}_6^-$ ,  $\text{AsF}_6^-$ ,  $\text{SbF}_6^-$ ,  $\text{F}(\text{HF})_n^-$ ,  $\text{ZnCl}_3^-$ ,  $\text{CuCl}_2^-$ ,  $\text{SnCl}_3^-$ ,  $(\text{CF}_3\text{SO}_2)_2\text{N}^-$ ,  $(\text{C}_2\text{F}_5\text{SO}_2)_2\text{N}^-$ ,  $\text{C}(\text{CF}_3\text{SO}_2)_3^-$ ,  $\text{CF}_3\text{CO}_2^-$ ,  $\text{CF}_3\text{SO}_3^-$ ,  $\text{CH}_3\text{SO}_3^-$ ,  $(\text{CF}_3\text{SO}_2)_3\text{C}^-$ ,  $\text{CF}_3\text{CF}_2\text{CF}_2\text{CO}_2^-$ , and  $\text{CF}_3\text{CF}_2\text{CF}_2\text{CF}_2\text{SO}_3^-$ . Recently, the anions  $\text{NbF}_6^-$  and  $\text{TaF}_6^-$ , forming ionic liquids with  $[\text{EMIM}]^+$ , have been reported (46). Other anions in ionic liquids include organics, such as  $\alpha$ -cyano-4-hydroxycinnamate and sinapinate (39).

The anions determine the chemical properties of ionic liquids to a large extent. For example, the following ionic liquids, in which the cation is the same and the anions are not, behave totally different from one another:

$[\text{BMIM}]\text{Al}_2\text{Cl}_7$ : hygroscopic;

$[\text{BMIM}]\text{PF}_6$ : hydrophobic;

$[\text{BMIM}]\text{BF}_4$ : has cation-dependent water miscibility.

More specifically, Visser and Rogers (50) showed some examples of the possible effects of cations and anions in their affinities toward water (Fig. 3).

Although the difference in miscibility with water between the  $\text{BF}_4^-$  and  $\text{PF}_6^-$  anions for the same cation remains unexplained, a recent measurement showed differences in the surface tension ( $\gamma$ ) values among ionic liquids of the two anions. The  $\gamma$  value is higher for  $[\text{BMIM}]\text{PF}_6$  than that for  $[\text{BMIM}]\text{BF}_4$ . By increasing the alkyl chain length resulted in a decrease in the  $\gamma$  value for ionic liquids of both anions, approaching values characteristic of long-chain alkanes (51).

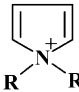
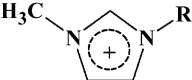
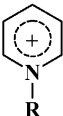
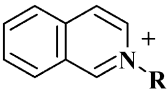
Cations			
			
1,1'-alkylpyrolium [C <sub>n</sub> pyr] <sup>+</sup>	1-alkyl-3-methylimidazolium [C <sub>n</sub> mim] <sup>+</sup>	N-alkylpyridinium [C <sub>n</sub> py] <sup>+</sup>	N-alkylisoquinolinium [C <sub>n</sub> isoq] <sup>+</sup>
Anions			
PF <sub>6</sub> <sup>-</sup> , N(SO <sub>2</sub> CF <sub>3</sub> ) <sub>2</sub> <sup>-</sup> , N(SO <sub>2</sub> CF <sub>2</sub> CF <sub>3</sub> ) <sub>2</sub> <sup>-</sup>	BF <sub>4</sub> <sup>-</sup>	NO <sub>3</sub> <sup>-</sup> , Cl <sup>-</sup> , ClO <sub>4</sub> <sup>-</sup>	
Water-immiscible	Cation dependent	Water miscible	

FIG. 3. Water miscibilities of representative ionic liquids. Reproduced with permission from Visser and Rogers (50).

The miscibility of an ionic liquid with water or an organic solvent has often been regarded as an important property of the ionic liquid. However, it should be clarified that a solvent that is regarded as immiscible with an ionic liquid should not be misunderstood as completely insoluble in it (although some organic solvents that have limited solubilities in ionic liquid have often been described as immiscible with the ionic liquids). Some ionic liquids that are regarded as immiscible in water are hygroscopic, such as [BMIM]PF<sub>6</sub>, which dissolves up to 1% water (52). Some of this water is even retained on drying (53).

The miscibility with water depends on the nature of the anions, the temperature, and the length of the alkyl chain in the dialkylimidazolium cation. For the same [BMIM]<sup>+</sup> ion, the BF<sub>4</sub><sup>-</sup>, MeSO<sub>4</sub><sup>-</sup>, CF<sub>3</sub>SO<sub>3</sub><sup>-</sup>, CF<sub>3</sub>CO<sub>2</sub><sup>-</sup>, CH<sub>3</sub>CO<sub>2</sub><sup>-</sup>, NO<sub>3</sub><sup>-</sup>, and halide salts display complete miscibility with water at 25°C. However, upon cooling of the [BMIM][BF<sub>4</sub>]/water solution to 4°C, a water-rich phase separates out. Similarly, changing the [BMIM]<sup>+</sup> ion to a longer-chain 1-hexyl-3-methylimidazolium [HMIM]<sup>+</sup> leads to a BF<sub>4</sub><sup>-</sup>-containing ionic liquid with a low miscibility with water at room temperature. Apparently, an increase in the length of an alkyl chain tends to decrease the water solubility because of the increased hydrophobicity of the cation. On the other hand, the ionic liquids incorporating [BMIM]<sup>+</sup> with the anions PF<sub>6</sub><sup>-</sup>, SbF<sub>6</sub><sup>-</sup>, NTf<sub>2</sub><sup>-</sup>, or BR<sub>4</sub><sup>-</sup> have very low miscibility with water, whereas the shorter, symmetric substituted 1,3-dimethylimidazolium cation with PF<sub>6</sub><sup>-</sup> gives a water-soluble ionic liquid (1).

Metal halides readily form ionic liquids by reacting with organohalide precursors such as pyridinium chloride or imidazolium chloride. The ionic liquids obtained from metal halides typically allow high ratios of the metal halide to the organic chloride precursor, thus forming polynuclear anions. For examples, Al<sub>2</sub>Cl<sub>7</sub><sup>-</sup>, Al<sub>3</sub>Cl<sub>10</sub><sup>-</sup>, Au<sub>2</sub>Cl<sub>7</sub><sup>-</sup>, Fe<sub>2</sub>Cl<sub>7</sub><sup>-</sup>, Sb<sub>2</sub>F<sub>11</sub><sup>-</sup>, Zn<sub>2</sub>Cl<sub>5</sub><sup>-</sup>, and Zn<sub>3</sub>Cl<sub>7</sub><sup>-</sup> form from their corresponding halide precursors (54). When a stoichiometric ratio of precursors is used, mononuclear halide anions are formed, such as AlCl<sub>4</sub><sup>-</sup>, ZnCl<sub>3</sub><sup>-</sup>, CuCl<sub>2</sub><sup>-</sup>, and SnCl<sub>3</sub><sup>-</sup>. The polynuclear anions can be viewed as the products of the reaction of the corresponding Lewis acid (e.g., AlCl<sub>3</sub>) with the mononuclear anion (e.g., AlCl<sub>4</sub><sup>-</sup>). Ionic liquids with a metal halide in sub-stoichiometric ratio to the aminoorganic halide

precursor can also be formed (e.g., [BMIM]Cl-[BMIM]AlCl<sub>4</sub>). Such ionic liquids are basic and function as basic media in catalysis (55). The metal halide-containing ionic liquids in general tend to be particularly water sensitive, except for most that contain fluoride and a few that contain chloride.

A limitation of aluminum-containing ionic liquids arises from their moisture sensitivity. Moreover, most transition metal complexes and organic reactants are not unreactive in the presence of the chloroaluminate compounds. These ionic liquids react with water in a highly exothermic manner, with the formation of hydrogen chloride and a white precipitate.

As a strong polar proton donor, water is strongly absorbed in most ionic liquids. In the extreme case, it is fully miscible with ionic liquids, such as [BMIM]BF<sub>4</sub> and [BMIM]CF<sub>3</sub>CO<sub>2</sub><sup>-</sup>. Even the hydrophobic ionic liquids can pick up a low concentration of water, resulting in a reduced absorption affinity for some organic compounds (27). The presence of water may, therefore, influence the performance of an ionic liquid in catalytic applications.

Of particular interest is the trifluoromethylsufonylamide anion, NTf<sub>2</sub><sup>-</sup> (56,57), which gives salts with thermal stability at temperatures up to 400°C. Because of the delocalization of the negative charge, the anion is probably less associated with the cation and more mobile than the triflate anion. It is important that NTf<sub>2</sub><sup>-</sup> is hydrolytically stable, in contrast to PF<sub>6</sub><sup>-</sup> (58).

The number of anions used in ionic liquids is growing rapidly. Among the recent additions are [B{C<sub>6</sub>H<sub>4</sub>[SiMe<sub>2</sub>C<sub>8</sub>H<sub>17</sub>]-4}<sub>4</sub>]<sup>-</sup> and [B(C<sub>6</sub>H<sub>4</sub>{SiMe<sub>2</sub>(CH<sub>2</sub>CH<sub>2</sub>C<sub>6</sub>F<sub>13</sub>)}-4)<sub>4</sub>]<sup>-</sup> (59). Their salts with [BMIM]<sup>+</sup> have melting points near -20°C, with a liquid range of about 200°C. The bulky lipophilic substituents dramatically enhance the solubility of the imidazolium borates in hexane and reduce their relative polarities. These unique properties make these ionic liquids interesting as amphiphilic ionic liquids with low polarities.

## D. PHYSICAL AND CHEMICAL PROPERTIES

### D.1. *Melting Point*

The melting points of ionic liquids are sensitive to the presence of impurities, such as halides, CO<sub>2</sub>, water, and organics (60,61). Water and organics dramatically reduce the melting points of a number of quaternary alkylammonium tetrafluoroborate ionic liquids. For example, dry [Bu<sub>4</sub>N]BF<sub>4</sub> has a melting point of about 160°C, but this dropped to about 80°C in the presence of water and to 55°C in the presence of toluene (60). Therefore, the reported melting points serve only as a general guide, and the temperature at which a liquid forms in a biphasic system can be sharply reduced by the presence of the other phase.

*D.1.1. Chloride-Containing Ionic Liquids.* The melting points of some typical [AMIM]Cl compounds are shown in Table I. Except for dimethylimidazolium chloride, which has a melting point above 120°C, the higher-alkyl [AMIM]Cl ionic liquids melt at temperatures below 100°C.



TABLE I  
Melting Points of Some Typical [AMIM]Cl Ionic Liquids

R group	Melting point of compound (°C)
Methyl	124.5–128
Ethyl	87
Propyl	58–66
Butyl	65–69

*D.1.2. N-alkylpyridinium-Containing Ionic Liquids.* The melting point of *N*-alkylpyridinium chloride increases from 70 to 80°C when the alkyl chain is lengthened from C<sub>12</sub> to C<sub>18</sub>. The melting point of *N*-alkylpyridinium [NiCl<sub>4</sub>]<sup>2-</sup> changes only from 80 to 86°C as the substituent changes from C<sub>12</sub> to C<sub>18</sub> (62).

*D.1.3. N,N-dialkylpyrrolidinium-Containing Ionic Liquids.* The ionic liquids incorporating pyrrolidinium ions show a clear trend of symmetry related melting points; those with the smaller symmetrical cations such as [(CH<sub>3</sub>)<sub>2</sub>C<sub>4</sub>H<sub>8</sub>N]<sup>+</sup> have relatively high melting points, whereas those with the larger, less symmetrical cations such as [(CH<sub>3</sub>)(*n*-C<sub>4</sub>H<sub>9</sub>)C<sub>4</sub>H<sub>8</sub>N]<sup>+</sup> are glass-forming liquids at room temperature (63).

The compound with the lowest melting point among the *N,N*-dialkylpyrrolidinium tetrafluoroborate family is [(CH<sub>3</sub>)(*n*-C<sub>3</sub>H<sub>7</sub>)C<sub>4</sub>H<sub>8</sub>N]BF<sub>4</sub>, which has a melting point of 64°C, as does *N*-methyl-*N*-propylpyrrolidinium tetrafluoroborate. The melting point is sufficiently low to enable the application of this compound in syntheses at temperatures above 70°C (64).

*D.1.4. Alkylimidazolium-Containing Ionic Liquids.* This group constitutes the most thoroughly investigated ionic liquids. Holbrey and Seddon (65) reported the physical properties of the ionic liquids [AMIM]BF<sub>4</sub> and [AMIM]PF<sub>6</sub> for a wide range of alkyl chain lengths. The melting points of these two types of ionic liquids are shown in Fig. 4. The results point to three regions of distinct melting points. In the region of short alkyl chain length, the symmetry of the cations prevails, resulting in higher melting points for highly symmetric alkyl substituents. The ionic liquids [1-methyl-3-methyl-IM]BF<sub>4</sub><sup>-</sup> and [1-ethyl-3-methyl-IM]PF<sub>6</sub><sup>-</sup> have melting points above room temperature. As the symmetry decreases with the increase in the length of the 3-alkyl chain, the melting point decreases to a minimum. The anion PF<sub>6</sub><sup>-</sup> is larger than BF<sub>4</sub><sup>-</sup>; the difference in melting points associated with this size difference appears primarily in the compounds with shorter alkyl chains. With a large increase in the length of the alkyl chain, the aliphatic part of the compound becomes dominant, as reflected in the high melting points.

The melting points of 1,2,3,4 = substituted imidazolium-containing ionic liquids with various substituent alkyl groups on the imidazolium ring and with various anions (Fig. 5) were investigated by Hagiwara and Ito (36). The authors concluded that there was no clear correlation between the melting points and the structures, although most of the salts were found to have melting points below 25°C. In general, however, the compounds containing symmetric cations such as



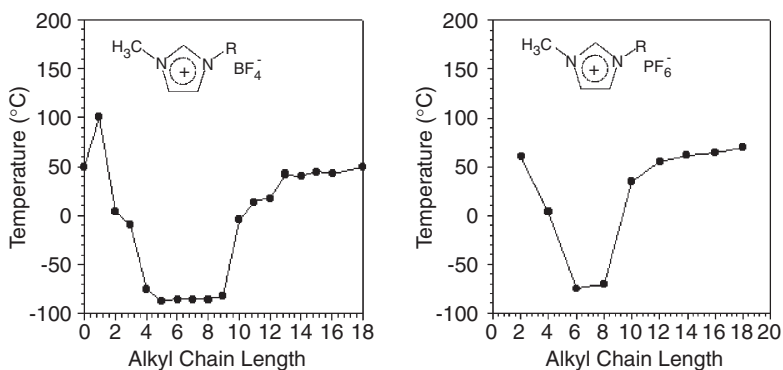


FIG. 4. Melting points of [AMIM]BF<sub>4</sub> and [AMIM]PF<sub>6</sub> of varying alkyl chain lengths. Reproduced with permission from Holbrey and Seddon (65).

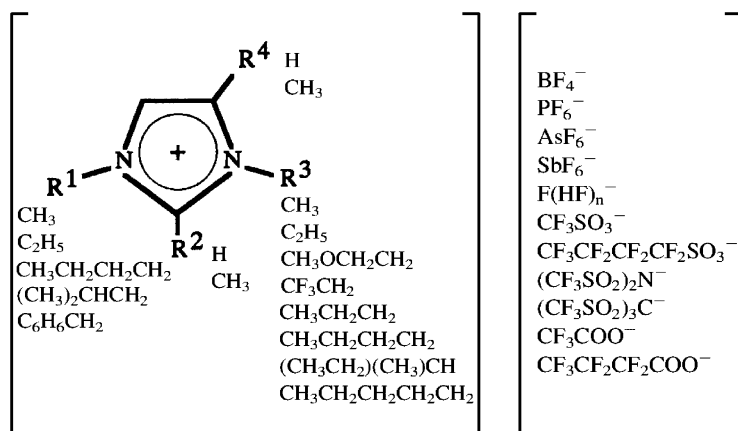


FIG. 5. 1,2,3,4-Substituted imidazolium-containing ionic liquids with various anions. Reproduced with permission from Hagiwara and Ito (36).

1,3-dimethyl and 1,3-diethylimidazolium exhibit higher melting points than those containing asymmetric cations (66). The anions were found to have a more pronounced effect on the melting point than the cations; for example, salts containing CF<sub>3</sub>CO<sub>2</sub><sup>-</sup> exhibited relatively low melting temperatures. Some of the salts do not crystallize but instead exhibit transitions to glasses. Methylation at C(2) (i.e., the CH<sub>2</sub> at the 2 position in the imidazolium ring was methylated) was found to increase the melting point, leading Hagiwara and Ito to suggest that the effect of van der Waals interactions involving the methyl groups dominates over electrostatic interactions via the more active hydrogen on C(2).

The dominant effect of anions on the melting points of [EMIM]<sup>+</sup>-containing ionic liquids is shown clearly in the data of Table II (66,67). The melting point ranges from 70°C for [EMIM][HSO<sub>4</sub>] to -45°C for [EMIM][MeCO<sub>2</sub>]. The salts of [EMIM]<sup>+</sup> with other anions have melting points spread through the whole range.

TABLE II  
Melting Point of [EMIM]-Containing Ionic Liquids with Corresponding Anions

Anion	HSO <sub>4</sub> <sup>-</sup>	PF <sub>6</sub> <sup>-</sup>	NO <sub>2</sub> <sup>-</sup>	NO <sub>3</sub> <sup>-</sup>	NfO <sup>-</sup>	NTf <sub>2</sub> <sup>-</sup>	TfO <sup>-</sup>	TA	MeCO <sub>2</sub> <sup>-</sup>
m.p. (°C)	70	60	55	38	28	-4	-9	-14	-45

*D.1.5. Quaternary Ammonium-Containing Ionic Liquids.* McFarlane *et al.* (63) investigated ionic liquids made of quaternary alkylammonium bis(trifluoromethylsulfonyl) imide, [R<sub>1</sub>R<sub>2</sub>R<sub>3</sub>R<sub>4</sub>N][CF<sub>3</sub>SO<sub>2</sub>]<sub>2</sub>N, with three of the alkyl chain lengths varied independently from one to four carbon atoms each and the remaining one varying from one to eight carbon atoms. It was concluded that, again, the melting points of the compounds are symmetry dependent:

- (1) The compounds containing highly symmetrical cations have melting points well above the room temperature, with most being higher than 100°C.
- (2) The compounds containing ammonium cations of lower symmetry have melting point below room temperature; some are glass forming.

*D.1.6. AlCl<sub>3</sub>-Containing Ionic Liquids.* AlCl<sub>3</sub>-containing ionic liquids are among the most widely investigated of all ionic liquids. A liquid state is maintained at room temperature for compositions between 33 and 67 mol% AlCl<sub>3</sub> in the mixture of AlCl<sub>3</sub> and [EMIM]Cl/AlCl<sub>3</sub> (Fig. 6).

The melting points of [1,3-dialkylimidazolium]AlCl<sub>4</sub> decrease with an increase in the alkyl chain length up to C<sub>4</sub>; symmetry does not appear to be important, as [1-methyl-3-methyl-IM]AlCl<sub>4</sub> has a much higher melting point (125°C) than [1-butyl-3-butyl IM][AlCl<sub>4</sub>]<sup>-</sup> (55°C) (8). Ionic liquids made by mixing [EMIM]Cl with AlCl<sub>3</sub> exhibit Lewis acid–base properties, which can be controlled by varying the ratio of the two components. The mole fraction of AlCl<sub>3</sub>,  $x_{\text{AlCl}_3}$ , is often used to express the relative content of AlCl<sub>3</sub> in the ionic liquids prepared from a mixture of AlCl<sub>3</sub> with [1,3-dialkylimidazolium]Cl. The ionic liquids with  $x > 0.5$  are acidic, and those with  $x < 0.5$  are basic.

The Lewis acid–base properties of these ionic liquids are determined by the chloroaluminate species. The equilibrium of the chloroaluminate liquid is primarily described by two equilibria at  $x_{\text{AlCl}_3}$  below 0.67:



The equilibrium (1) dominates in basic ionic liquids, where  $x_{\text{AlCl}_3} < 0.5$ ; the equilibrium (2) dominates in acidic ionic liquids, where  $x_{\text{AlCl}_3} > 0.5$ . This means that over much of the liquid range the anions present in significant quantities are Cl<sup>-</sup>, AlCl<sub>4</sub><sup>-</sup>, and Al<sub>2</sub>Cl<sub>7</sub><sup>-</sup>, and their relative amounts are controlled by the equilibrium:



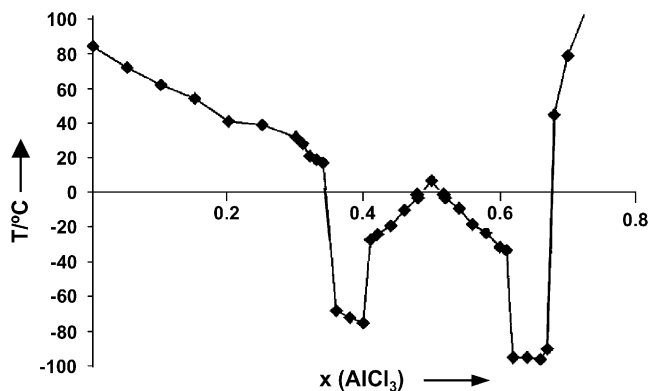


FIG. 6. Experimental phase diagram for [EMIM]Cl/AlCl<sub>3</sub>. Reproduced with permission from Fannin *et al.* (8).

The heptachloroaluminate ion is a strong Lewis acid, and chloride ion is the conjugate Lewis base. The basic ionic liquids, in which equilibrium (1) dominates, are light green in color, and the acidic ones, in which equilibrium (2) dominates, are darker and brownish in color (23). The acidic ionic liquids in this family are less viscous than the basic ones.

## D.2. Stability

Thermal stability has been reported for several liquids containing the [EMIM]<sup>+</sup> ion. A thermogravimetric investigation showed that its salts with CF<sub>3</sub>SO<sub>3</sub><sup>−</sup> and (CF<sub>3</sub>SO<sub>2</sub>)<sub>2</sub>N<sup>−</sup> are stable at temperatures up to 400°C, and the salt-containing CF<sub>3</sub>CO<sub>2</sub><sup>−</sup> is stable up to 150°C (66). The salt-containing BF<sub>4</sub><sup>−</sup> starts to lose weight at 300°C. Thus, it is expected that the thermal stability of dialkylimidazolium cations is relatively high, and the choice of the anions often determines the decomposition temperature.

The thermal properties of a number of ionic liquids with multiple alkyl substituted imidazolium cations and various anions were characterized by differential-scanning calorimetry (DSC) and thermographic analysis (TGA) measurements (68). Many of these salts are liquids at sub-ambient temperatures. The ionic liquids form glasses at low temperatures and have minimal vapor pressures at temperatures up to their thermal decomposition temperature (>400°C). The decomposition temperatures of these imidazolium salts were inferred to be insensitive to the presence of oxygen, as similar thermal decomposition behavior was observed in O<sub>2</sub> and N<sub>2</sub> environments. Thermal decomposition is endothermic when the anions are inorganic and exothermic when they are the organics (C<sub>2</sub>F<sub>5</sub>SO<sub>2</sub>)<sub>2</sub>N<sup>−</sup> and (CF<sub>3</sub>SO<sub>2</sub>)<sub>2</sub>N<sup>−</sup>. This exothermicity is likely to be a consequence the sulfonyl groups. Halide anions drastically reduce the thermal stability of these salts (<300°C). The imidazolium cations are thermally more stable than the tetraalkylammonium cations. The relative anion stability follows the order PF<sub>6</sub><sup>−</sup> > BF<sub>4</sub><sup>−</sup> > AsF<sub>6</sub><sup>−</sup> ≫ I<sup>−</sup>, Br<sup>−</sup>, Cl<sup>−</sup>.

The stability of dialkylimidazolium cation-containing ionic liquids can be a problem even at moderate temperatures in the presence of some reagents or catalysts. For example, when CsF and KF were used in the ionic liquid [BMIM]PF<sub>6</sub> to perform a halogen exchange reaction in an attempt to replace Br<sup>−</sup> from bromocarbons with F<sup>−</sup>, it was found that alkyl elimination from the [BMIM] cation took place, forming methyl imidazole, 1-butene, 1-fluorobutane, and other unidentified products at 150°C overnight (69). The fluoride ion acted as a base that promotes elimination or substitution processes.

The hydrolysis and decomposition of [BMIM]PF<sub>6</sub> ionic liquid in the presence of water and metal catalysts have also been reported (70–72). The decomposition of the ionic liquid occurs only in the presence of both water and the transition-metal precursor [e.g., (Ir(cod)Cl)<sub>2</sub> or RhCl<sub>3</sub>]. The presence of SnCl<sub>2</sub> was found to cause the decomposition of the PF<sub>6</sub><sup>−</sup> ion by water alone (73). When hydrolysis occurs, HF is formed as a decomposition product, and it can change the course of a catalytic reaction. In the absence of water, such metal precursors can be reduced in H<sub>2</sub> at 75°C to form ionic liquid-stabilized nanoparticles (12,74).

### D.3. Polarity

The polarities of various ionic liquids were measured by investigating the solvent–solute interactions using solvatochromic dyes (66,75). The polarity of the ionic liquid [BMIM]BF<sub>4</sub> is in the range of 0.6–0.7 on the normalized polarity scale, which sets the value for tetramethylsilane at 0.0 and that for water at 1.0 (76). Toluene (0.1) and MTBE (0.35) are less polar. The data indicate that the polarities of 1,3-dialkylimidazolium salts incorporating the PF<sub>6</sub><sup>−</sup>, BF<sub>4</sub><sup>−</sup>, CF<sub>3</sub>SO<sub>3</sub><sup>−</sup>, and NTf<sub>2</sub><sup>−</sup> ions can be compared to that of the short-chain primary alcohols, with a slightly lower polarity for the salts consisting of NTf<sub>2</sub><sup>−</sup> ion. The polarities of 1-alkyl-3-methylimidazolium-containing ionic liquids were found to be similar to those of short-chain alcohols, with the polarity decreasing somewhat as the length of the alkyl chain increases (77,78). The anion appears to have little effect on the polarity of the ionic liquid. 1-Butylpyridinium tetrafluoroborate exhibited a lower polarity than the imidazolium salts. Tetraalkylammonium derivatives are relatively non-polar, whereas those containing cations of the type [NH<sub>x</sub>R<sub>(4−x)</sub>]<sup>+</sup> (where  $x \geq 1$ ) are considerably more polar.

However, it is emphasized that the reported polarity values do not provide a rigorous basis for a prediction of the behavior of ionic liquids in catalysis, as the measurements of polarity values are particularly dependent on the methods used; in some cases the values are not consistent. For example, in one report the polarity of selected ionic liquids was stated to increase in the order [BMIM]PF<sub>6</sub> < [BMIM]Tf<sub>2</sub>N < [OMIM]PF<sub>6</sub> (75), whereas in another the order was just the opposite (77). In any case, the differences are small.

### D.4. Viscosity

Viscosities of ionic liquids are several tens to hundreds times higher than that of water at room temperature. The structure of the cation strongly influences viscosity; longer alkyl chains in the cation make the liquid more viscous. The viscosity of an

ionic liquid is governed by the van der Waals interactions and hydrogen bonding (66). Both the structure and basicity of the anion also affect the viscosity; a decrease in the size of the anion decreases the van der Waals interaction but increases the electrostatic interaction through hydrogen bonding. A low viscosity was found for the ionic liquid EMIMF(HF) $_n^-$ , which was attributed to the highly basic anion, suggesting that the effect of the van der Waals interaction dominates over the electrostatic interactions.

The temperature dependence of viscosity of 23 room-temperature ionic liquids was investigated. The size and symmetry of the cations and anions were shown to have a marked effect on viscosity (79).

The viscosity of 1-alkyl-3-methylimidazolium salts can be lowered by using a highly branched and compact alkyl chain in the cation, or, more important, by changing the nature of the anion (80). For a given cation, the viscosity decreased in the following order:  $\text{Cl}^- > \text{PF}_6^- > \text{BF}_4^- \approx \text{NO}_3^- > \text{NTf}_2^-$ . With  $[\text{BMIM}]^+$  as the cation, the viscosity at 20°C decreased as the size of the organic anion decreased:  $n\text{-C}_4\text{F}_5\text{SO}_3^-$  (373 cP)  $\gg n\text{-C}_3\text{F}_7\text{CO}_2^- \gg \text{C}_6\text{F}_5\text{SO}_3^- > \text{CF}_3\text{CO}_2^- > (\text{CF}_3\text{SO}_2)\text{N}^-$  (52 cP) (66).

When the ionic liquids are made from mixtures of  $[\text{AMIM}]\text{Cl}$  and  $\text{AlCl}_3$ , the effect of alkyl chain length on the viscosity is much less than that of the anionic species. There is also a strong dependence of the viscosity on the mole fraction of  $\text{AlCl}_3$  in the ionic liquid. Ionic liquids incorporating the chloride anion have the highest viscosity. The chloride anion prevails when the  $\text{AlCl}_3$  fraction in the mixture is less than 0.5 (81). A sharp change in the viscosity is observed when the fraction of  $\text{AlCl}_3$  is changed from a value of about 0.5. The viscosity is essentially determined by the ability of the ionic liquid to form hydrogen bonds and the strength of the van der Waals interactions. Among the anions  $\text{Cl}^-$ ,  $\text{AlCl}_4^-$ , and  $\text{Al}_2\text{Cl}_7^-$ ,  $\text{Cl}^-$  allows the strongest hydrogen bonding and  $\text{Al}_2\text{Cl}_7^-$  the lowest (this anion is also referred to as non-coordinating).

The viscosity of  $[\text{AMIM}]\text{X}$ -type ionic liquids ( $\text{X}$  = anion) in general increases with the alkyl chain length and is dependent on the anion (25). For example, the ionic liquids  $[\text{C}_n\text{-MIM}]\text{PF}_6$  are much more viscous than their  $\text{Tf}_2\text{N}$  analogs. Viscosity values for  $[\text{C}_n\text{-MIM}]\text{Tf}_2\text{N}$  with  $n$  in the range of 2–10 and for  $[\text{C}_n\text{-MIM}]\text{PF}_6$  with  $n$  in the range of 4–9 are shown in Fig. 7. There is an almost linear dependence of viscosity on the length of the alkyl chain for  $[\text{C}_n\text{-MIM}]\text{Tf}_2\text{N}$ , but the dependence is more complex for  $[\text{C}_n\text{-MIM}]\text{PF}_6$ .

The viscosities of several  $[\text{AMIM}]^+$ -containing ionic liquids were found to decrease markedly as the temperature increased. For example (Fig. 8), the viscosity at 50°C is only 20–35% of that at 25°C (25).

#### D.5. Solubility of Species in Ionic Liquids

The solubility of a reactant in an ionic liquid affects the performance of the ionic liquid as a catalyst and that of a catalyst dispersed in an ionic liquid. However, there are only a few reports about the solubilities of species in ionic liquid media. The solubility values of typical molecules of interest, as described below, are based on a limited number of reports.

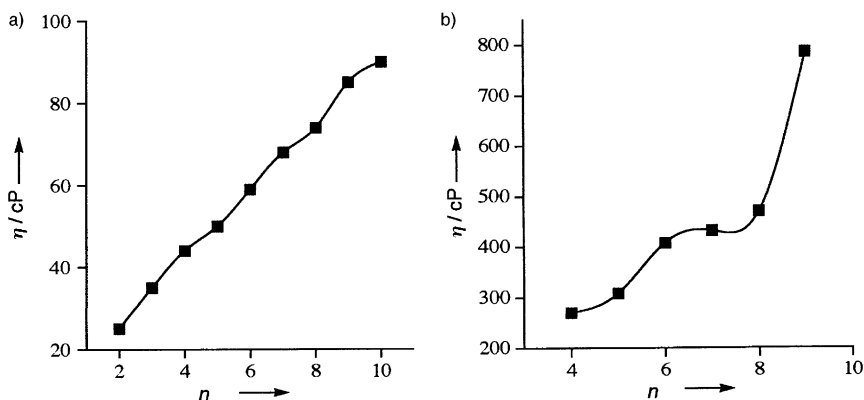


FIG. 7. Influence of the 1-alkyl group on the viscosity of the ionic liquids (a)  $[C_n\text{-MIM}]\text{Tf}_2\text{N}$  and (b)  $[C_n\text{-MIM}]\text{PF}_6$  at room temperature. Reproduced with permission from Dzyuba and Bartsch (25).

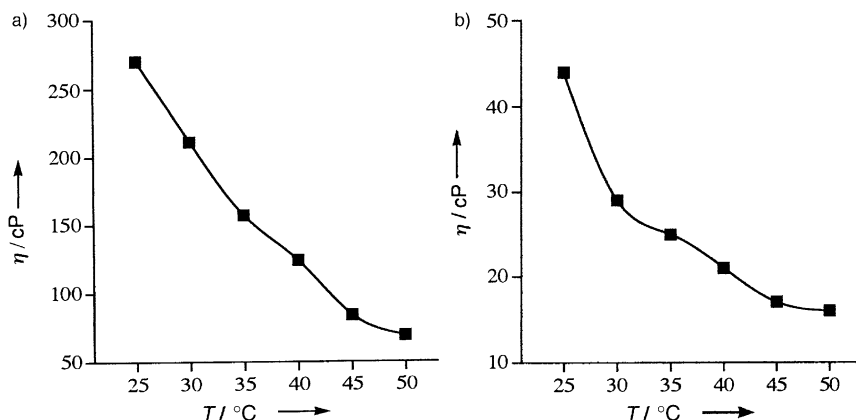


FIG. 8. Influence of temperature on the viscosity of (a)  $[C_4\text{-MIM}]\text{PF}_6$  and (b)  $[C_4\text{-MIM}]\text{NTf}_2$ . Reproduced with permission from Dzyuba and Bartsch (25).

**D.5.1. Hydrogen.** Hydrogen solubility at  $20^{\circ}\text{C}$  in the ionic liquids  $[\text{BMIM}]\text{PF}_6$  and  $[\text{BMIM}]\text{BF}_4$  was determined by Berger *et al.* (82), with the goal of correlating the solubility with the catalytic activity and enantioselectivity in the asymmetric hydrogenation of (Z)  $\alpha$ -acetamido cinnamic acid. The measurements showed that the solubility of  $\text{H}_2$  in  $[\text{BMIM}]\text{BF}_4$  is higher than that in  $[\text{BMIM}]\text{PF}_6$  by a factor of more than 3 at 50 atm. As expected, the amount of  $\text{H}_2$  dissolved increased with pressure. In  $[\text{BMIM}]\text{BF}_4$ , the  $\text{H}_2$  solubility is 0.15 mol/L at 50 atm.

**D.5.2. Oxygen.** The solubility of  $\text{O}_2$  in  $[\text{BMIM}]\text{PF}_6$  is very low,  $<0.2$  mmol/L, much lower than that of  $\text{O}_2$  in  $\text{CH}_3\text{CN}$  (9.1 mmol/L) (83).

**D.5.3. Carbon Monoxide.** The solubility of CO in ionic liquids is crucial for carbonylation reactions. However, quantitative measurements are not yet available. In

the butoxycarbonylation of iodobenzene or 4-bromoacetophenone in [TBA]Br with a palladium complex catalyst, the authors noted that a CO partial pressure exceeding 1 atm was needed and that the butoxyester yield increased with increasing CO partial pressure (84).

**D.5.4. Carbon Dioxide and Lower Alkanes.** Carbon dioxide has a remarkably high solubility in ionic liquids (22). For example, about 0.5 mol fraction of CO<sub>2</sub> was present in [BMIM]PF<sub>6</sub> at 40°C and 50 bar, although the total volume increased by only 10% as a result of the CO<sub>2</sub> addition.

Brennecke *et al.* (22) compared the Henry's law constants of several gases in [BMIM]PF<sub>6</sub> with those in toluene and methanol. The results (Fig. 9) show that CO<sub>2</sub> has a much higher solubility in the ionic liquid than in the organic solvent.

The solubility of CO<sub>2</sub> in ionic liquids is strongly dependent on the water content. Saturating [BMIM]PF<sub>6</sub> with water (it contained up to 2.3 wt% water) reduced the CO<sub>2</sub> solubility from 0.54 mol fraction (0.15 wt% water) to only 0.13 mol fraction at 57 bar and 40°C (30). When water is present in excess, CO<sub>2</sub> has also been found to induce the separation of water from ionic liquids (85).

Although CO<sub>2</sub> is highly soluble in ionic liquids, there is no appreciable ionic liquid solubility in the CO<sub>2</sub> phase in the supercritical state (29).

**D.5.5. Solubility of Organic Molecules.** The miscibility of ionic liquids with organic solvents was measured qualitatively by mixing equal volumes of the two (23). Table III provides a guide (which is only rough) to the selection of a solvent.

[BMIM]PF<sub>6</sub> is thermally stable and shows solubility in organic solvents with dielectric constants higher than 7 (except water) (Table III). Ionic liquids formed from mixtures of [BMIM]Cl and AlCl<sub>3</sub> are reactive with some solvents; the reactivity is dependent on the ratio of AlCl<sub>3</sub> to imidazolium chloride. Acidic chloroaluminate ionic liquid is highly reactive, and there are only a few solvents that do not react with it. In acetone, toluene, and tetrahydrofuran, solvation takes place to some degree, but

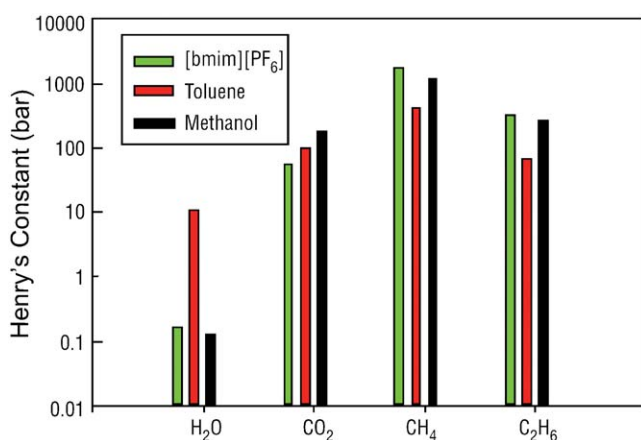


FIG. 9. Henry's law constants (bar) for H<sub>2</sub>O, CO<sub>2</sub>, CH<sub>4</sub>, and C<sub>2</sub>H<sub>6</sub> in [BMIM]PF<sub>6</sub>, toluene, and methanol. Reproduced with permission from Brennecke and Maginn (22).

TABLE III  
Miscibilities of Various Compounds in [BMIM]PF<sub>6</sub>, [BMIM]AlCl<sub>4</sub>, and [BMIM]Al<sub>2</sub>Cl<sub>7</sub>

Solvent	$\epsilon$	[BMIM]PF <sub>6</sub>	[BMIM]Cl-AlCl <sub>3</sub>	[BMIM]Cl-Al <sub>2</sub> Cl <sub>6</sub>
Water	80.1	I	R	R
Propylene carbonate	64.4	M	M	M
Methanol	33.0	M	R	R
Acetonitrile	26.6	M	M	M
Acetone	20.7	M	M	R
Methylene chloride	8.93	M	M	M
Tetrahydrofuran	7058	M	M	R
Trichloroethylene	3.39	I	I	I
Carbon disulfide	2.64	I	I	I
Toluene	2.38	I	I	I
Hexane	1.90	I	I	I

The interactions of the various compounds with the respective solvents, according to the following key: M = miscible; R = reactive; I = immiscible (23).

only when the ionic liquid is acidic. This observation shows that solvents with donor or acceptor properties may act differently in acidic and basic liquids.

It is possible to change the solubility of an organic compound in an ionic liquid by tuning the structure of the ionic liquid. For example, the solubility of 1-hexene in *N,N*-dialkylimidazolium- and in *N,N*-methylethylpyrrolidinium-containing ionic liquids increases with an increase in the length of the alkyl chain of the cation. This pattern is as expected, as the increase in the carbon chain length increases the aliphatic fraction in the ionic liquid. Surface tension measurements indicate that the surface tension approaches the values for alkanes with increasing the alkyl chain length in [AMIM]PF<sub>6</sub> (51). The effect of anions on solubility is also dramatic. For example, the solubility of hexene is strongly dependent on the nature of the anion associated with the cation [BMIM]<sup>+</sup>, in the following order: BF<sub>4</sub><sup>-</sup> ≈ NO<sub>3</sub><sup>-</sup> < PF<sub>6</sub><sup>-</sup> < CF<sub>3</sub>SO<sub>3</sub><sup>-</sup> < CF<sub>3</sub>COO<sup>-</sup> < NTf<sub>2</sub><sup>-</sup> (41).

The solubilities of organic compounds such as alkanes, cycloalkanes, alkenes, aromatic hydrocarbons, saturated alkylamines, and N- and S-containing aromatic compounds in several ionic liquids were reported recently (86). The solubilities in the ionic liquid [TMAC]Al<sub>2</sub>Cl<sub>7</sub> are listed in Table IV.

The solubilities of aromatic compounds in the ionic liquid are dramatically higher than those of saturated compounds. Benzene has a solubility of 4.9 mol/mol of ionic liquid, and thiophene has a solubility of 6.7 mol/mol of ionic liquid. A dramatic steric effect was observed on the solubility of aromatics; the alkyl-substituted aromatics showed reduced solubility. Although the solubility of hexene in the ionic liquid is considerably lower than that of the aromatics, it is still measurably higher than that of hexane. Similar structure-solubility relationships characteristic of organic molecules were observed with the ionic liquids [BMIM]BF<sub>4</sub>, [BMIM]PF<sub>6</sub>, and [EMIM]BF<sub>4</sub> (Fig. 10) (27).

The solubility of an aromatic compound is dependent on the nature of the ionic liquid, mainly on the sizes of the anion and cation. Increasing the size of the anion and the alkyl chain length leads to a large increase in the solubility of the aromatic



TABLE IV  
Solubilities of Organic Compounds in  $[TMAC]Al_2Cl_7$ ; TMAC = Trimethylammoniumchloride

Organic compound	Solubility (mol/mol IL)
2-Methylpentane	0
Hexene	0.12
Benzene	4.9
Toluene	2.8
m-Xylene	2.24
Ethylbenzene	2.0
Trimethylbenzene	2.0
2-Methylpropylthiol	1.2
Thiophene	6.7
2-Methylthiophene	1.0

IL refers to ionic liquid (86).

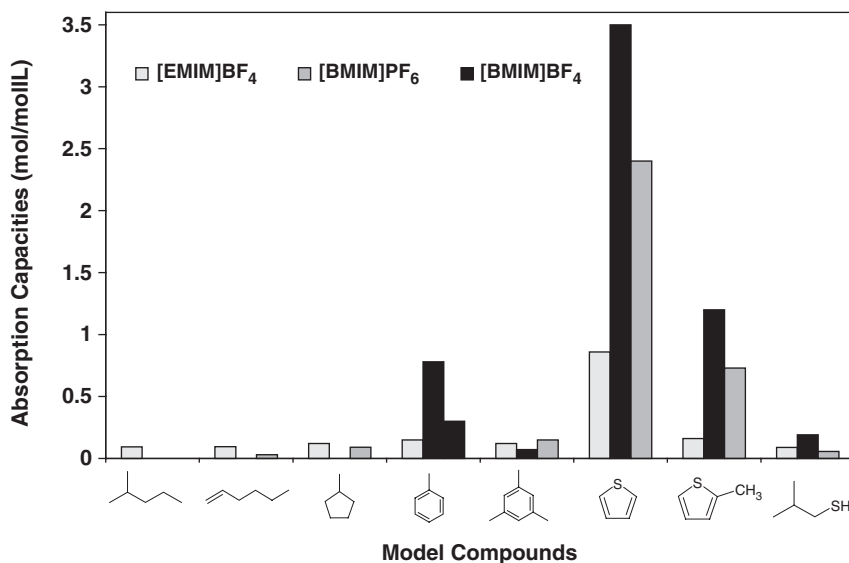


FIG. 10. Solubilities of model organic compounds in  $[EMIM]BF_4$ ,  $[BMIM]PF_6$ , and  $[BMIM]BF_4$ . Reproduced with permission from Zhang and Zhang (27).

compound. Thus, the solubility of an aromatic compound in the ionic liquids shown in Table V is higher in  $[TMAC]Al_2Cl_7$  than in other ionic liquids, because  $Al_2Cl_7^-$  is the largest anion among the three ionic liquids.

An increase in the number of alkyl substituents on an aromatic ring markedly reduces the solubility of the aromatic compound in  $[BMIM]BF_4$ ,  $[BMIM]PF_6$ , and chloroaluminate-containing ionic liquids (27). For example, the solubility of trimethylbenzene in  $[BMIM]PF_6$  is 10-fold less than that of toluene. Similarly, the solubility of 2-methylthiophene in this ionic liquid is three times less than that of thiophene.

TABLE V  
Solubilities of Nitrogen-Containing Compounds in [BMIM]BF<sub>4</sub> (89)

Compound	Solubility in [BMIM]BF <sub>4</sub> , mol/mol of [BMIM]BF <sub>4</sub>
Pyridine	Fully miscible
Piperidine	0.72
2-Picoline	Fully miscible
2-Methylpiperidine	0.23

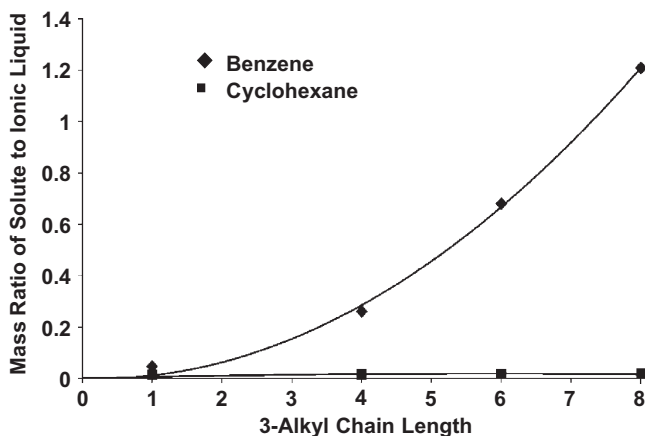


FIG. 11. Miscibility of benzene and of cyclohexane in the ionic liquids [C<sub>x</sub>MIM]BF<sub>4</sub> (where  $x = 1$  [MMIM];  $x = 4$  [BMIM];  $x = 6$  [HMIM]; and  $x = 8$  [OMIM]) at 20°C. Reproduced with permission from Dyson *et al.* (88).

The length of an alkyl chain in a conjugated molecule has also a significant effect on the solubility of the compound. For example, methyl acrylate is fully miscible with [BMIM]PF<sub>6</sub>, but butyl acrylate is only partially miscible, simply because of the increased alkyl chain length of the ester (87).

The solubility of benzene and of cyclohexane in [AMIM]BF<sub>4</sub> with various lengths of the alkyl chain in the cation of the ionic liquid was reported (88). The results of Fig. 11 show that the solubility of benzene increases with an increase in the alkyl chain length, but, surprisingly, the solubility of cyclohexane is little affected by varying the chain length.

N-containing compounds, whether saturated or not, have higher solubilities than hydrocarbons in [BMIM]BF<sub>4</sub>, as shown in Table V. Remarkably, the aromatic N-compounds are fully miscible with these ionic liquids (29,89).

The strong affinity of ionic liquids for aromatics has been attributed to the formation of liquid clathrates (90–92). Liquid clathrates (93) are semi-ordered liquids containing complex salt hosts. They are formed by associative interactions between aromatic molecules and salt ions, which separate cation–anion-packing interactions to a sufficient degree that localized cage structures are formed. Although the aromatic compounds are highly soluble in the ionic liquid phase, the

concentration of the ionic liquid in the aromatic hydrocarbon phase is generally very low (e.g., below the  $^1\text{H}$  NMR detection limit) (91). Some ionic liquid–aromatic combinations favor the formation of liquid clathrate phases (92).

Molecular dynamic simulations representing benzene in [MMIM]Cl and [MMIM]PF<sub>6</sub> established a correlation of the (high) solubility of benzene in ionic liquids with the strong electrostatic field around the aromatic molecule associated with the  $\pi$ -electrons. The high polarizability of benzene also contributes to the high solubility (94).

The typical liquid clathrate is characterized by (a) a low viscosity relative to that of a neat ionic liquid, (b) immiscibility with excess aromatic solvents, and (c) non-stoichiometric compositions. The formation of air- and water-stable liquid clathrates has been reported for the compositions consisting of aromatic hydrocarbons (e.g., benzene, toluene, and xylenes) and common salts of [AMIM]<sup>+</sup> cation with the anions PF<sub>6</sub><sup>−</sup>, [Tf<sub>2</sub>N]<sup>−</sup>, BF<sub>4</sub><sup>−</sup>, and Cl<sup>−</sup> (91).

Structure–solubility relationships can be used to predict the behavior of the hydrogenation reactions in an ionic liquid. For example (88), the hydrogenation of aromatics in ionic liquids is much faster than that in the aqueous systems because of the higher solubilities of the aromatics in ionic liquids than in water.

In general, the solubilities of alcohols in ionic liquids are high and those of ionic liquids in alcohols are low. The phase behavior of alcohols and ionic liquids depends on the length and branching of the alkyl chain of the alcohol and the anion of ionic liquid (95). An upper critical solution temperature (UCST, a measure of the temperature at which phase separation starts to occur on cooling) was observed for all the combinations of alcohols and ionic liquids. An increase in the alkyl chain length of the alcohol resulted in an increase in the UCST, consistent with the general trend of decreased solubility of alcohols in ionic liquids with increased alcohol aliphatic chain length. Increased branching of the alkyl chain in the alcohol results in higher solubility of the alcohol in the ionic-liquid-rich phase. On the other hand, an increase in the alkyl chain length in the cation of the ionic liquid leads to a decrease in the UCST. Replacement of the hydrogen at the C2 position of the imidazolium ring with a methyl group results in an increase in the UCST. The choice of the anion was also shown to have a large influence on the UCST. The effect of anion on the UCST was found to be related to the ability of the anion to accept a hydrogen bond. In the solutions of alcohols and a family of ionic liquids incorporating the cation [BMIM]<sup>+</sup>, the UCST decreased with an increase in the hydrogen bond strength, reflecting the relative affinity for alcohols of the anions: (CN)<sub>2</sub>N<sup>−</sup> > CF<sub>3</sub>SO<sub>3</sub><sup>−</sup> > (CF<sub>3</sub>SO<sub>2</sub>)<sub>2</sub>N<sup>−</sup> > BF<sub>4</sub><sup>−</sup> > PF<sub>6</sub><sup>−</sup>.

**D.5.6. Solubilities of Catalysts.** The solubility of the catalyst in an ionic liquid is a crucial parameter for the ionic liquid dispersed catalyst systems. When a catalyst is not fully dissolved in the ionic liquid, the reaction may occur to a significant degree in the organic phase.

The solubility of a Lewis acidic salt in an ionic liquid is dependent on the nature of both the salt and the ionic liquid. Hydrophobic ionic liquids have lower solubilities for such salts. For example, metal triflates such as Sc(TfO)<sub>3</sub> readily dissolve

in the hydrophilic ionic liquid [BMIM]BF<sub>4</sub>. But in the hydrophobic liquid [BMIM]PF<sub>6</sub>, it remains in a separate phase, being present as a suspension (96).

An organometallic catalyst that is soluble in water may not be soluble in some ionic liquids. For example, the well-known water-soluble metal-containing salts incorporating the ligand tri(*m*-sulfonyl)triphenyl phosphine trisodiums (tppts) are commonly applied in organic-aqueous biphasic catalysis because the catalysts inherit high solubility of the ligands in the aqueous phase. This salt is not soluble in [BMIM]PF<sub>6</sub>, although it is soluble in [BMIM]BF<sub>4</sub>. The modification of the catalyst by replacement of some of the ligands with an imidazolium ligand eliminates this solubility issue. The tri(*m*-sulfonyl)triphenyl phosphine tris(1-butyl-3-methylimidazolium) salt (tppti) is soluble in both [BMIM]BF<sub>4</sub> and [BMIM]PF<sub>6</sub> (97).

#### D.6. Brønsted Acidic Ionic Liquids

The reaction of 1-alkyl-3-methyl imidazolium chloride [AMIM]Cl and hydrogen fluoride gives a family of non-volatile liquids, [AMIM]F-2.3HF. The liquid is stable in air and, unlike HF, the liquids can even be stored in a glass container (98). The [AMIM]F-2.3HF ionic liquids have relatively high conductivities and low viscosities relative to many other ionic liquids. IR- and NMR-spectroscopic measurements suggest the existence of fluorohydrogenate anions such as H<sub>2</sub>F<sub>3</sub><sup>-</sup> and H<sub>3</sub>F<sub>4</sub><sup>-</sup>, with which HF is rapidly exchanged (98,99). [EMIM]F-HF, which has a melting point of 50°C, was made by crystallization from the HF-deficient ionic liquid obtained by thermal decomposition of the liquid [EMIM]F-2.3HF. [EMIM]F-HF, a solid at room temperature, was found to have a layered structure by the high-energy synchrotron X-ray radiation. This structure is partially preserved even in the liquid state at higher temperatures (100).

Ionic liquids with Brønsted acidity have also been prepared from neutral liquids, such as [BMIM]BF<sub>4</sub> and [BMIM]PF<sub>6</sub>, by dissolving well-known Brønsted acids, *p*-toluenesulfonic acid (TsOH), pyridinium *p*-toluenesulfonate (PPTS), and triphenyl phosphine hydrobromide (TPP.HBr) (101). The strong acidities of the catalysts are maintained in the liquids.

In the BASF BASIL process that utilizes *N*-methylimidazole to scavenge HCl byproduct, the acidic ionic liquid *N*-methylimidazolium chloride [HMIM]Cl was formed, with a melting point of 75°C (13,102). Recently, the group of Brønsted acidic ionic liquids with the same cation was extended to include other anions, such as BF<sub>4</sub><sup>-</sup>, TfO<sup>-</sup>, and TsO<sup>-</sup>. The melting point of the salt is between 30 and 109°C. Strong hydrogen bonding in the tosylate salt was characterized by IR spectroscopy.

Dissolving a strong acid like HCl in a strong Lewis acidic chloroaluminate ionic liquids (e.g., [EMIM]Al<sub>2</sub>Cl<sub>7</sub>) resulted in the formation of superacidic proton donors, according to quantitative ultraviolet (UV) spectroscopic measurements (103). In comparison with the acid strength of 100% sulfuric acid, the acidity of the HCl-[EMIM]Al<sub>2</sub>Cl<sub>7</sub> is much greater, as shown in Fig. 12 (104). The superacidity was ascribed to the non-solvated protons from the equilibrium  $\text{HCl} + \text{Al}_2\text{Cl}_7^- \rightleftharpoons [\text{H}]_{\text{non-solvated}}^+ + 2 \text{AlCl}_4^-$ . A TSIL with strong Brønsted acidity, [(C<sub>6</sub>H<sub>5</sub>)<sub>3</sub>(C<sub>3</sub>H<sub>6</sub>SO<sub>3</sub>H)P]OTf, was shown to have strong acidity for Fisher esterification. The catalyst was reused in multiple cycles with high yields (105).

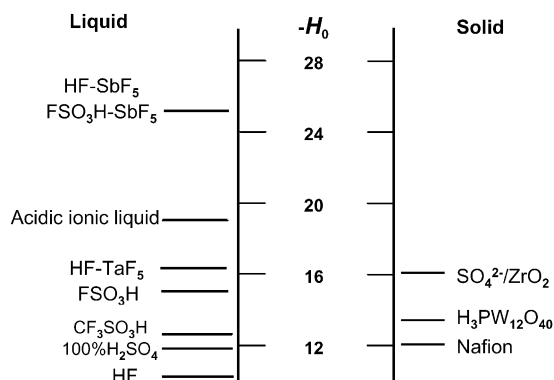


FIG. 12. Acid strength of [Al<sub>2</sub>Cl<sub>7</sub>]-ionic liquid in comparison with those of the conventional acids. Reproduced with permission from Hussey (104).

#### D.7. Basic Ionic Liquids

Ionic liquids of chloroaluminates with alkylpyridinium and dialkylimidazolium at AlCl<sub>3</sub> molar fractions ( $x$ ) less than 0.5 have been reported to have Lewis basicity. Although it has been well recognized that acidic chloroaluminate-containing ionic liquids degrade rapidly when even a small amount of water is present (with the formation of solid aluminum hydroxide species), the Lewis basic chloroaluminate ionic liquids of butylpyridinium are stable in water and have been used to catalyze water-forming reactions, such as the esterification of alcohols and carboxylic acids (106). Particularly remarkable is that the Lewis basic ionic liquids were reused for multiple cycles by simply evaporating the water after each run. The basic ionic liquid was not degraded at the reaction temperature range 30–100°C. For the esterification reaction, the authors emphasized two key factors regarding the use of the Lewis basic ionic liquid. The molar ratio of aluminum chloride/butylpyridine chloride must be  $<1$ . The aluminum chloride-containing ionic liquids are stable enough to resist degradation by water as long as the molar ratio of aluminum chloride/butylpyridine chloride is  $<1$ . It is also important that alcohol be added to the ionic liquid prior to the introduction of the organic acid. The advantage of such a reaction system is that the esters produced are not soluble in the ionic liquid and are therefore readily isolated.

Similar to the method of modifying neutral ionic liquids with strong Brønsted acids, a Lewis basic ionic liquid was also obtained by adding conventional base, such as NaOH, into the neutral ionic liquid. However, the solubility of the base in the ionic liquid is not high, and part of the [BMIM]PF<sub>6</sub> was converted to a solid phase, probably because of the anion exchange between PF<sub>6</sub><sup>-</sup> and OH<sup>-</sup> (107,108).

It has been noted that imidazolium ions are not inert. Under mild basic conditions, they are deprotonated to give reactive nucleophiles. For reactions in basic media, the C2 hydrogen of the imidazolium ring can be replaced with an alkyl group. In one study, the C2 hydrogen was substituted by a methyl group. Ionic liquids based on the C2 methylated imidazolium cation were evaluated for the

preparation of C9-aldehyde via aldol condensation reactions (109). The ionic liquid phases were treated with a concentrated solution of sodium hydroxide. The resulting mixtures were compared with an aqueous base containing sodium hydroxide. The hydroxyl concentration of the aqueous solution and that of the ionic liquid phase were both adjusted to 1 M, which corresponds to a conventional concentration for an aldol catalyst system (4 wt% NaOH). The resultant-basified ionic liquid catalyst was reported to successfully catalyze the aldol condensation reaction.

A weak base such as glycine added to [HMIM]PF<sub>6</sub> has also been reported to catalyze a Knoevenagel reaction of malononitrile and benzaldehyde (110). A KOH-treated [BMIM]PF<sub>6</sub> also provides a suitable medium for the Corey–Chaykovsky epoxidation of enones and cyclopropanation of aldehydes using trimethyl sulfonium iodide (111).

### D.8. Impurities

*D.8.1. Effect of Impurities.* High purity is essential for the application of ionic liquids to many catalytic processes (1), as the physical and chemical properties of ionic liquids can be significantly altered by the presence of impurities (53,112). Halide impurities can have a detrimental effect on transition metal-catalyzed reactions, largely because of the strong coordinating effect of the halide ions. The presence of water can reduce the density and the viscosity but can also modify the chemical properties. In some cases (e.g., PF<sub>6</sub><sup>−</sup>-containing ionic liquids), trace amounts of water can cause the decomposition of the anion and the formation of HF. The presence of trace acid can cause unwanted reactivity. As halide ions coordinate to transition metal centers, they block reactive coordination sites and lead to side reactions and catalyst deactivation (112,113). Therefore, substantial efforts in research have been devoted to synthesizing halide-free ionic liquids by avoiding halide precursors (114). It has proved to be extremely difficult to remove the final traces of chloride impurities from the ionic liquids.

*D.8.2. F<sup>−</sup> Impurity.* It has been observed that [MIM]SbF<sub>6</sub> produced a small amount of fluoride ion over time because of its sensitivity to air. Furthermore, residual chloride impurities have been found to exert a large influence on the physical properties of ionic liquids (115).

*D.8.3. Cl<sup>−</sup> Impurity.* Trace amounts of chloride impurities, which may be present at levels between 0.1 and 0.5 mol/kg, have significant effects on the physical properties of ionic liquids, such as viscosity and density. Increases in viscosity are of particular concern in biphasic processes because of the formation of emulsions that affect the interface between the two phases (88).

The largely negative effect of Cl<sup>−</sup> impurity was determined in benzene hydrogenation with a ruthenium complex as the pre-catalyst (115). The hydrogenation activities of the catalyst in water, halide-containing [BMIM]BF<sub>4</sub>, and “halide-free” [BMIM]BF<sub>4</sub> were compared. Whereas 50% higher activity in the “halide-free” ionic liquid was observed over that in water, the activity is even lower in the halide-containing ionic liquid than in water. The hydrogenation of other arene compounds showed similar trends in the three systems. Even a pre-catalyst,

$[\text{H}_4\text{Ru}_4(\eta^6\text{-C}_6\text{H}_6)](\text{BF}_4)_2$ , that was not expected to be sensitive to poisoning by halide impurities showed a significant increase in the turnover rate when the cluster was immobilized in the “halide-free”  $[\text{BMIM}]\text{BF}_4$ .

A systematic investigation of the effect of  $\text{Cl}^-$  impurity was reported for a metal-catalyzed Michael addition of acetylacetone to methyl vinyl ketone in  $[\text{BMIM}]\text{BF}_4$  (116). The time required for the completion of the reaction was used as a measure of the effect of  $\text{Cl}^-$ . With a  $\text{Ni}(\text{acac})_2 \cdot 2\text{H}_2\text{O}$  catalyst, the Michael addition was completed in 2, 5, and 9 h when the ionic liquid contained 0, 0.62, and 1.62%  $\text{Cl}^-$ , respectively.

Various sources of  $\text{Cl}^-$  impurity were found to inhibit the reaction to different degrees. Chloride from  $\text{NaCl}$  was more detrimental than that from  $[\text{BMIM}]\text{Cl}$ , as the former favorably exchanges with the acac ligand at the metal complex, resulting in the formation of tetrachloride metal (II) anion.

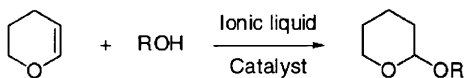
In certain cases, the halide impurities could be countered by using additives that serve to bind the halides, but this is not always a desired solution. In the rhodium-catalyzed polymerization of phenylacetylene (117), it was shown that the deleterious effect of halide impurities can be nullified by the addition of  $\text{NEt}_3$  co-catalyst to a  $\text{Rh}(\text{diene})(\text{acac})$ -containing catalyst.

## IV. Ionic Liquids as Catalysts

### A. BRØNSTED ACID CATALYSIS IN IONIC LIQUIDS

Because ionic liquids are in general weakly coordinating, they display low nucleophilicity. Such an environment favors the stabilization of electron-deficient intermediates (1). This unique property allows ionic liquids to be used as non-solvating media for the stabilization of strongly acidic species. It is this property that has given rise to the superacidity of non-solvated protons in acidic  $[\text{AMIM}]\text{Al}_2\text{Cl}_7$  (103).

Several authors reported the use of ionic liquids containing protonic acid in catalysis (118–120). For example, strong Brønsted acidity in ionic liquids has been reported to successfully catalyze tetrahydropyranylation of alcohols (120). Tetrahydropyranylation is one of the most widely used processes for the protection of alcohols and phenols in multi-step syntheses. Although the control experiments with the ionic liquids showed negligible activity in the absence of the added acids, high yields of product were obtained with the ionic liquid catalysts TPPTS or  $\text{TPP} \cdot \text{HBr} \cdot [\text{BMIM}]\text{PF}_6$ . By rapid extraction of the product from the acidic ionic liquid phase by diethyl ether, the reaction medium was successfully reused for 22 cycles without an appreciable activity loss. A gradual loss of the catalyst and a reduced volume of the ionic liquid were noted, however, as a consequence of transfer to the extraction solvent.



As the process was carried out at a low temperature (18°C), decomposition of the ionic liquids caused by the presence of the strong acids did not appear to be a serious problem.

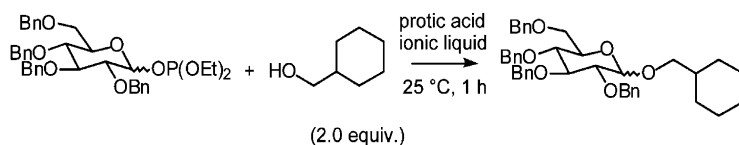
In another example, a catalytic amount of a Brønsted acid such as  $\text{H}_3\text{PO}_4$  was dissolved in  $[\text{NRR}'_3][\text{NTf}_2]$  ( $\text{R} = \text{hexyl}$ ,  $\text{R}' = \text{butyl}$ ) (119). The catalyst was applied for the condensation reaction of alcohols, which usually requires strongly acidic media and dehydrating conditions. The condensation of veratryl alcohol was facilitated because the water that formed was continuously removed as vapor, which assisted in driving the reaction to high yields. The product (cyclotrimeratrylene) separation, however, required the addition of a co-solvent.

When a Brønsted acid having a conjugated base identical to the anion of an ionic liquid is mixed with the ionic liquid, the complication of anion compatibility is avoided (121). For example, the ionic liquids  $[\text{HMIM}]\text{Tf}_2\text{N}$  and  $[\text{HMIM}]\text{TfO}$  ( $\text{H} = \text{hexyl}$ ) are suitable reaction media for protonic acid-catalyzed glycosidation of glucopyranosyl diethyl phosphite and alcohols (Scheme 2), because they have low viscosity, good hydrophobicity, and high solubility for the glycosyl donor and several glycosyl acceptors.  $\text{HOTf}$  and  $\text{HNTf}_2$  are excellent choices of Brønsted acids for these ionic liquids because of their anion compatibility. Therefore, a low dose of  $\text{HOTf}$  and  $\text{HNTf}_2$  at 0.01–1% was selected with the corresponding ionic liquids of the same anion. Compared to reactions in diethyl ether, toluene, acetonitrile, and dichloromethane, the highest yield (91%) was obtained with the ionic liquid containing protonic acid at 25°C in an hour. The product obtained from the ionic liquid catalyst showed the highest  $\beta$ -stereoselectivity among the solvents evaluated.

Chloride-free ionic liquid was essential for the high activity; the addition of only 5 mol%  $[\text{BMIM}]\text{Cl}$  led to a significant decrease in the yield because of the basicity of  $[\text{BMIM}]\text{Cl}$  (122). Remarkably, this acid–ionic liquid combination could be reused many times for the glycosidations without any loss in efficiency.

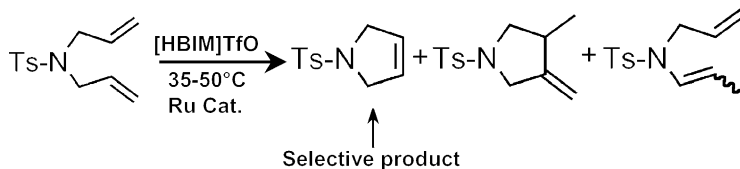
Brønsted acidic ionic liquids  $[\text{HMIM}]\text{BF}_4$ ,  $[\text{HMIM}]\text{TfO}$ , and  $[\text{HMIM}]\text{TsO}$  are effective for proton- and metal-assisted catalytic processes such as the dimerization of methyl acrylate and ring-closure metathesis (Scheme 3) (123). For example, the acidic  $[\text{HBIM}]\text{BF}_4$  in association with the  $[\text{Ru}(=\text{C}=\text{C}=\text{CPh}_2)(p\text{-cymene})(\text{PCy}_3)\text{Cl}][\text{OTf}]$  catalyst afforded a dramatic increase in the activity (100%) and selectivity (100%) for the ring-closure metathesis of *N,N*-diallyltosylamide.

Changing the ionic liquid anion to triflate leads to a further increase in the activity with no loss of selectivity (Scheme 3). The reaction product could be removed by extraction with diethyl ether.



SCHEME 2.





SCHEME 3.

Ionic liquids made from ethylamines and  $\text{AlCl}_3$  were reported to be active catalysts for the alkylation of 2-methylnaphthalene with long-chain mixed alkenes ( $\text{C}_{11-12}$ ) at ambient temperature (124). The catalytic activity of the ionic liquids follows the order  $\text{EtNH}_3\text{Cl}/\text{AlCl}_3$  ( $x = 0.71$ ),  $< \text{Et}_2\text{NH}_2\text{Cl}/\text{AlCl}_3$  ( $x = 0.71$ ),  $< \text{Et}_3\text{NHCl}/\text{AlCl}_3$  ( $x = 0.71$ ). The  $\text{AlCl}_3$  molar ratio ( $x$ ) to the alkylamines is a key to determining the catalytic activity. The optimal conditions for the alkylation reaction were observed to occur at an aromatic hydrocarbon to alkene molar ratio of 4:1 and at a cyclohexane to 2-methylnaphthalene molar ratio of 2:1 in the presence of 7% of catalyst at  $60^\circ\text{C}$ . More than 90% alkene conversion and 100% selectivity for the desired monoalkyl methylnaphthalene product were observed. The reaction was completed rapidly, and the product appeared to be stable over extended reaction times.

## B. LEWIS ACIDIC IONIC LIQUIDS

### B.1. Non-Chloroaluminate Lewis-Acid-Catalyzed Reactions

**B.1.1. Friedel–Crafts Acylation.** Acylation reactions have been carried out in acidic chloroaluminate(III) ionic liquids (125,126). The regioselectivities and reaction rates are comparable to the best known for the traditional acylations. However, the consumption of the ionic liquid as a catalyst was high, as in the industrial process that is carried out with  $\text{AlCl}_3$ .

The ionic liquids made of ferric chloride and tin chloride displayed good properties as alternative catalysts in the acylation reactions (127). For the acylation of mesitylene with acetylchloride and for the acylation of anisole with acetylanhydride, the best results were obtained with a ferric chloride-containing ionic liquid. The conversions were much higher, and the selectivity obtained was in the same range relative to those observed with the Al- and Sn-chloride-containing ionic liquids.

*In-situ* IR-spectroscopic characterization of the Friedel–Crafts acylation of benzene in ionic liquids derived from  $\text{AlCl}_3$  and  $\text{FeCl}_3$  showed that the mechanism of the reaction in ionic liquids was the same as that in 1,2-dichloroethane (128). The immobilization of ferric chloride-containing ionic liquid onto solid supports (e.g., silica and carbon) however failed to catalyze the acylation reaction, because leaching was a serious problem. When the reaction was carried out with gas-phase reactants, catalyst deactivation was observed.

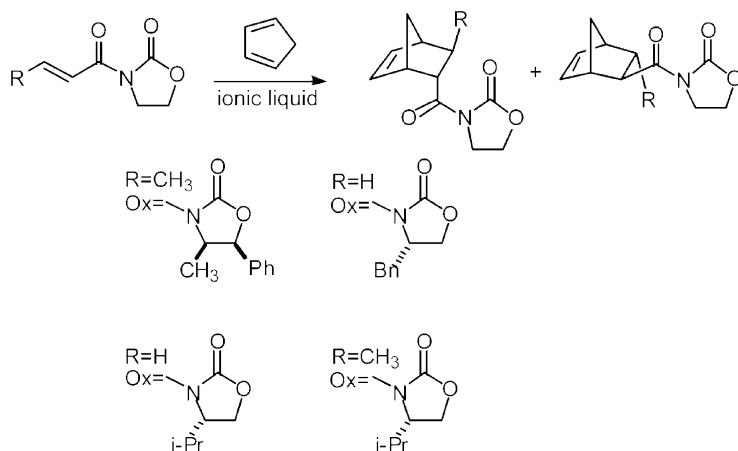
**B.1.2. Diels–Alder Reactions.** The Diels–Alder reaction is one of the reactions that has been most thoroughly investigated with ionic liquids (1). Adding a Lewis acidic catalyst such as  $\text{Sc}(\text{OTf})_3$  to ionic liquids improves endo selectivity (129). Ionic liquid co-solvent was found to activate the Lewis-acidic  $\text{Sc}(\text{OTf})_3$  catalyst in

the Diels–Alder reaction of linoleate with methyl vinyl ketone. Addition of the Lewis acid and ionic liquid [BMIM]BF<sub>4</sub> to a non-polar solvent like CH<sub>2</sub>Cl<sub>2</sub> led to a drastically shortened reaction time. Chloroaluminate-containing ionic liquids were found to be active but unselective for this reaction (96).

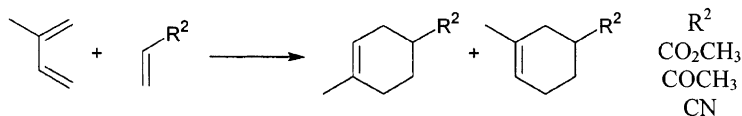
Varying the alkyl group in the [AMIM]<sup>+</sup> ion is a convenient method for tuning the ionic liquid performance in catalytic applications (130). This approach was used in a Diels–Alder reaction involving [AMIM]Tf<sub>2</sub>N ionic liquids. The 1-alkyl-3-methylimidazolium bis(trifluoromethylsulfonyl)imides (in which alkyl = C<sub>3</sub>H<sub>7</sub>, C<sub>10</sub>H<sub>21</sub>, C<sub>6</sub>H<sub>5</sub>CH<sub>2</sub>, CH<sub>3</sub>O(CH<sub>2</sub>)<sub>2</sub>, and HO(CH<sub>2</sub>)<sub>2</sub>) are less viscous liquids at room temperature. In the Diels–Alder reaction of cyclopentadiene with methyl acrylate, a correlation between the stereoselectivity (*endo/exo*) of the reaction and the polarity of the ionic liquid was observed; a greater polarity resulted in a higher *endo/exo* ratio. The hydroxy-containing ionic liquid has a higher polarity than [C<sub>10</sub>MIM]NTf<sub>2</sub>, and therefore resulted in a better stereoselectivity.

Unusually high diastereoselectivity and enantioselectivity in Diels–Alder reactions were achieved in ionic liquids at room temperature (131). The selectivity rivals that of the reaction in conventional solvents, for which a low temperature (e.g., –78°C) is needed. Furthermore, the rate of the reaction is much higher in the ionic liquids than in the conventional solvents, because the reaction is carried out at room temperature in ionic liquids.

In another investigation, 1% ZnCl<sub>2</sub> in hydrogen butylimidazolium tetrafluoroborate ([HBIM]BF<sub>4</sub>) and 1,3-dibutylimidazolium tetrafluoroborate ([DBIM]BF<sub>4</sub>) were found to be effective catalysts for the Diels–Alder reaction. The Diels–Alder reactions of acryloyl oxazolidinones and cyclopentadiene proceed well in [HBIM]BF<sub>4</sub> without ZnCl<sub>2</sub>, but for the reaction of crotonyl oxazolidinone with cyclopentadiene, the presence of 1% ZnCl<sub>2</sub> in [DBIM]BF<sub>4</sub> gave the highest rate, with a 68% yield to the cyclo adduct in a 92:8 *endo/exo* ratio (Scheme 4). For comparison, Zn(OAc)<sub>2</sub> or ZnCl<sub>2</sub> in the conventional solvents CH<sub>2</sub>Cl<sub>2</sub> or Et<sub>2</sub>O resulted in rather low yields (only 2–13%) to the desired product.



SCHEME 4.



SCHEME 5.

In the same work, it was demonstrated that 1%  $\text{ZnCl}_2$  in  $[\text{DBIM}]\text{BF}_4$  gave 55–97% yields and very high diastereoselectivities (*endo/exo* ratio of 100:0) to cycloadducts of chiral oxazolidinones at room temperature. For comparison, 1.4 equivalent of  $\text{Et}_2\text{AlCl}$  in  $\text{CH}_2\text{Cl}_2$  gave a modest 62% cyclo adduct, with a poor *endo/exo* ratio (*endo/exo* in 48:52).

A number of other ionic liquids have also been evaluated for Diels–Alder reactions, but mostly with model systems. Phosphonium tosylates were shown to be good catalysts at temperatures of 80–100°C for the Diels–Alder reaction of isoprene with oxygen-containing dienophiles, resulting in high regioselectivity, even in the absence of Lewis acids (Scheme 5) (132). The Lewis acid  $\text{ZnI}_2$  in  $[\text{BMIM}]\text{PF}_6$ , showed good activity and regioselectivity, even at a much milder reaction temperature (20°C) (133).

Earlier works included investigations of  $[\text{EMIM}]\text{PF}_6$ ,  $[\text{EMIM}]\text{BF}_4$ ,  $[\text{EMIM}]\text{TfO}$ ,  $[\text{BMIM}][\text{ClO}_4]$ ,  $[\text{OEMIM}]\text{Cl}/\text{AlCl}_3$ , and  $[\text{BMIM}]\text{TfO}$  (17,133–135). The addition of a Lewis acid (e.g.,  $\text{Sc}(\text{TfO})_3$ ) to ionic liquids promotes Diels–Alder reactions for high product yield (129).

## B.2. Chloroaluminate-Catalyzed Reactions

**B.2.1. Alkylation.** Lewis acidic ionic liquids have been extensively investigated as replacements for  $\text{AlCl}_3$  as catalysts for the alkylation of aromatics with alkenes. The ionic liquids have strong Lewis acidity and also allow easy handling of the acid in liquid state. An aromatic starting molecule typically has excellent solubility in the ionic liquids, and the alkylated products have a much lower solubility (27). Therefore, the Lewis acidic ionic liquids provide good opportunities for the formation of products that have not undergone multiple alkylations. The prevention of exposure to moisture during reaction and product separation is critical to allow for multiple reuse of the liquid catalysts.

In the alkylation of benzene with 1-dodecene, complete conversion of 1-dodecene was reached within 5 min in the presence of several strong Lewis acidic ionic liquids (as well as a reference  $\text{AlCl}_3$  catalyst) (136). However, the product distributions were different. Anhydrous  $\text{AlCl}_3$  was characterized by much lower selectivity for the 2-substituted isomer than the ionic liquid consisting of  $[\text{EMIM}]\text{Cl}-\text{AlCl}_3$ . With benzene in present large excess, dialkylated benzene and products of isomerization and oligomerization of 1-dodencene were not observed. A higher selectivity to the 2-substituted dodecyl isomer was observed with the ionic liquids, in contrast to the  $\text{AlCl}_3$ . The results were explained on the basis of stabilization of carbenium ion intermediates by the ionic liquids.

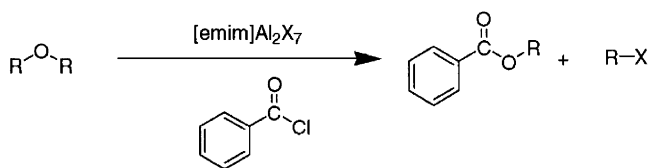
The alkylation of isobutane with 2-butene in ionic liquid media was investigated with [AMIM] halide–aluminum chloride-containing ionic liquids (137). A systematic investigation of the effect of the alkyl group in the [AMIM]<sup>+</sup> ion showed that a larger alkyl group on the ion (e.g., [C<sub>8</sub>MIM]) gives a higher activity than a smaller one (e.g., C<sub>6</sub> or C<sub>4</sub>MIM) with the same anionic composition in the ionic liquids; the effect is attributed to a high solubility of reactants in the former. Among ionic liquids with various halide groups, bromides ([C<sub>8</sub>MIM]Br/AlCl<sub>3</sub>) showed the highest activity. The characterization of the ionic liquids with <sup>27</sup>Al NMR and FTIR spectroscopies indicated the formation of [Al<sub>2</sub>Cl<sub>6</sub>Br]<sup>−</sup>, which associates with the hydrogen atom at the C(2) position of an imidazolium cation, resulting in strong Brønsted acid. The optimum catalytic activity was observed at 80°C; at a higher reaction temperature (120°C), the ionic liquid was characterized by lower activity and trimethylpentane selectivity, because the solubility of the reactants and Brønsted acid sites were reduced by the decomposition of imidazolium cation. Remarkably, when the ionic liquid [C<sub>8</sub>MIM]Br/AlCl<sub>3</sub> was compared with sulfuric acid under optimum conditions, it was found that the two catalysts are similar in performance, with the ionic liquid, however, showing a higher activity and a lower-TMP selectivity.

**B.2.2. Dialkyl Ether Cleavage.** Varying the mole fraction of AlCl<sub>3</sub> in an ionic liquid can optimize reactions that are sensitive to the strength of Lewis acidity. When the ionic liquids [EMIM]Cl/AlCl<sub>3</sub> were applied for the acylative cleavage of dialkyl ethers (Scheme 6), the reaction was found to be sensitive to the bulk Lewis acidity of the ionic liquid solvent (138).

The acylative cleavage of the cyclic ether tetrahydrofuran showed an excellent yield (95%) to 4-iodobutylbenzoate when fully acidic ionic liquid [EMIM]Al<sub>2</sub>Cl<sub>7</sub> was used, but the yield to di-functionalized product (61%) suffered when the mildly acidic halogenoaluminate ionic liquid (which has a mole fraction of AlCl<sub>3</sub> (x) at a value of 0.52) was used as the solvent. In contrast, for 1,5-dimethyltetrahydrofuran and tetrahydropyran, a good yield to the cleavage products was obtained when the mildly acidic chloroaluminate was used.

In recent work a serendipitous discovery showed that strongly acidic chloroaluminate-containing ionic liquids, whether in combination with trialkylammonium or with dialkylimidazolium cations, are active and selective for the cleavage of aromatic methyl ethers, even at temperatures <40°C. The ionic liquids are consistently better catalyst than AlCl<sub>3</sub> for this type of reaction (139).

Good selectivity in alkene (ethylene or butene) alkylation with isoparaffins has been reported for acidic chloroaluminates (140). The ionic liquids have also been



SCHEME 6.

applied to the alkylation of benzene and to the polymerization of isobutylene (141,142).

It was recently demonstrated that a chloroaluminate ionic liquid is well suited to the Pechmann synthesis of coumarins, which are well-known anticoagulants and are also used in a number of other applications (143). The reaction involves the condensation of phenols with  $\beta$ -ketonic esters in the presence of an acid catalyst (144). When conventional acid catalysts (e.g., sulfuric acid, trifluoroacetic acid, or aluminum chloride) are used (145), large excess of the conventional acid catalysts was necessary for the reaction. For this reaction, it was reported that the acidic chloroaluminate ionic liquid corresponding to an  $\text{AlCl}_3$  mole fraction ( $x$ ) of 0.67 gave a maximum yield. The reaction time was drastically reduced with most of the substrates. An excellent yield of coumarins was observed, even under ambient conditions. In contrast, a high temperature was needed in conventional preparation with  $\text{AlCl}_3$  in nitrobenzene to drive the reaction to completion. Another advantage of the strongly acidic ionic liquid is that no detectable undesired product from demethylation of 3-methoxyphenol was observed at temperatures  $< 30^\circ\text{C}$ . As the traditional method requires high temperatures, demethylation has been a significant issue.

### C. BASIC IONIC LIQUIDS AND RELATED REACTIONS

#### C.1. Aldol Reaction

Aldol condensation is one of the basic organic transformations for the formation of C–C bonds. The most promising approach leading to stereoselective aldol reactions involves the use of small organic molecules that mimic enzymes (146). Proline has been demonstrated to be a catalyst for asymmetric direct intermolecular aldol condensation. A strong solvent influence on the enantiopurity of the products was observed; anhydrous DMSO has been found to be the most suitable solvent (147). To enable catalyst reuse,  $[\text{BMIM}]\text{PF}_6$  was evaluated as a solvent to isolate proline. The resulting catalyst was effective for the conversion of a large number of 2- and 4-substituted benzaldehydes. Aldol products were obtained in good yields (61–94%) with satisfactory enantioselectivities (61–93% ee). The  $[\text{BMIM}]\text{PF}_6$  catalyst was shown to be recyclable and, in many cases the product yield and enantiopurity were comparable to those obtained with the fresh catalyst (148).

In similar works, a number of  $[\text{AMIM}]^+$ -containing ionic liquids were evaluated for proline-catalyzed aldol reactions. The catalyst in the ionic liquid with  $\text{Cl}^-$  as the anion was characterized by a higher reaction rate than the ionic liquids with the anions  $\text{BF}_4^-$  and  $\text{PF}_6^-$ , but elimination products affected the yields in the latter ionic liquids (149).

Several NaOH-treated ionic liquids for self- and cross-aldol condensation reactions of propanal provide an interesting example illustrating improved product selectivity in a system in which competing reactions take place (109). In the self-aldol condensation reaction of propanal, 2-methylpent-2-enal is formed. The reaction progresses through an aldol intermediate and produces the unsaturated aldehyde. The NaOH-treated ionic liquid  $[\text{BDMIM}]\text{PF}_6^-$  gave the highest product

selectivity (82%), identical to the selectivity obtained with an aqueous base. However, with the NaOH-treated [BMIM] PF<sub>6</sub><sup>-</sup> ionic liquid, although a quantitative conversion of propanal was also observed, a large amount of higher-boiling aldehydes was also produced. The results indicate the role of an increased solubility of the C<sub>6</sub> aldehyde products in the ionic liquid, favoring the formation of higher-boiling side products via cross-aldol condensation reactions. High selectivity for C<sub>6</sub> aldehydes such as 2-methylpentanal is essential for the subsequent synthesis of 2,4-dimethylhept-2-enal, as described below.

Following a selective hydrogenation of the self-condensation product, a cross-aldol condensation reaction was carried out by reacting 2-methylpentanal with propanal. The selectivity for the desired 2,4-dimethylhept-2-enal product was 20% higher with the NaOH-containing ionic liquid than with aqueous NaOH. The increased selectivity was attributed to the higher solubility of the starting material 2-methylpentanal in the ionic liquid. In the aqueous NaOH, the substrate propanal is fully soluble, but the other substrate, 2-methylpentanal, has only limited solubility. Even with a four-fold excess of 2-methylpentanal to compensate for the low solubility, the product selectivity was only 60%. The major competing reaction is the self-condensation of propanal to form 2-methylpent-2-enal. By carrying out the same reaction under identical conditions in the basic [BMIM]BF<sub>4</sub> ionic liquid phase, the competing reaction was reduced markedly, and the product selectivity for the desired 2,4-dimethylhept-2-enal increased to 80%.

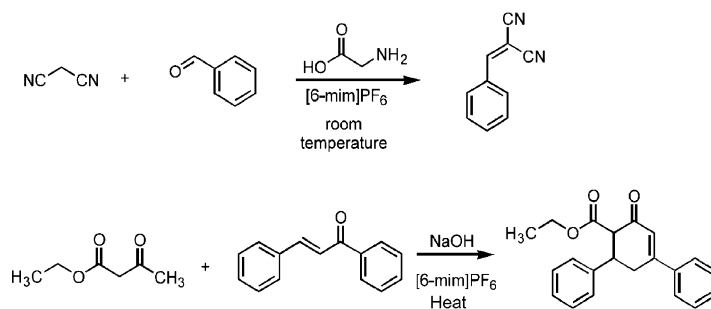
### C.2. Knoevenagel Condensation

The Lewis acidity of a catalyst for the Knoevenagel condensation of substituted benzaldehydes with ethyl malonate was tuned by simply varying the apparent mole fraction of AlCl<sub>3</sub> (150). The rate of the Knoevenagel reaction relative to the consecutive competing Michael reaction, which consumes the Knoevenagel product and ethyl malonate, depends on the mole fraction  $x$  of AlCl<sub>3</sub> in the ionic liquid [BMIM]Cl/AlCl<sub>3</sub>. At  $x = 0.5$ , the ionic liquid catalyzes the Knoevenagel reaction. With an increase in  $x$  from 0.5 to 0.67, the Michael reaction becomes important.

An organic base in an ionic liquid was also found to be effective for a Knoevenagel reaction. Glycine was added to the ionic liquid [HMIM]PF<sub>6</sub> as the base catalyst. The reaction proceeded at room temperature in air without the need for rigorous drying of the ionic liquid. Glycine and the reactants malononitrile and benzaldehyde dissolved readily in the ionic liquid. The product was extracted from the ionic liquid phase with an immiscible co-solvent, toluene (110).

### C.3. Robinson Annulation

The Robinson annulation of ethyl acetoacetate and *trans*-chalcone was investigated with pulverized NaOH in [BMIM]PF<sub>6</sub> as the base catalyst at 100°C (110). The mixture was neutralized before extraction with toluene. The product, 6-ethoxycarbonyl-3,5-diphenyl-2-cyclohexenone, was obtained by purification in a silica gel chromatography column. A yield of 48% was obtained (Scheme 7). The ionic liquid could be recycled and reused with no diminution of product yield. The C2 position in imidazolium cations is an acidic proton donor and may have reacted



SCHEME 7.

with the base catalysts to form imidazolidene carbenes (151,152). It was therefore suggested that the active bases in the Knoevenagel and Robinson annulation reactions are carbenes.

#### D. NEUTRAL IONIC LIQUIDS AS CATALYSTS

Neutral ionic liquids such as [AMIM]BF<sub>4</sub> and [AMIM]PF<sub>6</sub> function as catalysts for a limited number of reported reactions. The purities of such ionic liquids have been a concern. Because unknown impurities could give misleading results, care needs to be taken in the preparations (153).

The ionic liquid [BMIM]BF<sub>4</sub> was reported to catalyze the selective ring opening of epoxides with aryl amines for the synthesis of corresponding  $\beta$ -amino alcohols under mild and neutral conditions with excellent yields and high regioselectivity (154). These reactions have traditionally been carried out with large excesses of the amines at elevated temperatures, resulting in low regioselectivity. Metal amides, metal triflates, and transition metal halides have been developed to perform the epoxide ring opening with amines under mild conditions (155–157). Undesirable side reactions include the rearrangement of the oxiranes to allyl alcohols under basic conditions and polymerization under strongly acidic conditions.

In the presence of [BMIM]Br, aryl oxiranes are cleaved by a variety of amines, giving exclusively a regioselective product from benzylic attack. Other epoxides (including glycidyl aryl ethers, glycidyl alkyl ethers, and esters), alkyl oxiranes, and cycloalkyl epoxides are also converted. Remarkably, all the reactions were found to proceed efficiently at ambient temperature with high regioselectivity. The product yields reached 80–90% in a few hours.

The products were weakly soluble in the ionic phase. They were separated by extraction with ether. The viscous ionic liquid could be reused in five runs without any loss of activity after thorough washing with ether and drying at 80°C after each run. In contrast, the reaction did not proceed in the polar organic solvents DMF and *N*-methylpyrrolidine, even at higher temperatures (75–80°C). The ionic liquids [Bu<sub>4</sub>N]Cl and [BMIM]Cl were also found to be ineffective.

The ionic liquid [BMIM]BF<sub>4</sub> was found to efficiently catalyze the three-component coupling reactions of aldehydes, amines, and homophthalic anhydride under ambient conditions to give the corresponding *cis*-isoquinolonic acids in excellent yields with



high *cis*-selectivity (158). There was a slow decrease in activity observed in consecutive tests with recycled ionic liquid, but the activity of the ionic liquid became consistent in runs with no decrease in yield when the recycled ionic liquid was activated at 80°C under vacuum. In contrast, several Lewis acids (such as  $\text{BF}_3 \cdot \text{OEt}_2$ ,  $\text{TiCl}_4$ , and  $\text{SnCl}_4$ ) were decomposed or deactivated by amines and water during imine formation.

[BMIM] $\text{BF}_4$  and [BMIM] $\text{PF}_6$  were used as catalysts to activate aryl halides for nucleophilic substitution reactions with secondary amines at room temperature. The corresponding arylamines were obtained in high yields (159).

Tetraalkylammonium bromide was found to be a good catalyst for the conjugate addition of thiols to  $\alpha,\beta$ -unsaturated nitriles, carboxylic esters, ketones, aldehydes, and nitro alkenes. The reactions proceeded rapidly and gave high yields of products (typically, 90%) (160).

## V. Ionic Liquids as Catalyst Carriers

### A. CHARACTERISTICS OF IONIC LIQUID CATALYST CARRIERS

#### A.1. *Inert Catalyst Carriers*

In general, ionic liquids are weakly coordinating, and typically, they are chemically inert. Therefore, they are suitable catalyst carriers for a wide variety of catalysts, including organometallics and Lewis acids, which are applicable in many conventional homogeneous catalytic reactions. Nearly inert ionic liquids have also been used as media to prepare and isolate metal nanoclusters, such as Ir and Rh (12). Metal nanoclusters can be stabilized in the ionic liquid phase; the extraction of gold nanoclusters from an aqueous phase into an imidazolium-containing ionic liquid phase has been reported (161).

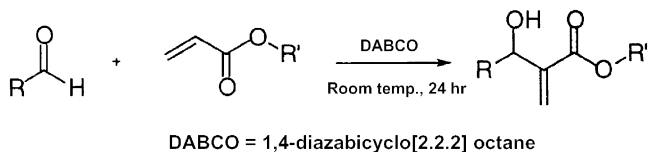
It is emphasized that not all ionic liquids are inert. Caution must be exercised particularly regarding the acidity of C2 groups in  $[\text{AMIM}]^+$ . This position can be substituted with an alkyl group, making the cations inert (Section III.D.7).

#### A.2. *Stabilization of Transition States*

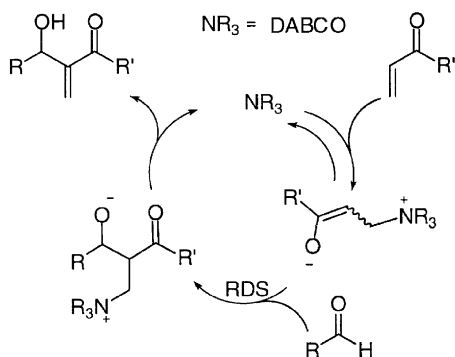
Because many of them are nearly inert, ionic liquids have been used to stabilize highly polar or ionic transition states. Ionic liquids provide favorable media for the formation and stabilization of intermediates in reactions that proceed through charged intermediates. An example is the Baylis–Hillman reaction catalyzed by 1,4-diazabicyclo (222).octane (DABCO) (Scheme 8) (162).

In the proposed mechanism (Scheme 9), the rate-determining step is the reaction between aldehyde and enolate. In the absence of a solvent, a major issue with this reaction is the typical low rate and the need for a high concentration of catalyst (usually DABCO). It was reported recently that, under basic conditions, the ionic liquid [BDMIM][ $\text{PF}_6$ ] is inert and that the Baylis–Hillman reaction in [BDMIM] $\text{PF}_6$  proceeds smoothly with better yields than in [BMIM] $\text{PF}_6$  (163).





SCHEME 8.



SCHEME 9.

A remarkable increase in the rate was observed when the reaction was conducted in ionic liquids instead of  $\text{CH}_3\text{CN}$  (Fig. 13). The rate increased by 11 times in  $[\text{BMIM}]\text{BF}_4$  and 34 times in  $[\text{BMIM}]\text{PF}_6$ . Furthermore, the product yield was significantly enhanced in  $[\text{BMIM}]\text{PF}_6$  (65%), and this value is considerably higher than that in  $\text{CH}_3\text{CN}$  (35%) and is comparable to that of characterizing the neat reaction. The enhanced reaction rates in the ionic liquids were attributed to a shift in the equilibrium favoring stabilization of the zwitterionic intermediate.

### A.3. Lewis Acidity

Lewis acidity is readily obtained in ionic liquids by selecting the anionic species or by dispersing a Lewis acid in an anionic liquid. Several types of Lewis acids and their catalytic applications are reviewed below.

Lewis acidic  $\text{InCl}_3$  was dispersed and isolated in several ionic liquids for the tetrahydropyranylation of cinnamyl alcohol with 3,4-dihydro-2H-pyran (164). Tetrahydropyranylation is one of the most widely used processes for the protection of alcohols and phenols in multi-step syntheses of complex natural products. With 5-mol%  $\text{InCl}_3$  dispersed in  $[\text{BMIM}]\text{PF}_6$ , the desired tetrahydropyranyl (THP) derivative was obtained in 92% yield. Similarly, a wide range of hydroxy compounds was converted to the corresponding THP ethers in excellent yields. The reactions proceeded efficiently at ambient temperature with high chemoselectivity. The reaction conditions were mild enough to avoid isomerization of multiple bonds during pyranlation of allylic and propargylic systems. The reaction medium was also

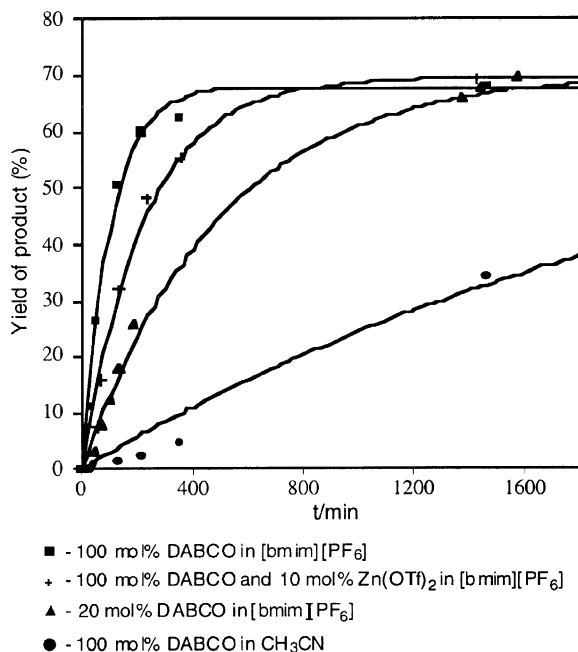


FIG. 13. Effect of the ionic liquid [BMIM]PF<sub>6</sub> on catalysis of the Baylis–Hillman reaction. Reproduced with permission from Rosa *et al.* (162).

highly selective for the protection of hydroxyl groups in the presence of highly acid-sensitive protecting groups, such as epoxides and acetals, which is difficult to achieve under the more severe conventional conditions. The catalyst was also effective for the reaction of alcohols with 2,3-dihydrofuran at ambient temperature with high chemoselectivity. The tetrahydrofuranyl ether products were isolated in high yields (about 90%) after 3–6 h. [BMIM]BF<sub>4</sub> was also effective for the same reaction. [BMIM]Cl and *n*-Bu<sub>4</sub>NCl are poor solvents for the reaction. In these ionic liquids, stronger interactions between InCl<sub>3</sub> and Cl<sup>−</sup> are expected, as InCl<sub>3</sub> has been reported to form ionic liquids with [EMIM]Cl (165).

Enhanced reaction rates, improved yields, and high functional group compatibility are the features demonstrated by these ionic liquids. The products are weakly soluble in the ionic phase, so that they are easily separated by simple extraction with ether.

Metal triflate Lewis acids can also be dispersed in ionic liquids for catalytic applications. Acetylation of alcohols with acetic anhydride and acetic acid has been reported with Cu(OTf)<sub>2</sub>, Yb(OTf)<sub>3</sub>, Sc(OTf)<sub>3</sub>, In(OTf)<sub>3</sub>, HfCl<sub>4</sub>·(THF)<sub>2</sub>, and InCl<sub>3</sub> in ionic liquids that consist of [BMIM]<sup>+</sup> and the anions BF<sub>4</sub><sup>−</sup>, PF<sub>6</sub><sup>−</sup>, or SbF<sub>6</sub><sup>−</sup> (166). With 1 mol% acid, all the catalysts in [BMIM]PF<sub>6</sub> showed >99% acetylation products in acetyl anhydride acetylation of benzyl alcohol. Sc(OTf)<sub>3</sub> showed the best yield with recycling, with a 25% drop in yield after two cycles. A relatively long reaction period was needed to obtain a high yield (95–98%) for the acetylation of benzyl alcohol with acetic acid, indicating that the activities of the catalysts were

low for this reaction. The ionic liquids [BMIM]BF<sub>4</sub> and [BMIM]SbF<sub>6</sub> were less effective solvents than [BMIM]PF<sub>6</sub> for the catalysts used for acetylation with acetic acid.

Non-chlorinated Lewis acids, such as scandium triflate, were found to be good catalysts for Friedel–Crafts alkylation reactions (167). Although no aromatic hydrocarbon alkylation occurred in CH<sub>2</sub>Cl<sub>2</sub>, [BMIM]PF<sub>6</sub>, Sc(OTf)<sub>3</sub> catalyzed the alkylation of benzene with high yields of the monoalkylated product. The lower acidity of the ionic liquid led to fewer byproducts and therefore higher yields. The products were separated by simple decantation and the catalyst was reused.

In another example, a catalytic amount of cerium triflate hydrate was dispersed and isolated in [BMIM]PF<sub>6</sub> for the direct formation of tetrahydropyranol derivatives. The reaction involves a simple homoallyl alcohol and an aldehyde. When an organic solvent such as chloroform was employed, an undesired ether derivative formed as the major product. In the ionic liquid, however, the desired tetrahydropyranol was exclusive. Although the yield was moderate, this example constitutes the first relatively facile and direct formation of the synthetically useful pyranol derivative; the only effective catalyst reported is the ionic liquid (168).

#### A.4. Dispersion and Isolation of Organometallic Catalysts

Many organometallic catalysts are soluble in ionic liquids, especially including ionic compounds. Neutral species, such as Wilkinson's catalyst, are also soluble to some extent in ionic liquids (169). There are numerous examples illustrating the dispersion and isolation of organometallic catalysts in ionic liquids; a list of examples is given in a recent review (1).

Often in the literature, the term “catalyst immobilization” has been used to describe the dispersion and retention of a catalyst in an ionic liquid, although it is generally understood that the catalyst in the ionic liquid is not truly immobilized as it is on a solid support surface; the term “catalyst immobilization” is avoided in this context here.

A primary incentive for the use of ionic liquids as media for transition-metal catalyzed reactions is the opportunity to recycle expensive catalysts and ligands and at the same time preventing contamination of the products by the catalysts and the ligands. There are many examples demonstrating the retention and recycling of organometallic catalysts by the use of ionic liquids. The principle is simply the retention of ionic or polar catalytic species in the ionic liquid without the need for specially designed ligands. An example is alkene hydrogenation catalyzed by the complexes [HRh(PPh<sub>3</sub>)<sub>2</sub>(L<sub>2</sub>)]PF<sub>6</sub> in [BMIM]BF<sub>4</sub> (170). The cluster [H<sub>4</sub>Ru<sub>4</sub>(C<sub>6</sub>H<sub>6</sub>)<sub>4</sub>](BF<sub>4</sub>) is also soluble and stable in [BMIM]BF<sub>4</sub> (170). In the presence of H<sub>2</sub>, it probably forms [H<sub>6</sub>Ru<sub>4</sub>(C<sub>6</sub>H<sub>6</sub>)<sub>4</sub>](BF<sub>4</sub>)<sub>2</sub>, which is an active arene hydrogenation catalyst.

#### A.5. Ligand Partitioning Effects

When the active catalyst species is not charged, partitioning of transition metal complexes into the organic phase can be controlled by using functionalized ligands. For example, organophosphorus ligands have been used widely as ligands for

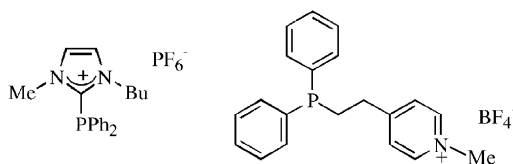
asymmetric hydrogenation catalysts. To protect the metal complexes from leaching from an ionic liquid during the reaction and separation steps, some charged phosphorus ligands have been designed; two examples are shown in Scheme 10 (171,172).

Other ligands chosen by a similar strategy were also reported (173,174). They have been used to retain rhodium complexes in ionic liquids for alkene hydroformylation.

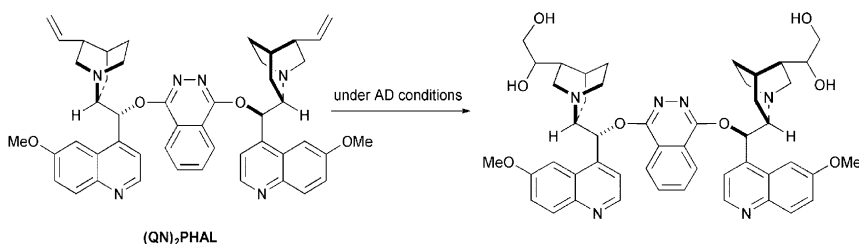
$\text{OsO}_4$  is a well-investigated catalyst for asymmetric dihydroxylation (AD) of alkenes, particularly for chiral drugs and fine chemicals (175). The high cost of osmium and chiral ligands, combined with the high toxicity and volatility of the osmium component, have made their large-scale industrial application difficult (176,177). Possible product contamination by osmium leaching from homogeneous systems has restricted the use of the catalyst for AD reactions in industry (178).

A specific ligand design strategy was implemented for favorable partitioning of the catalyst  $\text{OsO}_4$  in ionic liquids (179). It involved the selection of a pre-ligand, which strongly coordinates to the oxide catalyst. The pre-ligand, containing  $\text{C}=\text{C}$  bonds, was converted into a new dihydroxylated ligand *in situ* during the catalytic AD reaction of the reactant stilbene. The dihydroxylated ligand showed a remarkable strength of coordination to  $\text{OsO}_4$  as well as strong affinity for the ionic ligands. High activity was obtained with the catalyst.

By taking advantage of the polarity of  $[\text{BMIM}]\text{PF}_6$ , the pre-ligand,  $[(\text{QN})_2\text{PHAL}]$  (Scheme 11), with highly polar groups, was selected for its compatibility with the ionic liquid. This ligand showed excellent performance with  $\text{OsO}_4$  when it was applied for the AD of the model compound stilbene under standard conditions in the ionic liquid. The  $[(\text{QN})_2\text{PHAL}]$  ligand itself was further converted *in situ* with the reactant into a new bis-cinchona alkaloid ligand. The new ligand produced a dramatic improvement in the recyclability of the two catalyst



SCHEME 10.



SCHEME 11.

components. The recovered ionic liquid phase containing osmium and the new bis-cinchona alkaloid ligand were reused with no detectable leaching, even at much reduced catalyst loadings (0.1 mol% vs. > 1 mol% in comparable systems). The same ligand in combination with a catalyst,  $\text{K}_2\text{OsO}_2(\text{OH})_4/\text{K}_3\text{Fe}(\text{CN})_6$ , in a biphasic  $[\text{BMIM}]\text{PF}_6/\text{H}_2\text{O}$  reaction system and a monophasic  $[\text{BMIM}]\text{PF}_6/\text{H}_2\text{O}/t\text{-BuOH}$  system for the AD reaction of 1-hexene was also reported (180). The multiple cycle test results consistently showed the remarkable partitioning of the  $\text{OsO}_4$  catalyst in the  $[\text{BMIM}]\text{PF}_6$  ionic liquid through the favorable partitioning of the ligand. Most significant is a remarkable reduction of Os contamination in the product.

#### A.6. Ligand Effects of Ionic Liquids

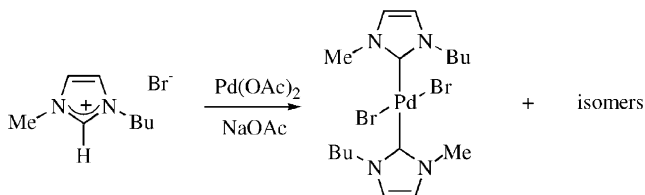
In general, a significant advantage of using ionic liquids for the stabilization of organometallic catalysts is their weak coordinating effect. Therefore, stronger ligand effects imposed by halide impurities in ionic liquids should be avoided.

However, the bromide ion in  $[\text{BMIM}]\text{Br}$  or  $[\text{TBA}]\text{Br}$  has been found to become beneficial when used to stabilize the noble metal catalysts that are prone to form zerovalent nanoparticles, which could agglomerate further under reaction conditions, resulting in the loss of the catalysts (84).

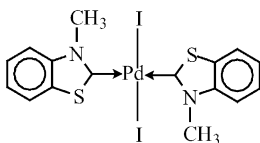
To prevent the loss of palladium as palladium black, two groups independently reported the use of a halide ion and the active nature of the acidic C2 groups in  $[\text{AMIM}]^+$ . In one case,  $[\text{TBA}]\text{Br}$  was used. The anion and the cation of  $[\text{TBA}]\text{Br}$  played a double role in the catalyst. The bromide ion, by reacting to give a rather unstable 14-electron complex,  $\text{L}_2\text{Pd}^0$ , led to an anionic, more stable, and catalytically active 16-electron complex,  $[\text{TBA}]^+[\text{L}_2\text{Pd}^0\text{Br}]^-$ . The formation of this large complex, by imposing a Coulombic barrier for collision, impedes the growth of clusters into metal particles. This catalyst has been shown to be successful in the Heck reaction of bromoaromatics with 3-hydroxy-2-methylenealkanoates to give  $\beta$ -arylketones (181).

The ligand effect of the halides on the stabilization of the metal catalyst, however, follows the efficacy order:  $\text{Br}^- > \text{Cl}^- \approx \text{I}^-$ . Although the  $\text{I}^-$  ion is a weaker ligand than  $\text{Br}^-$ ,  $\text{Cl}^-$  is too strong, so that the accessibility of the metal center by reactant is hindered. When a palladium complex catalyst was placed in a bromide-containing ionic liquid, the catalyst was shown to be stable for the Heck reactions without precipitation of the metals.  $[\text{TBA}]\text{Br}$  performed better than  $[\text{BMIM}]\text{Br}$ ; the structural difference between  $[\text{NBu}_4]^+$  and  $[\text{BMIM}]^+$  accounts for the difference, with the  $\text{Br}^-$  being more strongly coordinated in  $[\text{NBu}_4]\text{Br}$  due to a weak association with the bulky tetrahedral ammonium ion than the  $\text{Br}^-$  associated with the planar  $[\text{BMIM}]^+$  ion. Therefore,  $\text{Br}^-$  in  $[\text{TBA}]\text{Br}$  is a stronger ligand for the metal than the  $\text{Br}^-$  in  $[\text{BMIM}]\text{Br}$  (182).

Another strategy was successfully implemented by synthetic deprotonation of the acidic C2 group of the imidazolium cation by basic ligands of metal complexes, forming carbenes (Scheme 12). When  $\text{Pd}(\text{OAc})_2$  was heated in the presence of  $[\text{BMIM}]\text{Br}$ , a mixture of palladium imidazolylidene complexes formed. The palladium carbene complexes have been shown to be active and stable catalysts for the



SCHEME 12.



SCHEME 13.

Heck and C–C coupling reactions (183). The highest activity and stability of palladium was observed in the ionic liquid [BMIM]Br.

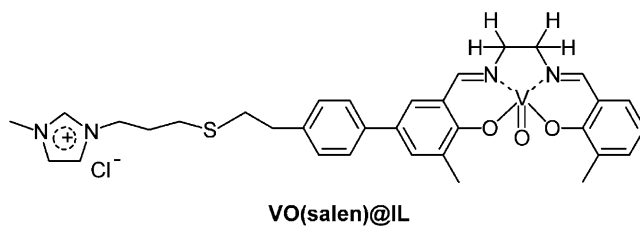
A similar palladium catalyst with benzothiazole ligands has been shown to be stable at high temperatures in the presence of oxygen and moisture (Scheme 13). This catalyst is active for C–C coupling reactions, both in conventional solvents and in ionic liquids such as [TBA]Br (182,184). For the Heck arylation of 3-hydroxy-2-methylenealkanoates using the ionic liquid [TBA]Br as a solvent, the stability of the catalyst in the ionic liquid makes its recycling feasible. For example, in only 3 g of [TBA]Br, after three cycles, 8 g of bromobenzene was processed with a total number of turnovers of about 1700, thus making the whole process economically viable (185). Isolated in [TBA]Br (m.p. 110°C), the catalyst gave a good yield to methoxycarbonylation from organic halides (84). The catalyst in the same ionic liquid was also reported to be active for the arylation allylic alcohols to give  $\beta$ -arylated carbonyl compounds (186).

#### A.7. Ionic Tagging of Active Catalysts

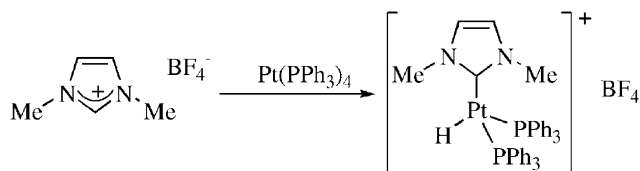
According to a different approach to tailoring a catalyst for the desired ionic character, the catalyst was modified by the attachment of an imidazolium ion. This approach was demonstrated for a vanadyl salen complex, VO(salen)@IL (Scheme 14) (187).

The modified catalyst is insoluble in conventional organic solvents but totally miscible with imidazolium-containing ionic liquids. The catalyst showed high activity for the cyanosilylation of aldehydes and, as expected, remained isolated in the ionic liquid phase after use (for more details, see Section V.A.12).

Another example is the ionic tagging of a ruthenium carbene catalyst for ring-closing alkene metathesis. A  $[-(\text{CH}_2)_4\text{-MIM}]^+\text{PF}_6^-$  moiety was built into the structure of the catalyst, which enabled the long-term retention of the catalyst in the [BMIM]PF<sub>6</sub> ionic liquid for multiple recycles (188).



SCHEME 14.



SCHEME 15.

The carbene complexes can also be formed by direct oxidative addition of zerovalent metal to an ionic liquid. The oxidative addition of a C–H bond has been demonstrated by heating [MMIM]BF<sub>4</sub> with Pt(PPh<sub>3</sub>)<sub>4</sub> in THF, resulting in the formation of a stable cationic platinum carbene complex (Scheme 15) (189). An effective method to protect this carbene–metal–alkyl complex from reductive elimination is to perform the reaction with an imidazolium salt as a solvent.

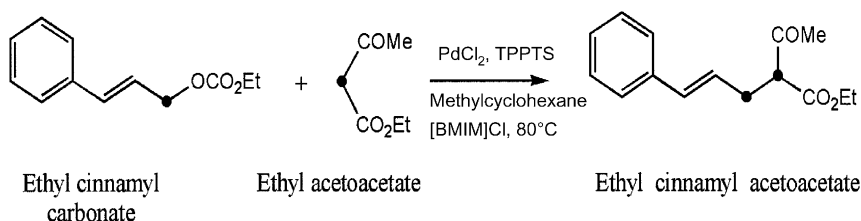
Although most anions in ionic liquids are known to be generally weakly coordinating, including the Al<sub>2</sub>Cl<sub>7</sub><sup>−</sup> anion, a special case of ligand replacement involving chloroaluminate anions was reported recently for the oligomerization of ethylene catalyzed by nickel(II)–diiminophosphorane complex catalysts with an alkylaluminum co-catalyst (190). A three-fold enhancement of catalytic activity was observed, resulting from the replacement of the diiminophosphorane ligands by organoaluminate anions, AlCl<sub>4−x</sub>Et<sub>x</sub>. The authors proposed that these chloroaluminate counteranions displace tightly bound chelates such as diiminophosphoranes from the active metal center.

#### A.8. Hydrophobicity-Aided Catalysis

The effect of hydrophobicity of some ionic liquids was explored (119) in a recent example of a condensation synthesis involving a quaternary ammonium amide. The water produced was continuously removed from the reaction mixture, producing a much higher yield than had previously been possible for this reaction in other media.

#### A.9. Enhanced Reaction Rate Due to Increased Substrate Solubility

There are many reports of benefits resulting from high solubilities of substrates. One example is the biphasic Trost Tsuji coupling (Scheme 16) involving [BMIM]Cl



SCHEME 16.

and methylcyclohexane (191).  $\text{PdCl}_2$  was readily dissolved in the ionic liquid phase, providing a precursor for zerovalent palladium for the subsequent formation of the  $\text{Pd/TPPTS}$  complex catalyst (TPPTS = triphenylphosphinetrisulphonate, sodium salt). A 10-fold increase in catalytic activity was observed relative to that of a butyronitrile/water system because of the higher solubility of the substrates in the ionic liquid. Enhanced selectivity was also in part the result of the suppression of the formation of cinnamyl alcohol and phosphonium salts.

A similar example is the monophasic reaction of 3-acetoxy-1,3-diphenylpropene with dimethyl malonate in  $[\text{BMIM}]\text{BF}_4$  (192). The product was obtained in 91% yield after 5 h at room temperature with a  $\text{Pd}(\text{OAc})_2/\text{PPh}_3$  catalyst and  $\text{K}_2\text{CO}_3$  as the base.

A unique opportunity was created for the carbonylation of alkylamines or aromatic amines with  $\text{CO}_2$  in  $\text{CsOH}$ -treated  $[\text{BMIM}]\text{Cl}$ , as both reactants have sufficient solubility in the ionic liquid. The products are symmetric urea derivatives. Yields >90% were obtained from the carbonylation of alkylamines, but lower yields were obtained with aromatic amines. The products precipitated when water was added (193).

#### A.10. Solubility-Aided Product Selectivity

The reduced product solubility in ionic liquids provides a convenient control of the reaction equilibrium favoring high product selectivity by limiting consumption of the product in consecutive reactions. The properties of ionic liquids can be specifically tailored to achieve this goal.

Control of the molecular weight of products of polycondensation reactions by the use of ionic liquids as solvents has been reported (194), exemplified by the polycondensation of diethyloctane-1,8-dicarboxylate and 1,4-butanediol with the celite-supported lipase *Pseudomonas cepacia* (PS-C) in  $[\text{BMIM}]\text{PF}_6$ . In a search for an alternative solvent for the enzymatic polycondensation (which has been investigated extensively in conventional organic solvents (195)),  $[\text{BMIM}]\text{PF}_6$  was found to be an excellent medium for the reaction. The polymer product (after precipitation with methanol) had an average molecular weight of 2230. Even after a prolonged incubation time, the average molecular weight of the polymer obtained at room temperature was limited to about 2270, but reaction at  $60^\circ\text{C}$  gave a molecular weight of about 5400. In control experiments carried out under identical conditions in the ionic liquid, no reaction was observed in the absence of the enzyme.

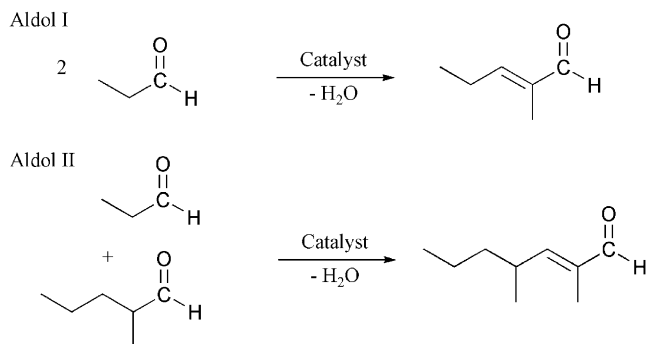


An interesting feature of this enzymatic polymerization in [BMIM]PF<sub>6</sub> is that the polymeric material exhibited remarkably narrow polydispersity values,  $M_w/M_n = 1.04\text{--}1.03$ , a value that was maintained in the seven-day test. The authors related this value to the insolubility of the polymer formed in the ionic liquid after it exceeds a certain molecular weight limit. This observation opens the possibility of tailoring ionic liquids with varying solvating abilities for structural manipulation of desired polymeric material.

Similar indications of narrow polydispersities were reported for the polymerization of ethylene, propylene, butylenes, pentene, hexene, and octene with TiCl<sub>4</sub> in [BMIM]AlCl<sub>4</sub><sup>−</sup> having a small excess of AlCl<sub>3</sub> (196). The oligomers were formed in up to 98% total yield after 4 h at 60°C. The products were easily decanted from the reaction mixture. Interestingly, oligomers with similar molar mass were obtained independent of the monomer used. Furthermore, the oligomerizations were unexpectedly selective and yielded narrow, monomodal polydispersity ( $D = 1.4\text{--}2.5$ ). Depending on the reaction temperature, values of  $M_w = 1290\text{--}1620$  g/mol and  $M_n = 530\text{--}970$  g/mol were determined for polyethylene, and values of  $M_w = 650\text{--}1340$  g/mol and  $M_n = 440\text{--}890$  g/mol were determined for polymers of higher 1-alkenes. In contrast, propylene polymerization in toluene under similar conditions yielded a broad trimodal polydispersity ( $D = 95$ ), and a higher value of  $M_w = 97\,900$  g/mol ( $M_n = 1030$  g/mol). The polymer obtained from the ionic liquid had a higher degree of branching than that from toluene. A possible rationalization of the results is that growing non-polar hydrocarbon chain started to float on the reaction medium whenever a certain chain length was reached, so that no further coordination to the active catalyst in the ionic liquid could occur.

When self-condensation of one of the reactants competes with the desired intermolecular reaction, such as,  $2A \rightarrow C$  and  $A + B \rightarrow E$ , where E is the desired product, it is obvious that the rate of the second reaction is improved by increasing the availability (or solubility) of B in a solvent. The principle has been demonstrated with a cross aldol condensation reaction, as shown in Scheme 17 (109).

Aqueous base (e.g., NaOH or basic ion-exchange resin) has been used for Aldol reactions. In this case, the performance of the ionic liquids containing 1 mol% NaOH was compared with that of water with the same NaOH content. In the Aldol



SCHEME 17.

II reaction under similar conditions at temperatures between 80 and 100°C and with a four-fold excess of 2-methylpentanal (to compensate for the low solubility), the selectivity for the Aldol II product (80%) was 20% higher in [BMIM]BF<sub>4</sub>/NaOH than in the water/NaOH system, both at 100% propanal conversion. The increased selectivity was attributed to the higher solubility of the reactant 2-methylpentanal in the ionic liquid phase than in the water phase. The higher solubility of 2-methylpentanal effectively suppressed the self-aldol condensation in the ionic liquid.

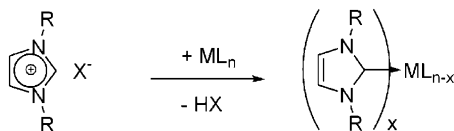
#### A.11. *Effect of Co-Solvents*

Catalysis in ionic liquids also offers flexibility in the control of the reaction kinetics and selectivity that is otherwise difficult to achieve in heterogeneous systems. Co-solvents markedly affect product selectivity. An example is the dimerization of ethylene to give butenes in a two-phase system involving Ni(II) complexes as catalysts that are soluble in [BMIM]Cl/AlCl<sub>3</sub> (in the presence of AlEtCl<sub>2</sub>). With [Ni(MeCN)<sub>6</sub>][BF<sub>4</sub>]<sub>2</sub> as the catalyst, the use of toluene as a co-solvent was essential for the ethylene dimerization activity and selectivity. The main product was but-1-ene. When heptane was used as the organic solvent (or none was used), a mixture of higher ethylene oligomers formed (197). Aromatics generally have higher solubilities in ionic liquids than alkanes. In all cases, the products are easily removed by decantation. The nickel complex remains almost quantitatively in the ionic liquid phase, allowing for multiple uses of the catalyst without changes in selectivity or turnover frequency (TOF).

#### A.12. *Structural Effects of Cations*

Although ionic liquids have been considered weakly coordinating for most organometallic catalysts that are isolated in the liquids, it has been noted that negatively charged metal complexes can be rendered inactive as a result of the exchange of counter ions of the complexes with the cations of the ionic liquids. For example, K<sub>3</sub>Co(CN)<sub>5</sub> is a catalyst that selectively hydrogenates conjugated dienes. Hydrogenation of butadiene with this catalyst in [BMIM]BF<sub>4</sub> at 25°C gave a 100% yield of but-1-ene (198). However, the catalyst turned completely inactive after the reaction; [BMIM]<sub>3</sub>Co(CN)<sub>5</sub> had formed as an inactive complex. This complex forms at room temperature in the absence of hydrogen and butadiene. The interaction of [BMIM]<sup>+</sup> with Co(CN)<sub>5</sub><sup>3-</sup> was strong and prevented coordination of the dienes to the metal center.

In another example, RuCl<sub>2</sub>(PPh<sub>3</sub>)<sub>3</sub> in [BMIM]Cl was shown to be a much less active catalyst than this complex in the ionic liquids [R<sub>4</sub>N]Cl or [R<sub>4</sub>N]OH for the aerobic oxidation of alcohol (199). The weaker association of the bulky tetraalkylammonium cation than the planar [BMIM] cation with the anion appears to be the principal reason for the difference.



SCHEME 18.

#### A.13. Reactivity of Proton at C2 Position in Imidazolium Ion

The strong acidity of the proton at the C2 position of a  $[\text{AMIM}]^+$  ion has been well recognized (183). This cation can react with palladium complexes to form inactive 1,3-dialkylimidazol-2-ylidene palladium complexes (200), as confirmed in a study of the conventional  $\text{Pd}(\text{OAc})_2/\text{PPh}_3/\text{base}$  catalyst in ionic liquids for the telomerization of butadiene with methanol at  $85^\circ\text{C}$  (201).

Although such catalyst systems are known to have rather high productivities for the reaction, the addition of several equivalents of 1,3-dialkylimidazolium salts per equivalent of palladium leads to complete deactivation of the catalyst, which was attributed to the formation of highly stable palladium imidazolylidene complexes (Scheme 18).

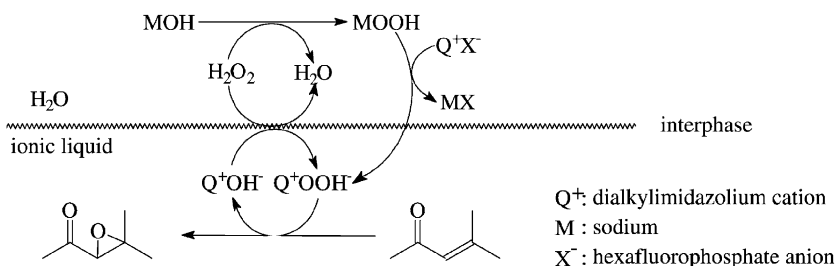
The detrimental effect of the reactive proton-donor group in the  $[\text{AMIM}]^+$  ion was further confirmed by the use of an ionic liquid with the proton at the C2 position replaced by a methyl group. The palladium catalyst in  $[\text{BDMIM}]\text{PF}_6$  showed high activity and selectivity in a biphasic system that allowed reaction with multiple recycles and little loss of activity.

#### A.14. Phase Transfer Effect

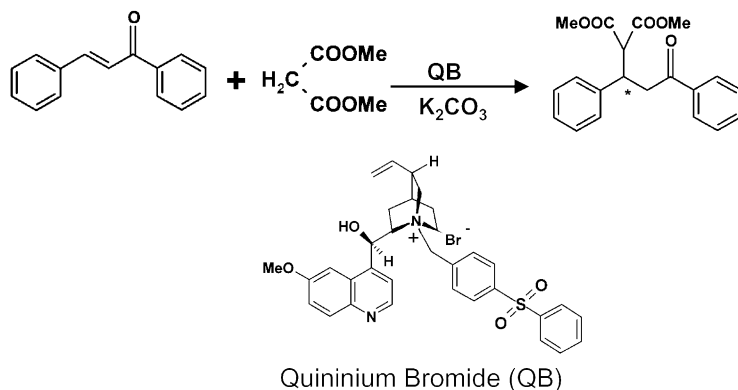
A biphasic system consisting of the ionic liquid  $[\text{BMIM}]\text{PF}_6$  and water was used for the epoxidation reactions of  $\alpha,\beta$ -unsaturated carbonyl compounds with hydrogen peroxide as an oxidant at room temperature (202). This biphasic catalytic system compared favorably with the traditional phase transfer catalysts. For example, under similar conditions ( $15^\circ\text{C}$  and a substrate/ $\text{NaOH}$  ratio of five), the  $[\text{BMIM}]\text{PF}_6/\text{H}_2\text{O}$  biphasic system showed a mesityl oxide conversion of 100% with 98% selectivity to  $\alpha,\beta$ -epoxyketone, whereas the phase-transfer catalyst with tetrabutylammonium bromide in a  $\text{CH}_2\text{Cl}_2/\text{H}_2\text{O}$  biphasic system gave a conversion of only 5% with 85% selectivity.

The new ionic liquid/ $\text{H}_2\text{O}$  system has also been shown to be highly effective for the epoxidation of various  $\alpha,\beta$ -unsaturated carbonyl compounds.  $[\text{BMIM}]\text{PF}_6$  retained almost all of its original activity for the epoxidation of mesityl oxide, even after eight repeated uses.

A mass-transfer model was proposed to account for the function of the  $[\text{BMIM}]\text{PF}_6/\text{water}$  biphasic system in the reaction (Scheme 19). According to this model, a small quantity of  $[\text{BMIM}]\text{PF}_6$  dissolved in water exchanged its anion with  $\text{H}_2\text{O}_2$  to form  $\text{Q}^+\text{OOH}^-$ , which was transferred into the  $[\text{BMIM}]\text{PF}_6$  phase to initiate the epoxidation reaction. In this reaction system, the ring-opening



SCHEME 19.



SCHEME 20.

hydrolysis of  $\alpha,\beta$ -epoxyketones was suppressed, resulting in the high selectivity to  $\alpha,\beta$ -epoxyketones.

In this system, although the pH was optimized to minimize the decomposition of  $\text{H}_2\text{O}_2$ , a four-fold excess  $\text{H}_2\text{O}_2$  had to be used to allow a high conversion of the reactants.

A chiral phase transfer catalyst was dissolved in ionic liquid media for the enantioselective Michael reaction of dimethyl malonate with 1,3-diphenylprop-2-en-1-one with  $\text{K}_2\text{CO}_3$  (203). The phase-transfer catalyst was a chiral quininium bromide (Scheme 20). The reaction proceeded rapidly with good yield and good enantioselectivity at room temperature in all three ionic liquids investigated, [BMIM] $\text{PF}_6$ , [BMIM] $\text{BF}_4$  and [BPy] $\text{BF}_4$ . In the asymmetric Michael addition, the enantioselectivity or the reaction in [BPy] $\text{BF}_4$  was the same as in conventional organic solvents.

## B. CATALYTIC REACTIONS

The applications of ionic liquids in catalysis have expanded widely to include reactions with an extremely broad diversity. Ionic liquids have been evaluated for

A Grubbs-type ruthenium complex and a Hoveyda ruthenium complex were compared under similar conditions for recycled activity. Both the reference catalysts showed a large drop in metathesis activity in the subsequent tests. For example, a Grubbs-type ruthenium alkylidene catalyst showed a drop of nearly 50% conversion in the second run.

### B.2. Dimerization of Dienes

An active catalyst can sometimes be made simply *in situ* for the target reaction, avoiding a pre-synthesis step.  $[\text{Fe}(\text{NO})_2\text{Cl}]_2$  in  $[\text{BMIM}]\text{BF}_4$  or  $[\text{BMIM}]\text{PF}_6$  was *in situ* treated with a reducing agent,  $\text{Zn}(0)$ ,  $(\text{Et})_2\text{AlCl}$ , or *n*-butyllithium for the 1,3-butadiene cyclodimerization reaction (Scheme 22), (206).

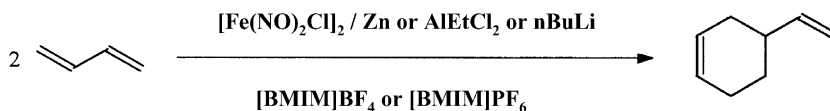
The resulting complex remained dissolved in the biphasic catalytic system. The 4-vinyl-1-cyclohexene product, obtained with 100% selectivity in  $[\text{BMIM}]\text{PF}_6$ , was continuously separated from the reaction mixture by decantation, allowing the reuse of the remaining catalyst solution. The 1,3-butadiene conversion in the biphasic system was higher than that observed in homogeneous systems. Because the unconjugated product has a lower solubility in the ionic liquids than the conjugated butadiene feed, continuous separation of product contributes to the increased reaction rate in the ionic liquid.

The presence of  $\text{PPh}_3$  reduced the TOF from about 1400 to about  $210 \text{ h}^{-1}$ , which is of the same order of magnitude as that obtained under homogeneous conditions (207). The weak nucleophilic nature of the ionic liquid was again found to be essential, as it does not compete with the butadiene reactant for the coordination site at the metal complex.

### B.3. Olefin Dimerization

Some nickel(II) complexes catalyze the dimerization of lower alkenes. Several investigators have explored the role of ionic liquids in promoting the performance of Ni(II) complex catalysts (208). For example, in the oligomerization of butenes in  $[\text{BMIM}]\text{Cl}/\text{AlCl}_3$  (209), more than the stoichiometric ratio of  $\text{AlCl}_3$  to  $[\text{BMIM}]\text{Cl}$  was used, with an additional about 10% of ethylaluminumdichloride (EADC). The EADC induced the formation of a cationic nickel hydride complex in the ionic liquid. The complexes  $[\text{Ni}(\text{MeCN})_6](\text{BF}_4)_2$  and  $\text{NiCl}_2(\text{PBu}_3)_2$  were both active catalysts for the reaction. Only a small amount of ionic liquids (6%) was used with respect to liquid butene. The catalyst was modified in the ionic liquid by adding a promotional ligand directly to the system without involving a pre-synthesis step; the addition of  $\text{PCy}_3\text{CS}_2$  led to the formation of a mixed  $\text{Ni-CS}_2\text{-PCy}_3$  complex that gave a much-improved TOF and higher dimer selectivity than when a  $\text{PR}_3$  ligand was used.

The complex  $[(\text{methallyl})\text{NiPh}_2\text{PCH}_2\text{PPh}_2(\text{O})][\text{SbF}_6]$  was found to be stable and active for ethylene oligomerization in  $\text{PF}_6^-$ -containing ionic liquids. The high electrophilicity of an unaltered Ni center in the liquid was suggested to be responsible for the activity of the catalyst (210).



SCHEME 22.

#### B.4. Suzuki Coupling

[BMIM]BF<sub>4</sub> was applied to a Suzuki reaction. The active catalyst was a tricoordinated [Pd(PPh<sub>3</sub>)<sub>2</sub>(Ar)][X] complex that formed after oxidative addition of aryl halide to [Pd(0)(PPh<sub>3</sub>)<sub>4</sub>] (211). The hydrophobic ionic liquid does not compete with the unsaturated organic substrate for the electrophilic active metal center.

Robust air-stable systems for Suzuki coupling reactions of a bromobenzene with tolylboronic acid at 110°C in the presence of Na<sub>2</sub>CO<sub>3</sub> were obtained by adding a substituted imidazole and (CH<sub>3</sub>CN)<sub>2</sub>PdCl<sub>2</sub> as a palladium(II) source to ionic liquids (212). Initiation by heating the palladium source and the imidazole in ionic liquids was required to generate a completely colorless catalytic solution prior to the reaction. Without the initiation, the yields were low. The catalytic activity and stability in the ionic liquids were strongly dependent on the nature of the imidazole ligands and on the natures of the ionic liquid. Extensive catalyst decomposition occurred in the catalytic system including [BMPy][N(SO<sub>2</sub>CF<sub>3</sub>)<sub>2</sub>], [BMIM]BF<sub>4</sub>, and molecular solvents. The reactivities of various stable solutions depend both on the cation and the anion of the ionic liquid, with the most active ones being [BMIM][PF<sub>6</sub>] and [BMIM][OSO<sub>2</sub>CF<sub>3</sub>]. The use of 1-phenylimidazole and 1-methylbenzimidazole further improved the reactivity, yielding the most active catalysts in [BMIM]BF<sub>4</sub>.

#### B.5. Hydrogenation

The rate of hydrogenation of aromatics and unsaturated hydrocarbons with a catalyst in ionic liquids is often controlled by hydrogen solubility in the liquids. Satisfactory activities can be achieved under high pressures of H<sub>2</sub>. In a rhodium-catalyzed hydrogenation of 1-pentene, the ionic liquid [BMIM]SbF<sub>6</sub> gave hydrogenation rates nearly five times higher than those of comparable homogeneous reactions in acetone. The TOF in [BMIM]SbF<sub>6</sub> is considerably higher than that in [BMIM]PF<sub>6</sub> and [BMIM]BF<sub>4</sub> (112).

Enantioselective hydrogenation in ionic liquids is worthy of attention because of the prospects for efficient reuse of metal complexes with expensive chiral ligands. The opportunities and challenges involved in the application of ionic liquids for chiral synthesis have been assessed recently (213).

With a rhodium complex catalyst containing a chiral ligand dispersed in [BMIM]SbF<sub>6</sub>, the enantioselective hydrogenation of  $\alpha$ -acetamidocinnamic acid to (*S*)-phenylalanine was achieved with 64% enantiomeric excess (112). [RuCl<sub>2</sub>(*S*)-BINAP]<sub>2</sub>•NEt<sub>3</sub> in [BMIM]BF<sub>4</sub> for (*S*)-naproxen synthesis gave 80% ee from 2-(6-methoxy-2-naphthyl) acrylic acid and isopropyl alcohol (214).

Remarkable activity and enantioselectivity in asymmetric hydrogenation of aromatic ketones were reported when ionic liquids were used as solvents for a rhodacarborane catalyst precursor having an alkene ligand, [closo-1,3{ $\mu$ -( $\eta^2$ -3-CH<sub>2</sub>=CHCH<sub>2</sub>CH<sub>2</sub>)}-3-H-3-PPh<sub>3</sub>-3,1,2-RhC<sub>2</sub>B<sub>9</sub>H<sub>10</sub>] (215). In ionic liquids ([OMIM]BF<sub>4</sub>, [BMIM]PF<sub>6</sub>, and a new ionic liquid consisting of 1-carbadodecaborate ions and *N*-*n*-butylpyridinium (BPy) cation, [BPy][CB<sub>11</sub>H<sub>12</sub>]) in the presence of the optically active  $\text{R}^*$ -BINAP ligand, the rhodium complex catalyst (0.1 mol%) gave 97–99.5% ee for the asymmetric hydrogenation of acetophenone and ethyl

benzoformate. In contrast, the TOF observed with the same catalyst in THF was less than half of that obtained in the ionic liquids, and the ee was much lower. The catalyst in ionic liquids allowed multiple reuse without degradation or loss.

Hydrogen solubility in the ionic liquids limits catalyst performance, as was demonstrated in the asymmetric hydrogenation of (*Z*)- $\alpha$ -acetamidocinnamic acid by Rh(I)-complex catalysts in [BMIM]PF<sub>6</sub> and [BMIM]BF<sub>4</sub> (82). The conversion increased with the solubility of molecular hydrogen. At a low H<sub>2</sub> pressures, the conversions and enantioselectivity were both low. At 50 atm, hydrogen is more soluble in *iso*-propanol (IPA) than in [BMIM]BF<sub>4</sub>, and the solubility in [BMIM]BF<sub>4</sub> is less than one-third of that in [BMIM]PF<sub>6</sub>. The solubility limitations clearly affected the conversion of the substrate, which was 99, 73, and 26%, respectively, in IPA, [BMIM]PF<sub>6</sub>, and [BMIM]BF<sub>4</sub> after the same time. The enantioselectivity followed a similar trend. Recycle of the catalyst–ionic liquid systems was possible, but catalyst leaching became obvious over four cycles.

Biphasic systems containing an ionic liquid and supercritical CO<sub>2</sub> have been used effectively for catalytic hydrogenation of alkenes. The ionic liquid phase containing the catalyst could be reused (216).

A number of positively charged organometallic clusters that were originally developed for the biphasic aqueous-organic arene hydrogenation are also effective for this reaction in ionic liquids, but with improved results because of the higher solubility of the arenes and hydrogen in the liquids (e.g., [BMIM]BF<sub>4</sub>) than in the aqueous system. However, the chloride impurity in [BMIM]BF<sub>4</sub> was found to have a detrimental effect on the activity of the catalyst formed from Ru( $\mu^6$ -C10H14)(pta)Cl<sub>2</sub> (pta = 1,3,5-triaza-7-phosphadamantane), (88,170).

Many low-oxidation-state transition metal cluster carbonyls, such as [Hf(CO)<sub>11</sub>]<sup>−</sup>, [HWOs<sub>3</sub>(CO)<sub>14</sub>]<sup>−</sup>, [H<sub>3</sub>Os<sub>4</sub>(CO)<sub>12</sub>]<sup>−</sup>, and [Ru<sub>6</sub>C(CO)<sub>16</sub>]<sup>2−</sup>, are highly soluble in ionic liquids. Some of these clusters in ionic liquids are active for the hydrogenation of alkenes (217). In [BMIM]BF<sub>4</sub>, the rates of hydrogenation catalyzed by some cluster catalysts (notably [HWOs<sub>3</sub>(CO)<sub>14</sub>]<sup>−</sup> and [H<sub>3</sub>Os<sub>4</sub>(CO)<sub>12</sub>]<sup>−</sup>) were more than three times those observed with the clusters in organic solvents; the improved activity was attributed to the increased stability of the cluster species in the ionic liquids. The ionic liquids also give rise to higher regioselectivity in the hydrogenation of cyclic dienes to monoenes relative to what has been observed for the reactions in organic solvents. For example, benzene was not hydrogenated by [Ru<sub>6</sub>C(CO)<sub>16</sub>]<sup>2−</sup> in the ionic liquid at 100°C and 50.7 atm of H<sub>2</sub>. However, 1,4-cyclohexadiene and 1,5-cyclooctadiene were hydrogenated to the corresponding monoenes with about 90% selectivity.

The formation of nanoparticles of noble metal (e.g., Rh, Ir, and Pt) in ionic liquids has been demonstrated by the reduction in hydrogen of soluble precursors at mild temperatures (12,74,218). Particles with a narrow distribution of diameters formed (about 2.0–2.5 nm). The nanoparticles were dispersed in [BMIM]PF<sub>6</sub>. They were recovered in solventless state and used for liquid–liquid biphasic, homogeneous, or heterogeneous hydrogenation of alkenes and arenes with high activity under mild conditions (75°C and 4 atm). The recovered noble metal nanoparticles could be redispersed several times in the ionic liquid and were claimed to have undergone no significant loss in catalytic activity. The flexibility in making and



recovering the noble metal nanoparticles from the ionic liquid appears to be a potential advantage. It was shown that for solventless hydrogenation of cyclohexene and of benzene that the metal nanoparticle catalysts exhibited significantly higher activity than  $\text{PtO}_2$  at  $75^\circ\text{C}$ .

### B.6. Oxidation

The use of gaseous oxygen as an oxidant in ionic liquids also appears to be limited by its low solubility, for example, in  $[\text{BMIM}]\text{PF}_6$  for the oxidation of aromatic aldehydes to give carboxylic acids (219). Hydrogen peroxide and organoperoxide, with their higher solubilities, have been used efficiently for enzymatic oxidation (220).

To overcome some solubility limitations, some organic solvents can be mixed with ionic liquids to achieve a more nearly homogeneous systems. Product separation could then be realized by extraction or by distillation of organic solvent from the mixed solvent containing the ionic liquids. This strategy was demonstrated in the epoxidation of alkenes with  $\text{PhI}(\text{OAc})_2$  as an oxidant with a manganese(III) porphyrin catalyst, [*meso*-tetrakis(pentafluorophenyl) porphinato]manganese(III) chloride, for which a  $[\text{BMIM}]\text{PF}_6/\text{CH}_2\text{Cl}_2$  mixture was used as the solvent at room temperature (221,222). The ionic liquid  $[\text{BMIM}]\text{PF}_6$  was selected for the model system because it is stable in the presence of both oxygen and water. To dissolve the reactants fully in the ionic liquid, a small amount of  $\text{CH}_2\text{Cl}_2$  was added to the ionic liquid. In such a system,  $\text{CH}_2\text{Cl}_2$  improves the solubility of the substrates.

For several alkene substrates, the yield of the epoxide product was lower when the reactions were carried out in pure  $\text{CH}_2\text{Cl}_2$  than in a mixed solvent system consisting of  $[\text{BMIM}]\text{PF}_6/\text{CH}_2\text{Cl}_2$  (3:1, v/v). The catalyst was also highly active for the epoxidation of aromatic alkenes. Although  $\text{PhIO}$  is an oxidant commonly used in organic solvents, it was found that the use of  $\text{PhI}(\text{OAc})_2$  under the same conditions in the mixed solvent led to higher yields of the epoxides.

The unconsumed reactants and products were both easily removed from the reaction mixture by extraction with *n*-hexane, which is not miscible with  $[\text{BMIM}]\text{PF}_6$ . The brown-red ionic liquid phase containing the catalyst was reused five times with  $\text{PhI}(\text{OAc})_2$  as the oxidant. The recovered catalyst gave catalytic activity comparable to that of the original. In epoxidation of styrene and of cyclohexene, both catalytic activity and selectivity fell slightly after five reuses. In the conversion of hept-1-ene, the reused catalyst showed the same activity and selectivity as the fresh catalyst, and the catalyst was shown to be unchanged after the reaction.

In the aerobic oxidation of the non-activated aliphatic primary and secondary alcohols to the corresponding aldehydes and ketones, co-catalysts or other additives are normally required (223–226). The catalytic aerobic oxidation of aromatic aldehydes to the corresponding carboxylic acids with  $\text{Ni}(\text{acac})_2$  in ionic liquids was the first example of an aerobic oxidation in ionic liquids (227).

The effect of cations and anions of several ionic liquids was investigated for the performance of several catalyst precursors, including  $\text{RuCl}_3$  and  $\text{RuCl}_2(\text{PPh}_3)_3$ , for aerobic oxidation of alcohols (199). The catalysts in the neutral ionic liquids

[BMIM]BF<sub>4</sub> and [BMIM]PF<sub>6</sub>, and in KOH-treated [BMIM]PF<sub>6</sub>, were essentially inactive. Among the ionic liquids investigated, only those containing tetraalkylammonium ions showed a large positive effect on the catalyst activity. The reaction was fast and selective at 80°C with 1 mol% catalyst. As expected, the reactivity of aliphatic alcohols was lower than that of aromatic alcohols. The reaction proceeded without any over-oxidation of the aldehyde product to the corresponding acid. No co-catalyst was necessary. The product could be easily isolated and the catalyst reused.

In basic tetraalkylammonium chloride ionic liquids, the active catalyst was suggested to form from the dissociation of the chloride ligand of RuCl<sub>2</sub>(PPh<sub>3</sub>)<sub>3</sub> in the base. The effect of the cation became evident as the catalyst in tetraalkylammonium chloride was much more active than that in [BMIM]Cl. It is known that the bulky tetraalkylammonium cation is weaker in its association with the chloride anion than a planar [BMIM] cation. Therefore, it was concluded that the ionic liquids giving the best catalytic activity appeared to be tetraalkylammonium hydroxide, which melts at approximately room temperature.

The low solubility of oxygen in most ionic liquids limits its application in oxidation catalysis in these liquids. However, oxidation by H<sub>2</sub>O<sub>2</sub> or organoperoxide is not subject to this limitation when the ionic liquids are properly chosen. An example of catalytic oxidation is the methyltrioxorhenium (MTO)-catalyzed epoxidation of alkenes with the urea-H<sub>2</sub>O<sub>2</sub> adduct in [EMIM]BF<sub>4</sub> (228). High conversions and yields were obtained.

A study of electro-assisted biomimetic activation of molecular oxygen by a chiral Mn(salen) complex in [BMIM]PF<sub>6</sub> showed that a highly reactive oxomanganese(V) intermediate could transfer its oxygen to an alkene (229).

An electron-deficient manganese(III) porphyrin complex was reported to catalyze the oxidation of alkanes by PhI(OAc)<sub>2</sub> in mixed [BMIM]PF<sub>6</sub>/CH<sub>2</sub>Cl<sub>2</sub> at room temperature (230). Cyclic alkanes were oxidized to secondary alcohols and ketone. A highly active and short-lived intermediate, Mn<sup>V</sup>=O, was observed in the ionic liquid, whereas in CH<sub>2</sub>Cl<sub>2</sub> the same reaction gave only a less-active intermediate, Mn<sup>IV</sup>=O.

Metalloporphyrins have been widely investigated as biomimetic catalysts for various oxidation reactions using hydrogen peroxide in homogeneous organic and aqueous reaction media (231). A means for stabilization and reuse of the expensive catalysts is essential for the practical application of the metalloporphyrins. A charged anionic water-soluble Fe(III) porphyrin catalyst, tetrakis(2A,6A-dichloro-3A-sulfonatophenyl) porphyrinato iron(III), was reported to be formed in the ionic liquid [BMIM]Br for the oxidation of selected alkenes with H<sub>2</sub>O<sub>2</sub> (232). In the biphasic system, the catalyst showed higher activity in the ionic liquid for the epoxidation of alkenes than that in conventional solvents. The feasibility of recycling the expensive metalloporphyrin catalyst from the reaction mixture was confirmed.

### B.7. Dihydroxylation

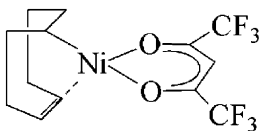
Osmium-catalyzed oxidation is one of the most useful routes to dihydroxylation of alkenes to give the corresponding diols. This oxidation proceeds in the presence

of catalytic amounts of  $\text{OsO}_4$  with a cooxidant (233). To prevent product contamination by the toxic osmium oxide catalyst, a ligand design has been applied for the immobilization of  $\text{OsO}_4$  in the ionic liquid  $[\text{BMIM}]\text{PF}_6$ , so that 0.1% of the catalyst could be stabilized in the ionic liquid for multiple hydroxylations (179). The  $\text{OsO}_4$  catalyst itself can be isolated directly in the  $[\text{BMIM}]\text{BF}_4$ , but a much higher  $\text{OsO}_4$  loading is required (5%) (234). It was reported that the ionic liquid effectively suppressed the volatility and toxicity of  $\text{OsO}_4$  in dihydroxylation of several alkenes. The catalyst together with the ionic liquid  $[\text{EMIM}]\text{BF}_4$  was used five times with little loss of the performance of the catalyst; results showed a consistent yield of dihydroxylated product in the range of 93–96%. The  $\text{OsO}_4$  isolated in the ionic liquid was applied to several substrates, including mono-, di-, and tri-substituted aliphatic alkenes and aromatic alkenes. In all cases, the desired diols were obtained in high yields (179).

### B.8. Olefin Dimerization

Significant interest has developed recently in the dimerization of alkenes in ionic liquid media. IFP's Dimersol<sup>®</sup> process produces isooctenes from *n*-butenes, which are used as a starting material for isononanol production. The Difasol process, based on a continuous biphasic system involving ionic liquids, has been under commercial development recently. A key to the process is the lower solubility of the dimer products than of the monomer feed in the ionic liquid, resulting in minimized formation of trimers and oligomers. Significant activities in research have also led to a broadening in the range of alkenes that can be used and in the control of product selectivity.

An excellent demonstration of the tunability of ionic liquids for catalysis is provided by an investigation of the dimerization of 1-butene (235). A  $\text{Ni}(\text{cod})(\text{hfacac})$  catalyst (Scheme 23) was evaluated for the selective dimerization of 1-butene after it was dissolved in various chloroaluminate ionic liquids. Earlier work on this reaction with the same catalyst in toluene led to the observations of low activity and difficult catalyst separation. In ionic liquids of varying acidity, little catalytic activity was found. However, a remarkable activity was achieved by adding a weak buffer base to an acidic ionic liquid. The reaction took place in a biphasic reaction mode with facile catalyst separation and catalyst recycling. A high selectivity to the dimer product was obtained because of a fast extraction of the  $\text{C}_8$  product from the ionic liquid phase, with the minimization of consecutive reaction to give trimers. Among a number of weak base buffers, a chinoline was chosen. The catalyst performance was compared with that in toluene. The catalytic TOF at 90°C in toluene was



SCHEME 23.

500 h<sup>-1</sup> with a dimer selectivity of 85% and a linearity of 75%; in contrast, the TOF in the buffered ionic liquid at 25°C was 1240 h<sup>-1</sup> with a dimer selectivity of 98% and a linearity of 64%. In a continuous loop reactor, an ionic liquid catalyst after 3 h of reaction still showed a TOF of 2700 h<sup>-1</sup> and a dimer selectivity of 98%. Unsubstituted pyridine gave poorer activity than a sterically hindered pyridine, because the former can coordinate to the active metal center better than the latter. The function of the buffering base was to neutralize excess acid through the reaction  $\text{Al}_2\text{Cl}_7^- + \text{base} \rightarrow \text{AlCl}_3\text{-base} + \text{AlCl}_4^-$ .

Another investigation of 1-butene dimerization involved the use of cationic nickel complexes,  $\text{Ni}(\text{MeCN})_6[\text{BF}_4]_2$ ,  $[\text{Ni}(\text{MeCN})_6][\text{AlCl}_4]_2$ ,  $[\text{Ni}(\text{MeCN})_6][\text{ZnCl}_4]$ , and  $[\text{Ni}(\text{PhCN})_6][\text{BF}_4]_2$  in a slightly acidic mixture  $[\text{BMIM}]\text{Cl}/\text{AlCl}_3$  (the mol fraction of  $\text{AlCl}_3$  was 0.57) with 10%  $\text{EtAlCl}_2$  (236). The activity was dependent on the nature of the catalyst precursor. The  $[\text{Ni}(\text{MeCN})_6][\text{AlCl}_4]_2$  and  $[\text{Ni}(\text{MeCN})_6][\text{ZnCl}_4]$  catalysts were most active. The lower activity of the nickel- $\text{BF}_4$  complex was attributed to the reactive interaction of the  $\text{BF}_4^-$  ligand with alkylaluminum dichloride, resulting in less active species. A TOF of up to 2.2 s<sup>-1</sup> was observed under mild reaction conditions (1.08 atm and 8°C); between 93 and 96% octenes were produced with a branching index of 1.2–1.3. A cationic nickel hydride complex was proposed to be the catalytically active species. The products were easily separated from the reaction mixture by decantation, and the recovered ionic catalyst solution showed little loss in performance.

In an investigation of the dimerization of 1-butene, the addition of  $\text{PCy}_3\text{-CS}_2$  to the  $[\text{Ni}(\text{MeCN})_6][\text{BF}_4]_2$  catalyst in an ionic liquid was found to give a much-improved TOF and higher dimer selectivity than  $\text{PCy}_3$ . A mixed  $\text{Ni-CS}_2\text{-PR}_3$  complex was suggested to have formed. The catalyst was reusable (209).

Olefin dimerization is a highly exothermic reaction. The reaction temperature of the two-phase system needs to be controlled to minimize the formation of higher oligomers. The activity of  $\text{NiCl}_2(\text{PCy}_3)_2$  in  $[\text{BMIM}]\text{Cl}/\text{AlCl}_3$  (the  $\text{AlCl}_3$  mol fraction was 0.55) was so high that the reaction temperature could not be controlled, leading to reduced selectivity to butanes.  $[\text{Ni}(\text{MeCN})_6][\text{BF}_4]_2$  showed improved selectivity, but with compromised activity. Conducting the reaction at a lower temperature (–10°C) afforded exclusively dimeric products, and higher oligomers were formed at 25°C (197).

### B.9. Dimerization of Dienes

Chloroaluminate-free ionic liquids have been used for dimerization of dienes, as these ionic liquids are more stable and easier to handle than the moisture-sensitive ionic liquid chloroaluminate(III). In one example, a mixture of  $[\text{BMIM}]\text{BF}_4/\text{water}$  (1:1 v/v) was used as the medium in the hydrodimerization of 1,3-butadiene catalyzed by  $[\text{BMIM}]_2[\text{PdCl}_4]$  (237). In addition to the dimer, 1,3,6-octatriene and 2,7-octadienol were produced. However, by using  $\text{PdCl}_2/\text{PPh}_3$  as a catalyst in  $[\text{BMIM}][\text{X}]$  ( $\text{X} = \text{BF}_4$ ,  $\text{PF}_6$ ,  $\text{CF}_3\text{SO}_3$ ), the dimer, 1,3,6-octatriene, was obtained exclusively (238).

The cyclodimerization of 1,3-butadiene and isoprene by zinc reduction of an iron nitrosyl complex dispersed in  $[\text{BMIM}]\text{BF}_4$  (and alternatively  $[\text{BMIM}]\text{PF}_6$ ) showed

much a improved butadiene conversion and TOF ( $1404 \text{ h}^{-1}$ ) relative to those obtained under homogeneous conditions (TOF of  $213 \text{ h}^{-1}$ ) (206). In the presence of diethylaluminum chloride, some linear oligomers of 1,3-butadiene were formed. The nature of the ionic liquid affected the reactivity. At  $10^\circ\text{C}$ , higher values of TOF were observed for reaction in [BMIM]BF<sub>4</sub> than for reaction in [BMIM]PF<sub>6</sub>. At  $50^\circ\text{C}$ , the trend was reversed. The presence of PPh<sub>3</sub> led to lower catalytic activities. This observation was attributed to the formation of iron phosphine species that are less active in the cyclodimerization reaction, as in single-phase butadiene cyclodimerization (207).

#### B.10. Oligomerization and Polymerization

The replacement of diiminophosphorane ligand in a nickel(II)–diiminophosphorane catalyst by an alkylchloroaluminate anion was observed in a biphasic system (190), when the catalyst was used for the oligomerization of ethylene in a [BMIM]Cl/AlCl<sub>3</sub> ionic liquid with alkylaluminum as co-catalyst in the presence of cyclohexane as a separate organic solvent phase). After repeated reuse of the ionic liquid-catalyst system, a three-fold enhancement in the catalytic activity was observed, and the selectivity approached a constant value. The authors suggested that organoaluminate anions replaced the diiminophosphorane ligands in the coordination sphere of the active nickel species, leading to a unique active species. The chloroaluminate anions were proposed to be (AlCl<sub>4-x</sub>Et<sub>x</sub>), arising from the equilibrium between AlCl<sub>4</sub><sup>-</sup> and AlEt<sub>2</sub>Cl. The  $\alpha$ -diiminophosphorane ligands were progressively displaced by the organoaluminate species, giving rise to more active but less selective nickel complexes containing organoaluminate anions as ligands.

Reports of alkene oligomerization reactions from several groups suggest that the ionic liquids have a significant influence on the product molecular weight and polydispersity. In one case, (nbd)Rh(acac) was used as a catalyst for the polymerization of phenylacetylene in the ionic liquids [BMIM]BF<sub>4</sub> and [BuPy]BF<sub>4</sub> at  $25^\circ\text{C}$  (239). Quantitative yields of poly(phenylacetylene) (PPA) with high yields of the *cis* product (95–100%) were obtained within 5 min with this catalyst in either [BMIM]BF<sub>4</sub> or [BuPy]BF<sub>4</sub>. A large excess of co-catalyst, triethylamine, was needed to activate the catalyst. The molecular weight of the poly(phenylacetylene) obtained in the reaction with the (nbd)Rh(acac) catalyst depends on the ionic liquid in which the  $r \times n$  takes place. The polymer formed in [BMIM]BF<sub>4</sub> had a molecular weight of about 196 000 Da, whereas that formed in [BuPy]BF<sub>4</sub> had a molecular weight of about 100 000 Da. Similar observations were made with the catalyst [(nbd)RhCl]<sub>2</sub>. In contrast, when the catalyst was (cod)Rh(acac), the product molecular weight was much lower (<60 000 Da) in either ionic liquid. Excellent polydispersities (3.5–10.5) were observed for all the polymers, as was observed for alkene polymerization in ionic liquids (196). The catalysts in the ionic liquids were reused without significant losses in the activity after the PPA separation by toluene extraction.

The production of 1-alkenes from ethylene oligomerization was carried out with high selectivity in ionic liquids in the presence of a cationic nickel complex catalyst ( $\eta^3$ -methallyl)-[bis(diphenylphosphino)methane-monoxide- $\kappa^2$ -P,O]nickel(II) hexafluoroantimonate, [(mall)-Ni(dppmo)]SbF<sub>6</sub> (240). The overall reaction rate of

$[(\text{mall})\text{Ni}(\text{dppmO})]\text{SbF}_6$  in  $[\text{AMIM}]\text{PF}_6$  was found to decrease with increasing alkyl chain length in the cation of the ionic liquid, an observation that was attributed to the higher solubility of internal alkene products in ionic liquids with longer alkyl chains. The increased product solubility in the ionic liquid with respect to that in the organic extraction solvent led to a reduced rate of product extraction from the ionic liquid phase. The increased product concentration in the ionic liquid phase further inhibits the solubility of ethylene. With short alkyl chain, such as in  $[\text{BMIM}][\text{PF}_6]$ , the fast extraction of products and side products from the ionic liquid phase, due to their higher distribution coefficient in the organic extraction phase, accounted for the high rate of the reaction. The oligomers were also found to be much shorter in the biphasic system as a consequence of restricted ethylene availability at the nickel center of the catalyst in the ionic liquid. In summary, the observed results are affected by a combination of fast oligomerization kinetics, relatively low ethylene solubility in the ionic liquid, and limited mass transfer of ethylene into the ionic catalyst solution.

Radical polymerization in ionic liquids was investigated with the goal of learning how to prepare electrically conducting blends of polymers (241). Ionic liquids were investigated for atom transfer radical polymerization (ATRP) (242). Catalysts for the ATRP process are typically copper salts with amine ligands. Interest in ionic liquids for the polymerization chemistry is related to the low solubility of the catalyst in the organic medium and the need to separate catalyst residue from the resulting polymer. In the initial work with  $\text{CuBr}/N$ -propyl-2-pyridylmethanimine as a catalyst for methyl methacrylate ATRP, the reaction was relatively fast. The resulting polymer was essentially free of catalyst residue.

The use of organic amine ligands was shown to be unnecessary when proper ionic liquids were applied for the ATRP (243). In this case,  $\text{FeBr}_2$  in the ionic liquid, 1-butyl-3-methylimidazolium dibutylphosphonate ( $[\text{BMIM}][\text{BDP}]$ ), formed an efficient catalytic system for the ATRP of methyl methacrylate (MMA). The iron-catalyzed reaction was carried out in the absence of an added organic complexing ligand. Similarly, the presence of a ligand was not necessary in copper-catalyzed polymerization of MMA when the ionic liquid was  $[\text{BMIM}][\text{BDP}]$ , although it was necessary when the anion was chloride or carbonate. The catalyst dispersed in the ionic liquids was recovered and reused for subsequent polymerizations.

Related work was done with variously substituted acrylates in an ionic liquid (87). It was found that the solubility of both monomers and polymers depends on the chain length of the alkyl group linked to the ester. Methyl acrylate and its polymer are soluble in  $[\text{BMIM}]\text{PF}_6^-$ . However, butyl acrylate (BA) is only partially soluble, and the corresponding polymer is insoluble in the ionic liquid. The ATRP of BA in the ionic liquid proceeded under biphasic conditions with the catalyst,  $\text{CuBr}/\text{pentamethyldiethylenetriamine}$ , dissolved in the ionic liquid phase. Relatively low-molecular-weight polymer was formed. In this case, as the polymer was insoluble in the ionic liquid, it was spontaneously separated from the ionic liquid phase free of copper contamination. Furthermore, an undesirable side-reaction was significantly reduced in the ionic-liquid-phase ATRP (87).



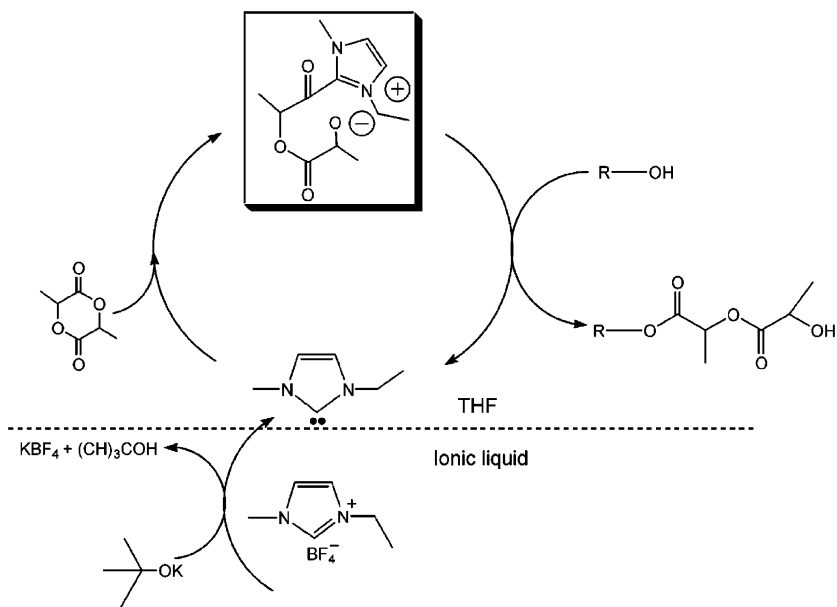
In an extension of the work to chiral chemistry (244), the imidazolium cation of the ionic liquid was modified to carry a chiral substituent. The high cost of the chiral cation could be justified as the chiral ionic liquid, [MBMIM\*]PF<sub>6</sub>, can be reused. In the ATRP of soluble methyl acrylate, a small effect of the chiral ionic liquid on the polymer tacticity was observed. The use of a chiral ionic liquid as a solvent could lead to applications in other areas of catalysis. The synthesis of imidazolium-containing ionic liquids functionalized with chiral natural amino acids has already been reported (245), as have less expensive chiral ionic liquids (246).

The broad applicability of ATRP in the ionic liquid [BMIM]PF<sub>6</sub> was shown by extending it to the polymerization of N-substituted maleimides with styrene. The ATRP was initiated with dendritic polyaryl ether 2-bromoisobutyrate as the initiator at room temperature. The dendritic-linear block copolymers formed in the ionic liquid were characterized by low polydispersity ( $1.05 < M_w/M_n < 1.32$ ) and were used as macroinitiators for chain-extension polymerization, suggesting the living nature of the polymerization (247).

A success was reported in the use of sterically unhindered imidazolium cation-containing ionic liquids as metal-free precatalysts for living polymerization. A lead came from investigations of a wide range of *in-situ*-generated N-heterocyclic carbenes as nucleophilic catalysts for the ring-opening polymerization (ROP) of lactides and lactones. Among the catalysts, the less sterically demanding carbenes were found to be more active for ROP than their sterically encumbered analogs for lactone polymerization. The short-chain alkyl imidazolium ion-containing ionic liquids are good candidate pre-catalysts for the ROP reactions (248). The dialkylimidazolium ions are also known to be carbene precursors after losing the C2 proton.

Therefore, it is not surprising that [BMIM]BF<sub>4</sub> proved to be a good pre-catalyst for the ROP. The reaction was conducted in neat ionic liquid or in a biphasic system including THF. In the biphasic system (Scheme 24), the polymerization proceeded in an immiscible mixture of [BMIM]BF<sub>4</sub> and THF. The activation of [BMIM]BF<sub>4</sub> *in situ* with potassium *tert*-butoxide generated the carbene catalyst, which was then extracted into the organic phase to begin the ROP catalysis. High-molecular-weight polylactides ( $M_n > 24\,000$  g/mol) with relatively narrow polydispersities (PDI = 1.4) were routinely achieved in >95% yield within 10 min. This reaction constituted a phase-transfer catalytic ROP whereby the reactive carbene was generated *in situ* in the ionic liquid, migrated to the organic phase, and induced the ROP. The polymerization was readily terminated by the addition of [R<sub>3</sub>NH]BF<sub>4</sub>, which regenerated the imidazolium precursor. The polymer was readily separated from the ionic liquid, allowing the reuse of the ionic liquid.

The suitability of ionic liquids (e.g., [EMIM]BF<sub>4</sub>, [BMIM]PF<sub>6</sub>, or [OMIM]Tf<sub>2</sub>N) for free-radical polymerization was explored (249). The homopolymerization of 1-vinyl-2-pyrrolidinone in [BMIM]PF<sub>6</sub> or that of 4-vinylpyridine in [OMIM]Tf<sub>2</sub>N resulted in polymers with  $M_w$  of 162 500 and 71 500 g/mol, respectively. However, detectable ionic liquid residues were retained in the isolated polymers, even after repeated precipitations from methanol, which is known to dissolve the ionic liquid. The residue may limit the usefulness of ionic liquids as the media for free-radical polymerizations.



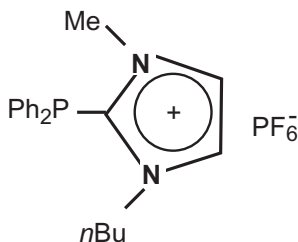
SCHEME 24.

### B.11. Carbonylation/Hydroformylation

The platinum-catalyzed hydroformylation of ethylene in [Et<sub>4</sub>N]SnCl<sub>3</sub> (m.p. 78°C) was first conducted in 1972 (250). Recently, (PPh<sub>3</sub>)<sub>2</sub>PtCl<sub>2</sub> in slightly Lewis-acidic chlorostannate ionic liquids showed remarkably high *n/i* selectivity and good activity at 120°C and 90 atm of CO/H<sub>2</sub> for the hydroformylation of 1-octene, but the activity for methyl-3-pentenoate hydroformylation was much lower (251). The platinum catalyst dissolved in the ionic liquids was found to be more stable than for the same reaction in conventional organic solvents. No leaching of platinum from the ionic liquid was observed. The low solubility of CO in the ionic liquid appeared to limit the reaction rate; therefore, the use of a higher pressure was suggested.

The NMR spectroscopy of PtCl<sub>2</sub> with a diphosphine ligand, [bdpp, 2,4-bis(diphenylphosphino)pentane], was used to follow the formation of platinum complexes in the presence of triphenylphosphine (PPh<sub>3</sub>) and SnCl<sub>2</sub> in the ionic liquid [BMIM]PF<sub>6</sub> (73). The spectra showed that the addition of PPh<sub>3</sub> to PtCl<sub>2</sub>(bdpp) resulted in the formation of [Pt(bdpp)(PPh<sub>3</sub>)Cl]<sup>+</sup> as a minor component in the ionic liquid. This component turned into the major component in the presence of tin(II) chloride with the formation of the trichlorostannate counterion. The tin(II) halide insertion was shown to depend on the size of the platinum ligand chelate. In the absence of PPh<sub>3</sub>, SnCl<sub>2</sub> insertion led to the formation of PtCl(SnCl<sub>3</sub>)(bdpp) and further to Pt(SnCl<sub>3</sub>)<sub>2</sub>(bdpp). However, in the presence of PPh<sub>3</sub>, [Pt(bdpp)(PPh<sub>3</sub>)Cl]<sup>+</sup> became a major component. The oxidative stability of the catalyst/ionic liquid system





SCHEME 25.

was confirmed. No phosphine dioxides or hemioxides were obtained, even after exposure of the samples to air for a week. What was of concern was the partial decomposition of the  $\text{PF}_6^-$  ion by a small amount of water in the presence of  $\text{SnCl}_2$ .

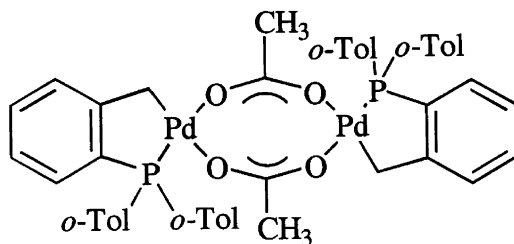
To prevent leaching of catalysts with phosphine ligands from the ionic liquid, a number of imidazolium phosphine ligands were tailor-made to favor retention of the catalyst. One of the ligands (Scheme 25) was used for biphasic hydroformylation of 1-octene at  $100^\circ\text{C}$  and 30 atm. It was made by *in situ* mixing of  $\text{Rh}(\text{CO})_2(\text{acac})$  with two equivalents of the ligand in  $[\text{BMIM}]\text{PF}_6$ . A TOF of 552 was observed (252). The close proximity of the positive charge to the phosphorus atom is inferred to have led to a large enhancement in the catalytic activity.

### B.12. Heck Cross-Coupling

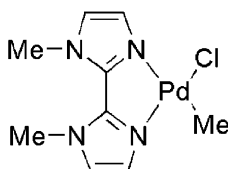
Palladium-catalyzed Heck reactions are important in synthetic organic chemistry (253,254). Under conventional reaction conditions, a palladium black deposit was formed from the deterioration of the homogeneous palladium complex catalyst after the reaction. Recovery and recycle of the palladium catalyst are usually not realistic.

In contrast, ionic liquids have been reported to be suitable solvents for Heck reactions because the products can be readily separated from the ionic liquids containing the homogeneous palladium catalysts. An early test with a palladium complex in ionic liquids showed remarkably improved recyclability of the catalyst (255), but palladium black still formed after several runs with recycled catalyst.

The choice of an ionic liquid was shown to be critical in experiments with  $[\text{NBu}_4]\text{Br}$  (TBAB, m.p.  $110^\circ\text{C}$ ) as a catalyst carrier to isolate a cyclometallated complex homogeneous catalyst, *trans*-di( $\eta$ -acetato)-bis[*o*-(di-*o*-tolylphosphino)benzyl] dipalladium (II) (Scheme 26), which was used for the Heck reaction of styrene with aryl bromides and electron-deficient aryl chlorides. The  $[\text{NBu}_4]\text{Br}$  displayed excellent stability for the reaction. The recycling of 1 mol% of palladium in  $[\text{NBu}_4]\text{Br}$  after the reaction of bromobenzene with styrene was achieved by distillation of the reactants and products from the solvent and catalyst *in vacuo*. Sodium bromide, a stoichiometric salt byproduct, was left in the solvent–catalyst system. High catalytic activity was maintained even after the formation of visible palladium black after a fourth run and after the catalyst phase had turned more viscous after the sixth run. The decomposition of the catalyst and the formation of palladium



SCHEME 26.



SCHEME 27.

black could have been caused by prolonged use, intrinsic catalyst instability, or NaBr byproduct-promoted catalyst destabilization. Palladium nanoparticles allow the regio- and stereospecific Heck reactions with very high values of TON and TOF. Furthermore, TBAB enhances, by solvation, the formation and reactivity of carbanions (256).

When another palladium complex, diiodobis(1,3-dimethylimidazolium-2-ylidene)palladium(II), was used as a catalyst (257), it resulted in a large improvement in catalyst stability in the same ionic liquid. The Heck reaction performed better in the ionic liquid than in organic solvents such as dimethylfuran (DMF). In the reaction of bromobenzene with styrene, the yield of stilbene was increased from 20% in DMF to 99% in  $[\text{NBu}_4][\text{Br}]$ . The ionic liquid showed excellent solubility for all the reacting molecules.

Other Pd(II) complexes with imidazole-like ligands were also specifically synthesized for improved solubility in ionic liquids (258). The catalysts were applied for the Heck Coupling of iodobenzene with *n*-butyl acrylate in  $[\text{BMIM}]\text{PF}_6$  in the presence of  $\text{Et}_3\text{N}$  at  $120^\circ\text{C}$ . One catalyst (Scheme 27) was especially well retained without any loss of activity even at fairly low catalyst loading (0.2 mol%) for more than five repeated uses. In all cases, >99% yield was achieved within 1 h.

In experiments with a supported palladium catalyst, Pd/C, satisfactory yields were obtained without the use of phosphine ligands for the Heck reactions of aryl iodide with acrylonitrile, styrene, and methyl methacrylate in the ionic liquid  $[\text{BMIM}]\text{PF}_6$  (259). The addition of triethylamine improved the yields. The Pd/C remained in the ionic liquid only. The ionic liquid containing Pd/C can be reused as

a catalyst. The accumulation of triethylammonium iodide caused partial loss of catalytic activity, but it could be recovered to the same degree as in a fresh system by washing the ionic liquid layer with water.

Okubo *et al.* (260) reported that Pd(II)/SiO<sub>2</sub> was a more effective catalyst than Pd/C when two equivalents of triethylamine base were added to the same ionic liquid; one equivalent was not sufficient. The reaction was carried out without phosphine ligands. The unreduced Pd(II)/SiO<sub>2</sub> catalyst with two equivalents of base in [BMIM]PF<sub>6</sub> was more active than the supported palladium catalysts in DMF. Furthermore, the stability of [BMIM]PF<sub>6</sub> also improved with the addition of triethylamine.

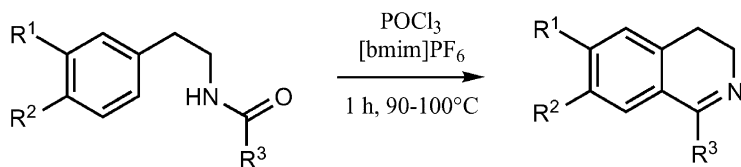
The salt Pd(OAc)<sub>2</sub> was dispersed in a toluene-[Bu<sub>4</sub>N]BF<sub>4</sub> biphasic system as a ligand-free catalyst for the Heck coupling of arylhalides with butyl acrylate in the presence of Et<sub>3</sub>N or K<sub>2</sub>CO<sub>3</sub> at 90°C. The results were comparable to those observed with systems including phosphine ligands. Although the reaction medium can be separated from the products, the formation of palladium black after the first run led to reduced activity in subsequent tests. It appears that the ligand-free catalyst can be effective in the biphasic systems, but the loss of the palladium catalyst is a problem (60).

### B.13. Alkoxyacylation

A butoxycarbonylation reaction was conducted in a liquid–liquid biphasic system under process conditions, but the removal of the product was conducted in a liquid–solid biphasic system at a lower temperature (84). Iodobenzene or 4-bromoacetophenone reacted with CO at a pressure of 1–8 atm in the presence of a palladium–benzothiazole complex catalyst in the ionic liquid [TBA]Br (m.p. = 110°C) in the presence of Et<sub>3</sub>N base. The catalyst/ionic liquid system was recycled by extractive removal of the butyl ester product with diethyl ether. The solid residue, containing the catalyst, [TBA]Br, and Et<sub>3</sub>N.HBr, remained effective in subsequent carbonylation tests. After each cycle, the yields were still close to the initial value. A slight decrease in yield was attributed to a loss of catalyst during handling.

### B.14. Cyclodehydration Reaction

An ionic liquid was used to simplify an otherwise complicated multiple-step cyclodehydration process. POCl<sub>3</sub> was used as a dehydrating reagent in the Bischler–Napieralski reaction for the synthesis of isoquinolines (Scheme 28) (261). In the traditional synthesis, β-phenylethanamides is cyclodehydrated to give 3,4-dihydroisoquinolines with any of a wide range of dehydrating agents, and the



SCHEME 28.

process involves toxic chlorinated and high-boiling-point solvents (e.g., 1,2-dichloroethane, 1,1',2,2'-tetrachloroethane, chlorobenzene, or dioxane) at elevated temperatures (262). With phosphorus oxychloride as a dehydrating reagent, black gummy products are typically obtained, which require extensive purification and several recrystallization steps with decolorizing charcoal to reach an acceptable product purity. In the ionic liquid, [BMIM]PF<sub>6</sub>, the cyclodehydration proceeded well at 90–100°C for 1 h, giving a much higher yield than when the other solvents were used. Steps usually needed for purification were eliminated, and the product, recovered by extraction, was of excellent purity. The reaction also worked well for the cyclization of other amides.

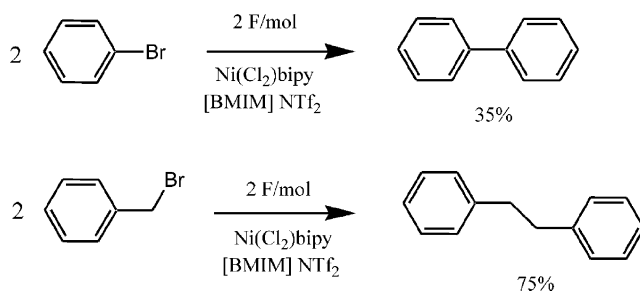
### C. ELECTROCATALYSIS IN IONIC LIQUIDS

Ionic liquids were originally developed for applications as low-temperature electrolytes because of their excellent electrical conductivity. Although they are likely to be suitable media for electrocatalysis of organic reactions, so far only few electrochemical reactions have been carried out in ionic liquids.

A recent report suggested the viability of electrochemical catalysis for organic synthesis (263). Several ionic liquids were applied for the preparative electrocatalytic homocouplings of PhBr and PhCH<sub>2</sub>Br, yielding biphenyl and 1,2-diphenylethane (Scheme 29). All the liquids chosen showed similar ranges of accessible cathodic potentials ( $E \leq -2.1$ – $-2.9$  V) vs. a silver quasi-reference electrode. Various anions were tested (BF<sub>4</sub><sup>-</sup>, PF<sub>6</sub><sup>-</sup>, Tf<sub>2</sub>N<sup>-</sup>, and CH<sub>3</sub>SO<sub>3</sub><sup>-</sup>), and the ionic liquid that was preferred was [BMIM]Tf<sub>2</sub>N, because of its hydrophobicity (water can interfere in the chemistry).

The complexes Ni(BF<sub>4</sub>)<sub>2</sub>(bipy)<sub>3</sub> and NiCl<sub>2</sub>(bipy), the reduction of which occurs at potentials in the range of  $-1.1$  to  $-1.8$  V, were used as catalysts in the ionic liquid medium.

In the presence of PhBr and PhCH<sub>2</sub>Br, both Ni(BF<sub>4</sub>)<sub>2</sub>(bipy)<sub>3</sub> and NiCl<sub>2</sub>(bipy) showed classical catalytic behavior. A peak for the product of the first oxidative addition of the reduced nickel complex appeared at  $E_p = -1.4$  to  $-1.5$  V when the reactant was Ar(Ni)Br. In this case, the electrochemical catalysis was carried out by maintaining the potential of the working electrode at  $E = -1.4$  V vs. silver.



SCHEME 29.

The product of the electrochemical reaction was extracted with cyclohexane. The yields observed in the reactions of PhBr and PhCH<sub>2</sub>Br were 35 and 75%, respectively. In the reaction of PhCH<sub>2</sub>Br, no toluene was formed, indicating that the process was highly selective and that the reduction of the halogenated substrate was avoided. It was further verified that, at the end of the electrolysis, the catalytic system completely regained its reversibility. The nickel(II) catalyst remained totally in the ionic liquid after the extraction of products, and the catalyst system was reusable.

The formation of conducting polymers upon the oxidation of benzene and pyrrole in ionic liquids has also been reported.(264).

## VI. Supported Ionic Liquid Catalysis

Supporting ionic liquids in the pores of solid materials offers the advantage of high surface areas between the reactant phase and that containing the supported liquid catalyst. This approach is particularly useful for reactants with less than desired solubility in the bulk liquid phase. Another incentive for using such catalysts is that they can be used in continuous processes with fixed-bed reactors (265). The use of an ionic liquid in the supported phase in addition to an active catalyst can help to improve product selectivity, with the benefit being similar to what was shown for biphasic systems. However, care has to be taken to avoid leaching the supported liquids, particularly when the reactants are concentrated in a liquid phase.

The ionic liquid [BMIM][Al<sub>2</sub>Cl<sub>7</sub>] on various porous supports (Al<sub>2</sub>O<sub>3</sub>, SiO<sub>2</sub>, TiO<sub>2</sub>, ZrO<sub>2</sub>, or zeolites) was evaluated for the alkylation of aromatics (including benzene, toluene, naphthalene, and phenol) with dodecene (266). Only the SiO<sub>2</sub>-supported ionic liquid was active for the alkylation of benzene. The benzene–dodecene alkylation was carried out at 80°C with SiO<sub>2</sub> (from two sources) containing 6 wt.% ionic liquid. Dodecene conversions as high as almost 100% were achieved with a selectivity of more than 99% for monoalkylated products within the first 30 min of the reaction. In this reaction, benzene itself was used as the solvent (the molar ratio of benzene to dodecene was 10:1).

Leaching of the ionic liquid from the support was negligible. However, deactivation was observed, caused by moisture present during product separation (which can be minimized with proper care) and by oligomerization of dodecene on the catalyst surface. Unfortunately, both factors cause irreversible loss of catalytic activity.

A supported ionic liquid containing a rhodium complex was used for a hydrogenation reaction (267). A catalyst was dissolved in a 6-Å layer of [BMIM]PF<sub>6</sub> (25%), which was confined within the pores of a silica gel. The catalyst was [Rh(nbd)(PPh<sub>3</sub>)<sub>2</sub>]PF<sub>6</sub> (nbd = norboradiene, PPh<sub>3</sub> = triphenylphosphine). Although the supported material could be handled as a solid, the active species was dissolved in the ionic liquid in the pores, and the catalysis was homogeneous (Fig. 14). The supported ionic liquid catalyst was used in a batch reactor and displayed high activity for the hydrogenation of hexene-1, cyclohexene, and 2,3-dimethyl-2-butene. The initial rate constant was 11.2 min<sup>-1</sup> when supported ionic

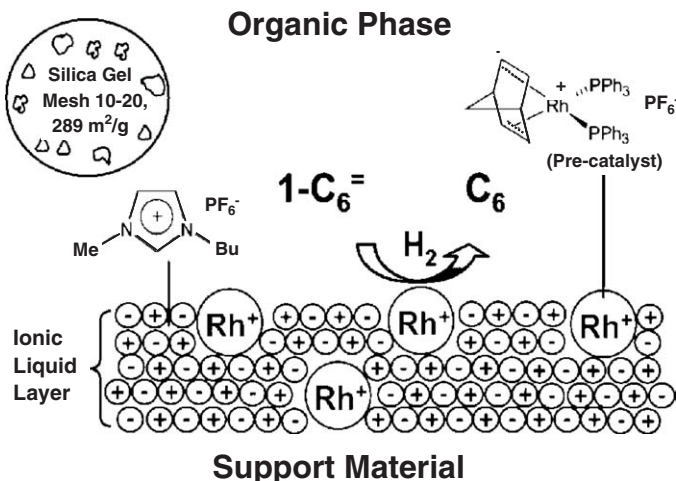


FIG. 14. Confined ionic liquid phase containing rhodium complex on the surface of a silica gel support material. Reproduced with permission from Mehnert (267).

liquid catalyst operated at 30°C. This activity compares favorably to the value of 0.4 min<sup>-1</sup> observed for the catalyst in acetone operated at 50°C. The rate of the reaction with the supported catalyst was 110 times that observed with the unsupported biphasic ionic liquid system under similar conditions. The superior performance of the supported catalyst over the unsupported one was attributed to a concentration effect: most of the reaction occurs near the interface between the ionic liquid layer and the organic phase, and the concentration of the active rhodium species is significantly enriched at the interface of a high-surface area support in comparison to the biphasic system.

It is also remarkable that the rhodium complex catalyst in the supported ionic liquid showed long-term stability, being used for 18 batches without any significant loss of activity. It was confirmed that no rhodium metal clusters were formed. However, acetone could be used to remove the ionic layer and its presence led to a total loss of activity.

The first fixed-bed application of a supported ionic liquid-phase catalyst was hydroformylation of propylene, with the reactants concentrated in the gas phase (265). The catalyst was a rhodium-sulfoxantphos complex in two ionic liquids on a silica support. The supported ionic liquid phase catalysts were conveniently prepared by impregnation of a silica gel with Rh(acac)(CO) and ligands in a mixture of methanol and ionic liquids, [BMIM]PF<sub>6</sub> and [BMIM][*n*-C<sub>8</sub>H<sub>17</sub>OSO<sub>3</sub>], under an argon atmosphere.

With this preparation method, a high ligand/Rh ratio (10 or 20) was shown to be essential for catalyst activity and for high *n/i* ratios in the product aldehyde. In the presence of ionic liquid, the *n/i* ratio was as much as 23.7, compared to a value of 16.9 observed in the absence of ionic liquids. Surprisingly, an L/Rh ratio of 2.5 resulted in an inactive catalyst. The catalytic activity and selectivity decreased steadily during the 5-h test, independent of the type of ionic liquid and the L/Rh ratio.

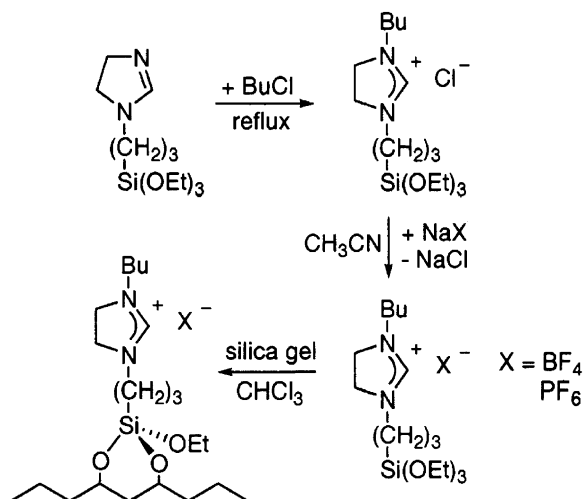


FIG. 15. Preparation of surface-anchored ionic liquid phases. Reproduced with permission from Mehnert *et al.* (97).

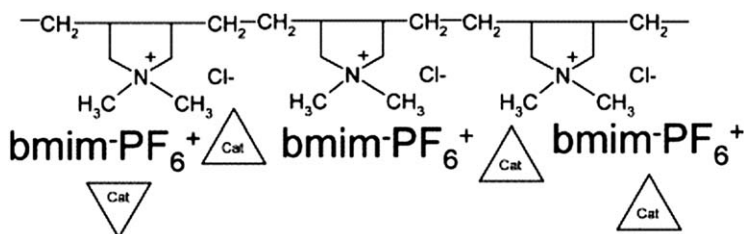


FIG. 16. Poly[diallyldimethylammonium chloride]. Reproduced with permission from Wolfson *et al.* (268).

An ionic liquid was fully immobilized, rather than merely supported, on the surface of silica through a multiple-step synthesis as shown in Fig. 15 (97). A ligand tri(*m*-sulfonyl)triphenyl phosphine tris(1-butyl-3-methyl-imidazolium) salt (tppti) was prepared so that the catalyst, formed from dicarbonylacetylacetonate rhodium and the ligand ( $P/Rh = 10$ ), could be soluble in both [BMIM]BF<sub>4</sub> and [BMIM]PF<sub>6</sub>. The supported ionic liquid-catalyst systems showed nearly three times higher rate of reaction (rate constant = 65 min<sup>-1</sup>) than a biphasic system for the hydroformylation of 1-hexene at 100°C and 1500 psi in a batch reactor, but the *n/i* selectivity was nearly constant the same for the two (~2.4). Unfortunately, both the supported and the biphasic ionic liquid systems exhibited similar metal leaching behavior.

Work with supported ionic liquids was extended to a cationic polymer, poly(diallyldimethylammonium chloride), which has quaternary ammonium functional groups (Fig. 16) (268). The extra-structural counter anion is Cl<sup>-</sup>. The polymer was applied to simultaneously incorporate an ionic liquid and a transition-metal catalyst via a simple mixing of the components. Wilkinson's catalyst and [BMIM]PF<sub>6</sub> were

impregnated onto the polymer and applied for hydrogenation of 2-cyclohexen-1-one and 1,3-cyclooctadiene. The value of the TOF observed with this supported catalyst was comparable to that observed with a homogeneous system but higher than that observed with the biphasic ionic liquid systems. The catalyst system could be re-used. However, the ionic liquid and the catalyst were leached out through a solvent that was miscible with the ionic liquid.

A similar strategy was followed with a catalyst that was made by direct polymerization of imidazolium ionic liquid monomers, followed by a subsequent anion exchange (269). It was used for the synthesis of 1-vinyl-3-alkyl-imidazolium halides (e.g., [ViEIM]Br (Vi = vinyl)). After the polymerization in chloroform at 60°C, poly(ViEIM)Br and poly(ViBIM)Br were obtained. Other anions were introduced via ligand exchange, replacing Br<sup>-</sup>. The solubility measurement of the cationic polymers containing various anions showed that, among the anions investigated (except Br<sup>-</sup> and Cl<sup>-</sup>), the polymers with BF<sub>4</sub><sup>-</sup>, PF<sub>6</sub><sup>-</sup>, TfO<sup>-</sup>, Tf<sub>2</sub>N<sup>-</sup>, and a few other anions are generally hydrophobic.

## VII. Biocatalysis in Ionic Liquid Media

Ionic liquids have drawn increasing interest as biotransformation media (21,270). In contrast to polar organic solvents, ionic liquids of higher polarity do not deactivate enzymes. Instead, in a number of investigations, high polarity in ionic liquids appeared to even lead to improved enzymatic performance (271). Furthermore, good solubility of polar substrates in ionic liquids can create a favorable situation for the biotransformations.

In general, hydrophobic ionic liquids, [BMIM]Tf<sub>2</sub>N, [BMIM]PF<sub>6</sub>, and [OMIM]PF<sub>6</sub>, provide environments that are less disruptive of the structures of biocatalysts than molecular solvents of similar polarity, methanol or DMSO (220).

An ionic liquid can be used as a pure solvent or as a co-solvent. An enzyme-ionic liquid system can be operated in a single phase or in multiple phases. Although most research has focused on enzymatic catalysis in ionic liquids, application to whole cell systems has also been reported (272). Besides searches for an alternative non-volatile and polar media with reduced water and organic solvents for biocatalysis, significant attention has been paid to the dispersion of enzymes and microorganisms in ionic liquids so that repeated use of the expensive biocatalysts can be realized. Another incentive for biocatalysis in ionic liquid media is to take advantage of the tunability of the solvent properties of the ionic liquids to achieve improved catalytic performance. Because biocatalysts are applied predominantly at lower temperatures (occasionally exceeding 100°C), thermal stability limitations of ionic liquids are typically not a concern. Instead, the solvent properties are most critical to the performance of biocatalysts.

Some general trends have started to appear correlating the properties of some ionic liquids to performance in biocatalysis (273), but conflicting observations have also been reported. The inconsistency of the performance of some systems could arise from the presence of impurities in the ionic liquids (or possibly in the substrates).



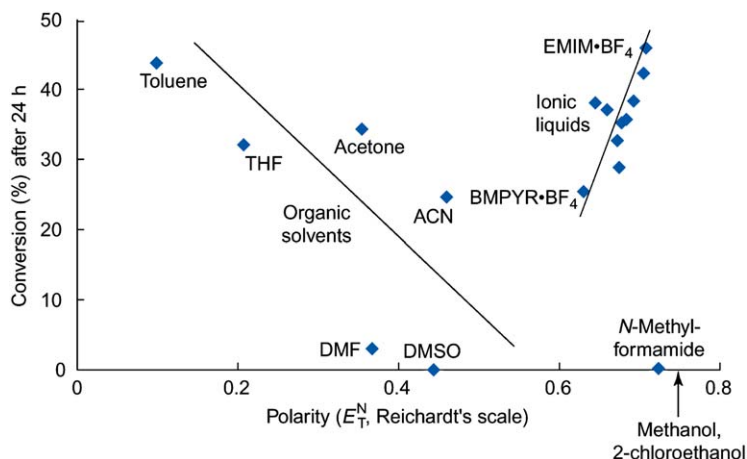


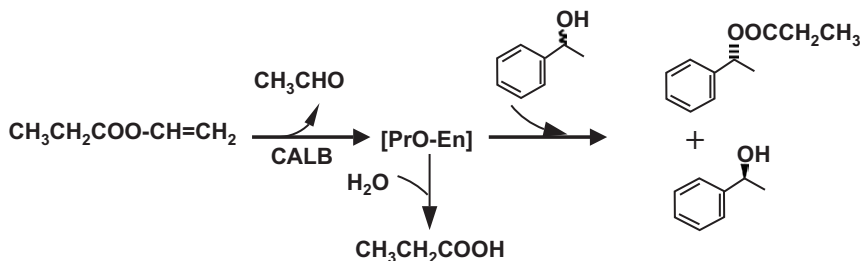
FIG. 17. Conversion in *Pseudomonas cepacia* lipase (PCL)-catalyzed reactions as a function of the solvent polarity (water = 1; trimethylsilane = 0). Reproduced with permission from Park and Kazlauskas (273).

In a recent review, some positive attributes of ionic liquids in biocatalysis were discussed (273). An example was given, which compares the enzymatic performance of *Pseudomonas cepacia* lipase (PCL)-catalyzed reactions as a function of the solvent polarity in both organic and ionic solvents, as shown in Fig. 17. The PCL shows no activity in organic solvents in the polarity range of the ionic liquids, but it is active in the ionic liquids.

It has often been found that enzymes retain their activity when suspended in ionic liquids of low hydrogen bond basicity, but they are inactive in those with high hydrogen bond basicity (e.g.,  $\text{Cl}^-$ ,  $\text{NO}_3^-$ , and acetate-containing ionic liquids) (274). Some recent biocatalytic reactions are discussed below, with an emphasis on the function of the ionic liquids in enzyme catalysis.

#### A. TRANSESTERIFICATION

Biphasic systems consisting of ionic liquids and supercritical  $\text{CO}_2$  showed dramatic enhancement in the operational stability of both free and immobilized *Candida antarctica* lipase B (CALB) in the catalyzed kinetic resolution of *rac*-1-phenylethanol with vinyl propionate at 10 MPa and temperatures between 120 and 150°C (Scheme 30) (275). Hydrophobic ionic liquids, [EMIM]Tf<sub>2</sub>N or [BMIM]Tf<sub>2</sub>N, were shown to be essential for the stability of the enzyme in the biotransformation. Notwithstanding the extreme conditions, both the free and isolated enzymes were able specifically to catalyze the synthesis of (*R*)-1-phenylethyl propionate. The maximum enantiomeric excess needed for satisfactory product purity (ee > 99.9%) was maintained. The (*S*)-1-phenylethanol reactant was not esterified. The authors suggested that the ionic liquids provide protection against enzyme denaturation by  $\text{CO}_2$  and heat. When the free enzyme was used, [EMIM]Tf<sub>2</sub>N appeared to be the best ionic liquid to protect the enzyme, which



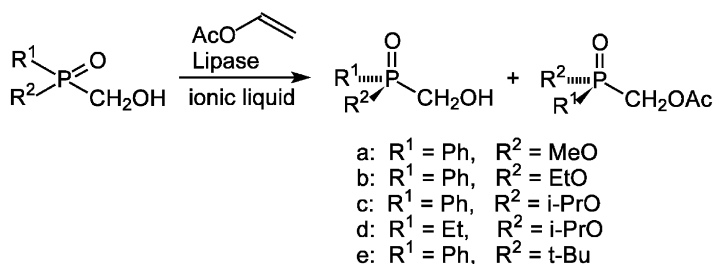
SCHEME 30.

was characterized by a half-life corresponding to 15 cycles. The observed effects of ionic liquids were attributed to the dual functions of the ionic liquids. First, they act as solvents, providing adequate microenvironments for the catalytic action of the enzyme (active catalytic conformation). Second, ionic liquids function as liquid supports, providing favorable multipoint enzyme-ionic liquids interactions (ionic, hydrogen, van der Waals, etc.) in a flexible supramolecular net able to maintain the active protein conformation in these highly denaturative conditions (276). The removal of residual water from the ionic liquids by  $\text{CO}_2$  purging was found to improve the product selectivity by preventing the hydrolysis of enzyme-propionate intermediate to propionic acid.

The hydrophobic ionic liquid  $[\text{BMIM}]\text{PF}_6$  has been consistently shown to provide the desired conformational flexibility to enzymes without drastically altering their catalytically active conformations. Therefore, this ionic liquid has been widely studied as a suitable medium for enzymatic transformations.

The hydrophobicity of ionic liquids was found to be particularly beneficial for lipase PS-C-catalyzed transesterification of 2-hydroxymethyl-1,4-benzodioxane in the presence of vinyl acetate (277). The hydrophobic  $[\text{BMIM}]\text{PF}_6$  functioned as a better promotional medium than methylene chloride and hydrophilic  $[\text{BMIM}]\text{BF}_4$ , with either supported or unsupported enzyme for the catalytic transesterifications. The ionic liquid not only acted as a medium but also as a permanent host for the enzymes, so that the enzyme-ionic liquid system could be recycled several times without substantial diminution in lipase activity.

The beneficial effect of the hydrophobicity of  $[\text{BMIM}]\text{PF}_6$  was shown to extend to other enzymes; a remarkably enhanced enantioselectivity was observed for lipases AK and *Pseudomonas fluorescens* for the kinetic resolution of racemic *P*-chiral hydroxymethanephosphinates (Scheme 31) (278). The *ee* values of the recovered alcohols and the acetates were about 80% when the enzymatic reactions were conducted in the hydrophobic  $[\text{BMIM}]\text{PF}_6$ . In contrast, there was little enantioselectivity (<5%) observed with the enzymes in hydrophilic  $[\text{BMIM}]\text{BF}_4$ . The lack of stereoselectivity in  $[\text{BMIM}]\text{BF}_4$  was attributed to the high miscibility of  $[\text{BMIM}]\text{BF}_4$  with water. The relatively hydrophilic ionic liquid is capable of stripping off the essential water from the enzyme surface, leading to insufficient hydration of the enzyme and a consequently strong influence on its performance (279).



SCHEME 31.

[BMIM]BF<sub>4</sub>, which is fully miscible with water, may undergo such undesirable interactions with various kinds of enzymes.

In a similar investigation, transesterification reactions of vinyl acetate with alcohols in [BMIM]BF<sub>4</sub> and [BMIM]PF<sub>6</sub> in the presence of immobilized lipases CALB and PS-C were found to proceed with higher enantioselectivities than in THF or toluene, with the best result again being observed with [BMIM]PF<sub>6</sub> (280).

In a recent study of protease  $\alpha$ -chymotrypsin transesterification reactions, several ionic liquids ([EMIM]BF<sub>4</sub>, [EMIM]Tf<sub>2</sub>N, [BMIM]BF<sub>4</sub>, [BMIM]PF<sub>6</sub>, and [MTOA]Tf<sub>2</sub>N) were used as the isolation media for the enzyme. Among these ionic liquids, [EMIM]BF<sub>4</sub> showed the least activity, and [BMIM]PF<sub>6</sub> offered the best stabilization of the enzyme (281).

Although [BMIM]BF<sub>4</sub> has been evaluated as an isolation medium for lipase-catalyzed biotransformations, the general experience with it has not been favorable, relative to that with other ionic liquids, such as [BMIM]PF<sub>6</sub>. However, excellent performance was recently reported for [BDMIM]BF<sub>4</sub> when it was used to host *Candida antarctica* (Novozym 435) for the enantioselective transesterification of 5-phenyl-1-penten-3-ol (+ and -) with vinyl acetate. The working hypothesis was that the oligomerization of acetaldehyde may be caused by the C2 proton of the [BMIM]<sup>+</sup> ion because of the unfavorable acidity of this group (226). In contrast, the cation in [BDMIM]BF<sub>4</sub> lacks this acidity.

The rate of the reaction in [BDMIM]BF<sub>4</sub> was superior to that in [BMIM]BF<sub>4</sub>. It is significant that no drop in the reaction rate was observed in the [BDMIM]BF<sub>4</sub> system after 10 repeated uses of the enzyme, whereas the reaction rate was significantly reduced when the reaction was conducted in [BMIM]BF<sub>4</sub> or in [BMIM]PF<sub>6</sub> (282). [BDMIM]BF<sub>4</sub> was found to be the best solvent for the recycled use of the enzyme under normal pressure conditions when vinyl acetate was used as the acyl donor. No reaction took place when [BDMIM]PF<sub>6</sub> was used as the solvent in the lipase-catalyzed reaction. (The [BDMIM]PF<sub>6</sub> was purified with particular care to rule out the possibility of contamination.) The replacement of the C2 proton of [BMIM]PF<sub>6</sub> by a methyl group was therefore concluded to have a large influence on its biocatalytic compatibility.

The polarity of an ionic liquid has been inferred to affect the activity of enzymes in it. Lozano *et al.* (276) attributed the differences in CALB activity in various ionic

liquids to the effect of solvent polarity; higher ionic liquid polarity led to greater transesterification rates. However, the importance of ionic liquid polarity was questioned in a recent study (220). It was argued that the differences in polarity of the ionic liquids were small, and—indeed contradictory values have been reported (75,226). Therefore, correlations of enzyme activity with the polarities of ionic liquids were suggested to be inappropriate for lipases and proteases (220). Instead, the authors pointed to the relationship between the enzyme's activity in water and the type of ionic liquid (283).

The presence of small amounts of water was found to be essential even for hydrophobic ionic liquids (284). When  $\alpha$ -chymotrypsin (in the form of salt-free lyophilized powder) was applied for the transesterification of *N*-acetyl-L-phenylalanine ethyl ester with 1-propanol in the dry ionic liquids [BMIM]PF<sub>6</sub> and [OMIM]PF<sub>6</sub>, little enzymatic activity was observed. The maximum activity was observed when 0.5 vol% water was added to the ionic liquids. Supercritical CO<sub>2</sub> was also sufficient to activate the enzyme in dry ionic liquids. The addition of water to the supercritical CO<sub>2</sub>-ionic liquid system further enhanced the enzymatic activity.

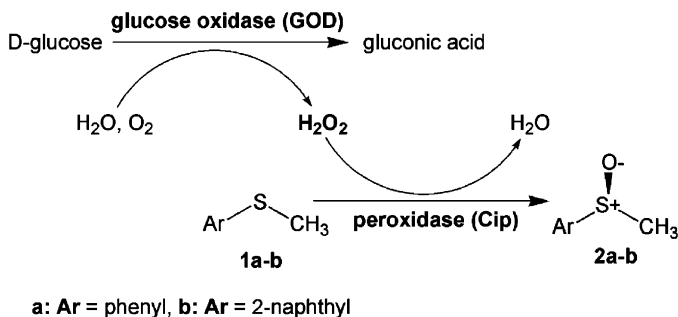
## B. OXIDATION

Fe(III) protoporphyrin chloride (hemin), microperoxidase-11 (MP-11), and cytochrome *c* (cyt-*c*) demonstrated substantial peroxidase activity for the oxidation of 2-methoxyphenol with H<sub>2</sub>O<sub>2</sub> and *tert*-BuOOH as the oxidant in ionic liquids [OMIM]PF<sub>6</sub> < [BMIM]PF<sub>6</sub> < [BMIM][Tf<sub>2</sub>N] (220). The non-coordinating, weak nucleophilic nature of the ionic liquids may have accelerate the peroxidase reaction by stabilizing the highly charged iron-peroxo or -oxo intermediates generated in the rate-limiting step of the reaction, thereby resulting in a substantial rate enhancement.

Although solvent polarity may influence the site of radical localization within the porphyrin ring, which can potentially alter the reactivity (285,286), the solvent coordinating ability and nucleophilicity and specific ligand effects are particularly important in determining peroxidase activity.

The hemin activity increased in the order [OMIM]PF<sub>6</sub> < [BMIM]PF<sub>6</sub> < [BMIM][Tf<sub>2</sub>N]. This order was correlated with the viscosities of the ionic liquids (682, 450, and 69 cP) rather than their polarity. The peroxidase activities of cyt-*c*, MP-11, and hemin were found not to be influenced by water.

[BMIM]PF<sub>6</sub> was applied to a bi-enzymatic system for the chemo- and stereoselective oxidation of organosulfide (ee = 92%), as shown in Scheme 32 (287). In this system, the peroxidase was used to catalyze the oxidation of the sulfides. Because the peroxidases could be deactivated by an excess of hydrogen peroxide, glucose oxidase (GOD) was used to generate *in situ* a continuous flux of hydrogen peroxide from glucose by the use of oxygen from the air. The reaction proceeded well with the addition of 5–10% water. The bi-enzyme/[BMIM]PF<sub>6</sub>/H<sub>2</sub>O system offered high operational stability. In such a system, all substrates including glucose, gluconic acid, and sulfides are dissolved in the ionic liquids. After extraction of the products, the system remained active; however, product inhibition was observed.



SCHEME 32.

### C. ALDOL REACTIONS

On the basis of encouraging work in the development of L-proline-DMSO and L-proline-ionic liquid systems for practical asymmetric aldol reactions, an aldolase antibody 38C2 was evaluated in the ionic liquid [BMIM]PF<sub>6</sub> as a reusable aldolase-ionic liquid catalytic system for the aldol synthesis of  $\alpha$ -chloro- $\beta$ -hydroxy compounds (288). The biocatalytic process was followed by chemical catalysis using Et<sub>3</sub>N in the ionic liquid [BMIM]TfO at room temperature, which transformed the  $\alpha$ -chloro- $\beta$ -hydroxy compounds to the optically active (70% ee)  $\alpha,\beta$ -epoxy carbonyl compounds. The aldolase antibody 38C2-ionic liquid system was also shown to be reusable for Michael additions and the reaction of fluoromethylated imines.

### D. GALACTOSYLATION REACTIONS

In the synthesis of *N*-acetylglucosamin from lactose and *N*-acetylglucosamine with  $\beta$ -galactosidase (289,290), the addition of 25 vol% of the water-miscible ionic liquid [MMIM][MeSO<sub>4</sub>] to an aqueous system was found to effectively suppress the side reaction of secondary hydrolysis of the desired product. As a result, the product yield was increased from 30 to 60%. Product separation was improved, and the reuse of the enzymatic catalyst became possible. A kinetics investigation showed that the enzyme activity was not influenced by the presence of the ionic liquids. The enzyme was stable under the conditions employed, allowing its repeated use after filtration with a commercially available ultrafiltration membrane.

When the water-miscible ionic liquid [MMIM][MeSO<sub>4</sub>] was used as a neat medium for the enzymatic transformations, however, poorer performance was observed. For the kinetic resolution of *rac*-1-phenylethanol by transesterification with vinyl acetate with a set of different lipases dispersed in the pure ionic liquid, it was found that [MMIM][MeSO<sub>4</sub>] was among the poorest media for the enzymes (291). It has been recognized that some water-miscible ionic liquids in the pure form are denaturants (21), but, when they are used in the presence of excess water, their tendency to

denature the enzymes disappeared. Similar results have been observed for other systems as well (284,292).

### VIII. Conclusions and Perspective

The catalytic applications of ionic liquids have grown rapidly in the preceding decade as the number of new ionic liquids has continued to expand. From an environmental point of view, the lack of vapor pressure has made ionic liquids highly attractive as replacements for conventional solvents for homogeneous catalysis. Although no other liquid material could be greener than water as a reaction medium, the inertness of many ionic liquids toward the most-known catalysts has made possible applications that are otherwise not feasible in water. Other unique properties of ionic liquids, including the high thermal stability, broad liquid range, the tunable acidity, and the excellent retention of polar or charged catalysts, have made ionic liquids suitable media for a broad range of catalytic applications. The tunability of a wide spectrum of properties of ionic liquids has allowed for task-specific applications. Reusable catalyst–ionic liquid systems made possible by facile catalyst–product separation have provided economic incentives for the development of such systems for new processes and as replacements for existing ones. Most reported investigations have been carried out in batch operations, but it has also been possible to use continuous processes that allow for product separation and reuse of catalyst–ionic liquid combinations (235).

On the basis of the desirable liquid properties, ionic liquids have been reported for a broad range of catalytic applications. The applications include the use of ionic liquids as active catalysts and as carrier phases for organometallic catalysts and for solid catalysts. The reaction system can be controlled so that reaction occurs in a single phase, or in a biphasic or triphasic system. Improved selectivity has often been observed in such systems relative to what is attained in conventional organic solvents, and activity improvements over those attainable in aqueous biphasic systems have also often been observed. In general, the solubility of a less-soluble reactant in the ionic liquids tends to limit the rate of the desired reaction. The partitioning of products in biphasic systems aids selectivity to desired products by limiting consecutive reactions. The tunable solubility of organic molecules in ionic liquids, either by the modification of the structure of the ionic liquid or by the addition of a co-solvent, (293–295) could in prospect be used to achieve desired reaction rates and selectivities.

The replacement of conventional catalytic processes for purification of mixtures by processes involving extraction with ionic liquids has also been envisioned. For example, the extractive removal of sulfur compounds from fuels has shown promising leads for high selectivity for aromatic sulfur compounds, and removal of such compounds has been a major challenge in conventional heterogeneous hydrodesulfurization catalysis (27,296).

The use of chiral ionic liquids for the synthesis of enantioselective compounds could allow important applications, although research activity in this area has been relatively low. The possibility of reusing the ionic liquids is particularly attractive. Recyclable ionic liquids containing expensive catalysts are expected to enable catalytic processes that are otherwise cost prohibitive.

Promising developments of ionic liquids for biocatalysis reflect their enhanced thermal and operational stabilities, sometimes combined with high regio- or enantioselectivities. Ionic liquids are particularly attractive media for certain biotransformations of highly polar substrates, which cannot be performed in water owing to equilibrium limitations (297).

It must be recognized that the understanding and the full characterization of some ionic liquids are still limited, and there are a number of limitations that must be kept in mind. Some ionic liquids are moisture sensitive, particularly a number of metal halide-containing ionic liquids, such as chloroaluminates. Those containing  $\text{BF}_4^-$  and  $\text{PF}_6^-$  are prone to hydrolysis, generating HF in the presence of water at elevated temperatures and particularly in the presence of metal catalysts (41,294). The presence of impurities can have a detrimental effect on the catalyst performance. A small loss of ionic liquid into the products may necessitate costly purification steps. The cost of ionic liquids has also limited the commercial development of catalytic processes for commodity chemicals.

Most important, there is significant uncertainty regarding the toxicity and potential environmental impact of some ionic liquids. Structural similarities between some ionic liquids and either herbicides or plant growth regulators have been pointed out (298). The anti-microbial activities of ionic liquids have been correlated with the alkyl chain length in the imidazolium ion; the longer chain length resulted in greater anti-microbial activity (299,300). Therefore, a full assessment of the toxicity of ionic liquids still falls behind the application tests. In view of possible product contamination and the issues of disposal of ionic liquids after repeated use, it is prudent to design processes using ionic liquids that have well-established toxicity profiles.

## References

1. Olivier-Bourbigou, H., and Magna, L., *J. Mol. Catal. A Chem.* **182**, 419 (2002).
2. Wilkes, J.S., in "Ionic Liquids in Synthesis" (P. Wasserscheid and T. Welton, Eds.), Wiley-VCH, Weinheim, 2003.
3. Herrmann, W.A., and Cornils, B., *Angew. Chem. Int. Ed.* **36**, 1049 (1997).
4. Cornils, B., and Herrmann, W.A. (Eds.), "Applied Homogeneous Catalysis with Organometallic Compounds." Wiley-VCH, Weinheim, 1996.
5. Cornils, B., *Org. Process Res. Dev.* **2**, 121 (1998).
6. Horvath, H., Cornils, B., and Herrmann, W.A. (Eds.), "Aqueous-Phase Organometallic Catalysis: Concepts and Applications." VCH, Weinheim, 1998.
7. Horvath, I.T., *J. Mol. Catal. A Chem.* **116**, 1 (1997).
8. Fannin, A.A., Floreani, D.A., King, L.A., Landers, J.S., Piersma, B.J., Stech, D.J., Vaugh, R.L., Wilkes, J.S., and Williams, J.L., *J. Phys. Chem* **88**, 2614 (1984).
9. Davis, J.H., Forrester, K.J., and Merrigan, T., *Tetrahedron Lett* **39**, 8955 (1998).
10. Davis, J.H., and Forrester, K.J., *Tetrahedron Lett.* **40**, 1621 (1999).

11. Zhao, D., Wu, M., Kou, Y., and Min, E., *Catal. Today* **74**, 157 (2002).
12. Fonseca, G.S., Umpierre, A.P., Fichtner, P.F.P., Teixeira, S.R., and Dupont, J., *Chem. Eur. J.* **9**, 3263 (2003).
13. Freemantle, M., *Chem. Eng. News* **81**(13), 9 (2003).
14. Olivier-Bourbigou, H., Chodorge, J.-A., and Travers, P., *Petrol. Technol. Quart. Autumn* **141**, (1999).
15. Olivier, H., *J. Mol. Catal. A Chem.* **146**, 285 (1999).
16. Gordon, C.M., *Appl. Catal. A Gen.* **222**, 101 (2001).
17. J.D. Holbrey, K.R. Seddon., *Clean Prod. Proc.* 223 (1999).
18. Zhao, H., and Malhotra, S.V., *Aldrichem. Acta* **35**(3), 75 (2002).
19. Wasserscheid, P., and Keim, W., *Angew. Chem. Int. Ed.* **39**, 3772 (2000).
20. Kragl, U., Eckstein, M., and Kaftzik, N., *Curr. Opin. Biotechnol.* **13**(6), 565 (2002).
21. van Rantwijk, F., Lau, R.M., and Sheldon, R.A., *Trends Biotechnol.* **21**, 131 (2003).
22. Brennecke, J.F., and Maginn, E.J., *AIChE J.* **47**(11), 2384 (2001).
23. Koel, M., *Proc. Est. Acad. Sci. Chem.* **49**, 145 (2000).
24. Augustine, R.L., Tanielyan, S.K., Anderson, S., and Yang, H., *Chem. Commun.* 1257 (1999).
25. Dzyuba, S.V., and Bartsch, R.A., *Chem. Phys. Chem.* **3**, 161 (2002).
26. Dyson, P.J., Ellis, D.J., and Welton, T., *Can. J. Chem.* **79**, 705 (2001).
27. Zhang, R., and Zhang, Z.C., *Green Chem.* **4**, 376 (2002).
28. Keim, W., Vogt, D., Waffenschmidt, H., and Wasserscheid, P., *J. Catal.* **186**, 481 (1999).
29. Blanchard, L.A., and Brennecke, J.F., *Ind. Eng. Chem. Res.* **40**, 287 (2001).
30. Blanchard, L.A., Gu, Z., and Brennecke, J.F., *J. Phys. Chem. B.* **105**, 2437 (2001).
31. Scurto, A.M., Aki, S.N.V.K., and Brennecke, J.F., *J. Am. Chem. Soc.* **124**, 10276 (2002).
32. Bates, E.D., Mayton, R.D., Ntai, I., and Davis, J.H. Jr., *J. Am. Chem. Soc.* **124**(6), 927 (2002).
33. Reetz, M.T., Wiesenhöfer, W., Franciò, G., and Leitner, W., *Adv. Synth. Catal.* **345**, 1221 (2003).
34. Schäfer, T., Rodrigues, C.A., Carlos, A.M.A., and Crespo, J.G., *Chem. Commun.* 1622 (2001).
35. Carmichael, A.J., Hardacre, C., Holbrey, J.D., Seddon, K.R., and Nieuwenhuyzen, M., *Proc. Electrochem. Soc.* **99**, 209 (2000).
36. Hagiwara, R., and Ito, Y., *J. Fluorine Chem.* **105**, 221 (2000).
37. Rogers, R., and Seddon, K. (Eds.), "ACS Symposium Series 858, American Chemical Society." Washington, DC, 2003.
38. Brown, R.J., Dyson, P.J., Ellis, D.J., and Welton, T., *Chem. Commun.* 1862 (2001).
39. Anderson, J.L., Ding, J., Welton, T., and Armstrong, D.W., *J. Am. Chem. Soc.* **124**, 14247 (2002).
40. Xu, W., Wang, L.M., Nieman, R.A., and Angell, C.A., *J. Phys. Chem.* **107**, 11749 (2003).
41. Huddleston, J.G., Visser, A.E., Reichert, W.M., Willauer, H.D., Broker, G.A., and Rogers, R.D., *Green Chem.* **3**, 156 (2001).
42. Wilkes, J.S., *J. Mol. Catal. A Chem.* **214**, 11 (2004).
43. Marsh, K.N., Boxall, J.A., and Lichtenthaler, R., *Fluid Phase Equil.* **219**, 93 (2004).
44. Platts, J.A., *Phys. Chem. Chem. Phys.* **2**, 3115 (2000).
45. Swatloski, R.P., Spear, S.K., Holbrey, J.D., and Rogers, R.D., *J. Am. Chem. Soc.* **124**, 4974 (2002).
46. Matsumoto, K., Hagiwara, R., and Ito, Y., *J. Fluorine Chem.* **115**, 133 (2002).
47. Kimizuka, N., and Nakashima, T., *Langmuir* **17**, 6759 (2001).
48. Abbott, A.P., Capper, G., Davies, D.L., Munro, H.L., Rasheed, R.K., and Tambyrajah, V., *Chem. Commun.* 2010 (2001).
49. Lall, S.I., Mancheno, D., Castro, S., Shteto, V., Cohen, J.I., and Engel, R., *Chem. Commun.* 2413 (2000).
50. Visser, A.E., and Rogers, R.D., *J. Solid State Chem.* **171**, 109 (2003).
51. Law, G., and Watson, P.R., *Chem. Phys. Lett.* **345**, 1 (2001).
52. Visser, A.E., in "Ionic liquids: Industrial Applications to Green Chemistry," *ACS Symposium Series 818* (R.D. Rogers, and K.R. Seddon, Eds.), p. 289. 2002.
53. Seddon, K.R., Stark, A., and Torres, M.J., *Pure Appl. Chem.* **72**, 2275 (2000).
54. Hsiu, S., Huang, J.F., Sun, I.W., Yuan, C.H., and Shiea, J., *Electrochim. Acta.* **47**, 4367 (2002).
55. Hasan, M., Kozhevnikov, I.V., Siddiqui, M.R.H., Femoni, C., Steiner, A., and Winterton, N., *Inorg. Chem.* **40**, 795 (2001).



56. H. Matsumoto, H. Kageyama, Y. Miyazaki, *Chem. Lett.* 182 (2001).
57. MacFarlane, D.R., Sun, J., Golding, J., Meakin, P., and Forsyth, M., *Electrochim. Acta.* **45**, 1271 (2000).
58. Dominey, L.A., Koch, V.R., and Blakley, T.J., *Electrochim. Acta.* **37**, 1551 (1992).
59. Broeke, J.v.d., Stam, M., Lutz, M., Kooijman, H., Spek, A.L., Deelman, B.-J., and vanKoten, G., *Eur. J. Inorg. Chem.* 2798 (2003).
60. Zou, G., Wang, Z., Zhu, J., Tang, J., and He, M.Y., *J. Mol. Catal. A Chem.* **206**, 193 (2003).
61. Kazarian, S.G., Sakellarios, N., and Gordon, C.M., *Chem. Commun.* 1314 (2002).
62. Bowlas, C.J., Bruce, D.W., and Seddon, K.R., *Chem. Commun.* 1625 (1996).
63. McFarlane, D.R., Sun, J., Golding, J., Meakin, P., and Forsyth, M., *Electrochim. Acta.* **45**, 1271 (2000).
64. Forsyth, S., Golding, J., MacFarlane, D.R., and Forsyth, M., *Electrochim. Acta.* **46**, 1753 (2001).
65. Holbrey, J.D., and Seddon, K.R., *J. Chem. Soc. Dalton Trans.* **13**, 2133 (1999).
66. Bonhôte, P., Dias, A.-P., Armand, M., Papageorgiou, N., Kalyanasundaram, K., and Grätzel, M., *Inorg. Chem.* **35**, 1168 (1996).
67. Wilkes, J.S., and Zaworotko, M.J., *J. Chem. Soc., Chem. Commun.* 965 (1992).
68. Ngo, H.L., LeCompte, K., Hargens, L., and McEwen, A.B., *Thermochim. Acta.* **357**, 97 (2000).
69. Murray, C.B., Sandford, G., and Korn, S.R., *J. Fluorine Chem.* **123**, 81 (2003).
70. Pelletier, P., Durand, J., and Cot, L., *Z. Anorg. Allg. Chem.* **581**, 190 (1990).
71. Clark, H.R., Clark, R., and Jones, M.M., *Inorg. Chem.* **10**, 28 (1971).
72. Dupont, J., Silva, S.M., and de Souza, R.F., *Catal. Lett.* **77**, 131 (2001).
73. Rangits, G., Petocz, G., Berente, Z., and Kollár, L., *Inorg. Chim. Acta.* **35**, 3301 (2003).
74. Dupont, J., Fonseca, G.S., Umpierre, A.P., Fichtner, P.F.P., and Texeira, S.R., *J. Am. Chem. Soc.* **124**, 4228 (2002).
75. Carmichael, A.J., and Seddon, K.R., *J. Phys. Org. Chem.* **13**, 591 (2000).
76. Reichardt, C., *Chem. Rev.* **94**, 2319 (1994).
77. Muldoon, M.J., Gordon, C.M., and Dunkin, I.R., *J. Chem. Soc. Perkin Trans.* **2**, 433 (2001).
78. Aki, S.N.V.K., Brennecke, J.F., and Samanta, A., *Chem. Commun.* **413**, 5 (2001).
79. Okoturo, O.O., and VanderNoot, T.J., *J. Electroanal. Chem.* **568**, 167 (2004).
80. Swartling, D., Ray, L., Compton, S., and Ensor, D., *Bull. Biochem. Biotechnol.* **13**, 1 (2000).
81. Fannin, A.A. Jr., Floreani, D.A., King, L.A., Landers, J.S., Piersma, B.J., Stech, D.J., Vaughn, R.L., Wilkes, J.S., and Williams, J.L., *J. Phys. Chem.* **88**, 2614 (1988).
82. Berger, A., de Souza, R.F., Delgado, M.R., and Dupont, J., *Tetrahedron Asymmetry.* **12**, 1825 (2001).
83. Álvaro, M.A., Ferrer, B., García, H., and Narayana, M., *Chem. Phys. Lett. Lett.* **362**, 435 (2002).
84. Calò, V., Giannoccaro, P., Nacci, A., and Monopoli, A., *J. Organomet. Chem.* **645**, 152 (2002).
85. A.M. Scurto, S.N.V.K. Aki, J.F. Brennecke, *Chem. Commun.* 572 (2003).
86. Zhang, Q., Zhang, Z.C., 4th International Colloquium Fuels, 486 (2003).
87. Biedron, T., and Kubisa, P., *Macromol. Rapid Commun.* **22**, 1237 (2001).
88. Dyson, P.J., Ellis, D.J., Henderson, W., and Laurenczya, G., *Adv. Synth. Catal.* **345**, 216 (2003).
89. Zhang, R., and Zhang, Z.C., *Ind. Eng. Chem. Res.* **43**, 614 (2004).
90. Zawodzinski, T.A.O., *Inorg. Chem.* **28**, 1710 (1989).
91. J.D. Holbrey, W.M. Reichert, M. Nieuwenhuyzen, O. Sheppard, C. Hardacrebc, R.D. Rogers, *Chem. Commun.* 476 (2003).
92. J.K.D. Surette, L. Green, R.D. Singer, *Chem. Commun.* 2753 (1996).
93. Steed, J.W., and Atwood, J.L., in "Supramolecular Chemistry" p. 707. Wiley, Chichester, 2000.
94. Hanke, C.G., Johansson, A., Harper, J.B., and Lynden-Bell, R.M., *Chem. Phys. Lett.* **374**, 85 (2003).
95. Crosthwaite, J.M., Aki, S.N.V.K., Maginn, E.J., and Brennecke, J.F., *J. Phys. Chem. B* **108**, 5113 (2004).
96. Behr, A., Naendrup, F., and Nave, S., *Eng. Life Sci.* **3**, 8 (2003).
97. Mehnert, C.P., Cook, R.A., Dispenziere, N.C., and Afeworki, M., *J. Am. Chem. Soc.* **124**, 12932 (2002).
98. Hagiwara, R., Hirashige, T., Tsuda, T., and Ito, Y., *J. Fluorine Chem.* **99**, 1 (1999).

99. Hagiwara, R., Hirashige, T., Tsuda, T., and Ito, Y., *J. Electrochem. Soc.* **149**, D1 (2002).
100. Matsumoto, K., Hagiwara, R., Ito, Y., Kohara, S., and Suzuya, K., *Nucl. Instr. Meth. Phys. Res. B* **199**, 29 (2003).
101. Branco, L., and Afonso, C.A.M., *Tetrahedron* **57**, 4405 (2001).
102. Maase, M. "American Chemical Society Meeting." New York, 2003. Abstract.
103. Smith, G.P., Dworkin, A.S., Pagni, R.M., and Zingg, S.P., *J. Am. Chem. Soc.* **111**, 525 (1989).
104. Hussey, C.L., *Adv. Molten Salt Chem.* **5**, 185 (1983).
105. Forbes, D.C., and Weaver, K.J., *J. Mol. Catal. A Chem.* **214**, 129 (2004).
106. Deng, Y., Shi, F., Beng, J., and Qiao, K., *J. Mol. Catal. A Chem.* **165**, 33 (2001).
107. Aggarwal, V.K., Emme, I., and Mereu, A. *Chem. Commun.* 1612 (2002).
108. Wuyts, A.W.S., De Vos, D.E., Vankelecom, I.F.J., and Jacobs, P.A., *Tetrahedron Lett.* **43**, 8107 (2002).
109. C.P. Mehnert, N.C. Dispenziere, R.A. Cook, *Chem. Commun.* 1610 (2002).
110. Morrison, D.W., Forbes, D.C., and Davis, J.H. Jr., *Tetrahedron Lett.* **42**, 6053 (2001).
111. Chandrasekhar, S., Narasimulu, C., Jagadeshwar, V., and Reddy, K.V., *Tetrahedron Lett.* **44**, 3629 (2003).
112. Chauvin, Y., Mussman, L., and Olivier, H., *Angew. Chem. Int. Ed.* **34**, 2698 (1995).
113. Sheldon, R., *Chem. Commun.* 2399 (2001).
114. Olivier, H., and Favre, F., US Pat. 6,245,918 (2001).
115. Anderson, J.L., Ding, J., Welton, T., and Armstrong, D.W., *J. Am. Chem. Soc.* **124**, 14247 (2002).
116. Gallo, V., Mastroiilli, P., Nobile, C.F., Romanazzi G., Suranna, G.P., and Trans, D., *J. Chem. Soc.* 4339 (2002).
117. Mastroiilli, P., Nobile, C.F., Gallo, V., Suranna, G.P., and Giannandrea, R., Proceedings of 4th Tokyo Conference on "Advanced Catalytic Science and Technology", Vol. IP420, Tokyo, 2002.
118. Laali, K.K., and Gettewert, V.J., *J. Org. Chem.* **66**, 35 (2001).
119. Scott, J.L., MacFarlane, D.R., Raston, C.L., and Teoh, C.M., *Green Chem.* **2**, 123 (2000).
120. Branco, L., and Afonso, C.A.M., *Tetrahedron* **57**, 4405 (2001).
121. Sasaki, K., Nagai, H., Matsumura, S., and Toshima, K., *Tetrahedron Lett.* **44**, 5605 (2003).
122. Aggarwal, A., Lancaster, N.L., Sethi, A.R., and Welton, T., *Green Chem.* **4**, 517 (2002).
123. Picquet, M., Tkatchenko, I., Tommasi, I., Wasserscheid, P., and Zimmermann, J., *Synth. Catal.* **345**, 959 (2003).
124. Zhao, Z.K., Li, Z.S., Wang, G.R., Qiao, W.H., and Cheng, L.B., *Appl. Catal. A Gen.* **262**, 69 (2004).
125. Adams, C.J., Earle, M.J., Roberts, G., and Seddon, K.R., *Chem. Commun.* 2097 (1998).
126. Boon, J.A., Levisky, J.A., Pflug, J.L., and Wilkes, J.S., *J. Org. Chem.* **51**, 480 (1986).
127. Valkenberg, M.H., deCastro, C., and Hölderich, W.F., *Appl. Catal. A Gen.* **215**, 185 (2001).
128. Csihony, S., Mehdi, H., and Horvath, I.T., *Green Chem.* **3**, 307 (2001).
129. Song, C.E., Roh, E.J., Lee, S.G., Shim, W.H., and Choi, J.H., *Chem. Commun.* 1122 (2001).
130. Dzyuba, S.V., and Bartsch, R.A., *Tetrahedron Lett.* **43**, 4657 (2002).
131. Meracz, I., and Oh, T., *Tetrahedron Lett.* **44**, 6465 (2003).
132. Ludley, P., and Karodia, N., *Tetrahedron Lett.* **42**, 2011 (2001).
133. Fischer, T., Sethi, A., Welton, T., and Woolf, J., *Tetrahedron Lett.* **40**, 793 (1999).
134. Earle, M.J., McCormac, P.B., and Seddon, K.R., *Green Chem.* 23 (1999).
135. Lee, C.W., *Tetrahedron Lett.* **40**, 2461 (1999).
136. Qiao, K., and Deng, Y., *J. Mol. Catal. A Chem.* **171**, 81 (2001).
137. Yoo, K.V., Namboodiri, V.V., Varma, R.S., and Smirniotis, P.G., *J. Catal.* **222**, 511 (2004).
138. Green, L., Hemeon, I., and Sing, R.D., *Tetrahedron Lett.* **41**, 1343 (2000).
139. Kemperman, G.J., Roeters, T.A., and Hilberink, P.W., *Eur. J. Org. Chem.* 1681 (2003).
140. Chauvin, Y., Hirschauer, A., and Olivier, H., *J. Mol. Catal.* **92**, 155 (1994).
141. Sherif, F.G., Shyyu, L., and Greco, C.C., US Pat. 5,824,832 (1998).
142. Golezinski, M., Birss, V.I., and Galuszka, J.J., *Ind. Eng. Chem. Res.* **32**, 1795 (1993).
143. Potdar, M.K., Mohile, S.S., and Salunkhe, M.M., *Tetrahedron Lett.* **42**, 9285 (2001).
144. Sethna, S., and Phadke, R., *Org. React.* **7**, 1 (1953).
145. S.M. Sethna, N.M. Shah, R.C. Shah, *J. Chem. Soc.* **228**, 2 (1938).
146. Gröger, H., and Wilken, J., *Angew. Chem. Int. Ed.* **40**, 529 (2001).

147. List, B., Lerner, R.A., and Barbas, C.F. III, *J. Am. Chem. Soc.* **122**, 2395 (2000).
148. Kotrusz, P., Kmentová, I., Gotov, B., Toma, S., and Solcániová, E., *Chem. Commun.* 2510 (2002).
149. Loh, T.P., Feng, L.C., Yang, H.Y., and Yang, J.Y., *Tetrahedron Lett.* **43**, 8741 (2002).
150. Harjani, J.R., Nara, S.J., and Salunkhe, M.M., *Tetrahedron Lett.* **43**, 1127 (2002).
151. Blanchard, L.A., Hancu, D., Beckman, E.J., and Brennecke, J.F., *Nature*. **399**, 28 (1999).
152. Joule, J.A., Mills, K., and Smith, G.F., "Heterocyclic Chemistry." 3rd Edition Chapman & Hall, London, 1995.
153. Wassersheid, P., in ACS Fall Meeting 2003. Abstract.
154. Yadav, J.S.S., Reddy, B.V., Basak, A.K., and Narsaiah, A.V., *Tetrahedron Lett.* **44**, 1047 (2003).
155. Das, U., Crousse, V., Kesavsn, V., Daniele, B.D., and Begue, J.P., *J. Org. Chem.* **65**, 6749 (2000).
156. Curini, M., Epifano, F., Marcotullio, M.C., and Rosati, O., *Eur. J. Org. Chem.* 4149 (2001).
157. Harrak, Y., and Pujol, M.D., *Tetrahedron Lett.* **43**, 819 (2002).
158. Yadav, J.S., Reddy, B.V.S., Raj, K.S., and Prasad, A.R., *Tetrahedron* **59**, 1805 (2003).
159. Yadav, J.S., Reddy, B.V.S., Basak, A.K., and Narsaiah, A.V., *Tetrahedron Lett.* **44**, 2217 (2003).
160. Ranu, B.C., Dey, S.S., and Hajra, A., *Tetrahedron* **59**, 2417 (2003).
161. Itoh, H., Naka, K., and Chujo, Y., *J. Am. Chem. Soc.* **126**, 3026 (2004).
162. Rosa, J.N., Afonso, C.A.M., and Santos, A.G., *Tetrahedron* **57**, 4189 (2001).
163. Hsu, J.-C., Yen, Y.-H., and Chu, Y.-H., *Tetrahedron Lett.* **45**, 4673 (2004).
164. Yadav, J.S., Reddy, B.V.S., and Gnaneshwar, D., *New J. Chem.* **27**, 202 (2003).
165. Yang, J., Tian, P., He, L.L., and Xu, W.G., *Fluid Phase Equil.* **204**, 295 (2003).
166. Lee, S., and Park, J.H., *J. Mol. Catal. A Chem.* **194**, 49 (2003).
167. Song, C.E., Roh, E.J., Shim, W.H., and Choi, J.H., *Chem. Commun.* 1695 (2000).
168. Keh, C.C.K., *Tetrahedron Lett.* **43**, 4993 (2002).
169. Suarez, P.A.Z., Dullius, J.E.L., Einloft, S., de Souza, R.F., and Dupont, J., *Polyhedron* **15**, 1217 (1996).
170. Dyson, P.J., Ellis, D.J., Parker, D.G., and Welton, T., *Chem. Commun.* (1999).
171. Sirieix, J., Ossberger, M., Betzemeier, B., and Knochel, P., *Synlett* 1613 (2000).
172. Favre, F., Olivier-Bourbigou, H., Commereuc, D., and Saussine, L., *Chem. Commun.* 1360 (2001).
173. Wasserscheid, P., Waffenschmidt, H., Machnitzki, P., Kotsieper, K.W., and Stelzer, O., *Chem. Commun.* 451 (2001).
174. Brasse, C.C., Englert, U., Salzer, A., Waffenschmidt, H., and Wasserscheid, P., *Organometallics* **19**, 3818 (2000).
175. Song, C.E., and Lee, S., *Chem. Rev.* **102**, 3495 (2002).
176. Choudary, B.M., Chowdari, N.S., Kantam, M.L., and Raghavan, K.V., *J. Am. Chem. Soc.* **123**, 9220 (2001).
177. Choudary, B.M., Chowdari, N.S., Jyothi, K., and Kantam, M.L., *J. Am. Chem. Soc.* **124**, 5341 (2002).
178. Lu, X., Xu, Z., and Yang, G., *Org. Process Res. Dev.* **4**, 575 (2000).
179. Song, C.E., Jung, D., Roh, E.J., Lee, S., and Chi, D.Y., *Chem. Commun.* 3038 (2002).
180. Branco, L.C., and Afonso, C.A.M., *Chem. Commun.* 3036 (2002).
181. Calò, V., Nacci, A., Lopez, L., and Napola, A., *Tetrahedron Lett.* **42**, 4701 (2001).
182. Calò, V., Nacci, A., Monopoli, A., Lopez, L., and di Cosmo, A., *Tetrahedron* **57**, 6071 (2001).
183. Xu, L., Chen, W., and Xiao, J., *Organometallics* **19**, 1123 (2000).
184. Calò, V., Nacci, A., Lopez, L., and Mannarini, N., *Tetrahedron Lett.* **41**, 8973 (2000).
185. Calò, V., Nacci, A., Lopez, L., and Napola, A., *Tetrahedron Lett.* **28**, 4701 (2001).
186. Calò, V., Nacci, A., Monopoli, A., Spinelli, M., *Eur. J. Org. Chem.* 1382 (2003).
187. Baleizaõ, C., Gigante, B., Garcia, H., and Corma, A., *Tetrahedron Lett.* **44**, 6813 (2003).
188. Yao, Q., and Zhang, Y., *Angew. Chem. Int. Ed.* **115**, 3517 (2003).
189. McGuinness, D.S., Cavell, K.J., and Yates, B.F., *Chem. Commun.* 355 (2001).
190. Bernardo-Gusmão, K., Queiroz, L.F., de Souza, R.F., Leca, F., Loup, C., and Réau, R., *J. Catal.* **219**, 59 (2003).
191. de Bellefon, C., Pollet, E., and Grenouillet, P., *J. Mol. Catal.* **145**, 121 (1999).

192. Chen, W., Xu, L., Chatterton, C., and Xiao, J., *Chem. Commun.* 1247 (1999).
193. Shi, F., Deng, Y., SiMa, T., Peng, J., Gu, Y., and Qiao, B., *Angew. Chem. Int. Ed.* **42**, 3257 (2003).
194. Nara, S.J., Harjani, J.R., Salunkhe, M.M., Mane, A.T., and Wadgaonkar, P.P., *Tetrahedron Lett.* **44**, 1371 (2003).
195. Gross, R.A., Kumar, A., and Kalra, B., *Chem. Rev.* **101**, 2097 (2001).
196. Stenzel, O., Brüll, R., Wahner, U.M., Sanderson, R.D., and Raubenheimer, H.G., *J. Mol. Catal. A Chem.* **192**, 217 (2003).
197. Einloft, S., Dietrich, F.K., de Souza, R.F., and Dupont, J., *Polyhedron* **15**, 3257 (1996).
198. Suarez, P.A.Z., Dullius, J.E.L., Einloft, S., de Souza, R.F., and Dupont, J., *Inorg. Chim. Acta.* **255**, 207 (1997).
199. Wolfson, A., Wuyts, S., De Vos, D.E., Vankelecom, I.F.J., and Jacobs, P.A., *Tetrahedron Lett.* **43**, 8107 (2002).
200. Mathews, C.J., Smith, P.J., Welton, T., White, A.J.P., and Williams, D.J., *Organometallics* **20**, 3848 (2001).
201. Magna, L., Chauvin, Y., Niccolai, G.P., and Basset, J.-M., *Organometallics* **22**, 4418 (2003).
202. Wang, B., Kang, Y.R., Yang, L.M., and Suo, S., *J. Mol. Catal. A Chem.* **203**, 29 (2003).
203. Dere, R.T., Pal, R.R., Patil, P.S., and Salunkhe, M.M., *Tetrahedron Lett.* **44**, 5351 (2003).
204. Howarth, J., James, P., and Dai, J., *J. Mol. Catal. A Chem.* **214**, 143 (2004).
205. Ranu, B.C., and Dey, S.S., *Tetrahedron* **60**, 4183 (2004).
206. Ligabue, R.A., Dupont, J., and de Souza, R.F., *J. Mol. Catal. A Chem.* **169**, 11 (2001).
207. Leroy, E., Huchette, D., Mortreux, A., and Petit, F., *Nouv. J. Chim.* **4**, 173 (1980).
208. Chauvin, Y., Gilbert, B., and Guibard, I., *J. Chem. Soc. Chem. Commun.* 1715 (1990).
209. Chauvin, Y., Olivier, H., Wyrvalski, C.N., Simon, L.C., and de Souza, R.F., *J. Catal.* **165**, 275 (1997).
210. Wasserscheid, P., Gordon, C.M., Hilgers, C., Muldoon, M.J., and Dunkin, I.R., *Chem. Commun.* 1186 (2001).
211. Mathews, C.J., Smith, P.J., and Welton, T., *Chem. Commun.* 1249 (2000).
212. Mathews, C.J., Smith, P.J., and Welton, T., *J. Mol. Catal. A Chem.* **214**, 27 (2004).
213. Baudequin, C., Baudoux, J., Levillain, J., Cahard, D., Gaumont, A.-C., and Plaquevent, J.-C., *Tetrahedron Asymmetry* **14**, 3081 (2003).
214. Monteiro, A.L., Zinn, F.K., de Souza, R.F., and Dupont, J., *Tetrahedron Asymmetry* **8**, 177 (1997).
215. Zhu, Y., Carpenter, K., Ching, C.B., Bahnmueller, S., Chan, P.K., Srid, V.S., Kee, L.W., and Hawthorne, M.F., *Angew. Chem. Int. Ed.* **42**, 3792 (2003).
216. Liu, F., Abrams, M.B., Baker, R.T., and Tumas, W., *Chem. Commun.* 433 (2001).
217. Zhao, D., Dyson, P.J., Laurenczy, G., and McIndoe, J.S., *J. Mol. Catal. A Chem.* **214**, 19 (2004).
218. Scheeren, C.W., Machado, G., Dupont, J., Fichtner, P.F.P., and Texeira, S.R., *Inorg. Chem.* **42**, 4738 (2003).
219. Howarth, J., *Tetrahedron Lett.* **41**, 6627 (2000).
220. Laszlo, J.A., and Compton, D.L., *J. Mol. Catal. B Enzyme* **18**, 109 (2002).
221. Li, Z., and Xia, C.G., *Tetrahedron Lett.* **44**(10), 2069 (2003).
222. Li, Z., Xia, C.G., and Ji, M., *Appl. Catal. A General* **252**, 17 (2003).
223. Lenz, R., and Ley, S.V., *J. Chem. Soc. Perkin Trans.* **1**, 3291 (1997).
224. Hinnen, B., and Ley, S.V., *J. Chem. Soc. Perkin Trans.* **1**, 1907 (1997).
225. Dijkstra, A., Gonzales, A.M., Mairta, A., Payaras, I., Arends, I.W.C.E., and Sheldon, R.A., *J. Am. Chem. Soc.* **123**, 6826 (2001).
226. Welton, T., *Chem. Rev.* **99**, 8 (1999).
227. Howarth, J., *Tetrahedron Lett.* **41**, 6627 (2000).
228. Owens, G.S., and Abu-Omar, M.M., *Chem. Commun.* 1165 (2000).
229. Gaillon, L., and Bedioui, F., *Chem. Commun.* 1458 (2001).
230. Li, Z., Xia, C.G., and Xu, C.Z., *Tetrahedron Lett.* **44**, 9229 (2003).
231. Meunier, B., *Chem. Rev.* **92**, 1411 (1992).
232. Srinivas, K.A., Kumar, A., and Chauhan, S.M.S., *Chem. Commun.* 2456 (2002).
233. Vanrheenen, V., Kelly, R.C., and Cha, D.Y., *Tetrahedron Lett.* **17**, 1973 (1976).
234. Yanada, R., and Takemoto, Y., *Tetrahedron Lett.* **43**, 6849 (2002).

235. Wasserscheid, P., and Eichmann, M., *Catal. Today* **66**, 309 (2001).
236. Simon, L.C., Dupont, J., and de Souza, R.F., *Appl. Catal. A Gen.* **175**, 215 (1998).
237. Dullius, J.E.L., Suarez, P.A.Z., Einloft, S., de Souza, R.F., Dupont, J., Fischer, J., and De Cian, A., *Organometallics* **17**, 815 (1998).
238. Silva, S.M., Suarez, P.A.Z., de Souza, R.F., and Dupont, J., *Polym. Bull.* **40**, 401 (1998).
239. Mastrorilli, P., Nobile, C.F., Gallo, V., Suranna, G.P., and Farinola, G., *J. Mol. Catal. A Chem.* **184**, 73 (2002).
240. Wasserscheid, P., Hilgers, C., and Keim, K., *J. Mol. Catal. A Chem.* **214**, 83 (2004).
241. Noda, A., and Watanabe, M., *Electrochim. Acta* **14**, 1265 (2000).
242. Carmichael, A.J., Haddleton, D.M., Bon, S.A.F., and Seddon, K.R., *J. Chem. Soc. Chem. Commun.* 1237 (2000).
243. Sarbu, T., and Matyjaszewski, K., *Macromol. Chem. Phys.* **202**, 3379 (2001).
244. Biedron, T., and Kubisa, P., *Polym. Int.* **52**, 1584 (2003).
245. Bao, W., Wang, Z., and Li, Y., *J. Org. Chem.* **68**, 591 (2003).
246. Handy, S.T., *Chem. Eur. J.* **9**, 2938 (2003).
247. Zhao, Y.L., Chen, C.F., and Xi, F., *J. Polym. Sci. Part A Polym. Chem.* **41**, 2156 (2003).
248. Nyce, G.W., Glauser, T., Connor, E.F., Möck, A., Waymouth, R.M., and Hedrick, J.L., *J. Am. Chem. Soc.* **125**, 3046 (2003).
249. Snedden, P., Cooper, A.I., Scott, K., and Winterton, N., *Macromolecules* **36**, 4549 (2003).
250. Parshall, G.W., *J. Am. Chem. Soc.* **94**, 8716 (1972).
251. Wasserscheid, P., and Waffenschmidt, H., *J. Mol. Catal. A Chem.* **164**, 61 (2000).
252. Brauer, D.J., Kottsieper, K.W., Liek, C., Stelzer, O., Waffenschmidt, H., and Wasserscheid, P., *J. Organomet. Chem.* **630**, 177 (2001).
253. Heck, R.F., and Nolley, J.P. Jr., "Palladium Reagents in Organic Synthesis." Academic Press, New York, 1985.
254. Beletskaya, I.P., and Cheprakov, A.V., *Chem. Rev.* **100**, 3009 (2000).
255. Herrmann, W.A., and Böhm, V.P.W., *J. Organomet. Chem.* **572**, 141 (1999).
256. Calò, V., Nacci, A., and Monopoli, A., *J. Mol. Catal. A Chem.* **214**, 45 (2004).
257. Bohm, V.P.W., and Hermann, W.A., *Chem. Eur. J.* **6**, 1017 (2000).
258. Park, S.B., and Alper, H., *Org. Lett.* **5**, 3210 (2003).
259. Hagiwara, H., Shimizu, Y., Hoshi, T., Suzuki, T., Ando, M., Okubo, K., and Yokoyama, C., *Tetrahedron Lett.* **42**, 4349 (2001).
260. Okubo, K., Shirai, M., and Yokoyama, C., *Tetrahedron Lett.* **43**, 7115 (2002).
261. Judeh, Z.M.A., Ching, C.B., Bu, J., and McCluskey, A., *Tetrahedron Lett.* **43**, 5089 (2002).
262. Siegfried, M.A., Hilpert, H., Rey, M., and Dreiding, A.S., *Helv. Chim. Acta* **63**, 938 (1980).
263. Mellah, M., Gmouh, S., Vaultier, M., and Jouikov, V., *Electrochem. Commun.* **5**, 591 (2003).
264. Sekiguchi, K., Atobe, M., and Fuchigami, T., *Electrochem. Commun.* **4**, 881 (2002).
265. Riisager, A., Wasserscheid, P., and van Hal, R.a.F.R., *J. Catal.* **219**(2), 452 (2003).
266. DeCastro, C., Sauvage, E., Valkenberg, M.H., and Hölderich, W.F., *J. Catal.* **196**, 86 (2000).
267. Mehnert, C.P., Mozeleski, E.J., and Cook, R.A., *Chem. Commun.* 3010 (2002).
268. Wolfson, A., Vankalecom, I.F.J., and Jacobs, P.A., *Tetrahedron Lett.* **44**, 1195 (2003).
269. Marcilla, R., Blazquez, J.A., Rodriguez, J., Pomposo, J.A., and Mecerreyes, D., *J. Polym. Sci. Part A Polym. Chem.* **42**, 208 (2004).
270. Kragl, U., Eckstein, M., and Kaftzik, N., *Curr. Opin. Biotechnol.* **13**, 565 (2002).
271. Persson, M., and Bornscheuer, U.T., *J. Mol. Catal. B Enzyme* **22**, 21 (2003).
272. Howarth, J., James, P., and Dai, J.F., *Tetrahedron Lett.* **42**, 7517 (2001).
273. Park, S., and Kazlauskas, R.J., *Curr. Opin. Biotechnol.* **14**, 432 (2003).
274. Kaar, J.L., Jesionowski, A.M., Berberich, J.A., Moulton, R., and Russell, A.J., *J. Am. Chem. Soc.* **125**, 4125 (2003).
275. Lozano, P., De Diego, T., Carrie, D., Vaultier, M., and Iborra, J.L., *Biotechnol. Prog.* **19**, 380 (2003).
276. Lozano, P., De Diego, T., Carrie, D., Vaultier, M., and Iborra, J.L., *Biotechnol. Lett.* **23**, 1529 (2001).
277. Nara, S.J., Harjani, J.R., and Salunkhe, M.M., *Tetrahedron Lett.* **43**, 2979 (2002).
278. Kielbasinski, P., Albrycht, M., Luczak, J., and Mikolajczyk, M., *Tetrahedron Asymmetry* **13**, 735 (2002).

279. Yang, Z., and Russell, A. J., in "Enzymatic Reactions in Organic Media," (A. M. P. Koskinen, and A. M. Klibanov, Eds.), pp. 43–69. Blackie Academic & Professional, London, 1996.
280. Kim, K.W., Song, B., Choi, M.Y., and Kim, M.J., *Org. Lett.* **10**, 1507 (2001).
281. Lozano, P., de Diego, T., Guegan, J.P., Vaultier, M., and Ilorra, J.L., *Biotechnol. Bioeng.* **75**, 564 (2001).
282. Itoh, T., Akasaki, E., Kudo, K., and Shirakami, S., *Chem. Lett.* 262 (2001).
283. Laszlo, J.A., and Compton, D.L., in "Ionic Liquids, Industrial Applications for Green Chemistry" (R. D. Rogers and K. R. Seddon, Eds.), p. 387. American Chemical Society, Washington, DC, 2002.
284. Laszlo, J.A., and Compton, D.L., *Biotech. Bioeng.* **75**, 82 (2001).
285. Weiss, R., Mandon, D., Wolter, T., Trautwein, A.X., Mütter, M., Bill, E., Gold, A., Jayaraj, K., and Terner, J.J., *Biol. Inorg. Chem.* **1**, 377 (1996).
286. Osman, A.M., Boeren, S., Boersma, M.G., Veeger, C., and Rietjens, C.M., *Proc. Natl. Acad. Sci. USA.* **94**, 4295 (1997).
287. Okrasa, K., Guibé-Jampel, E., and Therisod, M., *Tetrahedron Asymmetry* **14**, 2487 (2003).
288. Kitazume, T., Jiang, Z., Kasai, K., Mihara, Y., and Suzuki, M., *J. Fluorine Chem.* **121**, 205 (2003).
289. Kaftzik, N., Wasserscheid, P., and Kragl, U., *Organ. Proc. Res. Dev.* 553 (2002).
290. Kragl, U., Kaftzik, N., Schöfer, S.H., Eckstein, M., Wasserscheid, P., and Hilgers, C., *Chem. Today.* **19**, 22 (2001).
291. Schöfer, S.H., Kaftzik, N., Wasserscheid, P., and Kragl, U., *Chem. Commun.* **425**, 5 (2001).
292. Berberich, J.A., Kaar, J.L., and Russell, A.J., *Biotechnol. Prog.* **19** 1029 (2003); Laszlo, J.A., and Compton, D.L., *Biotech. Bioeng.* **75** 82 (2001).
293. Boesmann, A., Francio, G., Janssen, E., and Wasserscheid, P., *Angew. Chem. Int. Ed.* **40**, 2697 (2001).
294. Brennecke, J.F., *J. Am. Chem. Soc.* **124**, 10276 (2002).
295. Swatloski, R., Visser, A.E., Reichert, W.M., Broker, G.A., Farina, L.M., Holbery, J.D., and Rogers, R.D., *Chem. Commun.* 2070 (2001).
296. Zhang, S., and Zhang, Z.C., *ACS Fuel Division Preprints.* **47**(2), 449 (2002).
297. Eckstein, M., and Kaftzik, N., *Curr. Opin. Biotechnol.* **13**, 565 (2002).
298. Jastorff, B., Stormann, R., Ranke, J., Molter, K., Stock, F., Oberheitmann, B., Hoffmann, J., Nuchter, M., Ondruschka, B., and Filser, J., *Green Chem.* **5**, 136 (2003).
299. Pernak, J., Sobaszekiewicz, K., and Mirskw, I., *Green Chem.* 52 (2003).
300. Fadeev, A.G., and Meagher, M.M., *Chem. Commun.* 295 (2001).

# Optimization of Alkaline Earth Metal Oxide and Hydroxide Catalysts for Base-Catalyzed Reactions

A. CORMA and S. IBORRA

*Instituto de Tecnología Química CSIC-UPV, Universidad Politécnica de Valencia, Avda. de los Naranjos s/n, 46023 Valencia, Spain*

This review is a summary of the work done and potential opportunities for inexpensive and easily accessible base catalysts, such as alkaline earth metal oxides and hydroxides, as well as alkali metals and oxides supported on alkaline earth metal oxides. Preparation methods of these materials, as well as characterization of basic sites are reported. An extensive review of their catalytic applications for a variety of organic transformations including isomerization, carbon–carbon and carbon–oxygen bond formation, and hydrogen transfer reactions is presented.

**Abbreviations:**  $a_B^-$ , activity of the base; *AV*, anion vacancy; *CS*, Claisen–Schmidt; *DMSO*, dimethyl sulfoxide; *DNB*, 1, 2-dinitrobenzene; *DTA*, differential thermal analysis; *DTG*, differential thermal gravimetric; *EBH*, 5-ethylidenebicyclo-[2.2.1]-hept-2-ene; *EPR*, Electrón paramagnetic resonance; *F*, neutral bulk F center consisting of two electrons trapped in anion vacancy in oxides;  $F^+$ , positively charged bulk F center consisting of one electron trapped in anion vacancy in oxides; *IMO*, Isomesityl oxide; *IP*, isophorone; *IR*, infrared; *MBOH*, 2-methyl-3-buten-2-ol; *MEG*, 3-ethylidene-3-methylglutaric acid di-methyl ester; *MO*, mesityl oxide; *MPVO*, Meerwein–Pondorff–Verley and Oppenauer; *OCM*, oxidative coupling of methane; *TBMPHE*, 2, 6-di-*t*-butyl-4-methylphenol; *TEMPO*, 2, 2, 6, 6-tetramethyl-1-piperidinyloxy; *TG*, thermal gravimetric; *TPD*, temperature-programed desorption; *VBH*, 5-vinylbicyclo-[2.2.1]-hept-2-ene; *W–H*, Wittig–Horner; *wt%*, weight percentage; *XANES*, X-ray absorption near-edge structure; *XPS*, X-ray photoelectron spectroscopy; *XRD*, X-ray diffraction.

## I. Introduction

It is rewarding to see that researchers in catalysis are increasingly paying attention to solid base catalysts (1–4). Their work is leading to the discovery and, especially, to the improvement of such catalysts, many of which perform better than conventional homogeneous catalysts, such as hydroxides of alkali metals typified by NaOH. Although the recent research is increasing our fundamental knowledge of base catalysis, its reflection on industrial catalysis is still limited. No doubt it is difficult to compete economically with NaOH; many existing processes are well suited to operation with this catalyst, with appropriate treatment of the effluents. Thus, the practitioners of many of today's processes perceive no economic incentive

for replacement of NaOH by solid catalysts, which besides being relatively expensive, suffer from deactivation and the required regeneration.

It appears to us that the way forward to further industrial application of solid base catalysts may emerge from the discovery of unusual selectivity effects or new reactions that require well-balanced base and acid–base pair sites with relatively inexpensive solid catalysts that last long enough to process large quantities of reactants per unit mass of catalyst.

Thus, we focus in this review on a series of relatively inexpensive and easily accessible base catalysts, such as alkaline earth metal oxides and hydroxides, as well as alkali metals and oxides supported on alkaline earth metal oxides. We believe that the possibilities offered by solid base catalysts can be markedly enhanced if more researchers working in materials synthesis were to take these as the starting point and develop new synthesis methods to prepare well structured, high-surface-area alkaline earth materials. Building from this foundation, the present review is intended as a summary of what has been done and potential opportunities. Our hope is that this review will serve as a starting point for experts in catalyst synthesis, who, after seeing the many potential catalytic applications of these materials, will become interested in expanding their possibilities by developing the materials further.

## II. Surface Basicity and Base Strength of Alkaline Earth Metal Oxides

The surface basicity of a solid catalyst can be defined in a way analogous to that applied to conventional bases. Thus, a surface Lewis base site is one that is able to donate an electron pair to an adsorbed molecule. If we take the definition of surface basicity in a more general way, it could be said that the active surface corresponds to sites with relatively high local electron densities. This general definition will include not only Lewis basicity but also single electron donor sites. We emphasize that the literature of heterogeneous catalysis often reports that both single-electron and electron-pair donor sites exist on basic catalysts.

Concerning the nature of Lewis basic sites, little work has been done to establish general rules and models, except for alkaline earth metal oxides and zeolites. With respect to the former, i.e., the nature of oxygen Lewis basic sites on alkaline earth metal oxide catalysts, a charge-density model predicts that the strength of the sites decreases in the order:  $\text{O}^{2-} > \text{OH}^- > \text{H}_2\text{O} > \text{H}_3\text{O}^+$ .

In the case of oxide catalysts or alkali metal-doped oxide catalysts, basic surface sites can be generated by decarboxylation of a surface metal carbonate; exchange of hydroxyl hydrogen ions by electropositive cations; thermal dehydroxylation of the catalyst surface; condensation of alkali metal particles on the surface; and reaction of an alkali metal with an anion vacancy (AV) to give  $\text{F}^+$  centers (e.g.,  $\text{Na} + \text{AV} \rightarrow \text{Na}^+ + \text{e}^-$ ).

Coluccia *et al.* (5) proposed a model of the MgO surface that shows Mg–O ion pairs of various coordination numbers (Fig. 1). MgO has a highly defective surface structure showing steps, edges, corners, kinks, etc., which provide  $\text{O}^{2-}$  sites of low



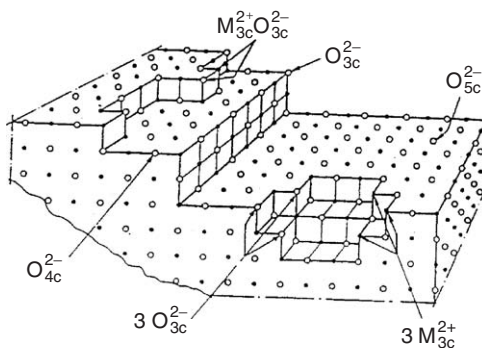


FIG. 1. Model of MgO surface (5).

coordination numbers. These low-coordinated  $O^{2-}$  sites ( $O^{2-}_{(5c)}$  on faces,  $O^{2-}_{(4c)}$  on edges, and  $O^{2-}_{(3c)}$  on corners) are expected to be responsible for the presence of basic sites with different strengths. Base strength of surface  $O^{2-}$  sites increases as the coordination number becomes lower. Thus,  $Mg^{2+}_{(3c)}O^{2-}_{(3c)}$  sites are the most reactive, adsorb  $CO_2$  most strongly, and should be able to dissociate molecules with  $pK_a$  values higher than 30, such as ammonia, ethene, and benzene (6).

In the case of oxides of alkali metals, the basic sites able to abstract protons from a reactant molecule are those associated with  $O^{2-}-M^{2+}$  ion pairs and OH groups, whereas the adjacent metal ion acts to stabilize the resultant anionic intermediate. However, the surfaces of these materials, when they are in contact with the atmosphere, are covered with  $CO_2$ , water, and in some cases oxygen. Because the surface basic sites become exposed when the oxide is pre-treated at high temperature, an important catalyst preparation variable in the case of alkaline earth metal oxides is the treatment temperature. The influence of temperature on the generation of basic sites is related to the progressively lower surface coordination number that results from increasing the treatment temperature. This temperature certainly influences not only the total number of such sites, but also the base site strength (7). Thus, as the treatment temperature increases, the molecules adsorbed on the surface are successively desorbed according to the strength of the interaction with the basic sites. The basic sites that appear on the surfaces by treatment at high temperatures have to be stronger than those created at lower temperatures.

According to Hattori (7), evacuation of MgO at high temperature (673–1273 K) leads to the appearance of three different types of basic sites exposing  $O^{2-}$  ions with different coordination numbers. The existence of sites with different structures, and therefore with different base strengths, is reflected in the variation of the catalytic activities for various reactions (8) as a function of the catalyst treatment temperature. The catalytic activity increases with increasing treatment temperature to give maximum activities at different temperatures, depending on the type of reaction (2). In a classical investigation, Tanabe (4) presented the effect of treatment temperature on the total basicity and reactivity of CaO (Fig. 2).

It is notable that the presence of basic sites with  $H_- \leq 26.5$  have been claimed when calcining  $CaCO_3$  at 1173 K and  $Sr(OH)_2$  at 1123 K (9).

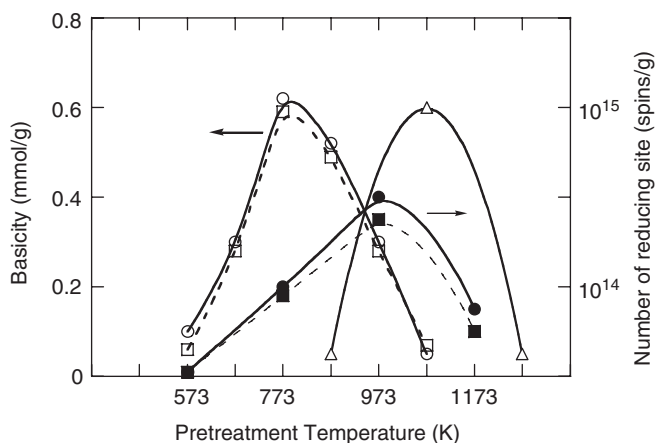


FIG. 2. Dependence of basicity and catalytic activity on calcination temperature of CaO: (○) Basic sites with  $H_- > 15$ ; (□) relative activity for Tishchenko reaction of benzaldehyde; (●) number of reducing sites; (■) activity for styrene polymerization; and (Δ) relative propene hydrogenation activity (4).

According to the model presented above, different types of basic sites of different nature and base strength exist on the surfaces of alkaline earth metal oxides. Therefore, these materials show heterogeneity with respect to the basic sites and with respect to catalysis. This statement implies that if several reactions compete that require basic sites of different strength, two MgO samples with different relative populations of sites  $O_{(5c)}^{2-}$ ,  $O_{(4c)}^{2-}$ , and  $O_{(3c)}^{2-}$  should give different selectivities. It becomes apparent that the population of basic sites and consequently the activity and selectivity of the catalyst can also be changed by control of the size and shape of the MgO crystals through the preparation procedure, because this controls the relative number of atoms located at corners, terraces or faces, i.e.,  $O_{(3c)}^{2-}$ ,  $O_{(4c)}^{2-}$ , and  $O_{(5c)}^{2-}$ .

If a correlation between the nature of the various sites and their catalytic activities and/or selectivities has to be established, methods for characterizing the different basicities will be required. Therefore, in the following sections, we discuss the methods for preparation of alkaline earth metal oxides as well as the principal characterization techniques used to evaluate their basicities.

### III. Synthesis of High-Surface-Area Alkaline Earth Metal Oxides

Alkaline earth metal oxides are generally prepared by thermal decomposition of alkaline earth compounds, such as hydroxides, chlorides, sulfates, and carbonates.

The most general methodology followed to prepare alkaline earth metal oxides as basic catalysts consists of the thermal decomposition of the corresponding hydroxides or carbonates in air or under vacuum. Decomposition of hydroxides is frequently used to prepare MgO and CaO, whereas BaO and SrO are prepared from the corresponding carbonates as precursor salts. Preparation of alkaline earth metal

oxides with high surface areas is especially important when the oxide has to be used as basic catalyst, because the catalytic activity will depend on the number and strength of the basic sites accessible to the reactant molecules, which is dependent on the accessible surface area.

From the available data, only MgO has been synthesized with high surface areas (usually between 130 and 300 m<sup>2</sup>/g) whereas for CaO, SrO, and BaO only very low surface areas have been achieved (around 60, 10, and 2 m<sup>2</sup>/g, respectively) (10–12). For the preparation of high-surface-area MgO, the decomposition of magnesium salts such as oxalates, hydroxycarbonates, sulfates, etc. has been selected frequently, with the thermal decomposition of Mg(OH)<sub>2</sub> being the most common method. Magnesium hydroxide precursors are obtained by treating commercial MgO (which usually has a low surface area, 10–40 m<sup>2</sup>/g) with water for several hours (13–15). In other cases, Mg(OH)<sub>2</sub> is prepared by precipitation starting from aqueous solutions of magnesium salts (MgNO<sub>3</sub>, MgSO<sub>4</sub>) and alkaline aqueous solutions (KOH or NH<sub>4</sub>OH) as precipitating agents (16–20).

A variety of variables influence the final surface area of the resultant MgO. Thus, the surface area is strongly dependent on the nature of the precursor salt (20–22), (e.g., magnesium hydroxide, carbonate, hydroxycarbonate, oxalate, etc.). Matsuda *et al.* (23) investigated the preparation of MgO starting from three different precursors, namely, magnesium hydroxycarbonate (MgCO<sub>3</sub>–Mg(OH)<sub>2</sub>), magnesium oxalate, and magnesium hydroxide, each of which was decomposed at 823 K for 20 h in air. The authors reported surface areas of 59, 140, and 85.7 m<sup>2</sup>/g for the MgO obtained from the hydroxycarbonate, oxalate, and Mg(OH)<sub>2</sub>, respectively. On the other hand, MgO prepared under identical conditions from different samples of magnesium hydroxide showed different properties (24–27). For instance, Bancquart *et al.* (28) reported that MgO prepared by decomposition of Mg(OH)<sub>2</sub> synthesized by precipitation from Mg(NO<sub>3</sub>)<sub>2</sub> with NH<sub>4</sub>OH and calcined in air at 723 K for 12 h, had a surface area of 150 m<sup>2</sup>/g, whereas when the Mg(OH)<sub>2</sub> was prepared by hydration of a commercial MgO, the surface area was lower (102 m<sup>2</sup>/g). Matsuda *et al.* (23) prepared Mg(OH)<sub>2</sub> by the alkaline precipitation method starting from various magnesium salts, such as nitrate, sulfate, chloride, and acetate. They found that the final surface area of the MgO depended on the nature of the starting salt used to prepare the Mg(OH)<sub>2</sub>. Table I shows that Mg(OH)<sub>2</sub> prepared from the acetate decomposes to give the MgO with the highest surface area, followed by nitrate and sulfate, whereas MgCl<sub>2</sub> gives samples with very low surface areas.

TABLE I

*Influence of the Salt Used to Prepare Mg(OH)<sub>2</sub> Precursor on the Surface Area of the Resultant MgO (23)*

Magnesium salt precursor	Surface area of MgO (m <sup>2</sup> /g)
Mg(NO <sub>3</sub> ) <sub>2</sub>	85.7
MgSO <sub>4</sub>	86.3
MgCl <sub>2</sub>	19.0
Mg(CH <sub>3</sub> COO) <sub>2</sub>	117

In the preparation of MgO from chloride salt precursors, it was observed that the presence of any residual chloride had a detrimental effect on the surface area of the resultant MgO (29). This effect has been related to the ability of chloride to aid sintering and grain growth in the oxide (30).

The higher surface areas of the MgO samples obtained by the decomposition of oxalate and of the  $\text{Mg}(\text{OH})_2$  prepared from magnesium acetate (Table I) are attributed to the evolution of gases during the decomposition of organic groups in magnesium salts. It was later reported (31) that the decomposition of the oxalate at 873 K for 5 h under vacuum gives MgO with a surface area of  $474 \text{ m}^2/\text{g}$ . Conditions of the thermal decomposition such as pre-treatment time of the sample, temperature, gas environment, and outgassing procedures strongly affect the sample morphology and surface uniformity of MgO (25).

Potential parameters influencing the preparation of MgO by thermal decomposition of magnesium hydroxide prepared from various magnesium salts have been thoroughly investigated by Choudhary *et al.* (18). These authors also found that the surface area and basicity of MgO obtained from magnesium hydroxide strongly depend on the magnesium salt precursor, precipitating agent, precipitation conditions (concentration of magnesium salt, pH, temperature), mode of mixing, aging period, and calcination temperature (873–1173 K). Analysis of the magnesium hydroxide decomposition process, using TG, DTG, and DTA techniques showed that the conditions of preparation of magnesium hydroxide strongly influence the thermal decomposition in the preparation of active MgO (19).

Several researchers have examined the possibility of synthesizing MgO powders from liquid precursors by a sol–gel route involving the hydrolysis and condensation of magnesium ethoxide (32–35). Interesting results were reported by Klabunde *et al.* (36–38) using a method involving the formation of  $\text{Mg}(\text{OH})_2$  gel (from  $\text{Mg}(\text{OCH}_3)_2$  in a methanol–toluene solvent mixture), which was submitted to a supercritical drying process in an autoclave giving a  $\text{Mg}(\text{OH})_2$  aerogel. This material had a surface area of  $1000 \text{ m}^2/\text{g}$  and a crystallite size of 3.5 nm. Heat treatment of this precursor at 773 K under vacuum yielded the dehydrated MgO with a  $500 \text{ m}^2/\text{g}$  surface area and 4.5 nm crystallite size.

#### IV. Characterization of the Number and Strength of Basic Sites

The surface acidity of solids has been investigated in much detail by a large number of physicochemical techniques, but determination of basicity in solids is a more difficult task and has been investigated much less. Methods for characterizing basic surfaces were reviewed by Tanabe (39), Forni (40), and, more recently, Hattori (2), and Barthomeuf (41). In broad terms, the main techniques that are used frequently are the following: titration, spectroscopic investigations, and test reactions. These methods, in conjunction with adsorption and temperature-programmed desorption (TPD) of probe molecules, give information about the nature, number, strength, and reactivity of basic sites on solid catalysts.

### A. TITRATION METHODS

The number of basic sites of different strengths can be evaluated by titration using organic acids (benzoic acid, acrylic acid, phenol, etc.) in water or organic solvents (42,43). The general methodology involves suspension of the solid in a solvent such as benzene or cyclohexane in the presence of a Hammett indicator (BH). The indicator is adsorbed on the catalyst in its conjugated base form ( $B^-$ ), which is then titrated with the organic acid. The amount of organic acid required is a measure of the number of sites that have a base strength corresponding to the  $pK_a$  value of the indicator.

The strength of the basic sites can be expressed on a scale given by the  $H_-$  function defined by the equation

$$H_- = pK_a + \log[B^-]/[BH],$$

where  $pK_a$  is the  $pK_a$  value of the indicator BH, and  $[BH]$  and  $[B^-]$  are the concentration of the indicator and its conjugated base, respectively. This method has been widely applied to assess the basicities of a variety of oxides and hydroxides. For instance, Take *et al.* (9) reported that MgO and CaO have basic sites stronger than  $H_- = 26$ , whereas SrO is less basic ( $H_- < 18$ ). Matsuda *et al.* (23) measured the basicity of various MgO samples prepared from six different kinds of magnesium salts, finding that MgO samples prepared from magnesium chloride, sulfate, or carbonate have base strengths lower than  $H_- = 22$ , whereas MgO samples prepared from nitrate, oxalate, or acetate have basic sites characterized by values of  $H_-$  exceeding 27.

However, although this method has been applied widely, the use of Hammett indicators is highly controversial, especially when they are used to give quantitative results. For instance, one has to take into account the fact that an indicator can change color by reactions different from acid-base reactions. Moreover, in some cases the titration solution may dissolve the surface of the solid catalyst. In both cases, the number of basic sites will be overestimated. To summarize, although the Hammett indicators are still used for evaluating the basicity of solids, researchers must be aware that this technique is intrinsically inappropriate. Indeed, although the use of the  $H_-$  function is adequate for homogeneous solutions of bases, neither  $a_B$  nor the surface basicity function  $H_-$  has an explicit physical meaning for solids. Therefore, the application of Hammett indicators to characterize the catalytic properties of solid bases can be misleading.

### B. SPECTROSCOPIC METHODS

Techniques such as X-ray photoelectron spectroscopy (XPS) and electron paramagnetic resonance (EPR) spectroscopy, have been applied to determine the basic properties of solids (2). The usefulness of XPS is based on the fact that the electron-pair donating ability of a solid base may be directly related to the  $O_{1s}$  binding energy. A good correlation between effective oxygen charge and the  $O_{1s}$  binding energy was found for single metal oxides (44). EPR, combined with the adsorption

of probe molecules such as tetracyanoethylene and perylene, has been used to measure electron-donor sites on MgO and Al<sub>2</sub>O<sub>3</sub>, respectively (45,46). Two types of electron-donor sites were observed on MgO, depending on the treatment temperature. After treatment at lower temperatures, the basic sites are hydroxyl groups, whereas after treatment at higher temperatures, the basic sites are the Lewis basic sites O<sup>2-</sup>. This result is important and is taken into account below in the assessment of catalytic results when a goal is to determine the nature of the basic active sites.

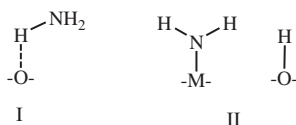
Among the spectroscopic techniques, one of the most widely used to characterize the basic properties of alkaline earth metal oxides is infrared (IR) spectroscopy of adsorbed probe molecules (41,47–49); this is described below.

### B.1. Infrared Spectroscopy of Adsorbed Probe Molecules

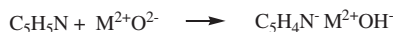
Adsorption of a specific probe molecule on a catalyst induces changes in the vibrational spectra of surface groups and the adsorbed molecules used to characterize the nature and strength of the basic sites. The analysis of IR spectra of surface species formed by adsorption of probe molecules (e.g., CO, CO<sub>2</sub>, SO<sub>2</sub>, pyrrole, chloroform, acetonitrile, alcohols, thiols, boric acid trimethyl ether, acetylenes, ammonia, and pyridine) was reviewed critically by Lavalley (50), who concluded that there is no universally suitable probe molecule for the characterization of basic sites. This limitation results because most of the probe molecules interact with surface sites to form strongly bound complexes, which can cause irreversible changes of the surface. In this section, we review work with some of the probe molecules that are commonly used for characterizing alkaline earth metal oxides.

CO, ammonia, and pyridine are suitable probe molecules for characterizing structural defects on metal oxides that are strongly basic. CO acts as a Lewis acid, interacting at low temperature with basic O<sup>2-</sup> sites to lead to the formation of (CO<sub>2</sub>)<sup>2-</sup> species on the surface. Such an interaction has been observed on alkaline earth-metal oxides evacuated at high temperature (51,52). Moreover, results characterizing adsorption of CO on lanthana (53) indicate that the strongest basic sites responsible for CO adsorption may correspond to structural defects, such as edges and steps, where the oxygen ions have low coordination numbers.

Ammonia and pyridine are frequently used as probe molecules for the characterization of acidic surfaces, but they also adsorb on strongly basic sites. Tsyganenko *et al.* (54) proposed various species resulting from NH<sub>3</sub> adsorption on basic solids (Scheme 1). The formation of species I corresponds to hydrogen bonding to a basic surface oxygen, and species II, formed by dissociation to give NH<sub>2</sub><sup>-</sup> and hydroxyl species, involves an acid–base site. Such adsorption requires sites of the greatest coordinative unsaturation, such as M<sub>(3c)</sub><sup>2+</sup>O<sub>(3c)</sub><sup>2-</sup>, which are those located at the edges of the crystals.



SCHEME 1.



SCHEME 2.

Species I were observed on MgO and CaO, and species II were observed on MgO, CaO, and SrO as well as on hydroxylated MgO (55). They were monitored by the  $\text{NH}_2^-$  absorption band in the region near  $1550\text{ cm}^{-1}$  (55–57). Dissociative chemisorption has also been reported for pyridine on  $\text{M}^{2+}\text{O}^{2-}$  pairs in low coordination on alkaline earth metal oxides (Scheme 2).

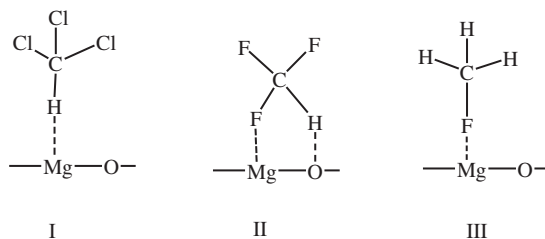
It was found that proceeding in the series from MgO to CaO to SrO, the ease of formation of  $\text{C}_5\text{H}_4\text{N}^-$  ions increased, in agreement with the increasing basicity of the oxides (58).

Acetonitrile has been shown to be a particularly useful probe molecule, being capable of co-coordinating to Lewis or Brønsted acid and base sites. On acid sites,  $\text{CH}_3\text{CN}$  forms N-bonded  $\sigma$  complexes, and the  $\nu(\text{CN})$  wavenumber increases. On the other hand, the hydrogen atoms of the methyl group present a proton-donor character, so that the interaction with basic sites leads to the formation of carbanion species  $^-\text{CH}_2\text{CN}$  that occur on Lewis sites and evidence the strong basicity of the  $\text{O}^{2-}$  sites. Acetonitrile can also interact with Brønsted basic sites, forming anionic acetamide species, as a result of the nucleophilic attack of a surface  $\text{OH}^-$  group on a coordinated acetonitrile molecule (59). However, one must be aware that the participation of basic  $\text{O}^{2-}$  sites in the formation of acetamide species cannot be ruled out (50). Accordingly, acetonitrile has been very useful for characterization of various metal oxides (58).

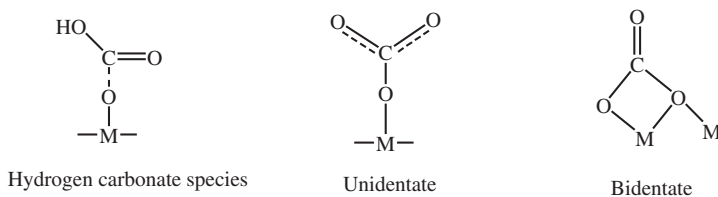
Monofluoro-, trifluoro-, and trichloromethane, as well as acetylene and methylacetylene, also undergo hydrogen-bonding interactions with Lewis basic sites. The experimental frequency shifts of the C–H stretching modes of these CH acids can be correlated with the hydrogen-bond acceptor strength of the  $\text{O}^{2-}$  and hence regarded as a measure of the strength of the basic sites. A detailed investigation carried out by Huber and Knözinger (60) of the adsorption of these types of molecules on MgO showed that the adsorption of  $\text{CHCl}_3$  and  $\text{CDCl}_3$  results in the formation of a type I complex, with the CH (CD) mode being shifted to lower wave numbers. A red shift of  $36\text{ cm}^{-1}$  was observed for the hydrogen-bonded  $\text{O}^{2-}\text{H}-\text{CCl}_3$  complex. However, the stronger CH acid trifluoromethane forms an adsorption complex (type II) in which hydrogen interacts with the basic oxygen sites, and simultaneously one of the fluorine atoms is associated with an  $\text{Mg}^{2+}$  site. Adsorbed  $\text{CH}_3\text{F}$  on MgO retains the  $\text{C}_{3v}$  symmetry, and therefore the most likely adsorption complex is  $\text{Mg}^{2+}\text{F}-\text{CH}_3$  (type III) (Scheme 3).

The spectral behavior of CO bonded to metal atoms (metal carbonyls) has been used to characterize the surface of solids (61). For instance, it is known that metal carbonyl interacts with surface site of metal oxides and zeolites to form a Lewis-type adduct where a CO ligand of the metal carbonyl interacts (via the oxygen atom) with surface OH groups or with co-ordinatively unsaturated metal ions (surface Lewis acid sites) (62,63). On the other hand, thermal treatment of the metal carbonyl support adducts lead to loss of CO with formation of subcarbonyls, which are anchored to the support (64,65). Papile *et al.* (66) reported the characterization





SCHEME 3.



SCHEME 4.

of rhenium subcarbonyls on MgO powder by IR spectroscopy, which were prepared by adsorption and decomposition of  $\text{Re}_2(\text{CO})_{10}$ . The presence of different surface ligands bonded to the rhenium as  $\text{O}^{2-}$  (via the  $\nu_{\text{CO}}$  frequencies) were identified in highly dehydroxylated MgO samples, whereas on MgO hydroxylated samples, surface ligands corresponding to HO- groups were detected. Surface subcarbonyl species of the type  $\text{Re}(\text{CO})_3\{\text{OMg}\}_3$ ,  $\text{Re}(\text{CO})_3\{\text{HOMg}\}_3$ ,  $\text{Re}(\text{CO})_3\{\text{HOMg}\}_2\{\text{OMg}\}$  (where the braces denote groups terminating the bulk MgO) were identified on the different MgO samples.

$\text{CO}_2$  is one of the probe molecules that have been used extensively to characterize the basic centers of the surfaces of alkali oxides and mixed oxides.  $\text{CO}_2$  is adsorbed in various forms, and IR spectroscopy becomes a highly informative technique to probe the nature of surface sites involved in the adsorption (48,67). Thus, formation of hydrogen carbonate species (Scheme 4) is characteristic of the presence of basic hydroxyl groups, but  $\text{CO}_2$  adsorption on Lewis sites leads to the formation of unidentate and bidentate carbonate species. In the adsorption state of unidentate carbonate, only the surface oxygen atoms participate, whereas in the adsorption state involving the bidentate species, the participation of a metal ion is required. Bidentate and unidentate carbonates have been assigned to  $\text{CO}_2$  adsorbed on sites with intermediate and high base strengths, respectively (68).

## B.2. Thermal Methods of Adsorbed Probe Molecules

In general, spectroscopic techniques and, in particular IR spectroscopy of adsorbed probe molecules such as the ones mentioned above, provide information about the nature of the basic sites on oxide surfaces. However, they do not give information about the number and strength distribution of the basic sites on a solid



base catalyst. To determine the number and strength distribution of the basic sites, the spectroscopic techniques must be coupled with TPD, gravimetric (20,69), volumetric (67), and/or microcalorimetric measurements of adsorbed probe molecules. For example, calorimetric measurements accompanying adsorption of CO<sub>2</sub> have been applied extensively to investigate the basicities of solid surfaces. In these measurements, CO<sub>2</sub> adsorption is usually tracked by calorimetry and by CO<sub>2</sub> uptake. The heat of adsorption of CO<sub>2</sub> can be taken as a measure of the base strength of the adsorption sites, and a strength distribution of basic sites is obtained by using the differential heat of adsorption as a function of coverage. Except when chemisorption of CO<sub>2</sub> leads to the formation of bulk carbonates, the amount of CO<sub>2</sub> chemisorbed is considered to be a good measure of the density of basic sites.

Temperature-programmed desorption of the probe molecules is frequently used to measure the number and strength of basic sites, and the most commonly used probe molecule is CO<sub>2</sub>. According to this method, the strength of the basic sites is represented by the desorption temperature, and the peak area in the TPD plot determines the number of basic sites (13,39,48,70–72). However, although this method accounts successfully for the relative strength and number of basic sites of various catalysts for which the TPD has been measured under the same conditions, it is difficult to express the measurements of basicity in a definite scale and to determine the number of basic sites quantitatively. Thus, TPD measurements of alkaline earth metal oxides carried out under the same conditions showed that the strength of basic sites increases in the order MgO < CaO < SrO < BaO, whereas the number of basic sites per gram of catalyst increases in the order BaO < SrO < MgO < CaO (73).

Data representing the number of basic sites on MgO have been reported by various authors on the basis of gravimetric, volumetric, and CO<sub>2</sub>-TPD techniques. Relying on volumetric techniques based on the measurement of the irreversible adsorption of CO<sub>2</sub> at room temperature using the double-isotherm method (14), Di Cosimo *et al.* (74) reported that the number of basic sites on MgO was 1.83 μmol/m<sup>2</sup>. This value is close to that reported by Auroux and Gervasini (67), 1.45 μmol/m<sup>2</sup>, whereas Philipp and Fujimoto (75) found a value of 4.31 μmol/m<sup>2</sup> using a similar gaseous volumetric technique. By the method of CO<sub>2</sub> TPD, the number of basic sites measured for MgO is higher than that obtained by the double-isotherm method because of the different evacuation procedures used in the latter method. Thus, Mackenzie *et al.* (76) reported a value of 4.4 μmol/m<sup>2</sup>; Kurokawa *et al.* (77) reported 2.4 μmol/m<sup>2</sup>; and Diez *et al.* (74) 2.33 μmol/m<sup>2</sup>. In summary, the values reported are generally in good agreement, although differences in sample preparation procedures and the characterization techniques can give different numbers of basic sites.

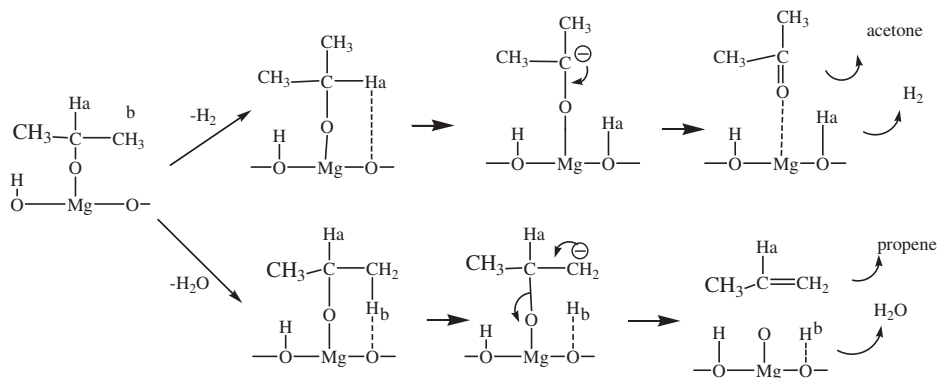
### C. CATALYTIC TEST REACTIONS

Several catalytic test reactions have been used for indirect characterization of acid and base properties of solids (78). Among them, decomposition of alcohols such as 2-propanol (79,80), 2-methyl-3-butyn-2-ol (81,82), 2-methyl-2-butanol (83), cyclohexanol (84), phenyl ethanol (85), and *t*-butyl alcohol (86) have been investigated. In

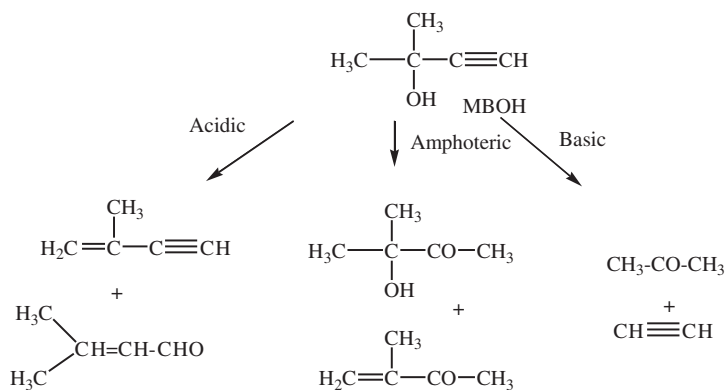
particular, the decomposition of 2-propanol is a reaction that has been employed extensively to investigate the acid–base properties of catalysts containing alkaline earth metals (74,87–90). This alcohol undergoes three types of competitive reactions when contacted with an acidic or basic solid: (i) intramolecular dehydration yielding propene and water, (ii) intermolecular dehydration giving isopropyl ether and water, and (iii) dehydrogenation to give acetone and hydrogen. Ai (91) claimed that the dehydration of 2-propanol takes place exclusively on acid sites, whereas its dehydrogenation involves both acidic and basic sites. Dehydration and dehydrogenation can proceed through different mechanisms, depending on the acid–base nature of the catalysts. All the proposed mechanisms for the decomposition of 2-propanol rely on the same assumption, namely, that the interaction is between the alcohol and the acid–base pair of the catalyst (74,86,90,92). When the catalyst has a larger number of acidic sites, decomposition of 2-propanol leads predominantly to dehydration through an E1 mechanism, whereas dehydrogenation takes place to a limited extent only via an E1cB mechanism. In solids with a large number of basic sites, it was suggested that both dehydrogenation and dehydration take place via an E1cB mechanism (71,90,93), whereby the former reaction predominates over the latter. The interaction between a basic site and an alcohol molecule causes the abstraction of a proton from the OH group, forming a surface alkoxide intermediate. The subsequent abstraction of  $H_\alpha$  or  $H_\beta$  from the 2-propoxide anion intermediate leads to ketone or alkene formation, respectively (Scheme 5). Predominant formation of either ketone or alkene will therefore depend on the relative acidities of the groups incorporating  $H_\alpha$  and  $H_\beta$  protons and on the acid–base properties of the solid.

Although the specific role of each type of center (acid or base) in each process (dehydration–dehydrogenation) is still only incompletely elucidated, many authors have correlated the initial rates of dehydration and dehydrogenation with the acidity and basicity, respectively, of the solid. Thus, the number of basic sites has been correlated with the rate constants for dehydrogenation or with the ratio of the rate constants for dehydrogenation and dehydration (74,80,89,90,94).

However, because the dehydrogenation to acetone can also occur on redox sites and the dehydration reaction can also take place on strongly basic catalysts through



SCHEME 5.



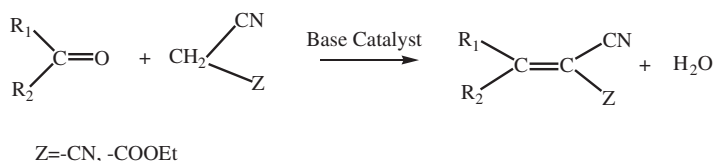
SCHEME 6.

an E1cB mechanism (93), researchers have sought other more suitable test reactions for the characterization of basic sites, such as the decomposition of 2-methyl-3-butyn-2-ol (MBOH) (17,82). Indeed, in the presence of basic sites (Lewis or Brønsted), MBOH decomposes into acetone and acetylene. This decomposition reaction is catalyzed only by basic sites, whereas acidic or amphoteric surfaces lead to completely different reaction products (Scheme 6).

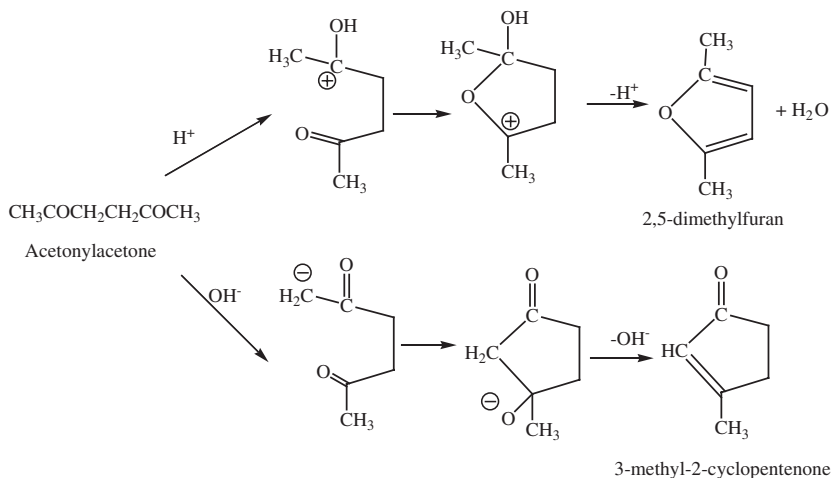
Aramendia *et al.* (22) investigated three separate organic test reactions such as, 1-phenyl ethanol, 2-propanol, and 2-methyl-3-butyn-2-ol (MBOH) on acid–base oxide catalysts. They reached the same conclusions about the acid–base characteristics of the samples with each of the three reactions. However, they concluded that notwithstanding the greater complexity in the reactivity of MBOH, the fact that the different products could be unequivocally related to a given type of active site makes MBOH a preferred test reactant. Unfortunately, an important drawback of the decomposition of this alcohol is that these reactions suffer from a strong deactivation caused by the formation of heavy products by aldolization of the ketone (22) and polymerization of acetylene (95). The occurrence of this reaction can certainly complicate the comparison of basic catalysts that have different intrinsic rates of the test reaction and the reaction causing catalyst decay.

### C.1. Knoevenagel Condensation

Because a base-catalyzed reaction involves the abstraction of a proton by the catalyst, one approach to measurement of the total number of basic sites and also the base strength distribution is to use the reactions of molecules with various  $\text{p}K_{\text{a}}$  values (96–100). For instance, the basic site distribution in calcined MgAl hydrotalcites was determined by Corma *et al.* (99), who used the Knoevenagel condensation (Scheme 7) between benzaldehyde and methylene active compounds with various  $\text{p}K_{\text{a}}$  values, i.e., ethyl cyanoacetate ( $\text{p}K_{\text{a}} = 9$ ), diethyl malonate ( $\text{p}K_{\text{a}} = 13.3$ ), and ethyl bromoacetate ( $\text{p}K_{\text{a}} = 16.5$ ). The authors found that this material has basic sites with  $\text{p}K_{\text{a}}$  values up to 16.5, although most of the basic sites



SCHEME 7.

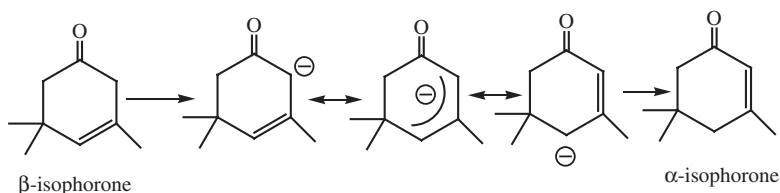


SCHEME 8.

were characterized by values in the range  $10.7 \leq \text{p}K_a \leq 13.3$ . Moreover, it was found that by increasing the Mg/Al ratio in the hydrotalcite, the number of basic sites with  $\text{p}K_a$  values between 9.0 and 13.3 increased, whereas the number of basic sites in the range 13.3–16.5 decreased.

### C.2. Acetylacetone Cyclization

Acetylacetone is a 1,4-diketone compound that can undergo both acid- and base-catalyzed intramolecular cyclization leading to very different products: furan by acid catalysis (101) and cyclopentenone by base catalysis (102) (Scheme 8). It was reported that in the presence of the acidic zeolite HZSM-5 at 623 K, acetylacetone gives 2,5-dimethyl furan in yields exceeding 97%. However, in the presence of NaZSM-5, a yield of 92.6% of 3-methyl-2-cyclopentenone was obtained (103,104). This monomolecular reaction requires a relatively high basicity, and it has been used as test reaction to confirm the basic properties of calcined hydrotalcites. Guida *et al.* (105) showed that on calcined MgAl hydrotalcites, acetylacetone gives 3-methyl-2-cyclopentenone as the only product in 65% yield after 14 h in a batch reactor at 573 K. The authors thus confirmed that for condensation reactions the condensation step is catalyzed only by the basic sites of the calcination product of the hydrotalcites.



SCHEME 9.

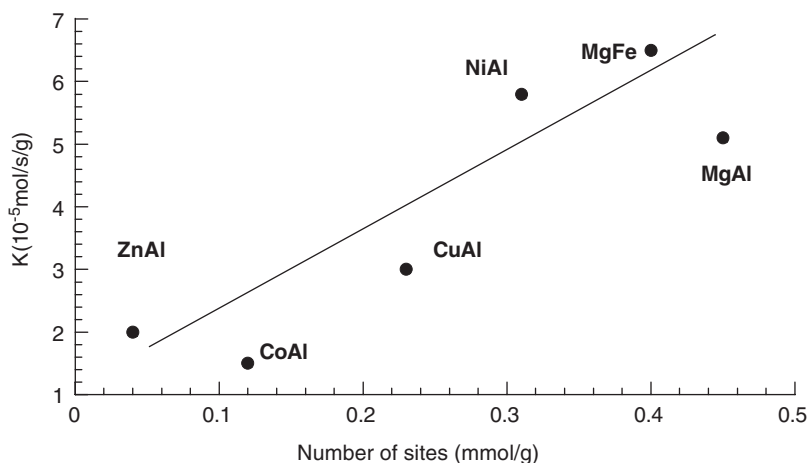


FIG. 3. Relationship between the rate constant ( $K$ ) for isophorone isomerization and the number of sites for  $\text{CO}_2$  adsorption on calcined hydrotalcites with various compositions (107).

### C.3. Isophorone Isomerization

Isomerization of  $\beta$ -isophorone to  $\alpha$ -isophorone has been represented as a model reaction for the characterization of solid bases (106,107). The reaction involves the loss of a hydrogen atom from the position  $\alpha$  to the carbonyl group, giving an allylic carbanion stabilized by conjugation, which can isomerize to a species corresponding to the carbanion of  $\alpha$ -isophorone (Scheme 9). In this reaction, zero-order kinetics has been observed at 308 K for many bases, and consequently the initial rate of the reaction is equal to the rate constant. The rate of isomerization has been used to measure the total number of active sites on a series of solid bases. Figueras *et al.* (106,107) showed that the number of basic sites determined by  $\text{CO}_2$  adsorption on various calcined double-layered hydroxides was proportional to the rate constants for  $\beta$ -isophorone isomerization (Fig. 3), confirming that the reaction can be used as a useful tool for the determination of acid–base characteristics of oxide catalysts.

## V. Stability of Anionic Intermediates

It is believed that base-catalyzed reactions occur through carbanionic intermediates. Thus, from a mechanistic viewpoint, which may also help to design better catalysts,

it is important to discuss thermodynamic (stability) and kinetic (persistence) properties of carbanionic intermediates. It is obvious that we want the carbanionic intermediate to be stable and persistent to allow the reaction to occur, but not so persistent that its average life time on the surface is so long that undesired reactions occur (including catalyst poisoning). We can influence the properties of the anionic intermediates by the choice of substituents and structural effects, solvent effects, and the catalyst.

The stabilizing influence of substituents attached directly to the carbanionic center is attributed to the polarizability of the second- or lower-row element. First-row substituents generally stabilize carbanions in aprotic media. Alkyl groups, as a rule, destabilize carbanions in protic solvents. On the other hand, substituents located far from the reactive site can stabilize an anion by inductive, polarization, and resonance effects. Conjugation may provide the strongest driving force for the stabilization of carbanions. This effect can work strongly to render a carbon acid more acidic, even in water. Structural factors such as planarity and hybridization strongly influence the stability of the carbanions. In general, the greater the s-character of the C–H bond to be broken, the more acidic the C–H group will be. For example, cyclopropane is more strongly acidic than methane, because its bonding results in each carbon atom effectively having  $sp^{2.28}$  hybridization (108). Anions that meet the Hückel ( $4n+2$   $\pi$ -electrons, where  $n$  is a whole number) rule for ground-state aromaticity are particularly acidic (109).

The ability of a solvent to stabilize a carbanion depends on its ability to disperse the negative charge through hydrogen bonding and charge transfer. Thus, depending on the effect desired, one should find the appropriate solvent for the reaction.

Furthermore, a catalyst can stabilize a carbanion not only through a stronger or weaker basicity of the site but by means of its coordination with the conjugated surface Lewis acid. It is apparent that the interplay between the acid and base pair can markedly help in the control of selectivity.

## VI. Catalytic Activity of Alkaline Earth Metal Oxides

Alkaline earth metal oxides have been used as solid base catalysts for a variety of organic transformations. Excellent reviews by Tanabe (4) and Hattori (2,3,7) provide detailed information about the catalytic behavior of alkaline earth metal oxides for several organic reactions of importance for industrial organic synthesis. In this section, we describe in detail reactions that have been reported recently to be catalyzed by alkaline earth metal oxides.

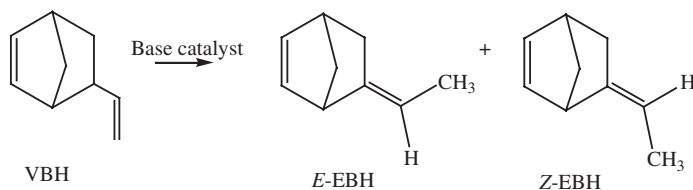
### A. ISOMERIZATION REACTIONS

Alkaline earth metal oxides are active catalysts for double bond isomerization. For example, SrO exhibits high activity and selectivity for the isomerization of  $\alpha$ -pinene to  $\beta$ -pinene (110). MgO and CaO have excellent activities for isomerization of 1-butene and 1,4-pentadiene and, particularly, for isomerization of compounds containing heteroatoms, such as allylamine or 2-propenyl ethers (111–115). Recently

it has been reported that alkaline earth metal oxides exhibit activities for double bond isomerization of 5-vinylbicyclo-[2.2.1]-hept-2-ene (VBH) (10). Isomerization of VBH leads to 5-ethylidenebicyclo-[2.2.1]-hept-2-ene (EBH) (Scheme 10), which is used as a co-monomer of ethene-propene synthetic rubber and is produced in industry by double bond isomerization of VBH using superbases, such as alumina promoted by sodium hydroxide and sodium (Na-NaOH/Al<sub>2</sub>O<sub>3</sub>) (116).

As in the case of double bond isomerization of butenes, the double bond isomerization of VBH is considered to be initiated by abstraction of an allylic proton from a tertiary carbon atom to give an allylic anion that may be stabilized by metal ions, yielding the *E*- and *Z*-EBH isomers.

Baba and Endou (117) reported that CaO is an active catalyst for isomerization of VBH to EBH when it is evacuated at temperatures above 800 K, whereas MgO did not show any activity for this process. However, some discrepancies have been reported by Kabashima *et al.* (10), who found that MgO, CaO, SrO, and BaO catalyze the isomerization of VBH to EBH, with the order of activity being CaO > MgO > SrO > BaO. This order in activity is attributed to the trends in base strength of oxides (BaO > SrO > CaO > MgO) and the surface area, the latter decreasing in the order MgO > CaO > SrO > BaO (Table II). The activity of the CaO was the highest among these alkaline earth metal oxides, and the activity of the MgO varied with the pre-treatment temperature, reaching a maximum it was 873 K;



SCHEME 10.

TABLE II  
Results Characterizing Isomerization of VBH to EBH on Alkaline Earth Metal Oxide Catalysts in a batch reactor (10)

Catalyst	Pre-treatment temp (K)	Surface area (m <sup>2</sup> /g)	Reaction temp (K)	Time (min)	Conversion (%)	<i>E/Z</i> <sup>a</sup> ratio
MgO	873	235	323	120	99.7	82/18
MgO	873	235	273	10	59.4	88/12
MgO	1073	223	273	60	14.7	—
CaO	1023	57	323	120	99.7	82/18
CaO	1023	57	273	10	99.7	87/13
SrO	1073	10	323	120	99.7	81/19
SrO	1073	10	273	10	23.5	—
BaO	1273	2	323	120	16.4	—

<sup>a</sup> *E*- and *Z*-ethylidene bicycle-[2.2.1]-hept-2-ene (EBH) isomers.

then a 99.7% conversion of VBH was observed after 2 h of reaction in a batch reactor at 323 K.

The pre-treatment temperature of MgO to give the maximum activity is higher by about 100 K for the double bond isomerization of VBH than for but-1-ene isomerization. Taking into account that the allylic hydrogen bonded to a tertiary carbon atom in VBH is more difficult to abstract than a secondary allylic hydrogen in but-1-ene, we infer that the results suggest that stronger basic sites are required for double bond isomerization of VBH than for double bond isomerization of but-1-ene.

On the other hand, the *E/Z* ratio was independent of the type of catalyst and the conversion and determined only by the reaction temperature, indicating that the interconversion of *E* and *Z* isomers is fast and that both conformers are in equilibrium during the reaction.

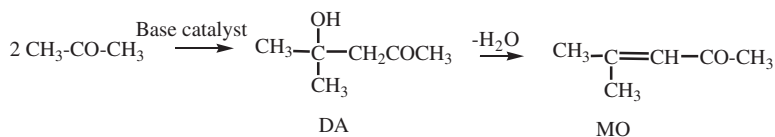
## B. CARBON–CARBON BOND FORMATION REACTIONS

### B.1. Aldol Condensations

One of the most thoroughly investigated aldol condensations is the self-condensation of acetone. This is an important industrial reaction for the production of diacetone alcohol (DA) (Scheme 11), which is valuable as a chloride-free solvent and an intermediate in the synthesis of industrially important products such as mesityl oxide (MO), isophorone, methyl isobutyl ketone, and 3,5-xyleneol. The reaction is exothermic, with the yield of DA decreasing with increasing reaction temperature; it is usually performed with NaOH or KOH as a basic catalyst (118).

It has been found that alkaline earth metal oxides are active for this process at 273 K, the order of activity being BaO > SrO > CaO > MgO (73), which is in good agreement with the order of basicity of the oxides. It was reported that the rate-determining step for this condensation is the formation of a new C–C bond between two molecules of acetone rather than the abstraction of a proton from the methyl group of the acetone. Moreover, when the catalyst was MgO, addition of CO<sub>2</sub> and water did not inhibit the aldol condensation. However, addition of small amounts of water or ammonia led to marked increases in activity and selectivity to diacetone alcohol, although pyridine had little effect on the catalytic behavior. It was suggested that the active sites for the aldol condensation are the basic OH groups retained on the surface of MgO or formed by dissociation of water resulting from the condensation process itself (119).

Recently, Di Cosimo *et al.* (14) investigated the self-condensation of acetone in the gas-phase at 573 K, with the catalysts being MgO or MgO promoted with alkali metal ions. On pure MgO, the acetone conversion was initially 17%, and this



SCHEME 11.

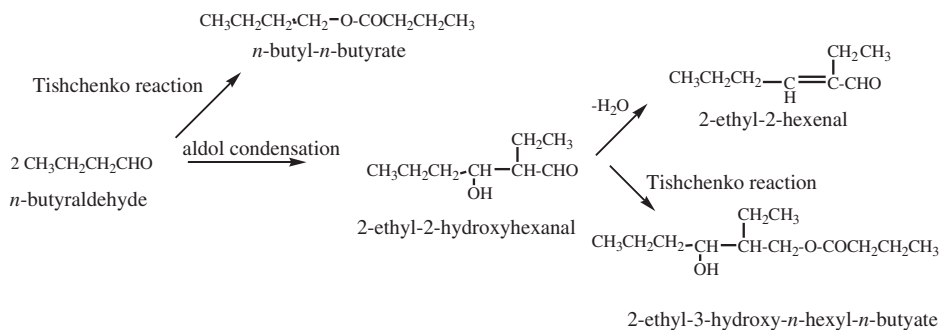


decreased to about 8% after 10 h of reaction with a selectivity to mesityl oxide (MO) of 67%. The decrease in the conversion was caused by a slow, progressive deactivation by coke. It is proposed that highly unsaturated compounds, such as phorone, which is produced by aldol condensation of mesityl oxide with acetone, remain strongly adsorbed on the catalyst surface, yielding heavier oligomeric compounds that block the basic active sites (120). Initial rates of conversion of acetone increased when MgO was promoted with alkali metals, but changes in selectivity were not observed. However, the addition of such promoters increased the rate of deactivation.

Condensation of butanol has been carried out on alkaline earth metal oxides at 273 K (13,121). This condensation reaction yields 2-ethyl-3-hydroxy-hexanal as a main product; other products, such as 2-ethyl-2-hexenal (arising from the dehydration of 2-ethyl-3-hydroxy-hexanal), *n*-butyl-*n*-butyrate (arising from the Tishchenko reaction of butyraldehyde), and 2-ethyl-3-hydroxy-*n*-hexyl butyrate (arising from the Tishchenko reaction of 2-ethyl-3-hydroxy-hexanal), are also formed (Scheme 12).

The order of activity per unit surface area was equal to that in the case of self-condensation of acetone and in agreement with the order of basicity of the solids, namely,  $\text{SrO} > \text{CaO} > \text{MgO}$ . However, the authors found that the rate-determining step for aldol condensation of *n*-butyraldehyde is the  $\alpha$ -hydrogen abstraction by the active sites, which are the surface  $\text{O}^{2-}$  ions. The differences in rate-determining step and active sites in the condensation of butyraldehyde and aldol condensation of the acetone were attributed to differences in acidity of the  $\alpha$ -hydrogen in the two molecules. CaO was slightly more active than MgO at 273 K; after a reaction time of 1 h, maximum conversions of 41% were observed with selectivities to 2-ethyl-3-hydroxy-hexanal and to the corresponding Tishchenko reaction product (2-ethyl-3-hydroxy-*n*-hexyl butyrate) of 39.8 and 56.9%, respectively.

Several cross-aldol condensations have been performed with alkaline earth metal oxides, including MgO, as a base catalyst. A general limitation of the cross-aldol condensation reactions is the formation of byproducts via the self-condensation of the carbonyl compounds, resulting in low selectivities for the cross-aldol condensation product. For example, the cross-condensation of heptanal with benzaldehyde, which leads to jasminaldehyde ( $\alpha$ -*n*-amylcinnamaldehyde), with a violet scent

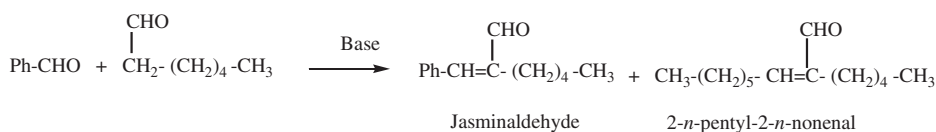


SCHEME 12.

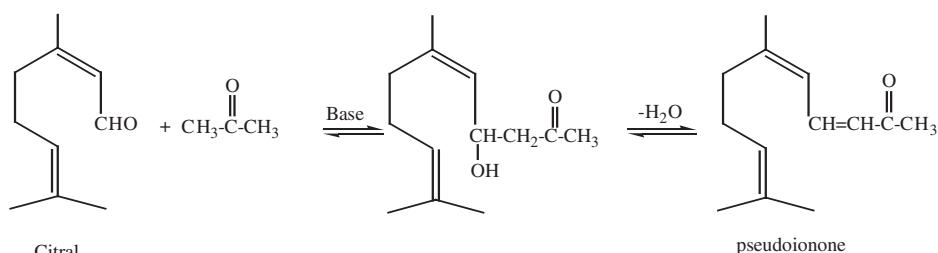
(Scheme 13), is carried out in the presence of sodium hydroxide or potassium hydroxide. In this process, heptanal is added slowly to the reaction mixture at moderate temperatures (122). In the synthesis of jasminaldehyde the most abundant undesired product results from the self-condensation of heptanal to form 2-*n*-pentyl-2-*n*-nonenal. Therefore, the general methodology for producing jasminaldehyde with high selectivity requires a low concentration of heptanal relative to benzaldehyde in the reaction mixture. This can be achieved by use of a high benzaldehyde/heptanal ratio or/and by slow addition of the heptanal to the reaction mixture. The reaction has been performed with various solid base catalysts (123,124), particularly MgO, which gave excellent conversions of heptanal (97%) at 398 K in the absence of a solvent (but the selectivity to jasminaldehyde was only 43%). A low selectivity was also reported (40%) for the cross-aldol condensation of acetaldehyde and heptanal catalyzed by MgO (125).

Another important example is the cross-aldol condensation of citral and acetone, which yields pseudoionone (Scheme 14), an intermediate in the commercial production of vitamin A. Numerous commercial routes to the preparation of pseudoionones are based on the aldol condensation using conventional homogeneous catalysts, such as aqueous alkali metal hydroxide solutions, alcoholates in alcohol or benzene solvents (126–129). The yields of the cross-condensation product vary between 50% and 80%, depending on the type of catalyst and conditions such as catalyst concentration, ratio of reagents, and temperature.

Noda *et al.* (130) evaluated the catalytic performance of solids such as CaO, MgO, and MgAl mixed oxide for the formation of pseudoionone. Working with a 1:1 molar ratio of reagents and 2 wt% of catalyst, the authors obtained the best results when the reactions were performed at 398 K and 3 bar with CaO and the mixed oxide; high conversions (98%) were observed with selectivities to pseudoionone close



SCHEME 13.



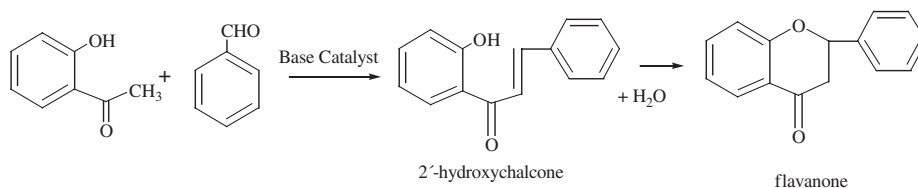
SCHEME 14.

to 70%. These pseudoionone yields are greater than those reported for the homogeneous reaction. MgO exhibited poor activity, and under these conditions only 20% citral conversion was obtained after 4 h in a batch reactor. However, Climent *et al.* (131), working at 336 K with a molar ratio of acetone to citral close to 3 and 16 wt% of catalyst (MgO), achieved 99% conversion and 68% selectivity to pseudoionone after 1 h.

### B.2. Claisen–Schmidt Condensation

The Claisen–Schmidt condensation between acetophenone and benzaldehyde derivatives is a valuable C–C bond-forming reaction that produces  $\alpha,\beta$ -unsaturated ketones (chalcones). Traditionally, this condensation is carried out at 323 K using 10–60 wt% of alkali hydroxides or sodium ethoxide over a period of 12–15 h (132,133). When the acetophenone derivative is a 2'-hydroxyacetophenone, the Claisen–Schmidt condensation yields a 2'-hydroxychalcone that can subsequently isomerize to flavanone, depending on the reaction conditions and the substituents on the aromatic rings (Scheme 15). Chalcones and flavanones belong to the flavonoid family, having found numerous applications as pesticides, photoprotectors in plastics, sun protection creams, food additives, and a plethora of interesting biological activities (antimalarial, anti-inflammatory, anticancer, diuretic, choleric, etc.) (132,134–137).

2'-Hydroxy chalcones and flavanones have been successfully synthesized with MgO as a solid base catalyst in a batch reactor at moderate temperatures (Scheme 15). Climent *et al.* (138) performed the Claisen–Schmidt reaction between 2'-hydroxyacetophenone and benzaldehyde in the absence of a solvent at 423 K; they reported a conversion of 40% after 1 h with 67% selectivity into chalcone. Drexler and Amiridis (139) measured kinetics of this reaction on MgO using DMSO as a solvent. The two reactions involved in this process (i.e., Claisen–Schmidt and the subsequent isomerization of the 2'-hydroxychalcone to flavanone) were investigated separately. The authors concluded that the condensation reaction is characterized by first-order kinetics in 2-hydroxyacetophenone and half-order kinetics in benzaldehyde, whereas hydroxychalcone cyclization is characterized by first-order kinetics. Activation energies of 40 and 24 kJ/mol were calculated for the two reactions, respectively. Influence of the solvent and the effects of substituent on the aromatic ring were investigated as the reaction was carried out on MgO at 433 K (140). When the reaction was performed with various *para*-substituted benzaldehydes, initial reaction rates increased with increasing Hammett constant, indicating that the reaction is favored by the presence of electron-accepting groups. When



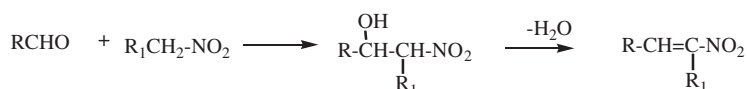
SCHEME 15.

nitrobenzene, benzonitrile, and tetralin were used as solvents, MgO exhibited poor activity, which may be attributed to competitive adsorption effects on the catalyst. However, dimethyl sulfoxide (DMSO) showed a strong promoting effect on the reaction, which was attributed to the ability of this dipolar aprotic solvent to weakly solvate anions and stabilize cations so that both become available for reaction. In this case, a conversion of 2-hydroxyacetophenone of 47% with a selectivity into flavanone of 78% was achieved after 30 min in a batch reactor. Further investigations (141) showed that DMSO significantly increases the rate of the subsequent isomerization of the 2'-hydroxychalcone intermediate to flavanone. Even the presence of small amounts of DMSO in other solvents such as benzonitrile and nitrobenzene, results in strong promotion of the flavanone synthesis. IR spectroscopic data indicated that the interaction of MgO with DMSO results in the formation of stable surface sulfate species, which affect the adsorption behavior of benzaldehyde and 2-hydroxyacetophenone.

### B.3. Nitroaldol Condensation

2-Nitroalkanol are intermediate compounds that are used extensively in many important syntheses (142). They can be converted by hydrogenation into  $\beta$ -aminoalcohols, which are intermediates for pharmacologically important chemicals such as chloroamphenicol and ephedrine. They are obtained by Henry's reaction by the condensation of nitroalkanes with aldehydes. The classical method for this transformation involves the use of bases such as alkali metal hydroxides, alkoxides,  $\text{Ba}(\text{OH})_2$ , amines, etc. (142–144). However, these catalysts give predominantly dehydrated products—nitroalkenes—which are susceptible to polymerization (Scheme 16). The reaction proceeds by the nucleophilic addition of the carbanion formed by the abstraction of a proton from the nitro compound to the carbon atom of the carbonyl group, finally forming the nitroaldol by abstraction of a proton from the catalyst.

Various nitro compounds have been condensed with carbonyl compounds in reactions catalyzed by alkaline earth metal oxides and hydroxides (145). It was found that the reactivities of the nitro compounds were in the order nitroethane > nitromethane > 2-nitropropane, and those of carbonyl compounds were propionaldehyde > isobutyraldehyde > pivalaldehyde > acetone > benzaldehyde > methyl propionate. Among the catalysts examined, MgO, CaO,  $\text{Ba}(\text{OH})_2$ , and  $\text{Sr}(\text{OH})_2$ , exhibited high activity for nitroaldol reaction of nitromethane with propionaldehyde. In reactions with these catalysts, the yields were between 60% (for MgO) and 26% (for  $\text{Sr}(\text{OH})_2$ ) at 313 K after 1 h in a batch reactor. On  $\text{Mg}(\text{OH})_2$ ,  $\text{Ca}(\text{OH})_2$ , and BaO, the yields were in the range of 3.8% (for BaO) and 17.5% (for  $\text{Mg}(\text{OH})_2$ ). Investigation of the influence of the pre-treatment



SCHEME 16.

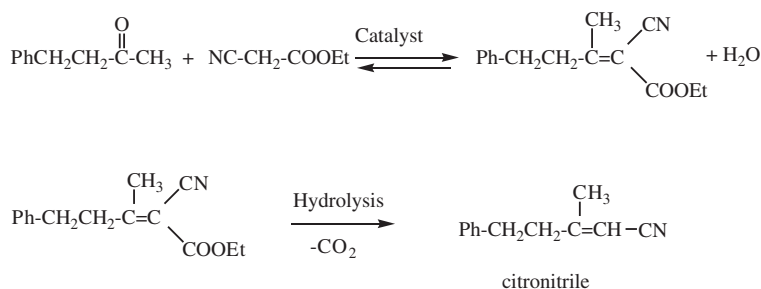
temperature of the solid showed that for MgO and CaO a considerable fraction of activity remained even after pre-treatment at low temperature (473 K), for which the transformation of Mg(OH)<sub>2</sub> into MgO is not complete and a large portion of the material is still in the form of Mg(OH)<sub>2</sub>. This result indicates that for the nitroaldol reaction the removal of the surface OH groups is not a pre-requisite to preparation of active catalysts. The nitroaldol reaction of nitromethane with propionaldehyde on MgO was barely poisoned by CO<sub>2</sub> and water. Nitromethane is so strongly acidic that it is able to compete for adsorption sites with CO<sub>2</sub> or water.

#### B.4. Knoevenagel Condensation

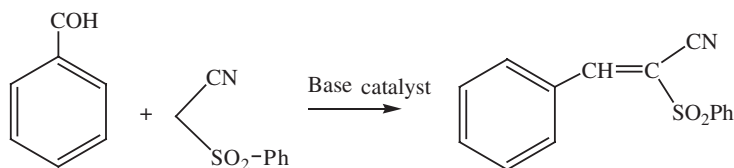
The Knoevenagel condensation is a cross-aldol condensation of a carbonyl compound with an active methylene compound leading to C–C bond formation (Scheme 7). This reaction has wide application in the synthesis of fine chemicals and is classically catalyzed by bases in solution (146,147).

An example of commercial interest is the synthesis of citronitrile (Scheme 17), a compound with a citrus-like odor, which is used in the cosmetics and fragrance industries. The first step in the synthesis of citronitrile is the Knoevenagel condensation of benzyl acetone and ethyl cyanoacetate. This condensation has been carried out with MgO and Al–Mg calcined hydrotalcites as catalysts (148). Similar results were obtained with the two solid catalysts, with yields of 75% of the Knoevenagel adduct.

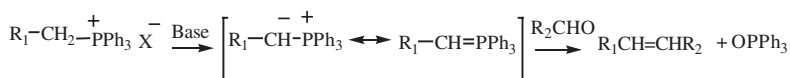
Sulfones are important intermediates in organic synthesis because they are useful as temporary activating groups for a variety of transformations, such as alkylation, acylation, and addition reactions. The method of choice for the synthesis of unsaturated arylsulfones is the Knoevenagel condensation of arylsulfonylalkanes with aldehydes. The condensation between aldehydes and phenylsulfonyl acetonitrile (Scheme 18) has been performed in the presence of various solid base catalysts (MgO, Cs-exchanged X zeolite, Al–Mg mixed oxide, and aluminophosphate oxinitride) at 373 K in the absence of solvents (149). The most active catalyst for this transformation was the aluminophosphate oxinitride, but MgO and the Al–Mg mixed oxide also were found to have excellent activity, yielding the Knoevenagel adduct in yields of 86% and 71%, respectively, after 2 h in a batch reactor.



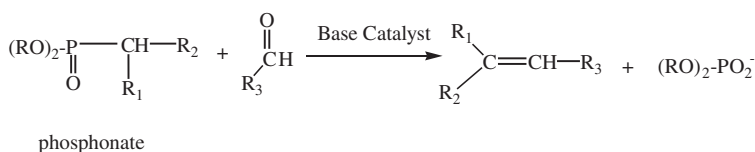
SCHEME 17.



SCHEME 18.



SCHEME 19.



SCHEME 20.

### B.5. Wittig and Wittig–Horner Reactions

The Wittig reaction is one of the most important reactions in organic chemistry for synthesizing alkenes with unambiguous positioning of the double bond. The process involves a reaction between a phosphonium ylide and an aldehyde or ketone (150). The reacting ylide is formed from a phosphonium salt in a solution of a base such as NaH, *t*-BuOK, or NaOH (151) (Scheme 19).

A variant of the Wittig reaction is the Wittig–Horner reaction, occasionally called the Wadsworth–Emmons reaction, which involves the condensation of an aldehyde or a ketone with a phosphonate (152) in the presence of a strong base such as NaOEt (153) or KOH (154) to give an alkene (Scheme 20). The main drawbacks associated with these transformations are the need to use equimolar amounts of base and reactant, leading to the formation of large amounts of undesired products. Moreover, other competitive reactions such as the Knoevenagel reactions or aldolization can take place, lowering the yield of the desired product.

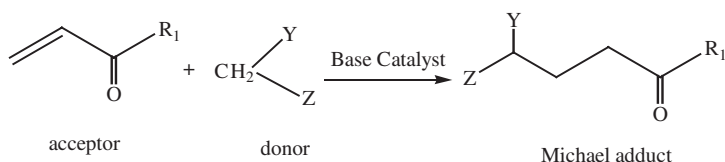
MgO has been reported to be an efficient basic catalyst for Knoevenagel, Wittig, and Wittig–Horner reactions for the preparation of alkenes at temperatures between 293 and 333 K (155). It has been observed that for the Wittig reaction the addition of a limited amount of water is necessary to increase the reaction yield; however, for the Knoevenagel condensation the addition of small amounts of water to MgO decreased the yield of alkene. The investigation of the Wittig–Horner reaction of diethylcyanomethylphosphonate with benzaldehyde showed that the competition between the Wittig–Horner reaction and the Knoevenagel reaction was dependent on the nature of the catalyst and on the presence of protic or dipolar aprotic solvents

or metal salts. Recently, competitive Wittig–Horner and Knoevenagel reactions of benzaldehyde with di-ethyl cyanomethylphosphonate and tetra-ethyl methylenediphosphonate on different solid base catalysts ( $\text{CsCO}_3$ ,  $\text{BaO}$ ,  $\text{Ca(OH)}_2$ ,  $\text{CaO}$ ,  $\text{MgO}$ ,  $\text{MgCl}_2$ ,  $\text{BaF}_2$ ,  $\text{KF}_2$ ,  $\text{CaF}_2$ , and  $\text{CsF}$ ) in the absence of a solvent have been reported (156). Tetra-ethyl methylenediphosphonate reacting with benzaldehyde at similar conditions gave only the product of Horner’s reaction. The basicity of the solid and the nature of the cation (mono or divalent) of the base strongly influence the ratio of products formed in the Horner/Knoevenagel reactions.

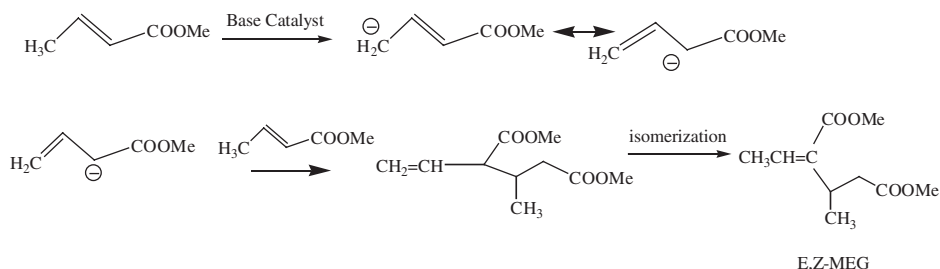
### B.6. Michael Addition

Another important reaction in synthetic chemistry leading to C–C bond formation is the Michael addition. The reaction typically involves a conjugate or nucleophilic 1,4-addition of carbanions to  $\alpha,\beta$ -unsaturated aldehydes, ketones, esters, nitriles, or sulfones (157) (Scheme 21). A base is used to form the carbanion by abstracting a proton from an activated methylene precursor (donor), which attacks the alkene (acceptor). Strong bases are usually used in this reaction, leading to the formation of byproducts arising from side reactions such as condensations, dimerizations, or rearrangements.

Dimerization of methyl crotonate has been carried out with alkaline earth metal oxides as basic catalysts (15). The reaction proceeds by Michael addition, which is initiated by abstraction of an allylic hydrogen of methyl crotonate by the basic site to form the allylic carbanion, which attacks a second methyl crotonate molecule at the  $\beta$ -position to form a methyl diester of 3-methyl-2-vinylglutaric acid. The diester undergoes a double bond migration to form the final *E*- and *Z*- isomers of 3-ethylidene-3-methylglutaric acid dimethyl ester (MEG) (Scheme 22).



SCHEME 21.



SCHEME 22.

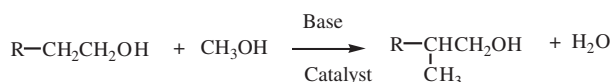
The reaction was performed at 323 K on various base catalysts (MgO, CaO, SrO, BaO, ZrO<sub>2</sub>, La<sub>2</sub>O<sub>3</sub>, KF/alumina, KOH/alumina, and KX zeolite). Among these catalysts, MgO exhibited the highest activity when it was pre-treated at 873 K. In this case, the conversion of methyl crotonate was 36.5% after a 2 h reaction time in a batch reactor with a selectivity into *E,Z*-MEG isomers of 93%. When higher pre-treatment temperatures were used, the catalytic activity of the MgO decreased sharply. However, MgO pre-treated at 673 K exhibited considerable activity for the Michael addition. Because at this pre-treatment temperature the catalyst still retains a large number of OH groups, it was assumed that basic hydroxyl groups can act as active sites.

The same authors (11) also investigated the Michael addition of nitromethane to  $\alpha,\beta$ -unsaturated carbonyl compounds such as methyl crotonate, 3-buten-2-one, 2-cyclohexen-1-one, and crotonaldehyde in the presence of various solid base catalysts (alumina-supported potassium fluoride and hydroxide, alkaline earth metal oxides, and lanthanum oxide). The reactions were carried out at 273 or 323 K; the results show that SrO, BaO, and La<sub>2</sub>O<sub>3</sub> exhibited practically no activity for any Michael additions, whereas MgO and CaO exhibited no activity for the reaction of methyl crotonate and 3-buten-2-one, but low activities for 2-cyclohexen-1-one and crotonaldehyde. The most active catalysts were KF/alumina and KOH/alumina for all of the Michael additions tested.

### B.7. Condensation of Alcohols

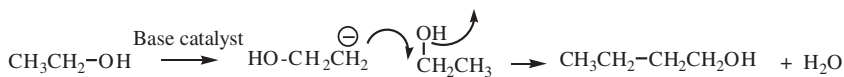
The Guerbet reaction is an important industrial process for increasing the carbon numbers of alcohols. Thus, a primary or secondary alcohol reacts with itself or another alcohol to produce a higher alcohol (Scheme 23). Alkaline earth metal oxides have been used as catalysts for the condensation of alcohols. Ueda *et al.* (158,159) reported the condensation of methanol with other primary or secondary alcohols having a methyl or methylene group at the  $\beta$ -position; they used MgO, CaO, and ZnO as catalysts. The reactions were performed with gas-phase reactants at 635 K; only MgO was found to be both active and selective (>80%).

Recently, Ndou *et al.* (160) reported the dimerization of ethanol to 1-butanol catalyzed by MgO, CaO, BaO, and modified MgO. The MgO catalyst exhibited the highest catalytic activity, giving conversions of 56% with 33% selectivity. Other compounds such as butanol, crotonal, butan-2-ol, and crotonol were also formed. A thorough investigation of the reaction using a variety of possible intermediates suggested that the dimerization reaction does not proceed primarily through the aldol condensation reaction, but rather involves a bimolecular condensation reaction via H abstraction from a  $\beta$ -C atom of ethanol to generate a nucleophilic center which attacks another ethanol molecule, resulting in OH displacement (i.e., dehydration) and C–C bond formation, giving butan-1-ol and water (Scheme 24). Activation of a

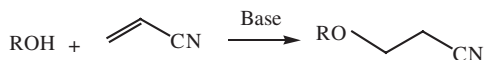


SCHEME 23.





SCHEME 24.



SCHEME 25.

$\beta$ -H atom appears to be the key step in the mechanism. It was suggested that ethanol reacts with the MgO surface, generating an ethoxide species and that it is this ion that presents an activated  $\beta$ -H atom.

### C. CARBON-OXYGEN BOND FORMATION REACTIONS

#### C.1. Cyanoethylation of Alcohols

Cyanoethylation of acrylonitrile with monohydric alcohols gives alkoxypropionitriles (Scheme 25). These nitriles can be converted into various types of carboxylic acids by hydrolysis, and they can be hydrogenated to give amines. Therefore, cyanoethylation of alcohols is an important reaction for the synthesis of drug intermediates and organic compounds of industrial interest.

The reaction is usually performed with homogeneous basic catalysts such as alkali hydroxides, alkoxides, and tetraalkyl ammonium hydroxide (161,162). The mechanism accepted for this transformation starts with the abstraction by the base catalyst of a proton from the hydroxyl group of the alcohol to generate the alkoxide anion, which reacts with acrylonitrile to form the 3-alkoxypropanenitrile anion. The 3-alkoxypropanenitrile anion abstracts a proton from the catalyst to yield 3-alkoxypropane nitrile.

Cyanoethylation of various alcohols with acrylonitrile to form 3-alkoxypropanenitriles has been carried out efficiently in the presence of solid base catalysts such as alkali metal oxides and hydroxides at a temperature of 323 K (163,164). In cyanoethylation of methanol, conversions of 98% after a 2 h in a batch reactor were obtained with MgO, CaO, and SrO; in contrast, with BaO the conversion was only 68%. Among the alkaline earth metal hydroxides, the most active was Ba(OH)<sub>2</sub>, which gave a conversion of 68% under comparable conditions. The investigation of the influence of alcohol structure on reactivity showed that the order of the reactivity of alcohols varied with the type of catalyst. With the alkaline earth metal oxides the reactivity increased in the order methanol < ethanol < propan-2-ol. However, with magnesium hydroxide and calcium hydroxide, the order of the reactivity was the opposite. The order of reactivity can be explained by the acid-base pairs, i.e., the acidity of the alcohol and the basic strength of the catalyst. The results strongly suggest that the controlling step of the reaction is the abstraction of the proton from the alcohol when the active site is weakly basic. On the other hand, when the active sites are strongly basic, then the controlling step is the addition of

an alkoxy anion to acrylonitrile. The catalytic activities of solid bases were scarcely affected by exposure of the catalysts to air before use. This result is attributed to the strong adsorption of the alcohols on the basic sites competing with the adsorption of CO<sub>2</sub> and water.

### C.2. Conjugate Addition of Methanol to $\alpha,\beta$ -unsaturated Carbonyl Compounds

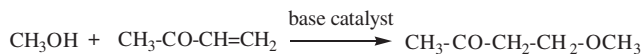
Conjugate addition of methanol to  $\alpha,\beta$ -unsaturated carbonyl compounds forms a new carbon–oxygen bond to yield valuable ethers (Scheme 26). Kabashima *et al.* (12) reported the conjugate addition of methanol to 3-buten-2-one on alkaline oxides, hydroxides, and carbonates at a temperature of 273 K. The activities of the catalyst follow the order alkaline earth metal oxides > alkaline earth metal hydroxides > alkaline earth metal carbonates. All alkaline earth metal oxides exhibited high catalytic activities and, as in alcohol condensations and nitroaldol reactions, their catalytic activities were not much affected by exposure to CO<sub>2</sub> and air.

The yields obtained after 10 min in a batch reactor with MgO, CaO, or SrO exceeded 92%, whereas with BaO the yield was lower (72%), probably because of its low surface area (2 m<sup>2</sup>/g). When alkaline earth hydroxides were used as basic catalysts, the yields were lower than for the corresponding oxides. The most active hydroxides were Sr(OH)<sub>2</sub> · 8H<sub>2</sub>O and Ba(OH)<sub>2</sub> · 8H<sub>2</sub>O, which gave the additional compound in yields of 75% and 70%, respectively, whereas carbonates were characterized by very poor activity. As observed for other reactions, the catalytic activity of MgO strongly depends on the pre-treatment temperature. A maximum in activity was observed when MgO was pre-treated at 673 K. At this temperature, decomposition of Mg(OH)<sub>2</sub> to MgO is not complete, and Mg(OH)<sub>2</sub> remains in the catalyst. It was suggested that the surface OH groups act as active sites, as for the Michael addition reactions described above.

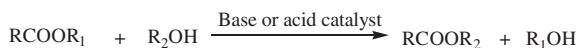
### C.3. Transesterification Reactions

Alcoholysis reactions of esters are important reactions for fine chemicals synthesis, involving the reaction of an alcohol with an ester. The reaction is catalyzed by both acids and bases. So far, the catalysts employed for alcoholysis have been mostly soluble, and solid catalysts have not been extensively investigated (Scheme 27).

Fatty acid methyl and ethyl esters derived from vegetable oils are valuable compounds for the production of fine chemicals for food, pharmaceutical, and cosmetic products. Moreover, they are considered to be a promising fuel for direct injection diesel engines. The classical method of fatty acid methyl and ethyl ester (FAME)



SCHEME 26.

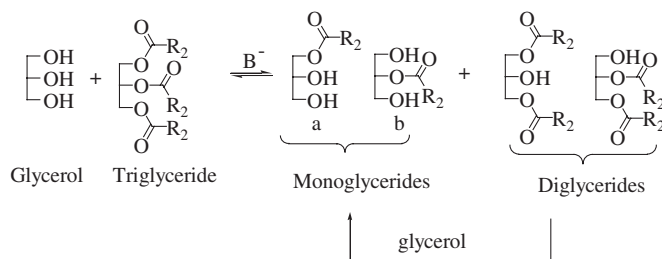


SCHEME 27.

preparation is based on triglyceride transesterification to methyl or ethyl esters. Sodium hydroxide dissolved in methanol is the usual catalyst; however, an important drawback associated with the use of soluble catalysts is that they must be neutralized and removed from the reaction products.

Peterson and Scarrah (165) reported the transesterification of rapeseed oil by methanol in the presence of alkaline earth metal oxides and alkali metal carbonates at 333–336 K. They found that although MgO was not active for the transesterification reaction, CaO showed activity, which was enhanced by the addition of MgO. In contrast, Leclercq *et al.* (166) showed that the methanolysis of rapeseed oil could be carried out with MgO, although its activity depends strongly on the pretreatment temperature of this oxide. Thus, with MgO pre-treated at 823 K and a methanol to oil molar ratio of 75 at methanol reflux, a conversion of 37% with 97% selectivity to methyl esters was achieved after 1 h in a batch reactor. The authors (166) showed that the order of activity was  $\text{Ba(OH)}_2 > \text{MgO} > \text{NaCsX zeolite} > \text{MgAl mixed oxide}$ . With the most active catalyst ( $\text{Ba(OH)}_2$ ), 81% oil conversion, with 97% selectivity to methyl esters after 1 h in a batch reactor was achieved. Gryglewicz (167) also showed that the transesterification of rapeseed oil with methanol could be catalyzed effectively by basic alkaline earth metal compounds such as calcium oxide, calcium methoxide, and barium hydroxide. Barium hydroxide was the most active catalyst, giving conversions of 75% after 30 min in a batch reactor. Calcium methoxide showed an intermediate activity, and CaO was the least active catalyst; nevertheless, 95% conversion could be achieved after 2.5 h in a batch reactor. MgO and  $\text{Ca(OH)}_2$  showed no catalytic activity for rapeseed oil methanolysis. However, the transesterification reaction rate could be enhanced by the use of ultrasound as well as by introduction of an appropriate co-solvent such as THF to increase methanol solubility in the phase containing the rapeseed oil.

As in the transesterification of vegetable oils with methanol, triglycerides react with glycerol to give fatty acid monoesters and diesters of glycerol (Scheme 28), which are valuable compounds with wide applications as emulsifiers in the food, pharmaceutical, and cosmetic industries. Commercial processes are carried out at temperatures above 473 K with soluble catalysts such as NaOH, KOH, or  $\text{Ca(OH)}_2$  (168). These industrial processes lead to mixtures of mono-, di-, and triesters, whereby the monoglyceride content is between 40% and 60% and distillation is necessary to obtain high-purity products and the process requires a neutralization step with formation of large amounts of salts.



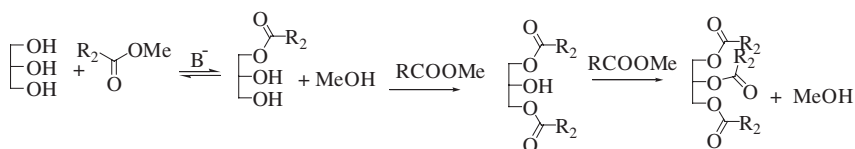
SCHEME 28.

Corma *et al.* (169) evaluated various solid-base catalysts (Cs-exchanged MCM-41, Cs-exchanged Sepiolite (96), MgO, and calcined hydrotalcites with various Al/Mg ratios) for the glycerolysis of triolein and rapeseed oil in the absence of a solvent. The results showed that the most active catalysts were MgO and calcined hydrotalcites with an Al/(Al+Mg) ratio of 0.20. The catalytic activity was directly related to the total basicity of the solid, whereas the selectivity to monoglycerides was found to depend principally on the triglyceride conversion. The authors showed that by using MgO as a solid base catalyst and optimizing the main process variables, such as temperature and the glycerol/oil ratio, it is possible to obtain 96% conversion of rapeseed oil with 68% selectivity to monoglycerides after 5 h in a batch reactor by working at 513 K with a glycerol/triglyceride molar ratio of 12. The final mixture composition, without further purification, meets the quality requirements established by the European Union for food applications.

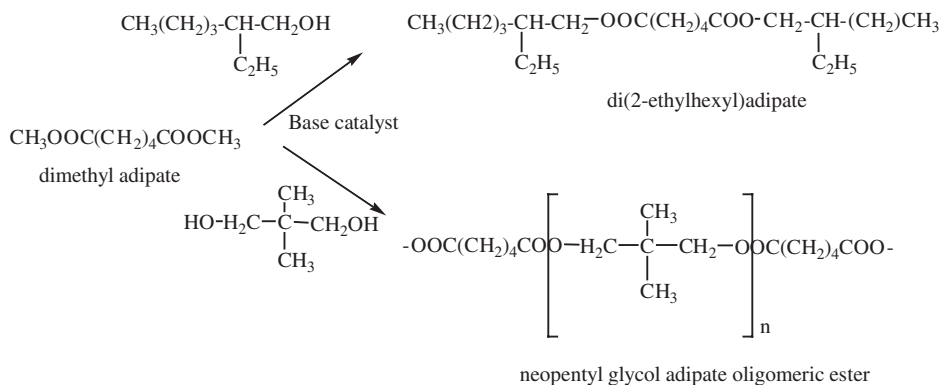
Monoglycerides can alternatively be prepared by glycerolysis of fatty acid methyl esters (Scheme 29). The use of fatty acid methyl esters has several advantages; for example, they are prepared from fats by fat methanolysis reactions and can be easily purified. Moreover, owing to the lower hydrophobic character than triglycerides, fatty methyl esters have high miscibility with glycerol, and the process can be carried out at lower temperatures (between 393 and 503 K), with the consequent efficiency advantage in energy use.

Bancquart *et al.* (28,170) showed that basic solid catalysts such as MgO, ZnO, CeO<sub>2</sub>, and La<sub>2</sub>O<sub>3</sub>, as well as MgO doped with alkali metals (Li/MgO and Na/MgO) are active catalysts for the transesterification of methyl stearate with glycerol. The reactions were performed at 493 K in the absence of a solvent, the order of activity being La<sub>2</sub>O<sub>3</sub> > MgO ≈ CeO<sub>2</sub> > ZnO, which correlates with the intrinsic basicity of these solids. The activity of MgO depends on the preparation method; thus, MgO prepared by hydration of a commercial MgO followed by calcination was the most active catalyst, giving conversions of 65% with selectivity to monoglycerides of 50% after 1.5 h in a batch reactor with equimolar ratios of reactants. The authors showed that in this process the nature of the oxide has a small effect on the selectivity to monoesters, with the distribution of the esters being similar to that obtained with homogeneous base catalysts.

By this approach, esters such as di(2-ethylhexyl) adipate and an oligomeric ester of neopentyl glycol have been synthesized recently by alcoholysis of dimethyl adipate ester and the corresponding alcohols, with alkaline earth metal compounds as the catalysts (171) (Scheme 30). These types of esters find application as lubricants, and it is suggested that they can be used as environment-friendly substitutes for petroleum-derived lubricants. The reactions were carried out with isooctane as a



SCHEME 29.



SCHEME 30.

solvent and refluxing reaction mixtures. The results show that the activity of the catalyst is related to its basicity. MgO does not show any activity for either transesterification reaction, whereas CaO gives yields of both diesters near 100% after 4 h in a batch reactor. A similar trend was found when alkaline earth hydroxides were used as catalysts. Mg(OH)<sub>2</sub> and Ca(OH)<sub>2</sub> were inactive, and Ba(OH)<sub>2</sub> exhibited high activity.

Alcoholysis of ester and epoxide with various basic catalysts including alkaline earth metal oxides and hydroxides was reported recently by Hattori *et al.* (172). Various alcohols were transesterified with ethyl acetate at 273 K. The results show that in the presence of strongly basic catalysts such as CaO, SrO, and BaO, propan-2-ol reacted much faster than methanol, whereas in the presence of more weakly basic catalysts such as MgO, Sr(OH)<sub>2</sub>·8H<sub>2</sub>O, and Ba(OH)<sub>2</sub>·8H<sub>2</sub>O, methanol reacted faster than propan-2-ol. This behavior agrees with the observations made for the cyanoethylation of alcohols with alkaline earth metal oxides and hydroxides as catalysts (163,164). Furthermore, the authors found that 2-methylpropan-2-ol reacted only on strongly basic catalysts and much more slowly than methanol and propan-2-ol. The observations can be attributed to the low acidity of this tertiary alcohol along with steric hindrance of the alkoxide anion for attacking the adsorbed ethyl acetate. When the alcoholysis was performed with propene oxide, alkaline earth metal oxides were found to be more reactive than hydroxides; the reactivity of the alcohols was in the order methanol > ethanol > propan-2-ol > 2-methylpropan-2-ol, regardless of the type of catalyst. An interesting result of this study was that the catalysts, were active after air exposure for alcoholysis of ester and epoxide. This result is probably caused by a strong adsorption of the alcohol, which competes favorably with CO<sub>2</sub> and water.

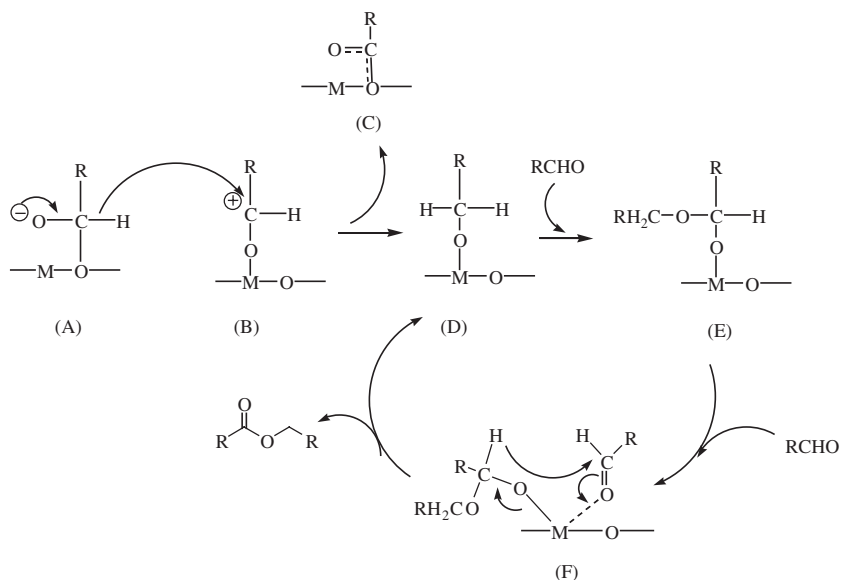
#### D. HYDROGEN TRANSFER REACTIONS

##### D.1. Tishchenko Reaction

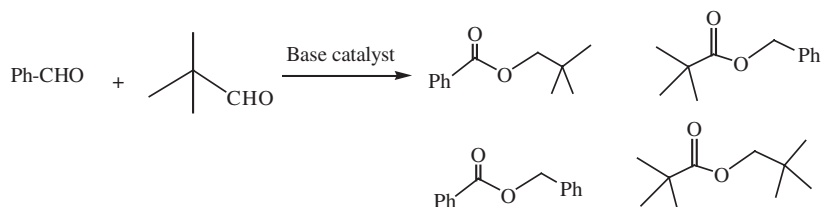
The Tishchenko reaction is a dimerization of aldehydes to the corresponding esters, which is classically carried out in homogeneous media using aluminum

alkoxides as catalysts (173–175). In 1974, Tanabe and Saito (176) found that alkaline earth metal oxides (MgO and CaO) that have both acidic and basic sites can catalyze the Tishchenko reaction of benzaldehyde. They proposed a mechanism which involves, as the first step, the adsorption of aldehydes onto the basic ( $O^{2-}$ ) and acidic sites (metal ions), resulting in the formation of the adsorbed intermediates (A) and (B), respectively (Scheme 31). In the second step, hydride transfer from (A) to (B) occurs to form the intermediate (C) and the active species (D) for the ester formation. The active species (D) attacks the electrophilic carbonyl carbon atom of an aldehyde to form the intermediate (E), which draws another aldehyde molecule onto metal ion (F), followed by hydride ion transfer to form the ester and the active species (D) (Scheme 31).

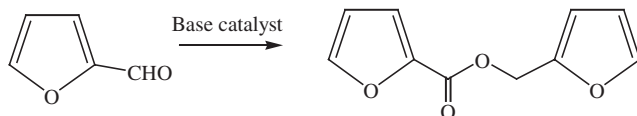
Mixed Tishchenko reactions with various aldehydes (a) benzaldehyde and pivalaldehyde, (b) pivalaldehyde and cyclopropanecarbaldehyde, and (c) cyclopropanecarbaldehyde and benzaldehyde have been investigated with various solid base catalysts including alkaline earth metal oxides (177). The reactions were performed at 353 K *in vacuo* without solvent using equimolar mixtures of two kinds of aldehydes. Alkaline earth metal oxides were the most active catalysts, and other solid base catalysts, such as  $La_2O_3$ ,  $ZrO_2$ , ZnO,  $\gamma$ -alumina, hydrotalcite, KF/alumina, and KOH/alumina, were all inactive for the mixed Tishchenko reaction of benzaldehyde and pivalaldehyde. Four product esters formed by cross- and self-esterification were found (Scheme 32 displays the four dimers formed in the Tishchenko reaction with benzaldehyde and pivalaldehyde). In all the combinations, the activity of the catalysts was found to increase in the order  $BaO \ll MgO < CaO < SrO$ . This result indicates that strongly basic sites and high surface areas are indispensable for high activity. Quantum chemical calculations of



SCHEME 31.



SCHEME 32.



SCHEME 33.

TABLE III

*Yields in the Tishchenko Reaction of Furfural on Alkaline Earth Metal Oxides in a Batch Reactor<sup>a</sup> (178)*

Catalyst	Catalyst pre-treatment temperature (K)	Surface area (m <sup>2</sup> /g)	Reaction temp (K)	Time (h)	Yield (%)
MgO	873	267	353	4	<1
CaO	873	48	353	4	61
CaO	873	48	353	6	78
SrO	1273	12	353	4	83
SrO	1273	12	353	6	95
SrO	1273	12	323	12	70
BaO	1273	2	353	4	0

<sup>a</sup> Reaction conditions: amount of furfural, 10 mmol; mass of catalysts, 100 mg.

the positive charges on the carbonyl carbon atoms of aldehydes and the structural parameters of the active species for the ester formations suggested that selectivities to the four Tishchenko dimers on MgO and CaO are determined primarily in the step of the nucleophilic addition of the active species (D) in Scheme 31 to the carbonyl carbon atoms of the aldehydes. Thus, the nucleophilic addition of the active species (D), having a less-hindered oxygen atom, over the aldehyde, having a more highly positively charged and sterically less-hindered carbonyl carbon atom, proceeds faster.

The Tishchenko reaction of furfural (Scheme 33) has been reported to be difficult when carried out by traditional homogeneous catalysis, but recently Seki *et al.* (178) obtained excellent results for the Tishchenko reaction of furfural and 3-furaldehyde (179) using CaO and SrO as catalysts.

The results obtained with the Tishchenko reaction of furfural using alkaline earth metal oxides as base catalysts are presented in Table III. Because the strength of basic sites increases in the order MgO < CaO < SrO < BaO, and the order of their acid strengths is the reverse (73), it was concluded that CaO and SrO—which have moderate acid and base sites in comparison with MgO and BaO—are appropriate

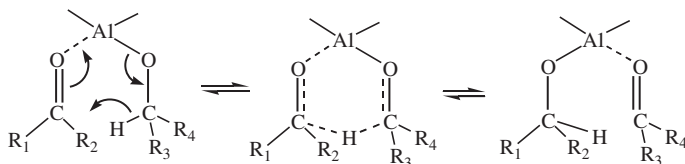




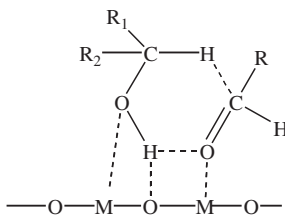
which both the carbonylic compound and the alcohol are coordinated to the metal center of the metal alkoxide catalyst. The reactant alcohol is coordinated as an alkoxide, and the activation of the carbonyl group by coordination to Al(III) initiates the hydride transfer reaction from the alkoxide to the carbonyl (Scheme 35).

However, the reaction requires a large excess of alkoxide (between 100% and 200%) that has to be neutralized with a strong acid. To overcome this drawback, various solid catalysts have been reported recently (186–188). Basic catalysts, comprising oxides and zeolites, have been used for this transformation (189); among them, special attention has been paid to MgO for catalytic transfer hydrogenations with vapor-phase reactants (190–193). Ivanov *et al.* (194) investigated the MPV reaction between ethanol and acetone on metal oxides having various acid–base pairs. They proposed a mechanism similar to that proposed for homogeneous catalysis, with the hydrogen transfer taking place via a concerted process involving a six-member intermediate with the alcohol and the carbonyl compound adsorbed on an acid–base pair. In the proposed mechanism, the alcohol adsorbs on the catalyst through a weak Lewis acid–strong base pair site, giving a surface-bound alkoxide, which leads to the transfer of a hydride ion that attacks the carbonyl group (Scheme 36).

The reaction of cyclopentanol in the presence of cyclohexanone at 623 K catalyzed by amorphous metal oxides and Cs-exchanged X zeolite was investigated by Berkani *et al.* (195). The reaction leads to alkenes and hydrogen transfer products, but it was found that the activities of the catalysts for dehydration of cyclopentanol and for the hydrogen transfer from cyclopentanol to cyclohexanone depend on their acid–base properties. Thus, MgO exhibited the highest activity for the hydrogen transfer reaction, followed by potassium impregnated on  $\gamma$ -Al<sub>2</sub>O<sub>3</sub> and CsNaX zeolites. The activities of the zeolites for hydrogen transfer increases with the basicity (i.e., with the Cs content). On the other hand, the acidities of the catalysts and their activities for dehydration follow the reverse trend. Moreover, addition of CO<sub>2</sub> to the carrier gas during the reaction inhibits only the hydrogen transfer reaction,



SCHEME 35.



SCHEME 36.

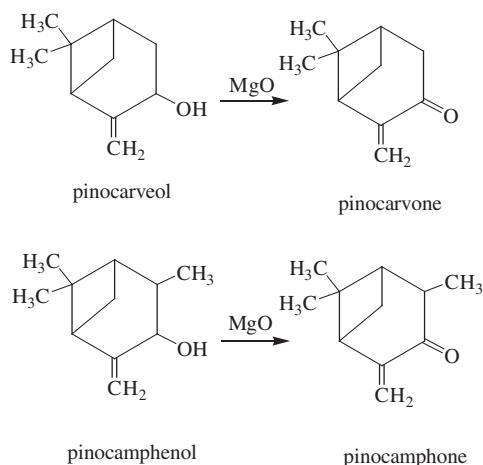
whereas the amount of cyclopentene remains constant. It was therefore concluded that hydrogen transfer occurs only on the basic sites of the catalysts and dehydration only on the acid sites.

The oxidation of 2-ethylhexan-1-ol to 2-ethyl-hexanal by the Oppenauer oxidation with aliphatic aldehydes such as acetaldehyde, propionaldehyde, and isobutyraldehyde has been investigated with gas-phase reactants and MgO as the catalyst (196). Reaction with propionaldehyde was found to be an effective synthetic route for 2-ethylhexanal preparation, whereas with acetaldehyde and isobutyraldehyde a gradual catalyst deactivation in a flow reactor was observed.

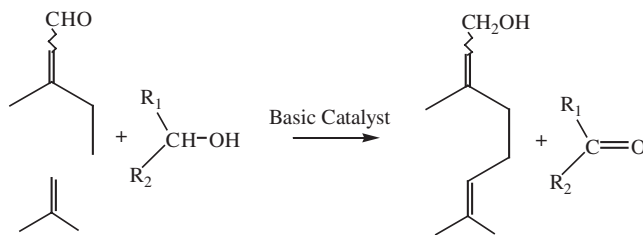
The same authors also reported the dehydrogenation of pinocarveol to pinocarvone and pinocampeol to pinocamphone catalyzed by MgO (197) (Scheme 37). Pinocampeol was oxidized to the corresponding ketone with yields in the range of 40%, whereas the yields of pinocarvone from pinocarvenol did not exceed 10%.

Although MgO appears to be an excellent catalyst for hydrogenation of ketones using secondary alcohols with reactants in the vapor phase, an important drawback of the reaction is that the MgO gradually deactivates, ultimately leading to a complete loss of activity. Szollosi and Bartok (198,199) showed that deactivation of MgO during the catalytic transfer hydrogenation of various ketones with propan-2-ol could be prevented by pre-treatment with chloromethanes. For instance, MgO subjected to treatment with chloroform retained its initial catalytic activity for as long as 65 h. It was suggested that modification of the MgO surface with chloroform resulted in blocking of the Lewis acid centers responsible for poisoning and also in the generation of surface OH groups with proper acidity for the reaction (200).

Alkaline earth metal oxides have also been used as basic catalysts for the MPV reaction with liquid-phase reactants. The reaction of benzaldehyde with ethanol in the presence of MgO, CaO, and mixed oxides obtained by calcination of double-layered hydroxides was investigated by Aramendia *et al.* (201). CaO, with the



SCHEME 37.



SCHEME 38.

highest density of basic sites, was found to be the most active catalyst for the process. Moreover, the MPV reaction was accompanied by two other competing reactions (aldol condensation and the Tishchenko cross-reaction). Data characterizing the MPV reaction of benzaldehyde with other alcohols showed that the highest conversions are obtained with secondary alcohols as hydrogen sources.

The same authors have reported the reduction of citral with alkanols and cycloalkanols to the Z- and E-alcohol isomers nerol and geraniol when MgO and CaO were used as catalysts (202) (Scheme 38). When the reactions were performed by refluxing the mixture with an alcohol/citral molar ratio of 20, excellent yields to the corresponding alcohol isomers were obtained. Various reducing alcohols were tested that gave the following sequence of reactivity: cycloalkanols > alkan-2-ols > alkan-3-ols. Reaction yield and selectivity on MgO and on CaO exceeded 95 and 85%, respectively, in all the experiments. The number and strength distribution of the basic sites on MgO and on CaO were determined by TPD of CO<sub>2</sub>; the total number of basic sites on MgO was almost three times greater than that on CaO. This result is reflected in the activity of MgO for the hydrogen transfer, which was higher than that of CaO.

Recently, the influence of the preparation method of various MgO samples on their catalytic activity in the MPV reaction of cyclohexanone with 2-propanol has been reported (202). The oxides were prepared by various synthetic procedures including calcination of commercially available magnesium hydroxide and magnesium carbonate; calcination of magnesium hydroxides obtained from magnesium nitrate and magnesium sulfate; sol-gel synthesis; and precipitation by decomposition of urea. It was concluded that the efficiency of the catalytic hydrogen transfer process was directly related to the number of basic sites in the solid. Thus, the MgO (MgO-2 sample in Table IV) prepared by hydration and subsequent calcination of a MgO sample that had been obtained from commercially available Mg(OH)<sub>2</sub> was the most basic and the most active for the MPV process, and the MgO samples with similar populations of basic sites exhibited similar activities (Table IV).

## VII. Zeolites and Mesoporous Aluminosilicates Modified with Alkaline Earth Metal Oxides

Because of their well-defined porous structures and spatial limitations, zeolites and mesoporous aluminosilicates are shape-selective catalysts. The availability of

TABLE IV

*Influence of Preparation Method of MgO on Catalytic Activity for the MPV Reaction of Cyclohexanone with 2-propanol in a Batch Reactor<sup>a</sup> (202)*

Catalyst precursor	MgO catalyst <sup>b</sup>	BET surface area (m <sup>2</sup> /g)	Number of basic sites (μmol CO <sub>2</sub> /g MgO)	$r_0^c$ (mmol/h/g)	Yield of cyclohexanol (%) after 46 h
Commercial Mg(OH) <sub>2</sub>	MgO-1	11.5	29	0.002	<5
Rehydration of MgO-1	MgO-2	110.8	257	0.130	88.9
Precipitation from Mg(NO <sub>3</sub> ) <sub>2</sub>	MgO-3	123.7	201	0.074	61.3
Precipitation from MgSO <sub>4</sub>	MgO-4	162.5	161	0.058	44.8
Sol-gel method	MgO-5	39.9	115	0.046	33.5
Precipitation by decomposition of urea	MgO-6	100.4	108	0.043	30.6
Calcination of MgCO <sub>3</sub>	MgO-7	71.2	173	0.066	69.2

<sup>a</sup> Reaction conditions: donor/acceptor ratio = 20 under refluxing conditions, 1 g of freshly calcined catalyst.

<sup>b</sup> MgO samples obtained by calcinations of Mg(OH)<sub>2</sub> in the air at 873 K for 2 h. MgO-7 was obtained by calcination at 873 K for 6 h.

<sup>c</sup>  $r_0$  = initial reaction rate.

shape-selective base catalysts is extremely desirable to enhance “atom utilization” and minimize the production of pollutants. Therefore, the preparation of strongly basic microporous and mesoporous aluminosilicates is attracting increasing attention. The exchange of zeolite protons by alkali and alkaline-earth cations (203,204) gives basic zeolites (98,205,206); the basic sites are the framework oxygen atoms, which are rich in electron density induced by the cations located nearby. As a consequence of the covalent nature of the bonding of the framework oxygen, only weakly basic sites are generated. Zeolites with stronger basic properties have been prepared by adding basic guest oxides into zeolites as hosts. Hathaway and Davis (207–209) and Kim *et al.* (210) reported that the introduction of excess alkali by decomposition of their salts and hydroxides in zeolite cavities resulted in the generation of active basic sites, which are much more active than those in alkali-exchanged zeolites for base-catalyzed reactions such as dehydrogenation of 2-propanol and alkylation of toluene with methanol. The authors proposed that the active basic sites are alkali metal oxides encapsulated in the zeolite cavities. Analogously, mesoporous molecular sieves (MCM-41) have been converted into basic materials by alkali cation exchange or by impregnation and subsequent thermal decomposition of alkali metal salts (211–214).

To prepare alkali- or alkaline earth-modified zeolites or mesoporous molecular sieves, identical general methodologies are used. Thus, alkaline earth cation-exchanged zeolites are prepared by exchange of the zeolite in the sodium form in aqueous solution of alkaline earth metal salts, followed by washing and calcination. Alkaline earth metal oxides loaded in zeolites are also prepared by impregnation of alkaline earth metal salts such as nitrates, acetates, or ethoxides followed by calcination (70,215,216).

Recently, Zhu *et al.* (217–220) reported the application of microwave radiation in dispersing MgO onto zeolites and mesoporous molecular sieves to generate strongly basic sites. Following this methodology, MgO was directly dispersed onto zeolites LTL, ZSM-5, beta, and the mesoporous molecular sieve MCM-48. The resulting materials were tested for the decomposition of 2-propanol and isomerization of *cis*-but-2-ene, with the results showing that the activity of supported MgO was strongly affected by the structure of the zeolite, with MgO/KLTL zeolite or MgO/NaLTL zeolite being the most active catalysts. For example, for isomerization of *cis*-but-2-ene at 273 K, the activity of a 2%MgO/KLTL zeolite sample exhibited an initial rate five times higher than a 5%MgO/K-beta zeolite sample, whereas a 5% MgO/NaZSM-5 was not active. The high basic activity exhibited by LTL zeolites was attributed to the geometric effect of their structure for absorbing microwaves in the irradiation process and the formation of special dispersed MgO.

#### A. CATALYTIC ACTIVITIES OF ALKALINE EARTH-MODIFIED ZEOLITES

Alkali metal ion-exchanged zeolites and occluded alkali metal oxide zeolites have been investigated extensively and applied as basic catalysts for a variety of organic transformations (1,41,221,222). Zeolites modified with alkaline earth compounds have been applied much less frequently as base catalysts for organic reactions.

In this section, we summarize recently reported organic transformations catalyzed by zeolites and mesoporous molecular sieves modified by alkaline earth metal oxides. Pillai (215) reported the alkylation of aniline with 2-propanol in the vapor phase at atmospheric pressure in the presence of alkali and alkaline earth metal ion (Li, Na, K, Ca, Sr, and Ba)-exchanged Y zeolites. Both N- and C-alkylated products were obtained, namely, *N*-isopropylaniline and *ortho*- and *para*-isopropylaniline isomers. Conversions of aniline were in the range of 7–18% at 623 K, with alkali earth metal ion-exchanged zeolites being more active than alkali metal ion-exchanged samples. Among the C-alkylated isomers, the *ortho* isomer was formed in higher yield than the *para* isomer, a result that was attributed to the proximity of the alkylating group on the catalyst surface to the *ortho* position of aniline. The authors found that the activities of the zeolites decrease as the cations become less electronegative, from Li to K and from Ca to Sr, with the C-alkylation selectivity decreasing in the same order, whereas the N-alkylation selectivity increases with increasing basicity of the ions. These results appear to be obvious because in the case of the alkaline earth-exchanged zeolites, it is well known that water can be hydrolyzed in association with the metal ions, resulting in the introduction of protons into the zeolite. Zeolite exchange by alkaline cations in aqueous media also leads to the exchange of some protons, unless the aqueous solution is basic. It

appears then that the weak acidity associated with these protons should be responsible for the C-alkylation.

Dumitriu *et al.* (223) reported the synthesis of acrolein by condensation of formaldehyde and acetaldehyde vapors using oxides (MgO, P<sub>2</sub>O<sub>5</sub>, B<sub>2</sub>O<sub>3</sub>, ZnO, and MoO<sub>3</sub>) deposited on HZSM-5, Y-zeolite, Al<sub>2</sub>O<sub>3</sub>, and SiO<sub>2</sub>. The investigation of the catalytic activity of these oxides supported on HZSM-5 showed that MgO gives the best performance, achieving 50% conversion at 673 K with an equimolar ratio of reagents. Moreover, it was observed that the selectivity to acrolein strongly depends on the nature of the support. MgO/SiO<sub>2</sub> and MgO/Y zeolite give higher conversions of acetaldehyde than MgO/ZSM-5; however, because of the formation of polycondensation products, crotonaldehyde, CH<sub>4</sub>, etc., the former are less selective than MgO/HZSM-5. The higher selectivity to acrolein exhibited by MgO/HZSM-5 was attributed to the spatial limitations of the zeolitic structure and probably to a cooperative effect of the basic centers of MgO and the acidic sites of the HZSM-5. With this zeolite as the support, there was an optimum MgO content (4 wt%) giving the highest yield (60%); an excess of magnesia hindered access of the reagents to the pores, with a decreased activity.

Ethylbenzene and styrene are traditionally obtained by the Friedel–Crafts alkylation of benzene with ethene. An attractive and novel route to obtain these compounds takes advantage of low-cost toluene produced from petroleum methane from natural gas; the reaction is the oxidative methylation of toluene, which proceeds only in the presence of basic catalysts (224). The basic active sites ensure the abstraction of hydrogen from toluene and methane, leading to the formation of methyl and benzyl radicals. Cross coupling of the radicals on the catalyst surfaces leads to the side-chain methylation of toluene to yield ethylbenzene and styrene (225). Kovacheva *et al.* (216,226–229) investigated the application of alkali earth metal oxides occluded in X zeolite for the oxidative methylation of toluene with methane. Reactions took place at temperatures between 973 and 1073 K, catalyzed by NaX zeolite loaded with MgO, CaO, SrO, and BaO. It was found that selectivities to styrene and ethylbenzene were similar (between 45 and 55%) for all samples; however, SrO- and BaO-modified zeolites were better catalysts than the others, giving higher toluene conversions. For example, at 1073 K, conversions of about 30% were measured with SrO- and BaO-modified zeolites, whereas conversions of only about 12% were measured with the others. TPD of CO<sub>2</sub> showed that the four samples exhibited strong basic sites of equal strength but different numbers. The amount of CO<sub>2</sub> desorbed increased with increasing the size of the alkali earth metal ion (i.e., from MgO/NaX zeolite to BaO/NaX zeolite). The higher basicity, as well as the higher catalytic activity observed in the presence of SrO/NaX zeolite and BaO/NaX zeolite was attributed to the highly electropositive character of the impregnated oxides relative to those of MgO/NaX zeolite and CaO/NaX zeolite.

Because BaO/NaX zeolite catalysts exhibited the best performance, further investigations have been carried out recently to characterize the oxidative methylation of toluene catalyzed by BaO-modified X- and Y-zeolites, mordenite, ZSM-5, silicalite, and ALPO<sub>4</sub>-5 (230). The authors found that activity and basicity of BaO-modified zeolites and zeolite-like catalysts depend on both the structural type and composition. Thus, for samples of the same structural type (BaO/NaX zeolite,

BaO/NaY zeolite, BaO/NaZSM-5, and BaO/silicalite), the activity and basicity depend on the composition, in other words, the lower the Si/Al ratio, the higher the activity and the higher the basicity. Moreover, it was found that the accessibility of the reagents to the BaO modifier also plays a decisive role in activity and basicity. The accessibility of the BaO was related to the structure of the zeolite, which determines the location of the BaO in the pores. Thus, in the large-pore X- and Y-zeolites, BaO particles easily migrate and fill the zeolite channels in such a way that the larger part of BaO remains partially hidden from the reagents, whereas the smaller pores of mordenite and ZSM-5 impede the migration of the formed BaO, making the BaO particles more accessible to the reagents. This interpretation is reflected in the catalytic activity; for example, conversions of 20 and 40% were achieved for BaO/NaX zeolite and BaO/NaZSM-5, respectively, at 1073 K.

Recently, a combinatorial investigation of alkylation of toluene with methanol to produce styrene with basic zeolites and alkaline earth catalysts was performed (231). The results of tests involving preparation and testing of more than 200 catalysts were modest, and these results emphasize that fine-tuning of the acid and base properties necessary to achieve better alkylation catalysts is not an easy task.

#### B. CATALYTIC ACTIVITY OF ALKALINE EARTH-MODIFIED MESOPOROUS MOLECULAR SIEVES

In the last decade, the mesoporous molecular sieve MCM-41 has been developed (232) and applied as a catalyst to many acid-catalyzed reactions (233). However, until now, comparatively few investigations of mesoporous molecular sieves as base catalysts have been reported (169,211–214,234,235). For example, sodium- and cesium-exchanged mesoporous MCM-41 were shown to be mildly selective, water-stable, recyclable catalysts for the base-catalyzed Knoevenagel condensation, and mesoporous MCM-41 containing intraporous cesium oxide particles prepared by impregnation with aqueous cesium acetate and subsequent calcination was found to have strong-base activity for the Michael addition (211,213) and rearrangement of *o*-phenylalkanals to phenyl alkyl ketones (212).

Recently, cross-aldol condensation of benzaldehyde with *n*-heptaldehyde to give jasminaldehyde (Scheme 13) has been reported; a mesoporous molecular sieve Al-MCM-41 with supported MgO was the catalyst. The reactions were carried out in a stirred autoclave reactor with a molar benzaldehyde/heptanal ratio of 10 at 373–448 K (236). The results show that Al-MCM-41 is catalytically active, and its activity is significantly increased by the deposition of MgO (Table V). Increasing the amount of deposited MgO on Al-MCM-41 decreases the surface area but enhances the catalyst basicity. The basicity is well correlated with the catalytic activity, although the selectivity to jasminaldehyde is not; the selectivity is essentially independent of temperature, pressure, time of the reaction, and conversion.

In addition to the results presented above, Jaenicke *et al.* (234) compared the activities of K<sub>2</sub>O, BaO, and K<sub>2</sub>O/La<sub>2</sub>O<sub>3</sub> incorporated in MCM-41 for the same reaction at 433 K with a benzaldehyde/heptanal molar ratio of 1.5. They found



TABLE V  
Cross-aldol Condensation of Benzaldehyde with Heptanal on Basic Catalysts<sup>a</sup> (236)

Catalyst	BET surface area (m <sup>2</sup> /g)	Base amount (mmol of CO <sub>2</sub> /g)	Conversion (%) after 2 h	Selectivity to jasminaldehyde (%)
Al-MCM-41	1032	—	9.4	41.6
5% MgO/Al-MCM-41	739	0.09	10.5	40.8
15% MgO/Al-MCM-41	726	0.11	20.5	35.5
20% MgO/Al-MCM-41	634	0.18	30.7	40.2
MgO	56	0.40	96.7	56.2

<sup>a</sup> Reaction conditions: Benzaldehyde/heptanal molar ratio = 10; temperature = 423 K; pressure, atmospheric.

that 10% BaO in MCM-41 exhibited very low activity (7.2% conversion after 2 h in a batch reactor); the best results were obtained with the most basic catalyst, the binary inorganic catalyst, K<sub>2</sub>O/La<sub>2</sub>O<sub>3</sub>-MCM-41, which gave a conversion of 61.9% with 53% selectivity to jasminaldehyde after 2 h. The authors claimed that the presence of the rare earth metal oxide improves the thermal stability of the material as well as the selectivity. Furthermore, much better results were obtained for the above reaction when MCM-41 was used as catalyst in a one-pot reaction in which, in order to minimize the self-condensation of heptanal, an intermediate heptanal dimethyl acetal was prepared and hydrolyzed *in situ* (237).

### VIII. Alkali Metal-Doped Alkaline Earth Metal Oxides

Promoter compounds are added to solid catalysts to induce enhancements in activity, selectivity, or lifetime. Alkali metals are used as promoters of many kinds of metal oxide catalysts, as their electron-donating ability leading to the enhancement of basicity of metal oxides is well known (238). Thus, Haag and Pines (239) observed that sodium metal deposited on alumina (Na/Al<sub>2</sub>O<sub>3</sub>) catalyzes isomerization of but-1-ene and pent-1-ene at room temperature. Researchers at Sumitomo Chemicals (116) developed base catalysts consisting of alkali metal hydroxide/alkali metal on alumina. These catalysts have basic sites with values corresponding to base strengths stronger than  $H_- = 37$ ; they are effective catalysts for low-temperature isomerization reactions such as the conversion of 5-vinylnorbornene to 5-ethylidenenorbornene; 2,3-dimethylbut-1-ene to 2,3-dimethylbut-2-ene; and safrole to isosafrole.

Kijenski and Malinowski reported that Na/MgO is a highly active catalyst for the isomerization of alkenes at 293 K and that the basic have base strengths stronger than those corresponding to  $H_- = 35$  (240,241).



### A. METHODS OF PREPARATION OF ALKALI METAL-DOPED ALKALINE EARTH METAL OXIDES

The preparation of alkali metal-doped alkaline earth metal oxides can generally be carried out by two different methods:

- (a) Chemical vapor deposition of the alkali metal (particularly Na and K) onto the alkaline earth hydroxide. This deposition is performed by heating the alkali metal to temperatures between 573 and 723 K under vacuum (242–245) or by mixing the alkaline earth oxide with an alkali metal azide salt ( $\text{NaN}_3$ ,  $\text{KN}_3$ , or  $\text{LiN}_3$ ) followed by decomposition of the azide by heating to about 673 K under vacuum (246–248). In both cases, the reaction of alkali metal vapor with the oxide surface gives solid super bases. According to Kijenskii and Malinowski (240,242) the term super base is used to denote a base strong enough to abstract a proton from hydrocarbon molecules such as triphenylmethane ( $\text{p}K_{\text{a}}$  of acid indicator equal to 33) or methane ( $\text{p}K_{\text{a}} = 40$ ). The base strength of a super base should therefore lie in the range of  $40 \geq H_- \geq 33$ . Later, Tanabe and Noyori (249) suggested that materials with base strengths corresponding to  $H_- = 26$  or stronger could be classified as super bases. In general, solid super bases are obtained when some metal oxides are treated with zero-valent alkali metals (116,250).
- (b) Impregnation of the alkali earth oxide with aqueous solutions of alkali metal salts or hydroxides ( $\text{NaOH}$ ,  $\text{KOH}$ ,  $\text{LiOH}$ ,  $\text{Li}_2\text{CO}_3$ , or  $\text{LiNO}_3$ ) followed by calcination at temperatures in the range of 733–1173 K (242,251,252).

Kijenski and Malinowski (242) reported properties and catalytic activities for isomerization of pent-1-ene to trans-pent-2-ene of catalysts prepared by doping of  $\text{MgO}$  with varying amounts of  $\text{NaOH}$  and catalysts prepared by evaporating sodium metal onto  $\text{MgO}$  pre-calcined at various temperatures. The numbers of basic sites of various strengths were determined by titrating the catalysts with benzoic acid solutions in benzene in the presence of appropriate Hammett indicators, and the one-electron donating or accepting properties of the catalysts were determined by adsorbing organic one-electron acceptors or donors, respectively, onto the catalyst and recording the EPR signals of the resulting ion radicals. The authors found that catalysts prepared by impregnating  $\text{MgO}$  with an aqueous solution of  $\text{NaOH}$  had acid–base properties close to those of pure  $\text{MgO}$ ; thus, the reaction of the  $\text{MgO}$  with sodium ions is inferred not to affect the maximum acid–base strength of the material, and only the number of centers is modified. The maximum concentration of both acid and base sites was attained for the catalyst containing 0.35 mmol of  $\text{Na}^+$  per gram of  $\text{MgO}$ . Moreover, it was found that the basicity of both pure  $\text{MgO}$  and  $\text{MgO}$  doped with  $\text{NaOH}$  decreased when the calcination temperature was increased, and for catalysts calcined at 1273 K, the strongest basic sites ( $27 \leq H_- \leq 33$ ) disappeared and the concentration of basic sites of lower strength decreased substantially. Furthermore, the one-electron donating properties of  $\text{MgO}$  underwent an insignificant change, and the maximum concentration of these sites that were able to reduce tetracyanoethene was found for the catalyst containing 0.35 mmol of  $\text{Na}^+$  per gram of  $\text{MgO}$ . However, the fact that the observed concentration of one-electron donor sites was much lower than the concentration of basic sites leads to the

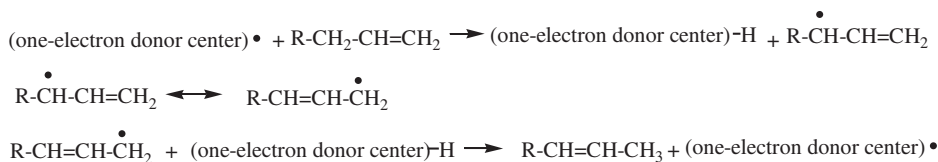
conclusion that there were two different types of sites, one responsible for one-electron donating properties and the other for the basic properties of the catalyst. On the other hand, catalysts prepared by evaporation of sodium metal onto MgO exhibited a greater number of basic sites than pure MgO and, moreover, basic sites of extreme strength ( $H_- > 35$ ). A high concentration of one-electron donor sites able to reduce nitrobenzene was detected in these materials.

Comparison of the results for catalytic isomerization of pent-1-ene to trans-pent-2-ene with the basic and one-electron donating properties of the catalysts led to the conclusion that two different reaction mechanisms operate in double bond isomerization reactions: (a) an ionic mechanism which involves proton abstraction from the alkene molecule by the super base site ( $pK_a = 37$  for pentenes) and (b) a free radical mechanism which involves the abstraction of a hydrogen atom from the alkene by the one-electron donor center (Scheme 39).

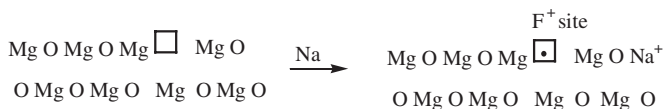
#### A.1. Alkaline Earth Metal Oxides Doped with Alkali Metals by Chemical Vapor Deposition

Investigations of the generation of super base sites on alkaline earth metal oxides by doping with alkali metals (246,247,253) led to the inference that when zero-valent alkali metals react with a metal oxide surface, the electron donated by the alkali metal to the oxide lattice resides in a defect site, such as an oxygen vacancy, generating a one-electron donor site ( $F^+$  center) (254,255) (Scheme 40).

The  $F^+$  sites can be observed by EPR spectroscopy. Matsushashi and Arata (253) investigated the relationship between the EPR signal intensity of the  $F^+$  center and the base catalytic activity for double bond migration of 3-methylbut-1-ene catalyzed by Na-doped MgO. The quantitative relationships indicated that the super base sites were generated by an induction effect of the electron released from the Na following its entrapment in the oxygen vacancy. Moreover, the maximum activity for the double bond migration was attained when two electrons were trapped in a single anion vacancy ( $F$  centers). It was also observed that the electrons trapped in the single anion vacancy activate several other sites (246). The authors concluded



SCHEME 39.



SCHEME 40.

that the  $F^+$  and  $F$  centers played the most important role in the formation of super base sites. Recently, they investigated (247) the concentration of super base sites generated on MgO, CaO, SrO, and BaO doped with Li, Na, and K by EPR spectroscopy with the aim of clarifying the role of the alkali metal ion in the generation of super base and adsorption sites. The catalytic activities of the solids were tested for the double bond migration of 4,4-dimethylpent-1-ene and 2,3-dimethylbut-1-ene at 273 K. A large increase in catalytic activity was observed with Na- and K-doped samples, whereas the increase in base catalytic activity relative to those of undoped oxides was very small for the other materials. The spin concentration of the paramagnetic  $NO_2^{2-}$  species generated by selective NO adsorption on strong basic sites and detected by EPR showed that the increased activity observed for Na- and K-doped MgO was caused by an increase in the number of sites. However, the promotion effect of electron(s) trapped in oxygen vacancies for the generation of super basic sites was very small on Li-doped MgO and on Li-, Na-, and K-doped CaO, SrO, and BaO. Thus, the authors concluded that when the ionic radius of the alkali metal is smaller than that of the oxide cation, the alkali cation adsorbs on the super basic sites (which are activated by trapped electron(s)), which consist of an assembly of three  $O^{2-}$  ions on the {111} microplane of the oxide. The electrical inductive effect is interfered by the adsorption of the alkali cation. In the case of Na- and K-doped MgO, the adsorption of the alkali cations on the super base site is unstable, because of the insufficient area on the three  $O^{2-}$  clusters for their adsorption, which forces the alkali cations to migrate, leading to an increase in the number of sites generated. On the basis of these results, the authors concluded that the ratio of ionic radii of the alkali metal and the alkaline earth metal must be 1.46 or greater to allow generation of super base sites.

As was shown above, the super base materials obtained by doping alkaline earth metal oxides with zero-valent alkali metals are efficient catalysts for isomerization reactions as well as alkylation reactions. Sun and Klabunde (244) reported that nanocrystalline MgO (prepared by the aerogel method) and doped with potassium metal has strongly basic sites that are active for isomerization of alkenes and alkylation of alkenes and toluene. The results show that undoped nanocrystalline MgO and fine crystalline MgO (prepared by coprecipitation) are not active for isomerization of pent-1-ene or 2,3-dimethylbut-1-ene at 273 K. However, the activity of a K-doped nanocrystalline sample was much higher than that of the K-doped crystalline MgO. Nearly 100% conversion was obtained for 10, 15, and 20% loadings of potassium for the doped nanocrystalline sample, whereas only 10% conversion was attained with the doped crystalline MgO having similar loadings. At higher temperatures (413–513 K), these catalysts are active for toluene–ethene and toluene–propene alkylation. Moreover, the catalysts were found to be active for propene–ethene alkylation at 413 K, giving pentenes and heptenes, with a maximum conversion at 483 K observed with the K-doped nanocrystalline sample. The number of basic sites and the base strength distribution of both doped samples were determined by titration methods. The total number of basic sites was closely correlated with the estimated number of ions that exist on edges/corners on the polyhedral crystallites of MgO. Only a fraction of these sites were basic enough to induce the alkylation reactions, and these sites were formed preferentially on

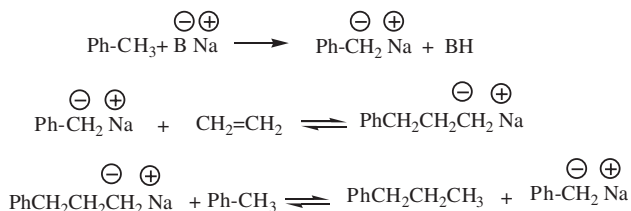
nanocrystalline MgO. It was observed that the surface concentration of strongly basic sites correlates well with the observed catalytic activities: K-doped nanocrystalline MgO > K-doped crystalline MgO. The authors suggested that trapped electrons near edge/corner sites could cause enhancements in basicity at these sites.

The side chain alkylation of alkyl benzenes is usually performed with alkenes as alkylating agents in the presence of strong-acid catalysts (256,257). The use of highly basic catalysts such as alkali metals, their hydrides, and sodium and potassium complexes for alkylation of alkylaromatic hydrocarbons has also been reported (256,257). The reaction mechanism proposed by Pines *et al.* (258) involves the addition of a benzylic carboanion to the alkene (Scheme 41).

Recently, alkylation of alkyl aromatic hydrocarbons such as toluene, ethylbenzene, cumene, and xylenes with ethene, propene, and 1,2-diphenylethene was investigated by Kijenski *et al.* (245), who used superbasic K-MgO and K-Al<sub>2</sub>O<sub>3</sub> catalysts at low temperature at atmospheric and elevated pressures. The reaction kinetics, EPR measurements of adsorbed intermediates, and the effects of poisoning determined by the radical trap TEMPO (2,2,6,6-tetramethyl-1-piperidinyloxy, free radical) led the authors to conclude that F<sup>+</sup> sites are the catalytically active centers. To demonstrate the importance of strong one-electron donor sites (F<sup>+</sup>) for the alkylation and the inactivity of strong two-electron donor centers, the ethylation of cumene, ethylbenzene, and toluene was carried out with MgO-10%NaOH. On this catalyst, strong basic two-electron donor sites (27 ≤ H<sub>2</sub> ≤ 33) were found, along with one-electron donor centers, which exhibited lower donor strengths than the F<sup>+</sup> centers on the superbasic surface of Na-MgO prepared by impregnation of MgO with NaOH. None of the investigated alkylbenzenes underwent alkylation. Moreover, the EPR spectra of the adsorbed reactants did not reveal radical or ion-radical activation of these species. These results indicate the necessity for participation of strong one-electron donor sites in the reaction and the impossibility of activating alkylation reactants ionically (i.e., by reactions involving two-electron donor sites). The authors suggested that alkylbenzenes and alkenes adsorb on independent surface sites in radical and/or ion-radical forms, which determine the reaction pathway.

#### A.2. Alkaline Earth Metal Oxides Doped with Alkali Metals Prepared by Impregnation

As stated above, a second route for the preparation of alkali-doped alkaline earth metal oxides is impregnation with aqueous solutions of alkali metal salts or hydroxides. As shown by Kijenski *et al.* (242), the resultant alkali metal-doped



SCHEME 41.

alkaline earth metal oxides exhibit lower basicities than those prepared by doping of the oxide with zero-valent metal. Lithium-doped MgO catalysts, first reported by Lunsford *et al.* (251,259), were prepared by impregnation of MgO with lithium salts (LiOH or LiCO<sub>3</sub>) followed by calcination. These materials are typical catalysts for the selective oxidation of alkanes, in particular for oxidative coupling of methane (OCM) (260). Several reviews of the catalytic oxidative coupling of methane have been reported since the 1980s (261–263). It is widely accepted that the catalytic activity for OCM is strongly correlated with the presence of oxygen anion species (e.g., O<sup>−</sup>, O<sub>2</sub><sup>2−</sup>, O<sup>2−</sup> etc.) formed by Li-doping (264,265).

Driscoll *et al.* (259,266) concluded that the catalytically active species for OCM are Li<sup>+</sup>-O<sup>−</sup> centers, which are equilibrated with surface O<sup>−</sup> centers via hole transport, because vacant hole sites are formed by Li doping in the surface and bulk. However, direct observation of the Li<sup>+</sup>-O<sup>−</sup> pairs is difficult, because they are present at high temperatures and are formed only in an O<sub>2</sub> atmosphere (267). It has been reported that O<sup>−</sup> species in other alkali-doped MgO catalysts are also active for OCM (265,268).

On the other hand, MgO contains a small number of various defect sites, including vacancies, ionic impurities, and trapped charge carriers. Voskresenkaya *et al.* (263) concluded that the formation of active oxygen anions for OCM results from the activation of oxidants by structural defects. When MgO is doped with Li, the substitution of Li<sup>+</sup> by Mg<sup>2+</sup> in the MgO lattice causes a loss of the characteristic crystal morphology of the precursor MgO, and the crystals now contain irregular grain boundary dislocations and dislocations in the bulk of the crystals, increasing the defect sites on the MgO. It has been found that the proposed mechanism for the active center formation (Li<sup>+</sup>-O<sup>−</sup> and vacant holes) (260) correlates with the formation of defect sites in/on Li-MgO. The characterization of these active defect sites has been carried out with various structural analytical techniques, such as EPR, (254,269,270) electron conductivity (271), XPS (272), XRD, and Mg K-edge XANES (273,274).

Besides oxidative coupling of methane and double bond isomerization reactions (242), a limited number of organic transformations have been carried out with alkali-doped alkaline earth metal oxides, including the gas-phase condensation of acetone on MgO promoted with alkali (Li, Na, K, or Cs) or alkaline earth (Ca, Sr, or Ba) (14,120). The basic properties of the samples were characterized by chemisorption of CO<sub>2</sub> (Table VI).

Promotion of MgO with alkali or alkaline earth metal ions (A) increases the amount of irreversibly held CO<sub>2</sub>, indicating that the promoter increases the concentration of surface basic sites. Moreover, the parameter M (mol CO<sub>2</sub>/mol of A) allows a comparison of the effect of the addition of various promoters on the basicity of MgO. Thus, it was observed that for each A-MgO series, M increased when the partial negative charge of oxygen in the pure A<sub>x</sub>O oxide increased. The value of the M parameter increases in the order Ca < Sr < Ba and Li < Na < K < Cs for alkaline earth- and alkali-promoted MgO, respectively. These results can be explained by taking into account the increase in the partial negative charge of oxygen ions in MgO resulting from the addition of alkaline earth or alkali metal ions of lower ionization potential than Mg. The specific increase of the number of

TABLE VI  
 Characterization of MgO and A-MgO catalysts (14)

Catalyst	Metal A loading ( $\mu\text{mol}/\text{m}^2$ )	Surface area ( $\text{m}^2/\text{g}$ )	Metal A ionic radius (Å)	CO <sub>2</sub> chemisorption		
				$n_i^a$ ( $\mu\text{mol}/\text{m}^2$ )	$n_i/n_T^b$	$M^c$ (mol of CO <sub>2</sub> /mol of A)
MgO	0.00	119	0.66	2.16	0.48	0.00
Ca/MgO	1.42	125	0.99	2.52	0.51	0.25
Sr/MgO	1.43	80	1.12	2.89	0.52	0.51
Ba/MgO	0.87	74	1.34	3.33	0.52	1.35
Li/MgO	18.50	81	0.68	4.60	0.71	0.13
Na/MgO	4.13	97	0.97	3.35	0.54	0.28
K/MgO	2.12	106	1.33	2.78	0.48	0.30
Cs/MgO	0.62	102	1.67	2.50	0.49	0.55

<sup>a</sup>  $n_i$  = number of moles of irreversibly held CO<sub>2</sub> per square meter;

<sup>b</sup>  $n_T$  = total number of moles of CO<sub>2</sub> adsorbed per square meter from the primary adsorption isotherm at 20 kPa;

<sup>c</sup> Values of  $M$  represent a measure of the effect that the addition of 1 mol of A has on increasing the CO<sub>2</sub> adsorption capacity of the MgO sample.

surface base sites would therefore be related to the electron-donating ability of the promoter—that is, the greater the electron-donor tendency of the promoter, the greater the number of generated basic sites. However, the basicity of the promoted oxide is not only influenced by the electron-donor properties of the alkali or alkaline earth metal, but, as reported by several authors (242,275,276), is also influenced by the loading of the promoter. Hence, the enhancement of the basicity of MgO observed by the addition of promoters results from a combination of the electron-donating ability of the A<sub>x</sub>O oxide and the concentration of the promoter in the sample.

The aldol condensation of acetone in the presence of these catalysts gave conversions between 17.9 and 12.6%, with the only products being mesityl oxide (MO), isomesityl oxide (IMO), and isophorone (IP). The activity of each promoted catalyst was higher than that of unpromoted MgO, and a good correlation was observed between the catalytic activity and the concentration of basic sites. All catalysts exhibited similar IP/(IMO + MO) selectivity ratios, except the Li–MgO sample, which gave larger yields of isophorone. Because the formation of isophorone requires the presence of strongly basic sites, the higher selectivity for formation of this compound indicates that the Li–MgO catalyst has stronger basic sites than the other doped samples.

Hur *et al.* (252,277,278) reported the use of alkali metal-doped MgO to catalyze the synthesis of acrylonitrile and propionitrile (278). Acrylonitrile is an important chemical, especially in the polymer industry; it is generally synthesized by the ammoxidation of propene catalyzed by multicomponent bismuth molybdates (279). An alternative method of synthesis of acrylonitrile is the reaction between methanol and acetonitrile (Scheme 42).



SCHEME 42.

This is a base-catalyzed reaction, and according to Kurokawa *et al.* (276) the conversion consists of three reactions: dehydrogenation of methanol to formaldehyde, cross-coupling between acetonitrile and formaldehyde, and dehydration of the intermediate to form acrylonitrile. This transformation has been performed with solid base catalysts such as alkali- and or alkaline earth metals supported on silica (280) and transition metal-promoted MgO (276,281). Hur *et al.* (278) investigated the catalytic activity of alkali metal-doped MgO catalysts, such as Li/MgO, Na/MgO, K/MgO, and Cs/MgO for the synthesis of acrylonitrile from methanol and acetonitrile in the temperature range 573–773 K. The catalysts were prepared by impregnation of MgO with aqueous solutions of the corresponding metal hydroxides followed by calcination at 873 K. The authors found that the order of activity was Na/MgO > K/MgO > Cs/MgO > Li/MgO. This order was explained on the basis of the ionic radius of the doped alkali metal ion. Kurokawa *et al.* (276) reported that the base strength of MgO increased when a transition metal ion with a radius larger than that of  $\text{Mg}^{2+}$  was incorporated into the MgO lattice, because it caused the localization of an electron on an oxygen atom. However, transition metal ions with radii markedly greater than that of  $\text{Mg}^{2+}$  caused a decrease in this effect, because the cation could not be effectively incorporated into the lattice. Such an explanation could also be applied to alkali metal-doped MgO. Thus, although the ionic radius of  $\text{Li}^+$  is similar to that of  $\text{Mg}^{2+}$ , the ionic radii of  $\text{K}^+$  and  $\text{Cs}^+$  are far greater than that of  $\text{Mg}^{2+}$ . Therefore, the base strengths of the catalysts were considered to decrease in the order Na/MgO > K/MgO > Cs/MgO > Li/MgO, in agreement with the order in catalytic activity. With the most active catalysts (Na/MgO) at 773 K and working under non-oxidative conditions (the reactions were carried out in the presence of  $\text{CO}_2$ ), the propionitrile yield was 49%, and the yield of acrylonitrile was only 5%. However, when the reactions were carried out under oxidative conditions the production of propionitrile (277) was suppressed and a maximum yield of 30% of acrylonitrile was obtained.

## IX. Alkaline Earth Metal Hydroxides

According to the Lewis theory, alkaline earth metal hydroxides are weaker bases than their oxides, the order of the strength of the basic sites being  $\text{Ba}(\text{OH})_2 > \text{SrO}(\text{OH})_2 > \text{Ca}(\text{OH})_2 > \text{Mg}(\text{OH})_2$ . The hydroxides have been used recently as solid catalysts for organic transformations, such as the conjugate addition of methanol to  $\alpha,\beta$ -unsaturated carbonyl compounds (12), cyanoethylation of alcohols (163,164), and transesterification reactions (166,167,171,172) which are described above. The extensive work of Sinisterra *et al.* (282) on the number and nature of sites and on the catalytic activity of the most basic alkali metal hydroxide,  $\text{Ba}(\text{OH})_2$ , is emphasized. It was found that commercial barium hydroxide octahydrate can be converted into



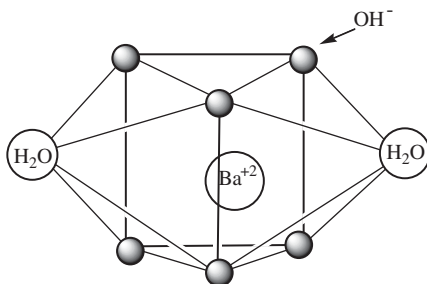


FIG. 4. Coordination sphere of  $\text{Ba}^{2+}$  in  $\text{Ba}(\text{OH})_2 \cdot \text{H}_2\text{O}$  cell lattice (283).

an active base catalyst by calcination in air at 473 K for 3 h (282). A complete investigation by thermal analysis, IR spectroscopy, and X-ray powder diffraction techniques (283) showed that this activated  $\text{Ba}(\text{OH})_2$  was in fact  $\beta\text{-Ba}(\text{OH})_2$  in the bulk and  $\text{Ba}(\text{OH})_2 \cdot \text{H}_2\text{O}$  on the surface. In the hydrate form, each  $\text{Ba}^{2+}$  ion is coordinated to six  $\text{OH}^-$  and two water molecules (Fig. 4).

The total basicity was determined by selective poisoning of the basic sites with benzoic acid ( $\text{p}K_{\text{a}} = 4.2$ ), and the number of strong basic sites was determined with 2,6-di-*t*-butyl-4-methylphenol (TBMPE,  $\text{p}K_{\text{a}} = 11.7$ ), which is a weak and hindered acid. The presence of strong basic sites was associated with unhindered surface  $\text{OH}^-$  groups, the negative charge of which is not compensated by the  $\text{Ba}^{2+}$  in the lattice. Thus, on the surface, the strongly basic sites could be the external  $\text{OH}^-$  groups hydrogen-bonded to the water. 1,2-Dinitrobenzene (DNB), which has a high electron affinity, was used to titrate the reducing sites of the catalyst. They may be negatively charged sites corresponding to  $\text{O}^{2-}$  ions formed during the calcination (176). The former would correspond to one-electron donor sites responsible for the catalytic activity exhibited by this solid for the Cannizzaro reaction (284), and the  $\text{O}^{2-}$  ions would act as basic and reducing sites. The titration results showed that only basic and reducing sites exist on the catalyst, and neither acid sites (tested for the adsorption of pyridine or cyclohexylamine) nor sites able to oxidize phenothiazine were present.

The strong basic sites associated with surface  $\text{OH}^-$  groups are responsible for the catalytic activity of the activated  $\text{Ba}(\text{OH})_2$  in organic reactions, such as the Michael addition (285). The authors showed, for example, that the Michael addition of diethyl malonate to chalcone catalyzed by activated  $\text{Ba}(\text{OH})_2$  yielded 95% of the Michael adduct. When  $\text{Ba}(\text{OH})_2$  was selectively poisoned with TBMPE, a conversion of only 5% was observed, however when  $\text{Ba}(\text{OH})_2$  was poisoned with DNB a conversion of 58% was obtained. The small poisoning effect of DNB indicates that only a small number of reducing sites with basic character (e.g.,  $\text{O}^{2-}$ ) can act in the process as basic sites. Thus, it was concluded that the basic sites responsible for the catalytic activity must be surface  $\text{OH}^-$  groups on the  $\text{Ba}(\text{OH})_2 \cdot \text{H}_2\text{O}$ .

A variety of organic reactions were reported to be catalyzed by the activated  $\text{Ba}(\text{OH})_2$  produced by calcination of  $\text{Ba}(\text{OH})_2 \cdot 8\text{H}_2\text{O}$  at 473 K. Some of the most important reactions, especially those leading to C–C bond formation, are summarized below.



## A. CATALYTIC REACTIONS ON ALKALINE EARTH METAL HYDROXIDES

A.1. *Aldol Condensations*

Aldol condensation of acetone is a well-known base-catalyzed reaction, and barium hydroxide is one of the catalysts for this reaction mentioned in textbooks. A family of barium hydroxide samples hydrated to various degrees determined by the calcination temperature (473, 573, 873, and 973 K) of the starting commercial  $\text{Ba}(\text{OH})_2 \cdot 8\text{H}_2\text{O}$  were reported to be active as basic catalysts for acetone aldol condensation (282,286). The reaction was carried out in a batch reactor equipped with a Soxhlet extractor, where the catalyst was placed. The results show that  $\text{Ba}(\text{OH})_2 \cdot 8\text{H}_2\text{O}$  is less active than any of the other activated  $\text{Ba}(\text{OH})_2$  samples, and the  $\text{Ba}(\text{OH})_2$  calcined at 473 K was the most active and selective catalyst for formation of diacetone alcohol, achieving nearly 58% acetone conversion after 8 h at 367 K in a batch reactor. When the reaction temperature was increased to 385 K, 78% acetone conversion with 92% selectivity to diacetone alcohol was obtained after 8 h. The yield of diacetone alcohol was similar to that described in the literature in applications with commercial barium hydroxide, but this catalyst required longer reaction times (72–120 h) (287). No deactivation of the catalyst was observed in the process, and it could be used at least 9 times without loss of activity.

A.2. *Claisen–Schmidt Condensation*

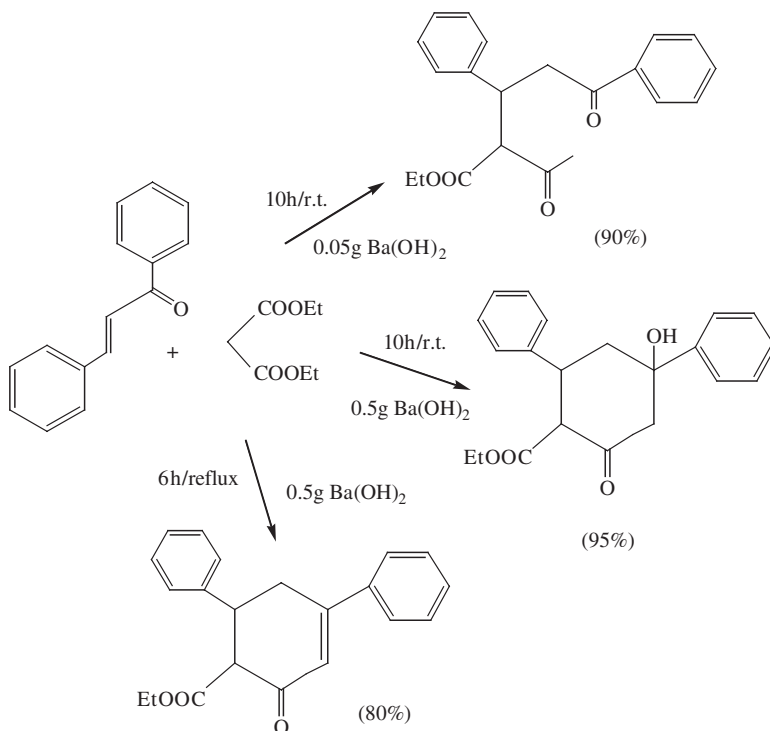
The activated  $\text{Ba}(\text{OH})_2$  was used as a basic catalyst for the Claisen–Schmidt (CS) condensation of a variety of ketones and aromatic aldehydes (288). The reactions were performed in ethanol as solvent at reflux temperature. Excellent yields of the condensation products were obtained (80–100%) within 1 h in a batch reactor. Reaction rates and yields were generally higher than those reported for alkali metal hydroxides as catalysts. Neither the Cannizzaro reaction nor self-aldol condensation of the ketone was observed, a result that was attributed to the catalyst's being more nucleophilic than basic. Thus, better selectivity to the condensation product was observed than in homogeneous catalysis under similar conditions. It was found that the reaction takes place on the catalyst surface, and when the reactants were small ketones, the rate-determining step was found to be the surface reaction, whereas with sterically hindered ketones the adsorption process was rate determining.

The condensation of 2-hydroxyacetophenone with benzaldehyde yielded exclusively 2'-hydroxy-chalcone, and the cyclization to flavanone was not observed. An investigation of the species adsorbed on the catalyst (289) suggested that CS condensation on the  $\text{Ba}(\text{OH})_2$  surface occurs via a very rigid transition state, whereby the OH group of 2-hydroxyacetophenone is bonded to the catalyst surface and placed at great distance from the carbonyl carbon atom of the aldehyde, making the cyclization of 2'-hydroxy-chalcone to flavanone difficult. Deactivation of the catalyst was not observed in the presence of moderate amounts of organic acids, such as benzoic, acrylic, or trichloroacetic acid.

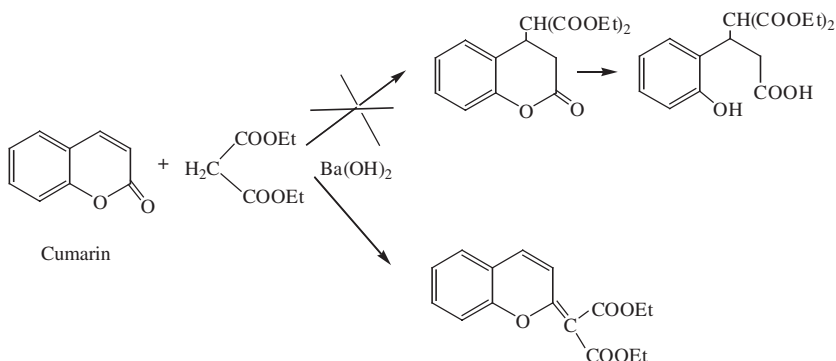
### A.3. Michael Additions

The activated  $\text{Ba}(\text{OH})_2$  catalyst was successfully used for the Michael reactions of chalcone with active methylene compounds (290), as well as for the Michael reaction of other benzylidene derivatives of acetone, butanone, 3-methylbutanone, 4-methyl-2-pentanone, and 3,3-dimethylbutanone with ethyl acetoacetate and diethyl malonate. The reaction with diethyl malonate gave good yields of the Michael adduct (between 65 and 93%), whereas with ethyl acetoacetate various products were obtained, depending on temperature and amount of catalyst (Scheme 43) (291). Thus, by varying the reaction conditions, it was possible to obtain a single product with practically 100% selectivity, the yields being higher than those obtained with soluble catalysts, such as KOH, NaOH, or piperidine.

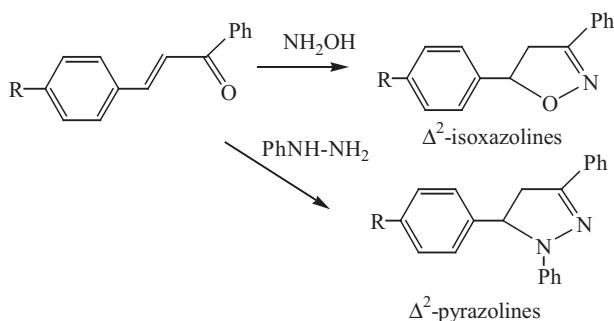
The Michael addition of nucleophiles to coumarins catalyzed by solid bases provides an interesting approach to the synthesis of 4-substituted 3,4-dihydrocoumarins, because with the conventional Michael catalysts the alkaline hydrolysis of the  $\delta$ -lactone predominates (Scheme 44). Results were obtained when the Michael addition of diethyl malonate to coumarin was catalyzed by the activated  $\text{Ba}(\text{OH})_2$  (292). An unusual 1,2-addition–elimination process at the  $\text{C}=\text{O}$  bond was observed. The mechanism of this reaction was explained on the basis of the microcrystalline structure of the catalyst. It was suggested that the rigid coumarin molecule interacts with the  $\text{Ba}^{2+}$  ions through the lone-pair electrons of both oxygen atoms of the



SCHEME 43.



SCHEME 44.



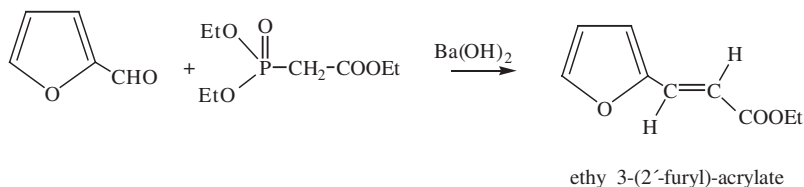
SCHEME 45.

lactone ring, which renders impossible the Michael addition but facilitates the 1,2-addition.

The synthesis of isoxazolines and pyrazolines via the Michael addition of hydroxylamine and phenyl hydrazine to chalcones and related enones was also reported with activated Ba(OH)<sub>2</sub> as a basic catalyst (293) (Scheme 45). In both cases, reactions were performed at reflux of ethanol, and excellent yields (65–80%) with 100% selectivity to the heterocyclic compounds were observed. Steric hindrance associated with the carbonyl compound as well as the electronic character of the substituents in the aromatic ring slightly affected the yields of the heterocyclic compounds.

#### A.4. Wittig–Horner Reaction

The Wittig–Horner (W–H) reaction is a versatile method for the synthesis of functionalized alkenes. The synthesis of 3-substituted ethyl acrylates and acrylonitriles, which are used as monomers in polymerization, were successfully carried out by the reaction of triethyl phosphonoacetate or cyanomethanephosphonate, respectively, with various aldehydes with activated Ba(OH)<sub>2</sub> as the catalyst in the presence of dioxane solvent at 343 K (294). As was observed for other basic solid



SCHEME 46.

TABLE VII

*Data Characterizing the Wittig–Horner Reaction between Furfural and Triethyl Phosphonoacetate in the Presence of Basic Catalysts in a Batch Reactor<sup>a</sup> (294)*

Catalyst	Reaction time (h)	Molar ratio catalyst/furfural	Yield (%) <sup>b</sup>
NaOH	1	0.66	93
KOH	1	0.66	83
K <sub>2</sub> CO <sub>3</sub>	1.5	0.66	96
Ba(OH) <sub>2</sub> · 8H <sub>2</sub> O	2.5	0.66	96
Activated Ba(OH) <sub>2</sub>	0.42	0.52	100

<sup>a</sup> Reaction conditions: dioxane (with 1.6% water) as a solvent at 343 K.

<sup>b</sup> Yield of ethyl-(2'-furyl)-acrylate.

catalysts, small amounts of water had to be added to increase the reaction rate. For example, the synthesis of ethyl-(2'-furyl)-acrylate (Scheme 46) was performed to give a yield and a selectivity of 100% each after 25 min in a batch reactor when 1.6 wt% of water was added to the dioxane. When anhydrous solvent was used, the catalytic activity was markedly lower (with a yield of 20% after 25 min).

It appears that the water plays an important role in the destruction of the 1,2-oxaphosphenate intermediate and in the regeneration of the catalytically active site. When the activity of activated Ba(OH)<sub>2</sub> was compared with that of other conventional basic catalysts, it was observed that the reaction times were dramatically reduced (Table VII). Moreover, no secondary reactions were observed with highly reactive aldehydes such as furfural and propanal.

Further investigations of the adsorption of phosphonates on the Ba(OH)<sub>2</sub> surface showed that with phosphonates characterized by high  $pK_a$  values (such as ketophosphonates, (EtO)<sub>2</sub>POCH<sub>2</sub>COR), dissolution of Ba(OH)<sub>2</sub> occurs, giving barium salts. The ylide produced on the catalyst surface goes to the liquid phase, where it reacts with the carbonyl compound, and therefore it can be considered that the process takes place in a homogeneous phase (295). However, when the phosphonate is weakly acidic (e.g., (EtO)<sub>2</sub>POCH<sub>2</sub>COOEt), the ylide remains adsorbed on the solid and is stabilized by the charge delocalization between the ylide and Ba<sup>2+</sup>. In this case, the reaction takes place only when the ylide has a geometry and charge distribution similar to those of the active site.

An investigation of the Wittig–Horner reaction taking place under sonochemical irradiation and catalyzed by the activated Ba(OH)<sub>2</sub> showed that the process could be markedly improved. The sonochemical process increased the reaction rate over

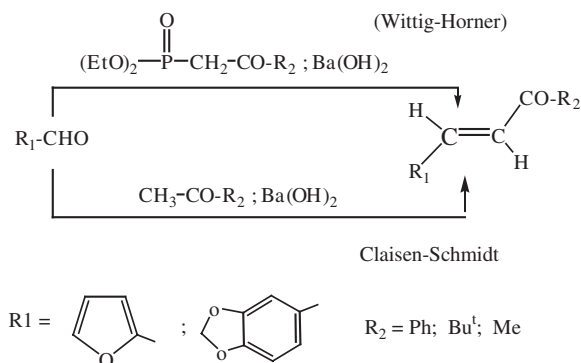
that observed in the absence of sonication, as has also been observed for other organic reactions. Thus, the sonochemical reaction took place even at room temperature, with a smaller catalyst mass and a shorter reaction time. Under these conditions, the yields were similar to those of the thermal process. Moreover, it was found that the necessary sonication time appears to be very short, because similar yields were obtained after 5 or 30 min. On the basis of an investigation of the nature of the adsorbed species, the authors postulated that an electron transfer mechanism was involved in the sonochemical catalytic process (296).

Synthesis of acyclic *E*- $\alpha$ -enones was performed according to the Wittig–Horner (297) and Claisen–Schmidt (298) approaches with activated  $\text{Ba}(\text{OH})_2$  as a basic catalyst (Scheme 47). The W–H reactions were carried out in the presence of dioxane solvent at 343 K, and yields higher than 90% were observed after reaction times between 10 and 30 min in a batch reactor. Under these conditions, owing to the dependence of the reaction course on the acidity of the phosphonate with barium hydroxide, the W–H reaction took place in a homogeneous phase.

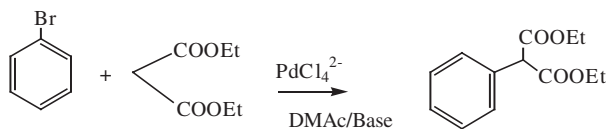
In the Claisen–Schmidt condensation at the same temperature and with ethanol solvent present, lower yields of  $\alpha$ -enones were observed. The best yield corresponds to condensation of the most reactive furfural with acetophenone, giving 95%  $\alpha$ -enone after 1 h in a batch reactor. A comparison of the results characterizing the two reactions led to the conclusion that the W–H reaction provides the more efficient and selective synthesis of  $\alpha$ -enones; however, the CS condensation provides the more economic approach.

#### A.5. Arylation of Carbonyl Compounds

As the last example of C–C bond-formation reactions catalyzed by alkaline earth hydroxides, we mention the recently reported  $\alpha$ -arylation of diethyl malonate in the presence of a palladium catalyst and a base in a separate phase (299). The arylation of carbonyl compounds is a carbon–carbon coupling reaction between an aryl halide and an enolate, which is usually catalyzed by palladium salts in the presence of an appropriate base (300,301). The arylation of diethyl malonate with bromobenzene (Scheme 48) was performed with tetrachloropalladate as the



SCHEME 47.



SCHEME 48.

TABLE VIII

*Results Obtained in the Arylation of Diethyl Malonate with Bromobenzene Catalyzed by  $\text{Na}_2\text{PdCl}_4$  and Various Solid Bases in a Batch Reactor (299)*

Base catalyst	Yield (%) <sup>a</sup>	Selectivity (%) <sup>b</sup>
MgO/Al <sub>2</sub> O <sub>3</sub>	16.5	92
MgO/Ga <sub>2</sub> O <sub>3</sub>	8.3	87
MgO/CaO	6.5	89
MgO	6.0	93
Ca(OH) <sub>2</sub>	96.1 <sup>c</sup>	94
Ba(OH) <sub>2</sub>	99.0 <sup>d</sup>	97
K <sub>2</sub> CO <sub>3</sub>	93.1	94
Na <sub>2</sub> CO <sub>3</sub>	41.7	91
Li <sub>2</sub> CO <sub>3</sub>	14.3	92

<sup>a</sup> Diethyl malonate yield after 24 h at 373 K.

<sup>b</sup> Selectivity for diethyl phenyl malonate.

<sup>c</sup> Yield after 20 h.

<sup>d</sup> Yield after 14 h.

catalyst, *N,N*-dimethylacetamide as a solvent, and various solid bases to obtain the enolate form.

Table VIII shows the conversions and selectivities obtained in this reaction with the various bases. Both calcium and barium hydroxide, as well as potassium carbonate, gave good yields and selectivities, particularly barium hydroxide, which gave conversions near 100% after 14 h in a batch reactor. Ba(OH)<sub>2</sub> was tested as a basic catalyst for the reaction with other aryl halides such as iodobenzene and chlorobenzene, and in both cases the yield and selectivity were also excellent.

## X. Conclusions and Future Opportunities

Although we have limited our consideration to alkaline earth metal oxides and hydroxides as base catalysts, it is evident that the number of reported investigations is very large. We perceive an emerging interest in materials science-oriented researchers in working on high-surface-area-modified alkaline earth metal oxides, which appear to offer attractive opportunities as basic catalysts. However, complementary approaches such as quantum chemical modeling of the basic sites and their interactions with reactants, have remained almost entirely neglected. In general, we perceive that fundamental investigations of the nature of basic surface sites appear to be much less sophisticated than fundamental investigations of acid sites.

It can be expected that solid bases could be successful for commercializing the alkylation of toluene with methanol as a route to styrene, or for selective alkene coupling. There is no doubt that achieving success in several important commercial processes will boost the field of solid base catalysis. Because it appears to be difficult to achieve superbasic organic resins, much more attention should be paid to enhancement of the base strengths of solid superbases. Further work should be done on supported alkali metals and mixed metal oxides. Development of new solid superbases will be improved by increasing our understanding of how alkali metal clusters (302–304) interact with supports and become stabilized.

We believe that an interesting advantage of solid bases with respect to the homogeneous ones is the possibility of tuning acidic and basic sites. The proper control of these pair sites can strongly influence activity and selectivity for some reactions through a cooperative effect (305–307). Cooperative effects of acid and base sites are particularly important in enzyme catalysis. Along the lines of dual functional catalysts, more emphasis should be placed on bifunctional hydrogenation-base catalysts, and oxidation-base catalysts. Finally, as we have noted, authors pay attention too infrequently to catalyst deactivation when working with base catalysts. This is most unfortunate, because commercialization of solid catalysts with enhanced basic strengths requires a good knowledge of the factors that influence catalyst stability.

## Acknowledgment

The authors thank the sponsors of CICYT project MAT2003-07945-C02-01.

## References

1. Ono, Y., and Baba, T., *Catal. Today* **38**, 321 (1997).
2. Hattori, H., *Chem. Rev.* **95**, 537 (1995).
3. Hattori, H., *Stud. Surf. Sci. Catal.* **21**, 319 (1985).
4. Tanabe, K., in "Catalysis by Acids and Bases" (B. Imelik, *et al.*, Eds.), Elsevier, Amsterdam, 1985.
5. Coluccia, S., and Tench, A.J., Proceedings of 7th International Congress for Catalysis, Tokyo, 1157, (1980).
6. Garrone, E., and Stone, F.S., 8th International Congress Catalysis, Berlin, Verlag Chemie III, 441 (1984).
7. Hattori, H., *Mater. Chem. Phys.* **18**, 533 (1988).
8. Tanabe, K., Misono, M., Ono, Y., and Hattori, H., in "New Solid Acids and Bases" p. 39. Kodansha-Elsevier, Amsterdam, 1989.
9. Take, J.I., Kikuchi, N., and Yoneda, Y., *J. Catal.* **21**, 164 (1971).
10. Kabashima, H., Tsuji, H., and Hattori, H., *React. Kinet. Catal. Lett.* **58**, 255 (1996).
11. Kabashima, H., Tsuji, H., Shibuya, T., and Hattori, H., *J. Mol. Catal., A: Chemical* **155**, 23 (2000).
12. Kabashima, H., Katou, T., and Hattori, H., *Appl. Catal., A: General* **214**, 121 (2001).
13. Tsuji, H., Yagi, F., Hattori, H., and Kita, H., *J. Catal.* **148**, 759 (1994).
14. Di Cosimo, J.I., Diez, V.K., and Apesteguia, C.R., *Appl. Catal., A: General* **137**, 149 (1996).
15. Kabashima, H., Tsuji, H., and Hattori, H., *Appl. Catal., A: General* **165**, 319 (1997).
16. Durgakumari, V., and Narayanan, S., *J. Mol. Catal.* **65**, 385 (1991).
17. Fouad, N.E., Thomasson, P., and Knozinger, H., *Appl. Catal., A: General* **194–195**, 213 (2000).
18. Choudhary, V.R., and Pandit, M.Y., *Appl. Catal.* **71**, 265 (1991).

19. Choudhary, V.R., Pataskar, S.G., Pandit, M.Y., and Gunjikar, V.G., *Thermochim. Acta* **194**, 361 (1992).
20. Choudhary, V.R., Rane, V.H., and Gadre, R.V., *J. Catal.* **145**, 300 (1994).
21. Choudhary, V.R., Pataskar, S.G., Zope, G.B., and Chaudhari, P.N., *J. Chem. Technol. Biotechnol.* **64**, 407 (1995).
22. Aramendia, M.A., Borau, V., Garcia, I.M., Jimenez, C., Marinas, A., Marinas, J.M., Porras, A., and Urbano, F.J., *Appl. Catal., A: General* **184**, 115 (1999).
23. Matsuda, T., Tanabe, J., Hayashi, N., Sasaki, Y., Miura, H., and Sugiyama, K., *Bull. Chem. Soc. Jpn.* **55**, 990 (1982).
24. Phillips, V.A., Opperhauser, H., and Kolbe, J.L., *J. Am. Ceram. Soc.* **61**, 75 (1978).
25. Shastri, A.G., Chae, H.B., Bretz, M., and Schwank, J., *J. Phys. Chem.* **89**, 3761 (1985).
26. Ardizzone, S., Bianchi, C.L., and Vercelli, B., *J. Mater. Res.* **13**, 2218 (1998).
27. Ardizzone, S., Bianchi, C.L., and Vercelli, B., *Appl. Surf. Sci.* **126**, 169 (1998).
28. Bancquart, S., Vanhove, C., Pouilloux, Y., and Barrault, J., *Appl. Catal., A: General* **218**, 1 (2001).
29. Leofanti, G., Solari, M., Tauszik, G.R., Garbassi, F., Galvano, S., and Schwank, J., *Appl. Catal.* **3**, 131 (1982).
30. Holt, T.E., Logan, A.D., Chakraborti, S., and Datye, A.K., *Appl. Catal.* **34**, 199 (1987).
31. Matsuda, T., Ishimatsu, K., and Sugimoto, M., *React. Kinet. Catal. Lett.* **44**, 63 (1991).
32. Lopez, T., Garcia-Cruz, I., and Gomez, R., *J. Catal.* **127**, 75 (1991).
33. Menon, M., Warren, J.L., and Bullard, J.W., *Ceram. Trans.* **95**, 217 (1998).
34. Lopez, T., Marmolejo, R., Asomoza, M., Solis, S., Gomez, R., Wang, J.A., Bokhimi, N.O., Navarrete, J., Llano, M.E., and Lopez, E., *Mater. Lett.* **32**, 325 (1997).
35. Bokhimi, M.A., Lopez, T., and Gomez, R., *J. Solid State Chem.* **115**, 411 (1995).
36. Utamapanya, S., Klabunde, K.J., and Schlup, J.R., *Chem. Mater.* **3**, 175 (1991).
37. Stark, J.V., Park, D.G., Lagadic, I., and Klabunde, K.L., *Chem. Mater.* **8**, 1904 (1996).
38. Klabunde, K.J., Stark, J., Koper, O., Mohs, C., Park, D.G., Decker, S., Jiang, Y., Lagadic, I., and Zhang, D.J., *J. Phys. Chem.* **100**, 12142 (1996).
39. Tanabe, K., "Solid Acids and Bases." Academic Press, New York, 1970.
40. Forni, L., *Catal. Rev.* **8**, 65 (1974).
41. Barthoomeuf, D., *Catal. Rev.-Sci. Eng.* **38**, 521 (1996).
42. Borodin, V.N., *Zh. Fiz. Khim.* **51**, 928 (1997).
43. Take, J.L., Nikichi, N., and Yoneda, Y., *J. Catal.* **21**, 164 (1971).
44. Gasteiger, J., and Marsili, M., *Tetrahedron Lett.* **3181**, (1978).
45. Che, M., Imelik, B., and Naccache, C., *J. Catal.* **24**, 328 (1972).
46. Flockhart, B.D., and Salem, M.A., *J. Colloid Interface Sci.* **103**, 76 (1985).
47. Paukshtis, E.A., and Yurchenko, E.N., *Russ. Chem. Rev.* **52**, 42 (1983).
48. Lavalley, J.C., *Trends Phys. Chem.* **2**, 305 (1991).
49. Knözinger, H., in "Handbook of Heterogeneous Catalysis." (G. Ertl, H. Knözinger, and J. Weitkamp, Eds.), Vol. 2, p. 707. Wiley-VCH, Weinheim, 1997.
50. Lavalley, J.C., *Catal. Today* **27**, 377 (1996).
51. Guglielminotti, E., Coluccia, S., Garrone, E., Cerruti, L., and Zecchina, A., *J. Chem. Soc. Faraday Trans. 1* **75**, 96 (1979).
52. Coluccia, S., Garrone, E., Guglielminotti, E., and Zecchina, A., *J. Chem. Soc. Faraday Trans. 1* **77**, 1063 (1981).
53. Tsyganenko, A.A., Lamotte, J., Gallas, J.P., and Lavalley, J.C., *J. Phys. Chem.* **93**, 4179 (1989).
54. Tsyganenko, A.A., Pozdnyakov, D.V., and Filimonov, V.N., *J. Mol. Struct.* **29**, 299 (1975).
55. Coluccia, S., Lavagnino, S., and Marchese, L., *J. Chem. Soc. Faraday Trans. 1: Phys. Chem. Cond. Phases* **83**, 477 (1987).
56. Coluccia, S., Garrone, E., and Borello, E., *J. Chem. Soc. Faraday Trans. 1* **79**, 607 (1983).
57. Kijenski, J., and Baiker, A., *Catal. Today* **5**, 1 (1989).
58. Zecchina, A., and Stone, F.S., *J. Catal.* **101**, 227 (1986).
59. Knözinger, H., Krietenbrink, H., Müller, H.D., and Schulz, W., in "Proceedings of the 6th International Congress for Catalysis." (G.C. Bond, P.E. Wells, and F.C. Tompkins, Eds.), The Chemical Society, London, 183, 1977.



60. Huber, S., and Knozinger, H., *J. Mol. Catal., A-Chemical* **141**, 117 (1999).
61. Hadjiivanov, K.I., and Vayssilov, G.N., *Adv. Catal.* **47**, 307 (2002).
62. Zecchina, A., and Arean, C.O., *Catal. Rev.-Sci. Eng.* **35**, 261 (1993).
63. Arean, C.O., Palomino, C.T., Platero, E.E., and Mentrui, M.P., *J. Chem. Soc.-Dalton Trans.* 873 (1997).
64. Okamoto, Y., and Kubota, T., *Microporous Mesopor. Mater.* **48**, 301 (2001).
65. Bremard, C., Denneulin, E., Depecker, C., and Legrand, P., *Stud. Surf. Sci. Catal.* **48**, 219 (1989).
66. Papile, C.J., and Gates, B.C., *Langmuir* **8**, 74 (1992).
67. Auroux, A., and Gervasini, A., *J. Phys. Chem.* **94**, 6371 (1990).
68. Kanno, T., and Kobayashi, M., in "Acid-base Catalysts II." (M. Misono, and Y. Ono, Eds.), Kodansha-Elsevier, Tokyo, 207, 1994.
69. Choudhary, V.R., and Rane, V.H., *Catal. Lett.* **4**, 101 (1990).
70. Tsuji, H., Yagi, F., Hattori, H., and Kitta, H., *Stud. Surf. Sci. Catal.* **75**, 1171 (1993).
71. Di Cosimo, J.L., Diez, V.K., Xu, M., Iglesia, E., and Apesteguia, C.R., *J. Catal.* **178**, 499 (1998).
72. Beres, A., Palinko, I., Kiricsi, I., Nagy, J.B., Kiyozumi, Y., and Mizukami, F., *Appl. Catal., A: General* **182**, 237 (1999).
73. Zhang, G., Hattori, H., and Tanabe, K., *Appl. Catal.* **36**, 189 (1988).
74. Diez, V.K., Apesteguia, C.R., and Di Cosimo, J.I., *Catal. Today* **63**, 53 (10-12-2000).
75. Philipp, R., and Fujimoto, K., *J. Phys. Chem.* **96**, 9035 (1992).
76. McKenzie, A.L., Fischell, C.T., and Davis, R.J., *J. Catal.* **138**, 547 (1992).
77. Kurokawa, H., Ueda, W., Morikawa, Y., Morooka, Y., and Ikawa, T., in "Acid-Base Catalysis." (K. Tanabe, H. Hattori, T. Yamaguchi, and T. Tanaka, Eds.), Kodansha, Tokyo, 93, 1989.
78. Tanabe, K., Misono, M., Ono, Y., and Hattori, H., "New Solid Acids and Bases." p. 260. Kodansha-Elsevier Amsterdam, 1989.
79. Ai, M., *J. Catal.* **40**, 318 (1975).
80. Gervasini, A., and Auroux, A., *J. Catal.* **131**, 190 (1991).
81. Lahousse, C., Bachelier, J., Lavalley, J.C., Laumonpernot, H., and LeGovic, A.M., *J. Mol. Catal.* **87**, 329 (1994).
82. Laumonpernot, H., Luck, F., and Popa, J.M., *Appl. Catal.* **78**, 213 (1991).
83. Davis, B., in "Adsorption and Catalysis on Oxide Surfaces." (M. Che, and G.C. Bond, Eds.), Elsevier, Amsterdam, 1985.
84. Bezouhanova, C.P., and Al-Zihari, M.A., *Catal. Lett.* **11**, 245 (1991).
85. Aramendia, M.A., Borau, V., Jimenez, C., Marinas, J.M., Porras, A., and Urbano, F.J., *React. Kinet. Catal. Lett.* **65**, 25 (1998).
86. Grisebach, H., and Moffat, J.B., *J. Catal.* **80**, 350 (1983).
87. Kurokawa, H., Kato, T., Ueda, W., Morikawa, Y., Morooka, Y., and Ikawa, T., *J. Catal.* **126**, 199 (1990).
88. Bordawekar, S.V., Doskocil, E.J., and Davis, R., *Catal. Lett.* **44**, 193 (1997).
89. Aramendia, M.A., Borau, V., Jimenez, C., Marinas, J.M., Porras, A., and Urbano, F.J., *React. Kinet. Catal. Lett.* **53**, 397 (1994).
90. Aramendia, M.A., Borau, V., Jimenez, C., Marinas, J.M., Porras, A., and Urbano, F.J., *J. Catal.* **161**, 829 (1996).
91. Ai, M., *J. Catal.* **40**, 327 (1975).
92. Williams, C., Makarova, M.A., Malysheva, L.V., Paukshtis, E.A., and Zamarev, K.I., *J. Chem. Soc. Faraday Trans.* **85**, 3473 (1990).
93. Gervasini, A., Fenyvesi, J., and Auroux, A., *Catal. Lett.* **43**, 19 (1997).
94. Tomczak, D.C., Allen, J.L., and Poeppelmeier, K.R., *J. Catal.* **146**, 155 (1994).
95. Audry, F., Hoggan, P.E., Saussey, J., Lavalley, J.C., Laumonpernot, H., and LeGovic, A.M., *J. Catal.* **168**, 471 (1997).
96. Corma, A., and Martin-Aranda, R.M., *J. Catal.* **130**, 130 (1991).
97. Climent, M.J., Corma, A., Fornes, V., Frau, A., Guil-Lopez, R., Iborra, S., and Primo, J., *J. Catal.* **163**, 392 (1996).
98. Corma, A., Martin-Aranda, R.M., and Sanchez, F., *J. Catal.* **126**, 192 (1990).
99. Corma, V., Fornes, V., Martin-Aranda, R.M., and Rey, F., *J. Catal.* **134**, 58 (1992).

100. Corma, A., Fornes, V., Martin-Aranda, R.M., Garcia, H., and Primo, J. *Appl. Catal.* **59**, 237 (1990).
101. Hurd, C.D., Edwards, O.E., and Roach, J.R., *J. Am. Chem. Soc.* **66**, 2013 (1994).
102. Hunsdiecker, H., *Chem. Ber.* **75**, 445 (1942).
103. Dessau, R.M., *Zeolites* **10**, 205 (1990).
104. Dessau, R.M., US Patent 5024919 (1991).
105. Guida, A., Lhouty, M.H., Tichit, D., Figueras, F., and Geneste, P., *Appl. Catal., A: General* **164**, 251 (1997).
106. Figueras, F., Lopez, J., Sanchez-Valente, J., Vu, T.T.H., Clacens, J.M., and Palomeque, J., *J. Catal.* **211**, 144 (2002).
107. Valente, J.S., Figueras, F., Gravelle, M., Kumbhar, P., Lopez, J., and Besse, J.P., *J. Catal.* **189**, 370 (2000).
108. Bent, H.A., *Chem. Rev.* **61**, 275 (1961).
109. Bordwell, F.G., Bausch, M.J., Branca, J.C., and Harrelson, J.A., *J. Phys. Org. Chem.* **1**, 225 (1988).
110. Ohnishi, R., and Tanabe, K., *Chem. Lett.* 207 (1974).
111. Tanabe, K., Yoshii, N., and Hattori, H., *J. Chem. Soc. Chem. Commun.* 464 (1971).
112. Morishige, K., Hattori, H., and Tanabe, K., *J. Chem. Soc. Chem. Commun.* 559 (1975).
113. Hattori, A., Hattori, H., and Tanabe, K., *J. Catal.* **65**, 245 (1980).
114. Matsuhashi, H., Hattori, H., and Tanabe, K., *Chem. Lett.* 341 (1981).
115. Matsuhashi, H., and Hattori, H., *J. Catal.* **85**, 457 (1984).
116. Suzukamo, G., Fukao, M., and Minobe, M., *Chem. Lett.* 585 (1987).
117. Baba, T., and Endou, T.H.H.O.Y., *J. Appl. Catal. A*, **97**, L19 (1993).
118. Salvapati, G.S., Ramanamurty, K.V., and Janardana Rao, M., *J. Mol. Catal.* **54**, 9 (1989).
119. Zhang, G., Hattori, H., and Tanabe, K., *Appl. Catal.* **40**, 183 (1988).
120. Di Cosimo, J.I., and Apesteguia, C.R., *J. Mol. Catal., A: Chemical* **130**, 177 (1998).
121. Zhang, G., Hattori, H., and Tanabe, K., *Bull. Chem. Soc. Jpn.* **62**, 2070 (1989).
122. Payne, L.S., EU Patent 0392579 (1990).
123. Climent, M.J., Corma, A., Fornes, V., Guil-Lopez, R., and Iborra, S., *Adv. Synth. Catal.* **344**, 1090 (2002).
124. Climent, M.J., Corma, A., Iborra, S., and Velty, A., *J. Mol. Catal., A: Chemical* **182–183**, 327 (2002).
125. Tichit, D., Lutić, D., Coq, B., Durand, R., and Tessier, R., *J. Catal.* **219**, 187 (2003).
126. Russel, A., and Kenyon, R.L., *Organic Synthesis* **3**, 380 (1996).
127. Lothar, J., Werner, H., Lothar, A., Manfred, S., and Juergen, S.H., EU Patent 62291 (1982).
128. Mitchell, P., US Patent 4874900 (1987).
129. Thomas, A.F., and Guntz-Dubini, R., *Helv. Chim. Acta* **59**, 2261 (1976).
130. Noda, C., Alt, G.P., Werneck, R.M., Henriques, C.A., and Monteiro, J.L.F., *Braz. J. Chem. Eng.* **15**, 120 (1998).
131. Climent, M.J., Corma, A., Iborra, S., and Velty, A., *Catal. Lett.* **79**, 157 (2002).
132. Dhar, D.N., "Chemistry of Chalcones and Related Compounds." Wiley, New York, 1981.
133. Harbone, J.B., and Mabry, T.J., "The Flavonoids: Advances in Research." Chapman & Hall, New York, 1982.
134. Ballesteros, J.F., Sanz, M.J., Ubeda, A., Miranda, M.A., Iborra, S., Paya, M., and Alcaraz, M.J., *J. Med. Chem.* **38**, 2794 (1995).
135. Li, R., Kenyon, G.L., Cohen, F.E., Chen, X., Gong, B., Dominguez, J.N., Davison, E., Kurzban, G., Miller, R.E., and Nuzman, E.O., *J. Med. Chem.* **38**, 5031 (1995).
136. Wattenberg, L.W., Coccia, J.B., and Galbraith, A.R., *Cancer Lett.* **83**, 165 (1994).
137. Yit, C.C., and Das, N.P., *Cancer Lett.* **82**, 65 (1994).
138. Climent, M.J., Corma, A., Iborra, S., and Primo, J., *J. Catal.* **151**, 60 (1995).
139. Drexler, M.T., and Amiridis, M.D., *Catal. Lett.* **79**, 175 (2002).
140. Hargrove-Leak, S.C., and Amiridis, M.D., *Catal. Commun.* **3**, 557 (2002).
141. Drexler, M.T., and Amiridis, M.D., *J. Catal.* **214**, 136 (2003).
142. Rosini, G., in "Comprehensive Organic Synthesis," (B.M. Trost and I. Fleming, Eds.), ch. 1.10, p. 2 Pergamon Press, Oxford, 1991.

143. Ballini, R., and Bosica, G., *Tetrahedron Lett.* **37**, 8027 (1996).
144. Luzzio, F.A., *Tetrahedron* **57**, 915 (2001).
145. Akutu, K., Kabashima, H., Seki, T., and Hattori, H., *Appl. Catal., A: General* **247**, 65 (2003).
146. Knoevenagel, E., *Chem. Ber.* **27**, 2345 (1984).
147. March, J., "Advanced Organic Chemistry." 4th Edition, Wiley-Interscience, John Wiley & Sons (1992).
148. Corma, A., Iborra, S., Primo, J., and Rey, F., *Appl. Catal., A: General* **114**, 215 (1994).
149. Climent, M.J., Corma, A., Guil-Lopez, R., Iborra, S., and Primo, J., *Catal. Lett.* **59**, 33 (1999).
150. Wittig, G., and Geissler, G., *Liebigs Ann. Chem.* **580**, 44 (1953).
151. Hwang, J.J., Lin, R.L., Shieh, R.L., and Jwo, J.J., *J. Mol. Catal. A-Chemical* **142**, 125 (1999).
152. Wadsworth, D.H., *Org. React.* **25**, 73 (1977).
153. Wadsworth, D.H., Schupp, O.E., Seus, E.J., and Ford, J.A., *J. Org. Chem.* **30**, 680 (1965).
154. Texier-Boullet, F., and Foucaud, A., *Synthesis*, 884 (1979).
155. Moison, H., Texier-Boullet, F., and Foucaud, A., *Tetrahedron* **43**, 537 (1987).
156. Hachemi, M., Puciova-Sebova, M., Toma, S., and Villemain, D., *Phosphorus, Sulfur Silicon Relat. Elem.* **113**, 131 (1996).
157. Bergmann, E.D., Ginsburg, D., and Pappo, R., *Org. React.* **10**, 179 (1959).
158. Ueda, W., Ohshida, T., Kuwabara, T., and Morikawa, Y., *Catal. Lett.* **12**, 97 (1992).
159. Ueda, W., Ohshida, T., Kuwabara, T., and Morikawa, Y., *J. Chem. Soc. Chem. Commun.* 1558 (1990).
160. Ndou, A.S., Plint, N., and Coville, N.J., *Appl. Catal. A-General* **251**, 337 (2003).
161. MacGregor, J.H., and Pugh, C., *J. Chem. Soc.* 535 (1945).
162. Unlermoheln, W.P., *J. Am. Chem. Soc.* **67**, 1505 (1945).
163. Kabashima, H., and Hattori, H., *Appl. Catal., A: General* **161**, L33 (1997).
164. Kabashima, H., and Hattori, H., *Catal. Today* **44**, 277 (1998).
165. Peterson, G.R., and Scarrah, W.P., *J. Am. Oil Chem. Soc.* **61**, 1593 (1984).
166. Leclercq, E., Finiels, A., and Moreau, C., *J. Am. Oil Chem. Soc.* **78**, 1161 (2001).
167. Gryglewicz, S., *Bioresour. Technol.* **70**, 249 (1999).
168. Sonntag, N.O.V., *J. Am. Oil Chem. Soc.* **59**, A795 (1982).
169. Corma, A., Iborra, S., Miquel, S., and Primo, J., *J. Catal.* **173**, 315 (1998).
170. Barrault, J., Pouilloux, Y., Clacens, J.M., Vanhove, C., and Bancquart, S., *Catal. Today* **75**, 177 (2002).
171. Gryglewicz, S., *Appl. Catal. A: General* **192**, 23 (2000).
172. Hattori, H., Shima, M., and Kabashima, H., *Stud. Surf. Sci. Catal.* **130D**, 3507 (2000).
173. Lin, L., and Day, A.R., *J. Am. Chem. Soc.* **74**, 5133 (1952).
174. Ogata, Y., and Kawasaki, A., *Tetrahedron* **25**, 929 (1969).
175. Saegusa, T., and Ueshima, T., *J. Org. Chem.* **33**, 3310 (1968).
176. Tanabe, K., and Saito, K., *J. Catal.* **35**, 247 (1974).
177. Seki, T., Kabashima, H., Akutsu, K., Tachikawa, H., and Hattori, H., *J. Catal.* **204**, 393 (2001).
178. Seki, T., Akutsu, K., and Hattori, H., *Chem. Commun.* 1000 (2001).
179. Seki, T., and Hattori, H., *Catal. Surv. Asia* **7**, 145 (2003).
180. Kabashima, H., Tsuji, H., Nakata, S., Tanaka, Y., and Hattori, H., *Appl. Catal., A: General* **194-195**, 227 (2000).
181. Handa, H., Baba, T., Sugisawa, H., and Ono, Y., *J. Mol. Catal. A-Chemical* **134**, 171 (1998).
182. Seki, T., Tachikawa, H., Yamada, T., and Hattori, H., *J. Catal.* **217**, 117 (2003).
183. Corma, A., and Garcia, H., *Chem. Rev.* **103**, 4307 (2003).
184. Graauw, C.F., Peters, J.A., van Beckum, H., and Huskens, J., *Synthesis* **10**, 1007 (1994).
185. Wilds, A.L., *Org. React.* **2**, 178 (1994).
186. Corma, A., Domine, M.E., and Valencia, S., *J. Catal.* **215**, 294 (2003).
187. van der Waal, J.C., Creighton, E.J., Kunkeler, P.J., Tan, K., and van Bekkum, H., *Top. Catal.* **4**, 261 (1997).
188. Corma, A., Domine, M.E., Nemeth, L., and Valencia, S., *J. Am. Chem. Soc.* **124**, 3194 (2002).
189. Creighton, E.J., Huskens, J., van der Waal, J.C., and van Bekkum, H., *Stud. Surf. Sci. Catal.* **108**, 531 (1997).

190. Kaspar, J., Trovarelli, A., Lenarda, M., and Graziani, M., *Tetrahedron Lett.* **30**, 2705 (1989).
191. Kijenski, J., Glinski, M., and Czarnecki, J., *J. Chem. Soc.-Perkin Trans.* **2**, 1695 (1991).
192. Kijenski, J., Rusczyński, J., Knedler, I., and Glinski, M., *React. Kinet. Catal. Lett.* **49**, 287 (1993).
193. Kaspar, J., Trovarelli, A., Zamoner, E., Farnetti, E., and Graziani, M., *Stud. Surf. Sci. Catal.* **59**, 253 (1991).
194. Ivanov, V.A., Bachelier, J., Audry, F., and Lavalley, J.C., *J. Mol. Catal.* **91**, 45 (1994).
195. Berkani, M., Lambertson, J.L., Marczewski, M., and Perot, G., *Catal. Lett.* **31**, 405 (1995).
196. Glinski, M., Kijenski, J., and Rusczyński, J., *React. Kinet. Catal. Lett.* **54**, 1 (1995).
197. Glinski, M., Kijenski, J., Gibka, J., and Gora, J., *React. Kinet. Catal. Lett.* **56**, 121 (1995).
198. Szollosi, G., and Bartok, M., *Appl. Catal. A-General* **169**, 263 (1998).
199. Szollosi, G., and Bartok, M., *Catal. Lett.* **59**, 179 (1999).
200. Szollosi, G., and Bartok, M., *J. Mol. Struct.* **483**, 13 (1999).
201. Aramendia, M.A., Borau, V., Jimenez, C., Marinas, J.M., Ruiz, J.R., and Urbano, F.J., *J. Colloid Interface Sci.* **238**, 385 (2001).
202. Aramendia, M.A., Borau, V., Jimenez, C., Marinas, J.M., Ruiz, J.R., and Urbano, F.J., *Appl. Catal., A-General* **244**, 207 (2003).
203. Barthomeuf, D., *J. Phys. Chem.* **88**, 42 (1984).
204. Mirodatos, C., Pichat, P., and Barthomeuf, D., *J. Phys. Chem.* **80**, 1335 (1976).
205. Corma, A., Martin-Aranda, R.M., and Sanchez, F., *Stud. Surf. Sci. Catal.* **59**, 503 (1991).
206. Corma, A., and Martin-Aranda, R.M., *Appl. Catal., A : General* **105**, 271 (1993).
207. Hathaway, P.E., and Davis, M.E., *J. Catal.* **116**, 263 (1989).
208. Hathaway, P.E., and Davis, M.E., *J. Catal.* **116**, 279 (1989).
209. Hathaway, P.E., and Davis, M.E., *J. Catal.* **116**, 497 (1989).
210. Kim, J.C., Li, H.X., Chen, C.Y., and Davis, M.E., *Microporous Mater.* **2**, 413 (1994).
211. Kloetstra, K.R., and vanBekkum, H., *J. Chem. Soc.-Chem Commun.* 1005 (1995).
212. Kloetstra, K.R., vandenBroek, J., and van Bekkum, H., *Catal. Lett.* **47**, 235 (1997).
213. Kloetstra, K.R., and van Bekkum, H., *Prog. Zeolite and Microporous Mater., Pts A-C* **105**, 431 (1997).
214. Kloetstra, K.R., vanLaren, M., and van Bekkum, H., *J. Chem. Soc.-Faraday Trans.* **93**, 1211 (1997).
215. Pillai, R.B.C., *J. Indian Chem. Soc.* **77**, 490 (2000).
216. Kovacheva, P., Predoeva, A., Arishtirova, K., and Vassilev, S., *Appl. Catal., A: General* **223**, 121 (2002).
217. Wang, Y., Zhu, J.H., Cao, J.M., Yuan, C., and Xu, Q.H., *Microporous Mesopor. Mater.* **26**, 175 (1998).
218. Zhu, J.H., Wang, Y., Chun, Y., Xing, Z., and Xu, Q.H., *Mater. Lett.* **35**, 177 (1998).
219. Zhu, J., Chun, Y., Wang, Y., and Xu, Q., *Catal. Today* **51**, 103 (1999).
220. Yan, X.W., Han, X.W., Cao, Y., Wei, Y.L., and Zhu, J.H., *Chin. J. Inor. Chem.* **18**, 1101 (2002).
221. Davis, R.J., Doscocil, E.J., and Bordawekar, S., *Catal. Today* **62**, 241 (2000).
222. Davis, R.J., *J. Catal.* **216**, 396 (2003).
223. Dumitriu, E., Hulea, V., Bilba, N., Carja, G., and Azzouz, A., *J. Mol. Catal.* **79**, 175 (1993).
224. Khan, A.Z., and Ruckenstein, E., *Appl. Catal. A-General* **102**, 233 (1993).
225. Osada, Y., Ogasawara, S., Fukushima, T., Shikada, T., and Ikariya, T., *J. Chem. Soc., Chem. Commun.* 1434 (1990).
226. Arishtirova, K.C., Predoeva, A.V., and Kovacheva, P.C., *Bulgarian Chem. Commun.* **32**, 352 (2000).
227. Arishtirova, K., Kovacheva, P., and Vassilev, S., *Appl. Catal. A-General* **213**, 197 (2001).
228. Kovacheva, P., Arishtirova, K., and Vassilev, S., *Appl. Catal. A-General* **210**, 391 (2001).
229. Kovacheva, P., and Arishtirova, K., *J. Environ. Prot. Ecol.* **3**, 196 (2002).
230. Arishtirova, K., Kovacheva, P., and Predoeva, A., *Appl. Catal. A-General* **243**, 191 (2003).
231. Serra, J.M., Corma, A., Farrusseng, D., Baumes, L., Mirodatos, C., Flego, C., and Perego, C., *Catal. Today* **81**, 425 (2003).
232. Kresge, C.T., Leonowicz, M.E., Roth, W.J., Vartuli, J.C., and Beck, J.S., *Nature* **359**, 710 (1992).
233. Corma, A., *Chem. Rev.* **97**, 2373 (1997).
234. Jaenicke, S., Chuah, G.K., Lin, X.H., and Hu, X.C., *Microporous Mesopor. Mater.* **35-36**, 143 (2000).

235. Rodriguez, I., Iborra, S., Corma, A., Rey, F., and Jorda, J.L., *Chem. Commun.* 593 (1999).
236. Yu, J.L., Shiau, S.Y., and Ko, A.N., *React. Kinet. Catal. Lett.* **72**, 365 (2001).
237. Climent, M.J., Corma, A., Guil-Lopez, R., Iborra, S., and Primo, J., *J. Catal.* **175**, 70 (1998).
238. Mross, W.D., *Catal. Rev.-Sci. Eng.* **25**, 591 (1983).
239. Haag, W.O., and Pines, H., *J. Am. Chem. Soc.* **82**, 387 (1960).
240. Malinowski, S., and Kijenski, J., in "Catalysis" (C. Kemball, and D.A. Downen, Eds.), Vol. 4, p. 130. The Royal Society of Chemistry, London, 1980.
241. Kijenski, J., and Malinowski, S., *React. Kinet. Catal. Lett.* **3**, 343 (1975).
242. Kijenski, J., and Malinowski, S., *J. Chem. Soc.-Faraday Trans. I* **74**, 250 (1978).
243. Kijenski, J., and Malinowski, S., *Bull. Acad. Pol. Sci., Ser. Sci. Chim.* **25**, 427 (1977).
244. Sun, N., and Klabunde, K.J., *J. Catal.* **185**, 506 (1999).
245. Kijenski, J., Radomski, P., and Fedorynska, E., *J. Catal.* **203**, 407 (2001).
246. Matsuhashi, H., and Klabunde, K.J., *Langmuir* **13**, 2600 (1997).
247. Matsuhashi, H., Oikawa, M., and Arata, K., *Langmuir* **16**, 8201 (2000).
248. Ushikubo, T., Hattori, H., and Tanabe, K., *Chem. Lett.* 649 (1984).
249. Tanabe, K., and Noyori, R., "Super Acids and Super bases," ch. 4. Kodansha Scientific, Tokyo, 1980.
250. Baba, T., Handa, H., and Ono, Y., *J. Chem. Soc.-Faraday Trans.* **90**, 187 (7-1-1994).
251. Ito, T., Wang, J.X., Lin, C.H., and Lunsford, J.H., *J. Am. Chem. Soc.* **107**, 5062 (1985).
252. Hur, J.M., Coh, B.Y., and Lee, H.I., *Catal. Today* **63**, 189 (2000).
253. Matsuhashi, H., and Arata, K., *J. Phys. Chem.* **99**, 11178 (1995).
254. Giamello, E., Ferrero, A., Coluccia, S., and Zecchina, A., *J. Phys. Chem.* **95**, 9385 (1991).
255. Ferrari, A.M., and Pacchioni, G., *J. Phys. Chem.* **99**, 17010 (1995).
256. Pines, H., and Stalick, W.M., "Base-Catalysed Reactions of Hydrocarbons and Related Compounds," p. 240 Academic Press, New York, 1981.
257. Pines, H., "The Chemistry of Catalytic Hydrocarbon Conversions," p. 139 Academic Press, New York, 1981.
258. Pines, H., Veseley, J.A., and Ipatieff, V.N., *J. Am. Chem. Soc.* **77**, 554 (1954).
259. Driscoll, D.J., Martir, W., Wang, J.X., and Lunsford, J.H., *J. Am. Chem. Soc.* **107**, 58 (1985).
260. Ito, T., and Lunsford, J.H., *Nature* **314**, 721 (1985).
261. Guzzi, L., VanSanten, R.A., and Sarma, K.V., *Catal. Rev.-Sci. Eng.* **38**, 249 (1996).
262. Lee, J.S., and Oyama, S.T., *Catal. Rev.-Sci. Eng.* **30**, 249 (1988).
263. Voskresenskaya, E.N., Roguleva, V.G., and Anshits, A.G., *Catal. Rev.-Sci. Eng.* **37**, 101 (1995).
264. Aika, K.I., and Lunsford, J.H., *J. Phys. Chem.* **81**, 1393 (1977).
265. Lin, C.H., Ito, T., Wang, J., and Lunsford, J.H., *J. Am. Chem. Soc.* **109**, 4808 (1987).
266. Driscoll, D.J., Martir, W., Wang, J.X., and Lunsford, J.H., "Adsorption and Catalysis on Oxide Surfaces," p. 403 Elsevier, Amsterdam, 1986.
267. Chen, Y., Tohver, H.T., Narayan, J., and Abraham, M.M., *Phys. Rev. B* **16**, 5535 (1977).
268. Zhang, H.S., Wang, J.X., Driscoll, D.J., and Lunsford, J.H., *J. Catal.* **112**, 366 (1988).
269. Maksimov, N.G., Selyutin, G.E., Anshits, A.G., Kondratenko, E.V., and Roguleva, V.G., *Catal. Today* **42**, 279 (1998).
270. Murphy, D., Giamello, E., and Zecchina, A., *J. Phys. Chem.* **97**, 1739 (1993).
271. Balint, I., and Aika, K., *Appl. Surf. Sci.* **173**, 296 (2001).
272. Peng, X.D., Richards, D.A., and Stair, P.C., *J. Catal.* **121**, 99 (1990).
273. Aritani, H., Yamada, H., Nishio, T., Imamura, S., Hasegawa, S., Tanaka, T., and Yoshida, S., *Chem. Lett.* 359 (1999).
274. Aritani, H., Yamada, H., Nishio, T., Shiono, T., Imamura, S., Kudo, M., Hasegawa, S., Tanaka, T., and Yoshida, S., *J. Phys. Chem. B* **104**, 10133 (2000).
275. Kanno, T., and Kobayashi, M., *Stud. Surf. Sci. Catal.* **90**, 207 (1994).
276. Kurokawa, H., Kato, T., Kuwabara, T., Ueda, W., Morikawa, Y., Morooka, Y., and Ikawa, T., *J. Catal.* **126**, 208 (1990).
277. Hur, J.M., Coh, B.Y., Lu, L., Kwon, H.H., and Lee, H.I., *Catal. Lett.* **69**, 237 (2000).
278. Hur, J.M., Kwon, H.H., and Lee, H.I., *React. Kinet. Catal. Lett.* **77**, 133 (2002).
279. Ogawa, T., Cedeno, R., and Inoue, M., *Polym. Bull.* **2**, 275 (1980).

280. Schlaefel, F.W., US Patent 3993888 (1976).
281. Kurokawa, H., Kato, T., Kuwabara, T., Ueda, W., Morikawa, Y., Morooka, Y., and Ikawa, T., *J. Catal.* **126**, 199 (1990).
282. Garcia Raso, A., Sinisterra, J.V., and Marinas, J.M., *React. Kinet. Catal. Lett.* **18**, 33 (1981).
283. Barrios, J., Rojas, R., Alcanrara, A.R., and Sinisterra, J.V., *J. Catal.* **112**, 528 (1988).
284. Fuentes, A., Marinas, J.M., and Sinisterra, J.V., *Tetrahedron Lett.* **28**, 2947 (1987).
285. Iglesias, M., Marinas, J.M., and Sinisterra, J.V., *Tetrahedron* **43**, 2335 (1987).
286. Barrios, J., Marinas, J.M., and Sinisterra, J.V., *Bull. Soc. Chim. Belg.* **95**, 107 (1986).
287. Connat, J.B., and Tuttle, N., *Org. Synth. Coll.* **1**, 199 (1994).
288. Sinisterra, J.V., Garciasaso, A., Cabello, J.A., and Marinas, J.M., *Synth.-Stuttgart* 502 (1984).
289. Aguilera, A., Alcantara, A.R., Marinas, J.M., and Sinisterra, J.V., *Can. J. Chem.* **65**, 1165 (1987).
290. Garcia-Raso, A., Garcia-Raso, J., Campaner, B., Mestres, R., and Sinisterra, J.V., *Synthesis* 1037 (1982).
291. Garciasaso, A., Garciasaso, J.A., Mestres, R., and Sinisterra, J.V., *React. Kinet. Catal. Lett.* **28**, 365 (1985).
292. Sinisterra, J.V., and Marinas, J.M., *Monatsh Chem.* **117**, 111 (1986).
293. Sinisterra, J.V., *React. Kinet. Catal. Lett.* **30**, 93 (1986).
294. Sinisterra Gago, J.V., Alcantara Leon, A.R., and Marinas Rubio, J.M., *J. Colloid Interface Sci.* **115**, 520 (1987).
295. Sinisterra, J.V., Marinas, J.M., Riquelme, F., and Arias, M.S., *Tetrahedron* **44**, 1431 (1988).
296. Sinisterra, J.V., Fuentes, A., and Marinas, J.M., *J. Org. Chem.* **52**, 3875 (1987).
297. Ibarra, C.A., Arias, S., Fernandez, M.J., and Sinisterra, J.V., *J. Chem. Soc.-Perkin Trans. 2*, 503 (1989).
298. Alvarez-Ibarra, C., Arias, M.S., Fernandez, M.J., Serrano, D., and Sinisterra, V., *J. Chem. Res. (S)* 326 (1992).
299. Aramendia, M.A., Borau, V., Jimenez, C., Marinas, J.M., Ruiz, J.R., and Urbano, F.J., *Tetrahedron Lett.* **43**, 2847 (2002).
300. Palucki, M., and Buchwald, S.L., *J. Am. Chem. Soc.* **119**, 11108 (1997).
301. Palucki, M., Wolfe, J.P., and Buchwald, S.L., *J. Am. Chem. Soc.* **119**, 3395 (1997).
302. Davis, R.J., *J. Catal.* **216**, 396 (2003).
303. Doskocil, E.J., and Mankidy, P.J., *Appl. Catal., A: General* **252**, 119 (2003).
304. Davis, R.J., *Res. Chem. Int.* **26**, 21 (2000).
305. Holderich, W.F., and Tjoe, J., *Appl. Catal. A-General* **184**, 257 (1999).
306. Tanabe, K., and Holderich, W.F., *Appl. Catal. A-General* **181**, 399 (1999).
307. Climent, M.J., Corma, A., Garcia, H., Guil-Lopez, R., Iborra, S., and Fornes, V., *J. Catal.* **197**, 385 (2001).

# Index

## A

Acetylacetone cyclization, 252–253  
 Acetyl-CoA synthetase (ACS), 16  
*Acinetobacter*, 58  
 Active catalysts, ionic tagging of, 197–198  
 Acylation reactions, 89–91  
 Adsorbed probe molecules  
   infrared spectroscopy of, 246–248  
   thermal methods of, 248–249  
 AlCl<sub>3</sub>-containing ionic liquids, 169  
 Aldolases, in directed evolution, 52–54  
 Aldol condensation reactions, 181, 188  
   in alkaline earth metal hydroxides, 289  
   in base catalysis, 256–259  
 Alkali metal-doped alkaline earth metal oxides, 280–287  
 Alkaline earth metal hydroxides, 287–294  
   catalytic reactions on, 289–294  
 Alkaline earth metal oxides  
   alkali metal-doped, 280–287  
   and hydroxide catalysts, for base catalyzed reactions, 239–294  
   catalytic activity of, 254–275  
   doped with alkali metals by chemical vapor deposition, 282–284  
   doped with alkali metals prepared by impregnation, 284–287  
   optimization of, 239–294  
   surface basicity and base strength of, 240–242  
   with high-surface-area, 242–244  
   zeolites and mesoporous aluminosilicates modified with, 275–280  
 Alkaline earth-modified zeolites, catalytic activities of, 277–279  
 Alkene hydroformylation  
   supported dendritic catalysts for, 115–119  
   water-soluble dendritic catalysts for, 129–130  
 Alkoxyacylation, in ionic liquids, 218  
 Alkylation, in Lewis acidic ionic liquids, 186–187  
 Alkylimidazolium-containing ionic liquids, 167–169  
 N-alkylpyridinium-containing ionic liquids, 167  
 Allylic substitution, using dendritic catalysts in a CFMR, 75–83  
 [AMIM]BF<sub>4</sub>, 167, 168, 177, 190  
 [AMIM]Cl, 166, 167, 172, 179

[AMIM]PF<sub>6</sub>, 167, 168, 175, 190, 213  
 Aminotransferases, in directed evolution, 52  
 Anionic intermediates, stability of, 253–254  
 Anions  
   hydrogen bond basicity of, 161–163  
   in ionic liquids, 164–166  
 Antipode resolution, 1  
 Arylation of carbonyl compounds, 293–294  
*Aspergillus niger*, 45, 60  
 ‘Assembly of designed oligonucleotides’ (ADO) method, 9  
 Asymmetric additions of diethylzinc to aldehydes, 108–113  
 Asymmetric borohydride reductions, 92–93  
 Asymmetric dialkyl zinc addition, 114–115  
 Asymmetric dihydroxylation (AD), 195  
 Asymmetric hydrogenation, 91–92  
 Asymmetric transformations, 10  
 Asymmetric transfer hydrogenation, 107–108  
 Atom transfer radical polymerization (ATRP), 213

## B

*Bacillus megaterium*, 60  
*Bacillus subtilis*, 3, 22  
*Bacillus subtilis* lipase A (BSLA), 41  
 Baeyer-Villiger (BV) reaction, 55–60  
   in stereoselective sulfoxidation, 58–60  
   mechanism of, 55  
 Base catalyzed reactions, alkaline earth metal oxide and hydroxide catalysts for, 239–294  
 BASF BASIL process, 156  
 Basic ionic liquids, 180–181  
   and related reactions, 188–190  
 Basic sites, number and strength of, characterization, 244–253  
 Batch processes, nanofiltration in, 89–99  
 [BDMIM]PF<sub>6</sub>, 191, 192  
 Beer–Lambert law, 25  
 Bidentate palladium complexes, 81  
 Bimetallic mechanism, 73, 134  
 BINAP core-functionalized dendrimers, 101, 142  
 BINOL ligands, 108–110, 122  
 Biocatalysis, in ionic liquid media, 223–229  
 Bis(cyclohexylphosphine), 100

Bis(*tert*-butylphosphine), 100  
 [BMIM]BF<sub>4</sub>, 162, 164, 166, 172, 175–182,  
   190–194, 199–203, 209–214, 222  
   and hydrogen bond basicity, 162  
   and Lewis acid, 185  
   and polarity of ionic liquids in, 171  
   hydrogen solubility in, 173  
   in dimerization of dienes, 205  
   in hydrogenation, 206–208  
   in Suzuki reaction, 206  
   in transesterification, 226  
 [BMIM]CF<sub>3</sub>CO<sub>2</sub>, 166  
 [BMIM]Cl, 162, 166, 174, 182–183, 190, 193, 198,  
   199, 201, 205, 209, 211  
   Knoevenagel condensation, 189  
 [BMIM]PF<sub>6</sub>, 160–165, 171, 176–182, 188–228  
   carbon dioxide and lower alkanes solubility in,  
     174  
   Henry's law constant in, 174  
   hydrogen solubility in, 173  
   Lewis acid in, 186  
   miscibilities of organic compounds in, 175  
 [BMIM]SbF<sub>6</sub>, 162, 194, 206  
 [BMIM]TfO, 162, 186, 228  
 Bovine serum albumin (BSA), 19  
 3-Bromo-2-methyl-propionic acid methyl  
   ester, 44  
 Brønsted acid catalysis, in ionic liquids, 182–184  
 [Bu<sub>4</sub>N]BF<sub>4</sub>, 166  
*Burkholderia cepacia* KWI-56 lipase, 43  
 Butene dimerization, 156  
 1-Butyl-3-methyl imidazolium [BMIM]  
 Butyryn test for lipase activity, 13–14

## C

*Candida antarctica* lipase B (CALB), 224, 226  
 Capillary array electrophoresis (CAE) assay, for  
   enantioselectivity, 28  
 Capillary electrophoresis (CE), 28  
 Carbon–carbon bond formation reactions, in base  
   catalysis, 256–265  
 Carbon dioxide and lower alkanes solubility, in  
   ionic liquids, 174  
 Carbon monoxide solubility, in ionic liquids, 173  
 Carbon–oxygen bond formation reactions,  
   265–269  
 Carbonylation, in ionic liquids, 215–216  
 Carbonylation, supported dendritic catalysts for,  
   120–121  
 Cassette mutagenesis, 7  
 Catalysis  
   dendrimers in, 71–147  
   in ionic liquids, 153–229  
 Catalyst immobilization, 194

Catalyst recycling  
   in dendrimer-supported catalysts, 75–133  
   using nanofiltration, 75–89  
   using nanofiltration, in batch processes, 89–99  
 Catalysts, *also see individual entries*  
   ionic liquids as, 182–191  
   isolation of, in ionic liquids, 158–159  
   recycling and product separation, in ionic  
     liquids, 159–160  
   solubility of, in an ionic liquid, 178–179  
 Catalytic test reactions, for determination of acid  
   base properties, 249–253  
 Cations  
   in ionic liquids, 163–164  
   structural effects of, 201–202  
 Chemical vapor deposition method, 282–284  
 Chloride-containing ionic liquids, 166–167  
 Chloroaluminate-catalyzed reactions, 186–188  
 Circular dichroism (CD) assay, for  
   enantioselectivity, 28–30  
 Citrate synthase (CS), 15  
 Claisen–Schmidt condensation, 259–260  
   in alkaline earth metal hydroxides, 289  
<sup>13</sup>C-labeling, 23–25  
 Cl<sup>–</sup> impurity, in ionic liquids, 181–182  
 Column chromatography, dendritic catalyst  
   recovery by, 113–115  
 Combinatorial asymmetric transition metal  
   catalysis, 10  
 Combinatorial multiple-cassette mutagenesis  
   (CMCM), 34  
 Complete active-site saturation test (CAST), 41  
 Condensation of alcohols, in base catalysis,  
   264–265  
 Conjugate addition of methanol, 266  
 Continuous-flow membrane reactor (CFMR), 73  
   covalently functionalized dendrimers in, 75–82  
   hydrovinylation using dendritic catalysts in,  
     83–85  
   nanofiltration in, using catalyst recycling, 75–89  
   Nickel-catalyzed Kharasch addition in, 85–86  
   non-covalently functionalized dendrimers, in,  
     82–83  
   Rhodium-catalyzed hydrogenation in, 86–89  
 Core-functionalized dendrimers, 99, 101, 142  
 Co-solvents, effect of, 201  
 Covalently functionalized dendrimers, in a  
   CFMR, 75–82  
 Crotylpalladium chloride complexes, 81  
 Cyanoethylation of alcohols, 265–266  
 Cyclodehydration reaction, 218–219  
 β-Cyclodextrin derivatives (β-CDs), 28  
 Cyclohexanone monooxygenases (CHMO), 27,  
   55–59



Cymeneruthenium chloride dendritic catalysts, 101  
 Cytochrome P450 enzymes, in directed evolution, 60–61

## D

'Degenerate homoduplex recombination' method, 9  
 Dendrimer-bound Pd(II) complex for selective hydrogenations, 127–128  
 Dendrimer-encapsulated palladium nanoparticles, for hydrogenations, 130–131  
 Dendrimers, *see also individual entries*  
   as soluble supports, 133–144  
   as surface-functionalized catalysts, 72  
   catalyst recycling in, 75–133  
   hydrovinylation, using, 83–85  
   in a CFMR, 75–83  
   in catalysis, 71–146  
   in two-phase catalysis, 129–133  
   supported on a solid phase, 144–146  
   supported on montmorillonite, 128–129  
   water-soluble, dendritic catalysts 129–130  
 Dendritic catalyst recovery, by column chromatography, 113–115  
 Dendritic catalyst recycling  
   by precipitation, 99–113  
   by Stille couplings, Knoevenagel condensations, Michael addition reactions, 104–107  
 Dendritic effects in catalysis, 133–146  
*meso*-1,4-Diacetoxy-2-cyclopentene, 22, 41  
 Dialkyl ether cleavage, in Lewis acidic ionic liquids, 187–188  
*N,N*-dialkylpyrrolidinium-containing ionic liquids, 167  
*N,N*-diallyltosylamide, 183  
 Diastereomer formation, 2  
 1,4-Diazabicyclo (222) octane (DABCO), 191–192  
 1,3-Dibutylimidozolium tetrafluoroborate ([DBIM]BF<sub>4</sub>), 185  
 Diels–Alder reaction, 125, 126, 137, 184–186  
 Dienes, dimerization of, 205, 211–212  
 Difasol process, 156, 210  
 Dihydroxylation, in ionic liquids, 209–210  
 Dimerization, of dienes, 205, 211–212  
 Dimersol process, 156, 210  
 Dimethylfuran (DMF), 217  
 1,5-Dimethyltetrahydrofuran, 187  
*N*-Diphenylphosphinyl imines, 114, 141  
 Directed evolution  
   description, 4  
   experimental stages of, 4  
   gene mutagenesis methods in, 5–10

  of enantioselective enzymes as catalysts, 1–63  
   recombinant methods in, 7–10  
   to control enantioselectivity of enzymes, 31–61  
 DNA shuffling, 5, 8–9, 12, 34–37, 48, 52–54, 60

## E

E1cB mechanism, 250, 251  
 Electrocatalysis, in ionic liquids, 219–220  
 Electrospray ionization (ESI), 22  
 EMDee method, 15  
 [EMIM]Cl/AlCl<sub>3</sub>, 169, 170, 187  
 [EMIM]NbF<sub>6</sub>, 162  
 [EMIM]TaF<sub>6</sub>, 162  
 Enantiomeric excess (*ee*) assays/screening systems, 3, 10, 28–30, 49, 51, 53, 59  
   enzyme-coupled, 15–17  
   fluorescence based, 18–20  
   FTIR spectroscopy based, 25–26  
   GC or HPLC based, 10, 26–28  
   MS-based approaches to, 20–23, 45  
   NMR spectroscopy based, 23–25  
   UV/Vis-based, 11–17  
 Enantiomer regeneration, 2  
 Enantioselective enzymes  
   as catalysts in organic synthesis, 1–61  
   directed evolution as means to control, 30–61  
   experimental stages of, 4  
   reactions, assaying, 10–30  
 Enzyme-coupled *ee* screening systems, 15–17  
 Enzymes, as catalysts in asymmetric transformations, 2  
*Epicurian coli* XL1-red, 44  
 Epoxide hydrolase from *Aspergillus niger* (ANEH), 45–47  
 Epoxide hydrolases (EHs), 19, 45  
 Error-prone polymerase chain reaction (epPCR), 5, 9, 12, 26, 32–37, 41, 42, 45–48, 52–61  
   point mutations induced by, 5  
*Escherichia coli*, 3, 22, 27, 45, 48, 53, 60  
 Esterases, in directed evolution, 43–45  
 6-Ethoxycarbonyl-3,5-diphenyl-2-cyclohexenone, 189–190  
 Ethylaluminumdichloride (EADC), 205  
 5-Ethylidenebicyclo-[2.2.1]-hept-2-ene (EBH), 255  
 1-Ethyl-3-methylimidazolium [EMIM], *see individual entries*  
 Ethyl-*N,N*-dimethylaminopropylcarbodiimide (EDC), 141  
*rac*-Ethyl-3-phenylbutyrate, 43

## F

Family shuffling, 8  
 F<sup>−</sup> impurity, in ionic liquids, 181

Fluorescence-based assays, for enantioselectivity, 18–20  
 Focal point-functionalized dendrimers, 72  
 Fréchet's polybenzyl ether dendritic wedges, 101  
 Friedel–Crafts acylation, 184  
 FTIR spectroscopy, for lipases or esterases assaying, 25–26

## G

Galactosylation reactions, 228–229  
 Gas chromatography (GC) assays, for enantioselectivity, 26–28  
 Gene mutagenesis methods  
   directed evolution of, 4–9  
   based on point mutations, 5–6  
 Guerbet reaction, 264

## H

Heck and Sonogashira reaction, dendritic catalyst recycling by, 100–101  
 Heck cross-coupling, 216–218  
 Heck reaction, 100  
   and two-phase allylic aminations, using thermomorphic dendritic catalysts, 131–133  
   supported dendritic catalysts for, 120–121  
 Henry's law constants, 174  
 Heptachloroaluminate ion, 170  
 Heterogeneous dendritic catalysts, recovery of, 115–129  
 High- and medium-throughput screening systems, for enantioselectivity assay, 10–30  
 High-surface-area alkaline earth metal oxides, 242–244  
 Horse-liver alcohol dehydrogenase (HLDH), 18  
 'Hot region', in cassette mutagenesis, 7  
 'Hot spots', in epPCR screening process, 7  
 HPLC assays, for enantioselectivity, 26–28  
 Hydantoinases, in directed evolution, 48  
 Hydroesterification, supported dendritic catalysts for, 120–121  
 Hydroformylation, 95–99  
   in ionic liquids, 215–216  
 Hydrogenation  
   dendrimer-encapsulated palladium nanoparticles for, 130–131  
 Hydrogen bond basicity, of anions, 161–163  
 Hydrogen butylimidazolium tetrafluoroborate ([HBIM]BF<sub>4</sub>), 185  
 Hydrogen solubility, in ionic liquids, 173  
 Hydrogen transfer reaction, 269–275  
 Hydrolases, in enantioselectivity of enzymes, 31–52

Hydrophobicity-aided catalysis, 198  
 Hydrovinylation, using dendritic catalysts in a CFMR, 83–85  
 Hydroxide and alkaline earth metal oxide catalysts, for base catalyzed reactions, 239–294  
 Hyperbranched macromolecules, *see* Dendrimers

## I

Imidazolin-2-ylidene carbene ligand, 113  
 Imidazolium ion, proton reactivity at, 202  
 Impregnation method, 284–287  
 Impurities effect, in ionic liquids, 181  
 Induced coupled plasma atomic emission spectroscopy (ICP-AES), 78  
 Inert catalyst carriers, 191  
 Infrared spectroscopy of adsorbed probe molecules, 246–248  
 Ionic liquid media, biocatalysis in, 223–229  
 Ionic liquids *see also individual entries*  
   as catalysts, 182–191  
   Brønsted acid catalysis in, 182–184  
   catalysis in, 153–229  
   catalysis in, general features, 156–158  
   electrocatalysis in, 219–220  
   for catalysis and process engineering, 156–160  
   Lewis acidic ionic liquids, 184–188  
   ligand effects of, 196–197  
   neutral ionic liquids as catalysts, 190–191  
   structure and properties of, 160–182  
 Ionic liquid catalyst carriers, 191–220  
   characteristics of, 191–203  
 Ionic tagging of active catalysts, 197–198  
 Isolation of catalysts, in ionic liquids, 158–159  
 Isomerization reactions, in alkaline earth metal oxides, 254–256  
 Isophorone isomerization, 253  
 Isotope labeling, 20  
 ITCHY method, in directed evolution, 9

## K

D-2-Keto-3-deoxy-6-phospho-gluconate (KDPG) aldolase, 53  
 Kharasch addition, 93–95, 134, 135  
 Knoevenagel condensation, 189  
   dendritic catalyst recycling by, 104–107  
   for basic properties determination, 251–252  
   in base catalysis, 261–262  
 Koshland model, 39

**L**

- Lewis acid catalysts, Scandium cross-linked dendrimers as, 124–127
- Lewis acidity, in ionic liquids, 184–188, 192–194
- Lid structural unit, 41
- Ligand partitioning effects, 194–196
- ‘Ligand tuning’, 2
- Lipase-catalyzed hydrolysis of esters, 32, 33
- Lipase- or esterase-catalyzed reactions, screening systems for, 11–14
- Lipases, from *Pseudomonas aeruginosa*, 31–43

**M**

- L-Malate dehydrogenase (L-MDH), 15
- Mass spectrometry (MS) assays, for enantioselectivity, 20–23
- Meerwein–Ponndorf–Verley and Oppenauer (MPVO) reaction, 272–275
- Melting point, of ionic liquids, 166–170
- Membrane reactors, 72, 74
- Mesoporous molecular sieve, alkaline earth-modified, 279–280
- Metalloporphyrins, 209
- Metal triflate Lewis acids, 194
- Metathesis, dendritic catalyst recovery by, 113–114
- 4-Methoxycyclohexanone, 57
- (*S,R*)-1-Methoxy-2-propylacetate, 15
- $\alpha$ -Methylbenzylamine, 59
- 2-Methyl-3-butyn-2-ol (MBOH), 249, 251
- N*-methylimidazole, 156
- N*-methylimidazolium chloride, 156
- Michael addition, 182, 203, 204, 228
  - dendritic catalyst recycling by, 104–107
  - in alkaline earth metal hydroxides, 290–291
  - in base catalysis, 263–264
- Michaelis–Menten complex, 39
- [MIM–C<sub>2</sub>H<sub>5</sub>OCH<sub>3</sub>]Br, 163
- [MIM–CH<sub>3</sub>OCH<sub>3</sub>]Br, 163
- MM/QM study, 38, 39
- Molecular biological gene mutagenesis methods, 1
- Monoamine oxidases, in directed evolution, 59–60
- Montmorillonite, dendrimers supported on, 128–129
- Mukaiyama aldol addition, 125, 126
- Mutant nitrilases, 23

**N**

- NAD(P)H, 16, 55
- Nanofiltration, 73
  - in batch processes, 89–99
- Neutral ionic liquids, as catalysts, 190–191

- Nickel-catalyzed Kharasch addition, in a CFMR, 85–86
- Nitrilases, in directed evolution, 49–50
  - L-amino acids from, 49
- Nitroaldol condensation, 260–261
- p*-Nitrophenyl esters
  - kinetic resolution of, 12–13
  - Quick-E-Test for, 13–14
- p*-Nitrophenyl glycidyl ether, 48
- Non-chlorinated Lewis acids, 194
- Non-chloroaluminate Lewis-acid-catalyzed reactions, 184–186
- Non-covalently functionalized dendrimers, in CFMR, 82–83
- Nuclear magnetic resonance (NMR) assays, for enantioselectivity, 23–25

**O**

- Octadecyl methyl acrylate, 75
- Olefin dimerization, 205
  - in ionic liquids, 210–211
- Olefin metathesis, 204
- Oligomerization, in ionic liquids, 212–215
- Organic molecules solubility, in ionic liquids, 174–178
- Organometallic catalysts, dispersion and isolation of, 194
- Oxidases, in directed evolution, 54–61
- Oxidation
  - dendritic catalyst recycling by, 102–104
  - in ionic liquid media, 208–209, 227–228
  - supported dendritic catalysts for, 120–121
- Oxygen solubility, in ionic liquids, 173

**P**

- Palladium nanoparticles, for hydrogenations, 130–131
- Pd(OAc)<sub>2</sub>, 100, 106
- Periodate-coupled fluorogenic *ee* assay, 20
- Periphery-functionalized dendrimers, 72–73, 133, 134
- Phase transfer catalysts (PTC), 128
- Phase transfer effect, in ionic liquid catalyst carrier, 202–203
- Phenyl acetone monooxygenase (PAMO), 57
- Phenylacetylene-containing dendrimers, 142
- 3-Phenylbutyric acid ethyl ester, 44
- Phenylcyclohexanone monooxygenase (PCHMO), 57
- rac*-1-Phenyl ethyl acetate, 24
- Phosphine-functionalized carbosilane dendrimers, 76
- Phosphotriesterases, in directed evolution, 51–52

Physical and chemical properties, of ionic liquids, 166–182  
 Platinum carbene complex, 198  
 Point mutations, gene mutagenesis methods based on, 5–7  
 Polarity, of ionic liquids, 171  
 Polyamidoamine (PAMAM) dendrimers, 92, 97, 120, 121, 129–130, 141–146  
 Polybenzyl ether dendritic wedges, 107  
 Poly[diallyldimethylammoniumchloride], 222  
 Polyhedral oligomeric silsesquioxane (POSS) dendrimers, 135  
 Polymerization, in ionic liquids, 212–215  
 Polyoxometalate (POM) dendrimers, 102–103  
 Poly(phenylacetylene) dendrimers, 114  
 Precipitation, dendritic catalyst recycling by, 99–113  
 Product selectivity, solubility-aided, 199–201  
 Product separation and catalyst recycling, in ionic liquids, 159–160  
 Propene, hydroformylation of, 97  
*Pseudomonas aeruginosa*, 11, 26, 31–43, 48  
*Pseudomonas cepacia* (PS-C), 199  
*Pseudomonas cepacia* lipase (PCL), 224  
*Pseudomonas diminuta*, 51  
*Pseudomonas fluorescens* (PFE), 43, 44, 225  
 Pyridinium *p*-toluenesulfonate (PPTS), 179

## Q

[(QN)<sub>2</sub>PHAL], 195  
 Quaternary ammonium-containing ionic liquids, 169  
 Quick-E-Test, 13–14

## R

Random insertion and deletion (RID) method, 9  
 Recombinant methods, in directed evolution, 7–10  
 Rhodium-catalyzed hydrogenation, in a CFMR, 86–89  
 Ring-closing metathesis (RCM), 113, 204  
 Ring-opening polymerization (ROP), 214  
 Robinson annulation, 189–190  
 [R<sub>1</sub>R<sub>2</sub>R<sub>3</sub>R<sub>4</sub>N][CF<sub>3</sub>SO<sub>2</sub>]<sub>2</sub>N, 169

## S

Scandium cross-linked dendrimers, as Lewis acid catalysts, 124–127  
 Selective hydrogenations, dendrimer-bound Pd(II) complex for, 127  
 Sequence saturation mutagenesis (SeSaM), 6  
 Size-exclusion chromatography (SEC), 82

Sodium diethyl 2-methylmalonate, 76, 79  
 Solid phase, dendrimers supported on, 144–146  
 Solubility-aided product selectivity, 199–201  
 Solubility of species, in ionic liquids, 173–179  
 Soluble supports, dendrimers as, 133–144  
 Sonogashira reaction, 100  
 Spectroscopic methods, for basic properties determination, 245–249  
 Stability, of ionic liquids, 170–171  
 Staggered extension process (StEP), 8  
 Stereoselective sulfoxidation, CHMO in, 58–59  
 Stille couplings, dendritic catalyst recycling by, 104–107  
 Substrate solubility, reaction rate, 198–199  
 Supercritical CO<sub>2</sub> (scCO<sub>2</sub>), 160  
 Supported dendritic catalysts  
   for alkene hydroformylation, 115–119  
   for carbonylation, hydroesterification, oxidation, and Heck reactions, 120–121  
 Supported ionic liquid catalysis, 220–223  
 Surface basicity and base strength, of alkaline earth metal oxides, 240–242  
 Surface-enhanced resonance Raman scattering (SERRS), 30  
 Suzuki coupling, 206  
 ‘Synthetic shuffling’ method, 9

## T

TADDOL moiety, 122  
 Tagatose-1,6-bisphosphate aldolase, 54  
 Task-specific ionic liquids (TSILs), 160  
 [TBA]Br, 174, 196–197, 218  
 Temperature-programmed desorption (TPD), 244, 249  
 Template switching, 8  
 Tetrahydropyranyl (THP), 192  
 Tetra(polyoxometalate) dendrimers, 102  
 Texanol, 97  
 Thermal methods of adsorbed probe molecules, 248–249  
*Thermobifida fusca*, 57  
 Tishchenko reaction, 269–272  
 Titration methods, for number of basic sites evaluation, 245  
 [TMAC]Al<sub>2</sub>Cl<sub>7</sub>, 175–176  
*p*-Toluenesulfonic acid (TsOH), 179  
 Transesterification, 224–227  
   in base catalysis, 266–269  
 Transition states, stabilization of, 191–192  
 Triethylamine, 156  
 Triethylammonium chloride, 156  
 Trimethylammoniumchloride (TMAC), *see individual entries*

Tri(*m*-sulfonyl)triphenyl phosphine tris(1-butyl-3-methylimidazolium) salt (tppti), 179  
 Tri(*m*-sulfonyl)triphenyl phosphine trisodiums (tppts), 179  
 Triphenyl phosphine hydrobromide (TPP.HBr), 179  
 Triphenylphosphinetrisulphonate (TPPTS), 199  
 Two-phase allylic aminations and Heck reactions, 131–133  
 Two-phase catalysis, dendritic catalysts in, 131–133

## U

Umbelliferone, 18, 19, 20  
 UV/Vis-based *ee* assays, 11–17

## V

5-Vinylbicyclo-[2.2.1]-hept-2-ene (VBH), 255

Viscosity, of ionic liquids, 171–172  
 VO(salen)@IL, 197–198

## W

Wadsworth–Emmons reaction, 262  
 Water-soluble dendritic catalysts, for alkene hydroformylation, 129–130  
 Wittig and Wittig–Horner reactions, 262–263  
 Wittig–Horner (W–H) reaction, 291–293  
 WT EH, crystal structure of, 46

## Z

Zeolites  
     and mesoporous aluminosilicates, modified with alkaline earth metal oxides, 275–280  
     modified with alkaline earth compounds, 277–279

# Contents

CONTRIBUTORS . . . . .	xi
PREFACE . . . . .	xiii

## Directed Evolution of Enantioselective Enzymes as Catalysts for Organic Synthesis

*M.T. Reetz*

I. Introduction . . . . .	2
II. Mutagenesis Methods . . . . .	5
A. Methods Based on Point Mutations . . . . .	5
B. Recombinant Methods . . . . .	7
III. High- and Medium-Throughput Screening Systems for Assaying the Enantioselectivity of Enzymatic Reactions . . . . .	10
A. UV/Vis-Based ee Assays . . . . .	11
1. Assay for Screening Lipases or Esterases in the Kinetic Resolution of Chiral p-Nitrophenyl Esters . . . . .	11
2. Quick-E-Test in the Lipase- or Esterase-Catalyzed Kinetic Resolution of Chiral p-Nitrophenyl Esters . . . . .	13
3. Screening Systems for Lipase- or Esterase-Catalyzed Reactions Based on pH-Indicators . . . . .	14
4. Enzyme-Coupled ee Screening Systems . . . . .	15
5. Other UV/Vis-Based ee Assays . . . . .	17
B. Assays Using Fluorescence . . . . .	18
C. Assays Based on Mass Spectrometry . . . . .	20
D. Assays Based on NMR Spectroscopy . . . . .	23
E. Assays Based on FTIR Spectroscopy for Assaying Lipases or Esterases . . . . .	25
F. Assays Based on Gas Chromatography or HPLC . . . . .	26
G. Assays Based on Capillary Array Electrophoresis . . . . .	28
H. Assays Based on Circular Dichroism . . . . .	28
I. Other ee Assays . . . . .	30
IV. Examples of Directed Evolution as a Means to Control the Enantioselectivity of Enzymes . . . . .	30
A. Hydrolases . . . . .	31
1. Lipase from <i>Pseudomonas Aeruginosa</i> . . . . .	31
2. Other Lipases . . . . .	41
3. Esterases . . . . .	43
4. Epoxide Hydrolases . . . . .	45
5. Hydantoinases . . . . .	48
6. Nitrilases . . . . .	49
7. Phosphotriesterases . . . . .	51
B. Aminotransferases . . . . .	52
C. Aldolases . . . . .	52
D. Oxidases . . . . .	54
1. Cyclohexanone Monooxygenases as Baeyer-Villigerases . . . . .	55
2. Cyclohexanone Monooxygenases in Stereoselective Sulfoxidation . . . . .	58

3. Monoamine Oxidases . . . . .	59
4. Cytochrome P450 Enzymes . . . . .	60
V. Conclusions and Perspective . . . . .	61
References . . . . .	62

## Dendrimers in catalysis

*Joost N. H. Reek, Silvia Arévalo, Rieko van Heerbeek, Paul C. J. Kamer  
and Piet W. N. M. van Leeuwen*

I. Introduction . . . . .	71
II. Catalyst Recycling in Applications of Dendrimer-Supported Catalysts . . . . .	75
A. Catalyst Recycling using Nanofiltration in a Continuous-Flow Membrane Reactor . . . . .	75
1. Allylic Substitution using Dendritic Catalysts in a CFMR . . . . .	75
2. Hydrovinylation using Dendritic Catalysts in a CFMR . . . . .	83
3. Nickel-Catalyzed Kharasch Addition in a CFMR . . . . .	85
4. Rhodium-Catalyzed Hydrogenation in a CFMR . . . . .	86
B. Catalyst Recycling using Nanofiltration in Batch Processes . . . . .	89
1. Acylation Reactions . . . . .	89
2. Asymmetric Hydrogenation . . . . .	91
3. Asymmetric Borohydride Reductions . . . . .	92
4. Kharash Addition . . . . .	93
5. Hydroformylation . . . . .	95
C. Dendritic Catalyst Recycling by Precipitation . . . . .	99
1. Heck and Sonogashira Reaction . . . . .	100
2. Hydrogenation . . . . .	101
3. Oxidation . . . . .	102
4. Stille Couplings, Knoevenagel Condensations, and Michael Addition Reactions . . . . .	104
5. Asymmetric Transfer Hydrogenation . . . . .	107
6. Asymmetric Additions of Diethylzinc to Aldehydes . . . . .	108
D. Catalyst Recovery by Column Chromatography . . . . .	113
1. Metathesis . . . . .	113
2. Asymmetric Dialkyl Zinc Addition . . . . .	114
E. Recovery of Heterogeneous Dendritic Catalysts . . . . .	115
1. Supported Dendritic Catalysts for Alkene Hydroformylation . . . . .	115
2. Supported Dendritic Catalysts for Carbonylation, Hydroesterification, Oxidation, and Heck Reactions . . . . .	120
3. Supported Dendritic Catalysts for the Asymmetric Addition of Diethylzinc . . . . .	121
4. Scandium Cross-Linked Dendrimers as Lewis Acid Catalysts . . . . .	124
5. Dendrimer-Bound Pd(II) Complex for Selective Hydrogenations . . . . .	127
6. Dendrimers Supported on Montmorillonite . . . . .	128
F. Dendritic Catalysts Applied in Two-Phase Catalysis . . . . .	129
1. Water-Soluble Dendritic Catalysts for Alkene Hydroformylation . . . . .	129
2. Dendrimer-Encapsulated Palladium Nanoparticles for Hydrogenations . . . . .	130
3. Two-Phase Allylic Aminations and Heck Reactions using Thermomorphic Dendritic Catalysts . . . . .	131
III. Dendritic effects in catalysis . . . . .	133
A. Dendrimers as Soluble Supports . . . . .	133
B. Dendrimers Supported on a Solid Phase . . . . .	144
IV. Conclusions . . . . .	146
References . . . . .	147

## Catalysis in Ionic Liquids

*Z. Conrad Zhang*

I. Introduction . . . . .	154
II. Ionic Liquids for Catalysis and Process Engineering . . . . .	156
A. General Features of Ionic Liquids in Catalysis . . . . .	156
B. Isolation of Catalysts . . . . .	158
C. Product Separation and Catalyst Recycling . . . . .	159
III. Structures and Properties of Ionic Liquids . . . . .	160
A. Hydrogen Bond Basicity of Anions . . . . .	161
B. Cations . . . . .	163
C. Anions . . . . .	164
D. Physical and Chemical Properties . . . . .	166
1. Melting Point . . . . .	166
2. Stability . . . . .	170
3. Polarity . . . . .	171
4. Viscosity . . . . .	171
5. Solubility of Species in Ionic Liquids . . . . .	172
6. Brønsted Acidic Ionic Liquids . . . . .	179
7. Basic Ionic Liquids . . . . .	180
8. Impurities . . . . .	181
IV. Ionic Liquids as Catalysts . . . . .	182
A. Brønsted Acid Catalysis in Ionic Liquids . . . . .	182
B. Lewis Acidic Ionic Liquids . . . . .	184
1. Non-Chloroaluminate Lewis-Acid-Catalyzed Reactions . . . . .	184
2. Chloroaluminate-Catalyzed Reactions . . . . .	186
C. Basic Ionic Liquids and Related Reactions . . . . .	188
1. Aldol Reaction . . . . .	188
2. Knoevenagel Condensation . . . . .	189
3. Robinson Annulation . . . . .	189
D. Neutral Ionic Liquids as Catalysts . . . . .	190
V. Ionic Liquids as Catalyst Carriers . . . . .	191
A. Characteristics of Ionic Liquid Catalyst Carriers . . . . .	191
1. Inert Catalyst Carriers . . . . .	191
2. Stabilization of Transition States . . . . .	191
3. Lewis Acidity . . . . .	192
4. Dispersion and Isolation of Organometallic Catalysts . . . . .	194
5. Ligand Partitioning Effects . . . . .	194
6. Ligand Effects of Ionic Liquids . . . . .	196
7. Ionic Tagging of Active Catalysts . . . . .	197
8. Hydrophobicity-Aided Catalysis . . . . .	198
9. Enhanced Reaction Rate Due to Increased Substrate Solubility . . . . .	198
10. Solubility-Aided Product Selectivity . . . . .	199
11. Effect of Co-Solvents . . . . .	201
12. Structural Effects of Cations . . . . .	201
13. Reactivity of Proton at C2 Position in Imidazolium Ion . . . . .	202
14. Phase Transfer Effect . . . . .	202
B. Catalytic Reactions . . . . .	203
1. Olefin Metathesis . . . . .	204
2. Dimerization of Dienes . . . . .	205
3. Olefin Dimerization . . . . .	205
4. Suzuki Coupling . . . . .	206
5. Hydrogenation . . . . .	206



6. Oxidation . . . . .	208
7. Dihydroxylation . . . . .	209
8. Olefin Dimerization . . . . .	210
9. Dimerization of Dienes . . . . .	211
10. Oligomerization and Polymerization . . . . .	212
11. Carbonylation/Hydroformylation . . . . .	215
12. Heck Cross-Coupling . . . . .	216
13. Alkoxy carbonylation . . . . .	218
14. Cyclodehydration Reaction . . . . .	218
C. Electrocatalysis in Ionic Liquids . . . . .	219
VI. Supported Ionic Liquid Catalysis . . . . .	220
VII. Biocatalysis in Ionic Liquid Media . . . . .	223
A. Transesterification . . . . .	224
B. Oxidation . . . . .	227
C. Aldol Reactions . . . . .	228
D. Galactosylation Reactions . . . . .	228
VIII. Conclusions and Perspective . . . . .	229
References . . . . .	230

## **Optimization of Alkaline Earth Metal Oxide and Hydroxide Catalysts for Base-Catalyzed Reactions**

*A. Corma and S. Iborra*

I. Introduction . . . . .	239
II. Surface Basicity and Base Strength of Alkaline Earth Metal Oxides . . . . .	240
III. Synthesis of High-Surface-Area Alkaline Earth Metal Oxides . . . . .	242
IV. Characterization of the Number and Strength of Basic Sites . . . . .	244
A. Titration Methods . . . . .	245
B. Spectroscopic Methods . . . . .	245
1. Infrared Spectroscopy of Adsorbed Probe Molecules . . . . .	246
2. Thermal Methods of Adsorbed Probe Molecules . . . . .	248
C. Catalytic Test Reactions . . . . .	249
1. Knoevenagel Condensation . . . . .	251
2. Acetylacetone Cyclation . . . . .	252
3. Isophorone Isomerization . . . . .	253
V. Stability of Anionic Intermediates . . . . .	253
VI. Catalytic Activity of Alkaline Earth Metal Oxides . . . . .	254
A. Isomerization Reactions . . . . .	254
B. Carbon-Carbon Bond Formation Reactions . . . . .	256
1. Aldol Condensations . . . . .	256
2. Claisen-Schmidt Condensation . . . . .	259
3. Nitroaldol Condensation . . . . .	260
4. Knoevenagel Condensation . . . . .	261
5. Wittig and Wittig-Horner Reactions . . . . .	262
6. Michael Addition . . . . .	263
7. Condensation of Alcohols . . . . .	264
C. Carbon-Oxygen Bond Formation Reactions . . . . .	265
1. Cyanoethylation of Alcohols . . . . .	265
2. Conjugate Addition of Methanol to $\alpha,\beta$ -unsaturated Carbonyl Compounds . . . . .	266
3. Transesterification Reactions . . . . .	266

D. Hydrogen Transfer Reactions . . . . .	269
1. Tishchenko Reaction. . . . .	269
2. Meerwein-Pondorff-Verley and Oppenauer Reactions. . . . .	272
VII. Zeolites and Mesoporous Aluminosilicates Modified with Alkaline Earth Metal Oxides . . . . .	275
A. Catalytic Activities of Alkaline Earth-Modified Zeolites . . . . .	277
B. Catalytic Activity of Alkaline Earth-Modified Mesoporous Molecular Sieves. . . . .	279
VIII. Alkali Metal-Doped Alkaline Earth Metal Oxides . . . . .	280
A. Methods of Preparation of Alkali Metal-Doped Alkaline Earth Metal Oxides. . . . .	281
1. Alkaline Earth Metal Oxides Doped with Alkali Metals by Chemical Vapor Deposition . . . . .	282
2. Alkaline Earth Metal Oxides Doped with Alkali Metals Prepared by Impregnation . . . . .	284
IX. Alkaline Earth Metal Hydroxides . . . . .	287
A. Catalytic Reactions on Alkaline Earth Metal Hydroxides . . . . .	289
1. Aldol Condensations . . . . .	289
2. Claisen-Schmidt Condensation . . . . .	289
3. Michael Additions. . . . .	290
4. Wittig-Horner Reaction . . . . .	291
5. Arylation of Carbonyl Compounds. . . . .	293
X. Conclusions and Future Opportunities . . . . .	294
Acknowledgement . . . . .	295
References . . . . .	295
INDEX . . . . .	303

# Contributors

*Numbers in parentheses indicate the pages on which the author's contributions begin.*

SILVIA ARÉVALO, *Van't Hoff Institute for Molecular Sciences, University of Amsterdam, Nieuwe Achtergracht 166, 1018 WV, Amsterdam, The Netherlands* (71)

Z. CONRAD ZHANG, *AKZO Nobel Chemicals, Inc., 1 Livingstone Avenue, Dobbs Ferry, New York 10522, USA* (153)

A. CORMA, *Instituto de Tecnología Química CSIC-UPV, Universidad Politécnica de Valencia, Avda. de los Naranjos s/n, 46023-Valencia, Spain* (239)

RIEKO VAN HEERBEEK, *Van't Hoff Institute for Molecular Sciences, University of Amsterdam, Nieuwe Achtergracht 166, 1018 WV, Amsterdam, The Netherlands* (71)

S. IBORRA, *Instituto de Tecnología Química CSIC-UPV, Universidad Politécnica de Valencia, Avda. de los Naranjos s/n, 46023-Valencia, Spain* (239)

PAUL C. J. KAMER, *Van't Hoff Institute for Molecular Sciences, University of Amsterdam, Nieuwe Achtergracht 166, 1018 WV, Amsterdam, The Netherlands* (71)

PIET W.N.M. VAN LEEUWEN, *Van't Hoff Institute for Molecular Sciences, University of Amsterdam, Nieuwe Achtergracht 166, 1018 WV, Amsterdam, The Netherlands* (71)

JOOST N. H. REEK, *Van't Hoff Institute for Molecular Sciences, University of Amsterdam, Nieuwe Achtergracht 166, 1018 WV, Amsterdam, The Netherlands* (71)

M. T. REETZ, *Max-Planck-Institut für Kohlenforschung, 45470 Mülheim/Ruhr, Germany* (1)

## Preface

In its 57 years of publication, *Advances in Catalysis* has emphasized heterogeneous catalysis, with only occasional chapters focused on homogeneous and biological catalysis. This volume is a departure and a signal of our intent to include more of the latter. In the preface to Volume 25 of this series, Paul Weisz offered the following challenge:

“Speaking of desirable goals, some years ago we resolved to help bring together the basically related knowledge of the catalytic and of the enzymatic researchers—but, alas, with little success. Common phenomena, laws, concepts, and mechanisms do exist, but are busily pursued by linguistically separated groups (like those who do Langmuir–Hinshelwood and those who do Michaelis–Menten kinetics, or those for which “substrate” not only has different but opposite connotations, etc.). These two areas of endeavor remain perfect examples of the ivory towers of Babel which often characterize scientific pursuits. We will continue to try to bridge a regrettable gap, but it will take editors *and* authors—authors fluent in both languages. We are looking for the rare talent ...”

Notwithstanding the stunning progress in catalysis since those words were written, they still ring true. Thus, one of our goals as editors, beyond increasing the scope of the *Advances*, is to encourage contributions that emphasize the unity of catalysis and highlight the ties between the traditionally distinct subcategories of homogeneous, heterogeneous, and biological catalysis, all of which are benefiting more and more from deeper understanding of catalyst structures and reaction processes at the molecular level.

The chapters in this volume illustrate how molecular concepts underlie catalysis. They illustrate how modern concepts of biology are influencing catalysis and catalyst discovery; how concepts of homogeneous and surface catalysis have merged (a theme that is evident in the preceding several volumes of the *Advances*), exemplified by dendrimer catalysts that have properties of both molecules and surfaces; and how concepts of molecular catalysis by bases have influenced the development of new solid-base catalysts and fundamental understanding of how they function.

The chapter by Reetz includes many examples and explanations of methods illustrating how directed evolution has been applied to prepare new enzyme catalysts. Directed evolution of enantioselective enzymes has emerged as a fundamentally new approach to asymmetric catalysis. It involves the combination

of gene mutagenesis, expression, and high-throughput testing to determine enantiomeric purity. The methods of directed evolution have been applied to improve catalytic properties such as activity, thermal stability, and resistance to hostile solvents, and even to reduce product inhibition and minimize the formation of undesired side products. Directed evolution is also beginning to have an impact on the engineering of proteins to cause them to catalyze reaction types different from those corresponding to their natural functions. Several examples of directed evolution of enantioselective and robust enzymes have emerged from industrial laboratories, and there seem to be good prospects of large-scale application of enzymes made by directed evolution.

The chapter by Zhang is an exhaustive summary of ionic liquids in catalysis. An ionic liquid, a salt with a melting point less than about 100°C, typically consists of an organic cationic with one or more heteroatoms such as N, P, or S and an inorganic or organic anion. The relative inertness of many ionic liquids makes them superior to water as solvents for many catalysts, and their low vapor pressures make them environmentally attractive replacements for organic solvents. Other appealing properties of ionic liquids include high thermal stabilities, broad ranges of temperatures over which they are liquids, and opportunities to tune their chemical properties by choice of the cationic and anionic components. Many of these liquids are easily separated from reaction products, and they have been used both in single-phase and biphasic catalysis. They have been the focus of extensive research in recent years and been shown to catalyze a broad range of reactions, with indications of potential industrial applications.

Nonetheless, the research in catalysis by ionic liquids is at an early stage, and questions remain regarding potential applications. For example, the solubility of a reactant in an ionic liquid may limit the rate of the desired reaction. Some ionic liquids are moisture-sensitive, particularly those containing metal halides. A small loss of ionic liquid into the products may necessitate costly purification steps. The cost of ionic liquids has also limited their applications, and there is significant uncertainty regarding the toxicity and potential environmental impact of some ionic liquids.

The chapter by Reek, Arevalo, van Heerbeek, Kamer, and van Leeuwen is a critical and thorough account of dendrimers in catalysis. These large, soluble, globular, hyperbranched macromolecules offer attractive new properties as catalysts and catalyst supports, combining characteristics such as selective swelling and uptake of some reactant molecules from mixtures (properties that are familiar from subjects such as catalysis by polymer gels and even by enzymes), combined with opportunities for efficient filtration with membranes to separate catalysts from fluid-phase products. The location of the catalytically active groups in the dendritic framework (e.g., at the core or near the periphery) is important in determining the catalytic properties, for example, by influencing the access of various reactants to these groups. Like other soluble catalysts, these can be used in a single-phase or in biphasic catalysis.

The common problems involved in recycle of soluble catalysts pertain to dendritic catalysts; one has to contend with decomposition of the dendrimer or the catalytic groups attached to it, dendrimer leaching, metal leaching, and catalyst

deactivation. Small changes in the dendritic architecture can have a great impact on the stability of a catalyst. Dendrimer supports are still relatively expensive, and it remains an open question whether dendritic catalysis can compete successfully in commercial applications.

For years, conventional acid and base catalysis has been carried out in industry with low-cost catalysts such as  $\text{H}_2\text{SO}_4$  and  $\text{KOH}$  in aqueous solutions. Environmental concerns with separation and disposal of these catalysts have led to their substantial replacement with solid acids and bases. The chapter by Corma and Iborra provides an assessment of the opportunities offered by solid-base catalysts, with an emphasis on alkaline earth metal oxides and hydroxides and structures formed from alkali metals and oxides supported on alkaline earth metal oxides. The authors include an extensive review of the catalytic applications of solid bases for organic transformations including isomerization, carbon–carbon and carbon–oxygen bond formation, and hydrogen transfer reactions, and they provide insightful comments about the opportunities for future applications of these catalysts. Their reasoning is molecular; they pose a challenge for materials scientists to synthesize high-area, well-structured, stable base catalysts on the foundation of molecular-scale understanding of the interactions of reactant molecules with groups on the catalyst surface. The authors highlight opportunities to tune surface acid–base pair sites to induce cooperative catalytic effects such as those known to be important in enzyme catalysis.

B.C. GATES  
H. KNÖZINGER